INHERITED PROTEIN GLYCOSYLATION DEFECTS IN HUMAN DISEASES

EDITED BY: Aleksandra Jezela-Stanek, Anna Tylki-Szymańska and Karolina Stepien

PUBLISHED IN: Frontiers in Genetics and Frontiers in Pediatrics

frontiers Research Topics

frontiers

ISSN 1664-8714
ISBN 978-2-88974-842-6
DOI 10.3389/978-2-88974-842-6

About Frontiers

Frontiers is more than just an open-access publisher of scholarly articles: it is a pioneering approach to the world of academia, radically improving the way scholarly research is managed. The grand vision of Frontiers is a world where all people have an equal opportunity to seek, share and generate knowledge. Frontiers provides immediate and permanent online open access to all its publications, but this alone is not enough to realize our grand goals.

Frontiers Journal Series

The Frontiers Journal Series is a multi-tier and interdisciplinary set of open-access, online journals, promising a paradigm shift from the current review, selection and dissemination processes in academic publishing. All Frontiers journals are driven by researchers for researchers; therefore, they constitute a service to the scholarly community. At the same time, the Frontiers Journal Series operates on a revolutionary invention, the tiered publishing system, initially addressing specific communities of scholars, and gradually climbing up to broader public understanding, thus serving the interests of the lay society, too.

Dedication to Quality

Each Frontiers article is a landmark of the highest quality, thanks to genuinely collaborative interactions between authors and review editors, who include some of the world's best academicians. Research must be certified by peers before entering a stream of knowledge that may eventually reach the public - and shape society; therefore, Frontiers only applies the most rigorous and unbiased reviews.
Frontiers revolutionizes research publishing by freely delivering the most outstanding research, evaluated with no bias from both the academic and social point of view. By applying the most advanced information technologies, Frontiers is catapulting scholarly publishing into a new generation.

What are Frontiers Research Topics?

Frontiers Research Topics are very popular trademarks of the Frontiers Journals Series: they are collections of at least ten articles, all centered on a particular subject. With their unique mix of varied contributions from Original Research to Review Articles, Frontiers Research Topics unify the most influential researchers, the latest key findings and historical advances in a hot research area! Find out more on how to host your own Frontiers Research Topic or contribute to one as an author by contacting the Frontiers Editorial Office: frontiersin.org/about/contact

INHERITED PROTEIN GLYCOSYLATION DEFECTS IN HUMAN DISEASES

Topic Editors:
Aleksandra Jezela-Stanek, National Institute of Tuberculosis and Lung Diseases (Poland), Poland
Anna Tylki-Szymańska, Children's Memorial Health Institute (IPCZD), Poland
Karolina Stepien, Salford Royal NHS Foundation Trust, United Kingdom

Citation: Jezela-Stanek, A., Tylki-Szymańska, A., Stepien, K., eds. (2022). Inherited Protein Glycosylation Defects in Human Diseases. Lausanne: Frontiers Media SA. doi: 10.3389/978-2-88974-842-6

Table of Contents

frontiers in Genetics

EDITORIAL
published: 14 March 2022
doi: 10.3389/fgene.2022.851438

Editorial: Inherited Protein Glycosylation Defects in Humans

Aleksandra Jezela-Stanek[1†], *Karolina M. Stepien*[2*†] *and Anna Tylki-Szymanska*[3]

[1]*Department of Genetics and Clinical Immunology, National Institute of Tuberculosis and Lung Diseases, Warsaw, Poland,* [2]*Adult Inherited Metabolic Disorders, Salford Royal NHS Foundation Trust, Salford, United Kingdom,* [3]*Department of Pediatric Nutrition and Metabolic Diseases, Children's Memorial Health Institute, Warsaw, Poland*

Keywords: congenital disorder of glycosylation, CDG, glycosylation, deglycosylation, GPIBD

Editorial on the Research Topic

Inherited Protein Glycosylation Defects in Humans Diseases

Facilitated by the wide availability of next-generation sequencing-based genetic testing such as whole exome sequencing (WES) or whole genome sequencing (WGS), the number of new diagnoses within rare diseases is constantly growing. Specifically, this editorial refers to inherited metabolic diseases resulting from defects in protein glycosylation, including congenital disorders of glycosylation (encompassing N-glycosylation, O-glycosylation, multiple glycosylation), disorders of glycosphingolipids, glycosylphosphatidylinositol (GPI)-anchored protein defects (GPIBDs), and deglycosylation disorders (CDDGs).

Congenital disorders of glycosylation (CDG), first reported in the medical literature in 1980 by Prof. Jaak Jaeken and colleagues (Jaeken, 2010), is a group of ~140 rare genetic, metabolic disorders resulting from defects in a complex chemical process known as glycosylation. This process involves myriad different genes, encoding a variety of proteins (called glycoproteins), such as enzymes and glycolipids, which have numerous important functions in nearly all tissue types (Jaeken et al., 1980). Consequently, CDG can affect any part of the human body and a predominant neurological deterioration is a frequent manifestation of the clinical spectrum (Paprocka et al., 2021). Because CDG can be associated with a multitude of symptoms and varies widely in severity, achieving a diagnosis based on clinical criteria is challenging. Molecular genetic testing offers the greatest accuracy toward pinpointing an underlying cause.

The goal of the "*Inherited Protein Glycosylation Defects in Human Diseases*" Research Topic was to raise awareness of and improve our understanding of genetic diseases resulting from defects in proteins glycosylation. We aimed to present a comprehensive picture of these disorders, ranging from: 1) clinical manifestation (in reference to specific internal organs), 2) genetic background, 3) underlying pathomechanisms, and 4) discussion of treatment options. The final topic issue has 14 published articles.

Contrary to a classical approach, wherein diagnostic analysis proceeds from phenotype to genotype, researchers are increasingly employing reverse genetics strategies, where the analysis proceeds from genotype to phenotype. As a consequence, reaching a genetic diagnosis is only the beginning of the clinical journey and can open up a plethora of complex considerations. For CDGs, GPIBDs, and CDDGs, geneticists and metabolic physicians face perpetual challenges regarding prediction of clinical manifestations, availability of natural history and/or availability of any treatment options. Consequently, and to overcome these challenges, a new genetic diagnosis can generate new basic science and clinical research opportunities, spark international collaboration and encourage researchers to share experience within the wider medical community. Furthermore, advocacy from patient organisations offer complementary advances toward improving diagnosis, shortening the lengthy diagnostic odyssey and decreasing mortality from these rare conditions (González-Domínguez et al.).

OPEN ACCESS

Edited and reviewed by:
Erica E. Davis,
Ann & Robert H. Lurie Children's Hospital of Chicago, United States

****Correspondence:***
Karolina M. Stepien
kstepien@doctors.org.uk

†These authors have contributed equally to this work

Specialty section:
This article was submitted to Genetics of Common and Rare Diseases, a section of the journal Frontiers in Genetics

Received: *09 January 2022*
Accepted: *25 February 2022*
Published: *14 March 2022*

Citation:
Jezela-Stanek A, Stepien KM and Tylki-Szymanska A (2022) Editorial: Inherited Protein Glycosylation Defects in Humans. Front. Genet. 13:851438. doi: 10.3389/fgene.2022.851438

Despite the advent of robust diagnostic technology, there are still regional limitations to WES and WGS access that are influenced by the local health economy. Given that rapid diagnosis can be hampered by poor access to specialist laboratories and tertiary metabolic centres, Lipinski and Tylki-Szymanska outlined diagnostic algorithms for a rapid and accurate diagnosis of CDGs in children based on their own clinical experience in Poland. Kosinski et al., however, outlined the difficulties of diagnosing a CDG prenatally, which highlights the need for including these disorders in the diagnostic paradigm of fetuses with certain ultrasound findings, such as diaphragmatic hernia.

Systematic employment of WES/WGS has uncovered hitherto unappreciated phenotype expansions of CDG. In one instance, liver involvement was observed in a congenital disorder of deglycosylation (Lipinski et al.), although it was not implicated previously as a core clinical feature. Clinical spectra of particular diseases were revisited; for example, Kamarus Jaman et al. emphasized ophthalmological abnormalities including early-onset retinal dystrophy and optic nerve hypoplasia as key clinical diagnostic features of SRD5A3-CDG in patients with a multisystem disorder with variable symptoms evolving over time. DOLK-CDG caused by a defect in dolichol kinase in which the congenital skin phenotype (often ichthyosis) is associated with variable extracutaneous features such as dilatated cardiomyopathy, epilepsy, microcephaly, visual impairment, and hypoglycemia are now shown to have a fatal course (Komlosi et al.). Other conditions such as PIGT and phosphomannomutase 2 deficiency (PMM2-CGD) have been better defined. The comprehensive analysis of a large cohort of both previously published and newly studied individuals with *PIGT* variants analysed by Bayat et al. broadens the phenotypic spectrum and presents evidence that p.Asn527Ser and p.Val528Met variants are associated with a mild phenotype and less severe outcomes, and *PIGT* may be considered as a new candidate gene for myoclonic, atonic epilepsy. Mercedes Serrano reported stroke-like episodes (SLE) as a manifestation of an expanded phenotype of PMM2-CDG. The characteristic but non-specific constellation of symptoms including migraine, focal neurologic deficits, hemispheric slow electroencephalogram (EEG) trace and refractory hyperpyrexia without laboratory signs of infection, are now shown to be suggestive of PMM2-CDG disorder.

Another recent report has shown expansion of the genotypic and phenotypic spectrum of another CDG. Abuduxikuer and Wang present four new cases affected with a previously unreported deleterious variant causing SLC35A2-CDG, and describe clinical complications of the condition in pregnancy (hypothyroidism and oligohydramnios). Taken together, the evolving clinical spectrum of CDGs makes it difficult to predict long-term prognosis and clinical outcomes in adulthood, therefore there is a need for long-term follow-up of these patients with multi-disciplinary specialists.

The prevalence of other CDG types remains unknown. To address this knowledge gap, Pajusalu and colleagues report the estimated prevalence of different N-linked protein glycosylation defects calculated from population allele frequencies (Pajusalu et al.). Although the CDG group involves at least 137 defects, they included only 27 autosomal recessive protein N-glycosylation affecting defects and excluded abnormalities that affect multiple glycosylation pathways. If all 27 defects are considered, the combined prevalence of CDGs in non-Finnish Europeans is 1:22,000. If FUK-CDG and MAN2B2-CDG are excluded (lack homozygous loss-of-function (LoF) variant carriers in Genome Aggregation Database (gnomAD)), the prevalence among Europeans is slightly lower and does not exceed one in 24,000.

Apart from CDGs, this Research Topic describes the prevalence and clinical manifestations of other inherited protein glycosylation defects such as POMT2-related defective O-mannosylglycosylation of α-dystroglycan (Chen et al.) and GM1-gangliosidosis caused by the reduced activity of β-Galactosidase which leads to the accumulation of both GM1 ganglioside and also its derivative, GA1, primarily in lysosomes of neuronal tissue (Nicoli et al.).

Beyond diagnostics, this Research Topic also discusses therapeutic options. Cellular models are the first step to the new therapeutic advances. In their original research, Sumya et al. described the cellular model for Conserved Oligomeric Golgi, an octameric protein complex that orchestrates intra-Golgi trafficking of glycosylation enzymes. Nicoli et al. described various experimental therapies for GM1-gangliosidosis tested on human cell lines. Understanding the cellular pathophysiology underlying this disease is essential toward developing therapeutic avenues. Mouse models have been instrumental for the pre-clinical testing of multiple therapies for GM1-gangliosidosis.

Recent therapeutic advances aimed both at the causative defect and secondary disease manifestations in CDGs were discussed by Park and Marquardt. Unfortunately, therapies are currently limited to only a few CDG subtypes and there is no strong evidence of their efficacy due to the lack of randomized controlled trials.

In conclusion, despite an improved understanding of pathophysiology of CDG, diagnosis within this disease group remains a challenge. However, an emergent availability of genome-editing techniques is opening a promising future for CDG patients who have received a molecular diagnosis. Therefore, the focus of future research should be on documenting long-term outcomes of adults affected with these conditions, and targeted therapeutic developments to attenuate symptoms.

AUTHOR CONTRIBUTIONS

All three guest editors drafted the editorial for the Research Topic.

REFERENCES

Jaeken, J. (2010). Congenital Disorders of Glycosylation. *Ann. N. Y. Acad. Sci.* 1214, 190–198. doi:10.1111/j.1749-6632.2010.05840.x

Jaeken, J., Vanderschueren-Lodeweyckx, M., Casaer, P., Snoeck, L., Corbeel, L., Eggermont, E., et al. (1980). Familial Psychomotor Retardation with Markedly Fluctuating Serum Prolactin, FSH and GH Levels, Partial TBG-Deficiency, Increased Serum Arylsulphatase A and Increased CSF Protein: a New Syndrome? *Pediatr. Res.* 14, 90179. doi:10.1203/00006450-198002000-00117

Paprocka, J., Jezela-Stanek, A., Tylki-Szymańska, A., and Grunewald, S. (2021). Congenital Disorders of Glycosylation from a Neurological Perspective. *Brain Sci.* 11 (1), 88. doi:10.3390/brainsci11010088

Conflict of Interest: The authors declare that the research was conducted in the absence of any commercial or financial relationships that could be construed as a potential conflict of interest.

Publisher's Note: All claims expressed in this article are solely those of the authors and do not necessarily represent those of their affiliated organizations, or those of the publisher, the editors and the reviewers. Any product that may be evaluated in this article, or claim that may be made by its manufacturer, is not guaranteed or endorsed by the publisher.

frontiers in Genetics

ORIGINAL RESEARCH
published: 11 May 2021
doi: 10.3389/fgene.2021.663643

Deep-Phenotyping the Less Severe Spectrum of *PIGT* Deficiency and Linking the Gene to Myoclonic Atonic Seizures

Allan Bayat[1,2], Manuela Pendziwiat[3,4], Ewa Obersztyn[5], Paula Goldenberg[6], Pia Zacher[7], Jan Henje Döring[8], Steffen Syrbe[8], Amber Begtrup[9], Artem Borovikov[10], Artem Sharkov[11], Aneta Karasińska[12], Maria Giżewska[13], Wendy Mitchell[14], Eva Morava[15], Rikke S. Møller[1,2] and Guido Rubboli[2,16]*

[1] *Institute for Regional Health Services, University of Southern Denmark, Odense, Denmark,* [2] *Department of Epilepsy Genetics and Personalized Medicine, Danish Epilepsy Centre, Dianalund, Denmark,* [3] *Department of Neuropediatrics, Children's Hospital, University Medical Center Schleswig-Holstein, University of Kiel, Kiel, Germany,* [4] *Institute of Clinical Molecular Biology, Christian-Albrechts-University of Kiel, Kiel, Germany,* [5] *Department of Medical Genetics, Institute of Mother and Child, Warsaw, Poland,* [6] *Division of Medical Genetics, Massachusetts General Hospital, Boston, MA, United States,* [7] *The Saxon Epilepsy Center Kleinwachau, Radeberg, Germany,* [8] *Department of General Pediatrics, Division of Child Neurology and Inherited Metabolic Diseases, Center for Pediatrics and Adolescent Medicine, University Hospital Heidelberg, Heidelberg, Germany,* [9] *GeneDx, Gaithersburg, MD, United States,* [10] *Research Centre for Medical Genetics, Moscow, Russia,* [11] *Veltischev Research and Clinical Institute for Pediatrics of the Pirogov Russian National Research Medical University, Moscow, Russia,* [12] *Department of Dermatology, The Nicolas Copernicus State Hospital, Koszalin, Poland,* [13] *Department of Pediatrics, Endocrinology, Diabetology, Metabolic Diseases and Cardiology of the Developmental Age, Pomeranian Medical University, Szczecin, Poland,* [14] *Department of Neurology, Keck School of Medicine, University of Southern California, Los Angeles, CA, United States,* [15] *Department of Clinical Genomics, Laboratory of Medicine and Pathology, Center for Individualized Medicine, Mayo Clinic, Rochester, MN, United States,* [16] *Department of Clinical Medicine, Faculty of Medical and Health Sciences, University of Copenhagen, Copenhagen, Denmark*

OPEN ACCESS

Edited by:
Karolina Stepien, Salford Royal NHS Foundation Trust, United Kingdom

Reviewed by:
Magdalena Sandu, Spitalul Clinic de Copii Doctor Victor Gomoiu, Romania
Ana Westenberger, University of Lübeck, Germany

***Correspondence:**
Allan Bayat
abaya@filadelfia.dk

Specialty section:
This article was submitted to Genetics of Common and Rare Diseases, a section of the journal Frontiers in Genetics

Received: *03 February 2021*
Accepted: *29 March 2021*
Published: *11 May 2021*

Citation:
Bayat A, Pendziwiat M, Obersztyn E, Goldenberg P, Zacher P, Döring JH, Syrbe S, Begtrup A, Borovikov A, Sharkov A, Karasińska A, Giżewska M, Mitchell W, Morava E, Møller RS and Rubboli G (2021) Deep-Phenotyping the Less Severe Spectrum of PIGT Deficiency and Linking the Gene to Myoclonic Atonic Seizures. Front. Genet. 12:663643. doi: 10.3389/fgene.2021.663643

The two aims of this study were (i) to describe and expand the phenotypic spectrum of *PIGT* deficiency in affected individuals harboring the c.1582G>A; p.Val528Met or the c.1580A > G; p.Asn527Ser variant in either homozygous or compound heterozygous state, and (ii) to identify potential genotype-phenotype correlations and any differences in disease severity among individuals with and without the *PIGT* variants. The existing literature was searched to identify individuals with and without the two variants. A detailed phenotypic assessment was performed of 25 individuals (both novel and previously published) with the two *PIGT* variants. We compared severity of disease between individuals with and without these *PIGT* variants. Twenty-four individuals carried the *PIGT* variant Val528Met in either homozygous or compound heterozygous state, and one individual displayed the Asn527Ser variant in a compound heterozygous state. Disease severity in the individual with the Asn527Ser variant was compatible with that in the individuals harboring the Val528Met variant. While individuals without the Asn527Ser or Val528Met variant had focal epilepsy, profound developmental delay (DD), and risk of premature death, those with either of the two variants had moderate to severe DD and later onset of epilepsy with both focal and generalized seizures. Individuals homozygous for the Val528Met variant generally became seizure-free on monotherapy

with antiepileptic drugs, compared to other *PIGT* individuals who were pharmaco-resistant. Two patients were diagnosed with myoclonic-atonic seizures, and a single patient was diagnosed with eyelid myoclonia. Our comprehensive analysis of this large cohort of previously published and novel individuals with *PIGT* variants broadens the phenotypical spectrum and shows that both Asn527Ser and Val528Met are associated with a milder phenotype and less severe outcome. Our data show that *PIGT* is a new candidate gene for myoclonic atonic epilepsy. Our genotype-phenotype correlation will be useful for future genetic counseling. Natural history studies of this mild spectrum of *PIGT*-related disorder may shed light on hitherto unknown aspects of this rare disorder.

Keywords: myoclonic-atonic seizures, generalized seizures, disease severity, developmental delay, glycosylphosphatidylinositol biosynthesis defects, inherited glycosylphosphatidylinositol-anchored protein (GPI-AP) deficiency

INTRODUCTION

Glycosylphosphatidylinositol (GPI) is a glycolipid that is synthetized and transferred to proteins in the membrane of the endoplasmic reticulum (Fujita and Kinoshita, 2012). The biogenesis of GPI-anchored proteins (GPI-APs) is a conserved post-translational mechanism in eukaryotes and is important for the attachment of these proteins to the cell membrane and for protein sorting, trafficking, and dynamics (Fujita and Kinoshita, 2012; Kinoshita and Fujita, 2016; Bayat et al., 2020b). GPI synthesis and GPI-AP modification are mediated by at least 31 genes, and pathogenic variants in 22 of these genes have so far been associated with human disease (Bellai-Dussault et al., 2019; Bayat et al., 2020b).

The *PIGT* gene encodes the phosphatidylinositol glycan class T protein that is part of the subunit of the heteropentameric GPI transamidase complex with *PIGK, PIGS, PIGT, PIGU,* and *PGAA1* that facilitates the attachment of GPI anchors to proteins (Ohishi et al., 2001, 2003).

Pathogenic germline missense and truncating variants in *PIGT* have been associated with a condition named "multiple congenital anomalies – hypotonia - seizures syndrome 3 (MCAHS3)" (OMIM 615398). Affected individuals share features such as epileptic seizures, severe to profound developmental delay (DD), intellectual disability (ID), and multiple congenital malformations of internal organs. Most individuals are non-verbal, non-ambulatory, and suffer from intractable epilepsy (Bayat et al., 2019). Generalized myoclonic and focal motor seizures with impaired awareness associated with various type of EEG epileptic abnormalities (focal sharp-slow wave, focal sharp spike/polyspikes wave, and generalized polyspikes-wave complexes) have been observed (Jezela-Stanek et al., 2020). While focal seizures with or without bilateral spreading have been described on several occasions (Bayat et al., 2019; Jezela-Stanek et al., 2020), reports of generalized seizures remain limited. Primary generalized seizures have so far only been described in a small number of individuals with a compound heterozygous variant at position Val528Met (Jezela-Stanek et al., 2020).

Individuals that are homozygous or compound heterozygous for the missense variant c.1582G > A; p.Val528Met have been reported to have a less severe phenotype (Pagnamenta et al., 2017; Bayat et al., 2019; Jezela-Stanek et al., 2020). This is currently the only variant reported to result in a milder phenotype. Amongst the 37 individuals described with *PIGT* deficiency (Kvarnung et al., 2013; Nakashima et al., 2014; Lam et al., 2015; Skauli et al., 2016; Knaus et al., 2018; Kohashi et al., 2018; Yang et al., 2018; Bayat et al., 2019; Mason et al., 2019; Jezela-Stanek et al., 2020; Jiao et al., 2020), only 13 individuals have been reported to harbor this variant in a homozygous or compound heterozygous state (Pagnamenta et al., 2017; Bayat et al., 2019; Jezela-Stanek et al., 2020). Our knowledge remains limited about the extent of DD and ID associated with this variant and about the natural history in adolescence and adulthood. Furthermore, a detailed comparison of symptoms in affected individuals with and without the p.Val528Met variant has yet to be done. More individuals are needed to better delineate the genotype-phenotype correlation and to investigate if other pathogenic variants can also be associated with a milder phenotype.

Here, we describe 13 novel individuals with a *PIGT* deficiency and 12 previously reported individuals (Bayat et al., 2019; Jezela-Stanek et al., 2020). We also present follow-up data on two of the 12 previously published individuals [P4 and P5 from Bayat et al. (2019)]. Of the 25 individuals, 24 harbored the Val528Met variant in either homozygous or compound heterozygous state, while one individual had a previously unreported c.1580A > G; p.Asn527Ser variant. We present a detailed phenotyping of the affected individuals and expand the known epilepsy semiology to include myoclonic-atonic seizures. We also compare the findings with those seen in previously published affected individuals without the two variants.

Abbreviations: AED, antiepileptic drugs; DD, developmental delay; EEG, electroencephalogram; ER, endoplasmatic reticulum; GPI, glycosylphosphatidylinositol; GPI-AP, glycosylphosphatidylinositol anchored protein; GPIBD, biosynthesis defects of the GPI anchor; ID, intellectual disability; MRI, magnetic resonance imaging; PIGT, phosphatidylinositol glycan class T protein; VPA, valproate.

MATERIALS AND METHODS

Individual Analysis

Subjects were identified and recruited either through their treating clinicians, self-referral, or GeneMatcher

(Sobreira et al., 2015). Basic medical information on birth parameters, epilepsy, developmental history, and physical examinations was collected from healthcare providers and/or families of affected individuals. Molecular testing results from exome sequencing were submitted by healthcare providers. In eight cases, individual videos provided by caregivers were also used to evaluate motor skills. All the videos submitted and evaluated were used with the written consent of guardians. Videos were evaluated by authors AB and GR.

The clinical findings of this cohort were compared to previously published individuals with *PIGT* deficiency who did not harbor either of the two variants. As the access to clinical data was limited in a substantial number of published individuals, we chose only to compare data on seizures and neurological development.

Standard Protocol Approvals, Registrations, and Individual Consent

The study was conducted in agreement with the Declaration of Helsinki and approved by the local ethics committee of the referring center. As all individuals were either minors or had cognitive impairment, their parents or legal guardians gave informed consent. The clinical information was collected through interviews with the families and/or from hospital records of the individuals and their family members. Videos were collected from either caregivers or healthcare providers.

Literature Search

We searched MEDLINE (PubMed) with the keywords epilepsy, GPI, GPI-AP, or GPI-anchored protein in combination with *PIGT* or phosphatidylinositol glycan class T protein (last PubMed search: January 2021). Any relevant references in the assessed articles, which were not found in the MEDLINE search, were further investigated. Only articles written in English and published after 1980 were included to ensure optimal data collection. Only cases with a confirmed molecular diagnosis were included.

Data Availability

Anonymized data, including data not published in this article, will be made available on request from any qualified investigator.

Genetic Identification and Analysis

All affected individuals were investigated by gene panels or exome sequencing ordered by healthcare providers. Variants were classified based on the 2015 joint guidelines from the American College of Medical Genetics and Genomics and the Association for Molecular Pathology (Richards et al., 2015). The protein-coding transcript used was NM_015937.6. We predicted the functional alteration of novel variants using polymorphism phenotyping-2 (PolyPhen-2) (Adzhubei et al., 2010) and SIFT (Sorting intolerant from tolerant) (Farheen et al., 2017), CADD[1], and mutationTaster[2].

[1]https://cadd.gs.washington.edu

[2]http://www.mutationtaster.org

RESULTS

Individuals and Families

We collected 13 living, novel *PIGT*-deficient individuals (8 males and 5 females) harboring either the Val528Met or the Asn527Ser variant. In addition, we present follow-up data for two previously published individuals [P4 and P5 published by Bayat et al. (2019)] 2 years after the initial publication. Fourteen individuals carried the Val528Met variant in either homozygous (n = 6) or compound heterozygous (n = 8) state, while a single individual had the Asn527Ser variant in a compound heterozygous state.

From the available literature, we identified ten previously reported individuals with the Val528Met variant [Decipher ID 258094 by Pagnamenta et al. (2017), P3 and P10 by Bayat et al. (2019), and P1-P7 by Jezela-Stanek et al. (2020)]. **Table 1** provides an overview of the clinical and genetic findings.

Part 1 of **Table 2** compares the clinical findings in the 25 individuals with the Val528Met or the Asn527Ser variant with those of 24 published individuals without these two *PIGT* variants (Kvarnung et al., 2013; Nakashima et al., 2014; Lam et al., 2015; Skauli et al., 2016; Knaus et al., 2018; Kohashi et al., 2018; Yang et al., 2018; Bayat et al., 2019; Mason et al., 2019; Jiao et al., 2020).

Phenotypic Analysis

In total, we evaluated the phenotypical features of 25 living individuals, including 15 novel and 10 previously published individuals (Bayat et al., 2020b; Jezela-Stanek et al., 2020).

Perinatal History

Few complications occurred during pregnancy. The 20-week ultrasound of one individual (P13) showed cardiac septal defects and decreased fetal movements while the other 24 patients did not exhibit any malformations on prenatal ultrasonography. The gestation length was at least 36 weeks (36–41 weeks) in all cases and was at term for the vast majority of deliveries. All children had either normal or increased birth parameters. The mean weight and length at birth were 3.9 kg (3.2–4.5 kg) and 54 cm (49–60 cm).

There were no reported stillbirth cases and no terminated pregnancies. Data on prenatal history are not shown.

Ophthalmological and Otological Features

Data on ophthalmological features were available for 22/25 (88%) individuals. Strabismus was diagnosed in 15/25 (60%), refractive error in 10/25 (40%), and cortical visual impairment (CVI) was evident in 7/25 (28%).

Individual P1 with the Asn527Ser variant had neither CVI, strabismus, nor a refractive error. Instead, he was diagnosed with features such as microphthalmia, posterior synechiae of the anterior chamber, partial angle closure, tight falciform retinal folds, peripheral avascular retina, retinal hemorrhage, and extensive vitreous membranes. Although one individual with the Asn527Ser variant exhibited ophthalmological features not previously described in *PIGT* deficiency, her overall phenotype was compatible with those found in affected individuals with the Val528Met variant. Exome sequencing found no additional

TABLE 1A | Clinical and genetic findings in 25 novel and previously published individuals with *PIGT* deficiency harboring the p.Asn527Ser or p.Val528Met variant in either homozygous or compound heterozygous state.

Families	**Family 1**	**Family 2**	**Family 3**	**Family 4**	**Family 5**	**Family 6**	**Family 7**	**Family 7**	**Family 8**	**Family 9**	**Family 10**	**Family 10**	**Family 10**
	Patient 1	**Patient 2**	**Patient 3**	**Patient 4**	**Patient 5**	**Patient 6**	**Patient 7**	**Patient 8**	**Patient 9**	**Patient 10**	**Patient 11**	**Patient 12**	**Patient 13**
cDNA change (NM_015937.6)	c.918dupC; c.1580A > G	c.769+2T > A; c.1582G > A	c.988C > T; c.1582G > A	c.988C > T; c.1582G > A	c.1127A > C; c.1582G > A	c.1342C > T; c.1582G > A	c.1519C > T; c.1582G > A	c.1519C > T; c.1582G > A	c.1520G > A; c.1582G > A	c.1582G > A; c.1582G > A	c.1582G > A; c.1582G > A	c.1582G > A; c.1582G > A	c.1582G > A; c.1582G > A
Amino acid change (NP_057021.2)	p.Val307Arg fsTer13; p.Asn527Ser	Splice site; p.Val528Met	p.Arg330Ter; p.Val528Met	p.Arg330Ter; p.Val528Met	p.His376Pro; p.Val528Met	p.Arg448Trp; p.Val528Met	p.Arg507Trp; p.Val528Met	p.Arg507Trp; p.Val528Met	p.Ala507Gln; p.Val528Met	p.Val528Met; p.Val528Met	p.Val528Met; p.Val528Met	p.Val528Met; p.Val528Met	p.Val528Met; p.Val528Met
Clinical significance	PATH; PATH	PATH: PATH	PATH; PATH	PATH; PATH	PATH; PATH	PATH; PATH	PATH; PATH	PATH; PATH	PATH; PATH	PATH; PATH	PATH; PATH	PATH; PATH	PATH; PATH
Heritage	Caucasian, African, Native American	Caucasian	Caucasian	Asian	Caucasian/African	Caucasian	Russian	Russian	Polish	Russian	Caucasian	Caucasian	Caucasian
Age at inclusion	2 years	16 years	28 years	6 years	2.6 years	6 years	8 years	22 years	3 years	6.5 years	11 years	4 years	2 years
Gender	Male	Male	Female	Female	Female	Female	Male	Female	Male	Female	Female	Female	Female
Seizures	Yes	Yes	Yes	Yes	No	Yes	Yes	Yes	No	Yes	Yes	Yes	No
Epilepsy diagnosis	Yes	Yes	Yes	No (febrile seizures only)	No	Yes	Yes	Yes	No	Yes	Yes	Yes	No
Age at seizure onset	Unknown	2 years 9 months	5 years 5 months	3 years	Not relevant	5 months	5 months	18 months	Not relevant	12 months	11 months	7 months	Not relevant
Non-epileptic myoclonic jerks	Unknown	Unknown	Yes (intractable to treatment)	No	No	No	Yes	No	No	No	Unknown	Unknown	Unknown
Seizure types during disease course	Single event with bilateral tonic–clonic seizure	Focal MS, focal hypomotor seizures with impaired awareness, FBTCS	FBTCS	Fever-induced bilateral tonic–clonic seizures	Not relevant	FBTCS	MAE, eyelid-myoclonia	MAE	Not relevant	Focal hypomotor seizures with impaired awareness, FBTCS	FBTCS	FBTCS	Unknown
Febrile seizures	No	No	Yes	Yes	Not relevant	Yes	No	No	Not relevant	Yes	No	No	No
Status epilepticus	No	No	Yes	No	Not relevant	No	No	No	Not relevant	N	No	No	Unknown
Current AED	None	None	LMT, VPA, CBD	None	Not relevant	LMT, VPA	None	None	Not relevant	LEV	VPA	VPA	None
Lifetime AED	None	LMT, TPM, LEV, VPA	LMT, VPA, CBD, CBZ, PHT, PMD, CLB	None	Not relevant	LMT, VPA	CBZ	CBZ and VPA	Not relevant	LEV	VPA	VPA	None
Overall antiepileptic drug response*	Not relevant	Very good	Partially good (free of epileptic seizures but not the non-epileptic myoclonic jerks)	Never used	Not relevant	Very good	Very good	Very good	Not relevant	Very good	Very good	Very good	Not relevant

(Continued)

TABLE 1A | Continued

Families	Family 1	Family 2	Family 3	Family 4	Family 5	Family 6	Family 7	Family 7	Family 8	Family 9	Family 10	Family 10	Family 10
	Patient 1	**Patient 2**	**Patient 3**	**Patient 4**	**Patient 5**	**Patient 6**	**Patient 7**	**Patient 8**	**Patient 9**	**Patient 10**	**Patient 11**	**Patient 12**	**Patient 13**
Age at sitting	Unknown butcan sit unaided	Unknown butcan sit unaided	19 months	2 years	22 months	2.5 years	2.5 years	2 years	13 months	4 years	3 years	2 years	1.5 years
Age at walking	Unknown but can walk unaided	Unknown but can walk unaided	8 years (assisted)	3 years (assisted)	Unable	4 years	Unable	4 years	27 months (assisted, short distances)	3 years	5 years	Unable	22 months (assisted)
Useful use of hands	Yes	Yes	Yes	Yes	Yes	Yes	Yes	Yes	Yes	Unknown	Yes	Yes	Yes
Age at first words	Unknown but can talk	Unknown but can talk	9 months	3 years	14 months (mama)	16 months	Only simple sounds	Only simple sounds	15 months	4 years	2.5 years	3 years	18 months
Present verbal ability	Understands simple sentences. Uses simple words	Understands simple sentences. Has a vocabulary of 100 single words. Dysarthric speech	Understands simple sentences. Replies with single words or short sentences. Dysarthric speech	Understands simple sentences. Has a vocabulary of 100 single words and in addition uses sign language	Nonverbal besides "mama"	Understands simple sentences. Uses 10 single words and has started to combine two words	Non-verbal	Non-verbal	Understands simple sentences. Single words, dysarthria. Uses sign language	Single words	Understands most sentences. Has a vocabulary of > 100 single words and can use short sentences. Dysarthric speech	Understands simple sentences. Uses 10 single words and has started to combine two words	Understands simple sentences. Uses a few words
Developmental delay	Moderate	Moderate	Moderate	Moderate–severe	Moderate–severe	Moderate	Severe	Severe	Moderate–severe	Moderate–severe	Moderate	Moderate–severe	Moderate–severe
Autism	No	No	No	No	No	No	No	No	No	No	No	No	No
Brain MRI results	Not performed	12 months: delayed myelination; 8 and 14 years: pronounced cerebellar atrophy	22 months: cerebellar atrophy; 11, 14, and 16 years: thinning of CC, progressive atrophy of cerebellum, pons, and mesencephalon; 25 years: hippocampal sclerosis	12 months: delayed, myelination	Not performed	Not performed	10 months: delayed myelination and enlargement of the subarachnoid spaces	15 years: cerebellar atrophy and thinning of CC	10 months: delayed myelination; 31 months: cortical and cerebellar atrophy	4 years: delayed myelination; 5 years: unremarkable	Not performed	Not performed	Not performed

**Overall antiepileptic drug response (very good = seizure-free; partially good = partially seizure-free on treatment; and poor = intractable seizures despite treatment).*

TABLE 1B | Clinical and genetic findings in novel and previously published individuals with *PIGT* deficiency harboring the p.Asn527Ser or p.Val528Met variant in either homozygous or compound heterozygous state.

Families	Family 11	Family 11	Family 12	Family 13	Family 14	Family 15	Family 16	Family 17	Family 18	Family 19	Family 20	Family 21
	Patient 14	**Patient 15**	**P1 (Jezela-Stanek et al., 2020)**	**P2 (Jezela-Stanek et al., 2020)**	**P3 (Jezela-Stanek et al., 2020)**	**P4 (Jezela-Stanek et al., 2020)**	**P5 (Jezela-Stanek et al., 2020)**	**P6 (Jezela-Stanek et al., 2020)**	**P7 (Jezela-Stanek et al., 2020)**	**P3 (Bayat et al., 2019)**	**P10 (Bayat et al., 2019)**	**Decipher ID 258094 (Pagnamenta et al., 2017)**
cDNA change (NM_015937.6)	c.1582G > A; c.1582G > A	c.1582G > A; c.1582G > A	c.1582G > A; c.1582G > A	c.1730dupC; c.1582G > A	c.1520G > A; c.1582G > A	c.494-2A > G; c.1582G > A	c.1582G > A; c.1582G > A	c.1096G > A; c.1582G > A	c.494-2A > G; c.1582G > A	c.494-2A, c.1582G > A;	c.1724_1725insC; c.1582G > A	c.1730dupC; c.1582G > A
Amino acid change (NP_057021.2)	p.Val528Met; p.Val528Met	p.Val528Met; p.Val528Met	p.Val528Met; p.Val528Met	p.Leu578fsTer 35; p.Val528Met	p.Ala507Gly; p.Val528Met	Splice site; p.Val528Met	p.Val528Met; p.Val528Met	p.Gly366TArg; p.Val528Met	Splice site; p.Val528Met	Splice site; p.Val528Met	p.Leu578fsTer35; p.Val528Met	p.Leu578fsTer35; Val528Met
Clinical significance	PATH; PATH	PATH; PATH	PATH; PATH	PATH; PATH	PATH; PATH	PATH; PATH	PATH; PATH	PATH; PATH	PATH; PATH	PATH; PATH	VUS;PATH	PATH; PATH
Heritage	Caucasian	Caucasian	Polish	Polish	Polish	Polish	Polish	Polish	Polish	Polish	Polish	Polish
Age at inclusion	2 years	7.5 years	Born 2019	Born 2017	Born 2017	Born 2016	Born 2011	Born 2013	Born 2003	5 years	4 years	Unknown
Gender	Female	Female	Female	Male	Male	Male	Female	Male	Female	Female	Female	Female
Seizures	Yes	Yes	Yes	Yes	Yes	Yes	Yes	Yes	Yes	Yes	Yes	Yes
Epilepsy diagnosis	Yes	Yes	No	No	Yes	Yes	Yes	No	No	Yes	Yes	Yes
Age at seizure onset	6 months	20 months	6 months	12 months	6 months	9 months	6 months	11 months	12 months	12 months	18 months	12 months
Non-epileptic myoclonic jerks	Yes	No	Unknown	Unknown	Unknown	Unknown	Unknown	Unknown	Unknown	Unknown	Unknown	Unknown
Seizure types during disease course	Atypical absences (generalized)	Atypical absences	Fever-induced tonic–clonic seizures of unknown onset	Fever-induced focal seizures with impaired awareness	Focal hypomotor seizures with impaired awareness, FBTCS	Absences, myoclonic jerks, and bilateral tonic–clonic seizures	Focal hypomotor seizures with impaired awareness, FBTCS, and generalized myoclonic jerks	Focal hypomotor seizures with impaired awareness	Focal hypomotor seizures with impaired awareness	Fever-induced tonic–clonic seizures of unknown onset	Bilateral tonic–clonic seizures of unknown onset	Bilateral tonic–clonic seizures of unknown onset
Febrile seizures	No	Yes	Yes (only)	Yes (only)	Yes	Yes	Yes	Yes (only)	Yes	Unknown	Unknown	Unknown
Status epilepticus	No	No	Unknown	Unknown	Unknown	Unknown	Unknown	Unknown	Unknown	Unknown	Unknown	Unknown
Current AED	LEV	LEV	None	Unknown	Unknown	Unknown	Unknown	Unknown	Unknown	Unknown	Unknown	Unknown
Lifetime AED	LEV	LEV	None	Unknown	Unknown	Unknown	Unknown	Unknown	Unknown	Unknown	Unknown	Unknown
Overall antiepileptic drug response*	Very good	Very good	Not relevant	Very good	Very good	Poor (intractable myoclonic jerks)	Good	Very good	Very good	Good	Good	Good
Age at sitting	1 year (with support)	3 years	Unable	25 months	18 months	30 months	2.5 years	2 years	2.5 years	Unknown	Unknown	Unknown
Age at walking	Unable	6 years (a few steps)	Unable	Unknown but can walk assisted	Unable	Unable	Unable	Unable	6 years (unassisted but short distances)	Unknown	Unknown	Unknown but can walk
Useful use of hands	Unknown	Unknown	Unknown	Unknown	Unknown	Unknown	Unknown	Unknown	Unknown	Unknown	Unknown	Unknown
Age at first words	Non-verbal	Non-verbal	Unknown	Unknown	Unknown	23 months	3.5 years	4.5 years	5 years	Unknown	Unknown	Unknown
Present verbal ability	Unknown	Understands simple sentences. Uses a communication device with eye movement control for words	Unknown	Unknown	Single words, dysarthria	Single words	Communicates through simple sentences, dysarthria	Single words	Single words, dysarthria	Unknown	Unknown	Unknown
Developmental delay	Severe	Severe	Unable to classify	Unable to classify	Unable to classify	Unable to classify	Unable to classify	Unable to classify	Unable to classify	Unable to classify	Unable to classify	Unable to classify
Autism	Unknown but has limited eye contact	No	Unknown	Unknown	Unknown	Unknown	Unknown	Unknown	Unknown	Unknown	Unknown	Unknown
Brain MRI results	Not performed	2 years: cerebellar atrophy	6 months: delayed myelination	10 months: delayed myelination, slight enlargement of pericerebral spaces	12 months: decreased white matter volume, enlargement of pericerebral spaces	12 months: decreased cerebral white matter volume including CC; 16 months: cortical–subcortical atrophy	8 months: delayed myelination and slight enlargement of pericerebral spaces; 3 years: cortical–subcortical and cerebellar vermis atrophy	Three times over 1 year: progressive cortical–subcortical atrophy, cerebellar vermis atrophy	12 months: normal; 11 and 16 years: progressive cerebral and cerebellar atrophy	Unknown age: cerebellar atrophy	4 years: progressive isolated cerebellar atrophy	Progressive isolated cerebellar atrophy

**Overall antiepileptic drug response (very good = seizure-free; partially good = partially seizure- free on treatment; and poor = intractable seizures despite treatment).*

Abbreviations: AED, antiepileptic drug; CBD, cannabidiol; CBZ, carbamazepine; CC, corpus callosum; EEG, electroencephalogram; FBTCS, focal to bilateral tonic–clonic seizure; LEV, levetiracetam; LMT, lamotrigine; MAE, myoclonic atonic epilepsy; MRI, magnetic resonance imaging; MS, myoclonic seizure; PATH, pathogenic; PHT, phenytoin; PIGT, phosphatidylinositol glycan class T protein; PMD, primidone; VPA, valproate; VUS, variant on unknown significance; TPM, topiramate.

explanation for the ophthalmological features. Functional testing by flow cytometry to determine the surface levels of GPI-APs (Knaus et al., 2018) was unfortunately unavailable for this subject. Such testing is needed in future patients with Asn527Ser variants to prove pathogenicity and to perform deep-phenotyping of the clinical features including any anomalies of the eyes.

Otological features have only rarely been addressed previously. We identified 2/25 (8%) individuals who had suffered from hearing disorders; one presented with a sensorineural deficit (P1), and the other with an unspecified impairment (P4) (no further data were available).

Cardiovascular and Gastrointestinal Features

While congenital heart defects have been associated with other pathogenic variants of the *PIGT* gene (Bayat et al., 2019), we cannot report any heart anomalies in individuals with Asn527Ser and Val528Met. Echocardiography was available in 10/25 individuals and was normal in all probands.

Data on gastrointestinal disturbances were available in 16/25 individuals. None of the individuals required a gastrostomy tube. Three individuals experienced feeding difficulties during the first 2 months of life, and four experienced gastroesophageal reflux and recurrent constipation.

Neurological and Behavioral Phenotype

Epileptic seizures were reported in 22/25 individuals (88%) [12 individuals from our cohort, Decipher ID 258094 (Pagnamenta et al., 2017) P1-P7 (Jezela-Stanek et al., 2020), P3 and P10 (Bayat et al., 2019)], but only 18 individuals fulfilled the diagnostic criteria for having epilepsy [11 individuals from our cohort, Decipher ID 258094 (Pagnamenta et al., 2017), P3-5 and P7 (Jezela-Stanek et al., 2020), P3 and P10 (Bayat et al., 2019)]. In 1/18 individuals (P1) only a single afebrile seizure was reported, but an epilepsy diagnosis was given due to the additional finding of interictal epileptic discharges on electroencephalogram (EEG). Four individuals [P1, P2, and P6 (Jezela-Stanek et al., 2020), and our P4] had febrile seizures as the only seizure type and did not reach an epilepsy diagnosis. Finally, febrile seizures were present in 13/25 (52%) individuals.

Age at seizure onset was available in all but one individual. The average time of onset was around 16 months of age (from 5 months to 5.5 years). Twelve individuals experienced their first epileptic seizure during the 5th to 12th month of life while the remaining children had an onset around the 2nd to 5th year of life (**Table 1**).

Seizure types were either focal (12/25) or primary generalized (9/25). The predominant seizure type was focal to bilateral tonic-clonic seizures, followed by primary generalized bilateral tonic-clonic seizures. Other generalized seizure types included atypical absences (3/25), myoclonic seizures (2/25), myoclonic-atonic seizures (2/25), and eyelid myoclonia (1/25). Only one individual experienced status epilepticus (P3).

Antiepileptic drugs (AEDs) were prescribed in 18/25 individuals. Pagnamenta et al. (2017) provided no data on AED treatment. Several of the individuals described by Jezela-Stanek et al. (2020) were taking AEDs despite only having febrile seizures and thereby not fulfilling the criteria for epilepsy; these authors provided no data on the type of AEDs used. Thus, a detailed description of types of AEDs prescribed in the 18 individuals was only possible for 10 individuals, all of whom fulfilled an epilepsy diagnosis. Six of these ten individuals became seizure-free on monotherapy with either valproate (VPA) or levetiracetam. Three of the ten individuals (P2, P3, and P6) became free of epileptic seizures on a combination of VPA and lamotrigine, but individual P3 had persistent non-epileptic myoclonic jerks. One individual (P7) became seizure-free on monotherapy with carbamazepine. Three of the ten individuals had been tapered off from their AED(s) and have been seizure-free for several years.

Comparison of symptoms seen in individuals homozygous for the Val528Met variant to those found in individuals compound heterozygous for Asn527Ser or Val528Met, revealed no convincing difference regarding onset of seizures, seizure types, and cognitive and developmental outcome. Although focal and primary generalized seizures were present in both subgroups, we noticed that atypical absence seizures were only present among the homozygous individuals and that homozygous individuals became seizure-free on monotherapy with AED. Compound heterozygous individuals typically needed a combination of AEDs to achieve seizure freedom. We also explored if it was possible to draw further genotype-phenotype conclusions within the group of 25 individuals (carrying the Asn527Ser or Val528Met variant) based on the annotation of the disease causing variant found on the other allel. In part 2 of **Table 2** the 25 individuals were divided in three groups: (i) individuals homozygous for the p.Val528Met variant, (ii) individuals compound heterozygous for a missense variant in addition to the p.Val528Met or p.Asn527Ser variant, and (iii) individuals compound heterozygous for a truncating variant in addition to the p.Val528Met or p.Asn527Ser variant. While the majority of individuals in the two first groups experienced seizures this was the case for all individuals in the third group. A small subset of individuals in all groups only experienced fever induced seizures and thus did not reach a formal diagnosis of epilepsy (**Table 2**, part 2). In all three groups 80–85% of individuals with seizures reached a formal diagnosis of epilepsy. In the first two groups the age of onset of seizures was around 9 months of life while seizures started around 2 years of age in the third group. Individuals carrying a disease causing missense variant on both allels were compatible in regard of the degree of DD. The overall seizure outcome across all groups was good as all but one individual became seizure free after treatment initiation of AEDs (**Table 2**).

Massive action myoclonia involving all four limbs and the trunk were observed in individual P3 without any clinical and polygraphic evidence of myoclonus at rest (**Supplementary Video 1**). This phenomenon started around the age of 8 years and became progressively worse and disabling during the course of the disease. No epileptic abnormalities were associated with the myoclonic phenomena on EEG (**Figure 1**).

The age range of the 25 individuals spanned from 27 months to 29 years. Degree of DD was as follows: moderate (5/25),

TABLE 2 | Brief clinical overview of all published individuals with *PIGT* deficiency.

	Part 1. Grouping of individuals (*n* = 49) based on whether they have the c.1582G>A; p.Val528Met or the c.1580A>G; p.Asn527Ser variant		**Part 2. Grouping of individuals (*n* = 25), with at least one copy of the c.1582G>A; p.Val528Met or the c.1580A>G; p.Asn527Ser variant, based on annotation of the disease causing variant on the other allel**		
	Individuals with the p.Val528Met or the p.Asn527Ser variant	Individuals without the p.Val528Met or the p.Asn527Ser variant	Individuals homozygous for the p.Val528Met variant	Individuals compound heterozygous for a missense variant in addition to the p.Val528Met or p.Asn527Ser variant	Individuals compound heterozygous for a truncating variant in addition to the p.Val528Met or p.Asn527Ser variant
Total number	25	24	8	7	10
Gender ratio (M/F)	9/16	14/10	0/8	4/3	4/6
Epileptic seizures	22/25 (88%)	24/24 (100%)	7/8 (87%)	5/7 (71%)	10/10 (100%)
Only febrile seizures	5/25 (20%)	1/24 (4%)	1/7 (15%)	1/5 (20%)	3/10 (30%)
Epilepsy diagnosis	17/22 (77%)	23/24 (96%)	6/7 (85%)	4/5 (80%)	8/10 (80%)
Average onset of seizures	16 months	6 months	9 months	9 months	23 months
Overall seizure outcome	Good (24/25, 96% seizure-free)	Bad (23/24, 96% intractable)	Good	Good	Good
Non-epileptic myoclonic jerks	2/25	Unknown	0/8	1/7	1/10
Degree of developmental delay	Moderate (5/25), moderate-severe (6/25), severe (4/25), unable to ascertain (10/25)	Profound (24/24, 100%)	Moderate (1/8), moderate-severe (3/8), severe (2/8), unable to ascertain (2/8)	Moderate (1/7), moderate-severe (2/7), severe (2/7), unable to ascertain (2/7)	Moderate (3/10), moderate-severe (1/10), severe (0/10), unable to ascertain (6/10)
Congenital hypotonia	24/25 (96%)	23/24 (96%)	7/8	7/7	10/10
Premature mortality	0/25 (0%)	3/23 (13%)	0/8	0/7	0/10
Landscape of disease causing variants	Patients with compound missense/truncating (*n* = 10), biallelic missense (*n* = 15), or biallelic truncating (*n* = 0) variants.	Patients with compound missense/truncating (*n* = 6), biallelic missense (*n* = 18), or biallelic truncating (*n* = 0) variants.			

moderate-severe (6/25), and severe (4/25). In 10 individuals [Decipher ID 258094 (Pagnamenta et al., 2017), P1–7 (Jezela-Stanek et al., 2020), and P3 and P10 (Bayat et al., 2019)], we were unable to obtain enough clinical data to assess the degree of DD, notably none of the individuals had profound DD (**Table 2**, part 1). Of the 25 individuals, 13 eventually learned to walk: 11 could walk short distances with walking aids or support from others, and two individuals learned to walk independently. The average age of independent walking was between the 3rd and 6th year of life. We were able to collect data on manual dexterity in 13 individuals. All individuals had purposeful use of hands and could eat autonomously using cutlery, play with bricks or puzzles, or use sign language. Information on verbal capabilities was obtained from 19 individuals. All 19 individuals comprehended simple sentences and 15/19 replied using single words. Two individuals, both homozygous for the Val528Met variant, could communicate with very simple sentences: one individual (P11) was even able to educate her younger affected sibling (P12) (**Supplementary Video 2**). Two individuals (currently 2 and 7.5 years of age) remained non-verbal. None of the patients were diagnosed with an autism spectrum disorder.

Electroencephalogram

EEG findings were available in five individuals with epilepsy (P2, P3, P7, P8, and P10). A poorly organized background activity was reported in two individuals, with burst of theta activity intermixed. Generalized epileptic discharges with frontal predominance were reported in two individuals (P8 and P10) at the age of 14 and 3 years, respectively. Occasional focal epileptic discharges were observed in individual P2 at the age of 3 years but were not detected after the age of 14 years, whereas isolated focal spikes were observed at the age of 10 months in individual P7. Individual P3, who exhibited action myoclonus, did not exhibit interictal epileptic abnormalities on routine EEG.

Brain Imaging

At least one brain MRI scan was performed in 18/25 individuals (**Table 1**), and 12 of those underwent repeated MRI scans. In six individuals, the first cerebral MRI was performed during the first year of life (in all cases between the 6th and 12th month of life). Delayed myelination was noted in all six individuals, while enlargement of the subarachnoid spaces was detected in three of them. There were no follow-up data on the delayed myelination

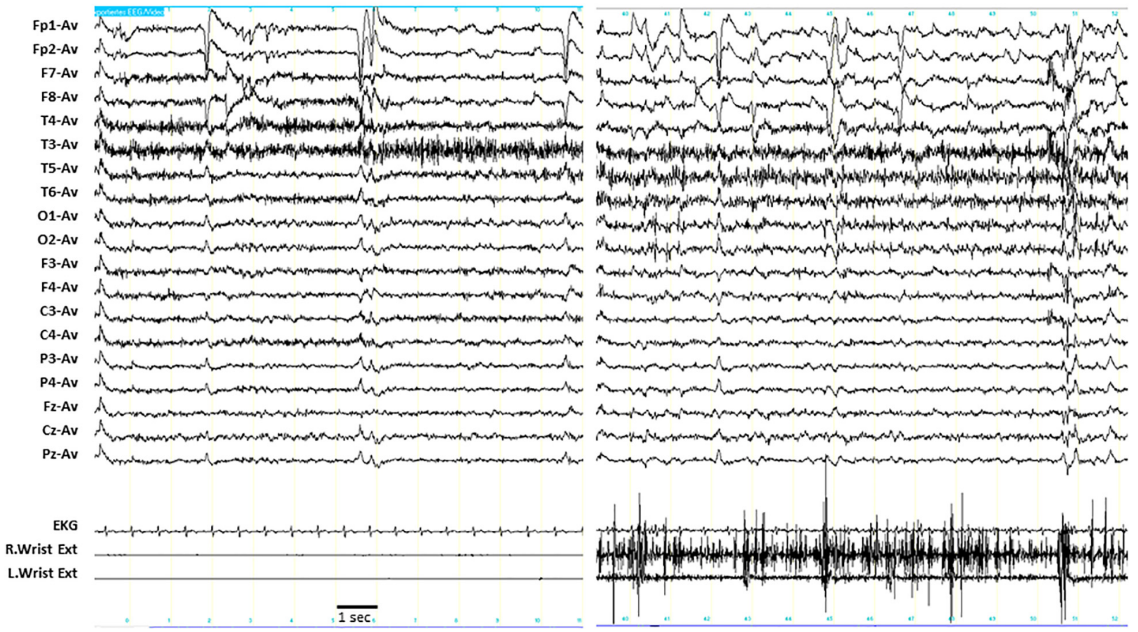

FIGURE 1 | EEG polygraphic recording in individual P3. **Left panel:** the individual is at rest. EEG does not show any epileptic abnormalities, and the myoclonic EMG activity is detectable in both wrist extensors. **Right panel:** the individual is maintaining a posture (outstretching her arms). The muscular contraction in both wrist extensors are fragmented by irregular, high amplitude, myoclonic potentials that are intermixed with brief silent periods, reproducing the EMG pattern of action myoclonus. No epileptic discharges associated with the myoclonic potentials were detectable in the EEG. Wrist Ext, wrist extensor; R, right; L, left.

described in our individuals P4 and P7, but the myelination was age-appropriate in the remaining four individuals.

MRI was performed in twelve individuals after the age of 1 year. Scans showed age-appropriate myelination associated with several developmental anomalies such as cerebellar atrophy (11/12) occasionally involving the brainstem (1/12), and abnormal corpus callosum (3/12). Additional MRI findings included prominent cortical and subcortical volume loss (7/12), enlargement of lateral and third ventricles (3/12), white matter immaturity (2/12), and a hippocampal sclerosis (1/12) (P3). In individual P10, the MRI detected delayed myelination at the age of 4 years, but the MRI scan a year later was unremarkable (**Table 1**).

We have previously shown that cerebral MRI findings of individuals with *PIGT* deficiency include delayed myelination, prominent cortical and subcortical volume loss with brainstem atrophy, atrophy of the cerebellum, and an abnormal corpus callosum (Bayat et al., 2019). This is compatible with the current results from our individuals with Asn527Ser and Val528Met. The natural history of the delayed myelination in other *PIGT* variants has to be delineated further, but the present study indicates that the myelination eventually becomes age-appropriate in individuals carrying Asn527Ser and Val528Met variants. Only one individual exhibited an unremarkable MRI at 5 years of age (P9). Only few *PIGT*-deficient individuals without those variants have been reported to have normal cerebral MRIs (Bayat et al., 2019). The examinations were done at a very early age, however, which might explain why no structural anomalies were found.

Molecular Results

From the complete dataset of the cohort of 25 individuals, 13 different variant sites emerged: seven missense variants, two splice site variants, and four truncating variants. The Val528Met variant has been reported in 29 out of 282.654 samples (0.0001026 allele frequency)[3]. In comparison, the Asn527Ser variant has only been reported once in 251.292 samples (0.000003979 allele frequency) and is predicted to be damaging by all four prediction tools (**Supplementary Table 1**) and likely to be damaging according to the ACMG guidelines (Richards et al., 2015). The clinical findings in the individual with the Asn527Ser was compatible with those harboring the Val528Met variant. While the previously published variant c.1724_1725insC; p.Leu578fsTer35 (Bayat et al., 2019) was classified as a variant of unknown significance, all remaining variants were predicted as either likely pathogenic or pathogenic (**Supplementary Table 1**).

DISCUSSION

In 2017, Pagnamenta et al. (2017) reported two individuals with *PIGT* deficiency: one was compound heterozygous for the variants Val528Met and Leu578*35, while the second was homozygous for the Glu237Gln. Western blot analysis showed that the expression of the mutant protein appeared to be reduced only for the truncating variant (8). *PIGT*-knockout

[3]https://gnomad.broadinstitute.org/

HEK293 cells were then transfected with wild-type or mutant *PIGT* cDNA. The largest fraction of CD59-rescued cells was observed with Val528Met, indicating highest residual functional activity (Pagnamenta et al., 2017). While the individual with the Glu237Gln was profoundly affected, the individual with the Val528Met and Leu578*35 variants was significantly less affected. This individual walked unaided but with an ataxic gate, understood spoken language but exhibited dysarthric speech, and attended a mainstream school with one-to-one support. This was the first evidence suggesting that the Val528Met is associated with a less severe phenotype, and our data give further support to this claim. Bayat et al. (2019) described four individuals harboring the Val528Met variant in either homozygous or compound heterozygous state, and in 2020 an additional seven individuals were described (Jezela-Stanek et al., 2020). Our knowledge of the phenotypical spectrum associated with homozygous and compound heterozygous Val528Met variants remains limited. We also have little insight into the natural history of this rare disorder. This is a challenge when counseling families with newly diagnosed children with Val528Met-related *PIGT* deficiency.

We compared the group of *PIGT* individuals with the Asn527Ser or the Val528Met (in either homozygous or compound heterozygous state) to a group of *PIGT* individuals without such variants (**Table 2**). In both groups (**Table 2**, part 1), the majority of individuals carried biallelic missense variants while there were no cases with biallelic truncations as this would likely not be compatible with life. We also explored potential genotype-phenotype correlations within the group of individuals with the Asn527Ser or Val528Met variant and grouped individuals based on the annotation of the disease causing variant found on the other allel (**Table 2**, part 2). In the group of individuals that were compound heterozygous for a truncating variant in addition to the p.Val528Met or p.Asn527Ser variant all experienced epileptic seizures with an average onset around 2 years of age. We were unable to detect other genotype-phenotype correlations based on the present dataset (**Table 2**, part 2). Studies of rare diseases are often conducted through a multicenter approach, and researchers are dependent on data provided by caregivers and other health care providers. This gives an unavoidable data collection bias as patients are evaluated by diverse health care providers with different medical backgrounds and levels of experience. In the current study, we aimed to reduce this bias by collecting videos of individuals with the two variants. These videos of eight individuals were used to give a more uniform evaluation of motor, verbal social, and cognitive skills. We found a more favorable outcome in our individuals, with less severe global DD, a considerably later onset of epilepsy, and no premature mortality (**Table 2**). While no individuals with the Asn527Ser and Val528Met variants were diseased, 3/24 (13%) individuals without the variants in question died prematurely (Bayat et al., 2019). Although the cumulative mortality rate is lower compared to what has been described in other genes involved in the GPI anchor synthesis (Bayat et al., 2020a), this finding gives more strength to the claim that the two *PIGT* variants are associated with a milder phenotype and a better prognosis.

Epilepsy was not a constant feature in our cohort although when present, it was treatment-responsive. While all previously identified individuals with different pathogenic variants had epilepsy and a more profound global DD, the individuals with Asn527Ser or Val528Met ranged from moderate to severe global DD (**Table 2**, part 1). We could also show that a minority of individuals with the Val528Met variant experienced only febrile seizures or had never had epileptic seizures (**Table 1**). Individuals with the two variants generally became seizure-free on monotherapy with AEDs, compared with other *PIGT* individuals that were drug-refractory (**Table 2**).

The comparison of individuals with homozygous Val528Met variants and those carrying compound heterozygous variants Asn527Ser and Val528Met lead to the conclusion that homozygosity is associated with a better outcome. Our study gives evidence to the claim that Asn527Ser- and Val528Met-related *PIGT* deficiency is associated with a mild to moderate "developmental and epileptic encephalopathy (DEE)", as compared to *PIGT*-related DEE caused by other pathogenic variants. A similar spectrum of symptoms ranging from mild to severe DEE is seen in the X-linked phosphatidylinositol glycan class A protein gene that is involved in one of the first steps of GPI anchor biosynthesis (Bayat et al., 2020b). As in other DEEs, co-existence of focal and generalized seizures in the same individual during a lifetime is a feature of *PIGT* deficiency. We presented five novel and two previously reported individuals [P4 and P5 (Jezela-Stanek et al., 2020)] with generalized seizures, such as myoclonic, atypical absence and tonic seizures. A detailed analysis of seizure semiology showed atypical absence seizures and bilateral tonic seizures, but it also revealed previously undetected seizure types such as myoclonic atonic seizures and eyelid-myoclonia. Myoclonic-atonic seizures are the distinguishing feature of myoclonic-atonic epilepsy (MAE), a rare epilepsy syndrome that occurs in 0.3–2.2% of children with epilepsy (Tang et al., 2020). Children with MAE usually have normal development prior to seizure onset at between 7 months and 6 years of age (Tang et al., 2020). Seizure types include myoclonic atonic, atonic, myoclonic, generalized tonic-clonic, atypical absence, and tonic seizures (Tang et al., 2020). Tang et al. (2020) showed that pathogenic genetic variants in *SYNGAP1, NEXMIF, SLC6A1, KCNA2*, *SCN2A, STX1B, KCNB1, MECP2, ASH1L, CHD4,* and *SMARCA2* are the cause of seizures in 14% of MAE individuals. Our data suggest that *PIGT* is a new candidate gene for MAE.

The eldest proband, a 29-year-old female individual with compound heterozygous *PIGT* variants (P3), exhibited action myoclonia. She first showed this symptom when she was 8 years old, and it has progressively worsened and has now become very disabling. Action myoclonia may have varying etiologies, including diseases such as Lance-Adams syndrome and the large group of progressive myoclonus epilepsies. It can be associated with epileptic EEG abnormalities (Tassinari et al., 1998), and its pathophysiological mechanisms suggest a cortical-subcortical dysfunction (Avanzini et al., 2016). It can also be associated with a cerebellar syndrome and be extremely disabling and difficult to treat, as described in individual P3. As this individual

was the oldest in our cohort, we cannot dismiss the possibility that myoclonus is a later manifestation in progression of PIGT deficiency syndrome.

While 22 individuals experienced seizures, only 18 of them fulfilled the clinical diagnosis of epilepsy (Fisher et al., 2014). Apart from our individual P5, who had the His376Pro and Val528Met variants and never had seizures, we found no differences in the *PIGT* variants among individuals with and without seizures. Our study provides a detailed and in-depth description of developmental features in patients with the less severe spectrum of *PIGT* deficiency, and we also offer a glimpse into the potential natural history in adulthood. Our data are important for caregivers and health care providers when dealing with uncertainties about what to expect in the future, but also when counseling families with infants newly diagnosed with *PIGT* deficiency related to the Val528Met variant. Further investigation is needed to better understand the natural history and to elucidate the relationship between the presence of seizures and seizure semiology and the pathogenic variants in the milder spectrum of *PIGT* deficiency.

DATA AVAILABILITY STATEMENT

The original contributions presented in the study are included in the article/**Supplementary Material**, further inquiries can be directed to the corresponding author/s.

ETHICS STATEMENT

The studies involving human participants were reviewed and approved by ethical committee of region Sjaelland. Written informed consent to participate in this study was provided by the participants' legal guardian/next of kin. Written informed consent was obtained from the individual(s), and minor(s)' legal guardian/next of kin, for the publication of any potentially identifiable images or data included in this article.

AUTHOR CONTRIBUTIONS

ABa and RM had the idea to write the article. ABa was responsible for collecting data from the medical records and writing the first draft of the manuscript. ABa was responsible for gathering relevant literature. GR evaluated the neurophysiological data. All authors were involved in the ongoing revision of the manuscript. All authors contributed to the revision of the final manuscript.

ACKNOWLEDGMENTS

The authors would like to thank the individuals and their families for their participation in our research. The authors also thank Claire Gudex for her contribution to editing the final draft of the article.

SUPPLEMENTARY MATERIAL

The Supplementary Material for this article can be found online at: https://www.frontiersin.org/articles/10.3389/fgene.2021.663643/full#supplementary-material

Supplementary Table 1 | Genetic overview, annotation, and classification of novel and previously published pathogenic variants in the phosphatidylinositol glycan class T protein gene.

Supplementary Video 1 | Video of individual P3 displaying action myoclonia of limbs and the whole body during motor tasks and the absence of myoclonia during rest.

Supplementary Video 2 | Video of individuals P11 and 12 showing motor, cognitive, and verbal capabilities.

REFERENCES

Adzhubei, I. A., Schmidt, S., Peshkin, L., Ramensky, V. E., Gerasimova, A., Bork, P., et al. (2010). A method and server for predicting damaging missense mutations. *Nat. Methods* 7, 248–249. doi: 10.1038/nmeth0410-248

Avanzini, G., Shibasaki, H., Rubboli, G., Canafoglia, L., Panzica, F., Franceschetti, S., et al. (2016). Neurophysiology of myoclonus and progressive myoclonus epilepsies. *Epileptic Disord* 18, 11–27. doi: 10.1684/epd.2016.0835

Bayat, A., Klovgaard, M., Johannesen, K. M., Stefan Barakat, T., Kievit, A., Montomoli, M., et al. (2020a). Deciphering the premature mortality in PIGA-CDG - An untold story. *Epilepsy Res.* 170:106530. doi: 10.1016/j.eplepsyres.2020.106530

Bayat, A., Knaus, A., Juul, A. W., Dukic, D., Gardella, E., Charzewska, A., et al. (2019). PIGT-CDG, a disorder of the glycosylphosphatidylinositol anchor: description of 13 novel patients and expansion of the clinical characteristics. *Genet. Med.* 21, 2216–2223. doi: 10.1038/s41436-019-0512-3

Bayat, A., Knaus, A., Pendziwiat, M., Afenjar, A., Barakat, T. S., Bosch, F., et al. (2020b). Lessons learned from 40 novel PIGA patients and a review of the literature. *Epilepsia* 61, 1142–1155. doi: 10.1111/epi.16545

Bellai-Dussault, K., Nguyen, T. T. M., Baratang, N. V., Jimenez-Cruz, D. A., and Campeau, P. M. (2019). Clinical variability in inherited glycosylphosphatidylinositol deficiency disorders. *Clin. Genet.* 95, 112–121. doi: 10.1111/cge.13425

Farheen, N., Sen, N., Nair, S., Tan, K. P., and Madhusudhan, M. S. (2017). Depth dependent amino acid substitution matrices and their use in predicting deleterious mutations. *Prog. Biophys. Mol. Biol.* 128, 14–23. doi: 10.1016/j.pbiomolbio.2017.02.004

Fisher, R. S., Acevedo, C., Arzimanoglou, A., Bogacz, A., Cross, J. H., Elger, C. E., et al. (2014). ILAE official report: a practical clinical definition of epilepsy. *Epilepsia* 55, 475–482. doi: 10.1111/epi.12550

Fujita, M., and Kinoshita, T. (2012). GPI-anchor remodeling: potential functions of GPI-anchors in intracellular trafficking and membrane dynamics. *Biochim. Biophys. Acta* 1821, 1050–1058. doi: 10.1016/j.bbalip.2012.01.004

Jezela-Stanek, A., Szczepanik, E., Mierzewska, H., Rydzanicz, M., Rutkowska, K., Knaus, A., et al. (2020). Evidence of the milder phenotypic spectrum of c.1582G > >A PIGT variant - delineation based on seven novel Polish patients. *Clin. Genet.* 98, 468–476. doi: 10.1111/cge.13822

Jiao, X., Xue, J., Gong, P., Bao, X., Wu, Y., Zhang, Y., et al. (2020). Analyzing clinical and genetic characteristics of a cohort with multiple congenital anomalies-hypotonia-seizures syndrome (MCAHS). *Orphanet. J. Rare Dis.* 15:78. doi: 10.1186/s13023-020-01365-0

Kinoshita, T., and Fujita, M. (2016). Biosynthesis of GPI-anchored proteins: special emphasis on GPI lipid remodeling. *J. Lipid Res.* 57, 6–24. doi: 10.1194/jlr.R063313

Knaus, A., Pantel, J. T., Pendziwiat, M., Hajjir, N., Zhao, M., Hsieh, T. C., et al. (2018). Characterization of glycosylphosphatidylinositol biosynthesis defects by

clinical features, flow cytometry, and automated image analysis. *Genome Med.* 10:3. doi: 10.1186/s13073-017-0510-5

Kohashi, K., Ishiyama, A., Yuasa, S., Tanaka, T., Miya, K., Adachi, Y., et al. (2018). Epileptic apnea in a patient with inherited glycosylphosphatidylinositol anchor deficiency and PIGT mutations. *Brain Dev.* 40, 53–57. doi: 10.1016/j.braindev.2017.06.005

Kvarnung, M., Nilsson, D., Lindstrand, A., Korenke, G. C., Chiang, S. C., Blennow, E., et al. (2013). A novel intellectual disability syndrome caused by GPI anchor deficiency due to homozygous mutations in PIGT. *J. Med. Genet.* 50, 521–528. doi: 10.1136/jmedgenet-2013-101654

Lam, C., Golas, G. A., Davids, M., Huizing, M., Kane, M. S., Krasnewich, D. M., et al. (2015). Expanding the clinical and molecular characteristics of PIGT-CDG, a disorder of glycosylphosphatidylinositol anchors. *Mol. Genet. Metab.* 115, 128–140. doi: 10.1016/j.ymgme.2015.04.007

Mason, S., Castilla-Vallmanya, L., James, C., Andrews, P. I., Balcells, S., Grinberg, D., et al. (2019). Case report of a child bearing a novel deleterious splicing variant in PIGT. *Med. (Baltimore)* 98:e14524. doi: 10.1097/MD.0000000000014524

Nakashima, M., Kashii, H., Murakami, Y., Kato, M., Tsurusaki, Y., Miyake, N., et al. (2014). Novel compound heterozygous PIGT mutations caused multiple congenital anomalies-hypotonia-seizures syndrome 3. *Neurogenetics* 15, 193–200. doi: 10.1007/s10048-014-0408-y

Ohishi, K., Inoue, N., and Kinoshita, T. (2001). PIG-S and PIG-T, essential for GPI anchor attachment to proteins, form a complex with GAA1 and GPI8. *EMBO J.* 20, 4088–4098. doi: 10.1093/emboj/20.15.4088

Ohishi, K., Nagamune, K., Maeda, Y., and Kinoshita, T. (2003). Two subunits of glycosylphosphatidylinositol transamidase, GPI8 and PIG-T, form a functionally important intermolecular disulfide bridge. *J. Biol. Chem.* 278, 13959–13967. doi: 10.1074/jbc.M300586200

Pagnamenta, A. T., Murakami, Y., Taylor, J. M., Anzilotti, C., Howard, M. F., Miller, V., et al. (2017). Analysis of exome data for 4293 trios suggests GPI-anchor biogenesis defects are a rare cause of developmental disorders. *Eur. J. Hum. Genet.* 25, 669–679. doi: 10.1038/ejhg.2017.32

Richards, S., Aziz, N., Bale, S., Bick, D., Das, S., Gastier-Foster, J., et al. (2015). Standards and guidelines for the interpretation of sequence variants: a joint consensus recommendation of the American College of medical genetics and genomics and the association for molecular pathology. *Genet. Med.* 17, 405–424. doi: 10.1038/gim.2015.30

Skauli, N., Wallace, S., Chiang, S. C., Baroy, T., Holmgren, A., Stray-Pedersen, A., et al. (2016). Novel pigt variant in two brothers: expansion of the multiple congenital anomalies-hypotonia seizures syndrome 3 phenotype. *Genes (Basel)* 7:108. doi: 10.3390/genes7120108

Sobreira, N., Schiettecatte, F., Valle, D., and Hamosh, A. (2015). GeneMatcher: a matching tool for connecting investigators with an interest in the same gene. *Hum. Mutat.* 36, 928–930. doi: 10.1002/humu.22844

Tang, S., Addis, L., Smith, A., Topp, S. D., Pendziwiat, M., Mei, D., et al. (2020). Phenotypic and genetic spectrum of epilepsy with myoclonic atonic seizures. *Epilepsia* 61, 995–1007. doi: 10.1111/epi.16508

Tassinari, C. A., Rubboli, G., and Shibasaki, H. (1998). Neurophysiology of positive and negative myoclonus. *Electroencephalogr. Clin. Neurophysiol.* 107, 181–195. doi: 10.1016/s0013-4694(98)00058-3

Yang, L., Peng, J., Yin, X. M., Pang, N., Chen, C., Wu, T. H., et al. (2018). Homozygous pigt mutation lead to multiple congenital anomalies-hypotonia seizures syndrome 3. *Front. Genet.* 9:153. doi: 10.3389/fgene.2018.00153

Conflict of Interest: ABe was employed by the company GeneDx.

The remaining authors declare that the research was conducted in the absence of any commercial or financial relationships that could be construed as a potential conflict of interest.

The handling editor declared a past co-authorship with the author MG.

frontiers in Genetics

BRIEF RESEARCH REPORT
published: 27 May 2021
doi: 10.3389/fgene.2021.658786

Four New Cases of SLC35A2-CDG With Novel Mutations and Clinical Features

Kuerbanjiang Abuduxikuer and Jian-She Wang**

Department of Hepatology, Children's Hospital of Fudan University, Shanghai, China

OPEN ACCESS

Edited by:
Aleksandra Jezela-Stanek, National Institute of Tuberculosis and Lung Diseases, Poland

Reviewed by:
Karyn Megy, University of Cambridge, United Kingdom
Muhammad Imran Naseer, King Abdulaziz University, Saudi Arabia

***Correspondence:**
Kuerbanjiang Abuduxikuer
k_abuduxikuer@fudan.edu.cn
orcid.org/0000-0003-0298-3269
Jian-She Wang
jshwang@shmu.edu.cn
orcid.org/0000-0003-0823-586X

Specialty section:
This article was submitted to Genetics of Common and Rare Diseases, a section of the journal Frontiers in Genetics

Received: *26 January 2021*
Accepted: *27 April 2021*
Published: *27 May 2021*

Citation:
Abuduxikuer K and Wang J-S (2021) Four New Cases of SLC35A2-CDG With Novel Mutations and Clinical Features. Front. Genet. 12:658786. doi: 10.3389/fgene.2021.658786

SLC35A2-CDG is a rare type of X-linked CDG with more than 60 reported cases. We retrospectively analyzed clinical phenotypes and *SLC35A2* genotypes of four cases of SLC35A2-CDG from four unrelated families of Han ethnicity in China. All patients had infantile onset epilepsies that were completely or partly resistant to multiple anti-epileptic medications or ketogenic diet. Three patients had severe developmental delay. All patients were female patients carrying *de novo* deleterious mutations in *SLC35A2* (NM_001042498.2) gene, including one canonical splice-site mutation (c.426+1G > A), one large deletion (c.-322_c.274+1del), and two frameshift mutations leading to premature stop codon (c.781delC/p.Arg289ValfsTer88 and c.601delG/p.Ala201GlnfsTer148). Novel clinical features in some of our patients include anemia, hypertriglyceridemia, hypertonia, small ears, extra folds on earlobes, and maternal oligohydramnios or hypothyroidism during pregnancy. In one patient, concomitant Marfan syndrome was confirmed for having positive family history, carrying a heterozygous known disease-causing mutation in FBN1 gene (c.7240C > T/p.Arg2414Ter), and presence of typical features (rachnodactyly, ventrical septal defect, and mitral valve regurgitation). In conclusion, we expanded clinical phenotype and genetic mutation spectrum of SLC35A2-CDG by reporting four new cases with novel pathogenic variants and novel clinical features.

Keywords: SLC35A2-CDG, UDP-galactose transporter, CDG-IIm, congenital disorders of glycosylation, Chinese

INTRODUCTION

Congenital disorder of glycosylation (CDG) is a rapidly expanding group of metabolic disorders of glycan biosynthesis or assembly. Most of more than 140 types of CDGs discovered so far have neurologic phenotype, and can affect any other organs or systems depending on the specific CDG types (Chang et al., 2018; Ng and Freeze, 2018). Located in Xp11.23, *SLC35A2* gene (OMIM*314375) encodes solute carrier family 35 member

2 protein (UDP−galactose transporter, SLC35A2) in humans responsible for transporting UDP-galactose from the cytosol to lumens of Golgi apparatus and endoplasmic reticulum for glycosylation (Ishida et al., 1996; Miura et al., 1996). Inactivation of SLC35A2 gene in mammalian cell models caused total absence of UDP−galactose traffic into the Golgi apparatus leading to synthesis of truncated glycans lacking galactose (Brändli et al., 1988; Ishida et al., 1999). In humans, SLC35A2-CDG (OMIM#300896, formerly known as CDG type IIm) is caused by heterozygous *de novo* mutations in *SLC35A* gene and mostly affect female gender due to X−chromosome inactivation. Clinical phenotypes include infantile-onset seizure, global development delay, facial dysmorphism, abnormal liver function, and skeletal abnormalities. Since the first report of SLC35A2-CDG in 2013 (Ng et al., 2013), 54 *de novo* variants from 63 cases have been reported in the literature (Kodera et al., 2013; Ng et al., 2013, 2019; EuroEPINOMICS-Res Consortium, Epilepsy Phenome/Genome Project, and Epi4K Consortium., 2014; Dörre et al., 2015; Bosch et al., 2016; Lopes et al., 2016; The Undiagnosed Disease Network, 2016; Evers et al., 2017; Kimizu et al., 2017; Westenfield et al., 2018; Yates et al., 2018; Miyamoto et al., 2019; Vals et al., 2019). However, no patient has been reported from mainland China in English literature. Here we report four new patients with typical features of SLC35A2-CDG from China, and expand genotypic as well as phenotypic features with novel findings.

MATERIALS AND METHODS

Patient Recruitment and Literature Analysis

The Ethics Committee of the Children's Hospital of Fudan University approved this study. We retrospectively analyzed clinical phenotype and *SLC35A2* genotype of four cases (P1–P4) from four unrelated families. Three patients (P1, P2, and P3), were treated in the Department of Hepatology, Children's Hospital of Fudan University from January, 2017 to July, 2020, and were asked to fill out questionnaire with phenotypes related to SLC35A2-CDG. P2 and P3 signed an informed consent before recommending oral D-galactose therapy. Pubmed searches were conducted at 11 June 2020 using key words such as SLC35A2, UDP-galactose transporter (species were filtered for humans), but no reports from Mainland China were found. We also conducted Chinese language literature search by using the CNKI (China Knowledge Resource Integrated Database[1]) and Wanfang Database[2] and collected a case report of SLC35A2-CDG (P4) in Chinese medical literature. We also analyzed all reported cases of SLC35A2-CDG in English literature.

Sequencing and Bioinformatics Analysis

SLC35A2 gene variants were identified either through whole exome sequencing (WES), panel sequencing, or CNV-seq analysis by using the NM_001042498.2 transcript and checked against the Human Gene Mutation Database (HGMD®) Professional[3]. P1 had trio-WES by FindRare (a commercial genetic testing company[4], using Illumina platform and NextGene V2.3.4 software) (**Figure 1A**). P2 had trio-WES with CNV-seq analysis in a commercial genetic testing company (Berry Genomics[5], using Verita Trekker® mutation site detection system and Enliven® Data Annotation and Interpretation System) (**Figure 1B**). P3 had Epilepsy panel sequencing with parental confirmation by a commercial medical testing company called Kangso Medical Inspection[6] (**Figure 1C**). P4 was reported to be identified through simultaneous WES of the index patient, parents, maternal grandmother, and maternal uncle using Illumina Nextseq 500 sequencer. Novelty of *SLC35A2* gene variants were checked against dbSNP152[7], 1000 Genome Database[8], Exome Variant Server[9], and gnomAD[10]. Location of large deletion on the *SLC35A2* gene is confirmed with Mutalyzer 2.0.30 Position Converter[11]. Pathogenicity of genetic variants were predicted by online tools such as MutationTaster[12], CADD[13], SIFT Indel[14], and M-CAP[15]. Effects of variants on gene splicing were predicted with BDGP/NNSplice[16], ESE Finder 3.0[17], Human Splicing Finder 3.1[18], MutationTaster (see text footnote 12), and ASSP (Alternative splice site predictor[19]). All variants were Sanger confirmed.

RESULTS

Case Profiles

All cases were Han Chinese, and the only child born to healthy non-consanguineous parents.

Abbreviations: ACTH, adrenocorticotropic hormone; AEDs, anti-epileptic drugs; AFP, alphafetoprotein; ALT, alanine aminotransferase; AST, aspartate aminotransferase; BAEP, brainstem auditory evoked potential; CDG, congenital disorders of glycosylation; CDT, carbohydrate-deficient transferrin test; CMV, cytomegalovirus; CNKI, China Knowledge Resource Integrated Database; CT, computed tomography; EEG, electroencephalogram; GGT, gamma-glutamyl transpeptidase; IUGR, intrauterine growth restriction; MRI, magnetic resonance imaging; NMD, non-sense-mediated mRNA decay; TSH, thyroid stimulating hormone; VEP, visual evoked potential.

[1]https://cnki.net

[2]www.wanfangdata.com.cn

[3]www.hgmd.cf.ac.uk/

[4]www.findrare.cn

[5]www.berrygenomics.com

[6]www.kangso.net

[7]www.ncbi.nlm.nih.gov/snp

[8]www.1000genomes.org/

[9]http://exac.broadinstitute.org

[10]http://gnomad.broadinstitute.org

[11]https://mutalyzer.nl/position-converter

[12]www.mutationtaster.org

[13]https://cadd.gs.washington.edu

[14]https://sift.bii.a-star.edu.sg/www/SIFT_indels2.html

[15]http://bejerano.stanford.edu/MCAP/

[16]www.fruitfly.org/seq_tools/splice.html

[17]http://krainer01.cshl.edu/cgi-bin/tools/ESE3/esefinder.cgi

[18]www.umd.be/HSF

[19]http://wangcomputing.com/assp/index.html

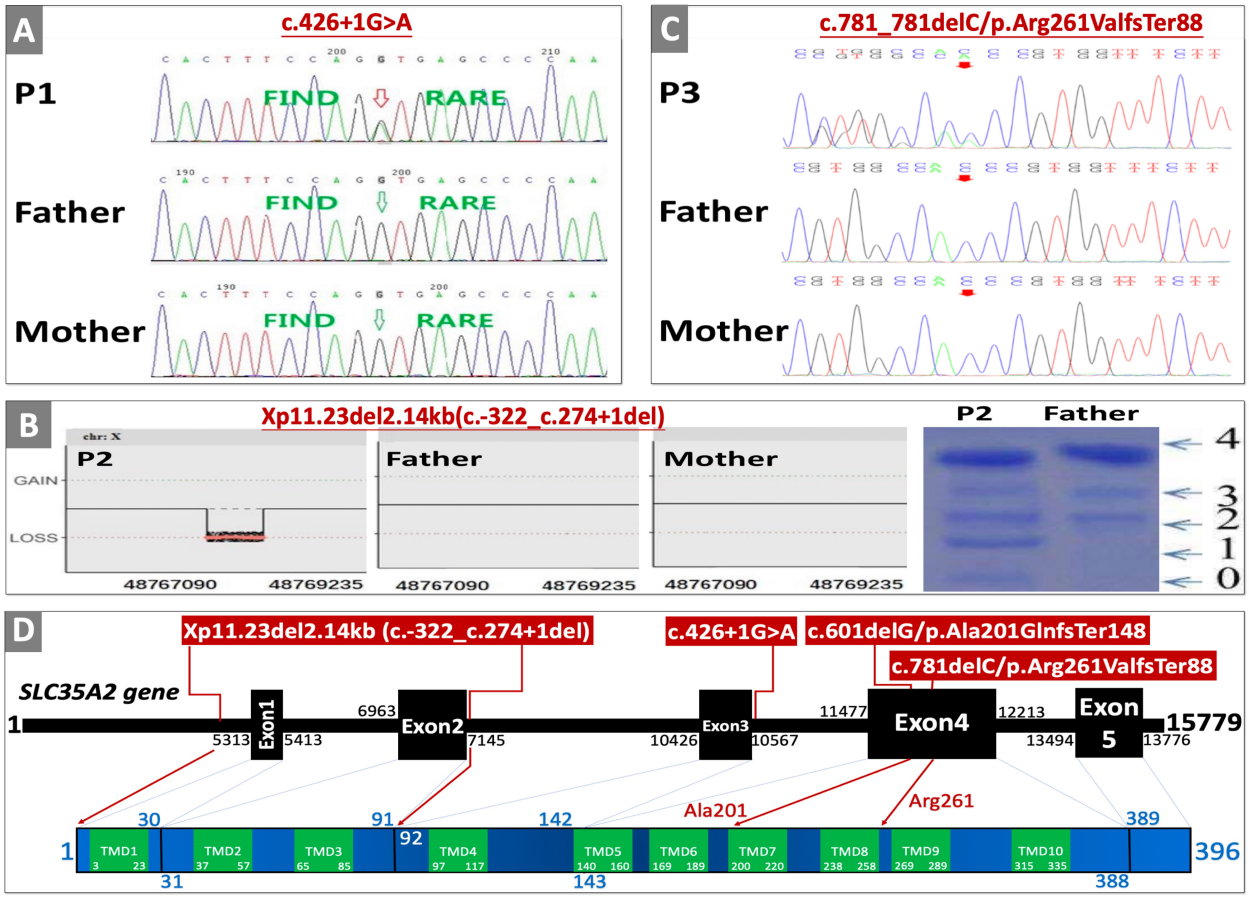

FIGURE 1 | Genetic testing, transferrin isoelectric focusing, cDNA changes, and effects on protein domain. **(A)** Sanger sequencing confirmation of P1. **(B)** Whole exome sequencing copy number variant (CNV) analysis result, and serum transferrin isoelectric focusing results of P2 (0, 1, 2, 3, and 4 are the numbers of sialic acid glycosylated with transferrin corresponding to transferrin not glycosylated with sialic acid, transferrin glycosylated with monosialic acid, disialic acid, trisialic acid, and tetrasialic acid). **(C)** Sanger sequencing confirmation of P3. **(D)** Location of variants on SLC35A2 gene with corresponding amino-acid location and transmembrane domains (TMD); *SLC35A2* gene NCBI reference sequence of NG_034300.1, transcript reference of NM_001042498.2, and protein reference of NP_001035963.1, and GRCh37/hg19 were used for cDNA and amino acid changes. Sanger sequencing confirmation of P4 and parents were published in the Chinese literature (Tian et al., 2020).

P1 was a full-term female born after uneventful pregnancy (except for mild oligohydramnios), and delivery was uncomplicated except for a lower birthweight (2,350 g, 1st centile by WHO standards). She presented with seizure at the age of 3 months, hypsarrhythmia in electroencephalogram (EEG) indicated infantile spasms. Seizures significantly improved after treatment with topiramate and vigabatrin. However, epilepsy was not controlled despite therapies with multiple anti-epileptic drugs (AEDs), adrenocorticotropic hormone (ACTH), and ketogenic diet. She was diagnosed with infantile spasm, epileptic encephalopathy, and psychomotor developmental delay. Brain MRI at the age of 5 months showed delayed myelination, slight enlargement of bilateral lateral ventricles and frontal subarachnoid spaces. At the age of 8.5 months, she still could not hold her head or roll over, eyes rarely follow objects, and rarely smiles. Weight is on the 8th centile (7.5 kg), while length is less than the 1st centile (59 cm). Other abnormal findings include mild microcytic normochromic anemia (hemoglobin 100 g/L, normal range 110–130 g/L) at the age of 7 months, and hypertriglyceridemia (2.98 mmol/L, normal range 0–1.7 mmol/L) with slight elevation of serum uric acid (412 μmol/L, normal range 140–390 umol/L) at the age of 1 year. Trio-WES identified a *de novo* canonical splice-site variant (c.426+1G > A) in *SCL35A2* gene (NM_001042498.2) (**Figure 1A**), and chromosome microarray analyses were negative for copy number variants. Normal findings include serum lactose, ammonia, creatine kinase, glucose, pyruvate, transaminases, profiles of amino-acid with acylcarnitine, cholesterol, folate, and vitamin B12 levels. This patient lost to follow-up before taking blood samples for glycosylation studies and recommending oral D-galactose therapy.

P2 is the first child of non-consanguineous parents born after full-term pregnancy (38 weeks and 2 days) with normal birthweight (2,950 g, 26th centile) and length (49 cm, 47th centile). Maternal history was positive for pre-conceptional

hyperthyroidism and hypothyroidism during pregnancy. Newborn period was uneventful except for significant hyperbilirubinemia and phototherapy. She presented with hypertonia, developmental delay, and seizures at the age of 5 months. EEG showed hypsarrhythmia and multifocal discharges on both temporal and occipital lobes. Physical examination was positive for increased muscle tone on extremities, smaller left ear with extra folds on both earlobes. Seizures were not responsive to topiramate and sodium valproate, but could be partly controlled with ACTH therapy. EEG at the age of 7 months was abnormal. Other abnormal findings include mild hypertransaminasemia (ALT/AST 42/52U/L, normal range 0–30 U/L), and mild lactic acidosis (3.1 mmol/L, normal range 0–2 mmol/L). Trio-WES was negative, but chromosome microarray analysis identified a *de novo* large deletion leading to the absence of the exon 1 and exon 2 (Xp11.23del2.14kb, c.-322_c.274+1del) in the *SLC35A2* gene. She and her healthy father (as normal control) were screened for carbohydrate deficient transferrin by iso-electric focusing. When compared to her father's normal profile, P3 had increased levels of transferrin glycosylated with monosialic and asialic acids (**Figure 1B**). Normal findings include lymphocyte sub-population, creatine kinase, thyroid function test, electrocardiography, brain MRI, chest X-ray, T-spot TB test, full blood count, serum amino-acid with acylcarnitine profiling, and urine organic acids. She received gradual increase of oral D-galactose therapy (a health supplement produced by Vita-World GmbH, Germany[20]) starting with 0.5 g/kg*day (divided into five doses), and adding 0.5 g/kg*day in 6 weeks with a final dosage of 1.5 g/kg*day from the age of 11 months (as recommended by a clinical trial protocol, ClinicalTrials.gov Identifier: NCT02955264). When followed up at the age of 22 months, she achieved seizure control with minimal EEG abnormality with slight improvement in both motor and language skills.

P3 was a full-term female infant with normal birthweight (3,100 g, 38th centile) born to non-consanguineous parents. Neonatal period was uneventful except for phototherapy due to hyperbilirubinemia. She developed seizures at the age of 10 months, EEG results were suggestive of infantile spasm (intermittent hypsarrhythmia with focal sharp waves on temporal-occipital lobe). Infantile spasm improved with ketogenic diet, but there was no improvement on abnormal EEG pattern after 3 months. She was found to have *de novo* frameshift mutation (c.781delC/p.Arg289ValfsTer88) on trio-WES (**Figure 1C**). Normal test results included liver function test, serum cholesterol and triglyceride levels, renal function test, serum electrolytes, full blood count, serum amino-acids with acylcarnitine profiling, urine organic acids, and brain MRI. Psychomotor developmental milestones were within normal range. After signing an informed consent for glycosylation study and oral D-galactose treatment, parents send blood samples of the child and parents to our institution. Seizure activities are controlled 6 months after galactose therapy.

[20]https://vita-world24.de/ihre-ziele/jung-vital-schoen/117/d-galactose-500-g

P4 is a 10-month-old girl recently reported in the Chinese literature (Tian et al., 2020). She was born full-term to non-consanguineous parents after an uneventful first pregnancy and vaginal delivery. She had normal birthweight (3,200 g, 47th centile), length (49 cm, 47th centile), and head circumference (34 cm, 54th centile). She was diagnosed with infantile spasms and developmental delay at the age of 3 months. At the age of 10 months, she was found to have severe global developmental delay (inability to hold her head or sit, Gesell Developmental Schedules DQ score was 15, normal range: >65), hypotonia, ventrical septal defect on echocardiography, hypsarrhythmia on electroencephalography, and mega cisterna magna accompanied by a cyst on brain MRI. Simultaneous WESs were performed using blood samples from the index patient, parents, maternal uncle, and maternal grandmother (Genetic testing was done as part of the screening and diagnosis of Marfan syndrome within the family members). A *de novo* heterozygous frameshift mutation (c.601delG/p.Ala201GlnfsTer148) in *SLC35A2* gene was found in the index patient only. P4 was also diagnosed to have Marfan syndrome due to carrying a known disease causing mutation in *FBN1* gene (NM_000138, heterozygous c.7240C > T/p.Arg2414Ter, HGMD CM020137), having typical features (congenital heart disease with VSD with mitral valve regurgitation, and arachnodactyly), and positive family history (mother and maternal grandmother) (Loeys et al., 2010). Normal test results at the age of 10 months include body weight (8 kg, 32nd centile), head circumference (42 cm, 5st centile), chest radiography, abdominal ultrasound, full blood count, serum biochemistry (including liver function test, serum creatinine, electrolytes, glucose, and transferrin levels), blood coagulation profiling, blood amino acid with acyl carnitine profiling, and urine organic acid analysis, and chromosome karyotyping (46XX).

Clinical characteristics of patients from our cohort and previously reported cases are summarized in **Table 1**. None of those SLC35A2 variants are present in gnomAD including Chinese and East-Asian population. None of these variants had been reported to be associated with SLC35A2-CDG in English literature. All four variants were predicted to be damaging by various *in silico* pathogenicity prediction tools, and predicted to affect gene splicing by at least one splice-site prediction tool. On the other hand, splice-site, large deletion, and frameshift variants may also affect protein function by causing non-sense mediated mRNA decay or by skipping of exons during transcription. *SLC35A2* gene variants, carrier frequencies, and results of *in silico* prediction tools were provided in **Table 2**. Sanger sequencing or chromosome microarray testing results, transferrin iso-electric focusing results, location of variants on the gene, and predicted effect on protein domains were provided in **Figure 1**. We also provided pedigrees of all patients in **Figure 2**.

DISCUSSION

We presented four new patients with typical features of SLC35A2-CDG carrying *de novo* and deleterious mutations in *SLC35A2* gene.

TABLE 1 | Clinical characteristics of patients from our cohort and previous reports.

Clinical phenotypes	**Features in our report (underline, novel features)**				**Previously reported features in English literature**
Patient ID	**P1**	**P2**	**P3**	**P4**	
Gender, age	Female, 8.5 months	Female, 22 months	Female, 13 months	Female, 10 months	Female/Male 41/4 (Ng et al., 2019; Vals et al., 2019)
Growth percentiles	Weight 8th, height < 1st, Short stature	Weight 50th, head circumference 52nd	Weight 54th, height 37th	Weight 32nd, head circumference 5th	Short stature 67% (10/15) (The Undiagnosed Disease Network, 2016; Vals et al., 2019)
Developmental delay	Yes	Yes	None	Yes	100% (62/62) (Ng et al., 2019; Vals et al., 2019)
Hypotonia	–	No (hypertonia)	–	Yes	90% (54/60) (Ng et al., 2019; Vals et al., 2019)
Intellectual Disability	Yes	Yes	None	Yes	97% (29/30) (Ng et al., 2019; Vals et al., 2019)
Facial Dysmorphism	–	Smaller left ear with extra folds on both earlobes.	–	–	85% (53/62) (Ng et al., 2019; Vals et al., 2019)
Epilepsy	Yes	Yes	Yes	Yes	83% (52/63) (Ng et al., 2019; Vals et al., 2019)
Skeletal abnormalities	Short stature	–	–	Arachnodactyly due to Marfan syndrome	83% (43/52) Shortened limbs, short stature, contractures, scoliosis, clubfoot, pes adductus, and craniosynostosis (Ng et al., 2019; Vals et al., 2019)
Abnormal brain MRI	Yes (delayed myelination, enlargement of lateral ventricles and frontal subarachnoid spaces)	No	No	Yes (mega cisterna magna, and a brain cyst)	Cerebral atrophy (50%, 13/26), cerebellar atrophy (46%, 26/56), thin corpus callosum (39%, 23/56), and delayed/hypo-myelination (59%, 16/27) (Ng et al., 2019; Vals et al., 2019)
Gastrointestinal	–	–	–	–	Feeding problems (75%, 24/32), Gastric-tube feeding (69%, 22/32) (Dörre et al., 2015; Westenfield et al., 2018; Ng et al., 2019)
Failure to Thrive	Short stature	–	–	None	77% (23/30) (Ng et al., 2019)
Feeding problems	–	–	–	–	73% (22/30) (Ng et al., 2019)
Ocular abnormalities	Does not follow objects	–	–	–	75% (43/57), Cortical visual impairment, strabismus, refractive errors (Ng et al., 2019; Vals et al., 2019)
Skin	No	–	–	–	60% (18/30) Inverted nipples, hypo/hyper-pigmentation of the skin (Ng et al., 2019)
Liver	Neonatal hyperbilirubinemia	Neonatal hyperbilirubinemia	Neonatal hyperbilirubinemia	–	80% (24/30) Mildly elevated transaminases (ALT, AST, GGT) and AFP elevation, 40% (12/30) Neonatal hyperbilirubinemia (Ng et al., 2019)
Abnormal CDT	–	Yes	–	–	35% (11/30) Truncated N-glycans lacking galactose and terminal sialic acid (Ng et al., 2019; Vals et al., 2019)
Immunological	–	–	–	–	33% (10/30) (Ng et al., 2019)
Respiratory	–	–	–	–	33% (10/30) (Ng et al., 2019)
Heart	–	–	–	VSD and mitral valve regurgitation	27% (8/30) (Ng et al., 2019)
Hearing Loss	Does not follow sounds	–	–	–	23% (7/30), sensorineural hearing loss, impaired hearing (Ng et al., 2019)
Pregnancy complication	Conceptional oligohydramnios	Conceptional hypothyroidism	–	None	20% (fetal skeletal dysplasias, pericardial effusions, decreased fetal movements, breech presentation) (Ng et al., 2019)
Genital/Endocrine	None	–	–	–	17% (5/30), Premature signs of puberty, hypothyroidism, slight elevation of thyroid stimulating hormone and free T4) (Ng et al., 2019)
IUGR	Yes	None	–	None	13% (4/30) (Ng et al., 2019)
Kidney	Uric acidemia	–	–	None	3% (1/30) (Ng et al., 2019)
Other	Anemia, and hypertriglyceridemia		–	Marfan syndrome	tapering fingers (14%, 2/14), broad great toes or overlapped toes (20%, 3/15) (Dörre et al., 2015; Kimizu et al., 2017; Westenfield et al., 2018; Yates et al., 2018)

–, not available or not tested; AFP, alphafetoprotein; CDT, carbohydrate-deficient transferrin test; IUGR, intrauterine growth restriction; VSD, ventrical septal defect; Underline, novel features.

TABLE 2 | SLC35A2 gene mutations, carrier frequency, and *in-silico* pathogenicity prediction results.

Patients		P1	P2	P3	P4
Physical location (GRCh37/hg19)		chrX:48763668C > T	chrX:48767090-48769235del	chrX:48762405_48762405delG	chrX:48762585_48762585delC
Nucleotide change (NM_001042498.2)		c.426+1G > A	Xp11.23del2.14kb (c.-322_c.274+1del, deletion of exon1 and exon2)	c.781delC	c.601delG
Amino acid change		NA	NA	p.Arg261ValfsTer88	p.Ala201GlnfsTer148
Parental origin		*De novo*	*De novo*	*De novo*	*De novo*
Frequency in control population	1000G	0	0	0	0
	ExAC	0	0	0	0
	gnomAD	0	0	0	0
Pathogenicity (ACMG criteria; Richards et al., 2015)		Class 5 (PS2+PM2+PM4+PP3+PP4)	Class 5 (PS2+PS3+PM2+PM4+PP3+PP4)	Class 5 (PS2+PM2+PM4+PP3+PP4)	Class 5 (PS2+PM2+PM4+PP3+PP4)
In silico prediction of pathogenicity (Score)	Mutation Taster	Disease causing (1)	NA	Disease causing (1)	Disease causing (1)
	M-CAP	Possibly pathogenic (0.838)	NA	NA	NA
	CADD	Pathogenic (34)	NA	NA	NA
	SIFT Indel	NA	Non-sense Mediated Decay	Damaging	Damaging
Effect of variants on gene splicing	BDGP/NNSplice	Donor site affected	Donor and acceptor sites affected	Donor and acceptor sites affected	None
	ESE Finder 3.0	Broken WT Donor Site	Loss of BranchSite	ESE site affected	None
	HSF3.1	New Donor Site, New ESS Site	ESS Sites broken, New ESE Site	None	None
	Mutation Taster	Donor lost, Acc increased	NA	Acc increased	Donor increased/gained
	ASSP	None	None	None	None
Predicted effect		Splice variant	Large deletion	Frameshift,	Frameshift

ASSP, Alternative Splice Site Predictor; BDGP/NNSplice, Berkeley Drosophila Genome Project/Splice Site Prediction by Neural Network; ESE, exonic splicing enhancer; ESS, exonic splicing silencer; HSF, Human Splicing Finder; NA, not available or not applicable; Pathogenicity thresholds: MutationTaster (probability), M-CAP (> 0.025), CADD (> 20).

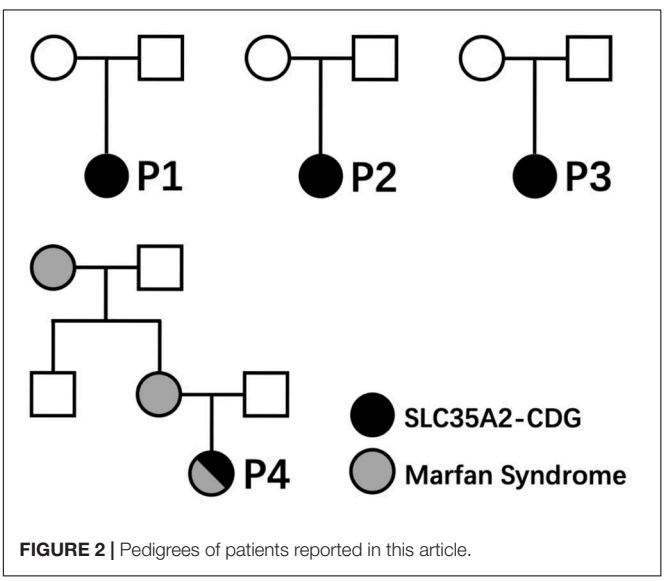

FIGURE 2 | Pedigrees of patients reported in this article.

Previously reported facial dysmorphisms included brachycephaly, coarse face, hypertelorism, high-set/broad/thick eyebrows, large blue irises, long narrow palpebral fissures, eversion of the lower lids, long eyelashes, epicanthal folds, low-set/posteriorly-rotated ears, mid-face hypoplasia, full cheek, depressed/broad nasal bridge, short nose, upturned nares, hypoplastic alae nasi, long, or short philtrum, thick lips, prominent cupid's bow, protruding tongue, fused tooth, enamel hypoplasia, high-arched palate, maxillary prognathism, and retrognathia (Kodera et al., 2013; Dörre et al., 2015; Westenfield et al., 2018). One patient in our cohort (P2) had smaller left ear with extra folds on both earlobes, a potentially new dysmorphism associated with SLC35A2-CDG.

Slight elevation of liver enzyme, hypothyroidism (Vals et al., 2019), and some fetal abnormalities (fetal skeletal dysplasias, pericardial effusion, decreased fetal movements, and breech presentation) (Ng et al., 2019) had been reported before. However, one patient (P1) in our cohort had anemia and hypertriglyceridemia, while another patient (P2) had hypertonia. All of which have never been reported in previous reports and could be novel phenotypes of SLC35A2-CDG. Previously reported pregnancy complications included fetal skeletal dysplasias, pericardial effusions, decreased fetal movements, and breech presentation. New findings on pregnancy complications in our cohort include conceptional oligohydramnios (P1) and conceptional hypothyroidism (P2). For the first time, we reported an SLC35A2-CDG patient with concomitant Marfan syndrome (P4).

Previously reported patients had various types of brain MRI abnormalities, including white matter abnormalities, cerebral/cerebellar/brainstem/pons atrophy, thin/short corpus callosum, delayed/hypo-myelination, frontal cortical dysplasia, diffusion abnormalities in mesencephalon/dentate, nucleus/cerebellar peduncule, Dandy-Walker malformation (congenital hydrocephalus affecting the cerebellum), arachnoidal pouch, periventricular frontal nodules, and enlarged lateral ventricle. P1 had delayed myelination, enlargement of lateral ventricles and frontal subarachnoid spaces the other hand, P4 had mega cisterna magna, and a brain cyst probably due to the coexistence of Marfan syndrome.

According to 2015 American College of Medical Genetics and Genomics (ACMG) guideline (Richards et al., 2015), c.426+1G > A (*de novo* PS2 + absent from controls PM2 + change in protein length PM4 + *in silico* evidence PP3 + phenotype match PP4), c.-322_c.274+1del (*de novo* PS2 + functional test PS3 + absent from controls PM2 + change in protein length PM4 + *in silico* evidence PP3 + phenotype match PP4), c.781delC/p.Arg261ValfsTer88 (*de novo* PS2 + absent from controls PM2 + change in protein length PM4 + *in silico* evidence PP3 + phenotype match PP4), and c.601delG/p.Ala201GlnfsTer148 (*de novo* PS2 + absent from controls PM2 + change in protein length PM4 + *in silico* evidence PP3 + phenotype match PP4) are all classified as Class 5 pathogenic variants. Two glycine (Gly202 and Gly214) and lysine residues (Lys78 and Lys297) are critical for transporter activity of SLC35A2 protein (Li and Mukhopadhyay, 2019). Transport activities in our patients could be completely absent due to Gly202/Gly214/Lys297 loss in P1 and P4 (143-388 amino acid residues could be absent due to loss of exon 4 caused by c.426+1G > A in P1, and amino acid sequence is completely changed beginning with Ala201 in P4 due to p.Ala201GlnfsTer148), Lys78 loss in P2 (1-91 amino acid residues could be absent due to exon 1 and exon 2 deletion caused by c.-322_c.274+1del), Lys297 loss in P3 (p.Arg261ValfsTer88). Canonical splice-site mutations (c.-322_c.274+1del), large deletions (c.781delC/p.Arg261ValfsTer88), and frameshift mutations (c.781delC/p.Arg261ValfsTer88 and c.601delG/p.Ala201GlnfsTer148) may also cause absence of the protein product through non-sense-mediated mRNA decay (NMD) (Hu and Ng, 2012). Previously, only two splice site mutations have been reported (c.274+2T > C and c.274+1T > C) to be associated with SLC35A2-CDG (Miyamoto et al., 2019; Ng et al., 2019). The c.426+1G > A variant in P1 is a canonical exon 3 splicing donor site mutation that usually causes skipping of Exon 4 during transcription and translation (Maszczak-Seneczko et al., 2011; Shibata et al., 2016; Anna and Monika, 2018) leading to loss of transmembrane domains (TMD) 5–10. All variants found in our patient caused amino acid changes in strictly conserved positions within TMDs in SLC35A2 protein by frameshifting or deletion, predicted to affect at least one feature of gene splicing, and predicted to be disease causing by multiple pathogenicity prediction tools (**Table 2**). In **Table 3**, we also listed all *SLC35A2* gene mutations reported so far.

TABLE 3 | Reported *SLC35A2* gene mutations (NM_001042498.2) in order of cDNA change.

cDNA change (NM_001042498.2)	Amino acid change	References
c.-322_c.274+1del	?	Current report
c.1A > G	Met1?	Ng et al., 2019
c.3G > A	Met1?	Ng et al., 2013
c.15_91+48delinsA	Gly8Serfs*9	Ng et al., 2013
c.124del	Val42Cysfs*53	Vals et al., 2019
c.164G > C	Arg55Pro	Ng et al., 2019; Vals et al., 2019
c.168C > A	Tyr56Ter	Ng et al., 2019
c.193_204del	Phe65_Thr68del	Ng et al., 2019
c.195C > A	Phe65Leu	Yates et al., 2018
c.211G > A	Val71Met	Ng et al., 2019
c.245G > T	Cys82Phe	The Undiagnosed Disease Network, 2016; Ng et al., 2019
c.262G > C	Ala88Pro	Vals et al., 2019
c.274+1G > A	?	Miyamoto et al., 2019
c.274+2T > C	?	Ng et al., 2019
c.302T > C	Leu101Pro	Ng et al., 2019
c.327T > G	Tyr106Ter	Yates et al., 2018
c.346G > C	p.Ala116Pro	Ng et al., 2019
c.348del	Val117Cysfs*27	Ng et al., 2019
c.353C > G	Pro118Arg	Ng et al., 2019
c.389A > G	Tyr130Cys	Ng et al., 2019; Vals et al., 2019
c.426+1G > A	?	Current report
c.433_434del	Tyr145Profs*76	Kodera et al., 2013
c.466_468delTCC	Ser156del	Vals et al., 2019
c.497_501dup	Gln168Glyfs*183	Ng et al., 2019
c.502C > T	Gln168Ter	EuroEPINOMICS-Res Consortium, Epilepsy Phenome/Genome Project, and Epi4K Consortium., 2014; Ng et al., 2019
c.515T > C	Leu172Pro	Yates et al., 2018
c.523C > T	Leu175Phe	Ng et al., 2019
c.523_525del	Leu175del	Ng et al., 2019
c.547C > T	Gln183Ter	Ng et al., 2019
c.562G > A	Gly188Ser	Ng et al., 2019
c.569dup	Gly191Argfs*31	Ng et al., 2019
c.601delG	Ala201Glnfs*148	Current report
c.617del	Val206Alafs*143	Ng et al., 2019
c.638C > T	Ser213Phe	Kodera et al., 2013
c.670C > T	Leu224Phe	Vals et al., 2019
c.683C > A	Ser228Ter	EuroEPINOMICS-Res Consortium, Epilepsy Phenome/Genome Project, and Epi4K Consortium., 2014
c.698T > C	Leu233Pro	Ng et al., 2019; Vals et al., 2019
c.747_757dup	Ala253Glyfs*100	Ng et al., 2019
c.753delG	Trp251Cysfs*98	Vals et al., 2019
c.772G > A	Val258Met	Lopes et al., 2016; Vals et al., 2019
c.781delC	Arg261Valfs*88	Current report
c.795del	Phe265Leufs*84	Ng et al., 2019
c.797G > T	Gly266Val	Dörre et al., 2015
c.800A > G	Tyr267Cys	Bosch et al., 2016; Vals et al., 2019
c.816G > A	Trp272Ter	Ng et al., 2019

(Continued)

TABLE 3 | Continued

cDNA change (NM_001042498.2)	Amino acid change	References
c.818G > A	Gly273Asp	Ng et al., 2019; Vals et al., 2019
c.831C > G	Asn277Lys	Evers et al., 2017
c.841G > A	Gly281Ser	Vals et al., 2019
c.841G > C	Gly281Arg	Vals et al., 2019
c.856del	Ala286Leufs*63	Ng et al., 2019
c.889A > G	Lys297Glu	Yates et al., 2018
c.908T > C	Leu303Pro	Ng et al., 2019
c.923C > T	Ser308Phe	Yates et al., 2018; Vals et al., 2019
c.935C > A	Ser312Tyr	Ng et al., 2019
c.944T > C	Leu315Pro	Ng et al., 2019
c.950delG	Gly317Alafs*32	Kimizu et al., 2017
c.972del	Phe324Leufs*25	Kodera et al., 2013
c.991G > A	Val331Ile	Ng et al., 2013, 2019; Westenfield et al., 2018; Vals et al., 2019

All patients were females in our cohort, and all carried deleterious mutations. Ng et al. (2013) calculated significantly more female patients with SLC35A2-CDG carried deleterious mutations (41%) than male patients (25%), indicating deleterious mutations might be less tolerated in male patients and retention of SLC35A2 protein functionality (either in the form of missense variant or mosaicism) might be needed for survival in male patients.

Transferrin isoelectric focusing (IEF) in some patients with SLC35A2-CDG showed type II patterns with increased levels of hypoglycosylated transferrins along with decreased level of tetrasialated transferrin (Ng et al., 2013; Dörre et al., 2015). However, transferrin IEF screening in some patients showed normal patterns during earlier or later years of disease course (9 out of 15) (Vals et al., 2019). P2 in our cohort had abnormal type II pattern with increased levels of asialated, monosialated, disialated, and trisialated transferrins. Mass spectrometry (MS) of N-glycans showed loss of galactose in one study (Vals et al., 2019), and partial loss of galactose and sialic acid of the N−linked glycans of serum transferrin was observed in other studies (Ng et al., 2013; Miyamoto et al., 2019).

Assays using Streptolysin-O-permeabilized fibroblasts from patients (Ng et al., 2013), glycoside−based UDP−galactose transport assays with primary fibroblast lines from patients (Ng et al., 2019), or a novel assay using the binding of bacterial Shiga toxins (Li and Mukhopadhyay, 2019) can be used to evaluate SLC35A2 enzyme activity. Deleterious mutations in our cohort have high likelihood of leading to complete loss of enzyme activity. Effects of variants found in our patients on enzyme activity need to be confirmed by similar assays.

There is no disease-specific treatment for SLC35A2-CDG that proven to be effective, but oral galactose supplementation may improve residual enzyme activity by providing extra substrate. Dörre et al. (2015) reported reduced seizure activity and improved transferrin IEF pattern after 100 days of oral galactose therapy (1 g/kg*day, divided into five doses) in a 6-months-old infant. Same efficacy may be achieved when the galactose was administered as a single morning dosage without having additional side effect (Witters et al., 2020). P2 and P3 achieved seizure control with minimal EEG abnormality after gradual increase of oral D-galactose up to 1.5 g/kg*day (starting with 0.5 g/kg*day and adding 0.5 g/kg*day in 6 weeks). P4 had improved motor development, reduced seizure activity, and improved EEG patterns after receiving 1 g/kg*day (divided to eight doses in a day) of oral galactose supplement.

Due to retrospective nature of this study, some limitations could not be avoided. Limitations in our study include lack of functional studies to confirm effects of mutations on protein function, N-glycan analysis for the confirmation of glycosylation defect, and transferrin IEF for P1, P3, and P4 for the screening of glycosylation defect. Nevertheless, we believe that the available information should be sufficient for the diagnosis of SLC35A2-CDG.

In summary, we expanded genotypic and phenotypic spectrum of SLC35A2-CD by reporting first four patients with novel *SLC35A2* gene variants and novel phenotypes from mainland China.

DATA AVAILABILITY STATEMENT

The original contributions presented in the study are included in the article/supplementary material, further inquiries can be directed to the corresponding author/s.

ETHICS STATEMENT

The studies involving human participants were reviewed and approved by the Ethics Committee of the Children's Hospital of Fudan University. Written informed consent to participate in this study was provided by the participants' legal guardian/next of kin. Written informed consent was obtained from the individual(s), and minor(s)' legal guardian/next of kin, for the publication of any potentially identifiable images or data included in this article.

AUTHOR CONTRIBUTIONS

J-SW and KA designed the study, approved the final submission, and clinically managed patients. KA collected clinical and genetic data, performed *in-silico* prediction, conducted literature search, summarized relevant information, and wrote the manuscript. Both authors contributed to the article and approved the submitted version.

FUNDING

This work was supported by the National Natural Science Foundation of China (81873543 and 81570468 to J-SW).

REFERENCES

Anna, A., and Monika, G. (2018). Splicing mutations in human genetic disorders: examples, detection, and confirmation. *J. Appl. Genet.* 59, 253–268. doi: 10.1007/s13353-018-0444-7

Bosch, D. G., Boonstra, F. N., de Leeuw, N., Pfundt, R., Nillesen, W. M., de Ligt, J., et al. (2016). Novel genetic causes for cerebral visual impairment. *Eur. J. Hum. Genet.* 24, 660–665. doi: 10.1038/ejhg.2015.186

Brändli, A. W., Hansson, G. C., Rodriguez-Boulan, E., and Simons, K. (1988). A polarized epithelial cell mutant deficient in translocation of UDP-galactose into the Golgi complex. *J. Biol. Chem.* 263, 16283–16290. doi: 10.1016/s0021-9258(18)37590-2

Chang, I. J., He, M., and Lam, C. T. (2018). Congenital disorders of glycosylation. *Ann. Transl. Med.* 6:477.

Dörre, K., Olczak, M., Wada, Y., Sosicka, P., Grüneberg, M., Reunert, J., et al. (2015). A new case of UDP-galactose transporter deficiency (SLC35A2-CDG): molecular basis, clinical phenotype, and therapeutic approach. *J Inherit Metab Dis.* 38, 931–940. doi: 10.1007/s10545-015-9828-6

EuroEPINOMICS-Res Consortium, Epilepsy Phenome/Genome Project, and Epi4K Consortium. (2014). De novo mutations in synaptic transmission genes including DNM1 cause epileptic encephalopathies. *Am. J. Hum. Genet.* 95, 360–370.

Evers, C., Staufner, C., Granzow, M., Paramasivam, N., Hinderhofer, K., Kaufmann, L., et al. (2017). Impact of clinical exomes in neurodevelopmental and neurometabolic disorders. *Mol. Genet. Metab.* 121, 297–307. doi: 10.1016/j.ymgme.2017.06.014

Hu, J., and Ng, P. C. (2012). Predicting the effects of frameshifting indels. *Genome Biol.* 13:R9.

Ishida, N., Miura, N., Yoshioka, S., and Kawakita, M. (1996). Molecular cloning and characterization of a novel isoform of the human UDP-galactose transporter, and of related complementary DNAs belonging to the nucleotide-sugar transporter gene family. *J. Biochem.* 120, 1074–1078. doi: 10.1093/oxfordjournals.jbchem.a021523

Ishida, N., Yoshioka, S., Iida, M., Sudo, K., Miura, N., Aoki, K., et al. (1999). Indispensability of transmembrane domains of Golgi UDP-galactose transporter as revealed by analysis of genetic defects in UDP-galactose transporter-deficient murine had-1 mutant cell lines and construction of deletion mutants. *J. Biochem.* 126, 1107–1117. doi: 10.1093/oxfordjournals.jbchem.a022556

Kimizu, T., Takahashi, Y., Oboshi, T., Horino, A., Koike, T., Yoshitomi, S., et al. (2017). A case of early onset epileptic encephalopathy with de novo mutation in SLC35A2: clinical features and treatment for epilepsy. *Brain Dev.* 39, 256–260. doi: 10.1016/j.braindev.2016.09.009

Kodera, H., Nakamura, K., Osaka, H., Maegaki, Y., Haginoya, K., Mizumoto, S., et al. (2013). De novo mutations in SLC35A2 encoding a UDP-galactose transporter cause early-onset epileptic encephalopathy. *Hum. Mutat.* 34, 1708–1714. doi: 10.1002/humu.22446

Li, D., and Mukhopadhyay, S. (2019). Functional analyses of the UDP-galactose transporter SLC35A2 using the binding of bacterial Shiga toxins as a novel activity assay. *Glycobiology* 29, 490–503. doi: 10.1093/glycob/cwz016

Loeys, B. L., Dietz, H. C., Braverman, A. C., Callewaert, B. L., De Backer, J., Devereux, R. B., et al. (2010). The revised Ghent nosology for the Marfan syndrome. *J. Med. Genet.* 47, 476–485. doi: 10.1136/jmg.2009.072785

Lopes, F., Barbosa, M., Ameur, A., Soares, G., de Sá, J., Dias, A. I., et al. (2016). Identification of novel genetic causes of Rett syndrome-like phenotypes. *J. Med. Genet.* 53, 190–199.

Maszczak-Seneczko, D., Olczak, T., Wunderlich, L., and Olczak, M. (2011). Comparative analysis of involvement of UGT1 and UGT2 splice variants of UDP-galactose transporter in glycosylation of macromolecules in MDCK and CHO cell lines. *Glycoconj J.* 28, 481–492. doi: 10.1007/s10719-011-9348-z

Miura, N., Ishida, N., Hoshino, M., Yamauchi, M., Hara, T., Ayusawa, D., et al. (1996). Human UDP-galactose translocator: molecular cloning of a complementary DNA that complements the genetic defect of a mutant cell line deficient in UDP-galactose translocator. *J. Biochem.* 120, 236–241. doi: 10.1093/oxfordjournals.jbchem.a021404

Miyamoto, S., Nakashima, M., Ohashi, T., Hiraide, T., Kurosawa, K., Yamamoto, T., et al. (2019). A case of de novo splice site variant in SLC35A2 showing developmental delays, spastic paraplegia, and delayed myelination. *Mol. Genet. Genomic Med.* 7:e814.

Ng, B. G., and Freeze, H. H. (2018). Perspectives on glycosylation and its congenital disorders. *Trends Genet.* 34, 466–476. doi: 10.1016/j.tig.2018.03.002

Ng, B. G., Buckingham, K. J., Raymond, K., Kircher, M., Turn.er, E. H., He, M., et al. (2013). University of Washington Center for Mendelian Genomics, Freeze HH. Mosaicism of the UDP-galactose transporter SLC35A2 causes a congenital disorder of glycosylation. *Am. J. Hum. Genet.* 92, 632–636. doi: 10.1016/j.ajhg.2013.03.012

Ng, B. G., Sosicka, P., Agadi, S., Almannai, M., Bacino, C. A., Barone, R., et al. (2019). SLC35A2-CDG: functional characterization, expanded molecular, clinical, and biochemical phenotypes of 30 unreported Individuals. *Hum. Mutat.* 40, 908–925.

Richards, S., Aziz, N., Bale, S., Bick, D., Das, S., Gastier-Foster, J., et al. (2015). Standards and guidelines for the interpretation of sequence variants: a joint consensus recommendation of the American College of Medical Genetics and Genomics and the Association for Molecular Pathology. *Genet. Med.* 17, 405–424. doi: 10.1038/gim.2015.30

Shibata, A., Okuno, T., Rahman, M. A., Azuma, Y., Takeda, J., Masuda, A., et al. (2016). IntSplice: prediction of the splicing consequences of intronic single-nucleotide variations in the human genome. *J. Hum. Genet.* 61, 633–640. doi: 10.1038/jhg.2016.23

The Undiagnosed Disease Network, (2016). Available online at: https://undiagnosed.hms.harvard.edu/participants/participant-012/ (accessed November 18, 2016).

Tian, Y., Hou, C., Wang, X., Zhu, H., Cao, B., Li, X., et al. (2020). Clinical characteristics analysis of a child with West syndrome caused by SLC35A2 gene mutation in a Marfan syndrome family and literature review. *J. Clin. Pediatr.* 38, 302–305.

Vals, M. A., Ashikov, A., Ilves, P., Loorits, D., Zeng, Q., Barone, R., et al. (2019). Clinical, neuroradiological, and biochemical features of SLC35A2-CDG patients. *J. Inherit. Metab. Dis.* 42, 553–564. doi: 10.1002/jimd.12055

Westenfield, K., Sarafoglou, K., Speltz, L. C., Pierpont, E. I., Steyermark, J., Nascene, D., et al. (2018). Mosaicism of the UDP-Galactose transporter SLC35A2 in a female causing a congenital disorder of glycosylation: a case report. *BMC Med. Genet.* 19:100.

Witters, P., Tahata, S., Barone, R., Õunap, K., Salvarinova, R., Grønborg, S., et al. (2020). Clinical and biochemical improvement with galactose supplementation in SLC35A2-CDG. *Genet. Med.* 22, 1102–1107. doi: 10.1038/s41436-020-0767-8

Yates, T. M., Suri, M., Desurkar, A., Lesca, G., Wallgren-Pettersson, C., Hammer, T. B., et al. (2018). SLC35A2-related congenital disorder of glycosylation: defining the phenotype. *Eur. J. Paediatr. Neurol.* 22, 1095–1102. doi: 10.1016/j.ejpn.2018.08.002

Conflict of Interest: The authors declare that the research was conducted in the absence of any commercial or financial relationships that could be construed as a potential conflict of interest.

frontiers in Genetics

REVIEW
published: 07 June 2021
doi: 10.3389/fgene.2021.674722

Diaphragmatic Hernia as a Prenatal Feature of Glycosylphosphatidylinositol Biosynthesis Defects and the Overlap With Fryns Syndrome – Literature Review

Przemyslaw Kosinski[1†], Milena Greczan[2] and Aleksandra Jezela-Stanek[3†]*

[1] 1st Department of Obstetrics and Gynecology, Medical University of Warsaw, Warsaw, Poland, [2] Department of Pediatrics, Nutrition, and Metabolic Diseases, Children's Memorial Health Institute, Warsaw, Poland, [3] Department of Genetics and Clinical Immunology, National Institute of Tuberculosis and Lung Disease, Warsaw, Poland

OPEN ACCESS

Edited by:
Thomas Schaible, University of Heidelberg, Germany

Reviewed by:
Magdalena Sandu, Spitalul Clinic de Copii Doctor Victor Gomoiu, Romania
Charlotte Bendixen, University Hospital Bonn, Germany

***Correspondence:**
Aleksandra Jezela-Stanek
jezela@gmail.com

† These authors have contributed equally to this work

Specialty section:
This article was submitted to Genetics of Common and Rare Diseases, a section of the journal Frontiers in Genetics

Received: *01 March 2021*
Accepted: *14 May 2021*
Published: *07 June 2021*

Citation:
Kosinski P, Greczan M and Jezela-Stanek A (2021) Diaphragmatic Hernia as a Prenatal Feature of Glycosylphosphatidylinositol Biosynthesis Defects and the Overlap With Fryns Syndrome – Literature Review. Front. Genet. 12:674722. doi: 10.3389/fgene.2021.674722

Fryns syndrome is an autosomal recessive multiple congenital anomaly syndrome, with diaphragmatic defects and secondary lung hypoplasia as cardinal features. Despite it was reported first in 1979, its exact etiology has not been established to date. With this review, we would like to draw attention to the prenatal presentation of multiple congenital anomalies syndromes, resulting from defects in the synthesis of glycosylphosphatidylinositol anchors, to be considered in a prenatal assessment of fetuses with DH and Fryns-like phenotype.

Keywords: glycosylphosphatidylinositol biosynthesis defects, GPIBDs, congenital diaphragmatic hernia, CDH, Fryns syndrome

INTRODUCTION

Fryns syndrome (FRNS, %229850) is an autosomal recessive multiple congenital anomaly syndrome. It was reported first in 1979 in two siblings with numerous congenital anomaly, including coarse facies, diaphragmatic hernia, absence of lung lobulation, and distal limb deformities (Fryns and Van den Berghe, 1979). To date, the exact etiology of FRNS (FS) has not been established, and genetic heterogeneity remains highly probable. From the clinical perspective, diaphragmatic defects and secondary lung hypoplasia are cardinal features (Fryns, 1987).

Congenital diaphragmatic hernia (CDH) is a developmental discontinuity of the diaphragm. As a result, the abdominal viscera may herniate into the chest and leads to lung hypoplasia. It occurs in approximately 1 in 3,000 live births but results in high morbidity and mortality, in neonatal and infancy period (Wynn et al., 2014). The most common localization is the posterolateral left side of the diaphragm (75–90% of cases), but the defect can also be right-sided (10–15% of cases) or even bilateral (1–2% of cases) (Deprest et al., 2011). The pulmonary vasculature malformation are the main cause of CDH-related pulmonary hypertension (Sluiter et al., 2012). Moreover, increased vascular resistance and decreased surface area for gas exchange are observed (Hislop and Reid, 1976).

Unfortunately, the pathogenesis of CDH has not been established definitively, and encompass wide range of genetic disorders, from chromosomal defects, noted in at least 10–30% cases,

including polyploidies, trisomy 18, partial trisomy 5, partial trisomy 20 or tetrasomy 12p (Pallister-Killian syndrome) (Graham and Devine, 2005; Pober, 2008; Kosinski and Wielgos, 2017) to monogenic syndromes (as Apert, CHARGE, Coffin-Siris, Goltz, Swyer, Brachmann-Cornelia De Lange, Simpson-Golabi-Behmel, Donnai-Barrow, Mathew-Wood, Jarcho-Levin, and Fraser). The influence of genetics in CDH was recently reviewed by Yu et al. (2020). This comprehensive review explains the genetic contributions to CDH are highly heterogeneous and suggests CDH genes are often transcription factors, genes involved in cell migration or the components of extracellular matrix. In cases of multiple abnormalities, malformations may occur in all major organ systems (Pober et al., 2005; Pober, 2007; Taylor et al., 2009). Since the etiology of CDH varies and is difficult to establish, with this review, we would like to draw attention to the prenatal presentation of multiple congenital anomalies syndromes, resulting from defects in the synthesis of glycosylphosphatidylinositol (GPI) anchors, as a possible cause, and to be considered in a prenatal assessment of fetuses with DH and Fryns-like phenotype.

DIAPHRAGMATIC HERNIA AS A MANIFESTATION OF FRYNS SYNDROME

In 1987 following criteria were suggested by Fryns (1987) to establish the diagnosis of FRNS: polyhdramnios, often occurring in the presence of normal fetal growth, in an infant with characteristic facial dysmorphism – a coarse face, a broad flat nasal bridge (but a large nose anteriorly), a short upper lip, a small jaw, a cleft lip and palate, and poorly shaped auricles with attached earlobes. The phalanges are distally hypoplastic with rudimentary and dysplastic nails. The cardinal features within internal organs are diaphragmatic defects with secondary lung hypoplasia. Moreover, malrotation of the intestine, duodenal or multiple atresias and a bicornuate uterus may be noted. Cloudy corneas, facial hirsutism and pulmonary segmentation defects all help in establishing the diagnosis. The eye findings in the syndrome were reviewed by Pierson et al. (2004), who found corneal clouding in nine out of 15 patients, anophthalmia in two and retinal dysplasia in two. Subtle skeletal abnormalities are also part of the condition (Kershisnik et al., 1991; Tsukahara et al., 1995).

Fryns (1995) points out that growth parameters may be above the 75th centile at birth with apparent macrocephaly. The author suggested that the finding of diaphragmatic hernia with intrauterine growth retardation is against the diagnosis (Fryns, 1995). Vargas et al. (2000) described discordant phenotype for diaphragmatic hernia in monozygotic twins. A few cases have survived the neonatal period and are severely retarded (Bamforth et al., 1989; Cunniff et al., 1990; Hanssen et al., 1992; Van Hove et al., 1995). Dingens and Fryns (1999) reported that the girl first described by Hanssen et al. (1992) had died at the age of 10 years in status epilepticus. She was found to have hematometra.

The individual presented by Davis and Samarakkody (2002) (with no facial photographs available), was diagnosed with Fryns syndrome based on constellation of physical anomalies, as coarse facial feature, fifth digits' hypoplasia and nail absence, tricuspid regurgitation, diaphragmatic defects, as well as Hirschsprung's disease. The finding of a diaphragmatic defect and renal abnormalities might alert the astute investigator to the possibility of this syndrome, but note that Siebert et al. found that 13–27% of infants with a diaphragmatic defect had a urinary tract anomaly (Siebert et al., 1990). Willems et al. (1991) reported a possible case with the diaphragm reduced to a fibrous web without an overt hernia. In some cases CDH might be the only ultrasound abnormality detected prenatally.

In a review of 23 patients with a diaphragmatic hernia (Congenital Diaphragmatic Hernia Study Group, 2002), seven patients underwent surgical repair at an average age of 7.5 days (range, 6 h to 14 days); the mortality rate was as high as 83% in patients with both CDH and FS compared to 33% in patients with unilateral isolated CDH (Neville et al., 2002).

McPherson et al. reported a case of Pallister-Killian syndrome (resulted from mosaic isochromosome 12p) with some Fryns syndrome features (facial dysmorphism and digital anomalies) and pointed out the possibility of diagnostic challenge (McPherson et al., 1993). Stratton et al. (1994) and Rodriguez et al. (1994) noted similar cases with Pallister–Killian syndrome and re-emphasized the latter point.

Three cases have had osteochondrodysplasia (mostly delayed ossification) (Kershisnik et al., 1991; Slavotinek et al., 2005). Wilgenbus et al. (1994) reported two fetuses with features of the condition where there were no diaphragmatic hernias, but one of them had severe lung hypoplasia. Bartsch et al. (1995) reported similar two more cases with Fryns syndrome but without lateral diaphragmatic defects. Records of 1,833 liveborn patients with CDH from 83 hospitals revealed Fryns syndrome in 23 cases witch constitutes for 1.3% (Neville et al., 2002). On the other hand, CDH among Fryns syndrome patients is present in approximately 76% to 89% of reported cases (Cunniff et al., 1990; Van Hove et al., 1995).

While Ramsing et al. (2000) delineated three fetuses between 15 and 31 weeks of gestation with FS features (Cases 3–5). They also reported a family where two fetuses had a more severe form or a different condition (Cases 1 and 2). Several cases have been reported with features of the discussed condition and chromosome aberrations, including duplication of 1q24–31 (Clark and Fenner-Gonzales, 1989), terminal 6q deletion (Krassikoff and Sekhon, 1990), a submicroscopic deletion of 1q41–42 (Kantarci et al., 2006) and partial trisomy 22 (Dean et al., 1991). It should be noted that mosaic trisomy 9 also shares these features. Ladonne et al. (1996) reported a case of trisomy 22 with features of Fryns syndrome. de Beaufort et al. (2000) presented a patient with some features of the condition who had a partial trisomy 22. There is an excellent review by Slavotinek describing diagnostic features of Fryns syndrome (Slavotinek, 2004).

Based on previously published articles, Lin et al. (2005) suggested a definition of the Fryns phenotype, encompassing the combination of six criteria: diaphragmatic defects, pulmonary hypoplasia, recognizable facial features, distal digital hypoplasia,

TABLE 1 | Summary of reported to date cases with Fryns syndrome phenotype due to glycosylphosphatidylinositol biosynthesis defects (GPIBDs).

References: no. of cases, sex	Prenatal clinical features	Postnatal clinical features	Genotype
***PIGN* gene (cytogenetic location: 18q21.33 phenotype: Multiple congenital anomalies-hypotonia-seizures syndrome 1 MIM 614080)**			
Alessandri et al., 2018: 3			
Patient 2, female	Polyhydramnios	Dysmorphic facial features, cloudy corneas and terminal hypoplasia of V digits with fingernails absence; right-sided diaphragmatic hernia (diagnosed by chest X-ray) presented with refractory hypoxemia and died at 24 h of life	Deletion-spanning exons 5–7 of *PIGN*
Patient 5, female	22 WG: left diaphragmatic hernia associated with bilateral pyelectasis and polyhydramnios	Hypoplasia of of hands and feet's distal phalanges, hirsutism and facial dysmorphism, small, low set and dysplastic ears, small nose with a flat nasal bridge, and macrostomia	Frameshift variant in *PIGN* [NM_176787.4:c.(421dup), p.(Ile141Asnfs*10)]
Patient 6, male (brother of Patient 5)	Left diaphragmatic hernia and polyhydramnios, with dilated and hyperechogenic kidneys	Microcephaly, symmetric growth retardation, hypoplastic distal phalanges and nails (of hands and feet), micropenis, wide and short neck, facial dysmorphic features: anteverted nares, macrostomia, a posterior cleft palate, and dysplastic ears; ventricular septal defect and two bilobed and hypoplastic lungs	As above
McInerney-Leo et al., 2016: 3			
NSGC-7.3, female	15 WG: omphalocele, left-sided CDH 17 WG: right-sided cleft lip, cystic and mildly echogenic kidneys, and pulmonary hypoplasia	Pregnancy was terminated	Stop mutation in exon 21 (NM_176787.4: c.1966C > T: p.Glu656X) and a splice site mutation following exon 18 (NM_176787.4: c.1674 + 1G > C) in the *PIGN* gene
NSGC-7.4, male (brother of NSGC-7.3)	13 WG: left-sided diaphragmatic hernia, omphalocele, kidneys anomalies, pulmonary hypoplasia, and unilateral cleft lip; increased nuchal translucency (3.39 mm, >95th centile for gestation)	Pregnancy was terminated	As above
Individual COLL-2.3, female	13 WG: raised nuchal translucency (8 mm, >95% centile), cystic hygroma, and fetal ascites 15 WG: severe septated cystic hygromata, a small exomphalos, moderately hyperechogenic bowel, echogenic kidneys, femur length on the 5th centile	Autopsy: facial dysmorphism (with hypertelorism), distal phalanges of V fingers; multiple internal organ malformations: brain, lungs and heart, bilateral posterior diaphragmatic herniae	Stop mutation in exon 9 of *PIGN* (NM 176787.4: c.694A > T, p.Lys232X)
Brady et al., 2014: 1			
Male		Pregnancy was terminated at 16 WG due to DH	Homozygous splice site mutation in *PIGN*: (NM_012327.5:exon16: c.1574fl1G > A; NM_176787.4:exon17: c.1574fl1G > A).
***PIGA* gene (cytogenetic location: Xp22.2 phenotype: Multiple congenital anomalies-hypotonia-seizures syndrome 2 MIM 300868)**			
Bayat et al., 2020: 1			
Patient 3, male (his sibling, patients 2, had craniofacial dysmorphic features, brachytelephalangy with nail hypoplasia, but no CDH)		Pregnancy was terminated at 16 weeks of gestation due to a severe CDH	Splice site variant c.-63 + 1G > C in *PIGA*

(Continued)

TABLE 1 | Continued

References: no. of cases, sex	Prenatal clinical features	Postnatal clinical features	Genotype
***PIGV* gene (cytogenetic location: 1p36.11 phenotype: Hyperphosphatasia with mental retardation syndrome 1 MIM 239300)**			
Reynolds et al., 2017: 1			
Sibling 1, female (sibling 2: elevated alkaline phosphatase, providing further evidence for a diagnosis of HPMRS, not Fryns syndrome)	20 WG: left-sided diaphragmatic hernia, head to lung ratio of 0.68, pelviectasis, heart anomaly (not confirmed as a result of DH) 32 WG: polyhydramnios	Coarsening of face, broad nasal base, prominent globes, V-shaped concha, and overfolded ear helix, telecanthus, broad mouth, hypoplastic V finger with absent nails	Compound Heterozygous variants within the *PIGV* gene [NM_017837.3]: a A maternally inherited missense variant in exon 3 [c.1022 C > A; p. Ala341Glu (GCA > GAA)] and a paternally inherited missense variant in Exon 4 [c.1253 C > A; p.Ala418Asp (GCT > GAT)]

associated anomalies (polyhydramnios, cloudy corneas, cleft lip/palate and genitourinary, cardiovascular and cerebral malformations), and affected sibs. The presence of four among mentioned characteristics may provide a strict clinical definition of FS, while three constitute a broad definition of FS. To date, no gene had been clearly associated with FS. Thus the diagnosis typically remains clinical after the exclusion of chromosomal aberrations using classical karyotyping and/or array comparative genomic hybridization (aCGH) (Jezela-Stanek et al., 2020).

FRYNS SYNDROME PHENOTYPE IN GLYCOSYLPHOSPHATIDYLINOSITOL BIOSYNTHESIS DEFECTS (GPIBDS)

Recently, several patients with syndromic CDH, harboring pathogenic variants in *PIGN* (Phosphatidyl Inositol Glycan Anchor Biosynthesis, Class N), *PIGA* (Phosphatidyl Inositol Glycan Anchor Biosynthesis, Class A), and *PIGV* (Phosphatidyl Inositol Glycan Anchor Biosynthesis, Class V) gene have been characterized (Longoni et al., 1993; Slavotinek, 1993; Brady et al., 2014; McInerney-Leo et al., 2016; Thompson and Cole, 2016; Reynolds et al., 2017; Alessandri et al., 2018; Witters et al., 2018; Bayat et al., 2020). These molecular diagnosed have expanded the genetic spectrum of Fryns-like phenotype to be part of congenital disorder of glycosylations (CDG), which encompass GPI-anchor biosynthesis defects (GPIBD).

Glycosylphosphatidylinositol is a phosphoglyceride that anchors proteins to the outer leaflet of the cellular membrane. GPIBDs form a group of heterogeneous diseases with a common underlying cause of inappropriate GPI-anchors biosynthesis or modification. Correct GPI biosynthesis and modification determine GPI-anchored proteins' expression on the cell surface and thus determines the proper antigen presentation, cell adhesion, and signal transduction (Alessandri et al., 2018). According to the clinical and laboratory findings, GPIBDs have been historically divided into two main subgroups: hyperphosphatasia with mental retardation syndrome (HPMRS) – a group of GPIBDs with elevated serum alkaline phosphatase activity (ALP) (mutations in *PIGV, PGAP2, PGAP3, PIGO, PIGW,* and *PIGY*) and multiple congenital anomalies hypotonia seizures (MCAHS) – with normal serum ALP (mutations in *PIGA*, *PIGN*, *PIGT).* However, the number of GPIBSDs that cannot be divided into these two groups is growing (Knaus et al., 2018). Accordingly, the terminology is questioned and no longer recommended.

PIGN-CDG and PIGA-CDG are MCAHS, characterized by severe developmental delay, early-onset intractable seizures, global hypotonia, congenital cardiac, gastrointestinal, renal and central nervous system (CNS) anomalies, nystagmus, failure to thrive and facial dysmorphism. In some individuals, brachytelephalangy with nail hypoplasia, joint contractures and CDH have also been described (Alessandri et al., 2018; Knaus et al., 2018). Surprisingly, ALP levels are elevated in some individuals with PIGA-CDG and borderline in some individuals with PIGN-CDG (Knaus et al., 2018).

PIGV-CDG is HPMRS (also known as Mabry syndrome), characterized by the constantly elevated ALP, intellectual disability, seizures with facial dysmorphia, brachytelephalangy and nail hypoplasia. In some individuals, Hirschprung disease, renal and anorectal malformations and CDH have been described (Reynolds et al., 2017).

No specific treatment is available so far for these conditions, and early death may occur.

The summary of described cases is presented in **Table 1**. Please note that the diagnoses cited by us are the original ones described in the discussed publications (that is why the terminology is diverse).

SUMMARY

Due to the complex nature and not fully recognized etiology of "Fryns syndrome", some confusion about the terminology exists. When it is a clinical entity, "Fryns-like phenotype" term should be used. Otherwise, Fryns syndrome is a disorder with presumed autosomal recessive inheritance. It is thus of primary importance to distinguish between a clinical or molecular diagnosis. In all individuals/fetuses within the spectrum of Fryns syndrome phenotype genetic diagnostics is rational.

It has to be underlined that a genetic abnormality must be suspected in each case of CDH diagnosed prenatally, when accompany with other malformations. Except for CDH, the clinical presentation of Fryns-like phenotype includes pulmonary hypoplasia, craniofacial dysmorphism, cleft lip/palate, brachytelephalangy accompany with nail hypoplasia, and various other internal organ malformations. Although no major genetic cause has been identified for FRNS, biallelic pathogenic variants in *PIGN*, *PIGV* and X-linked in *PIGA*, all encoding a component of the GPI-anchor biosynthesis pathway, have been identified in several probands with a phenotype fitting with FRNS.

During the genetic evaluation of fetuses that manifest developmental anomalies, it is mandatory to check for chromosomal aberrations (and perform karyotype and/or chromosomal microarray) and also to consider monogenic disorders (Committee on Genetics and the Society for Maternal-Fetal Medicine, 2016; Hay et al., 2018). All of the GPIBDs presented above, means caused by pathogenic variants in the *PIGN*, *PIGV*, and *PIGA* genes, are clinically very heterogenic and congenital malformations are not among their primary characteristics in many other affected individuals. All these syndromes belong to neurodevelopmental disorders and manifest predominantly with facial dysmorphism, global developmental disorders (especially speech and language), muscular hypotonia and seizures, as well as cerebral or cerebellar atrophy in PIGN-CDG, minor CNS anomalies in PIGA- and PIGV-CDG (Siebert et al., 1990; Knaus et al., 2018; Bayat et al., 2020).

Given the high mortality rate resulting from severe congenital malformations, reliable and early genetic diagnosis is crucial. It only allows for determining the recurrence risk (which is 25% for autosomal recessive disorder and even up to 50% for X-linked disorders, if the genetic status of mothers is unknown) and perform genetic testing in subsequent pregnancies. Thus, we propose to include GPI biosynthesis defects in the differential diagnosis during the prenatal evaluation of fetuses with diaphragmatic defects, especially in families with positive family history. When isolated cases are evaluated, the additional ultrasound features that may direct the diagnosis are large for gestational age, hypertelorism, cleft lip/palate, atrial/ventricular septal defects, urogenital anomalies and hand/feet abnormal positioning. However, we wonder how much safer it would be, keeping in mind the complexity of Fryns syndrome, to utilize the term "Fryns syndrome – like phenotype".

AUTHOR CONTRIBUTIONS

PK: manuscript writing and literature review. MG: manuscript writing. AJ-S: concept of the manuscript, writing, and literature review. All authors contributed to the article and approved the submitted version.

REFERENCES

Alessandri, J. L., Gordon, C. T., Jacquemont, M. L., Gruchy, N., Ajeawung, N. F., Benoist, G., et al. (2018). Recessive loss of function PIGN alleles, including an intragenic deletion with founder effect in La Reunion Island, in patients with Fryns syndrome. *Eur. J. Hum. Genet.* 26, 340–349. doi: 10.1038/s41431-017-0087-x

Bamforth, J. S., Leonard, C. O., Chodirker, B. N., Chitayat, D., Gritter, H. L., Evans, J. A., et al. (1989). Congenital diaphragmatic hernia, coarse facies, and acral hypoplasia: Fryns syndrome. *Am. J. Med. Genet.* 32, 93–99. doi: 10.1002/ajmg.1320320120

Bartsch, O., Meinecke, P., and Kamin, G. (1995). Fryns syndrome: two further cases without lateral diaphragmatic defects. *Clin. Dysmorphol.* 4, 352–358. doi: 10.1097/00019605-199510000-00012

Bayat, A., Knaus, A., Pendziwiat, M., Afenjar, A., Barakat, T. S., Bosch, F., et al. (2020). Lessons learned from 40 novel PIGA patients and a review of the literature. *Epilepsia* 61, 1142–1155.

Brady, P. D., Moerman, P., De Catte, L., Deprest, J., Devriendt, K., and Vermeesch, J. R. (2014). Exome sequencing identifies a recessive PIGN splice site mutation as a cause of syndromic congenital diaphragmatic hernia. *Eur. J. Med. Genet.* 57, 487–493. doi: 10.1016/j.ejmg.2014.05.001

Clark, R. D., and Fenner-Gonzales, M. (1989). Apparent Fryns syndrome in a boy with a tandem duplication of 1q24-31.2. *Am. J. Med. Genet.* 34, 422–426. doi: 10.1002/ajmg.1320340319

Committee on Genetics and the Society for Maternal-Fetal Medicine (2016). Committee opinion No. 682 summary: microarrays and next-generation sequencing technology: the use of advanced genetic diagnostic tools in obstetrics and gynecology. *Obstet. Gynecol.* 128, 1462–1463. doi: 10.1097/aog.0000000000001814

Congenital Diaphragmatic Hernia Study Group (2002). Available online at: https://med.uth.edu/pediatricsurgery/research/research-centers-and-programs/cdhsg/

Cunniff, C., Jones, K. L., Saal, H. M., and Stern, H. J. (1990). Fryns syndrome: an autosomal recessive disorder associated with craniofacial anomalies, diaphragmatic hernia, and distal digital hypoplasia. *Pediatrics* 85, 499–504.

Davis, C., and Samarakkody, U. (2002). Fryns syndrome: a surviving case with associated Hirschsprung's disease and hemidiaphragmatic agenesis. *J. Paediatr. Child Health* 38, 318–320. doi: 10.1046/j.1440-1754.2002.00820.x

de Beaufort, C., Schneider, F., Chafai, R., Colette, J. M., Delneste, D., and Pierquin, G. (2000). Diaphragmatic hernia and Fryns syndrome phenotype in partial trisomy 22. *Genet. Couns.* 11, 181–182.

Dean, J. C., Couzin, D. A., Gray, E. S., Lloyd, D. J., and Stephen, G. S. (1991). Apparent Fryns' syndrome and aneuploidy: evidence for a disturbance of the midline developmental field. *Clin. Genet.* 40, 349–352. doi: 10.1111/j.1399-0004.1991.tb03108.x

Deprest, J. A., Nicolaides, K., and Gratacos, E. (2011). Fetal surgery for congenital diaphragmatic hernia is back from never gone. *Fetal Diagn. Ther.* 29, 6–17. doi: 10.1159/000322844

Dingens, M., and Fryns, J. P. (1999). Hematometra and sudden death after status epilepticus in the adolescent female with Fryns syndrome. *Genet. Couns.* 10, 329–330.

Fryns, J. P. (1987). Fryns syndrome: a variable MCA syndrome with diaphragmatic defects, coarse face, and distal limb hypoplasia. *J. Med. Genet.* 24, 271–274. doi: 10.1136/jmg.24.5.271

Fryns, J. P. (1995). Prenatal diagnosis and long survival of Fryns syndrome. *Prenat. Diagn.* 15, 97–98. doi: 10.1002/pd.1970150125

Fryns, J. P., and Van den Berghe, H. (1979). Corneal clouding, subvalvular aortic stenosis, and midfacial hypoplasia associated with mental deficiency and growth retardation–a new syndrome? *Eur. J. Pediatr.* 131, 179–183. doi: 10.1007/bf00538941

Graham, G., and Devine, P. C. (2005). Antenatal diagnosis of congenital diaphragmatic hernia. *Semin. Perinatol.* 29, 69–76. doi: 10.1053/j.semperi.2005.04.002

Hanssen, A. M., Schrander-Stumpel, C. T., Thiry, P. A., and Fryns, J. P. (1992). Fryns syndrome: another example of non-lethal outcome with severe mental handicap. *Genet. Couns.* 3, 187–193.

Hay, S. B., Sahoo, T., Travis, M. K., Hovanes, K., Dzidic, N., Doherty, C., et al. (2018). ACOG and SMFM guidelines for prenatal diagnosis: is karyotyping really sufficient? *Prenat. Diagn.* 38, 184–189. doi: 10.1002/pd.5212

Hislop, A., and Reid, L. (1976). Persistent hypoplasia of the lung after repair of congenital diaphragmatic hernia. *Thorax* 31, 450–455. doi: 10.1136/thx.31.4.450

Jezela-Stanek, A., Mierzewska, H., and Szczepanik, E. (2020). Vertical nystagmus as a feature of PIGN-related glycosylphosphatidylinositol biosynthesis defects. *Clin. Neurol. Neurosurg.* 196:106033. doi: 10.1016/j.clineuro.2020.106033

Kantarci, S., Casavant, D., Prada, C., Russell, M., Byrne, J., Haug, L. W., et al. (2006). Findings from aCGH in patients with congenital diaphragmatic hernia (CDH): a possible locus for Fryns syndrome. *Am. J. Med. Genet. A* 140, 17–23. doi: 10.1002/ajmg.a.31025

Kershisnik, M. M., Craven, C. M., Jung, A. L., Carey, J. C., and Knisely, A. S. (1991). Osteochondrodysplasia in Fryns syndrome. *Am. J. Dis. Child* 145, 656–660. doi: 10.1001/archpedi.1991.02160060074024

Knaus, A., Pantel, J. T., Pendziwiat, M., Hajjir, N., Zhao, M., Hsieh, T. C., et al. (2018). Characterization of glycosylphosphatidylinositol biosynthesis defects by clinical features, flow cytometry, and automated image analysis. *Genome Med.* 10:3.

Kosinski, P., and Wielgos, M. (2017). Congenital diaphragmatic hernia: pathogenesis, prenatal diagnosis and management - literature review. *Ginekol. Pol.* 88, 24–30. doi: 10.5603/gp.a2017.0005

Krassikoff, N., and Sekhon, G. S. (1990). Terminal deletion of 6q and Fryns syndrome: a microdeletion/syndrome pair? *Am. J. Med. Genet.* 36, 363–364. doi: 10.1002/ajmg.1320360327

Ladonne, J. M., Gaillard, D., Carre-Pigeon, F., and Gabriel, R. (1996). Fryns syndrome phenotype and trisomy 22. *Am. J. Med. Genet.* 61, 68–70. doi: 10.1002/(sici)1096-8628(19960102)61:1<68::aid-ajmg13>3.0.co;2-u

Lin, A. E., Pober, B. R., Mullen, M. P., and Slavotinek, A. M. (2005). Cardiovascular malformations in Fryns syndrome: is there a pathogenic role for neural crest cells? *Am. J. Med. Genet. A* 139, 186–193. doi: 10.1002/ajmg.a.31023

Longoni, M., Pober, B. R., and High, F. A. (1993). "Congenital diaphragmatic hernia overview," in *GeneReviews((R))*, eds M. P. Adam, H. H. Ardinger, R. A. Pagon, S. E. Wallace, L. J. H. Bean, G. Mirzaa, et al. (Seattle, WA: Wiely).

McInerney-Leo, A. M., Harris, J. E., Gattas, M., Peach, E. E., Sinnott, S., Dudding-Byth, T., et al. (2016). Fryns syndrome associated with recessive mutations in PIGN in two separate families. *Hum. Mutat.* 37, 695–702. doi: 10.1002/humu.22994

McPherson, E. W., Ketterer, D. M., and Salsburey, D. J. (1993). Pallister-killian and fryns syndromes: nosology. *Am. J. Med. Genet.* 47, 241–245. doi: 10.1002/ajmg.1320470219

Neville, H. L., Jaksic, T., Wilson, J. M., Lally, P. A., Hardin, W. D. Jr., Hirschl, R. B., et al. (2002). Fryns syndrome in children with congenital diaphragmatic hernia. *J. Pediatr. Surg.* 37, 1685–1687. doi: 10.1053/jpsu.2002.36695

Pierson, D. M., Taboada, E., and Butler, M. G. (2004). Eye abnormalities in fryns syndrome. *Am. J. Med. Genet. A* 125A, 273–277. doi: 10.1002/ajmg.a.20520

Pober, B. R. (2007). Overview of epidemiology, genetics, birth defects, and chromosome abnormalities associated with CDH. *Am. J. Med. Genet. C Semin. Med. Genet.* 145C, 158–171. doi: 10.1002/ajmg.c.30126

Pober, B. R. (2008). Genetic aspects of human congenital diaphragmatic hernia. *Clin. Genet.* 74, 1–15. doi: 10.1111/j.1399-0004.2008.01031.x

Pober, B. R., Lin, A., Russell, M., Ackerman, K. G., Chakravorty, S., Strauss, B., et al. (2005). Infants with Bochdalek diaphragmatic hernia: sibling precurrence and monozygotic twin discordance in a hospital-based malformation surveillance program. *Am. J. Med. Genet. Part A* 138A, 81–88. doi: 10.1002/ajmg.a.30904

Ramsing, M., Gillessen-Kaesbach, G., Holzgreve, W., Fritz, B., and Rehder, H. (2000). Variability in the phenotypic expression of fryns syndrome: a report of two sibships. *Am. J. Med. Genet.* 95, 415–424. doi: 10.1002/1096-8628(20001218)95:5<415::aid-ajmg2>3.0.co;2-j

Reynolds, K. K., Juusola, J., Rice, G. M., and Giampietro, P. F. (2017). Prenatal presentation of Mabry syndrome with congenital diaphragmatic hernia and phenotypic overlap with Fryns syndrome. *Am. J. Med. Genet. A* 173, 2776–2781. doi: 10.1002/ajmg.a.38379

Rodriguez, J. I., Garcia, I., Alvarez, J., Delicado, A., and Palacios, J. (1994). Lethal Pallister-Killian syndrome: phenotypic similarity with Fryns syndrome. *Am. J. Med. Genet.* 53, 176–181. doi: 10.1002/ajmg.1320530211

Siebert, J. R., Benjamin, D. R., Juul, S., and Glick, P. L. (1990). Urinary tract anomalies associated with congenital diaphragmatic defects. *Am. J. Med. Genet.* 37, 1–5. doi: 10.1002/ajmg.1320370102

Slavotinek, A. (1993). "Fryns syndrome," in *GeneReviews((R))*, eds M. P. Adam, H. H. Ardinger, R. A. Pagon, S. E. Wallace, L. J. H. Bean, G. Mirzaa, et al. (Seattle, WA: Wiely).

Slavotinek, A. M. (2004). Fryns syndrome: a review of the phenotype and diagnostic guidelines. *Am. J. Med. Genet. A* 124A, 427–433. doi: 10.1002/ajmg.a.20381

Slavotinek, A. M., Robinson, H., and Steele, M. A. (2005). Fryns syndrome with osteochondrodysplasia. *Am. J. Med. Genet. A* 134, 454–456. doi: 10.1002/ajmg.a.30351

Sluiter, I., Veenma, D., van Loenhout, R., Rottier, R., de Klein, A., Keijzer, R., et al. (2012). Etiological and pathogenic factors in congenital diaphragmatic hernia. *Eur. J. Pediatr. Surg.* 22, 345–354.

Stratton, R. F., Moore, C. M., Popham, C. S., DuPont, B. R., and Mattern, V. L. (1994). Pallister-Killian and Fryns syndromes. *Am. J. Med. Genet.* 51:90. doi: 10.1002/ajmg.1320510124

Taylor, G. A., Atalabi, O. M., and Estroff, J. A. (2009). Imaging of congenital diaphragmatic hernias. *Pediatr. Radiol.* 39, 1–16. doi: 10.1007/s00247-008-0917-7

Thompson, M. D., and Cole, D. E. (2016). Recessive PIGN mutations in fryns syndrome: evidence for genetic heterogeneity. *Hum. Mutat.* 37:621. doi: 10.1002/humu.23016

Tsukahara, M., Sase, M., Tateishi, H., Saito, T., Kato, H., and Furukawa, S. (1995). Skeletal manifestations in Fryns syndrome. *Am. J. Med. Genet.* 55, 217–220. doi: 10.1002/ajmg.1320550213

Van Hove, J. L., Spiridigliozzi, G. A., Heinz, R., McConkie-Rosell, A., Iafolla, A. K., and Kahler, S. G. (1995). Fryns syndrome survivors and neurologic outcome. *Am. J. Med. Genet.* 59, 334–340. doi: 10.1002/ajmg.1320590311

Vargas, J. E., Cox, G. F., and Korf, B. R. (2000). Discordant phenotype in monozygotic twins with Fryns syndrome. *Am. J. Med. Genet.* 94, 42–45. doi: 10.1002/1096-8628(20000904)94:1<42::aid-ajmg9>3.0.co;2-6

Wilgenbus, K. K., Engers, R., Crombach, G., and Majewski, F. (1994). Two fetuses with Fryns syndrome without diaphragmatic defects. *J. Med. Genet.* 31, 962–964. doi: 10.1136/jmg.31.12.962

Willems, P. J., Keersmaekers, G. H., Dom, K. E., Colpaert, C., Schatteman, E., Vergote, I. B., et al. (1991). Fryns syndrome without diaphragmatic hernia? *Am. J. Med. Genet.* 41, 255–257.

Witters, P., Breckpot, J., Foulquier, F., Preston, G., Jaeken, J., and Morava, E. (2018). Expanding the phenotype of metabolic cutis laxa with an additional disorder of N-linked protein glycosylation. *Eur. J. Hum. Genet.* 26, 618–621. doi: 10.1038/s41431-017-0044-8

Wynn, J., Yu, L., and Chung, W. K. (2014). Genetic causes of congenital diaphragmatic hernia. *Semin. Fetal Neonatal Med.* 19, 324–330.

Yu, L., Hernan, R. R., Wynn, J., and Chung, W. K. (2020). The influence of genetics in congenital diaphragmatic hernia. *Semin. Perinatol.* 44:151169.

Conflict of Interest: The authors declare that the research was conducted in the absence of any commercial or financial relationships that could be construed as a potential conflict of interest.

frontiers in Pediatrics

ORIGINAL RESEARCH
published: 05 July 2021
doi: 10.3389/fped.2021.696918

Liver Involvement in Congenital Disorders of Glycosylation and Deglycosylation

Patryk Lipiński[1], *Anna Bogdańska*[2], *Piotr Socha*[3] *and Anna Tylki-Szymańska*[1]*

[1] Department of Pediatrics, Nutrition and Metabolic Diseases, Children's Memorial Health Institute, Warsaw, Poland, [2] Department of Biochemistry, Radioimmunology and Experimental Medicine, Children's Memorial Health Institute, Warsaw, Poland, [3] Department of Gastroenterology, Hepatology, Feeding Difficulties and Pediatrics, Children's Memorial Health Institute, Warsaw, Poland

Background: Congenital disorders of glycosylation (CDG) and NGLY1-CDDG (NGLY1-congenital disorder of deglycosylation) usually represent multisystem (especially neurovisceral) diseases with liver involvement reported in some of them. The aim of the study was to characterize the liver phenotype in CDG and NGLY1-CDDG patients hospitalized in our Institute, and to find the most specific features of liver disease among them.

Material and Methods: The study involved 39 patients (from 35 families) with CDG, and two patients (from two families) with NGLY1-CDDG, confirmed molecularly, for whom detailed characteristics of liver involvement were available. They were enrolled based on the retrospective analysis of their medical records.

Results: At the time of the first consultation, 13/32 patients were diagnosed with hepatomegaly; none of them with splenomegaly. As many as 23/32 persons had elevated serum transaminases, including 16 (70%) who had mildly elevated levels. During the long-term follow-up (available for 19 patients), serum transaminases normalized in 15/19 (79%) of them, including a spontaneous normalization in 12/15 (80%) of them. The GGT activity was observed to be normal in all study cases. Protein C, protein S and antithrombin activities in plasma were observed in 16 patients, and they were decreased in all of them.

Conclusions: It is necessary to conduct a long-term follow-up of liver disease in CDG to obtain comprehensive data.

Keywords: congenital disorder glycosylation, liver disease, hepatomegaly, coagulopathy, elevated serum transaminases, NGLY1-conegnital disorder of deglycosylation

OPEN ACCESS

Edited by:
Aleksandra Jezela-Stanek, National Institute of Tuberculosis and Lung Diseases (Poland), Poland

Reviewed by:
Delphine Borgel, Assistance Publique-Hôpitaux de Paris, France
Robert Smigiel, Division Pediatric Propedeutics and Rare Disorders Wroclaw Medical University, Poland

***Correspondence:**
Anna Tylki-Szymańska
a.tylki@ipczd.pl

Specialty section:
This article was submitted to Genetics of Common and Rare Diseases, a section of the journal Frontiers in Pediatrics

Received: *18 April 2021*
Accepted: *07 June 2021*
Published: *05 July 2021*

Citation:
Lipiński P, Bogdańska A, Socha P and Tylki-Szymańska A (2021) Liver Involvement in Congenital Disorders of Glycosylation and Deglycosylation. Front. Pediatr. 9:696918. doi: 10.3389/fped.2021.696918

INTRODUCTION

Glycosylation comprises the main process of the post-translational modification of most human proteins and is critical for physiological and pathological cellular functions. Congenital disorders of glycosylation (CDG) are a heterogeneous group of genetic defects in the synthesis of glycans and their attachment to proteins and lipids. Since the first description of phosphomannomutase 2 deficiency (PMM2-CDG), more than 130 CDG subtypes have been reported (1–3). On the other hand, deficiency of N-glycanase 1 (NGLY1) comprises the only one entity defined as congenital disorder of deglycosylation (CDDG) (4, 5).

N-glycanase 1 is a deglycosylating enzyme that cleaves N-glycans from misfolded glycoproteins during the endoplasmic reticulum (ER)-associated degradation (ERAD) process (6).

CDG and NGLY1-CDDG usually represent multisystem (especially neurovisceral) diseases with liver involvement reported in some of them (7). As observed in the severe phenotypes, sometimes associated with non-immune hydrops fetalis, the liver disease was usually part of multiple organ failure, leading to death in the 1st months of life (7, 8). In neurovisceral phenotypes, the liver disease was generally diagnosed based on elevated serum transaminases, independently from the neurological disease (7, 9, 10). However, both liver steatosis and fibrosis (and even cirrhosis) have been reported in the course of some of them (7, 11–13). There are also some subtypes, like MPI-CDG, TMEM199-CDG and CCDC115-CDG, with clinical and biochemical phenotype expressed mainly in the liver (no neurological involvement) (7, 14–19).

Since next-generation sequencing (NGS) became more widely available, an improvement in diagnostics has been observed, with more patients as well as new diseases being reported (1–3). However, the exact data on liver involvement in various CDG subtypes as well as NGLY1-CDDG are sparse and diverse, especially in relation to the long-term follow-up. There is also no general statement on whether the liver disease in various CDG and NGLY1-CDDG is clinically relevant.

The aim of the study was to characterize the liver phenotype in CDG and NGLY1-CDDG patients hospitalized in our Institute and to find the most specific features of liver involvement.

MATERIALS AND METHODS

The study involved 39 patients (from 35 families) with CDG, and two patients (from two families) with NGLY1-CDDG, confirmed molecularly. Detailed clinical, biochemical and molecular characteristics were recently published (20–22). All study patients were diagnosed and followed-up in Department of Pediatrics, Nutrition and Metabolic Diseases, Children's Memorial Health Institute, Warsaw, Poland.

The patients for whom detailed characteristics of liver involvement were available were enrolled in the study based on the clinical (physical examination), biochemical (aspartate and alanine aminotransferase, gamma-glutamyl transferase, serum total and direct bilirubin, internal normalized ratio, protein C and protein S activity, antithrombin activity), and histopathological (liver biopsy or autopsy) data.

The reference ranges of GGT in the 1st year of life were in accordance with Cabrera-Abreu and Green (23, 24). The upper limit of normal (ULN) for ALT was modified in accordance with Schwimmer et al. (25).

For the purpose of the study, of the levels of elevation of serum transaminases were divided into the following categories: mild elevation (<3 times of the ULN), moderate elevation (3–5 times of the ULN), severe elevation (>5 times of the ULN).

RESULTS

Overall Characteristics

A total of 32 patients were included in the study, including 10 PMM2-CDG, 4 SRD5A3-CDG, 3 ATP6AP1-CDG, 3 MPI-CDG, 3 ALG13-CDG, 3 ALG1-CDG, 1 ALG3-CDG, 1 PGM1-CDG, 1 DPAGT1-CDG, 1 ATPV0A2-CDG, and 2 NGLY1-CDDG.

In patients with MPI-CDG, the clinical and biochemical phenotype was mainly expressed in the liver, whereas in other cases, liver involvement was associated with neurological manifestation/neurovisceral disease (PMM2-CDG, SRD5A3-CDG, ALG13-CDG, ALG1-CDG, ALG3-CDG, DPAGT1-CDG, NGLY1-CDDG), cardiac involvement (dilated cardiomyopathy and progressive cardiac insufficiency in the patient with PGM1-CDG), *cutis laxa* in ATPV0A2-CDG, sensorineural hearing loss, glomerular and tubular dysfunction in ATP6AP1-CDG. One PMM2-CDG patient demonstrated a severe phenotype and succumbed to multiple organ failure at 2 months of age.

The characteristics of clinical, biochemical and histological liver phenotypes are summarized in **Table 1**.

Clinical and Biochemical Phenotype

At the time of the first consultation, 13/32 patients were diagnosed with hepatomegaly, including 8/10 with PMM2-CDG, 3/3 with MPI-CDG, 1/1 with PGM1-CDG, and 1/3 with ALG1-CDG. None of the persons was diagnosed with splenomegaly. Prolonged neonatal jaundice was not observed in the studied patients.

As many as 23/32 (72%) patients had elevated serum transaminases. Mild elevation was observed in 16 (70%) of them, moderate elevation in three cases (one with PGM1-CDG, one with SRD5A3-CDG, one with PMM2-CDG), and severe elevation in four patients (two with MPI-CDG, one with SRD5A3-CDG, one with PMM2-CDG). During the long-term follow-up (available for 19 persons), serum transaminases normalized in 15/19 (79%) of them, including 3 MPI-CDG patients on mannose supplementation therapy and 12 patients with other CDG and a spontaneous improvement. The same level of transaminase elevation was observed in 3/3 patients with ATP6AP1-CDG and 1/1 with PGM1-CDG.

The GGT activity was observed to be normal in all study patients. One person with PMM2-CDG had an elevated serum total bilirubin concentration with normal serum direct bilirubin.

Coagulation studies demonstrated an elevated INR in 1/30 patients (PMM2-CDG). Protein C, protein S and antithrombin activities in plasma were available in 16 cases, and they decreased in all of them. Two patients (one with PMM2-CDG and one with ALG1-CDG) with decreased plasma protein C, protein S and antithrombin activity developed thrombotic events (see **Table 1**).

Serum ceruloplasmin was tested in 6 patients (three with MPI-CDG, one with PMM2-CDG, one with PGM1-CDG, one with SRD5A3-CDG) and it was found to have decreased in one of them (PGM1-CDG). Wilson disease was excluded on the basis of low urinary copper excretion.

The prevalence of extra-hepatic manifestations of various CDG in our patients was recently published.

TABLE 1 | Biochemical and histological characteristics of liver disease in study patients with CDG/NGLY1-CDDG defined molecularly.

CDG/CDDG	Mutation and protein change	Age at first presentation and during follow-up	H/S	Laboratory analyses Liver biopsy (if performed) Other features
ALG1-CDG	c.773C>T, p.Ser258Leu/ c.1182C>G, p.Phe394Leu	3 mo Death	H (+) S (–)	3 mo – thromobotic event AST 80 ALT 85 INR 1.00 Alb 24 AT 12 Protein C 6.8 Protein S 33
ALG1-CDG	ALG1 c.773C>T, p.Ser258Leu/ c.1182C>G, p.Phe394Leu	1 mo	H (–) S (–)	AST 20 ALT 17 INR 1.15 Alb 21 Protein C 10.6 Protein S 32
		4 mo	H (–) S (–)	AST 23 ALT 9 INR 1.15 AT 15 Protein C 4.7 Protein S 24.4
ALG1-CDG	16p13.3 deletion in the *ALG1* gene	1 mo	H (–) S (–)	ALT 53 AST 49 INR 1.05 AT 30 Protein C 20 Protein S 42
		10 mo	H (–) S (–)	ALT 17 AST 29
ALG3-CDG	n.a.	10 mo	H (–) S (–)	AST 20 ALT 14 INR 0.99 Alb 39 AT 61 Protein C 54 Protein S 51
		10y 5mo	H (–) S (–)	AST 33 ALT 32 INR 0.95 Alb 43 AT 58 Protein C 52 Protein S 65
ALG13-CDG	c.320A>G, p.Asn107Ser, hmz *de novo*	12mo	H (–) S (–)	AST 44 ALT 29 INR 1.00
		4y	H (–) S (–)	AST 27 ALT 5 INR 0.9
ALG13-CDG	c.320A>G, p.Asn107Ser, hmz *de novo*	8mo	H (–) S (–)	ALT 16 AST 33 INR 1.03
		2y	H (–) S (–)	AST 31 ALT 5 Alb 43 INR 0.97
ALG13-CDG	c.320A>G, p.Asn107Ser, hmz *de novo*	6mo	H (–) S (–)	AST 22 ALT 12 INR 1.00
ATP6AP1-CDG (X-linked)	c.1284G>A, p.Met428Ile	8y	H (–) S (–)	AST 70 ALT 76 INR 1.05
		17y	H (–) S (–)	AST 61 ALT 55
		25y	H (–) S (–)	AST 54 ALT 46
ATP6AP1-CDG (X-linked)	c.1284G>A, p.Met428Ile	9y	H (–) S (–)	AST 64 ALT 39
		18y	H (–) S (–)	AST 46 ALT 51
ATP6AP1-CDG (X-linked)	c.1284G>A, p.Met428Ile	30y	H (–) S (–)	AST 68 ALT 52
		36y	H (–) S (–)	AST 57 ALT 48
ATPV0A2-CDG	c.2015T>A, p.Leu672X/ c.130delG, p.N43fsX55	1y9m	H (–) S (–)	AST 69 ALT 23 Alb 45 INR 1.01 Protein C 17 Protein S 38
DPAGT1-CDG	c.1117C>G, p. Pro373Ala/ c.1197T>A, p.Tyr399X	6mo Death	H (–) S (–)	AST 102 ALT 104
MPI-CDG	c.1193T>C, p. Ile398Thr, hmz	2y	H (+) S (–)	AST 196 ALT 365 INR 1.05 Protein C 41.4 Protein S 52.4 Ceruloplasmin 0,3 Liver biopsy–mild focal foamy degeneration of hepatocytes, without steatosis.
		4y	H (–) S (–)	On mannose supplementation therapy AST 41 ALT 70 AT 50
		9y	H (–) S (–)	On mannose supplementation therapy AST 24 ALT 21 INR 1,01 AT 76 Protein C 110 Protein S 124

(Continued)

TABLE 1 | Continued

CDG/CDDG	Mutation and protein change	Age at first presentation and during follow-up	H/S	Laboratory analyses Liver biopsy (if performed) Other features
MPI-CDG	c.1193T>C, p. Ile398Thr, hmz	12mo	H (+) S (–)	AST 168 ALT 355 ATIII 50 Protein C 52 Protein S 50 Ceruloplasmin 0.24
				Liver biopsy–Mild inflammatory infiltrates, mixed macro- and microvesicular steatosis of hepatocytes, foamy degeneration of hepatocytes.
		2y	H (+) S (–)	On mannose supplementation therapy AST 45 ALT 39
		14y 5mo	H (–) S (–)	On mannose supplementation therapy AST 21 ALT 19 AT 86 Protein C 81 Protein S 105
MPI-CDG	c.656G>A, p.Arg219Glu/ c.748G>A, p.Gly250Ser	12mo	H (+) S (–)	AST 77 ALT 60 AT 48,9 Ceruloplasmin 0.34
		4y 5mo	H (–) S (–)	Protein C 63,5 Protein S 60 AT 69
PGM1-CDG	c.988G>C, p.Gly330Arg/ c.1129G>A, p.Glu377Lys	4y	H (+) S (–)	AST 443 ALT 128
				Liver biopsy–fibrous thin strands between portal tracts, mild inflammatory infiltrates, mixed macro- and microvesicular steatosis of hepatocytes, foamy degeneration of hepatocytes.
		10y	H (+) S (–)	AST 269 ALT145 INR 1.02 Ceruloplasmin 0.16
		18y	H (+) S (–)	On galactose supplementation therapy AST 73 ALT 39 INR 1.14 AT 61
SRD5A3-CDG	c.292_293del p.Leu98ValfsX121/ c.292_293del p.Leu98ValfsX121	4mo	H (–) S (–)	AST 167 ALT 186 INR 1.24 Protein C 17 Protein S 38 AT 53
		4y 4mo	H (–) S (–)	AST 44 ALT 54 INR, GGTP—normal
SRD5A3-CDG	c.292_293del p.Leu98ValfsX121/ c.292_293del p.Leu98ValfsX121	6mo	H (–) S (–)	AST 214 ALT 291 INR 1.04 Protein C 34 Protein S 51 AT 39
		7y 8mo	H (–) S (–)	AST 18 ALT 13 INR 1.04 GGTP 30 Protein C 40 Protein S 47 AT 53
SRD5A3-CDG	c.424C>T, p.Arg142X/ c.424C>T, p.Arg142X	4mo	H (–) S (–)	ALT 70 AST 55 INR 1.15 GGTP 30 AT 18.3
		9y	H (–) S (–)	ALT 26 AST 26 INR, GGTP—normal
SRD5A3-CDG	c.424C>T, p.Arg142X/ c.489C>A, p.Tyr163X	1y 1mo	H (–) S (–)	ALT 114 AST 82 INR 1.03 GGTP 24 AT 45 Protein C 40 Protein S 47 Ceruloplasmin 28
				Liver biopsy–Mild inflammatory infiltrates, mixed macro- and microvesicular steatosis of hepatocytes, foamy cell degeneration of hepatocytes
		11y	H (–) S (–)	AST 51 ALT 58 INR, GGTP—normal
		17y 5mo	H (–) S (–)	AST 25 ALT 24 INR, GGTP—normal

(Continued)

TABLE 1 | Continued

CDG/CDDG	Mutation and protein change	Age at first presentation and during follow-up	H/S	Laboratory analyses Liver biopsy (if performed) Other features
PMM2-CDG	c.155T>G, p.Val52Gly/ c.640-23A>G, p.?	6mo	H (+) S (–)	AST 20 ALT 14
		8y	H (–) S (–)	AST 26 ALT 16 INR 0,95 AT 58 Protein C 113,6 Protein S 48
PMM2-CDG	c.422G>A, p.Arg141His/ c.691G>A, p.Val231Met	3mo	H (+) S (–)	AST 150 ALT 85 GGTP 25 INR 1.02
		9mo	H (+) S (–)	AST 90 ALT 22 GGTP 17 INR 1.00
		16y	H (–) S (–)	AST 25 ALT 10 GGTP 12 INR 0.99
PMM2-CDG	c.169G>A, p.Gly57Arg/ c.422G>A, p.Arg141His	5mo	H (+) S (–)	ALT 122 AST 149 GGTP 36 INR 1.02 Protein C 18 Protein S 53 AT 28
PMM2-CDG	c.422G>A, p.Arg141His/ c.484C>T, p.Arg162Trp	8y	H (–) S (–)	AST 26 ALT 13 GGTP 25 INR 1.00 Protein C 68 Protein S 62 AT 89 Ceruloplasmin 0,23
		16y	H (–) S (–)	ALT 17 AST 21 GGTP 15 INR 1.05 Protein C 75 Protein S 65 AT 82
PMM2-CDG	c.357C>A, p.Phe119Leu/ c.422G>A, p.Arg141His	4mo	H (+) S (–)	AST 210 ALT 146 GGTP 40 INR 1.04
		6mo	H (–) S (–)	AST 262 ALT 494 GGTP 32 INR 0.99
		6y	H (–) S (–)	AST 26 ALT 38 GGTP 23 INR 1.12
PMM2-CDG	c.24delC, p.C9AfsX27/ c.385G>A, p.Val129Met	Prenatal - NIHF		
		1mo	H (+) S (–)	AST 100 ALT 76 GGTP INR 0.99
		9mo death	H (+) S (–)	AST 110 ALT 120
PMM2-CDG	c.24delC, p.C9AfsX27/ c.691G>A, p.Val231Met	2mo death	H (+) S (–)	AST 100 ALT 114 INR 1.74
				Post mortem examination—liver cirrhosis, mixed macro- and microvesicular steatosis, cholestasis
PMM2-CDG	c.691G>A, p.Val231Met/ c.640-15479C>T (deep intronic splice site mutation)	2mo	H (+) S (–)	AST 320 ALT 500 INR 1.1 GGTP 20
		3 mo—thromobotic event		
		5mo	H (+) S (–)	ALT 326 AST INR, GGTP—normal
PMM2-CDG	c.422G>A, p.Arg141His/ c.691G>A, p.Val231Met	Prenatal – NIHF		
		2y	H (+) S (–)	AST 149 ALT 134 INR, GGTP—normal
PMM2-CDG	c.710C>G, p.Thr237Arg/ c.691G>A, p.Val231Met	2mo	H (+) S (–)	AST 58 ALT 45 INR 0.91 GGTP normal Alb 23 PLT 94 AT 15
		9mo	H (+) S (–)	AST 82 ALT 76 Alb 35 INR 1,25 AT 35
NGLY1-CDDG	c.1789+1G>A, p.?/ c.1063T>C, p.?	3y	H (–) S (–)	ALT 150 AST 125 GGTP 30 INR 1.05

(Continued)

TABLE 1 | Continued

CDG/CDDG	Mutation and protein change	Age at first presentation and during follow-up	H/S	Laboratory analyses Liver biopsy (if performed) Other features
				Liver biopsy–micro- as well as macrovesicular steatosis, minimal lobular fibrosis, amorphous periodic acid-Schiff staining positive diastases-digested material in the cytoplasm.
		7y	H (–) S (–)	ALT 28 AST 40 GGTP 30 INR 1.02
NGLY1-CDDG	c.250G>T, p.Glu84X/ c.1201A>T, p.Arg401X	1y 5mo	H (–) S (–)	ALT 126 AST 142 INR 1.07 GGTP 88

CDG, congenital disorder of glycosylation; CDDG, congenital disorder of deglycosylation; H, hepatomegaly; S, splenomegaly; "+", present; "–" absent; mo, months; y, years; AST, aspartate aminotransferase; ALT, alanine aminotransferase; INR, internal normalized ratio; GGTP, gamma-glutamyltranspeptidase; AT, antithrombin; NIHF, non-immune hydrops fetalis; hmz, homozygote.

Histological Phenotype

A liver biopsy was performed in five persons, including two with MPI-CDG, one with SRD5A3-CDG, one with PGM1-CDG, and one with NGLY1-CDDG. In one PMM2-CDG patient, the histopathological analysis comprised liver autopsy samples. Detailed histopathological studies were recently published (21, 23).

The foamy degeneration of hepatocytes and liver steatosis (micro- as well as macro-vesicular) were observed in 4 out of 5 CDG cases. In two of them, liver fibrosis was also found, including stage 4 (cirrhosis in the PMM2-CDG patient) and stage 2 (in the PGM1-CDG patient) according to the Batts and Ludwig classification, respectively. One of them (PMM2-CDG) also suffered from cholestasis with rosette formation around bile plugs. In two patients (SRD5A3-CDG and PGM1-CDG), apart from steatosis, mild inflammatory infiltrates were observed. There was no correlation between the person's age and histopathological features.

In the NGLY1-CDDG patient, the liver biopsy revealed moderate micro- and macro-vesicular steatosis as well as minimal lobular fibrosis. An amorphous periodic acid-Schiff-positive material digested by diastase was present in the cytoplasm.

Treatment

Four patients underwent specific monosaccharide supplementation therapy for CDG; PGM1-CDG patients were treated with oral galactose, while MPI-CDG patients with oral mannose. The exact data were recently published (20).

In the case of MPI-CDG patients, the clinical and biochemical features improved after the administration of mannose (normalization of serum transaminases, serum transferrin isoform values close to the reference range).

In the PGM1-CDG patient, the final diagnosis was established at the age of 10 years but the galactose supplementation did not start until the age of 16 years. Serum transferrin isoforms (but not serum transaminases) improved after galactose supplementation.

DISCUSSION

Liver involvement (disease) is observed in about one-third of inherited metabolic disorders such as CDG. It is unique due to the fact that the liver is one of the main areas of N-glycosylation in the body and most of serum glycoproteins are synthesized by liver hepatocytes (1–3).

Marques-da-Silva et al. (7) published a systematic review of the literature concerning liver involvement in CDG. The authors classified CDG based on liver involvement into two main groups: one with predominant/isolated liver involvement (MPI-CDG, CCDC115-CDG, TMEM199-CDG, ATP6AP1-CDG) and the other associated with liver disease (PMM2-CDG, ALG1-CDG, ALG3-CDG, ALG8-CDG, ALG9-CDG, PGM1-CDG).

Based on the results of our study and the literature review, we would like to propose another categorization/statement. In the great majority of CDG, the liver disease is not clinically significant; it manifests itself with hepatomegaly (less often) and mildly elevated serum transaminases (more often) in early infancy/childhood, which normalizes later in life. However, in the case of severe phenotypes (sometimes proceeded by non-immune hydrops fetalis) leading to early death, severe liver involvement is observed as part of multiple organ failure.

There is also a group of CDG, including MPI-CDG, CCDC115-CDG and TMEM199-CDG, in which the disease is mainly expressed in the liver (no neurological manifestation).

From the histological point of view, there is no typical pattern for liver disease in CDG as well as no correlation with the person's age. The most common histopathological finding in our cohort of CDG patients was the presence of liver steatosis. However, liver fibrosis, or even cirrhosis, was reported in PMM2-CDG, TMEM199-CDG, and NGLY1-CDDG.

As far as PMM2-CDG is concerned, liver involvement may occur as two distinct phenotypes. The first one comprises a severe neonatal/infantile liver failure (sometimes proceeded by non-immune hydrops fetalis) associated with an early-onset neurovisceral disease (9, 26–31). The histological examination usually shows signs of fibrosis or even cirrhosis (cholestasis and steatosis, as well) (26–31). The histopathological analysis of the liver in PMM2-CDG patients with neurological and multivisceral form, reported by De Lonlay et al., revealed fibrosis in all (4) patients with cirrhosis in of them (27). Portal fibrosis was also observed based on the histopathological evaluation of the liver in the patient reported by Aronica et al., who died at 1 month of age (28).

This was also clearly showed in our study on the example of one PMM2-CDG patient, who succumbed to multiple organ failure at 2 months of age. Liver autopsy samples revealed cirrhosis, mixed macro- and microvesicular steatosis (75% of hepatocytes), and cholestasis with rosette formation around bile plugs. It is interesting to note that no biochemical features of cholestasis were observed (normal GGT activity, mildly elevated serum total bilirubin concentration with normal serum direct bilirubin concentration).

The latter phenotype constitutes a non-progressive neurological disease with a mildly expressed liver disease in the form of hepatomegaly with elevated serum transaminases, which often improves with age, as observed in 9/10 PMM2-CDG patients (9, 10, 31). This is also consistent with the findings reported in other cohorts. Over time, the liver phenotype has a similar pattern to the neurological disease, which does not progress but even improves. We may only speculate about the cellular mechanisms of liver regeneration/compensation in the course of the disease.

In the study carried out by Witter et al. on 75 patients (61 patients with longitudinal follow-up data), a several-fold elevation of serum transaminases in infancy/childhood with their normalization during the follow-up was observed (10). Liver biopsies were rarely performed, but they usually showed liver steatosis (32–34).

In the case of CDG with the primary neurological phenotype (neurodevelopmental disorders), including ALG1-CDG, ALG3-CDG, ALG13-CDG, and DPAGT1-CDG, liver is affected in a minority of patients (7, 35–41). However, in the case of severe phenotypes (sometimes proceeded by non-immune hydrops fetalis) leading to early death, liver involvement is more commonly observed as part of multiple organ failure.

The liver autopsy conducted in the patient with ALG3-CDG, reported by Sun et al., who died at 19 days of life, showed bile duct plate malformations and moderate to severe steatosis (35).

MPI-CDG is special among others CDG due to the fact that it is mainly expressed in the liver (no neurological disease) and that it may be treated with the oral administration of mannose (42). Hepatomegaly is the most common clinical sign, sometimes associated with splenomegaly as the cause of the development of portal hypertension (42–48). So far, only one patient required liver transplantation due to chronic liver disease with the development of hepatopulmonary syndrome (43). The elevation of serum transaminases is a common abnormality in MPI-CDG, but GGT and serum bilirubin concentrations are often normal. Liver biopsy usually showed liver steatosis and fibrosis (12, 42–48). Congenital hepatic fibrosis (CHF) and ductal plate malformations were also depicted as distinct pathological liver biopsy findings for MPI-CDG (42–48). In the study of Damen et al., it was also reported that CHF may be the only sign of MPI-CDG for many years (12).

The administration of mannose improves the clinical and biochemical outcome (including serum transferrin isoforms); however, patients can still develop progressive liver fibrosis (42, 43, 45, 48).

As far as PGM1-CDG is concerned, liver involvement is observed in the multisystem phenotype (including congenital malformations, cardiomyopathy, variable endocrine and hematological abnormalities and no neurological disease); it has not been described in the muscular form of PGM1-CDG (7, 9, 14–16). Like in other CDG subtypes, elevated serum transaminases were observed in the majority of patients. There are some reports of liver biopsy findings, including steatosis, cholestasis and fibrosis; cirrhosis, however, was not reported (14–16, 49). In the study of Tegtmeyer et al., liver biopsy was performed in five patients and showed signs of steatosis, cholestasis, and fibrosis (16). An increased amount of glycogen was observed in two of these persons, and in one of them, electron microscopy revealed glycogen deposits in hepatocytes. In our previous study on histological and ultrastructural liver involvement in various CDG, significant ultrastructural abnormalities in hepatocytes with anomalies of the endoplasmic reticulum and mitochondria, and the accumulation of glycogen and lamellar deposits in cytoplasm were found in in the PGM1-CDG patient (21).

In the recently published paper on liver manifestations in 39 CDG patients, Starosta et al. found that 48.6% of those persons had elevated values of alanine aminotransferase and 70.3% of them had elevated values of aspartate aminotransferase (13). These parameters mostly increased during the first 5 years of life in most types of CDG (apart from ALG8-CDG, CCDC115-CDG, MPI-CDG, PGM1-CDG, and TMEM165-CDG patients), but they improved significantly afterwards. In our study, we observed a higher proportion of persons with an elevated level of serum transaminases. However, according to Starosta et al. and other authors, it normalized spontaneously in the majority of patients.

Cholestasis seems to be not a characteristic/typical feature of CDG; it was mostly reported in histopathological liver studies (there are no detailed data on the serum bilirubin concentration and gamma-glutamyl transferase activity). In the study of Starosta et al., 4 out of 39 patients had elevated levels of gamma-glutamyl transferase (GGT), including 3 PMM2-CDG cases and 1 PGM1-CDG case. In our study, there were no patients with elevated GGT values, and only 1 PMM2-CDG person was diagnosed with hyperbilirubinemia (normal serum direct bilirubin) with cholestasis in the liver biopsy specimens.

Coagulation abnormalities require a special attention in CDG. They typically affect both procoagulant and anticoagulant factors, in the case of which antithrombin deficiency, protein C and S deficiency, and factor XI deficiency were mainly observed, respectively (1–3, 50–53). Elevated serum transaminases observed in the majority of our CDG patients were associated with the presence of coagulation disorders, including protein C, protein S, and antithrombin deficiency. Similar observations were reported by Starosta et al. (13). However, only two patients developed thrombotic events.

In some of our CDG patients who had an elevated level of serum transaminases, a low level of ceruloplasmin and a lower serum copper concentration (less often), Wilson disease was suspected. Disturbances in copper metabolism in persons suffering from CDG type II, especially V-ATPase deficiencies, were reported in the literature (17–19, 54–56). The accumulation

of copper in the liver was described in the case of both TMEM199-CDG and CCDC115-CDG (17–19). Serum copper was low in 10 out of 11 patients with ATP6AP1-CDG reported by Jansen et al. (54). The mechanism of this phenomenon is not known but a partial loss of either or both of the copper transporting proteins ATP7A and ATP7B was raised (18).

Since the first report by Need et al., a total number of 34 patients with a congenital disorder of N-linked deglycosylation have been reported (57). The pattern of liver disease in NGLY1-CDDG seems to be similar to that in CDG. Elevated serum transaminases were reported in the majority of NGLY1-CDDG patients in early childhood and normalized in some of them (4, 5, 57–61). Rios-Flores et al. have recently reported on a 5-year-old patient with NGLY1-CDDG who presented a severe episode of acute liver failure (ALF) (62). This was the the first report of ALF in patients with NGLY1-CDDG. The authors claimed that ALF was a consequence of an impaired mitochondrial function. This observation was supported by previous reports of mitochondrial respiratory chain dysfunction in patients with NGLY1 deficiency (63).

In our recently published paper on NGLY1-CDDG, we suggested that every patient with developmental disability associated with a hyperkinetic movement disorder and alacrimia/hypolacrima should be tested for NGLY1-CDDG; an increase of serum transaminases and of the abovementioned biomarkers are in favor of this diagnosis (58). However, a detailed characteristics on liver involvement in NGLY1-CDDG is impossible due to insufficient data due to lack of follow-up in the majority of cases.

Liver biopsy have been reported in some patients. Among them, liver steatosis, fibrosis and also cirrhosis (two cases) have been described (59–61). One of the patients described by Lam et al. underwent orthotopic liver transplantation at 21 months of age for liver cirrhosis and presumed hepatocellular carcinoma. In some patients, including one of our NGLY1-CDDG patients, liver biopsy revealed a cytoplasmic storage of amorphous material (with staining properties similar to glycogen) or vacuolization in hepatocytes consistent with the storage (5). In our latest article, we put forward a hypothesis that the presence of cytoplasmic storage of amorphous periodic acid-Schiff positive material digested by diastases reflects the storage of misfolded and probably not degraded N-glycosylated proteins (21).

CONCLUSIONS

It is necessary to conduct a long-term follow-up of liver disease in CDG to obtain comprehensive data.

If CDG is suspected, the normalization of serum transaminases, which was observed in the majority of patients during the long-term observation, could diminish the suspicion of CDG.

Cholestasis was not observed as a characteristic feature of CDG.

DATA AVAILABILITY STATEMENT

The original contributions generated for this study are included in the article/supplementary material, further inquiries can be directed to the corresponding author/s.

ETHICS STATEMENT

The studies involving human participants were reviewed and approved by Ethics Committee of Children's Memorial Health Institute. Written informed consent to participate in this study was provided by the participants' legal guardian/next of kin. Written informed consent was not obtained from the individual(s) for the publication of any potentially identifiable images or data included in this article.

AUTHOR CONTRIBUTIONS

PL and AT-S: project administration and writing—review & editing. AT-S: supervision. PL, AB, PS, and AT-S: investigation. PL: writing—original draft. All authors contributed to the article and approved the submitted version.

FUNDING

This study was funded by the Children's Memorial Health Institute intramural grant S190/2020.

REFERENCES

1. Francisco R, Marques-da-Silva D, Brasil S, Pascoal C, Dos Reis Ferreira V, Morava E, et al. The challenge of CDG diagnosis. *Mol Genet Metab.* (2019) 126:1–5. doi: 10.1016/j.ymgme.2018.11.003
2. Péanne R, de Lonlay P, Foulquier F, Kornak U, Lefeber DJ, Morava E, et al. Congenital disorders of glycosylation (CDG): Quo vadis? *Eur J Med Genet.* (2018) 61:643–63. doi: 10.1016/j.ejmg.2017.10.012
3. Jaeken J, Peanne R. What is new in CDG? *J Inherit Metab Dis.* (2017) 40:569–86. doi: 10.1007/s10545-017-0050-6
4. Lam C, Wolfe L, Need A, Shashi V, Enns G. NGLY1-related congenital disorder of deglycosylation. In: Adam MP, Ardinger HH, Pagon RA, Wallace SE, Bean LJH, Stephens K, et al., editors. *GeneReviews®*. Seattle (WA): University of Washington, Seattle (1993–2019).
5. Enns GM, Shashi V, Bainbridge M, Gambello MJ, Zahir FR, Bast T, et al. Mutations in NGLY1 cause an inherited disorder of the endoplasmic reticulum-associated degradation pathway. *Genet Med.* (2014) 16:751–8. doi: 10.1038/gim.2014.61
6. Suzuki T, Huang C, Fujihira H. The cytoplasmic peptide:N-glycanase (NGLY1) - Structure, expression and cellular functions. *Gene.* (2016) 577:1–7. doi: 10.1016/j.gene.2015.11.021
7. Marques-da-Silva D, Dos Reis Ferreira V, Monticelli M, Janeiro P, Videira PA, Witters P, et al. Liver involvement in congenital disorders of glycosylation (CDG). A systematic review of the literature. *J Inherit Metab Dis.* (2017) 40:195–207. doi: 10.1007/s10545-016-0012-4
8. Makhamreh MM, Cottingham N, Ferreira CR, Berger S, Al-Kouatly HB. Nonimmune hydrops fetalis and congenital disorders of glycosylation: a systematic literature review. *J Inherit Metab Dis.* (2020) 43:223–33. doi: 10.1002/jimd.12162

9. Altassan R, Péanne R, Jaeken J, Barone R, Bidet M, Borgel D, et al. International clinical guidelines for the management of phosphomannomutase 2-congenital disorders of glycosylation: diagnosis, treatment and follow up. *J Inherit Metab Dis.* (2019) 42:5–28. doi: 10.1002/jimd.12082
10. Witters P, Honzik T, Bauchart E, Altassan R, Pascreau T, Bruneel A, et al. Long-term follow-up in PMM2-CDG: are we ready to start treatment trials? *Genet Med.* (2019) 21:1181–88. doi: 10.1038/s41436-018-0301-4
11. Grünewald S, Matthijs G, Jaeken J. Congenital disorders of glycosylation: a review. *Pediatr Res.* (2002) 52:618–24. doi: 10.1203/00006450-200211000-00003
12. Damen G, de Klerk H, Huijmans J, den Hollander J, Sinaasappel M. Gastrointestinal and other clinical manifestations in 17 children with congenital disorders of glycosylation type Ia, Ib, and Ic. *J Pediatr Gastroenterol Nutr.* (2004) 38:282–87. doi: 10.1097/00005176-200403000-00010
13. Starosta RT, Boyer S, Tahata S, Raymond K, Lee HE, Wolfe LA, et al. Liver manifestations in a cohort of 39 patients with congenital disorders of glycosylation: pin-pointing the characteristics of liver injury and proposing recommendations for follow-up. *Orphanet J Rare Dis.* (2021) 16:20. doi: 10.1186/s13023-020-01630-2
14. Wong SY, Gadomski T, van Scherpenzeel M, Honzik T, Hansikova H, Holmefjord KSB, et al. Oral D-galactose supplementation in PGM1-CDG. *Genet Med.* (2017) 19:1226–35. doi: 10.1038/gim.2017.41
15. Wong SY, Beamer LJ, Gadomski T, Honzik T, Mohamed M, Wortmann SB, et al. Defining the phenotype and assessing severity in phosphoglucomutase-1 deficiency. *J Pediatr.* (2016) 175:130–6. doi: 10.1016/j.jpeds.2016.04.021
16. Tegtmeyer LC, Rust S, van Scherpenzeel M, Ng BG, Losfeld ME, Timal S, et al. Multiple phenotypes in phosphoglucomutase 1 deficiency. *N Engl J Med.* (2014) 370:533–42. doi: 10.1056/NEJMc1403446
17. Girard M, Poujois A, Fabre M, Lacaille F, Debray D, Rio M, et al. CCDC115-CDG: a new rare and misleading inherited cause of liver disease. *Mol Genet Metab.* (2018) 124:228–35. doi: 10.1016/j.ymgme.2018.05.002
18. Vajro P, Zielinska K, Ng BG, Maccarana M, Bengtson P, Poeta M, et al. Three unreported cases of TMEM199-CDG, a rare genetic liver disease with abnormal glycosylation. *Orphanet J Rare Dis.* (2018) 13:4. doi: 10.1186/s13023-017-0757-3
19. Jansen JC, Timal S, van Scherpenzeel M, Michelakakis H, Vicogne D, Ashikov A, et al. TMEM199 deficiency is a disorder of Golgi homeostasis characterized by elevated aminotransferases, alkaline phosphatase, and cholesterol and abnormal glycosylation. *Am J Hum Genet.* (2016) 98:322–30. doi: 10.1016/j.ajhg.2015.12.011
20. Bogdańska A, Lipiński P, Szymańska-Rozek P, Jezela-Stanek A, Rokicki D, Socha P, et al. Clinical, biochemical and molecular phenotype of congenital disorders of glycosylation: long-term follow-up. *Orphanet J Rare Dis.* (2021) 16:17. doi: 10.1186/s13023-020-01657-5
21. Lipiński P, Cielecka-Kuszyk J, Czarnowska E, Bogdańska A, Socha P, Tylki-Szymańska A. Congenital disorders of glycosylation in children - histopathological and ultrastructural changes in the liver. *Pediatr Neonatol.* (2021) 62:278–83. doi: 10.1016/j.pedneo.2021.01.017
22. Lipiński P, Cielecka-Kuszyk J, Socha P, Tylki-Szymańska A. Liver involvement in NGLY1 congenital disorder of deglycosylation. *Pol J Pathol.* (2020) 71:66–68. doi: 10.5114/pjp.2020.92994
23. Fawaz R, Baumann U, Ekong U, Fischler B, Hadzic N, Mack CL, et al. Guideline for the evaluation of cholestatic jaundice in infants: joint recommendations of the North American society for pediatric gastroenterology, hepatology, and nutrition and the European society for pediatric gastroenterology, hepatology, and nutrition. *J Pediatr Gastroenterol Nutr.* (2017) 64:154–68. doi: 10.1097/MPG.0000000000001334
24. Cabrera-Abreu JC, Green A. Gamma-glutamyltransferase: value of its measurement in paediatrics. *Ann Clin Biochem.* (2002) 39:22–5. doi: 10.1258/0004563021901685
25. Schwimmer JB, Dunn W, Norman GJ, Pardee PE, Middleton MS, Kerkar N, et al. SAFETY study: alanine aminotransferase cutoff values are set too high for reliable detection of pediatric chronic liver disease. *Gastroenterology.* (2010) 138:1357–64. doi: 10.1053/j.gastro.2009.12.052
26. Wurm D, Hänsgen A, Kim YJ, Lindinger A, Baghai A, Gortner L. Early fatal course in siblings with CDG-Ia (caused by two novel mutations in the PMM2 gene): clinical, molecular and autopsy findings. *Eur J Pediatr.* (2007) 166:377–78. doi: 10.1007/s00431-006-0240-y
27. de Lonlay P, Seta N, Barrot S, Chabrol B, Drouin V, Gabriel BM, et al. A broad spectrum of clinical presentations in congenital disorders of glycosylation I: a series of 26 cases. *J Med Genet.* (2001) 38:14–9. doi: 10.1136/jmg.38.1.14
28. Aronica E, van Kempen AA, van der Heide M, Poll-The BT, van Slooten HJ, Troost D, et al. Congenital disorder of glycosylation type Ia: a clinicopathological report of a newborn infant with cerebellar pathology. *Acta Neuropathol.* (2005) 109:433–42. doi: 10.1007/s00401-004-0975-3
29. Edwards M, McKenzie F, O'callaghan S, Somerset D, Woodford P, Spilsbury J, et al. Prenatal diagnosis of congenital disorder of glycosylation type Ia (CDG-Ia) by cordocentesis and transferrin isoelectric focusing of serum of a 27-week fetus with non-immune hydrops. *Prenat Diagn.* (2006) 26:985–88. doi: 10.1002/pd.1543
30. Grünewald S. The clinical spectrum of phosphomannomutase 2 deficiency (CDG-Ia). *Biochim Biophys Acta.* (2009) 1792:827–34. doi: 10.1016/j.bbadis.2009.01.003
31. Schiff M, Roda C, Monin ML, Arion A, Barth M, Bednarek N, et al. Clinical, laboratory and molecular findings and long-term follow-up data in 96 French patients with PMM2-CDG (phosphomannomutase 2-congenital disorder of glycosylation) and review of the literature. *J Med Genet.* (2017) 54:843–51. doi: 10.1136/jmedgenet-2017-104903
32. Serrano M, de Diego V, Muchart J, Cuadras D, Felipe A, Macaya A, et al. Phosphomannomutase deficiency (PMM2-CDG): ataxia and cerebellar assessment. *Orphanet J Rare Dis.* (2015) 10:138. doi: 10.1186/s13023-015-0358-y
33. Bortot B, Cosentini D, Faletra F, Biffi S, De Martino E, Carrozzi M, et al. PMM2-CDG: phenotype and genotype in four affected family members. *Gene.* (2013) 531:506–9. doi: 10.1016/j.gene.2013.07.083
34. Al-Maawali AA, Miller E, Schulze A, Yoon G, Blaser SI. Subcutaneous fat pads on body MRI-an early sign of congenital disorder of glycosylation PMM2-CDG (CDG1a). *Pediatr Radiol.* (2014) 44:222–25. doi: 10.1007/s00247-013-2782-2
35. Sun L, Eklund EA, Chung WK, Wang C, Cohen J, Freeze HH. Congenital disorder of glycosylation id presenting with hyperinsulinemic hypoglycemia and islet cell hyperplasia. *J Clin Endocrinol Metab.* (2005) 90:4371–75. doi: 10.1210/jc.2005-0250
36. Lepais L, Cheillan D, Frachon SC, Hays S, Matthijs G, Panagiotakaki E, et al. ALG3-CDG: Report of two siblings with antenatal features carrying homozygous p.Gly96Arg mutation. *Am J Med Genet A.* (2015) 167A:2748–54. doi: 10.1002/ajmg.a.37232
37. Schollen E, Frank CG, Keldermans L, Reyntjens R, Grubenmann CE, Clayton PT, et al. Clinical and molecular features of three patients with congenital disorders of glycosylation type Ih (CDG-Ih) (ALG8 deficiency). *J Med Genet.* (2004) 41:550–6. doi: 10.1136/jmg.2003.016923
38. Vesela K, Honzik T, Hansikova H, Haeuptle MA, Semberova J, Stranak Z, et al. A new case of ALG8 deficiency (CDG Ih). *J Inherit Metab Dis.* (2009) 32(Suppl. 1):259–64. doi: 10.1007/s10545-009-1203-z
39. Höck M, Wegleiter K, Ralser E, Kiechl-Kohlendorfer U, Scholl-Bürgi S, Fauth C, et al. ALG8-CDG: novel patients and review of the literature. *Orphanet J Rare Dis.* (2015) 10:73. doi: 10.1186/s13023-015-0289-7
40. Eklund EA, Sun L, Westphal V, Northrop JL, Freeze HH, Scaglia F. Congenital disorder of glycosylation (CDG)-Ih patient with a severe hepato-intestinal phenotype and evolving central nervous system pathology. *J Pediatr.* (2005) 147:847–50. doi: 10.1016/j.jpeds.2005.07.042
41. Ng BG, Eklund EA, Shiryaev SA, Dong YY, Abbott MA, Asteggiano C, et al. Predominant and novel de novo variants in 29 individuals with ALG13 deficiency: clinical description, biomarker status, biochemical analysis, and treatment suggestions. *J Inherit Metab Dis.* (2020) 43:1333–48. doi: 10.1002/jimd.12290
42. Cechová A, Altassan R, Borgel D, Bruneel A, Correia J, Girard M, et al. Consensus guideline for the diagnosis and management of mannose phosphate isomerase-congenital disorder of glycosylation. *J Inherit Metab Dis.* (2020) 43:671–93. doi: 10.1002/jimd.12241
43. Janssen MC, de Kleine RH, van den Berg AP, Heijdra Y, van Scherpenzeel M, Lefeber DJ, et al. Successful liver transplantation and long-term follow-up in a patient with MPI-CDG. *Pediatrics.* (2014) 134:e279–83. doi: 10.1542/peds.2013-2732

44. Liem YS, Bode L, Freeze HH, Leebeek FW, Zandbergen AA, Paul Wilson J. Using heparin therapy to reverse protein-losing enteropathy in a patient with CDG-Ib. *Nat Clin Pract Gastroenterol Hepatol.* (2008) 5:220–24. doi: 10.1038/ncpgasthep1061
45. Westphal V, Kjaergaard S, Davis JA, Peterson SM, Skovby F, Freeze HH. Genetic and metabolic analysis of the first adult with congenital disorder of glycosylation type Ib: long-term outcome and effects of mannose supplementation. *Mol Genet Metab.* (2001) 73:77–85. doi: 10.1006/mgme.2001.3161
46. Mention K, Lacaille F, Valayannopoulos V, Romano S, Kuster A, Cretz M, et al. Development of liver disease despite mannose treatment in two patients with CDG-Ib. *Mol Genet Metab.* (2008) 93:40–3. doi: 10.1016/j.ymgme.2007.08.126
47. de Koning TJ, Nikkels PG, Dorland L, Bekhof J, De Schrijver JE, van Hattum J, et al. Congenital hepatic fibrosis in 3 siblings with phosphomannose isomerase deficiency. *Virchows Arch.* (2000) 437:101–5. doi: 10.1007/s004280000185
48. Hendriksz CJ, McClean P, Henderson MJ, Keir DG, Worthington VC, Imtiaz F, et al. Successful treatment of carbohydrate deficient glycoprotein syndrome type 1b with oral mannose. *Arch Dis Child.* (2001) 85:339–40. doi: 10.1136/adc.85.4.339
49. Morava E. Galactose supplementation in phosphoglucomutase-1 deficiency; review and outlook for a novel treatable CDG. *Mol Genet Metab.* (2014) 112:275–79. doi: 10.1016/j.ymgme.2014.06.002
50. Linssen M, Mohamed M, Wevers RA, Lefeber DJ, Morava E. Thrombotic complications in patients with PMM2-CDG. *Mol Genet Metab.* (2013) 109:107–11. doi: 10.1016/j.ymgme.2013.02.006
51. Brucker WJ, Croteau SE, Prensner JR, Cullion K, Heeney MM, Lo J, et al. An emerging role for endothelial barrier support therapy for congenital disorders of glycosylation. *J Inherit Metab Dis.* (2020) 43:880–90. doi: 10.1002/jimd.12225
52. López-Gálvez R, de la Morena-Barrio ME, López-Lera A, Pathak M, Miñano A, Serrano M, et al. Factor XII in PMM2-CDG patients: role of N-glycosylation in the secretion and function of the first element of the contact pathway. *Orphanet J Rare Dis.* (2020) 15:280. doi: 10.1186/s13023-020-01564-9
53. Mühlhausen C, Henneke L, Schlotawa L, Behme D, Grüneberg M, Gärtner J, et al. Mannose phosphate isomerase deficiency-congenital disorder of glycosylation (MPI-CDG) with cerebral venous sinus thrombosis as first and only presenting symptom: a rare but treatable cause of thrombophilia. *JIMD Rep.* (2020) 55:38–43. doi: 10.1002/jmd2.12149
54. Socha P, Vajro P, Lefeber D, Adamowicz M, Tanner S. Search for rare liver diseases: the case of glycosylation defects mimicking Wilson Disease. *Clin Res Hepatol Gastroenterol.* (2014) 38:403–6. doi: 10.1016/j.clinre.2014.04.012
55. Jansen EJ, Timal S, Ryan M, Ashikov A, van Scherpenzeel M, Graham LA, et al. ATP6AP1 deficiency causes an immunodeficiency with hepatopathy, cognitive impairment and abnormal protein glycosylation. *Nat Commun.* (2016) 7:11600. doi: 10.1038/ncomms11600
56. Van Damme T, Gardeitchik T, Mohamed M, Guerrero-Castillo S, Freisinger P, Guillemyn B, et al. Mutations in ATP6V1E1 or ATP6V1A cause autosomal-recessive cutis laxa. *Am J Hum Genet.* (2017) 100:216–27. doi: 10.1016/j.ajhg.2016.12.010
57. Need AC, Shashi V, Hitomi Y, Schoch K, Shianna KV, McDonald MT, et al. Clinical application of exome sequencing in undiagnosed genetic conditions. *J Med Genet.* (2012) 49:353–61. doi: 10.1136/jmedgenet-2012-100819
58. Lipiński P, Bogdańska A, Rózdzyńska-Swiatkowska A, Wierzbicka-Rucińska A, Tylki-Szymańska A. NGLY1 deficiency: novel patient, review of the literature and diagnostic algorithm. *JIMD Rep.* (2020) 51:82–8. doi: 10.1002/jmd2.12086
59. Heeley J, Shinawi M. Multi-systemic involvement in NGLY1-related disorder caused by two novel mutations. *Am J Med Genet A.* (2015) 167A:816–20. doi: 10.1002/ajmg.a.36889
60. Lam C, Ferreira C, Krasnewich D, Toro C, Latham L, Zein WM, et al. Prospective phenotyping of NGLY1-CDDG, the first congenital disorder of deglycosylation. *Genet Med.* (2017) 19:160–8. doi: 10.1038/gim.2016.75
61. Caglayan AO, Comu S, Baranoski JF, Parman Y, Kaymakçalan H, Akgumus GT, et al. NGLY1 mutation causes neuromotor impairment, intellectual disability, and neuropathy. *Eur J Med Genet.* (2015) 58:39–43. doi: 10.1016/j.ejmg.2014.08.008
62. Rios-Flores IM, Bonal-Pérez MÁ, Castellanos-González A, Velez-Gómez E, Bertoli-Avella AM, Bobadilla-Morales L, et al. Acute liver failure in a male patient with NGLY1-congenital disorder of deglycosylation. *Eur J Med Genet.* (2020) 63:103952. doi: 10.1016/j.ejmg.2020.103952
63. Kong J, Peng M, Ostrovsky J, Kwon YJ, Oretsky O, McCormick EM, et al. Mitochondrial function requires NGLY1. *Mitochondrion.* (2018) 38:6–16. doi: 10.1016/j.mito.2017.07.008

Conflict of Interest: The authors declare that the research was conducted in the absence of any commercial or financial relationships that could be construed as a potential conflict of interest.

The handling Editor declared a past co-authorship with several of the authors AT-S, PL, and PS.

frontiers in Genetics

ORIGINAL RESEARCH
published: 03 August 2021
doi: 10.3389/fgene.2021.692479

Phenotype and Genotype Study of Chinese *POMT2*-Related α-Dystroglycanopathy

*Xiao-Yu Chen[1], Dan-Yu Song[1], Li Jiang[2], Dan-Dan Tan[1], Yi-Dan Liu[1], Jie-Yu Liu[1], Xing-Zhi Chang[1], Guo-Gang Xing[3], Tatsushi Toda[4] and Hui Xiong[1]**

[1] Department of Pediatrics, Peking University First Hospital, Beijing, China, [2] Department of Neurology, Children's Hospital of Chongqing Medical University, Chongqing, China, [3] Department of Neurobiology, School of Basic Medical Sciences, Peking University Health Science Center, Beijing, China, [4] Department of Neurology, Graduate School of Medicine, The University of Tokyo, Tokyo, Japan

Objective: Alpha-dystroglycanopathy (α-DGP) is a subtype of muscular dystrophy caused by defects in the posttranslational glycosylation of α-dystroglycan (α-DG). Our study aimed to summarize the clinical and genetic features of *POMT2*-related α-DGP in a cohort of patients in China.

Methods: Pedigrees, clinical data, and laboratory tests of patients diagnosed with *POMT2*-related α-DGP were analyzed retrospectively. The pathogenicity of variants in *POMT2* were predicted by bioinformatics software. The variants with uncertain significance were verified by further analysis.

Results: The 11 patients, comprising eight males and three females, were from nine non-consanguineous families. They exhibited different degrees of muscle weakness, ambulation, and intellectual impairment. Among them, three had a muscle-eye-brain disease (MEB)-like phenotype, five presented congenital muscular dystrophy with intellectual disability (CMD-ID), and three presented limb-girdle muscular dystrophy (LGMD). Overall, nine novel variants of *POMT2*, including two non-sense, one frameshift and six missense variants, were identified. The pathogenicity of two missense variants, c.1891G > C and c.874G > C, was uncertain based on bioinformatics software prediction. *In vitro* minigene analysis showed that c.1891G > C affects the splicing of *POMT2*. Immunofluorescence staining with the IIH6C4 antibody of muscle biopsy from the patient carrying the c.874G > C variant showed an apparent lack of expression.

Conclusion: This study summarizes the clinical and genetic characteristics of a cohort of *POMT2*-related α-DGP patients in China for the first time, expanding the mutational spectrum of the disease. Further study of the pathogenicity of some missense variants based on enzyme activity detection is needed.

Keywords: dystroglycanopathy, mannosyltransferase, *POMT2*, genotype, phenotype

OPEN ACCESS

Edited by:
Karolina Stepien, Salford Royal NHS Foundation Trust, United Kingdom

Reviewed by:
Enrique Lin Shiao, University of California, Berkeley, United States
Dmitry Vlodavets, Pirogov Russian National Research Medical University, Russia

***Correspondence:**
Hui Xiong
xh_bjbj@163.com;
xionghui03582@pkufh.com

Specialty section:
This article was submitted to Genetics of Common and Rare Diseases, a section of the journal Frontiers in Genetics

Received: *08 April 2021*
Accepted: *09 July 2021*
Published: *03 August 2021*

Citation:
Chen X-Y, Song D-Y, Jiang L, Tan D-D, Liu Y-D, Liu J-Y, Chang X-Z, Xing G-G, Toda T and Xiong H (2021) Phenotype and Genotype Study of Chinese POMT2-Related α-Dystroglycanopathy. Front. Genet. 12:692479. doi: 10.3389/fgene.2021.692479

INTRODUCTION

Alpha-dystroglycanopathy (α-DGP) is a subtype of congenital muscular dystrophy (CMD) with autosomal recessive inheritance. It is caused by defective O-mannosylglycosylation of α-dystroglycan (α-DG), which is required for binding to extracellular matrix ligands, such as laminins, neurexin, and perlecan. At least 18 pathogenic genes associated with α-DGP have

been identified to date (Endo, 2015). *POMT2*, which encodes protein O-mannosyltransferase 2 (POMT2), is one of the pathogenic genes of α-DGP. It catalyzes the initial step in the biosynthesis of the α-DG O-mannosylation glycan chain, transferring mannose to serine or threonine residues (Willer et al., 2002). α-DGP shows high clinical and genetic heterogeneity. The most severe phenotype of *POMT2*-related α-DGP is Walker-Warburg syndrome [WWS, (OMIM 236670)], with an onset of intrauterine or after birth. WWS manifests as progressive muscle weakness and severe brain and eye abnormalities, such as lissencephaly, hydrocephalus, severe cerebellar involvement, complete or partial absence of the corpus callosum, congenital cataracts, glaucoma, and microphthalmia. Most patients cannot obtain ambulation ability and die before 1–3 years of age (Cormand et al., 2001; van Reeuwijk et al., 2005). The second severe phenotype is muscle-eye-brain disease [MEB, (OMIM 253280)], with milder brain structural abnormalities than WWS, including pachygyria, polymicrogyria, cerebellar, and brainstem dysplasia. A small number of MEB patients can acquire the ability to walk alone, although most patients have language and intellectual disability (Diesen et al., 2004). The intermediate phenotype is congenital muscular dystrophy with intellectual disability [CMD-ID, (OMIM 613156)]. Patients with this phenotype often have obvious intellectual and cognitive impairment, but their brain structure can be normal or only shows microcephaly and mild cerebral white matter changes (Godfrey et al., 2007). The mildest type of the disease is limb-girdle muscular dystrophy (LGMD) type 2N [LGMD2N, (OMIM 613158)], which presents a late onset and mild muscle weakness (Saredi et al., 2014; Østergaard et al., 2018). In this study, we summarized the results of clinical and mutational analyses of 11 *POMT2*-related α-DGP patients.

MATERIALS AND METHODS

Patients and Clinical Data

This study [2015(916)] was approved by the Ethics Committee of the Peking University First Hospital. Written informed consent was obtained from the individuals and legal guardians for participation in the study as well as for the publication of any potentially identifiable images or data included in this article.

The inclusion criteria for α-DGP were described in our previous study (Song et al., 2020). In this study, patients with molecular genetic results indicating *POMT2* variants were enrolled, and patients diagnosed with other types of CMD or with other gene variants were excluded.

The patients' clinical symptoms, physical examination results, and laboratory and molecular genetic tests were analyzed retrospectively.

Molecular Genetic Testing

Genomic DNA was extracted from peripheral blood lymphocytes of the patients and their parents for whole exome sequencing (WES). Sequencing analysis was based on the reference sequence of *POMT2* (NM_013382.5), and the candidate variant was confirmed by Sanger sequencing in family members. We used some disease association databases, including the Human Gene Mutation Database (HGMD[1]), Leiden Open Variation Database (LOVD[2]), ClinVar database[3], and 1,000 Genomes[4] to identify pathogenic, clinically reported or novel mutations. If WES data revealed differences in the number of sequence reads between the patients and control samples, the change was considered to be a copy number variant (CNV), which was then confirmed by quantitative polymerase chain reaction (qPCR). The pathogenicity of novel or clinically unreported variants was predicted by using three kinds of bioinformatics software: MutationTaster[5], PolyPhen2[6], and Provean[7].

Muscle Biopsy and Immunofluorescence Staining

Open biopsy of the quadriceps or biceps brachii was performed, and the samples were fixed in isopentane precooled in liquid nitrogen. Routine histochemical staining was performed. Frozen sections (6 μm) from the muscle biopsy specimens were fixed with 4% paraformaldehyde at room temperature for 10 min. Non-specific binding was reduced by a 1-h incubation with 10% goat serum (Solarbio, China) in phosphate-buffered saline (PBS). The sections were then incubated at 4°C overnight with α-DG glycosylation antibody, IIH6C4 (Millipore, United States, 1:200), and β-DG antibody (Abcam, United Kingdom, 1:200), washed three times with PBS and then incubated with a goat anti-mouse fluorescent antibody (Life Technologies Corporation, United States, 1:500) at room temperature for 1 h. Immunofluorescence staining was observed by using an Olympus Fluoview FV10i (Olympus, Japan).

Minigene Construction and Splicing Analysis

A hybrid minigene splicing assay *in vitro* was employed to evaluate the transcriptional effect of the variant on splicing. Wild-type and mutant minigene constructs comprising a genomic fragment spanning exon 17 to the exon 20 of *POMT2* were synthesized and cloned into the pcDNA 3.1 plasmid (Ge et al., 2019); the mutant minigene contains the variant c.1891G > C. Wild-type and mutant minigenes were transiently transfected into HEK-293 cells using Lipofectamine 3000 transfection reagent (Thermo Fisher Scientific, United States), and the cells were then incubated for 72 h before isolation of total RNA using TRIzol. cDNA was synthesized using 1 μg of RNA with a reverse transcription system kit (Promega, A3500, United States) and specific primers, including primers upstream in exon 17 (forward 5′-GGTCAATGACACAGATTTCCGA-3′) and downstream in exon 20 (reverse 5′-TAGGCAGTTCCCAGGAGCA-3′).

[1]http://www.hgmd.cf.ac.uk/ac/index.php
[2]http://www.dmd.nl/
[3]https://www.ncbi.nlm.nih.gov/clinvar/
[4]http://www.1000genomes.org/
[5]http://www.mutationtaster.org/
[6]http://genetics.bwh.harvard.edu/pph2/
[7]http://provean.jcvi.org/

RESULTS

Clinical Characteristics

A total of 11 *POMT2*-related α-DGP patients diagnosed by WES were enrolled. They come from non-consanguineous families, including eight males and three females. Among them, patients 4a and 5a were siblings, as were patients 7b and 8b. The patients were divided into three groups based on their clinical manifestations: MEB-like, CMD-ID, and LGMD2N. The clinical characteristics of these 11 patients were summarized in **Table 1**.

The MEB-like group includes patients 4a, 5a, and 10. Their age of onset was between 3 and 8 months old, manifesting as psychomotor developmental delay, microcephaly, and joint contractures. Their maximum mobile ability was only supported or unsupported sitting. Patients 4a and 5a were only able to speak simple words; patient 10 could pronounce two syllables unconsciously. In addition, the patients were only able to understand simple instructions. All of them had no abnormal history of birth. Physical examination revealed obvious myopathy appearances, small head circumferences, and prominently decreased muscle strength in the proximal limbs. In patient 4a, multiple joint contractures including interphalangeal, knee, and ankle joints and severe scoliosis occurred from 4 years old. Patient 5a presented with pseudohypertrophy of the forearm and gastrocnemius and knee joint contracture at the age of 5 years. Patient 10 showed a high palate arch and knee joint contracture at the age of 2 years. However, eye involvement in three children was not obvious, with only patient 10 exhibiting esotropia. Their serum creatine kinase (CK) levels were moderately elevated and fluctuated between 3,609 and 5,200 IU/L. Brain MRI showed cerebellar and brainstem dysplasia in patients 4a and 10 and obvious polymicrogyria in patient 10 (**Figure 1**). As the clinical and MRI data of these three patients were similar to MEB, but milder than it, we considered their phenotype to be MEB-like.

The CMD-ID group includes patients 1, 2, 7b, 8b, and 11. Their age of onset was between shortly after birth and 5 months of age. The symptoms initially manifested as motor developmental delays with different degrees of severity. The maximum motor capacity of patient 1 was running and jumping but worse than that of normal children of the same age; patient 2 could only sit without support. Patients 7b, 8b, and 11 were able to walk alone, albeit unstably, and patient 7b had lost his ambulant capacity at the age of 10 years due to severe knee and ankle joint contractures. All five patients exhibited intellectual disability. Patients 1 and 7b had difficulty learning at school and poor reading ability. Patients 2, 8b, and 11 were only able to understand simple instructions. Although patient 1's language development was generally normal, the remaining patients could only speak single words or short sentences. Physical examination revealed muscle weakness, which was dominant in the proximal lower limbs. Patient 7b exhibited pseudohypertrophy in the gastrocnemius muscle with a positive Gowers' sign and obvious knee and ankle joint contractures at the age of 10 years. Patient 2 displayed slight esotropia; the remaining patients showed no ocular involvement. Their CK levels ranged from 2,000 to 9,080 IU/L. Brain MRI of these patients showed no structural abnormalities, though patients 1 and 2 revealed an enlarged subarachnoid space or ventricle, and patients 7b and 8b showed abnormal white matter signals.

The LGMD2N group includes patients 3, 6, and 9. Their onset age ranged from 1 to 4 years old, with initial manifestations of abnormal or unstable gait and limb muscle weakness that were relatively milder than those of the patients above. They were susceptible to fatigue, although their daily activities were not affected, and they had poorer running and jumping abilities than normal individuals of the same age. All of them had difficulties learning at school and poor reading skills. The language development of the three patients was generally normal, but patient 6 had mild dysarthria, and patient 9 had poor language expression. Physical examination at the age of last follow-up revealed small head circumferences and slightly decreased muscle strength, which was proximally dominant, with no joint contractures. The patellar tendon reflex of patient 6 was weakened and that of patients 3 and 9 was not drawn out. They had no ocular involvement currently. CK levels ranged from 1,362 to 8,000 IU/L in these patients. Brain MRI indicated normal cerebral structure, though the posterior horns of the lateral ventricle of patient 6 were enlarged slightly, and patient 9 had abnormal white matter signals. Considering the late onset age, mild clinical symptoms, unlimited daily activities and lack of brain structural abnormalities of the three patients, we categorized them into the LGMD group. Notably, we found that all patients had learning difficulties through follow-up, as it was difficult for them to understand the contents of courses, and they had poor mathematical calculation and memory skills.

Molecular Genetic Analysis

A total of 15 different *POMT2* variants, including 9 novel variants and 6 known variants were identified in these 11 patients. No pathogenic CNVs were found. The genetic data for the 11 patients were summarized in **Table 1**. We performed pathogenicity prediction for the 11 unreported variants using bioinformatics software. Most of the variants are missense changes in highly conservative regions. Nine of these 11 variants are predicted to be deleterious or likely pathogenic, but the pathogenicity of 2 missense variants, c.1891G > C and c.874G > C, are uncertain (**Table 2**). Base G at position c.1891 is the last base in exon 18 of the *POMT2* gene, and a nucleotide change at this position would possibly affect the splicing of the transcript. The position c.874G is not particularly conservative, and this change may be benign based on the prediction of software. In order to confirm the pathogenicity of these two variants, we have conducted further research.

Muscle Pathology and Immunofluorescence Staining

Hematoxylin–eosin (HE) staining of the left biceps brachii biopsy of patient 6 showed muscular dystrophic changes with slightly increased variation in muscle fiber diameter, necrosis, and regeneration of muscle fibers accompanied by inflammatory cell infiltration (**Figure 2A**). In addition, obviously proliferated

TABLE 1 | Clinical characteristics of 11 *POMT2*-related alpha-dystroglycanopathy (α-DGP) patients.

Patient	1	2	3	4a	5a	6	7b	8b	9	10	11
Gender	Male	Male	Male	Female	Male	Female	Male	Male	Male	Male	Female
Last follow-up age	12 years	5 years	11 years	11 years	6 years	21 years	11 years	8 years	9 years	4 years	4 years
Onset age	3–4 months	After birth	4 years	4 months	8 months	18 months	3–4 months	3–4 months	3 years 5 months	3–4 months	5 months
Phenotype	CMD-ID	CMD-ID	LGMD	MEB-like	MEB-like	LGMD	CMD-ID	CMD-ID	LGMD	MEB-like	CMD-ID
Initial symptom	Developmental delay	Developmental delay	Abnormal gait	Developmental delay	Developmental delay	Walking unstably	Developmental delay	Developmental delay	Limbs weakness	Developmental delay	HyperCKemia
Maximal mobility	Run and jump (worse)	Sit without support	Run and jump (slightly poor)	Sit without support	Sit without support	Run (unstable)	Walk independently	Walk independently (unstable)	Run and jump	Sit with support	Walk independently
Joint contractures	No	Yes	No	Yes	Yes	No	Yes	Yes	No	Yes	No
Language development	Normal	Single word	Normal	Single word	Single word	Dysarthria	Words and short sentences	Words and short sentences	Poor expression	Unconscious syllables	Short sentences
Intelligence disability	Yes	Yes	Yes	Yes	Yes	Yes	Yes	Yes	Yes	Yes	Yes
Head circumference/ percentile	$<P_3$	$<P_{25}$	$<P_3$	$<P_3$	$<P_3$	$<P_3$	$<P_3$	NA	$<P_3$	$<P_3$	$<P_3$
CK (IU/L)	2,480–7,774	2,000–4,683	3,200–5,193	3,609–5,200	Not detected	2,760–8,000	6,808–9,080	4,956	1,362–2,204	3,656–4,602	3,152–4,347
Cardiovascular involvement	No	No	No	No	Not detected	No	No	No	No	No	No
Ocular involvement	No	Esotropia	No	No	No	No	No	No	No	Esotropia	No
Electromyogram	Myogenic change	Myogenic change	Not done	Myogenic change	Not done	Normal	Not done	Normal	Non-specific change	Not done	Myogenic change
Muscle biopsy	Muscular dystrophic change	Not done	Not done	Muscular dystrophic change	Not done	Muscular dystrophic change	Muscular dystrophic change	Not done	Slightly pathogenic change	Not done	Not done
Brain MRI	Slightly enlarged subarachnoid space, slightly deeper sulcus	Slightly enlarged bilateral ventricles	Normal	Cerebellar and brainstem dysplasia	Not done	Slightly enlarged posterior horn of the lateral ventricle	Extensive signal abnormalities in the white matter of the brain	Abnormal white matter signal in frontal and parietal lobe and periventricular	Abnormal white matter signal in posterior body of lateral ventricle	Polymicrogyria, cerebellar and brainstem dysplasia, cerebellar cysts, enlarged bilateral ventricles	Normal
Genetic test	c.287A > G p.(Tyr96Cys) c.551C > T p.(Thr184Met)	c.1237C > T p.(Arg413X) c.604T > G p.(Phe202Val)	c.479A > G p.(Tyr160Cys) c.287A > G p.(Tyr96Cys)	c.1521C > A p.(Tyr507X) c.227T > G p.(Leu76Trp)	c.1521C > A p.(Tyr507X) c.227T > G p.(Leu76Trp)	c.1891G > C p.(Gly631Arg) c.295C > T p.(Arg99Cys)	c.874G > C p.(Ala292Pro), homozygote	c.874G > C p.(Ala292Pro) homozygote	c.2176G > A p.(Gly726Arg) c.1261C > T p.(Arg421Trp)	c.1769_1772dupATCT p.(Leu592Ser fs*189) c.1769A > G p.(Tyr590Cys)	c.227T > G p.(Leu76Trp) c.1274G > A p.(Ser425Asn)

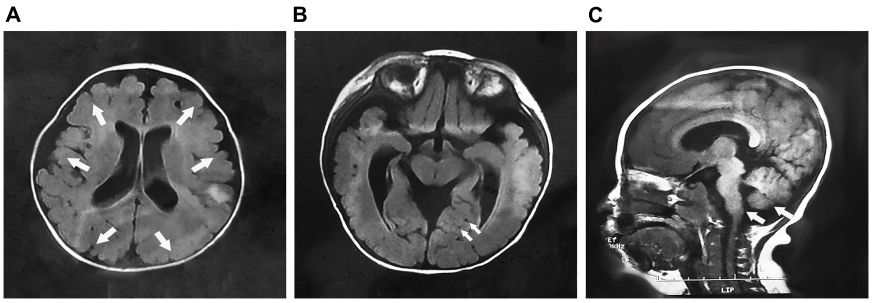

FIGURE 1 | The brain MRI of patient 10 at 7 months of age. **(A)** Cross-sectional imaging showed polymicrogyria in the frontal, temporal, parietal, and occipital regions (arrows); **(B)** multiple cysts were identified in the cerebellum (arrows); and **(C)** sagittal imaging showed the cerebellum and brainstem dysplasia (arrows).

lipids and connective tissue in the partial perimysium, increased variation in muscle fiber diameter, and some necrotic muscle fibers were detected in the muscle biopsy of the right quadriceps of patient 7b (**Figure 2B**). Based on immunofluorescence staining with an IIH6C4 antibody, the expression of glycosylated α-DG in the muscle cell membrane from patients was significantly defective compared to that in the control (**Figures 2A1–C3**). The staining of β-DG antibody was normal in both patients and the healthy control (**Figures 2A4–C4**).

TABLE 2 | Pathogenicity prediction results of clinically unreported *POMT2* variants.

Variants/software	Mutationtaster	PolyPhen 2	Provean
c.287A > G	Pathogenic	Probably damaging (score: 1)	Deleterious (score: −8.127)
p.(Tyr96Cys)			
c.1237C > T	Pathogenic	/	/
p.(Arg413X)			
c.479A > G	Pathogenic	Probably damaging (score: 1)	Deleterious (score: −6.068)
p.(Tyr160Cys)			
c.1521C > A	Pathogenic	/	/
p.(Tyr507X)			
c.227T > G	Pathogenic	Probably damaging (score: 0.999)	Deleterious (score: −4.154)
p.(Leu76Trp)			
c.1891G > C	Pathogenic	Benign (score: 0.001)	Neutral (score: 0.382)
p.(Gly631Arg)			
c.295C > T	Pathogenic	Probably damaging (score: 1)	Deleterious (score: −6.274)
p.(Arg99Cys)			
c.874G > C	Polymorphism	Possibly damaging (score: 0.564)	Neutral (score: −2.35)
p.(Ala292Pro)			
c.1769_1772dupATCT	Pathogenic	/	/
p.(Leu592Ser fs*189)			
c.1769A > G	Pathogenic	Probably damaging (score: 1)	Deleterious (score: −8.066)
p.(Tyr590Cys)			
c.1274G > A	Pathogenic	Probably damaging (score: 0.996)	Deleterious (score: −2.8)
p.(Ser425Asn)			

Minigene Assay Analysis

A minigene of *POMT2* carrying the c.1891G > C variant was constructed to verify the transcriptional consequences of the splice site change. An electropherogram of PCR products revealed the predicted size 402-bp band in the wild-type control, whereas a larger 1,500-bp band was observed in the mutant (**Figure 3A**). Sequencing of the PCR product showed that the intron between exons 18 and 19 was spliced retention, which suggested that the variant c.1891G > C affects splicing. Furthermore, we found a termination codon when analyzing the sequence of the retention intron 18, which probably resulted in the premature termination of the protein translation (**Figure 3B**).

DISCUSSION

As *POMT2* catalyzes the first step in O-mannosylation of α-DG, it is believed that *POMT2* mutations would cause severe phenotypes, and the first case of *POMT2*-related α-DGP presented the most severe phenotype of WWS, as expected (van Reeuwijk et al., 2005). With an increasing number of genetically diagnosed cases reported, a number of milder phenotypes of *POMT2*-related α-DGPs have been identified, such as MEB/FCMD-like (Godfrey et al., 2007), CMD-ID (Yanagisawa et al., 2007), and LGMD2N (Biancheri et al., 2007; Murakami et al., 2009; Saredi et al., 2014; Østergaard et al., 2018). However, due to the pleiotropic effects of the genes involved, there is no definite correlation between genotype and phenotype, and the same mutation site in different individuals may cause variable phenotypes. Although patients with *POMT2*-related α-DGP present variable phenotypes, they still have common features, including slowly progressive muscle weakness, predominantly in the proximal muscle group, elevated CK levels, and psychomotor retardation.

The development of next-generation sequencing technology enhances the diagnostic rate. Here, we summarize the characteristics of a *POMT2*-related α-DGP cohort in China. Their age of onset ranged from after birth to childhood. The phenotype included LGMD, CMD-ID, and MEB-like, but the

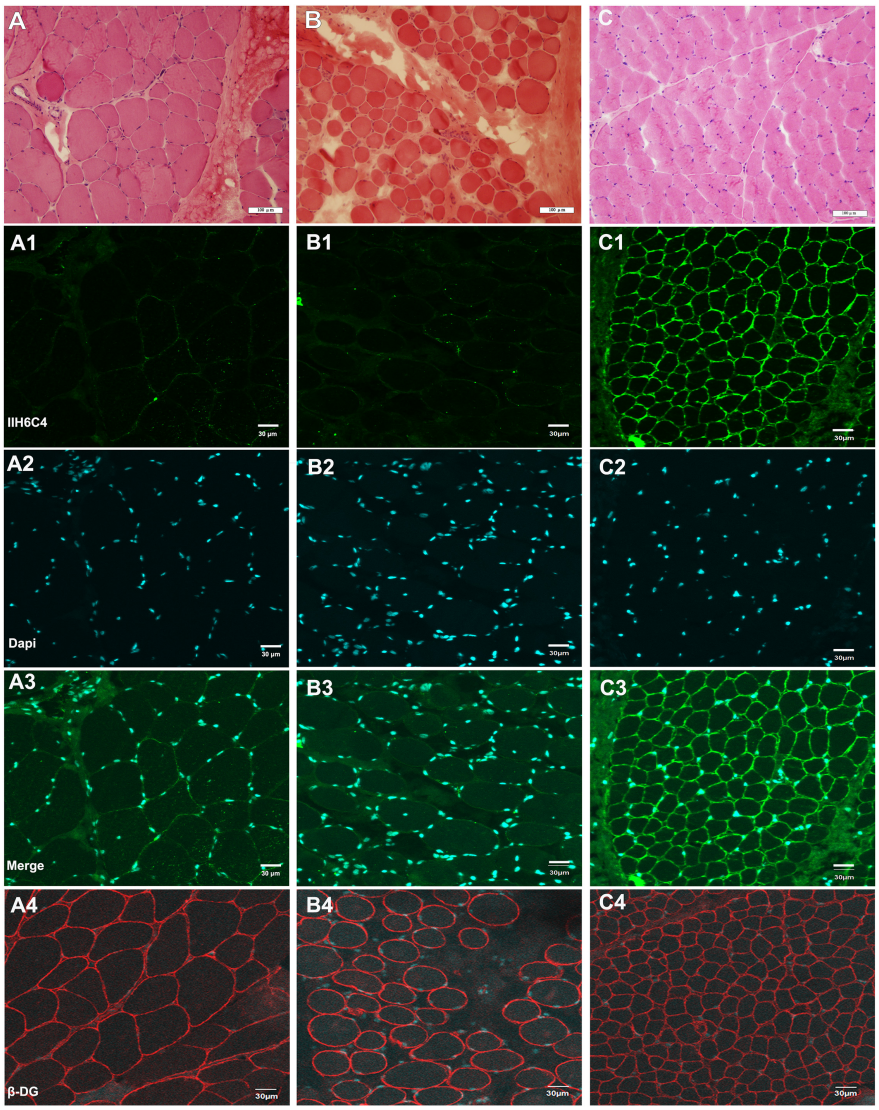

FIGURE 2 | Hematoxylin–eosin (HE) staining and immunofluorescence staining of IIH6C4 antibody of patients 6 and 7b **(A,B)** HE staining of patients 6, and 7b showed slightly increased variation of the muscle fiber diameter, and necrosis; **(C)** HE staining of the healthy control; **(A1,B1,C1)** Immunofluorescence staining of IIH6C4 antibody from patients 6, 7b, and the normal control, respectively; **(A2,B2,C2)** the staining of Dapi for cell nucleus of patients 6, 7b, and the normal control, respectively; **(A3,B3,C3)** the staining of merge, and the staining of patients 6 and 7b showed the expression of glycosylated α-DG in the cell membranes was much weaker than in the control; and **(A4,B4,C4)** the staining of β-DG antibody for patients 6, 7b, and the normal control, respectively.

most severe phenotype WWS was not seen in this cohort. All the patients developed slowly progressive muscle weakness and intellectual disability with varying degrees and no severe ocular involvement at the last follow-up. All of them had microcephaly and none of them has developed epilepsy to date, although some only exhibited white matter signal abnormalities on brain MRI and no brain structural abnormalities. Some studies have suggested that the results of brain MRI are not necessarily related to intellectual and cognitive impairment (Palmieri et al., 2011). In general, intellectual disability in α-DGP possibly results from defective α-DG glycosylation in neurons, inhibiting the long-term potentiation of the hippocampus and ultimately leading to learning and memory dysfunction (Satz et al., 2010).

POMT2 is a member of the protein O-mannosyltransferase family, and it is relatively conserved in different species from yeast to humans. The protein, containing nine transmembrane regions, catalyzes O-mannosylation, which is essential for skeletal muscle function and neuronal migration (Willer et al., 2002). Formation of a heterodimer with its homologous analog, POMT1, is necessary for *POMT2* to exert mannosyltransferase function (Manya et al., 2004). When synthesis of the glycosylated glycan chain is completed, α-DG can act as a receptor for the binding of many ligands in the extracellular matrix, and this receptor function plays a key role in stabilizing the cytoskeleton, completing material transportation, and signal transduction. The enzyme activity of *POMT2* depends on five N-glycosylation

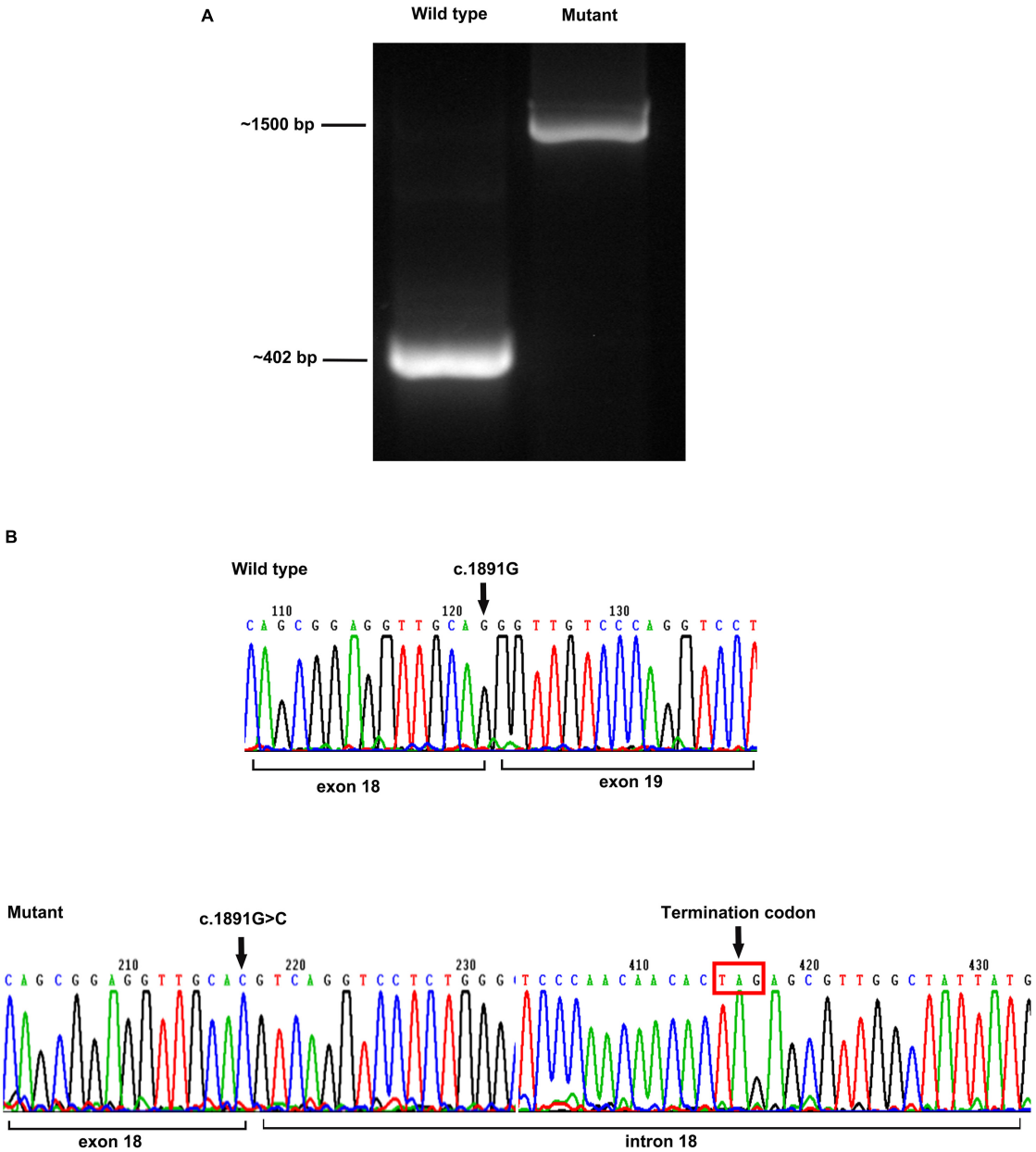

FIGURE 3 | Minigene assay analysis. **(A)** The size of an electropherogram of PCR product of the wildtype was around 402 bp, and the size of mutant was around 1,500 bp; and **(B)** sequencing of the cDNA revealed the intron 18 was spliced into the mutant, resulting to the premature appearance of termination codon.

sites, namely, Asn98, Asn330, Asn445, Asn528, and Asn583, which are all located on the luminal side of the endoplasmic reticulum. The last four sites are located in a large hydrophilic loop, containing amino acids 305–601, which are key areas that affect *POMT2* enzymatic activity (Manya et al., 2010). There are three presumed homologous domains in this hydrophilic loop, called the mannosyltransferase-3-phosphate inositol receptor-ryanodine receptor (M-IP3R-RyR, MIR) domain, each consisting of amino acids 318–381, 392–443, and 456–513 (**Figure 4**); these domains may also be important for the catalytic function of *POMT2* (Ponting, 2000).

As p.(Arg413X) in patient 2, p.(Tyr507X) in patients 4a and 5a, p.(Arg421Trp) in patient 9, p.(Leu592Ser fs*189), and p.(Tyr590Cys) in patient 10 in this study are located in the large hydrophilic loop or MIR domain of *POMT2*, they are likely to be pathogenic based on their position. Nonetheless, it is difficult to predict the effect of the remaining variants on protein function according to their sites. c.1891G > C/p.(Gly631Arg) in patient 6 is not located in an area critical for enzymatic activity, and the software analysis also predicted that it is possibly non-pathogenic. However, this variant is located at the end of exon 18, so we suspected it may affect splicing of *POMT2*. We then

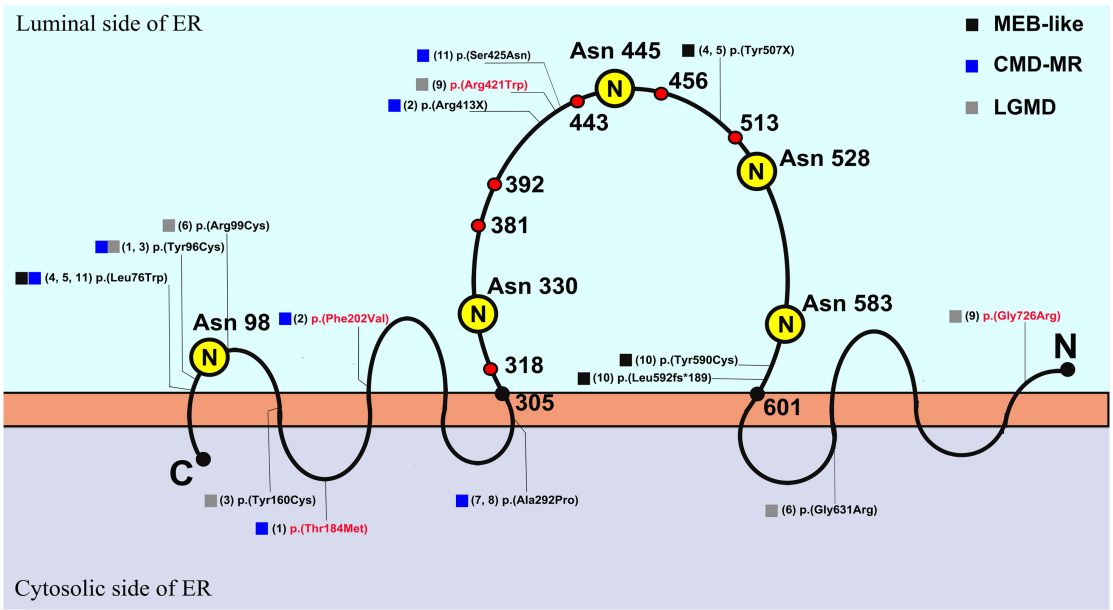

FIGURE 4 | The schematic diagram of *POMT2* (Manya et al., 2010) and the distribution of variants in this cohort. The capital letter *N* in yellow circle represented N-glycosylation sites, which are located on the amino acids of Asn 98, Asn 330, Asn 445, Asn 528, and Asn 583. The amino acids 305–601 represented the large hydrophilic loop, and it contains three presumed MIR domains, amino acid 318–381, 392–443, and 456–513, which are the important areas that affect enzymatic activity. The number in brackets represented the serial number of patients, and the variants in red font had been clinically reported; ER, endoplasmic reticulum; C, C terminal; N, N terminal.

constructed a minigene carrying the variant c.1891G > C to verify its pathogenicity. We confirmed that this missense change of the last base in exon 18 leads to a splicing change and premature termination of the protein translation. Homozygous c.874G > C in patients 7b and 8b was predicted to be polymorphic or benign, but immunofluorescence staining from patient 7b's skeletal muscle biopsy confirmed hypoglycosylation of α-DG, suggesting the pathogenicity of this variant.

Four compound heterozygous variants, p.(Thr184Met), p.(Phe202Val), p.(Gly726Arg), and p.(Arg421Trp), in our cohort have been reported previously. The phenotype of patient 1 with variants of p.(Thr184Met) and p.(Tyr96Cys) manifested as CMD-ID, though in a previous report, the phenotype of an individual also harboring heterozygous variants of p.(Thr184Met) and p.(Trp748Ser) was LGMD (Godfrey et al., 2007). Patient 2 carrying p.(Phe202Val) manifested as CMD-ID, consistent with a previous report about a homozygote of p.(Phe202Val) (Murakami et al., 2009). The phenotype of homozygous p.(Gly726Arg) in a previous report was WWS (Bouchet et al., 2007), and the heterozygous variant p.(Arg421Trp) caused variable phenotype (Punetha et al., 2016; Johnson et al., 2018). Patient 9, with a compound heterozygous variant of p.(Gly726Arg) and p.(Arg421Trp), presented the phenotype of LGMD. We marked the variant sites of our cohort on the *POMT2* protein schematic illustrated in **Figure 4**. In general, if the variant is located on the luminal side of the endoplasmic reticulum, especially on the large hydrophilic loop related to the enzyme activity of *POMT2*, it usually causes a more severe phenotype. If the variant is located on the cytoplasmic side, it may cause a milder phenotype due to the slight impact on the enzyme catalytic activity. However, this is not absolute, as clinical severity depends on how the mutation site affects protein function.

Our study broadens the mutational spectrum of *POMT2*-related α-DGP, but there is no clear correlation between genotype and phenotype. The main mutational types in this study were missense variants, and most of them were compound heterozygotes. It is difficult to determine the pathogenicity of a missense variant, even though it is located in the catalytic domain of the protein, as there may be some residual protein function. Hence, further study is needed to detect whether the enzymatic activity of *POMT2* is affected by the missense variants described here.

DATA AVAILABILITY STATEMENT

The datasets for this article are not publicly available due to concerns regarding participant/patient anonymity. Requests to access the datasets should be directed to the corresponding author.

ETHICS STATEMENT

The studies involving human participants were reviewed and approved by the Ethics Committee of the Peking University First Hospital. Written informed consent to participate in this study was provided by the participants' legal guardian/next of kin.

Written informed consent was obtained from the individual(s), and minor(s)' legal guardian/next of kin, for the publication of any potentially identifiable images or data included in this article.

AUTHOR CONTRIBUTIONS

X-YC: conceptualization, methodology, validation, investigation, and writing – original draft. D-YS: resources and formal analysis. LJ and Y-DL: resources. D-DT: formal analysis. J-YL and X-ZC: investigation. G-GX and TT: technique support. HX: writing, review and editing, supervision, project administration, and funding acquisition. All authors contributed to the article and approved the submitted version.

FUNDING

This work was supported by the National Natural Science Foundation of Beijing [No. 7212116]; the Development Program of China [No. 2016YFC0901505]; the National Natural Science Foundation of China [No. 81571220]; and the Beijing key laboratory of molecular diagnosis and study on pediatric genetic diseases [No. BZ0317].

ACKNOWLEDGMENTS

We appreciate all the patients and their families who have participated in this study.

REFERENCES

Biancheri, R., Falace, A., Tessa, A., Pedemonte, M., Scapolan, S., Cassandrini, D., et al. (2007). POMT2 gene mutation in limb-girdle muscular dystrophy with inflammatory changes. *Biochem. Biophys. Res. Commun.* 363, 1033–1037. doi: 10.1016/j.bbrc.2007.09.066

Bouchet, C., Gonzales, M., Vuillaumier-Barrot, S., Devisme, L., Lebizec, C., Alanio, E., et al. (2007). Molecular heterogeneity in fetal forms of type II lissencephaly. *Hum. Mutat.* 28, 1020–1027. doi: 10.1002/humu.20561

Cormand, B., Pihko, H., Bayes, M., Valanne, L., Santavuori, P., Talim, B., et al. (2001). Clinical and genetic distinction between Walker-Warburg syndrome and muscle-eye-brain disease. *Neurology* 56, 1059–1069. doi: 10.1212/wnl.56.8.1059

Diesen, C., Saarinen, A., Pihko, H., Rosenlew, C., Cormand, B., Dobyns, W. B., et al. (2004). POMGnT1 mutation and phenotypic spectrum in muscle-eye-brain disease. *J. Med. Genet.* 41:e115. doi: 10.1136/jmg.2004.020701

Endo, T. (2015). Glycobiology of alpha-dystroglycan and muscular dystrophy. *J. Biochem.* 157, 1–12. doi: 10.1093/jb/mvu066

Ge, L., Fu, X., Zhang, W., Wang, D., Wang, Z., Yuan, Y., et al. (2019). Recessive mutations in proximal I-band of TTN gene cause severe congenital multi-minicore disease without cardiac involvement. *Neuromuscul. Disord.* 29, 350–357. doi: 10.1016/j.nmd.2019.03.007

Godfrey, C., Clement, E., Mein, R., Brockington, M., Smith, J., Talim, B., et al. (2007). Refining genotype phenotype correlations in muscular dystrophies with defective glycosylation of dystroglycan. *Brain* 130, 2725–2735. doi: 10.1093/brain/awm212

Johnson, K., Bertoli, M., Phillips, L., Töpf, A., Van den Bergh, P., Vissing, J., et al. (2018). Detection of variants in dystroglycanopathy-associated genes through the application of targeted whole-exome sequencing analysis to a large cohort of patients with unexplained limb-girdle muscle weakness. *Skelet. Muscle* 8:23.

Manya, H., Akasaka-Manya, K., Nakajima, A., Kawakita, M., and Endo, T. (2010). Role of N-glycans in maintaining the activity of protein O-mannosyltransferases POMT1 and POMT2. *J. Biochem.* 147, 337–344. doi: 10.1093/jb/mvp170

Manya, H., Chiba, A., Yoshida, A., Wang, X., Chiba, Y., Jigami, Y., et al. (2004). Demonstration of mammalian protein O-mannosyltransferase activity: coexpression of POMT1 and POMT2 required for enzymatic activity. *Proc. Natl. Acad. Sci. U. S. A.* 101, 500–505. doi: 10.1073/pnas.0307228101

Murakami, T., Hayashi, Y. K., Ogawa, M., Noguchi, S., Campbell, K. P., Togawa, M., et al. (2009). A novel POMT2 mutation causes mild congenital muscular dystrophy with normal brain MRI. *Brain Dev.* 31, 465–468. doi: 10.1016/j.braindev.2008.08.005

Østergaard, S. T., Johnson, K., Stojkovic, T., Krag, T., De Ridder, W., De Jonghe, P., et al. (2018). Limb girdle muscular dystrophy due to mutations in POMT2. *J. Neurol. Neurosurg. Psychiatry* 89, 506–512.

Palmieri, A., Manara, R., Bello, L., Mento, G., Lazzarini, L., Borsato, C., et al. (2011). Cognitive profile and MRI findings in limb-girdle muscular dystrophy 2I. *J. Neurol.* 258, 1312–1320. doi: 10.1007/s00415-011-5930-3

Ponting, C. P. (2000). Novel repeats in ryanodine and IP3 receptors and protein O-mannosyltransferases. *Trends Biochem. Sci.* 25, 48–50.

Punetha, J., Kesari, A., Uapinyoying, P., Giri, M., Clarke, N. F., and Waddell, L. B. (2016). Targeted re-sequencing emulsion PCR panel for myopathies: results in 94 cases. *J Neuromuscul Dis.* 3, 209–225. doi: 10.3233/jnd-160151

Saredi, S., Gibertini, S., Ardissone, A., Fusco, I., Zanotti, S., Blasevich, F., et al. (2014). A fourth case of POMT2-related limb girdle muscle dystrophy with mild reduction of α-dystroglycan glycosylation. *Eur. J. Paediatr. Neurol.* 18, 404–408. doi: 10.1016/j.ejpn.2013.10.005

Satz, J. S., Ostendorf, A. P., Hou, S., Turner, A., Kusano, H., Lee, J. C., et al. (2010). Distinct functions of glial and neuronal dystroglycan in the developing and adult mouse brain. *J. Neurosci.* 30, 14560–14572. doi: 10.1523/jneurosci.3247-10.2010

Song, D., Dai, Y., Chen, X., Fu, X., Chang, X., Wang, N., et al. (2020). Genetic variations and clinical spectrum of dystroglycanopathy in a large cohort of Chinese patients. *Clin. Genet.* 99, 384–395. doi: 10.1111/cge.13886

van Reeuwijk, J., Janssen, M., van den Elzen, C., Beltran-Valero, de Bernabé, D., Sabatelli, P., et al. (2005). POMT2 mutations cause alpha-dystroglycan hypoglycosylation and Walker-Warburg syndrome. *J. Med. Genet.* 42, 907–912. doi: 10.1136/jmg.2005.031963

Willer, T., Amselgruber, W., Deutzmann, R., and Strahl, S. (2002). Characterization of POMT2, a novel member of the PMT protein O-mannosyltransferase family specifically localized to the acrosome of mammalian spermatids. *Glycobiology* 12, 771–783. doi: 10.1093/glycob/cwf086

Yanagisawa, A., Bouchet, C., Van den Bergh, P. Y., Cuisset, J. M., Viollet, L., Leturcq, F., et al. (2007). New POMT2 mutations causing congenital muscular dystrophy: identification of a founder mutation. *Neurology* 69, 1254–1260. doi: 10.1212/01.wnl.0000268489.60809.c4

Conflict of Interest: The authors declare that the research was conducted in the absence of any commercial or financial relationships that could be construed as a potential conflict of interest.

Publisher's Note: All claims expressed in this article are solely those of the authors and do not necessarily represent those of their affiliated organizations, or those of the publisher, the editors and the reviewers. Any product that may be evaluated in this article, or claim that may be made by its manufacturer, is not guaranteed or endorsed by the publisher.

frontiers in Genetics

ORIGINAL RESEARCH
published: 10 August 2021
doi: 10.3389/fgene.2021.719437

The Estimated Prevalence of N-Linked Congenital Disorders of Glycosylation Across Various Populations Based on Allele Frequencies in General Population Databases

Sander Pajusalu[1,2†], Mari-Anne Vals[1,3†], Laura Mihkla[1,2], Ustina Šamarina[2], Tiina Kahre[1,2] and Katrin Õunap[1,2]*

[1] Department of Clinical Genetics, Institute of Clinical Medicine, University of Tartu, Tartu, Estonia, [2] Department of Clinical Genetics, United Laboratories, Tartu University Hospital, Tartu, Estonia, [3] Children's Clinic, Tartu University Hospital, Tartu, Estonia

Congenital disorders of glycosylation (CDG) are a widely acknowledged group of metabolic diseases. PMM2-CDG is the most frequently diagnosed CDG with a prevalence as high as one in 20,000. In contrast, the prevalence of other CDG types remains unknown. This study aimed to analyze the estimated prevalence of different N-linked protein glycosylation disorders. We extracted allele frequencies for diverse populations from The Genome Aggregation Database (gnomAD), encompassing variant frequency information from 141,456 individuals. To identify pathogenic variants, we used the ClinVar database as a primary source. High confidence loss-of-function variants as defined by the LOFTEE algorithm were also classified as pathogenic. After summing up population frequencies for pathogenic alleles, estimated disease birth prevalence values with confidence intervals were calculated using the Bayesian method. We first validated our approach using two more common recessive disorders (cystic fibrosis and phenylketonuria) by showing that the estimated prevalences calculated from population allele frequencies were in accordance with previously published epidemiological studies. Among assessed 27 autosomal recessive N-glycosylation disorders, the only disease with estimated birth prevalence higher than one in 100,000 was PMM2-CDG (in both, all gnomAD individuals and those with European ancestry). The combined prevalence of 27 different N-glycosylation disorders was around one in 22,000 Europeans but varied considerably across populations. We will show estimated prevalence data from diverse populations and explain the possible pitfalls of this analysis. Still, we are confident that these data will guide CDG research and clinical care to identify CDG across populations.

Keywords: CDG, congenital disorders of glycosylation, *N*-glycosylation, prevalence, population allele frequencies

Edited by:
Karolina Stepien, Salford Royal NHS Foundation Trust, United Kingdom

Reviewed by:
Gregory M. Pastores, Mater Misericordiae University Hospital, Ireland
James O'Byrne, Mater Misericordiae University Hospital, Ireland

****Correspondence:***
Katrin Õunap
katrin.ounap@kliinikum.ee

† These authors have contributed equally to this work and share first authorship

Specialty section:
This article was submitted to Genetics of Common and Rare Diseases, a section of the journal Frontiers in Genetics

Received: *02 June 2021*
Accepted: *21 July 2021*
Published: *10 August 2021*

Citation:
Pajusalu S, Vals M-A, Mihkla L, Šamarina U, Kahre T and Õunap K (2021) The Estimated Prevalence of N-Linked Congenital Disorders of Glycosylation Across Various Populations Based on Allele Frequencies in General Population Databases. Front. Genet. 12:719437. doi: 10.3389/fgene.2021.719437

INTRODUCTION

Congenital disorders of glycosylation (CDG) are a growing group of metabolic diseases with at least 137 defects (Ondruskova et al., 2021). According to the International Classification of Inherited Metabolic Disorders (ICIMD) database, 32 are classified as N-linked protein glycosylation defects (Ferreira et al., 2021). Based on population allele frequencies, the expected birth prevalence of the most common PMM2-CDG could be as high as 1:20,000 (Schollen et al., 2000), and in later reports, 1:77,000 to 1:286,000 (Vals et al., 2018; Yildiz et al., 2020). Mainly at the expense of PMM2-CDG, type 1 defects are more frequently diagnosed than type 2 defects (Peanne et al., 2017; Medrano et al., 2019) but compared to PMM2-CDG, other defects occur much seldom. The estimated combined prevalence of CDG among the Saudi population is 14 per million (Alsubhi et al., 2017), whereas, in Poland, the prevalence is approximately one case per million (Lipinski et al., 2021). The worldwide individual prevalence of different defects remains unknown.

The emergence of large-scale population-based exome and genome sequencing studies and the aggregation into even more extensive cross-population databases like gnomAD makes allele frequency data available from more than 100,000 individuals across different populations (Karczewski et al., 2020). Disease prevalence can be estimated when these data are combined with clinical variant classification databases like ClinVar (Landrum et al., 2018) and variant loss-of-function predictions. This approach has been previously used on assessing disease prevalence of different limb-girdle muscular dystrophy subtypes across populations (Liu et al., 2019). Although direct calculations using the Hardy-Weinberg equation can be used, the methods developed by Liu et al. (2019) make use of more advanced Bayesian statistics to add confidence intervals on prevalence estimators.

This study aimed to analyze the estimated prevalence of N-linked protein glycosylation defects across different populations based on allele frequencies in general population databases.

MATERIALS AND METHODS

Only N-linked protein glycosylation defects with autosomal recessive inheritance patterns (27/32) were included in the analysis. The list was based on the ICIMD database (Ferreira et al., 2021). We extracted allele frequencies for different populations from The Genome Aggregation Database (gnomAD v2.1.1) (Karczewski et al., 2020), encompassing variant frequency information from 141,456 individuals. We defined variants as pathogenic if they were classified pathogenic or likely pathogenic in the ClinVar database (version 20210119) (Landrum et al., 2018) or were marked as high confidence loss-of-function (Moller et al., 2016) variants by the LOFTEE algorithm (Karczewski et al., 2020). In the case of conflicting annotations, high confidence LoF variants marked as (likely) benign in ClinVar were considered as non-pathogenic. Also, variants not passing all quality filters in the gnomAD variant call set were eliminated from counting toward the sum of pathogenic alleles.

The calculations were carried out across all seven gnomAD populations (African/African American, Latino/Admixed American, non-Finnish European, Finnish, Ashkenazi Jewish, East Asian, and South Asian). The number of individuals per population ranged from 5,185 (Ashkenazi Jewish) to 64,603 (non-Finnish European). In addition, we calculated prevalence estimates for the Estonian population (2,418 individuals), which is a subpopulation of non-Finnish Europeans. After obtaining population frequencies for pathogenic alleles, estimated disease birth prevalence values with confidence intervals were calculated using Bayesian statistics adapted from the previously published study by Liu et al. (2019). No manual variant curation was performed, and no gene-based exceptions were made to assure reproducibility and robustness (i.e., for PMM2-CDG, the p.Arg141His variant homozygotes were not excluded although known to be embryonically lethal). For validation, we used two common recessive disorders (cystic fibrosis and phenylketonuria) and compared the estimated disease prevalence with the data from epidemiological studies conducted in different populations.

RESULTS

The estimated prevalence from population allele frequencies of cystic fibrosis and phenylketonuria was in accordance with previously published data (**Supplementary Table 1**). Results from published epidemiological studies fell into 95% confidence intervals in non-Finnish European, Estonian, and Finnish populations, where reliable population prevalence is known.

The selected list of N-linked protein glycosylation defects, their estimated prevalence, and the number of reported cases is presented in **Table 1**. The full list of all defects in all assessed populations is shown in **Supplementary Table 2**.

PMM2-CDG showed the highest estimated prevalence counted from 71 different pathogenic variants, and it is more prevalent in European (1 in 27,000), Ashkenazi Jewish (1 in 20,000), and admixed American populations (1 in 64,000). All other N-linked protein glycosylation defects had a much lower prevalence.

FUK-CDG and MAN2B2-CDG, which are both only recently reported and classified as N-linked protein glycosylation defects, showed high estimated prevalence, especially in East-Asians where FUK-CDG prevalence was estimated at 1:12,000 and MAN2B2-CDG at 1:11,000.

The estimated prevalence of combined N-linked protein glycosylation defects in Europeans was one in 22,000 or one in 24,000 after excluding FUK-CDG and MAN2B2-CDG. In East-Asians, however, the total CDG prevalence was estimated at 1:5,613, dropping to 1:121,935 after excluding FUK-CDG and MAN2B2-CDG. CDG seems to be more common in Finnish (1:16,000) and Ashkenazi Jewish populations (1:14,000). In Estonians, the combined CDG birth prevalence is estimated at around 1:50,000.

TABLE 1 | N-linked protein glycosylation defects with highest estimated prevalence.

Defect	Population	Estimated prevalence	Reported patients (references)
PMM2-CDG	NFE	1:27,465 (1:24,014-1:31,804)	>900 (Altassan et al., 2019)
	FIN	1:18,745 (1:14,391-1:25,744)	
	EST	1:61,506 (1:30,827-1:213,327)	
	AFR	1:288,214 (1:177,276-1:582,250)	
	AMR	1:64,498 (1:47,771-1:93,421)	
	EAS	1:150,016 (1:94,205-1:290,357)	
	SAS	1:366,999 (1:229,546-1:716,111)	
	ASJ	1:19,908 (1:13,368-1:33,911)	
FUK-CDG	NFE	1:491,021 (1:376,701-1:675,057)	2 (Ng et al., 2018)
	FIN	1:20,817,888 (1:7,099,020-1:997,371,113)	
	EST	1:1,163,396 (1:371,284-1:113,077,583)	
	AFR	1:140,528 (1:92,099-1:250,277)	
	AMR	1:159,571 (1:110,439-1:257,822)	
	EAS	1:12,248 (1:9,355-1:16,948)	
	SAS	1:264,096 (1:170,511-1:483,909)	
	ASJ	1:255,447 (1:129,730-1:848,576)	
ALG6-CDG	NFE	1:623,512 (1:471,533-1:875,344)	101 (Peanne et al., 2017)
	FIN	1:31,451,234 (1:10,034,414-1:3,065,715,982)	
	EST	1:3,891,489 (1:1,025,904-1:1,609,067,019)	
	AFR	1:1,819,171 (1:898,773-1:6,624,417)	
	AMR	1:13,909,852 (1:5,657,192-1:128,018,704)	
	EAS	1:66,077,105 (1:17,423,193-1:27,292,863,020)	
	SAS	1:7,088,553 (1:3,056,117-1:46,137,181)	
	ASJ	1:17,848,406 (1:4,706,371-1:7,371,298,516)	
MAN2B2-CDG	NFE	1:787,319 (1:586,411-1:1,130,745)	1 (Verheijen et al., 2020)
	FIN	1:52,368,616 (1:15,379,043-1:10,698,108,148)	
	EST	1:1,945,432 (1:571,159-1:398,260,061)	
	AFR	1:399,033 (1:237,158-1:868,735)	
	AMR	1:995,113 (1:577,663-1:2,287,515)	
	EAS	1:11,323 (1:8,713-1:15,500)	
	SAS	1:104,832 (1:73,327-1:166,377)	
	ASJ	-	
ALG1-CDG	NFE	1:881,984 (1:651,920-1:1,281,505)	57 (Ng et al., 2016)
	FIN	1:4,775,806 (1:2,058,960-1:31,088,465)	
	EST	1:3,882,716 (1:1,023,873-1:1,603,070,711)	
	AFR	1:329,069 (1:199,633-1:684,648)	
	AMR	1:2,981,452 (1:1,514,011-1:9,907,069)	
	EAS	1:2,543,998 (1:1,124,720-1:14,579,668)	
	SAS	1:1,559,334 (1:828,918-1:4,508,711)	
	ASJ	1:47,656 (1:29,448-1:95,348)	
MPI-CDG	NFE	1:1,294,251 (1:930,944-1:1,962,331)	35 (Cechova et al., 2020)
	FIN	1:4,778,023 (1:2,059,807-1:31,111,585)	
	EST	1:11,654,073 (1:2,660,508-1:8,720,690,758)	
	AFR	1:8,630,916 (1:3,389,920-1:102,061,250)	
	AMR	1:22,366,551 (1:8,439,237-1:371,016,597)	
	EAS	1:13,209,464 (1:4,505,222-1:631,735,293)	
	SAS	1:12,962,840 (1:5,091,807-1:153,179,670)	
	ASJ	1:53,570,813 (1:12,229,235-1:40,091,239,613)	
ALG8-CDG	NFE	1:1,415,559 (1:1,011,381-1:2,169,560)	19 (Hock et al., 2015; Bastaki et al., 2018; Vuillaumier-Barrot et al., 2019)
	FIN	1:113,720 (1:76,487-1:193,148)	
	EST	1:1,167,178 (1:372,380-1:113,784,408)	
	AFR	1:467,544 (1:273,118-1:1,059,029)	
	AMR	1:2,983,716 (1:1,515,013-1:9,917,690)	
	EAS	1:5,516,877 (1:2,166,449-1:65,327,618)	
	SAS	1:8,491,922 (1:3,562,236-1:64,394,419)	
	ASJ	1:53,570,813 (1:12,229,235-1:40,091,239,613)	
ALG12-CDG	NFE	1:3,351,728 (1:2,231,972-1:5,796,068)	15 (Sturiale et al., 2019; Tahata et al., 2019; De la Morena Barrio et al., 2020; Lekka et al., 2021)
	FIN	1:7,006,414 (1:2,848,761-1:64,600,402)	
	EST	1:11,653,895 (1:2,660,472-1:8,720,505,722)	
	AFR	1:11,091,299 (1:4,185,867-1:183,600,265)	
	AMR	1:1,785,729 (1:967,871-1:4,889,276)	
	EAS	1:19,815,990 (1:6,323,450-1:1,927,830,733)	
	SAS	1:46,648,320 (1:14,885,720-1:4,538,726,166)	
	ASJ	1:17,888,161 (1:4,715,426-1:7,399,706,924)	
RFT1-CDG	NFE	1:4,002,089 (1:2,622,918-1:7,127,436)	17 (Abiramalatha et al., 2019; Quelhas et al., 2019)
	FIN	1:104,751,692 (1:27,620,721-1:43,268,721,479)	
	EST	1:3,882,747 (1:1,023,880-1:1,603,094,646)	
	AFR	1:6,903,683 (1:2,808,018-1:63,498,158)	
	AMR	1:694,726 (1:419,403-1:1,460,905)	
	EAS	1:19,816,478 (1:6,323,581-1:1,927,952,708)	
	SAS	1:5,130,463 (1:2,320,228-1:26,453,803)	
	ASJ	1:53,571,026 (1:12,229,292-1:40,091,317,606)	
MAN1B1-CDG	NFE	1:6,787,005 (1:4,228,673-1:13,348,564)	40 (Balasubramanian et al., 2019)
	FIN	1:104,751,828 (1:27,620,743-1:43,268,894,067)	
	EST	1:1,940,866 (1:570,034-1:396,154,895)	
	AFR	1:1,347,137 (1:692,613-1:4,304,308)	
	AMR	1:4,603,156 (1:2,204,053-1:18,769,689)	
	EAS	1:13,235,145 (1:4,512,603-1:635,115,108)	
	SAS	1:31,096,221 (1:10,605,563-1:1,487,347,436)	
	ASJ	-	
MOGS-CDG	NFE	1:9,149,993 (1:5,524,081-1:19,239,011)	12 (Anzai et al., 2021; Lo Barco et al., 2021)
	FIN	1:31,246,156 (1:9,968,990-1:3,045,708,636)	
	EST	-	
	AFR	1:5,305,643 (1:2,225,824-1:40,213,116)	
	AMR	1:29,725,472 (1:10,706,387-1:781,475,013)	
	EAS	1:6,817,673 (1:2,572,492-1:113,059,182)	
	SAS	1:3,889,994 (1:1,830,265-1:16,972,762)	
	ASJ	-	

Population abbreviations as defined in gnomAD: NFE, non-Finnish European; FIN, Finnish; EST, Estonian; AFR, African/African American; AMR, Latino/Admixed American; EAS, East Asian; SAS, South Asian; ASJ, Ashkenazi Jewish.

DISCUSSION

This study presents the estimated prevalence of different N-linked protein glycosylation defects calculated from population allele frequencies. As the CDG group involves at least 137 defects, we emphasize that we only included 27 autosomal recessive protein N-glycosylation affecting defects and excluded defects that affect multiple glycosylation pathways.

The used methods make several assumptions and do not take variant- and gene-specific properties into account. For example, the calculations assume that pathogenic variants are independent and not on the same allele. Also, Hardy-Weinberg equilibrium is assumed but may not be present in some populations with more consanguinity. All diseases are considered to result from the biallelic loss-of-function mechanism; however, we cannot exclude the possibility that for some CDG, only specific variants (e.g., certain missense variants) cause the disease.

Also, this method did not consider the possibility that some variant recombinants might not be compatible with life. Since we cannot exclude this phenomenon in these genes, the chance of p.Arg141His homozygosity was also included when calculating the estimated prevalence of PMM2-CDG. However, as seen from the subanalysis of the Estonian population, it does not change the prevalence that much. In Estonia, the estimated prevalence of PMM2-CDG with the exclusion of p.Arg141His homozygosity was 1:77,000, and with inclusion, 1:62,000 (Vals et al., 2018). This example shows that the estimated prevalence of different defects might be somewhat overrated.

On the other hand, some aspects can cause an underestimation of disease prevalence. For example, currently, the data relies on gnomAD variants, and thus ultra-rare pathogenic variants not seen in gnomAD are not counted toward prevalence estimation. Also, only small variants (single nucleotide substitutions and small indels) were included, and thus pathogenic copy-number variants (deletions) may raise the disease prevalence estimators. Regarding missense variants, only those classified as pathogenic in ClinVar were included, while some other missense, as well as synonymous, intronic, and regulatory variants, may truly be pathogenic but missed due to lack of such information in databases. Regarding missense variants, one possibility to improve the estimates would be to include variants with high pathogenicity predictions. However, as shown by Liu et al. (2019) and consistent with our experience (data not shown), this leads to an overestimation of prevalence. Thus, we did not include any missense variant prediction tools in our final calculations. To be on the conservative side, we eliminated all low-quality variants in gnomAD; however, some of them, especially indels, may be true and pathogenic. Of note, presented results rely on data extracted from two publicly available databases, ClinVar and gnomAD, at a single time point. If other databases would have been used, we expect to see slightly different results; however, confidence intervals are shown to address this variability. Moreover, as the databases update both allele frequencies and pathogenicity classifications, a follow-up study in the future is planned to investigate whether the prevalence estimates will change after some years.

Despite many pitfalls, the validation with two well-known recessive diseases—cystic fibrosis and phenylketonuria—proved the method's accuracy and usability for estimating the disease prevalence. From our previous epidemiological studies in Estonia, the prevalence of phenylketonuria is known to be 1:6,700 (Lillevali et al., 2018) correlating with the estimate from gnomAD data is 1:6,604 (95% CI 1:4,269-1:12,073). For cystic fibrosis, the birth prevalence in Estonia is 1:7,743 (Kahre, 2004) comparing well with the calculated estimate 1:8,482 (95% CI 1:5,351-1:16,269). For other well-studied populations like Europeans and Finnish, the data is in good correlation as well (**Supplementary Table 1**).

As shown in **Table 1**, compared to PMM2-CDG, all other N-linked protein glycosylation defects are less common. Still, our reported prevalence of different defects shows compliance with published clinical observations. In 2016, an informal inquiry was conducted in various European laboratories to evaluate the number of screening positive and molecularly confirmed CDG-I and CDG-II patients (Peanne et al., 2017). Based on their results, the most common type 1 N-glycosylation defect in Europe was PMM2-CDG, followed by ALG6-CDG, ALG1-CDG, and MPI-CDG. If we compare this distribution with non-Finnish Europeans, a similar pattern is seen with type 1 N-glycosylation defects. The most common type 2 N-glycosylation defects, according to the inquiry, were MAN1B1-CDG, MGAT2-CDG, and B4GALT1-CDG. In the non-Finnish European population, MAN1B1-CDG is followed by MOGS-CDG, which does not show an abnormal serum transferrin profile with routine CDG screening (De Praeter et al., 2000), and therefore was not reported by laboratories. Compared to these two defects, MGAT2-CDG and B4GALT1-CDG show a much lower prevalence.

Unexpectedly, two recently described defects, FUK-CDG and MAN2B2-CDG, showed the prevalence of higher than one per million. To date, FUK-CDG is described only in two individuals, whereas MAN2B2-CDG only in one (Ng et al., 2018; Verheijen et al., 2020). For *FUK,* we found 119, and for *MAN2B2*, 84 different possibly disease-causing alleles matching our definition of pathogenicity. Disagreement between relatively high estimated prevalence and the low number of reported cases could be explained by the phenomenon where homozygosity or compound heterozygosity of some variants may not be viable, as is the case with p.Arg141His homozygosity in *PMM2* (Matthijs et al., 1998). Also, *FUK* and *MAN2B2* are not included in smaller panels and are only identified by whole-exome sequencing. Theoretically, it may be the cause for the underdiagnosis of these defects to some extent. Notably, one of the pathogenic missense variants reported by Ng et al. (2018), NM_145059.3:c.2980A > C (p.Lys994Gln), reaches allele frequency of 0.002 in the East Asian population, and there is one homozygous individual present in gnomAD. Although mild phenotypes cannot be excluded in gnomAD individuals, also non-pathogenicity of this allele, at least in the homozygous state, should be considered. Of note, *FUK* and *MAN2B2* both lack homozygous LoF variant carriers in gnomAD, which hints that biallelic LoF may be an actual pathogenic mechanism for those genes.

Unlike FUK-CDG and MAN2B2-CDG, other recently described defects (GFUS-CDG, OSTC-CDG, and FUT8-CDG) show lower prevalence.

Although the individual prevalence of each N-linked protein glycosylation defect is very low, the combined prevalence for this group of CDG is notable. If all 27 defects are included, the combined prevalence in non-Finnish Europeans is one in 22,000. If we exclude FUK-CDG and MAN2B2-CDG, the prevalence in Europeans is slightly lower, one in 24,000. Compared to available data (Vals et al., 2018; Lipinski et al., 2021), the expected and observed prevalence differ. The lower observed prevalence might be somewhat underestimated because of undiagnosed patients due to different causes such as unrecognized phenotypes, negative screening results or limited access to different metabolic and molecular studies. In the Estonian population, the combined prevalence of 25 defects is 1:50,000. Therefore, with a yearly birth rate of 13,000–14,000, one individual with protein N-glycosylation defect should be born every 4 years correlating with our clinical data.

In summary, we broaden the knowledge about N-linked protein glycosylation disorders, which hopefully helps raise awareness about the prevalence of this CDG subgroup.

DATA AVAILABILITY STATEMENT

Publicly available datasets were analyzed in this study. These data can be found at: https://gnomad.broadinstitute.org/ and https://www.ncbi.nlm.nih.gov/clinvar/.

AUTHOR CONTRIBUTIONS

SP planned and conducted the study, carried out the statistical analysis, and compiled the manuscript. M-AV planned, conducted the study, analyzed the data, and compiled the manuscript. LM conducted literature review, analyzed the data, and reviewed the manuscript. UŠ and TK analyzed the data and reviewed the manuscript. KÕ planned and conducted the study and reviewed the manuscript. All authors contributed to the article and approved the submitted version.

FUNDING

This work was supported and funded by the Estonian Research Council grants PRG471 and MOBTP175.

SUPPLEMENTARY MATERIAL

The Supplementary Material for this article can be found online at: https://www.frontiersin.org/articles/10.3389/fgene.2021.719437/full#supplementary-material

REFERENCES

Abiramalatha, T., Arunachal, G., Muthusamy, K., and Thomas, N. A. (2019). Family with floppy neonates with severe respiratory insufficiency: A lethal phenotype of RFT1-CDG due to a novel mutation. *Eur. J. Med. Genet.* 62, 248–253. doi: 10.1016/j.ejmg.2018.07.023

Alsubhi, S., Alhashem, A., Faqeih, E., Alfadhel, M., Alfaifi, A., Altuwaijri, W., et al. (2017). Congenital disorders of glycosylation: The Saudi experience. *Am. J. Med. Genet. Part A* 173, 2614–2621.

Altassan, R., Peanne, R., Jaeken, J., Barone, R., Bidet, M., Borgel, D., et al. (2019). International clinical guidelines for the management of phosphomannomutase 2-congenital disorders of glycosylation: Diagnosis, treatment and follow up. *J. Inherit. Metab. Dis.* 42, 5–28.

Anzai, R., Tsuji, M., Yamashita, S., Wada, Y., Okamoto, N., Saitsu, H., et al. (2021). Congenital disorders of glycosylation type IIb with MOGS mutations cause early infantile epileptic encephalopathy, dysmorphic features, and hepatic dysfunction. *Brain Dev.* 43, 402–410. doi: 10.1016/j.braindev.2020.10.013

Balasubramanian, M., Johnson, D. S., and Study, D. D. D. (2019). MAN1B-CDG: Novel variants with a distinct phenotype and review of literature. *Eur. J. Med. Genet.* 62, 109–114. doi: 10.1016/j.ejmg.2018.06.011

Bastaki, F., Bizzari, S., Hamici, S., Nair, P., Mohamed, M., Saif, F., et al. (2018). Single-center experience of N-linked congenital disorders of glycosylation with a summary of molecularly characterized cases in arabs. *Ann. Hum. Genet.* 82, 35–47. doi: 10.1111/ahg.12220

Cechova, A., Altassan, R., Borgel, D., Bruneel, A., Correia, J., Girard, M., et al. (2020). Consensus guideline for the diagnosis and management of mannose phosphate isomerase-congenital disorder of glycosylation. *J. Inherit. Metab. Dis.* 43, 671–693. doi: 10.1002/jimd.12241

De la Morena Barrio, M. E., Sabater, M., de la Morena Barrio, B., Ruhaak, R. L., Minano, A., Padilla, J., et al. (2020). ALG12-CDG: An unusual patient without intellectual disability and facial dysmorphism, and with a novel variant. *Mol. Genet. Genomic Med.* 8:e1304.

De Praeter, C. M., Gerwig, G. J., Bause, E., Nuytinck, L. K., Vliegenthart, J. F., Breuer, W., et al. (2000). A novel disorder caused by defective biosynthesis of N-linked oligosaccharides due to glucosidase I deficiency. *Am. J. Hum. Genet.* 66, 1744–1756. doi: 10.1086/302948

Ferreira, C. R., Rahman, S., Keller, M., Zschocke, J., and Group, I. A. (2021). An international classification of inherited metabolic disorders (ICIMD). *J. Inherit. Metab. Dis.* 44, 164–177.

Hock, M., Wegleiter, K., Ralser, E., Kiechl-Kohlendorfer, U., Scholl-Burgi, S., Fauth, C., et al. (2015). ALG8-CDG: novel patients and review of the literature. *Orphanet J. Rare Dis.* 10:73.

Kahre, T. (2004). *Cystic fibrosis in Estonia*. Tartu: Tartu University Press.

Karczewski, K. J., Francioli, L. C., Tiao, G., Cummings, B. B., Alfoldi, J., Wang, Q., et al. (2020). The mutational constraint spectrum quantified from variation in 141,456 humans. *Nature* 581, 434–443.

Landrum, M. J., Lee, J. M., Benson, M., Brown, G. R., Chao, C., Chitipiralla, S., et al. (2018). ClinVar: improving access to variant interpretations and supporting evidence. *Nucleic Acids Res.* 46, D1062–D1067.

Lekka, D. E., Brucknerova, J., Salingova, A., Sebova, C., Ostrozlikova, M., Ziburova, J., et al. (2021). Congenital disorders of glycosylation - an umbrella term for rapidly expanding group of rare genetic metabolic disorders - importance of physical investigation. *Bratisl. Lek. Listy.* 122, 190–195. doi: 10.4149/bll_2021_030

Lillevali, H., Reinson, K., Muru, K., Simenson, K., Murumets, U., Mols, T., et al. (2018). Hyperphenylalaninaemias in estonia: genotype-phenotype correlation and comparative overview of the patient cohort before and after nation-wide neonatal screening. *JIMD Rep.* 40, 39–45. doi: 10.1007/8904_2017_61

Lipinski, P., Bogdanska, A., and Tylki-Szymanska, A. (2021). Congenital disorders of glycosylation: Prevalence, incidence and mutational spectrum in the Polish population. *Mol. Genet. Metab. Rep.* 27:100726. doi: 10.1016/j.ymgmr.2021.100726

Liu, W., Pajusalu, S., Lake, N. J., Zhou, G., Ioannidis, N., Mittal, P., et al. (2019). Estimating prevalence for limb-girdle muscular dystrophy based on public sequencing databases. *Genet. Med.* 21, 2512–2520. doi: 10.1038/s41436-019-0544-8

Lo Barco, T., Osanni, E., Bordugo, A., Rodella, G., Iascone, M., Tenconi, R., et al. (2021). Epilepsy and movement disorders in CDG: Report on the oldest-known MOGS-CDG patient. *Am. J. Med. Genet. Part A* 185, 219–222. doi: 10.1002/ajmg.a.61916

Matthijs, G., Schollen, E., Van Schaftingen, E., Cassiman, J. J., and Jaeken, J. (1998). Lack of homozygotes for the most frequent disease allele in carbohydrate-deficient glycoprotein syndrome type 1A. *Am. J. Hum. Genet.* 62, 542–550. doi: 10.1086/301763

Medrano, C., Vega, A., Navarrete, R., Ecay, M. J., Calvo, R., Pascual, S. I., et al. (2019). Clinical and molecular diagnosis of non-phosphomannomutase 2 N-linked congenital disorders of glycosylation in Spain. *Clin. Genet.* 95, 615–626. doi: 10.1111/cge.13508

Moller, R. S., Larsen, L. H., Johannesen, K. M., Talvik, I., Talvik, T., Vaher, U., et al. (2016). Gene panel testing in epileptic encephalopathies and familial epilepsies. *Mol. Syndromol.* 7, 210–219. doi: 10.1159/000448369

Ng, B. G., Rosenfeld, J. A., Emrick, L., Jain, M., Burrage, L. C., Lee, B., et al. (2018). Pathogenic variants in fucokinase cause a congenital disorder of glycosylation. *Am. J. Hum. Genet.* 103, 1030–1037. doi: 10.1016/j.ajhg.2018.10.021

Ng, B. G., Shiryaev, S. A., Rymen, D., Eklund, E. A., Raymond, K., Kircher, M., et al. (2016). ALG1-CDG: clinical and molecular characterization of 39 unreported patients. *Hum. Mutat.* 37, 653–660.

Ondruskova, N., Cechova, A., Hansikova, H., Honzik, T., and Jaeken, J. (2021). Congenital disorders of glycosylation: Still "hot" in 2020. *Biochim. Biophys. Acta Gen. Subj.* 1865:129751. doi: 10.1016/j.bbagen.2020.129751

Peanne, R., de Lonlay, P., Foulquier, F., Kornak, U., Lefeber, D. J., Morava, E., et al. (2017). Congenital disorders of glycosylation (CDG): Quo vadis? *Eur. J. Med. Genet.* 61, 643–663. doi: 10.1016/j.ejmg.2017.10.012

Quelhas, D., Jaeken, J., Fortuna, A., Azevedo, L., Bandeira, A., Matthijs, G., et al. (2019). RFT1-CDG: absence of epilepsy and deafness in two patients with novel pathogenic variants. *JIMD Rep.* 43, 111–116. doi: 10.1007/8904_2018_112

Schollen, E., Kjaergaard, S., Legius, E., Schwartz, M., and Matthijs, G. (2000). Lack of Hardy-Weinberg equilibrium for the most prevalent PMM2 mutation in CDG-Ia (congenital disorders of glycosylation type Ia). *Eur. J. Hum. Genet.* 8, 367–371. doi: 10.1038/sj.ejhg.5200470

Sturiale, L., Bianca, S., Garozzo, D., Terracciano, A., Agolini, E., Messina, A., et al. (2019). ALG12-CDG: novel glycophenotype insights endorse the molecular defect. *Glycoconj. J.* 36, 461–472. doi: 10.1007/s10719-019-09890-2

Tahata, S., Gunderson, L., Lanpher, B., and Morava, E. (2019). Complex phenotypes in ALG12-congenital disorder of glycosylation (ALG12-CDG): Case series and

review of the literature. *Mol. Genet. Metab.* 128, 409–414. doi: 10.1016/j.ymgme.2019.08.007

Vals, M. A., Pajusalu, S., Kals, M., Magi, R., and Ounap, K. (2018). The Prevalence of PMM2-CDG in estonia based on population carrier frequencies and diagnosed patients. *JIMD Rep.* 39, 13–17. doi: 10.1007/8904_2017_41

Verheijen, J., Wong, S. Y., Rowe, J. H., Raymond, K., Stoddard, J., Delmonte, O. M., et al. (2020). Defining a new immune deficiency syndrome: MAN2B2-CDG. *J. Allergy Clin. Immunol.* 145, 1008–1011. doi: 10.1016/j.jaci.2019.11.016

Vuillaumier-Barrot, S., Schiff, M., Mattioli, F., Schaefer, E., Dupont, A., Dancourt, J., et al. (2019). Wide clinical spectrum in ALG8-CDG: clues from molecular findings suggest an explanation for a milder phenotype in the first-described patient. *Pediatr. Res.* 85, 384–389. doi: 10.1038/s41390-018-0231-5

Yildiz, Y., Arslan, M., Celik, G., Kasapkara, C. S., Ceylaner, S., Dursun, A., et al. (2020). Genotypes and estimated prevalence of phosphomannomutase 2 deficiency in Turkey differ significantly from those in Europe. *Am. J. Med. Genet. Part A* 182, 705–712. doi: 10.1002/ajmg.a.61488

Conflict of Interest: The authors declare that the research was conducted in the absence of any commercial or financial relationships that could be construed as a potential conflict of interest.

Publisher's Note: All claims expressed in this article are solely those of the authors and do not necessarily represent those of their affiliated organizations, or those of the publisher, the editors and the reviewers. Any product that may be evaluated in this article, or claim that may be made by its manufacturer, is not guaranteed or endorsed by the publisher.

frontiers in Genetics

MINI REVIEW
published: 03 September 2021
doi: 10.3389/fgene.2021.734878

GM1 Gangliosidosis—A Mini-Review

*Elena-Raluca Nicoli[1], Ida Annunziata[2], Alessandra d'Azzo[2,3], Frances M. Platt[4], Cynthia J. Tifft[1,5] and Karolina M. Stepien[6,7]**

[1] Glycosphingolipid and Glycoprotein Disorders Unit, Medical Genetics Branch, National Human Genome Research Institute, National Institutes of Health, Bethesda, MD, United States, [2] Department of Genetics, St. Jude Children's Research Hospital, Memphis, TN, United States, [3] Department of Anatomy and Neurobiology, College of Graduate Health Sciences, University of Tennessee Health Science Center, Memphis, TN, United States, [4] Department of Pharmacology, University of Oxford, Oxford, United Kingdom, [5] Office of the Director, National Human Genome Research Institute, National Institutes of Health, Bethesda, MD, United States, [6] Adult Inherited Metabolic Disorders, Salford Royal NHS Foundation Trust, Salford, United Kingdom, [7] Division of Diabetes, Endocrinology and Gastroenterology, University of Manchester, Manchester, United Kingdom

GM1 gangliosidosis is a progressive, neurosomatic, lysosomal storage disorder caused by mutations in the *GLB1* gene encoding the enzyme β-galactosidase. Absent or reduced β-galactosidase activity leads to the accumulation of β-linked galactose-containing glycoconjugates including the glycosphingolipid (GSL) GM1-ganglioside in neuronal tissue. GM1-gangliosidosis is classified into three forms [Type I (infantile), Type II (late-infantile and juvenile), and Type III (adult)], based on the age of onset of clinical symptoms, although the disorder is really a continuum that correlates only partially with the levels of residual enzyme activity. Severe neurocognitive decline is a feature of Type I and II disease and is associated with premature mortality. Most of the disease-causing β-galactosidase mutations reported in the literature are clustered in exons 2, 6, 15, and 16 of the *GLB1* gene. So far 261 pathogenic variants have been described, missense/nonsense mutations being the most prevalent. There are five mouse models of GM1-gangliosidosis reported in the literature generated using different targeting strategies of the *Glb1* murine locus. Individual models differ in terms of age of onset of the clinical, biochemical, and pathological signs and symptoms, and overall lifespan. However, they do share the major abnormalities and neurological symptoms that are characteristic of the most severe forms of GM1-gangliosidosis. These mouse models have been used to study pathogenic mechanisms, to identify biomarkers, and to evaluate therapeutic strategies. Three *GLB1* gene therapy trials are currently recruiting Type I and Type II patients (NCT04273269, NCT03952637, and NCT04713475) and Type II and Type III patients are being recruited for a trial utilizing the glucosylceramide synthase inhibitor, venglustat (NCT04221451).

Keywords: GM1 gangliosidosis, glycoconjugates metabolism, beta galactosidase, gene therapy, mouse model

OPEN ACCESS

Edited by:
Desheng Liang,
Central South University, China

Reviewed by:
Baoheng Gui,
The Second Affiliated Hospital of Guangxi Medical University, China
Yao Zhang,
Peking University First Hospital, China
Konrad Sandhoff,
University of Bonn, Germany

***Correspondence:**
Karolina M. Stepien
kstepien@doctors.org.uk

Specialty section:
This article was submitted to Genetics of Common and Rare Diseases, a section of the journal Frontiers in Genetics

Received: *01 July 2021*
Accepted: *16 August 2021*
Published: *03 September 2021*

Citation:
Nicoli E-R, Annunziata I, d'Azzo A, Platt FM, Tifft CJ and Stepien KM (2021) GM1 Gangliosidosis—A Mini-Review. Front. Genet. 12:734878. doi: 10.3389/fgene.2021.734878

Abbreviations: BBB, Blood-brain barrier; β-GAL, β-galactosidase; EBP, Elastin binding protein; PPCA, Protective protein/cathepsin A; NEU1, α-neuraminidase 1; CNS, Central nervous system; CRISPR/Cas9, Clustered regularly interspaced short palindromic repeats and CRISPR-associated protein 9; TALEN, Transcription activator-like effector nucleases; ERT, Enzyme replacement therapy; EET, Enzyme enhancement therapy; SRT, Substrate reduction therapy; AAV, Adeno-associated virus; ICV, Intracerebroventricular; mTfR, Mouse transferrin receptor; *N*B-DNJ, *N*-butyldeoxynojirimycin; miglustat; NOEV, N-octyl-4-epi-β-valienamine; HGMD, Human Gene Mutation Database; Cer, Ceramide; GlcCer, Glucosylceramide; LacCer, Lactosylceramide; GA2, Asialo-GM2 (GalNAc1,4Gal1,4Glc1Cer); GA1, Asialo-GM1 (Gal1,3GalNAc1,4Gal1,4Glc1Cer); GM3, Neu5Ac2,3Gal1,4Glc1Cer; GM2, GalNAc1,4(Neu5Ac2,3)Gal1,4Glc1Cer; GM1a, GM1 [Gal1,3GalNAc1,4(Neu5Ac2,3)Gal1,4Glc1Cer]; Glc, Glucose; Gal, Galactose.

INTRODUCTION

Glycoconjugates play a key role in cellular function and are tightly regulated both in terms of biosynthesis and catabolism. β-Galactosidase (β-GAL) is a lysosomal hydrolase that cleaves β-linked galactose residues from the non-reducing end of glycan moieties found in various glycoconjugates. Reduction in β-GAL activity leads to the accumulation of GM1 ganglioside and its asialo derivative GA1, primarily in lysosomes of neuronal tissue (Caciotti et al., 2011; Jarnes Utz et al., 2017). The first description of GM1 and GA1 storage was made in a case of amaurotic idiocy (as it was then called), now called GM1 gangliosidosis (Jatzkewitz and Sandhoff, 1963). In addition to the storage of GM1 ganglioside, other glycoconjugates with β-galactose at the non-reducing end are detectable in high concentration in patients' urine, including N-linked glycans, and various O-linked glycans (Lawrence et al., 2019). These disease-related β-linked galactose-terminal oligosaccharides arise from the lysosomal breakdown of glycoproteins that are stored in the brain (Tsay and Dawson, 1976), liver (Holmes and O'Brien, 1978), and other biological fluids including urine (Brunetti-Pierri and Scaglia, 2008; Bruggink et al., 2012) and amniotic fluid (Piraud et al., 2017). The significant proportion of these soluble glycans are metabolites of incompletely degraded *N*-linked glycans, such as A1G1, A2G2, A3G3, and A4G4. The *N*-glycan metabolite A2G2 was proposed to be a surrogate glycan biomarker of GM1 gangliosidosis (Lawrence et al., 2019).

GM1 gangliosidosis is an example of a family of inherited metabolic disorders termed lysosomal storage diseases. The estimated incidence of GM1 gangliosidosis is 1:100,000–200,000 live births (Brunetti-Pierri and Scaglia, 2008). However, some forms of the disease appear to be more prevalent in specific geographical areas, including Southern Brazil and Japan and among the Roma (Yoshida et al., 1991; Severini et al., 1999; Sinigerska et al., 2006).

GM1 presents with a continuum of disease severity but patients are loosely classified based on the age of onset of the symptoms into Type I (infantile), Type II (late-infantile and juvenile) and Type III (adult). In principle, disease severity should inversely correlate with residual enzyme activity levels. However, β-GAL activity is mostly measured with the synthetic fluorogenic substrate 4-methyl-umbelliferyl-β-D-galactopyranoside, which may not be accurate enough to estimate the clinical course of the disease on the basis of the measured residual enzyme activity (Inui et al., 1990; Caciotti et al., 2011; Ferreira and Gahl, 2017; **Figure 1**).

Bi-allelic mutations in *GLB1* result in a reduction in β-GAL activity and the build-up of GM1 ganglioside in multiple tissues including the brain (Brunetti-Pierri and Scaglia, 2008; Karimzadeh et al., 2017; Rha et al., 2021) leading to severe neurodegeneration resulting in morbidity and premature mortality (Ferreira and Gahl, 2017). More than 200 disease-causing mutations have been identified across the *GLB1* gene, particularly in exons 2, 6, 15, and 16 (**Figure 2**).

A smaller subset of mutations predominantly near the 3′ end of *GLB1* can result in another lysosomal storage disease, Morquio B disease (mucopolysaccharidosis type IVB), which is characterized by primary lysosomal accumulation of the glycosaminoglycan keratan sulfate. Morquio B patients have predominantly skeletal abnormalities without the neurodegenerative aspects of GM1 gangliosidosis (Ferreira and Gahl, 2017). Cases with phenotypic features of both GM1 gangliosidosis and Morquio B disease have also been described (Mayer et al., 2009).

Distinct *GLB1* gene mutations that affect the affinity of the enzyme for the two main substrates, GM1 ganglioside and keratan sulfate, explain at least in part the different clinical manifestations and the degree and type of storage material (**Figure 2**).

Five murine models have been developed that mimic the human phenotype and have formed that basis of our current understanding of disease pathogenesis. They have also been instrumental in the trialing of new therapies.

Comprehensive reviews of GM1 gangliosidosis have been recently published (Regier et al., 1993; Breiden and Sandhoff, 2019; Lawrence et al., 2019; Lang et al., 2020; Rha et al., 2021). In this mini review, we will focus on the clinical spectrum of disease and genetic variants, our current understanding of disease pathogenesis, the utility of available animal models and approaches to therapy for these devastating disorders.

CLINICAL MANIFESTATIONS

Among the three subtypes of GM1 gangliosidosis, the infantile form is the most severe, with onset of symptoms before 6 months of age and death early in childhood (Jarnes Utz et al., 2017; Lang et al., 2020). One of the earliest signs that can be seen in infantile disease prenatally is hydrops fetalis, which is associated with many severe cases of LSDs (Stone and Sidransky, 1999), and should stimulate an investigation into the underlying causes of this phenotype (Iyer et al., 2021). The early diagnosis of infantile onset disease would have the greatest chance of successful therapeutic intervention.

Type II consists of late infantile and juvenile subtypes (**Figure 1**). Late infantile disease patients meet developmental milestones at 12 months but have onset of symptoms generally between 12 and 24 months. Patients quickly lose the ability to ambulate and have difficulty swallowing and handling secretions necessitating gastrostomy placement. Late infantile patients succumb to their illness by the mid second decade.

Juvenile patients have onset at 3–5 years of age, having learned to walk, run, and speak in sentences. The first symptoms may be unsteady gait, frequent falls, and "slurring" of speech progressing to ataxia and dysarthria. Children become unable to walk without assistance then lose the ability to walk. Dysarthria progresses to inability to swallow effectively and subsequent weight loss, necessitating gastrostomy tube placement. Children with juvenile onset disease can live into their 4th decade of life (Regier et al., 1993, 2016; Jarnes Utz et al., 2017).

Adult onset GM1 represents with an attenuated form with slower disease progression and very mild dysmorphic features (Suzuki et al., 2001) and greater clinical variability (Tonin et al., 2019). The onset of symptoms occurs in early

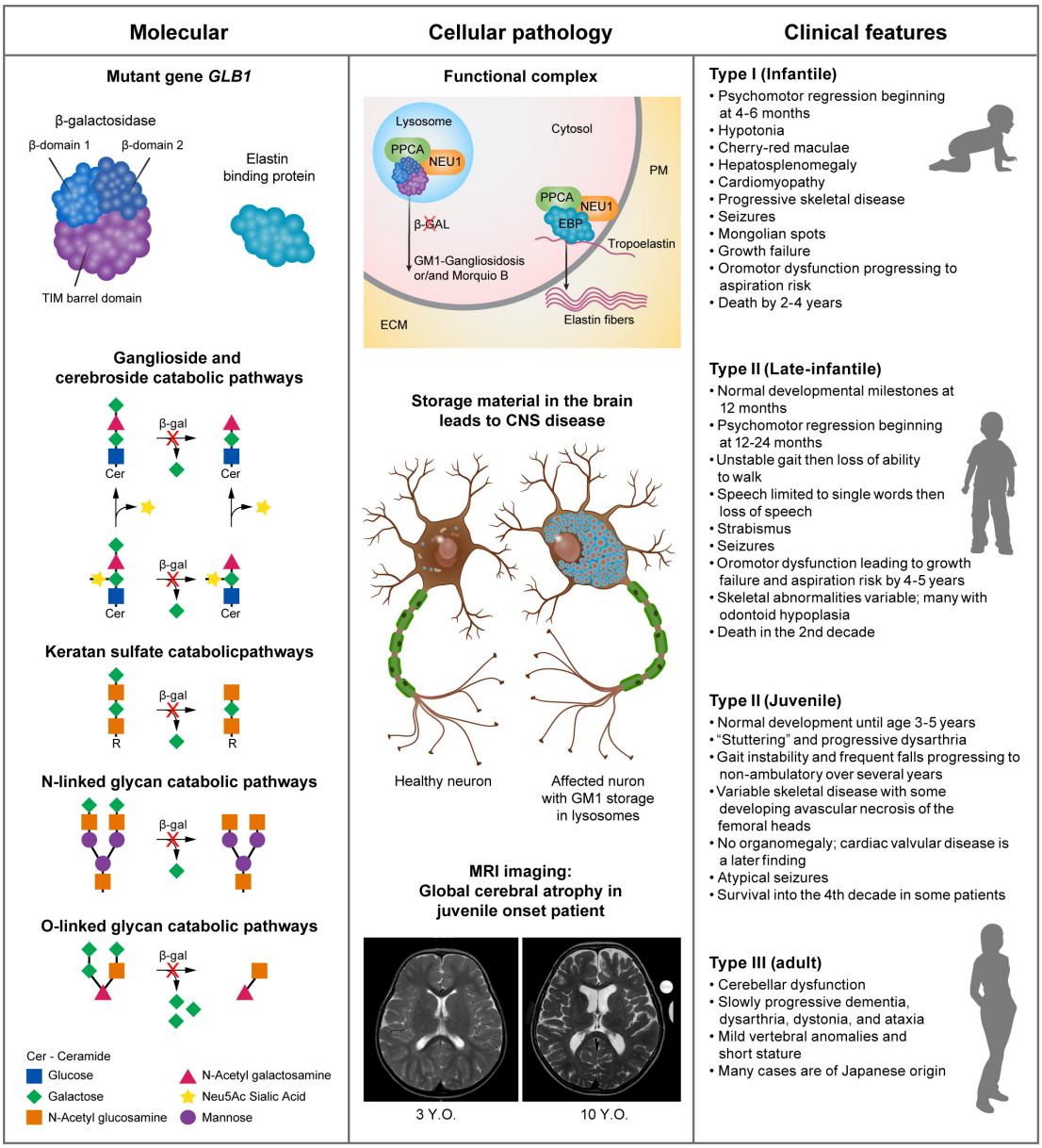

FIGURE 1 | Pathogenesis and clinical manifestations. Panel 1: human β-GAL is composed of a catalytic TIM barrel domain followed by β-domain 1 and β-domain 2 (Ohto et al., 2012). Mutations in the *GLB1* gene lead to impaired enzyme activity, which results in the progressive accumulation of complex gangliosides, specifically GM1. This, in turn, initiates a series of pathogenic events that ultimately lead to neurodegeneration (Kolter, 2012; Annunziata et al., 2018). Panel 2: through alternative splicing, the *GLB1* gene gives rise to two transcripts, one encoding the hydrolytic enzyme β-galactosidase and the other the elastin binding protein (EBP). The primary role of EBP is to chaperone the deposition of elastin fibers in the extracellular matrix (ECM). β-galactosidase (GLB1) and EBP are found in complex with PPCA and NEU1 in lysosomes and the plasma membrane (PM), respectively (Caciotti et al., 2005; Bonten et al., 2014). Panel 3: although GM1 gangliosidosis is a disease continuum it can be loosely divided into 3 types, with Type II having 2 subtypes. The common use of a synthetic fluorogenic substrate to measure β-GAL activity makes it difficult to establish an accurate correlation between residual enzyme activity and clinical outcome. This may also be complicated by the regulatory and post posttranslational mechanisms that influence GM1-ganglioside catabolism and may vary among patients (Breiden and Sandhoff, 2019). The main symptoms of the disease commonly found in each type/subtype are summarized.

childhood to late teens, as described in individuals of Japanese descent (Inui et al., 1990; Arash-Kaps et al., 2019).

Patients with all types of GM1 gangliosidosis can have variable skeletal disease including pectus carinatum with spine and rib changes that lead to restrictive lung disease (Ferreira et al., 2020). Radiographic changes can allow differentiation between the late-infantile and juvenile forms of Type II disease. Odontoid hypoplasia, as observed in all late infantile patients but not juvenile patients, requires cervical spine evaluation in late infantile patients prior to anesthesia, and anesthetic care

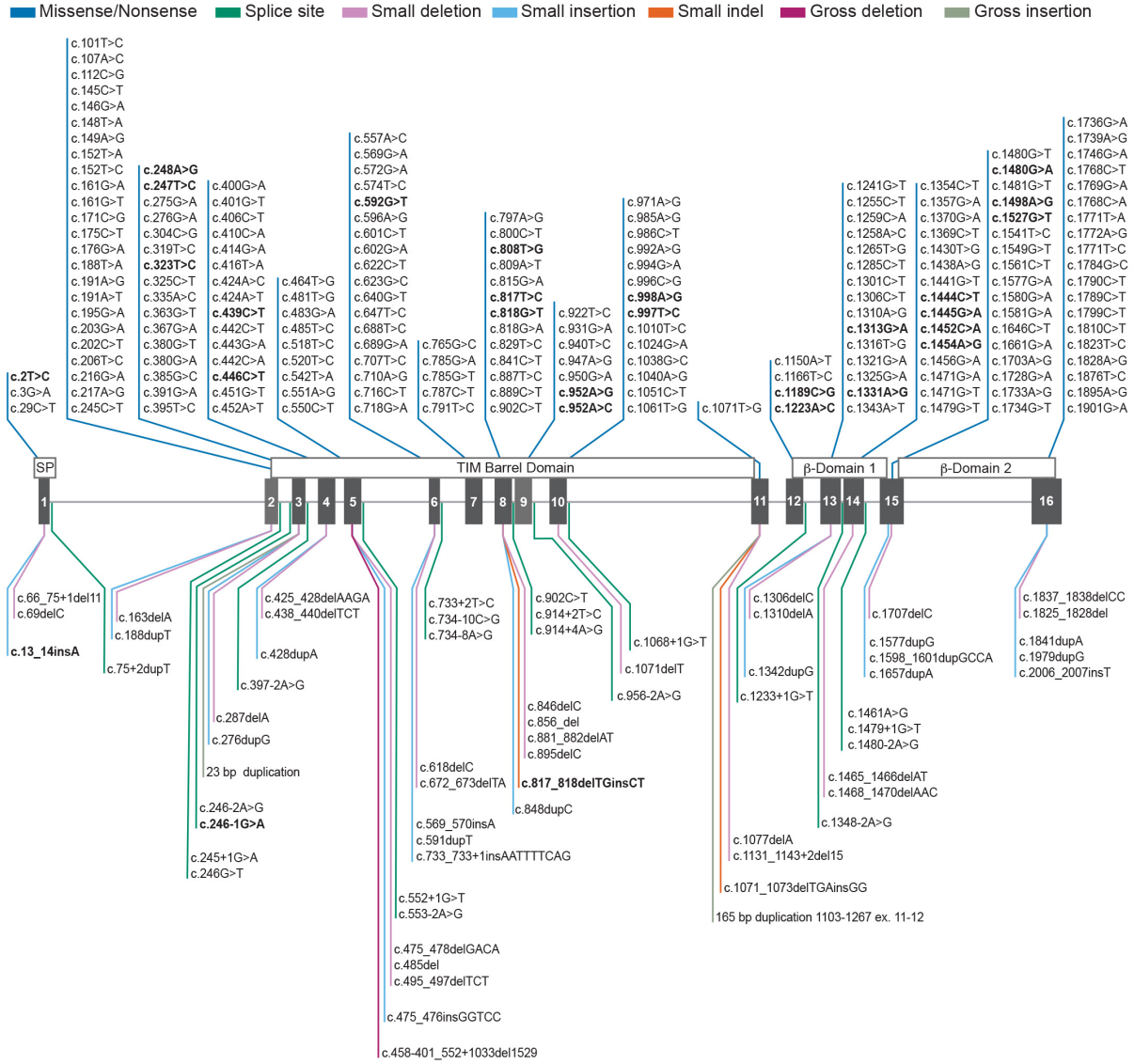

FIGURE 2 | Genotypes in GM1 gangliosidosis. Schematic representation of 261 *GLB1* variants with a reported phenotype of GM1-gangliosidosis and/or Morquio B registered in the database HGMD (2021) updated with the novel variants from Tebani et al. (2021). The *GLB1* gene is located on the short arm of chromosome 3 (3p21.33). GM1 gangliosidosis and Morquio B disease result from biallelic mutations in *GLB1* gene. Mutations affecting the catalytical site of the β-GAL enzyme may reduce or eliminate the degradation of GM1 substrate. *GLB1* cDNA sequence NM_000404.4; Ref SeqGene NG_009005.1; 194 Missense/Nonsense (dark blue), 20 Splicing substitutions (dark green), 25 small deletions (pink), 17 small insertion/duplications (light blue), 2 small indels (orange), 1 gross deletion (purple), 2 gross insertion/duplications (light green). Bold text represents GM1 gangliosidosis and/or Morquio B reported phenotypes. A summary of the 261 reported variants with a phenotype of GM1 gangliosidosis and/or Morquio B disease can be found at ***GLB1*** (HGMD, 2021; Tebani et al., 2021). The main domains of the protein are shown above the exons. For a full description on the clinical pathogenicity of each variant the database ClinVar (Landrum et al., 2018) provides information about genomic variation and its relationship to human health at ***GLB1*** (ClinVar, 2021).

optimally provided by pediatric anesthesiologists with experience in patients with cervical spine pathology to prevent perioperative morbidity or mortality (Ferreira et al., 2020).

The progressive nature of the neurological disease in GM1 gangliosidosis requires close monitoring. Biomarkers in blood, urine, and CSF biomarkers may be potentially useful in this regard (Gray-Edwards et al., 2017a,b; Rha et al., 2021). Disease progression can also be monitored using minimally invasive neuroimaging. In Type II disease both late infantile and juvenile patients demonstrate progressive atrophy in the cerebrum and cerebellum with greater variability and slower progression in the juvenile subtype. Quantitative magnetic resonance spectroscopy (MRS) shows increasing deficits of *N*-acetyl aspartate (NAA) across many brain regions with greater and swifter deficits seen in

the more rapidly progressive late infantile subtype (Regier et al., 2016). These biomarkers of disease progression also correlate with developmental progression of disease and may serve as useful outcome measures for clinical trials.

In contrast to GM1 gangliosidosis, Morquio B disease (**Figure 2**) patients do not have CNS disease but can have neurologic compromise due to underlying skeletal disease, such as spinal nerve compression (Abumansour et al., 2020).

GENOTYPES

There is a poor genotype-phenotype correlation in GM1 gangliosidosis demonstrated by the clinical variability in age of onset and progression of disease even between siblings with the same genotype. One can speculate that polymorphisms or mutations in the other genes of the β-GAL complex, protective protein/cathepsin A (PPCA) and neuraminidase 1 (NEU1) (see **Figure 1**) may account for this variability. An additional limitation to reach an accurate genotype-phenotype correlation is posed by the way the enzyme assay is commonly performed using a soluble fluorogenic substrate that does not reflect the topology and membrane microenvironment of the natural substrate, GM1 ganglioside. Moreover, regulatory, and post-translational mechanisms that modulate GM1 catabolism further hamper an accurate prediction of the clinical course of the disease in patients, if based only on residual enzyme activity against the synthetic substrate (Breiden and Sandhoff, 2019).

Most patients with GM1 gangliosidosis are compound heterozygotes and aside from biallelic null mutations that produce type I disease, it is difficult to attribute specific phenotypes to any single mutation. Generalizations based on crystallographic structure of the β-GAL enzyme have been attempted (Ohto et al., 2012). Mutations associated with type I/infantile onset GM1 gangliosidosis, for the most part, are located in the core protein region causing β-gal instability, whereas mutations associated with milder phenotypes, such as types II and III GM1 gangliosidosis, tend to be on the protein surface (Morita et al., 2009; Ohto et al., 2012; Rha et al., 2021). Recently, the determination of the 3D structure of murine β-gal in complex with PPCA has revealed that some mutations at conserved amino acid residues found in GM1 gangliosidosis patients affect formation of the complex (Gorelik et al., 2021). These findings further complicate genotype-phenotype correlation, in relation to the penetrance of specific disease phenotypes.

Out of the total 261 reported pathogenic variants associated with a phenotype of GM1 gangliosidosis and/or Morquio B disease, most of them are missense/nonsense (194), and the rest are splicing substitutions (20), small deletions (25), small insertion/duplications (17), small indels (2), gross insertion/duplications (2), and a single large deletion (**Figure 2**). The largest number of mutations are found in exons 2 (26 variants), 6 (23 variants), 15 (21 variants) and 16 (24 variants). Previous reports implicate exons 2, 6, and 15 (Brunetti-Pierri and Scaglia, 2008) as hot spots for mutations, however exon 16 also harbors multiple pathogenic variants.

MOUSE MODELS

The first two genetically engineered mouse models of GM1 gangliosidosis were reported in 1997 by two groups (Hahn et al., 1997) and (Matsuda et al., 1997a,b). These knockout mice were generated by homologous recombination at the murine *Glb1* locus that disrupted the gene by introducing a selectable marker cassette in either exon 6 or exon 15 (Hahn et al., 1997; Matsuda et al., 1997a,b). Both mouse models closely recapitulated the infantile/juvenile onset form of GM1 gangliosidosis and have been used extensively for studying disease pathogenesis and for testing therapeutic modalities (**Table 1**).

The β-$gal^{-/-}$ mice described by Hahn et al. (1997) showed substantial early neuronal loss in the brain and spinal cord (Tessitore et al., 2004). GM1 is abundant in the neuronal plasma membrane (PM) and is the only ganglioside that can influence Ca^{2++} transfer across membranes by interacting with Ca^{2+}-binding proteins (Ledeen and Wu, 2015; Annunziata et al., 2018). In β-$gal^{-/-}$ neurons impaired lysosomal degradation of GM1 results in the abnormal accumulation of the ganglioside in internal membranes, specifically those of the ER resulting in two pathogenic effects: (1) it enhances the flux of Ca^{2+} out of the ER, thereby altering ER Ca^{2+} levels, which activates an unfolded protein response (UPR) (Tessitore et al., 2004); and (2) it increases the number of membrane contact sites between the ER and mitochondria, known as mitochondria associated ER membranes (MAMs). These GM1-enriched microdomains mediate the abnormal flux of Ca^{2+} from the ER to the mitochondria, which ultimately results in mitochondria Ca^{2+} overload (Sano et al., 2009). The combination of these Ca^{2+}-dependent pathogenic events steers the simultaneous activation of UPR and mitochondria-mediated neuronal apoptosis (Tessitore et al., 2004; Sano et al., 2009). In addition, the progressive neurodegeneration in these mice elicits a widespread neuroinflammatory response, accompanied by the release of cytokines and chemokines in the brain interstitial fluid and the CSF (Jeyakumar et al., 2003; Sano et al., 2005), which likely accelerates CNS disease. This neuroinflammatory response was shown to favor the recruitment of genetically modified BM monocytes expressing a therapeutic β-*gal* enzyme, following *ex vivo* gene therapy in β-$gal^{-/-}$ mice (Sano et al., 2005) (see below).

With the development of new gene editing approaches, additional β-*gal* deficient mouse models have been more recently generated using either TALEN or CRISPR/Cas9 technologies (Przybilla et al., 2019; Eikelberg et al., 2020; Liu et al., 2021). Using CRISPR/Cas9 Przybilla et al. (2019) engineered a knock-out mouse model by introducing a deletion in exon 8 of the *Glb1* gene. Phenotypic alterations in these mice were evaluated using behavioral tests that showed profound neurocognitive impairment (Przybilla et al., 2019). In Eikelberg et al. (2020) described a knock-out model using TALENs to target exon 15 of *Glb1*. These mice display brain and spinal cord pathology, characterized by swelling of axons and loss of myelin, leading to abnormal electrophysiological activity of neurons (Eikelberg et al., 2020). This is the first electrophysiological study performed in a mouse model of the disease, showing abnormalities

TABLE 1 | Overview of developed GM1 gangliosidosis mouse models: characteristics and therapies tested.

	Genotype	*Glb1*$^{-/-}$ or *Glb1*^{tm1Adz}/knock-out (Hahn et al., 1997)	*Glb1*$^{-/-}$ or *Glb1*^{tm1Jmat}/knock-out (Matsuda et al., 1997a,b)	*Glb1*$^{-/-}$ or β-*gal*$^{-/-}$/knock-out (Przybilla et al., 2019)	*Glb1*$^{-/-}$/knock-out (Eikelberg et al., 2020)	*Glb1*$^{(G455R)}$/knock-i (Liu et al., 2021)
	Exon targeted	6	15	8	15	14
	Technology used to generate	Homologous recombination and embryonic stem cell technology	Homologous recombination and embryonic stem cell technology	CRISPR/Cas9	TALEN	CRISPR/Cas9
Evaluations	Life span	∼6–7 months	∼7–10 months	∼10 months	∼8 months is the last experimental timepoint reported	∼11 months
	Gross neurological and behavioral symptoms	∼4–5 months	∼6–8 months	∼6 months	∼3.5–4 months	∼4–8 months
	β-gal activity	∼0–2%	∼0–10%	∼0–13%	∼0–12%	∼0–3%
	mRNA status	Absent	n/a	n/a	Shortened mRNA	Retention of mutant mRNA
	GM1 levels compared to control	∼2–7×	∼4–6	∼2–4%	∼2–15×	∼4×
	Histopathology and morphologic analyses	At 3 weeks of age, swollen neurons containing storage material. At the EM level, neurons at the same age show pleiomorphic inclusions	Vacuolated lymphocytes in peripheral blood. No evident skeletal dysplasia. Degenerated neurons with distended cytoplasm and multilamellar and myelin-like inclusion bodies.	Impaired neurocognitive function (Barnes maze and spontaneous alteration T-maze tests)	Axonopathy and reduction of membrane resistance (electrophysiology and single cell electroporation experiments).	Inflammatory response and abnormal autophagy in the brains: CNS inflammation with activated microglia and abnormal autophagy
	Therapy	• ERT (Chen et al., 2020) • SRT (Jeyakumar et al., 2003; Kasperzyk et al., 2004, 2005; Elliot-Smith et al., 2008) • *Ex vivo* gene therapy (Sano et al., 2005) • *In vivo* gene therapy (Broekman et al., 2007; Baek et al., 2010; Weismann et al., 2015; Hinderer et al., 2020)	• ERT (Matsuda et al., 2003; Suzuki, 2006, 2008; Suzuki et al., 2007, 2012; Takai et al., 2013) • *In vivo* gene therapy (Takaura et al., 2003)	• ERT (Przybilla et al., 2021)	n/a	n/a

that the authors attribute to increased neuronal cell size and reduced membrane resistance. The most recent β-*gal* mutant mouse generated using CRISPR/Cas9 is a knock-in model that introduces a human missense mutation in exon 14 of *Glb1*, described in a patient with late-infantile GM1 gangliosidosis (Liu et al., 2021). The CNS phenotype in this model included impaired motor function, as well as extensive microgliosis, accompanied by activation of autophagy (Liu et al., 2021). The characteristics of available mouse models are summarized in **Table 1**.

THERAPEUTIC STRATEGIES

Until very recently, therapy for GM1 gangliosidosis was limited to symptomatic management. However, several experimental therapies have been trialed in murine (**Table 1**) and feline models (Gray-Edwards et al., 2017a,b, 2020). Since GM1 primarily affects the brain, targeted delivery must traverse the blood-brain barrier (BBB) or be delivered directly to the brain. Experimental therapies are discussed below.

Substrate Reduction Therapy

The rationale of Substrate Reduction Therapy (SRT) is to use small molecule inhibitors of enzymes responsible for the biosynthesis of stored substrates (Jeyakumar et al., 2002; Platt et al., 2018). For example miglustat, is a *N*-alkylated iminosugar that is a reversible competitive inhibitor of glucosylceramide synthase, the enzyme catalyzing the first committed step in the biosynthesis of most glycosphingolipids, including gangliosides (Platt et al., 1994). This approach aims to balance the rate of glycosphingolipid biosynthesis with the impaired rate of glycosphingolipid catabolism (Platt et al., 2001). Miglustat crosses the BBB and so can in principle be applied to treat glycosphingolipid storage diseases affecting the periphery and the brain (Cox et al., 2000; Kasperzyk et al., 2004, 2005; Patterson et al., 2007; Treiber et al., 2007; Ficicioglu, 2008). Miglustat was approved for treating type 1 Gaucher disease in 2002 and for Niemann-Pick disease type C in 2009 (Platt et al., 2018). Miglustat has also been proposed for the treatment of GM1 gangliosidosis. Indeed, miglustat reduced GM1 ganglioside in the central nervous system of a mouse model of GM1 gangliosidosis (Kasperzyk et al., 2004), and led to functional improvements and a decrease in brain inflammation (Kasperzyk et al., 2004; Treiber et al., 2007; Elliot-Smith et al., 2008).

Despite the demonstrated effectiveness of miglustat in other storage disorders, its use in GM1 gangliosidosis type II has been tested only in a few patients. In 2007, Tifft et al. (2007) reported that miglustat administration improved neurological functions in two patients with juvenile GM1 gangliosidosis (Tifft et al., 2007). Deodato et al. (2017) described similar neurological improvement in the juvenile form of the disease (Deodato et al., 2017). Stabilization and/or slowing of neurological progression in three of four patients was observed by Fischetto et al. (2020).

Miglustat combined with a ketogenic diet has been used to treat children with GM1 and GM2 gangliosidosis (ClinicalTrials.gov Identifier NCT02030015). The aim of this study was to learn if synergistic enteral regimen for treatment of the gangliosidoses will show improvement in overall survival and clinical benefits in neurodevelopmental abilities in children with gangliosidosis diseases. The Syner-G regimen may have prolonged lifespan, however, the small sample size and variability in other palliative care measures used by families prevented definitive conclusions to be drawn (Jarnes Utz et al., 2017).

Venglustat, another SRT drug chemically distinct from miglustat and designed specifically to cross the BBB is an orally available inhibitor of the enzyme glucosylceramide synthase (Peterschmitt et al., 2021). It is currently under study for GM1 gangliosidosis and several other LSDs in the same degradation pathway including late-onset GM2-gangliosidosis (Tay-Sachs and Sandhoff diseases), Fabry disease, and neuronopathic Gaucher disease (type III) (NCT04221451).

Enzyme Enhancement Therapy

Enzyme enhancement therapy (EET), also termed pharmacological chaperone therapy, has been proposed for GM1 (Matsuda et al., 2003; Suzuki, 2006). The aim is to use small molecules to stabilize potentially unstable or misfolded mutant proteins in the endoplasmic reticulum to enhance lysosomal delivery and increase half-life (Parenti, 2009). Small molecule chaperones that cross the BBB, would be a prerequisite for disorders with CNS involvement (Begley et al., 2008).

Several pharmacological chaperones including galactose, *N*-octyl-4-epi-β-valienamine (NOEV)alkylated or fluorinated derivates of *N*-butyldeoxynojirimycin (NB-DNJ), and (5aR)-5a-C-Pentyl-4-epiisofagomine have been tested against numerous *GLB1* mutant enzymes (Matsuda et al., 2003; Suzuki et al., 2007, 2012; Suzuki, 2008, 2014; Fantur et al., 2010; Takai et al., 2013; Parenti et al., 2015; Thonhofer et al., 2016; Front et al., 2017).

Treatment with NOEV, a galactose analog, at the early stage of the disease reduced disease progression and prolonged survival in a murine model of GM1 gangliosidosis (see **Table 1**; Suzuki, 2014; Parenti et al., 2015). The compound was determined to cross the BBB for CNS delivery (Suzuki, 2014).

Collectively, dozens of patient cell lines with missense mutations have been shown to be responsive to the chaperones listed above, in some cases resulting in greater than the 10–15% residual β-gal activity sufficient to avoid substrate accumulation (Leinekugel et al., 1992; Iwasaki et al., 2006).

Pharmacological chaperones have broad tissue distribution and can be given orally; major advantages for treatment (Front et al., 2017). In addition, they have been shown to work synergistically with other therapies, such as ERT (Kishnani et al., 2017).

Enzyme Replacement Therapy

Enzyme replacement therapy (ERT) as potential treatment for GM1 gangliosidosis was first tested using either a purified (Reynolds et al., 1978) or a recombinant (Samoylova et al., 2008) feline β-gal enzyme *in vitro*. Since β-gal cannot cross the BBB, several therapeutic "Trojan horse" strategies have been utilized, including creating fusion proteins of the enzyme with lectin subunit ribosome-inactivating toxin B (RTB) of ricin (Condori et al., 2016), and to the carboxyl terminus of the heavy

chain of a mouse chimeric monoclonal antibody against the mouse transferrin receptor (mTfR-GLB1) (Przybilla et al., 2021).

Encapsulation of β-gal enzyme into artificial nanoparticles to traverse the BBB has also been experimented *in vitro* (Gupta et al., 2017; Kelly et al., 2017). Mechanically breaching the BBB has been described by Chen et al. (2020) who used direct intracerebroventricular (ICV) injection of rhβ-gal to β-*gal*$^{-/-}$ mice, which led to normalization of neuropathology.

Stem Cell Transplantation

Stem cell transplantation (SCT) early in the course of disease may ameliorate symptoms in GM1 gangliosidosis (Sawada et al., 2009), although for optimal benefit, like Krabbe disease, the transplant would need to be undertaken in the first few weeks of life; a strong argument for universal newborn screening for GM1 disease. Although it could be successfully utilized in GM1 gangliosidosis and may reduce visceral features, the long-term correction of neurological symptoms is less likely. Improvement was observed in a 7-month GM1 gangliosidosis baby who after SCT developed normally until regression was noted at the age of 20–25 months (Shield et al., 2005). The risk of procedure-related mortality with transplantation has decreased with improvements in chemotherapy regimens and should be considered in cases of very early diagnosis with limited therapeutic options.

Gene Therapy

Pre-clinical studies in mouse models resulted in extended life expectancy, β-gal activity restoration and decreased storage levels in the CNS and peripheral organs (see **Table 1**). After the successful treatment in the mouse (Takaura et al., 2003; Broekman et al., 2007, 2009; Baek et al., 2010; Weismann et al., 2015) studies were extended to the feline model with dramatic response in widespread distribution of β-gal enzyme, improved function, and greatly extended lifespan (McCurdy et al., 2014; Gray-Edwards et al., 2017a,b). The dramatic improvement observed in the murine and feline models paved the way for *in vitro* studies in human cerebral organoids (Latour et al., 2019) and subsequent phase I clinical trials in patients with Type I and Type II disease. Three trials are currently recruiting: intravenous delivery of AAV9-GLB1 (ClinicalTrials.gov Identifier NCT03952637), LYS-GM101 administered via cisterna magna (ClinicalTrials.gov Identifier NCT04273269), and PBGM01 delivered via cisterna magna (ClinicalTrials.gov Identifier NCT04713475).

CONCLUSION

GM1 gangliosidosis is a severe LSD underpinned by complex pathophysiological mechanisms. Numerous disease causing *GLB1* mutations have been reported. However, genotype-phenotype correlation has been difficult to establish due in part to the way the enzyme is commonly assayed in patients' samples. In addition, the clinical outcome of the disease in patients may be strongly influenced by post-translational and regulatory mechanisms controlling GM1 catabolism that may vary from patient to patient. These caveats ask for further elucidation of the cellular pathophysiology underlying this disease that may improve our understanding of the fundamental cell biology of GM1 ganglioside and the enzyme complex that regulates its catabolism in the lysosome. Multiple mouse models of this disorder have been instrumental for the pre-clinical testing of multiple therapies, several of which are currently in clinical trials.

AUTHOR CONTRIBUTIONS

E-RN, KS, FP, CT, Ad'A, and IA were involved in designing the concept of the review and oversight. KS and E-RN drafted the manuscript. All authors reviewed the manuscript, read, and approved the final manuscript.

FUNDING

E-RN and CT work was supported by the Intramural Research Program of the National Human Genome Research Institute, NIH. FP was a Royal Society Wolfson Merit Award recipient and a Wellcome Trust Investigator in Science. Ad'A and IA work was funded in part by NIH grants CA021764, GM104981; the Assisi Foundation of Memphis and the American Lebanese Syrian Associated Charities (ALSAC).

ACKNOWLEDGMENTS

We thank Julia Fekecs and Darryl Leja—NHGRI medical illustrators.

REFERENCES

Abumansour, I. S., Yuskiv, N., Paschke, E., and Stockler-Ipsiroglu, S. (2020). Morquio-B disease: clinical and genetic characteristics of a distinct GLB1-related dysostosis multiplex. *JIMD Rep.* 51, 30–44. doi: 10.1002/jmd2.12065

Annunziata, I., Sano, R., and d'Azzo, A. (2018). Mitochondria-associated ER membranes (MAMs) and lysosomal storage diseases. *Cell Death Dis.* 9:328. doi: 10.1038/s41419-017-0025-4

Arash-Kaps, L., Komlosi, K., Seegraber, M., Diederich, S., Paschke, E., Amraoui, Y., et al. (2019). The Clinical and Molecular Spectrum of GM1 Gangliosidosis. *J. Pediatr.* 215, 152–157e153. doi: 10.1016/j.jpeds.2019.08.016

Baek, R. C., Broekman, M. L., Leroy, S. G., Tierney, L. A., Sandberg, M. A., d'Azzo, A., et al. (2010). AAV-mediated gene delivery in adult GM1-gangliosidosis mice corrects lysosomal storage in CNS and improves survival. *PLoS One* 5:e13468. doi: 10.1371/journal.pone.0013468

Begley, D. J., Pontikis, C. C., and Scarpa, M. (2008). Lysosomal storage diseases and the blood-brain barrier. *Curr. Pharm. Des.* 14, 1566–1580. doi: 10.2174/138161208784705504

Bonten, E. J., Annunziata, I., and d'Azzo, A. (2014). Lysosomal multienzyme complex: pros and cons of working together. *Cell. Mol. Life Sci.* 71, 2017–2032. doi: 10.1007/s00018-013-1538-3

Breiden, B., and Sandhoff, K. (2019). Lysosomal glycosphingolipid storage diseases. *Annu. Rev. Biochem.* 88, 461–485. doi: 10.1146/annurev-biochem-013118-111518

Broekman, M. L., Baek, R. C., Comer, L. A., Fernandez, J. L., Seyfried, T. N., and Sena-Esteves, M. (2007). Complete correction of enzymatic deficiency and neurochemistry in the GM1-gangliosidosis mouse brain by neonatal adeno-associated virus-mediated gene delivery. *Mol. Ther.* 15, 30–37. doi: 10.1038/sj.mt.6300004

Broekman, M. L., Tierney, L. A., Benn, C., Chawla, P., Cha, J. H., and Sena-Esteves, M. (2009). Mechanisms of distribution of mouse beta-galactosidase in the adult GM1-gangliosidosis brain. *Gene Ther.* 16, 303–308. doi: 10.1038/gt.2008.149

Bruggink, C., Poorthuis, B. J., Deelder, A. M., and Wuhrer, M. (2012). Analysis of urinary oligosaccharides in lysosomal storage disorders by capillary high-performance anion-exchange chromatography-mass spectrometry. *Anal. Bioanal. Chem.* 403, 1671–1683. doi: 10.1007/s00216-012-5968-9

Brunetti-Pierri, N., and Scaglia, F. (2008). GM1 gangliosidosis: review of clinical, molecular, and therapeutic aspects. *Mol. Genet. Metab.* 94, 391–396. doi: 10.1016/j.ymgme.2008.04.012

Caciotti, A., Donati, M. A., Boneh, A., d'Azzo, A., Federico, A., Parini, R., et al. (2005). Role of beta-galactosidase and elastin binding protein in lysosomal and nonlysosomal complexes of patients with GM1-gangliosidosis. *Hum. Mutat.* 25, 285–292. doi: 10.1002/humu.20147

Caciotti, A., Garman, S. C., Rivera-Colon, Y., Procopio, E., Catarzi, S., Ferri, L., et al. (2011). GM1 gangliosidosis and Morquio B disease: an update on genetic alterations and clinical findings. *Biochim. Biophys. Acta* 1812, 782–790. doi: 10.1016/j.bbadis.2011.03.018

Chen, J. C., Luu, A. R., Wise, N., Angelis, R., Agrawal, V., Mangini, L., et al. (2020). Intracerebroventricular enzyme replacement therapy with beta-galactosidase reverses brain pathologies due to GM1 gangliosidosis in mice. *J. Biol. Chem.* 295, 13532–13555. doi: 10.1074/jbc.RA119.009811

ClinVar (2021). *Xxxxxx*. Available online at: https://www.ncbi.nlm.nih.gov/clinvar/?term=GLB1[gene] (accessed June 25, 2021).

Condori, J., Acosta, W., Ayala, J., Katta, V., Flory, A., Martin, R., et al. (2016). Enzyme replacement for GM1-gangliosidosis: uptake, lysosomal activation, and cellular disease correction using a novel beta-galactosidase:RTB lectin fusion. *Mol. Genet. Metab.* 117, 199–209. doi: 10.1016/j.ymgme.2015.12.002

Cox, T., Lachmann, R., Hollak, C., Aerts, J., van Weely, S., Hrebicek, M., et al. (2000). Novel oral treatment of Gaucher's disease with N-butyldeoxynojirimycin (OGT 918) to decrease substrate biosynthesis. *Lancet* 355, 1481–1485. doi: 10.1016/S0140-6736(00)02161-9

Deodato, F., Procopio, E., Rampazzo, A., Taurisano, R., Donati, M. A., Dionisi-Vici, C., et al. (2017). The treatment of juvenile/adult GM1-gangliosidosis with Miglustat may reverse disease progression. *Metab. Brain Dis.* 32, 1529–1536. doi: 10.1007/s11011-017-0044-y

Eikelberg, D., Lehmbecker, A., Brogden, G., Tongtako, W., Hahn, K., Habierski, A., et al. (2020). Axonopathy and reduction of membrane resistance: key features in a new murine model of human GM1-gangliosidosis. *J. Clin. Med.* 9:1004. doi: 10.3390/jcm9041004

Elliot-Smith, E., Speak, A. O., Lloyd-Evans, E., Smith, D. A., van der Spoel, A. C., Jeyakumar, M., et al. (2008). Beneficial effects of substrate reduction therapy in a mouse model of GM1 gangliosidosis. *Mol. Genet. Metab.* 94, 204–211. doi: 10.1016/j.ymgme.2008.02.005

Fantur, K., Hofer, D., Schitter, G., Steiner, A. J., Pabst, B. M., Wrodnigg, T. M., et al. (2010). DLHex-DGJ, a novel derivative of 1-deoxygalactonojirimycin with pharmacological chaperone activity in human G(M1)-gangliosidosis fibroblasts. *Mol. Genet. Metab.* 100, 262–268. doi: 10.1016/j.ymgme.2010.03.019

Ferreira, C. R., and Gahl, W. A. (2017). Lysosomal storage diseases. *Transl. Sci. Rare Dis.* 2, 1–71. doi: 10.3233/TRD-160005

Ferreira, C. R., Regier, D. S., Yoon, R., Pan, K. S., Johnston, J. M., Yang, S., et al. (2020). The skeletal phenotype of intermediate GM1 gangliosidosis: clinical, radiographic and densitometric features, and implications for clinical monitoring and intervention. *Bone* 131:115142. doi: 10.1016/j.bone.2019.115142

Ficicioglu, C. (2008). Review of miglustat for clinical management in Gaucher disease type 1. *Ther. Clin. Risk Manag.* 4, 425–431. doi: 10.2147/tcrm.s6865

Fischetto, R., Palladino, V., Mancardi, M. M., Giacomini, T., Palladino, S., Gaeta, A., et al. (2020). Substrate reduction therapy with Miglustat in pediatric patients with GM1 type 2 gangliosidosis delays neurological involvement: a multicenter experience. *Mol. Genet. Genomic Med.* 8:e1371. doi: 10.1002/mgg3.1371

Front, S., Biela-Banas, A., Burda, P., Ballhausen, D., Higaki, K., Caciotti, A., et al. (2017). (5aR)-5a-C-Pentyl-4-epi-isofagomine: a powerful inhibitor of lysosomal beta-galactosidase and a remarkable chaperone for mutations associated with GM1-gangliosidosis and Morquio disease type B. *Eur. J. Med. Chem.* 126, 160–170. doi: 10.1016/j.ejmech.2016.09.095

Gorelik, A., Illes, K., Hasan, S. M. N., Nagar, B., and Mazhab-Jafari, M. T. (2021). Structure of the murine lysosomal multienzyme complex core. *Sci. Adv.* 7:eabf4155. doi: 10.1126/sciadv.abf4155

Gray-Edwards, H. L., Jiang, X., Randle, A. N., Taylor, A. R., Voss, T. L., Johnson, A. K., et al. (2017a). Lipidomic evaluation of feline neurologic disease after AAV gene therapy. *Mol. Ther. Methods Clin. Dev.* 6, 135–142. doi: 10.1016/j.omtm.2017.07.005

Gray-Edwards, H. L., Maguire, A. S., Salibi, N., Ellis, L. E., Voss, T. L., Diffie, E. B., et al. (2020). 7T MRI predicts amelioration of neurodegeneration in the brain after AAV gene therapy. *Mol. Ther. Methods Clin. Dev.* 17, 258–270. doi: 10.1016/j.omtm.2019.11.023

Gray-Edwards, H. L., Regier, D. S., Shirley, J. L., Randle, A. N., Salibi, N., Thomas, S. E., et al. (2017b). Novel biomarkers of human GM1 gangliosidosis reflect the clinical efficacy of gene therapy in a feline model. *Mol. Ther.* 25, 892–903. doi: 10.1016/j.ymthe.2017.01.009

Gupta, M., Pandey, H., and Sivakumar, S. (2017). Intracellular delivery of beta-galactosidase enzyme using arginase-responsive dextran sulfate/Poly-l-arginine capsule for lysosomal storage disorder. *ACS Omega* 2, 9002–9012. doi: 10.1021/acsomega.7b01230

Hahn, C. N., del Pilar Martin, M., Schroder, M., Vanier, M. T., Hara, Y., Suzuki, K., et al. (1997). Generalized CNS disease and massive GM1-ganglioside accumulation in mice defective in lysosomal acid beta-galactosidase. *Hum. Mol. Genet.* 6, 205–211. doi: 10.1093/hmg/6.2.205

HGMD (2021). *The Human Gene Mutation Database at the Institute of Medical Genetics in Cardiff*. Available online at: http://www.hgmd.cf.ac.uk/ac/gene.php?gene=GLB1. (Accessed June 25, 2021)

Hinderer, C., Nosratbakhsh, B., Katz, N., and Wilson, J. M. (2020). A single injection of an optimized adeno-associated viral vector into cerebrospinal fluid corrects neurological disease in a murine model of GM1 gangliosidosis. *Hum. Gene. Ther.* 31, 1169–1177. doi: 10.1089/hum.2018.206

Holmes, E. W., and O'Brien, J. S. (1978). Hepatic storage of oligosaccharides and glycolipids in a cat affected with GM1 gangliosidosis. *Biochem. J.* 175, 945–953. doi: 10.1042/bj1750945

Inui, K., Namba, R., Ihara, Y., Nobukuni, K., Taniike, M., Midorikawa, M., et al. (1990). A case of chronic GM1 gangliosidosis presenting as dystonia: clinical and biochemical studies. *J. Neurol.* 237, 491–493. doi: 10.1007/BF00314770

Iwasaki, H., Watanabe, H., Iida, M., Ogawa, S., Tabe, M., Higaki, K., et al. (2006). Fibroblast screening for chaperone therapy in beta-galactosidosis. *Brain Dev.* 28, 482–486. doi: 10.1016/j.braindev.2006.02.002

Iyer, N. S., Gimovsky, A. C., Ferreira, C. R., Critchlow, E. J., and Al-Kouatly, H. B. (2021). Lysosomal storage disorders as an etiology of nonimmune hydrops fetalis: a systematic review. *Clin. Genet.* 212, 281–290. doi: 10.1111/cge.14005

Jarnes Utz, J. R., Kim, S., King, K., Ziegler, R., Schema, L., Redtree, E. S., et al. (2017). Infantile gangliosidoses: mapping a timeline of clinical changes. *Mol. Genet. Metab.* 121, 170–179. doi: 10.1016/j.ymgme.2017.04.011

Jatzkewitz, H., and Sandhoff, K. (1963). On a biochemically special form of infantile amaturotic idiocy. *Biochim. Biophys. Acta* 70, 354–356. doi: 10.1016/0006-3002(63)90764-9

Jeyakumar, M., Butters, T. D., Dwek, R. A., and Platt, F. M. (2002). Glycosphingolipid lysosomal storage diseases: therapy and pathogenesis. *Neuropathol. Appl. Neurobiol.* 28, 343–357. doi: 10.1046/j.1365-2990.2002.00422.x

Jeyakumar, M., Thomas, R., Elliot-Smith, E., Smith, D. A., van der Spoel, A. C., d'Azzo, A., et al. (2003). Central nervous system inflammation is a hallmark of pathogenesis in mouse models of GM1 and GM2 gangliosidosis. *Brain* 126(Pt 4), 974–987. doi: 10.1093/brain/awg089

Karimzadeh, P., Naderi, S., Modarresi, F., Dastsooz, H., Nemati, H., Farokhashtiani, T., et al. (2017). Case reports of juvenile GM1 gangliosidosisis type II caused by mutation in GLB1 gene. *BMC Med. Genet.* 18:73. doi: 10.1186/s12881-017-0417-4

Kasperzyk, J. L., d'Azzo, A., Platt, F. M., Alroy, J., and Seyfried, T. N. (2005). Substrate reduction reduces gangliosides in postnatal cerebrum-brainstem and cerebellum in GM1 gangliosidosis mice. *J. Lipid Res.* 46, 744–751. doi: 10.1194/jlr.M400411-JLR200

Kasperzyk, J. L., El-Abbadi, M. M., Hauser, E. C., D'Azzo, A., Platt, F. M., and Seyfried, T. N. (2004). N-butyldeoxygalactonojirimycin reduces neonatal brain ganglioside content in a mouse model of GM1 gangliosidosis. *J. Neurochem.* 89, 645–653. doi: 10.1046/j.1471-4159.2004.02381.x

Kelly, J. M., Gross, A. L., Martin, D. R., and Byrne, M. E. (2017). Polyethylene glycol-b-poly(lactic acid) polymersomes as vehicles for enzyme replacement therapy. *Nanomedicine (Lond.)* 12, 2591–2606. doi: 10.2217/nnm-2017-0221

Kishnani, P., Tarnopolsky, M., Roberts, M., Sivakumar, K., Dasouki, M., Dimachkie, M. M., et al. (2017). Duvoglustat HCl increases systemic and tissue exposure of active acid alpha-glucosidase in pompe patients co-administered with alglucosidase alpha. *Mol. Ther.* 25, 1199–1208. doi: 10.1016/j.ymthe.2017.02.017

Kolter, T. (2012). Ganglioside biochemistry. *ISRN Biochem.* 2012:506160. doi: 10.5402/2012/506160

Landrum, M. J., Lee, J. M., Benson, M., Brown, G. R., Chao, C., Chitipiralla, S., et al. (2018). ClinVar: improving access to variant interpretations and supporting evidence. *Nucleic Acids Res.* 46, D1062–D1067. doi: 10.1093/nar/gkx1153

Lang, F. M., Korner, P., Harnett, M., Karunakara, A., and Tifft, C. J. (2020). The natural history of Type 1 infantile GM1 gangliosidosis: a literature-based meta-analysis. *Mol. Genet. Metab.* 129, 228–235. doi: 10.1016/j.ymgme.2019.12.012

Latour, Y. L., Yoon, R., Thomas, S. E., Grant, C., Li, C., Sena-Esteves, M., et al. (2019). Human GLB1 knockout cerebral organoids: a model system for testing AAV9-mediated GLB1 gene therapy for reducing GM1 ganglioside storage in GM1 gangliosidosis. *Mol. Genet. Metab. Rep.* 21:100513. doi: 10.1016/j.ymgmr.2019.100513

Lawrence, R., Van Vleet, J. L., Mangini, L., Harris, A., Martin, N., Clark, W., et al. (2019). Characterization of glycan substrates accumulating in GM1 Gangliosidosis. *Mol. Genet. Metab. Rep.* 21:100524. doi: 10.1016/j.ymgmr.2019.100524

Ledeen, R. W., and Wu, G. (2015). The multi-tasked life of GM1 ganglioside, a true factotum of nature. *Trends Biochem. Sci.* 40, 407–418. doi: 10.1016/j.tibs.2015.04.005

Leinekugel, P., Michel, S., Conzelmann, E., and Sandhoff, K. (1992). Quantitative correlation between the residual activity of beta-hexosaminidase A and arylsulfatase A and the severity of the resulting lysosomal storage disease. *Hum. Genet.* 88, 513–523. doi: 10.1007/BF00219337

Liu, S., Feng, Y., Huang, Y., Jiang, X., Tang, C., Tang, F., et al. (2021). A GM1 gangliosidosis mutant mouse model exhibits activated microglia and disturbed autophagy. *Exp. Biol. Med. (Maywood)* 246, 1330–1341. doi: 10.1177/1535370221993052

Matsuda, J., Suzuki, O., Oshima, A., Ogura, A., Naiki, M., and Suzuki, Y. (1997a). Neurological manifestations of knockout mice with beta-galactosidase deficiency. *Brain Dev.* 19, 19–20.

Matsuda, J., Suzuki, O., Oshima, A., Ogura, A., Noguchi, Y., Yamamoto, Y., et al. (1997b). Beta-galactosidase-deficient mouse as an animal model for GM1-gangliosidosis. *Glycoconj. J.* 14, 729–736.

Matsuda, J., Suzuki, O., Oshima, A., Yamamoto, Y., Noguchi, A., Takimoto, K., et al. (2003). Chemical chaperone therapy for brain pathology in G(M1)-gangliosidosis. *Proc. Natl. Acad. Sci. U.S.A.* 100, 15912–15917. doi: 10.1073/pnas.2536657100

Mayer, F. Q., Pereira Fdos, S., Fensom, A. H., Slade, C., Matte, U., and Giugliani, R. (2009). New GLB1 mutation in siblings with Morquio type B disease presenting with mental regression. *Mol. Genet. Metab.* 96:148. doi: 10.1016/j.ymgme.2008.11.159

McCurdy, V. J., Johnson, A. K., Gray-Edwards, H. L., Randle, A. N., Brunson, B. L., Morrison, N. E., et al. (2014). Sustained normalization of neurological disease after intracranial gene therapy in a feline model. *Sci. Transl. Med.* 6:231ra248. doi: 10.1126/scitranslmed.3007733

Morita, M., Saito, S., Ikeda, K., Ohno, K., Sugawara, K., Suzuki, T., et al. (2009). Structural bases of GM1 gangliosidosis and Morquio B disease. *J. Hum. Genet.* 54, 510–515. doi: 10.1038/jhg.2009.70

Ohto, U., Usui, K., Ochi, T., Yuki, K., Satow, Y., and Shimizu, T. (2012). Crystal structure of human beta-galactosidase: structural basis of Gm1 gangliosidosis and morquio B diseases. *J. Biol. Chem.* 287, 1801–1812. doi: 10.1074/jbc.M111.293795

Parenti, G. (2009). Treating lysosomal storage diseases with pharmacological chaperones: from concept to clinics. *EMBO Mol. Med.* 1, 268–279. doi: 10.1002/emmm.200900036

Parenti, G., Andria, G., and Valenzano, K. J. (2015). Pharmacological chaperone therapy: preclinical development, clinical translation, and prospects for the treatment of lysosomal storage disorders. *Mol. Ther.* 23, 1138–1148. doi: 10.1038/mt.2015.62

Patterson, M. C., Vecchio, D., Prady, H., Abel, L., and Wraith, J. E. (2007). Miglustat for treatment of Niemann-Pick C disease: a randomised controlled study. *Lancet Neurol.* 6, 765–772. doi: 10.1016/S1474-4422(07)70194-1

Peterschmitt, M. J., Crawford, N. P. S., Gaemers, S. J. M., Ji, A. J., Sharma, J., and Pham, T. T. (2021). Pharmacokinetics, pharmacodynamics, safety, and tolerability of oral venglustat in healthy volunteers. *Clin. Pharmacol. Drug Dev.* 10, 86–98. doi: 10.1002/cpdd.865

Piraud, M., Pettazzoni, M., Menegaut, L., Caillaud, C., Nadjar, Y., Vianey-Saban, C., et al. (2017). Development of a new tandem mass spectrometry method for urine and amniotic fluid screening of oligosaccharidoses. *Rapid Commun. Mass Spectrom.* 31, 951–963. doi: 10.1002/rcm.7860

Platt, F. M., d'Azzo, A., Davidson, B. L., Neufeld, E. F., and Tifft, C. J. (2018). Lysosomal storage diseases. *Nat. Rev. Dis. Primers* 4:27. doi: 10.1038/s41572-018-0025-4

Platt, F. M., Jeyakumar, M., Andersson, U., Priestman, D. A., Dwek, R. A., Butters, T. D., et al. (2001). Inhibition of substrate synthesis as a strategy for glycolipid lysosomal storage disease therapy. *J. Inherit. Metab. Dis.* 24, 275–290. doi: 10.1023/a:1010335505357

Platt, F. M., Neises, G. R., Dwek, R. A., and Butters, T. D. (1994). N-butyldeoxynojirimycin is a novel inhibitor of glycolipid biosynthesis. *J. Biol. Chem.* 269, 8362–8365.

Przybilla, M. J., Ou, L., Tabaran, A. F., Jiang, X., Sidhu, R., Kell, P. J., et al. (2019). Comprehensive behavioral and biochemical outcomes of novel murine models of GM1-gangliosidosis and Morquio syndrome type B. *Mol. Genet. Metab.* 126, 139–150. doi: 10.1016/j.ymgme.2018.11.002

Przybilla, M. J., Stewart, C., Carlson, T. W., Ou, L., Koniar, B. L., Sidhu, R., et al. (2021). Examination of a blood-brain barrier targeting beta-galactosidase-monoclonal antibody fusion protein in a murine model of GM1-gangliosidosis. *Mol. Genet. Metab. Rep.* 27:100748. doi: 10.1016/j.ymgmr.2021.100748

Regier, D. S., Kwon, H. J., Johnston, J., Golas, G., Yang, S., Wiggs, E., et al. (2016). MRI/MRS as a surrogate marker for clinical progression in GM1 gangliosidosis. *Am. J. Med. Genet. A* 170, 634–644. doi: 10.1002/ajmg.a.37468

Regier, D. S., Tifft, C. J., and Rothermel, C. E. (1993). "GLB1-related disorders," in *GeneReviews*, eds M. P. Adam, H. H. Ardinger, R. A. Pagon, S. E. Wallace, L. J. H. Bean, G. Mirzaa, et al. (Seattle, WA: University of Washington).

Reynolds, G. C., Baker, H. J., and Reynolds, R. H. (1978). Enzyme replacement using liposome carriers in feline Gm1 gangliosidosis fibroblasts. *Nature* 275, 754–755. doi: 10.1038/275754a0

Rha, A. K., Maguire, A. S., and Martin, D. R. (2021). GM1 gangliosidosis: mechanisms and management. *Appl. Clin. Genet.* 14, 209–233. doi: 10.2147/TACG.S206076

Samoylova, T. I., Martin, D. R., Morrison, N. E., Hwang, M., Cochran, A. M., Samoylov, A. M., et al. (2008). Generation and characterization of recombinant feline beta-galactosidase for preclinical enzyme replacement therapy studies in GM1 gangliosidosis. *Metab. Brain Dis.* 23, 161–173. doi: 10.1007/s11011-008-9086-5

Sano, R., Annunziata, I., Patterson, A., Moshiach, S., Gomero, E., Opferman, J., et al. (2009). GM1-ganglioside accumulation at the mitochondria-associated ER membranes links ER stress to Ca(2+)-dependent mitochondrial apoptosis. *Mol. Cell* 36, 500–511. doi: 10.1016/j.molcel.2009.10.021

Sano, R., Tessitore, A., Ingrassia, A., and d'Azzo, A. (2005). Chemokine-induced recruitment of genetically modified bone marrow cells into the CNS of GM1-gangliosidosis mice corrects neuronal pathology. *Blood* 106, 2259–2268. doi: 10.1182/blood-2005-03-1189

Sawada, T., Tanaka, A., Higaki, K., Takamura, A., Nanba, E., Seto, T., et al. (2009). Intracerebral cell transplantation therapy for murine GM1 gangliosidosis. *Brain Dev.* 31, 717–724. doi: 10.1016/j.braindev.2008.11.004

Severini, M. H., Silva, C. D., Sopelsa, A., Coelho, J. C., and Giugliani, R. (1999). High frequency of type 1 GM1 gangliosidosis in southern Brazil. *Clin. Genet.* 56, 168–169. doi: 10.1034/j.1399-0004.1999.560215.x

Shield, J. P., Stone, J., and Steward, C. G. (2005). Bone marrow transplantation correcting beta-galactosidase activity does not influence neurological outcome in juvenile GM1-gangliosidosis. *J. Inherit. Metab. Dis.* 28, 797–798. doi: 10.1007/s10545-005-0089-7

Sinigerska, I., Chandler, D., Vaghjiani, V., Hassanova, I., Gooding, R., Morrone, A., et al. (2006). Founder mutation causing infantile GM1-gangliosidosis in the Gypsy population. *Mol. Genet. Metab.* 88, 93–95. doi: 10.1016/j.ymgme.2005.12.009

Stone, D. L., and Sidransky, E. (1999). Hydrops fetalis: lysosomal storage disorders in extremis. *Adv. Pediatr.* 46, 409–440.

Suzuki, Y. (2006). Beta-galactosidase deficiency: an approach to chaperone therapy. *J. Inherit. Metab. Dis.* 29, 471–476. doi: 10.1007/s10545-006-0287-y

Suzuki, Y. (2008). Chemical chaperone therapy for GM1-gangliosidosis. *Cell. Mol. Life Sci.* 65, 351–353. doi: 10.1007/s00018-008-7470-2

Suzuki, Y. (2014). Emerging novel concept of chaperone therapies for protein misfolding diseases. *Proc. Jpn. Acad. Ser. B Phys. Biol. Sci.* 90, 145–162. doi: 10.2183/pjab.90.145

Suzuki, Y., Ichinomiya, S., Kurosawa, M., Matsuda, J., Ogawa, S., Iida, M., et al. (2012). Therapeutic chaperone effect of N-octyl 4-epi-beta-valienamine on murine G(M1)-gangliosidosis. *Mol. Genet. Metab.* 106, 92–98. doi: 10.1016/j.ymgme.2012.02.012

Suzuki, Y., Ichinomiya, S., Kurosawa, M., Ohkubo, M., Watanabe, H., Iwasaki, H., et al. (2007). Chemical chaperone therapy: clinical effect in murine G(M1)-gangliosidosis. *Ann. Neurol.* 62, 671–675. doi: 10.1002/ana.21284

Suzuki, Y., Oshima, A., and Nanba, E. (2001). "β-Galactosidase deficiency (β-galactosidosis): GM1 gangliosidosis and Morquio B disease," in *The Metabolic and Molecular Bases of Inherited Disease*, eds C. R. Shriver, A. L. Beaudet, W. S. Sly, and D. Valle (New York, NY: McGraw Hill), 3775–3809.

Takai, T., Higaki, K., Aguilar-Moncayo, M., Mena-Barragan, T., Hirano, Y., Yura, K., et al. (2013). A bicyclic 1-deoxygalactonojirimycin derivative as a novel pharmacological chaperone for GM1 gangliosidosis. *Mol. Ther.* 21, 526–532. doi: 10.1038/mt.2012.263

Takaura, N., Yagi, T., Maeda, M., Nanba, E., Oshima, A., Suzuki, Y., et al. (2003). Attenuation of ganglioside GM1 accumulation in the brain of GM1 gangliosidosis mice by neonatal intravenous gene transfer. *Gene Ther.* 10, 1487–1493. doi: 10.1038/sj.gt.3302033

Tebani, A., Sudrie-Arnaud, B., Dabaj, I., Torre, S., Domitille, L., Snanoudj, S., et al. (2021). Disentangling molecular and clinical stratification patterns in beta-galactosidase deficiency. *J. Med. Genet.* doi: 10.1136/jmedgenet-2020-107510 [Epub ahead of print].

Tessitore, A., del, P. M. M., Sano, R., Ma, Y., Mann, L., Ingrassia, A., et al. (2004). GM1-ganglioside-mediated activation of the unfolded protein response causes neuronal death in a neurodegenerative gangliosidosis. *Mol. Cell* 15, 753–766. doi: 10.1016/j.molcel.2004.08.029

Thonhofer, M., Weber, P., Santana, A. G., Fischer, R., Pabst, B. M., Paschke, E., et al. (2016). Synthesis of C-5a-chain extended derivatives of 4-epi-isofagomine: powerful beta-galactosidase inhibitors and low concentration activators of GM1-gangliosidosis-related human lysosomal beta-galactosidase. *Bioorg. Med. Chem. Lett.* 26, 1438–1442. doi: 10.1016/j.bmcl.2016.01.059

Tifft, C., Adams, D., and Morgan, C. (2007). 55 Miglustat improves function in patients with juvenile GM1 gangliosidosis. *Mol. Genet. Metab.* 4:24.

Tonin, R., Caciotti, A., Procopio, E., Fischetto, R., Deodato, F., Mancardi, M. M., et al. (2019). Pre-diagnosing and managing patients with GM1 gangliosidosis and related disorders by the evaluation of GM1 ganglioside content. *Sci. Rep.* 9:17684. doi: 10.1038/s41598-019-53995-5

Treiber, A., Morand, O., and Clozel, M. (2007). The pharmacokinetics and tissue distribution of the glucosylceramide synthase inhibitor miglustat in the rat. *Xenobiotica* 37, 298–314. doi: 10.1080/00498250601094543

Tsay, G. C., and Dawson, G. (1976). Oligosaccharide storage in brains from patients with fucosidosis, GM1-gangliosidosis and GM2-gangliosidosis (Sandhoff's disease). *J. Neurochem.* 27, 733–740. doi: 10.1111/j.1471-4159.1976.tb10401.x

Weismann, C. M., Ferreira, J., Keeler, A. M., Su, Q., Qui, L., Shaffer, S. A., et al. (2015). Systemic AAV9 gene transfer in adult GM1 gangliosidosis mice reduces lysosomal storage in CNS and extends lifespan. *Hum. Mol. Genet.* 24, 4353–4364. doi: 10.1093/hmg/ddv168

Yoshida, K., Oshima, A., Shimmoto, M., Fukuhara, Y., Sakuraba, H., Yanagisawa, N., et al. (1991). Human beta-galactosidase gene mutations in GM1-gangliosidosis: a common mutation among Japanese adult/chronic cases. *Am. J. Hum. Genet.* 49, 435–442.

Conflict of Interest: Ad'A holds the Jewelers for Children Endowed Chair in Genetics and Gene Therapy.

The remaining authors declare that the research was conducted in the absence of any commercial or financial relationships that could be construed as a potential conflict of interest.

Publisher's Note: All claims expressed in this article are solely those of the authors and do not necessarily represent those of their affiliated organizations, or those of the publisher, the editors and the reviewers. Any product that may be evaluated in this article, or claim that may be made by its manufacturer, is not guaranteed or endorsed by the publisher.

frontiers in Pediatrics

REVIEW
published: 03 September 2021
doi: 10.3389/fped.2021.715151

Congenital Disorders of Glycosylation: What Clinicians Need to Know?

Patryk Lipiński and Anna Tylki-Szymańska*

Department of Pediatrics, Nutrition and Metabolic Diseases, The Children's Memorial Health Institute, Warsaw, Poland

Congenital disorders of glycosylation (CDG) are a group of clinically heterogeneous disorders characterized by defects in the synthesis of glycans and their attachment to proteins and lipids. This manuscript aims to provide a classification of the clinical presentation, diagnostic methods, and treatment of CDG based on the literature review and our own experience (referral center in Poland). A diagnostic algorithm for CDG was also proposed. Isoelectric focusing (IEF) of serum transferrin (Tf) is still the method of choice for diagnosing N-glycosylation disorders associated with sialic acid deficiency. Nowadays, high-performance liquid chromatography, capillary zone electrophoresis, and mass spectrometry techniques are used, although they are not routinely available. Since next-generation sequencing became more widely available, an improvement in diagnostics has been observed, with more patients and novel CDG subtypes being reported. Early and accurate diagnosis of CDG is crucial for timely implementation of appropriate therapies and improving clinical outcomes. However, causative treatment is available only for few CDG types.

Keywords: congenital disorders of glycosylation, clinical presentation, isoelectric focusing of serum transferrin, next-generation sequencing, treatment

OPEN ACCESS

Edited by:
Huali Shen,
Fudan University, China

Reviewed by:
Yoshinao Wada,
Osaka Women's and Children's Hospital, Japan
Paul Lasko,
McGill University, Canada

****Correspondence:***
Patryk Lipiński
p.lipinski@ipczd.pl

Specialty section:
This article was submitted to Genetics of Common and Rare Diseases, a section of the journal Frontiers in Pediatrics

Received: *26 May 2021*
Accepted: *10 August 2021*
Published: *03 September 2021*

Citation:
Lipiński P and Tylki-Szymańska A (2021) Congenital Disorders of Glycosylation: What Clinicians Need to Know? Front. Pediatr. 9:715151. doi: 10.3389/fped.2021.715151

BACKGROUND

Congenital disorders of glycosylation (CDG), previously known as carbohydrate-deficient glycoprotein syndromes, constitute a group of inborn errors of metabolism (IEM) characterized by impaired synthesis and attachment of glycans to glycoproteins and glycolipids and impaired synthesis of glycosylphosphatidylinositol. Two main types of protein glycosylation are depicted, including N-glycosylation and O-glycosylation, while N-glycosylation is the most common type in the human body. So far, more than 150 CDG subtypes have been reported, while the phosphomannomutase-2 deficiency (PMM2-CDG) comprises the most common one (1–4).

Currently, CDG types are classified into defects in protein N-glycosylation, protein O-glycosylation, glycosphingolipid, and glycosylphosphatidylinositol (GPI) anchor glycosylation defects, and multiple glycosylation pathway defects (1–4).

CDG nomenclature is denoted by the affected gene name (non-italicized) followed by -CDG (i.e., PMM2-CDG, phosphomannomutase-2 deficiency) (1–4).

Most CDG types are autosomal recessive in inheritance, but autosomal dominant (i.e., EXT1/EXT2-CDG, GANAB-CDG, PRKCSH-CDG, POGLUT1-CDG, POFUT1-CDG) as well as X-linked (i.e., ALG13-CDG, PIGA-CDG, SLC35A2-CDG, ATP6AP1-CDG) forms have also been described (1–4).

This manuscript aims to provide a classification of the clinical presentation, diagnostic methods, and treatment of CDG based on the literature review and our own experience (referral center in Poland). A diagnostic algorithm for CDG was also proposed.

CLINICAL PRESENTATION

CDG are usually multisystem diseases with neurological manifestation observed in most patients (5, 6). Like in other IEM, depending on the disease severity (age of symptom onset), mild to severe phenotypes could be observed.

Most CDG patients presenting with an early-onset neurovisceral phenotype have some signs and symptoms since birth. Thus, a detailed clinical analysis, including a physical examination (i.e., craniofacial dysmorphia, birth body length, weight, and head circumference) as well as family and pregnancy history (i.e., regarding non-immune hydrops fetalis, NIHF), is essential in the context of further biochemical and molecular analyses. NIHF was commonly reported in PMM2-CDG, ALG9-CDG, and ALG8-CDG, and the presence of NIHF is associated with poor outcomes (7).

Neurological signs and symptoms include psychomotor retardation, hypotonia, microcephaly, epileptic seizures, ataxia, peripheral neuropathy, and stroke-like episodes (5, 6). Deficiencies in several glycosylation pathways comprise the cause of epilepsy, while in some of them (i.e., ALG1-CDG, ALG3-CDG, ALG11-CDG, ALG13-CDG, DPM1-CDG, DPM2-CDG, MPDU1-CDG, DPAGT1-CDG, RFT1-CDG, PIGA-CDG, PIGW-CDG, and PIGQ-CDG) the severe epileptic encephalopathies have been described (8–23). Besides cerebellar and cerebral atrophy, most CDG patients with epilepsy do not have characteristic brain malformations. However, O-glycosylation disorders are associated with neuronal migration defects, including lissencephaly, polymicrogyria, schizencephaly, and neuronal heterotopia (24). The cerebellum is commonly affected in PMM2-CDG, dystroglycanopathies, and SRD5A3-CDG, while the course of cerebellar ataxia is not progressive (25–28). Several CDG types, especially dystroglycanopathies, are connected with congenital muscular dystrophy (29–33).

In the majority of CDG, liver involvement is observed as a part of multisystem phenotype, presenting with elevated serum transaminases (more often) and hepatomegaly (less often) in early infancy/childhood, while serum transaminases could normalize later in life (34–36). In the case of severe neurovisceral phenotype leading to premature death, severe liver involvement is observed as part of multiple organ failure (i.e., COG7-CDG, ALG3-CDG) (37). There is also a group of CDG, including MPI-CDG, CCDC115-CDG, and TMEM199-CDG, in which the disease is expressed mainly in the liver (no neurological manifestation) (38–43). There is no typical histologic pattern for liver disease in CDG; liver fibrosis, or even cirrhosis, was reported in PMM2-CDG, MPI-CDG, and TMEM199-CDG (44).

About 20% of CDG were reported to exhibit heart disease in the form of pericardial effusion, cardiomyopathy, arrhythmias, and structural abnormalities (45, 46). Structural (valvular and septal) defects are predominant in patients with GPI-anchor biosynthesis defects and COG-CDG (47–49). Pericardial effusions are characteristic features of PMM2-CDG, while dilated cardiomyopathy is typical for PGM1-CDG and DK1-CDG (50–52).

Recurrent and severe infections as a part of immunodeficiency phenotype were reported in ALG12-CDG, ATP6AP1-CDG, EXTL3-CDG, G6PC3-CDG, MOGS-CDG, PGM3-CDG, and SLC35C1-CDG (53–60).

Some types of CDG, including ALG3-CDG, ALG6-CDG, ALG9-CDG, ALG12-CDG, PGM3-CDG, CSGALNACT1-CDG, SLC35D1-CDG, and TMEM-165, were reported with well-defined skeletal dysplasia (61–69). In addition, some skeletal abnormalities are also unique for some types of CDG, including Schneckenbecken dysplasia in SLC35D1-CDG, brachytelephalangy in PIGV-CDG and PIGO-CDG, pseudodiastrophic dysplasia in ALG12-CDG, Gillessen-Kaesbach and Nishimura skeletal dysplasia in ALG9-CDG, and Desbuquois dysplasia in PGM3-CDG (48, 70–72).

Some CDG also have unique characteristics in the form of a constellation of clinical symptoms), which may facilitate their recognition and shorten the diagnostic process, including:

- connective tissue involvement (*cutis laxa* in ATP6V0A2-CDG, COG7-CDG; inguinal hernias in ATP6AP1-CDG) (73–76);
- midline malformations, including palate/uvula cleft in PGM1-CDG; a constellation of congenital malformations, dilated cardiomyopathy, liver involvement, variable endocrine, and hematological abnormalities and no neurological disease in PGM1-CDG (38, 77);
- inverted nipples and abnormal fat distribution in PMM2-CDG; specific craniofacial dysmorphia in PMM2-CDG, including microcephaly, prominent forehead, flat nasal bridge, thin upper lip, and large ears; polycystic kidney disease and hyperinsulinemic hypoglycemia in PMM2-CDG due to a promotor defect (26, 78–80);
- cerebellar hypoplasia in PMM2-CDG, SRD5A3-CDG, dystroglycanopathies (25, 28);
- cerebellar ataxia and variable eye malformations, including optic disc hypoplasia and nystagmus in SRD5A3-CDG (28);
- achalasia and alacrima without adrenal insufficiency in GMPPA-CDG (81);
- severe immunodeficiency accompanied by a skeletal dysplasia in PGM3-CDG; immunodeficiency with the Bombay blood phenotype and severe growth and psychomotor retardation in leukocyte adhesion deficiency type II (known as SLC35C1-CDG) (57–59, 82, 83).

DIAGNOSTIC PROCESS

Since the introduction by Jaeken et al. (84), isoelectric focusing (IEF) of serum transferrin (Tf) is the method of choice for diagnosis of hypo-*N*-glycosylation disorders associated with sialic acid deficiency (1–4, 84, 85).

So far, several other laboratory techniques have been used for the separation and quantification of serum Tf isoforms, including high-performance liquid chromatography (HPLC), capillary

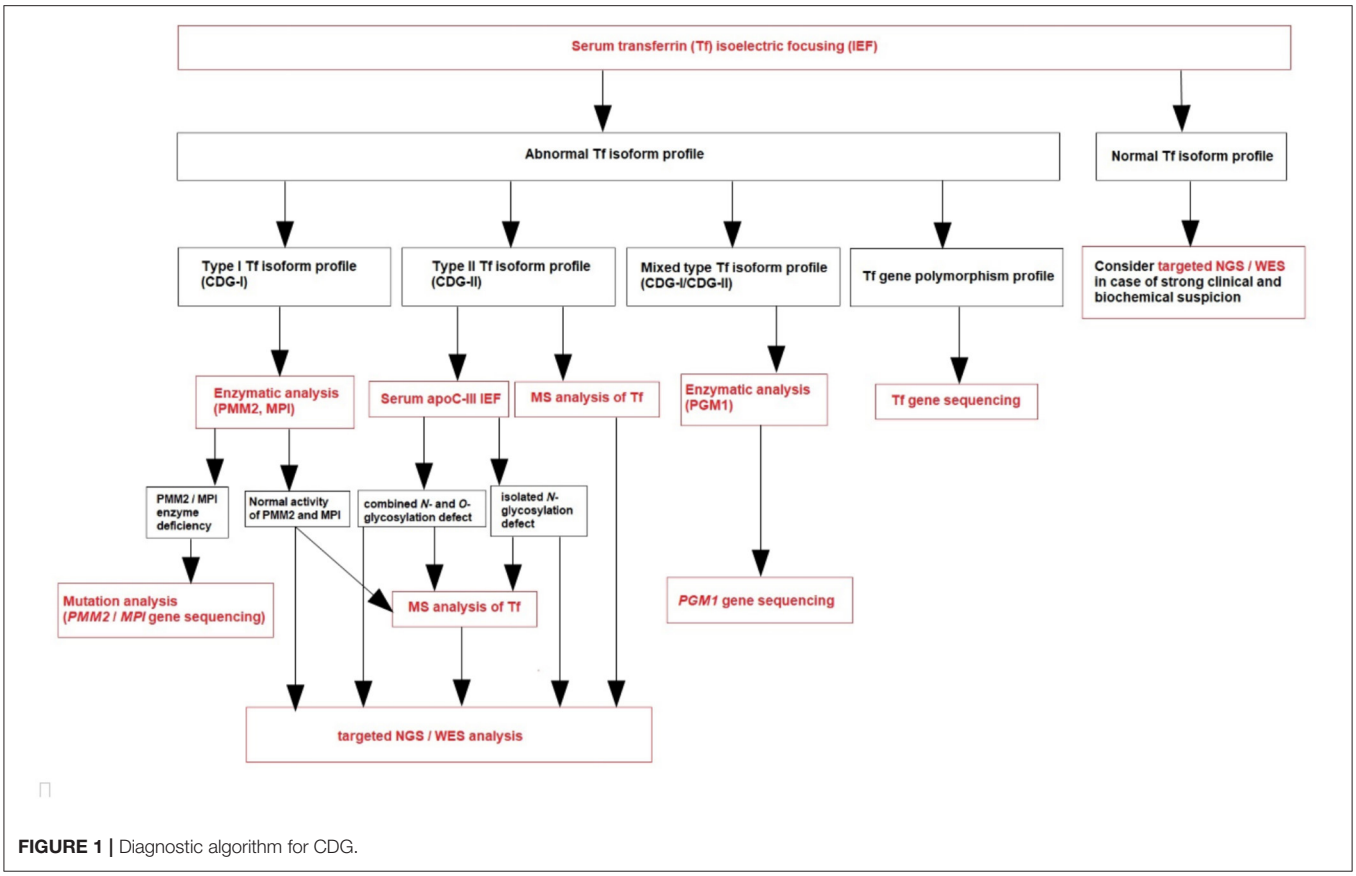

FIGURE 1 | Diagnostic algorithm for CDG.

zone electrophoresis (CZE), and mass spectrometry (MS) (86–94). Every diagnostic method has its own limitations. Both CZE and HPLC techniques are universal with low maintenance cost and suitable for CDG screening. An abnormal result should be further investigated by serum Tf IEF. In addition, serum Tf IEF is the most commonly used for diagnosis and monitoring of CDG, and thus considered as the reference method. Other techniques, including CZE and HPLC, can be adapted by the laboratories based on their equipment accessibility.

IEF of serum Tf from dried blood spot (DBS) samples was recently demonstrated as a reliable method for CDG screening (95, 96). DBS is firmly established in the analysis of various IEM, especially in the context of newborn screening programs across the world. However, there is a number of CDG for which there is no data regarding glycosylation abnormalities after birth and thus further studies are needed.

Based on our own experience (referral center in Poland), we create a diagnostic algorithm for CDG (**Figure 1**). We recommend to perform serum Tf IEF for an initial screening of glycosylation abnormalities in patients presenting with clinical and biochemical features listed in **Table 1**.

Transferrin (Tf) is a plasma iron transport protein with two asparagine N-glycosylation sites (Asn432 and Asn630), and the dominated isoform in healthy individuals is tetrasialo-Tf, while asialo- and monosialo-Tf isoforms are usually not detectable. A type 1 pattern (CDG-I) is associated with an increased asialo- and disialo-Tf, and decreased tetrasialo-Tf, indicating an assembly or transfer defect of the dolichol-linked glycan (85). A type 2 pattern (CDG-II) is associated with increased asialo-, monosialo-, disialo-, and trisialo-Tf, indicating a processing defect after glycan transfer in the ER or during Golgi glycosylation (85). PGM1-CDG presents features of the both types of serum Tf IEF patterns (mixed type, CDG-I/CDG-II).

TABLE 1 | Clinical and biochemical features requiring IEF of serum transferrin.

Non-immune hydrops foetalis (NIHF)
Inverted nipples, abnormal fat distribution
Connective tissue involvement (*cutis laxa*, inguinal hernias)
Unexplained multisystemic phenotype, including neurological manifestation
Non-progressive cerebellar ataxia
Severe epileptic encephalopathy
Elevated serum transaminases (especially with decreased antithrombin/protein C and S activity)
Liver steatosis/fibrosis/cirrhosis of unknown etiology
Recurrent pericardial effusion
Cardiomyopathy
Skeletal dysplasia (especially features of pseudodiastrophic dysplasia, Gillessen-Kaesbach and Nishimura skeletal dysplasia, Desbuquois dysplasia, brachytelephalangy)
Immunodeficiency

During CDG diagnostic process, it is important to exclude secondary causes of N-hypoglycosylation as well as Tf gene polymorphisms. Several Tf gene polymorphisms (i.e., transferrin B2 presenting with an elevated pentasialo-Tf solely or transferrin C2 resulting in increased trisialo-Tf solely) are known to result in a shifted IEF pattern, caused by pI differences of the polypeptide chain.

It is also known that untreated patients with classic galactosemia (galactose-1-phosphate uridyltransferase deficiency) and fructosemia (fructose 1-phosphate aldolase deficiency) have secondarily an abnormal serum Tf isoform profile that could resemble CDG-I. For example, Bogdańska et al. reported a study on 19 pediatric patients with primary liver disease and increased secondary asialo-Tf and monosialo-Tf isoforms; none of the patients had an elevated level of trisialo-Tf isoform (97). On the other hand, Jansen et al. published a study about secondary glycosylation defects in 961 adult patients qualified for LTx or with chronic liver disease. It showed that 247 patients (26%) had hyposialylation of serum Tf, while the majority of them (70%) had an increase in the trisialo-Tf isoform (98).

Normal serum Tf IEF profile does not exclude CDG—we should consider targeted next-generation sequencing (NGS) or whole-exome sequencing (WES) in case of a strong clinical and biochemical suspicion. PMM2-CDG due to promotor defect and several other CDG, like SLC35A1-CDG, SLC35A3-CDG, SEC23B-CDG, and PGM3-CDG, could show normal N-glycosylation profile. What is more, serum Tf IEF could be normal as well as abnormal in several others CDG, like ALG13-CDG, SLC35A2-CDG, RTF1-CDG, and SRD5A3-CDG (1–4, 85).

After the diagnosis of CDG-I based on serum Tf IEF, phosphomannomutase-2 (PMM2) and phosphomannose isomerase (PMI) activity should be measured in fibroblasts or leukocytes in the proper clinical context (1–4, 85). PMM2-CDG has the best-defined clinical phenotype and is by far the most frequent N-glycan assembly defect (99). PMI activity should be measured in case of clinical and biochemical presentation mainly expressed by the liver. If the clinical phenotype is not typical for PMM2-CDG and MPI-CDG, and in the case of normal PMM2 and PMI activity, plasma N-glycan analysis by MS (total plasma and/or intact transferrin glycoprofiling) could be done (1–4, 85). Nowadays, this is replaced by next-generation sequencing (NGS), including targeted NGS (panel of genes known to be involved in CDG) or whole exome sequencing (WES) (**Figure 1**). However, since NGS became more widely available, an improvement in diagnostics has been observed, with more patients and novel CDG subtypes being reported. These molecular analyses could take more time to result and be more expensive than laboratory CDG screening, although the high-throughput methods (like MS) are not routinely available (like in our center) and require both a qualified staff and comprehensive equipment.

After the diagnosis of CDG-II, IEF of serum apolipoprotein C-III (apoC-III) is recommended to perform (**Figure 1**) to distinguish between an exclusive N-glycosylation defect and a combined disorder of N- and O-glycosylation (1–4, 85). This analysis was described by Wopereis et al. in 2003 as a screening method for defects in the biosynthesis of the core 1 mucin-type O-glycans (100). However, some patients could also have an abnormal biosynthesis of core 1 O-glycans, including those with hemolytic uremic syndrome due to *Streptococcus pneumoniae*. Therefore, other laboratory methods have been developed parallel to serum Tf IEF, including serum apoC-III CZE.

Protein-linked glycan analysis should next be performed in attempt to identify the defective step, or targeted NGS, or WES (94).

Molecular analysis is necessary to confirm the final diagnosis of CDG and predict the possible genotype-phenotype correlation. However, the combination of MS with clinical exome sequencing (especially WES) is helpful to identify new CDG defects.

TREATMENT

An early diagnosis of CDG is crucial for the timely implementation of appropriate therapies. However, causative treatment is available only for few CDG types in the form of specific monosaccharide supplementation therapy (i.e., galactose for PGM1-CDG, fucose for SLC35C1-CDG, Mn^{2+} for TMEM165-CDG, or mannose for MPI-CDG) (101–103). For the majority of patients, only symptomatic treatment can be offered. The natural history for most CDG types is unknown (also due to lack of long-term follow-up); however, cerebellar ataxia in PMM2-CDG is not progressive, and patients could even slowly improve with age (26, 27).

Several therapeutic strategies were developed for PMM2-CDG, including mannose supplementation, inhibition of MPI, pharmacological chaperones, proteostasis regulators (celastrol), acetazolamide, and antisense therapy (104). To date, no causative treatment for PMM2-CDG exists. However, acetazolamide was reported to be well tolerated and effective for cerebellar syndrome (105). In addition, Taday et al. recently published a study on long-term oral mannose supplementation in 20 patients with PMM2-CDG (106). The therapy was tolerated well, and biochemical improvement was noted in the majority of patients.

Symptomatic treatment in PMM2-CDG includes:

- nutritional support (including percutaneous endoscopic gastrostomy placement) in failure-to-thrive patients;
- regular albumin infusions, octreotide therapy, or a diet rich in mid-chain fatty acids (MCTs) in protein-losing enteropathy;
- levothyroxine in the presence of decreased free thyroxine;
- fresh frozen plasma infusions to prevent bleeding episodes;
- pleural-pericardial window formation in recurrent pericardial effusion (26, 36).

The administration of mannose in MPI-CDG improves the clinical and biochemical outcome (including serum transferrin isoforms); however, patients can still develop progressive liver fibrosis (107–110). Mannose therapy in MPI-CDG was also discontinued in a few patients due to side effects (40). One reported patient with MPI-CDG required liver transplantation due to chronic liver disease with the development of hepatopulmonary syndrome (39).

Two patients with CCDC115-CDG underwent LTx; one rejected the transplant and died while the other is doing well, showing biochemical improvement of liver function tests and transferrin glycosylation profile (111).

Galactose therapy in PGM1-CDG is safe and associated with a significant improvement of *N*-glycosylation and clinical parameters (liver function tests, coagulation, blood glucose) (38, 77). Four patients with PGM1-CDG underwent heart transplantation, and all died due to cardiac disease-related complications. Three other patients reported by Tegtmeyer et al. were listed for heart transplantation (38).

Heart transplantation could be considered as a treatment option in other patients with cardiac involvement. It was performed in three patients with defects in dolichol synthesis (DOLK-CDG, DK1-CDG), despite supportive heart failure therapy (ACE inhibitors, β-blockers, and diuretics); one of them died unexpectedly 2 years after transplantation at the age of 16.5 years (51).

Besides PGM1-CDG, galactose supplementation showed promising results in SLC35A2-CDG, SLC39A8-CDG, and TMEM165-CDG (112–114).

Fucose supplementation in SLC35C1-CDG was reported to decrease infection rates, normalize neutrophil counts, and improve psychomotor development. However, it should be monitored carefully due to the risk of autoimmune and hemolytic reactions (115–117).

Uridine supplementation in CAD-CDG patients was reported to improve the clinical manifestation, including seizure cessation, cognitive and motor development, and normalization of biochemical parameters (118).

Hematopoietic stem cell transplantation was successfully applied to treat CDG with immunodeficiency in PGM3-CDG children (57).

AUTHOR CONTRIBUTIONS

PL and AT-S: project administration and writing—review and editing. AT-S: supervision. PL: writing—original draft. Both authors contributed to the article and approved the submitted version.

FUNDING

The study was funded by the Children's Memorial Health Institute intramural grant S190/2020.

REFERENCES

1. Jaeken J, Peanne R. What is new in CDG? *J Inherit Metab Dis.* (2017) 40:569–86. doi: 10.1007/s10545-017-0050-6
2. Francisco R. Marques-da-Silva D, Brasil S, Pascoal C, Dos Reis Ferreira V, Morava E, et al. The challenge of CDG diagnosis. *Mol Genet Metab.* (2019) 126:1–5. doi: 10.1016/j.ymgme.2018.11.003
3. Péanne R, de Lonlay P, Foulquier F, Kornak U, Lefeber DJ, Morava E, et al. Congenital disorders of glycosylation (CDG): Quo vadis? *Eur J Med Genet.* (2018) 61:643–63. doi: 10.1016/j.ejmg.2017.10.012
4. Ferreira CR, Altassan R, Marques-Da-Silva D, Francisco R, Jaeken J, Morava E. Recognizable phenotypes in CDG. *J Inherit Metab Dis.* (2018) 41:541–53. doi: 10.1007/s10545-018-0156-5
5. Makhamreh MM, Cottingham N, Ferreira CR, Berger S, Al-Kouatly HB. Nonimmune hydrops fetalis and congenital disorders of glycosylation: A systematic literature review. *J Inherit Metab Dis.* (2020) 43:223–33. doi: 10.1002/jimd.12162
6. Paprocka J, Jezela-Stanek A, Tylki-Szymańska A, Grunewald S. Congenital Disorders of Glycosylation from a Neurological Perspective. *Brain Sci.* (2021) 11:88. doi: 10.3390/brainsci11010088
7. Freeze HH, Eklund EA, Ng BG, Patterson MC. Neurological aspects of human glycosylation disorders. *Annu Rev Neurosci.* (2015) 38:105–25. doi: 10.1146/annurev-neuro-071714-034019
8. Fiumara A, Barone R, Del Campo G, Striano P. Jaeken J. Early-Onset Epileptic Encephalopathy in infants with different forms of Congenital Disorders of Glycosylation (CDG). *Brain Dev.* (2017) 39:366–67. doi: 10.1016/j.braindev.2016.11.008
9. Fiumara A, Barone R, Del Campo G, Striano P. Jaeken J. Electroclinical features of early-onset epileptic encephalopathies in congenital disorders of glycosylation (CDGs). *JIMD Rep.* (2016) 27:93–9. doi: 10.1007/8904_2015_497
10. Pereira AG, Bahi-Buisson N, Barnerias C, Boddaert N, Nabbout R, de Lonlay P, et al. Epileptic spasms in congenital disorders of glycosylation. *Epileptic Disord.* (2017) 19:15–23. doi: 10.1684/epd.2017.0901
11. Ng BG, Shiryaev SA, Rymen D, Eklund EA, Raymond K, Kircher M, et al. University of Washington Center for Mendelian Genomics, Matthijs G, Freeze HH. ALG1-CDG: clinical and molecular characterization of 39 unreported patients. *Hum Mutat.* (2016) 37:653–60.
12. Paketci C, Edem P, Hiz S, Sonmezler E, Soydemir D, Sarikaya Uzan G, et al. Successful treatment of intractable epilepsy with ketogenic diet therapy in twins with ALG3-CDG. *Brain Dev.* (2020) 42:539–45. doi: 10.1016/j.braindev.2020.04.008
13. Wu X, Rush JS, Karaoglu D, Krasnewich D, Lubinsky MS, Waechter CJ, et al. Deficiency of UDP-GlcNAc: Dolichol phosphate N-acetylglucosamine-1 Phosphate transferase (DPAGT1) causes a novel congenital disorder of glycosylation type Ij. *Hum Mutat.* (2003) 22:144–50. doi: 10.1002/humu.10239
14. Ng BG, Underhill HR, Palm L, Bengtson P, Rozet JM, Gerber S, et al. University of Washington Center for Mendelian Genomics, Freeze HH, Eklund EA. DPAGT1 deficiency with encephalopathy (DPAGT1-CDG): clinical and genetic description of 11 new patients. *JIMD Rep.* (2019) 44:85–92. doi: 10.1007/8904_2018_128
15. Barone R, Aiello C, Race V, Morava E, Foulquier F, Riemersma M, et al. DPM2-CDG: a muscular dystrophy-dystroglycanopathy syndrome with severe epilepsy. *Ann Neurol.* (2012) 72:550–8. doi: 10.1002/ana.23632
16. Ng BG, Eklund EA, Shiryaev SA, Dong YY, Abbott MA, Asteggiano C, et al. Predominant and novel de novo variants in 29 individuals with ALG13 deficiency: Clinical description, biomarker status, biochemical analysis, and treatment suggestions. *J Inherit Metab Dis.* (2020) 43:1333–48. doi: 10.1002/jimd.12290
17. Paprocka J, Jezela-Stanek A, Boguszewicz Ł, Sokół M, Lipiński P, Jamroz E, et al. The first metabolome analysis in children with epilepsy and ALG13-CDG resulting from c.320A>G variant. *Children (Basel).* (2021) 8:251. doi: 10.3390/children8030251
18. Galama WH. Verhaagen-van den Akker SLJ, Lefeber DJ, Feenstra I, Verrips A. ALG13-CDG with infantile spasms in a male patient due to a de novo ALG13 gene mutation. *JIMD Rep.* (2018) 40:11–6. doi: 10.1007/8904_2017_53
19. Chiyonobu T, Inoue N, Morimoto M, Kinoshita T, Murakami Y. Glycosylphosphatidylinositol (GPI) anchor deficiency caused by mutations in PIGW is associated with West syndrome and hyperphosphatasia with mental retardation syndrome. *J Med Genet.* (2014) 51:203–7. doi: 10.1136/jmedgenet-2013-102156

20. Bayat A, Knaus A, Pendziwiat M, Afenjar A, Barakat TS, Bosch F, et al. Lessons learned from 40 novel PIGA patients and a review of the literature. *Epilepsia.* (2020) 61:1142–55. doi: 10.1111/epi.16545
21. Kato M, Saitsu H, Murakami Y, Kikuchi K, Watanabe S, Iai M, et al. Mutations cause early-onset epileptic encephalopathies and distinctive features. *Neurology.* (2014) 82:1587–96. doi: 10.1212/WNL.0000000000000389
22. Johnstone DL, Nguyen TTM, Zambonin J, Kernohan KD, St-Denis A, Baratang NV, et al. Early infantile epileptic encephalopathy due to biallelic pathogenic variants in PIGQ: Report of seven new subjects and review of the literature. *J Inherit Metab Dis.* (2020) 43:1321–32. doi: 10.1002/jimd.12278
23. Martin HC, Kim GE, Pagnamenta AT, Murakami Y, Carvill GL, Meyer E, et al. Clinical whole-genome sequencing in severe early-onset epilepsy reveals new genes and improves molecular diagnosis. *Hum Mol Genet.* (2014) 23:3200–11. doi: 10.1093/hmg/ddu030
24. Schiller S, Rosewich H, Grünewald S, Gärtner J. Inborn errors of metabolism leading to neuronal migration defects. *J Inherit Metab Dis.* (2020) 43:145–55. doi: 10.1002/jimd.12194
25. Barone R, Fiumara A, Jaeken J. Congenital disorders of glycosylation with emphasis on cerebellar involvement. *Semin Neurol.* (2014) 34:357–66. doi: 10.1055/s-0034-1387197
26. Altassan R, Péanne R, Jaeken J, Barone R, Bidet M, Borgel D, et al. International clinical guidelines for the management of phosphomannomutase 2-congenital disorders of glycosylation: Diagnosis, treatment and follow up. *J Inherit Metab Dis.* (2019) 42:5–28. doi: 10.1002/jimd.12024
27. Serrano M, de Diego V, Muchart J, Cuadras D, Felipe A, Macaya A, et al. Phosphomannomutase deficiency (PMM2-CDG): ataxia and cerebellar assessment. *Orphanet J Rare Dis.* (2015) 10:138. doi: 10.1186/s13023-015-0358-y
28. Morava E, Wevers RA, Cantagrel V, Hoefsloot LH, Al-Gazali L, Schoots J, et al. Novel cerebello-ocular syndrome with abnormal glycosylation due to abnormalities in dolichol metabolism. *Brain.* (2010) 133:3210–20. doi: 10.1093/brain/awq261
29. Martin PT. The dystroglycanopathies: the new disorders of O-linked glycosylation. *Semin Pediatr Neurol.* (2005) 12:152–8. doi: 10.1016/j.spen.2005.10.003
30. Falsaperla R, Praticò AD, Ruggieri M, Parano E, Rizzo R, Corsello G, et al. Congenital muscular dystrophy: from muscle to brain. *Ital J Pediatr.* (2016) 42:78. doi: 10.1186/s13052-016-0289-9
31. Brancaccio A, A. molecular overview of the primary dystroglycanopathies. *J Cell Mol Med.* (2019) 23:3058–62. doi: 10.1111/jcmm.14218
32. Hu P, Yuan L, Deng H. Molecular genetics of the POMT1-related muscular dystrophy-dystroglycanopathies. *Mutat Res.* (2018) 778:45–50. doi: 10.1016/j.mrrev.2018.09.002
33. Godfrey C, Foley AR, Clement E, Muntoni F. Dystroglycanopathies: coming into focus. *Curr Opin Genet Dev.* (2011) 21:278–85. doi: 10.1016/j.gde.2011.02.001
34. Marques-da-Silva D, Dos Reis Ferreira V, Monticelli M, Janeiro P, Videira PA, Witters P, et al. Liver involvement in congenital disorders of glycosylation (CDG). A systematic review of the literature. *J Inherit Metab Dis. (*2017) 40:195–207. doi: 10.1007/s10545-016-0012-4
35. Starosta RT, Boyer S, Tahata S, Raymond K, Lee HE, Wolfe LA, et al. Liver manifestations in a cohort of 39 patients with congenital disorders of glycosylation: pin-pointing the characteristics of liver injury and proposing recommendations for follow-up. *Orphanet J Rare Dis.* (2021) 16:20. doi: 10.1186/s13023-020-01630-2
36. Bogdańska A, Lipiński P, Szymańska-Rozek P, Jezela-Stanek A, Rokicki D, Socha P, et al. Clinical, biochemical and molecular phenotype of congenital disorders of glycosylation: long-term follow-up. *Orphanet J Rare Dis.* (2021) 16:17. doi: 10.1186/s13023-020-01657-5
37. Spaapen LJ, Bakker JA, van der Meer SB, Sijstermans HJ, Steet RA, Wevers RA, et al. Clinical and biochemical presentation of siblings with COG-7 deficiency, a lethal multiple O- and N-glycosylation disorder. *J Inherit Metab Dis.* (2005) 28:707–14. doi: 10.1007/s10545-005-0015-z
38. Tegtmeyer LC, Rust S, van Scherpenzeel M, Ng BG, Losfeld ME, Timal S, et al. Multiple phenotypes in phosphoglucomutase 1 deficiency. *N Engl J Med.* (2014) 370:533–42. doi: 10.1056/NEJMoa1206605
39. Janssen MC, de Kleine RH, van den Berg AP, Heijdra Y, van Scherpenzeel M, Lefeber DJ, et al. Successful liver transplantation and long-term follow-up in a patient with MPI-CDG. *Pediatrics.* (2014) 134:e279–83. doi: 10.1542/peds.2013-2732
40. Damen G, de Klerk H, Huijmans J, den Hollander J, Sinaasappel M. Gastrointestinal and other clinical manifestations in 17 children with congenital disorders of glycosylation type Ia, Ib, and Ic. *J Pediatr Gastroenterol Nutr.* (2004) 38:282–87. doi: 10.1097/00005176-200403000-00010
41. Girard M, Poujois A, Fabre M, Lacaille F, Debray D, Rio M, et al. CCDC115-CDG: A new rare and misleading inherited cause of liver disease. *Mol Genet Metab.* (2018) 124:228–35. doi: 10.1016/j.ymgme.2018.05.002
42. Vajro P, Zielinska K, Ng BG, Maccarana M, Bengtson P, Poeta M, et al. Three unreported cases of TMEM199-CDG, a rare genetic liver disease with abnormal glycosylation. *Orphanet J Rare Dis.* (2018) 13:4. doi: 10.1186/s13023-017-0757-3
43. Jansen JC, Timal S, van Scherpenzeel M, Michelakakis H, Vicogne D, Ashikov A, et al. TMEM199 deficiency is a disorder of Golgi homeostasis characterized by elevated aminotransferases, alkaline phosphatase, and cholesterol and abnormal glycosylation. *Am J Hum Genet.* (2016) 98:322–30. doi: 10.1016/j.ajhg.2015.12.011
44. de Koning TJ, Nikkels PG, Dorland L, Bekhof J, De Schrijver JE, van Hattum J, et al. Congenital hepatic fibrosis in 3 siblings with phosphomannose isomerase deficiency. *Virchows Arch.* (2000) 437:101–5. doi: 10.1007/s004280000185
45. Marques-da-Silva D, Francisco R, Webster D, Dos Reis Ferreira V, Jaeken J, Pulinilkunnil T. Cardiac complications of congenital disorders of glycosylation (CDG): a systematic review of the literature. *J Inherit Metab Dis.* (2017) 40:657–72. doi: 10.1007/s10545-017-0066-y
46. Footitt EJ, Karimova A, Burch M, Yayeh T, Dupré T, Vuillaumier-Barrot S, et al. Cardiomyopathy in the congenital disorders of glycosylation (CDG): a case of late presentation and literature review. *J Inherit Metab Dis.* (2009) 32:S313–9. doi: 10.1007/s10545-009-1262-1
47. Knaus A, Pantel JT, Pendziwiat M, Hajjir N, Zhao M, Hsieh TC, et al. Characterization of glycosylphosphatidylinositol biosynthesis defects by clinical features, flow cytometry, and automated image analysis. *Genome Med.* (2018) 10:3. doi: 10.1186/s13073-017-0510-5
48. Carmody LC, Blau H, Danis D, Zhang XA, Gourdine JP, Vasilevsky N, et al. Significantly different clinical phenotypes associated with mutations in synthesis and transamidase+remodeling glycosylphosphatidylinositol (GPI)-anchor biosynthesis genes. *Orphanet J Rare Dis.* (2020) 15:40. doi: 10.1186/s13023-020-1313-0
49. D'Souza Z, Taher FS, Lupashin VV. Golgi inCOGnito: From vesicle tethering to human disease. *Biochim Biophys Acta Gen Subj.* (2020) 1864:129694. doi: 10.1016/j.bbagen.2020.129694
50. Görlacher M, Panagiotou E, Himmelreich N, Hüllen A, Beedgen L, Dimitrov B, et al. Fatal outcome after heart surgery in PMM2-CDG due to a rare homozygous gene variant with double effects. *Mol Genet Metab Rep.* (2020) 25:100673. doi: 10.1016/j.ymgmr.2020.100673
51. Kapusta L, Zucker N, Frenckel G, Medalion B, Ben Gal T, Birk E, et al. From discrete dilated cardiomyopathy to successful cardiac transplantation in congenital disorders of glycosylation due to dolichol kinase deficiency (DK1-CDG). *Heart Fail Rev.* (2013) 18:187–96. doi: 10.1007/s10741-012-9302-6
52. Fernlund E, Andersson O, Ellegård R, Årstrand HK, Green H, Olsson H, et al. The congenital disorder of glycosylation in PGM1 (PGM1-CDG) can cause severe cardiomyopathy and unexpected sudden cardiac death in childhood. *Forensic Sci Int Genet.* (2019) 43:102111. doi: 10.1016/j.fsigen.2019.06.012
53. Pascoal C, Francisco R, Ferro T, Dos Reis Ferreira V, Jaeken J, Videira PA, et al. and immune response: From bedside to bench and back. *J Inherit Metab Dis.* (2020) 43:90–124. doi: 10.1002/jimd.12126
54. Monticelli M, Ferro T, Jaeken J, Dos Reis Ferreira V, Videira PA. Immunological aspects of congenital disorders of glycosylation (CDG): a review. *J Inherit Metab Dis.* (2016) 39:765–80. doi: 10.1007/s10545-016-9954-9
55. Sturiale L, Bianca S, Garozzo D, Terracciano A, Agolini E, Messina A, et al. ALG12-CDG: novel glycophenotype insights endorse the molecular defect. *Glycoconj J.* (2019) 36:461–72. doi: 10.1007/s10719-019-09890-2

56. Chang J, Block TM, Guo JT. Viral resistance of MOGS-CDG patients implies a broad-spectrum strategy against acute virus infections. *Antivir Ther.* (2015) 20:257–9. doi: 10.3851/IMP2907
57. Stray-Pedersen A, Backe PH, Sorte HS, Mørkrid L, Chokshi NY, Erichsen HC, et al. PGM3 mutations cause a congenital disorder of glycosylation with severe immunodeficiency and skeletal dysplasia. *Am J Hum Genet.* (2014) 95:96–107. doi: 10.1016/j.ajhg.2014.05.007
58. Pacheco-Cuéllar G, Gauthier J, Désilets V, Lachance C, Lemire-Girard M, Rypens F, et al. Novel PGM3 mutation is associated with a severe phenotype of bone marrow failure, severe combined immunodeficiency, skeletal dysplasia, and congenital malformations. *J Bone Miner Res.* (2017) 32:1853–59. doi: 10.1002/jbmr.3173
59. Knapp KM, Luu R, Baerenfaenger M, Zijlstra F, Wessels HJCT, Jenkins D, et al. Biallelic variants in SLC35C1 as a cause of isolated short stature with intellectual disability. *J Hum Genet.* (2020) 65:743–50. doi: 10.1038/s10038-020-0764-4
60. Sadat MA, Moir S, Chun TW, Lusso P, Kaplan G, Wolfe L, et al. Glycosylation, hypogammaglobulinemia, and resistance to viral infections. *N Engl J Med.* (2014) 370:1615–25. doi: 10.1056/NEJMoa1302846
61. Murali C, Lu JT, Jain M, Liu DS, Lachman R, Gibbs RA, et al. Diagnosis of ALG12-CDG by exome sequencing in a case of severe skeletal dysplasia. *Mol Genet Metab Rep.* (2014) 1:213–9. doi: 10.1016/j.ymgmr.2014.04.004
62. Lepais L, Cheillan D, Frachon SC, Hays S, Matthijs G, Panagiotakaki E, et al. ALG3-CDG: Report of two siblings with antenatal features carrying homozygous p.Gly96Arg mutation. *Am J Med Genet A.* (2015) 167A:2748–54. doi: 10.1002/ajmg.a.37232
63. Tham E, Eklund EA, Hammarsjö A, Bengtson P, Geiberger S, Lagerstedt-Robinson K, et al. Novel phenotype in N-glycosylation disorders: Gillessen-Kaesbach-Nishimura skeletal dysplasia due to pathogenic variants in ALG9. *Eur J Hum Genet.* (2016) 24:198–207. doi: 10.1038/ejhg.2015.91
64. AlSubhi S, AlHashem A, AlAzami A, Tlili K, AlShahwan S, Lefeber D, et al. Further delineation of the ALG9-CDG phenotype. *JIMD Rep.* (2016) 27:107–12. doi: 10.1007/8904_2015_504
65. Sassi A, Lazaroski S, Wu G, Haslam SM, Fliegauf M, Mellouli F, et al. Hypomorphic homozygous mutations in phosphoglucomutase 3 (PGM3) impair immunity and increase serum IgE levels. *J Allergy Clin Immunol.* (2014) 133:1410–9. doi: 10.1016/j.jaci.2014.02.025
66. Vodopiutz J, Mizumoto S, Lausch E, Rossi A, Unger S, Janocha N, et al. Chondroitin Sulfate N-acetylgalactosaminyltransferase-1 (CSGalNAcT-1) Deficiency Results in a Mild Skeletal Dysplasia and Joint Laxity. *Hum Mutat.* (2017) 38:34–8. doi: 10.1002/humu.23070
67. Mizumoto S, Janecke AR, Sadeghpour A, Povysil G, McDonald MT, Unger S, et al. CSGALNACT1-congenital disorder of glycosylation: A mild skeletal dysplasia with advanced bone age. *Hum Mutat.* (2020) 41:655–67. doi: 10.1002/humu.23952
68. Zeevaert R, de Zegher F, Sturiale L, Garozzo D, Smet M, Moens M, et al. Bone dysplasia as a key feature in three patients with a novel congenital disorder of glycosylation (CDG) type ii due to a deep intronic splice mutation in TMEM165. *JIMD Rep.* (2013) 8:145–52. doi: 10.1007/8904_2012_172
69. Foulquier F, Amyere M, Jaeken J, Zeevaert R, Schollen E, Race V, et al. TMEM165 deficiency causes a congenital disorder of glycosylation. *Am J Hum Genet.* (2012) 91:15–26. doi: 10.1016/j.ajhg.2012.05.002
70. Rautengarten C, Quarrell OW, Stals K, Caswell RC, De Franco E, Baple E, et al. hypomorphic allele of SLC35D1 results in Schneckenbecken-like dysplasia. *Hum Mol Genet.* (2019) 28:3543–51. doi: 10.1093/hmg/ddz200
71. Horn D, Krawitz P, Mannhardt A, Korenke GC, Meinecke P. Hyperphosphatasia-mental retardation syndrome due to PIGV mutations: expanded clinical spectrum. *Am J Med Genet A.* (2011) 155A:1917–22. doi: 10.1002/ajmg.a.34102
72. Altassan R, Fox S, Poulin C, Buhas D. Hyperphosphatasia with mental retardation syndrome, expanded phenotype of PIGL related disorders. *Mol Genet Metab Rep.* (2018) 15:46–9. doi: 10.1016/j.ymgmr.2018.01.007
73. Dimitrov B, Himmelreich N, Hipgrave Ederveen AL, Lüchtenborg C, Okun JG, Breuer M, et al. Cutis laxa, exocrine pancreatic insufficiency and altered cellular metabolomics as additional symptoms in a new patient with ATP6AP1-CDG. *Mol Genet Metab.* (2018) 123:364–74. doi: 10.1016/j.ymgme.2018.01.008
74. Witters P, Breckpot J, Foulquier F, Preston G, Jaeken J, Morava E. Expanding the phenotype of metabolic cutis laxa with an additional disorder of N-linked protein glycosylation. *Eur J Hum Genet.* (2018) 26:618–21. doi: 10.1038/s41431-017-0044-8
75. Jansen EJ, Timal S, Ryan M, Ashikov A, van Scherpenzeel M, Graham LA, et al. ATP6AP1 deficiency causes an immunodeficiency with hepatopathy, cognitive impairment and abnormal protein glycosylation. *Nat Commun.* (2016) 7:11600. doi: 10.1038/ncomms11600
76. Van Damme T, Gardeitchik T, Mohamed M, Guerrero-Castillo S, Freisinger P, Guillemyn B, et al. Mutations in ATP6V1E1 or ATP6V1A cause autosomal-recessive cutis laxa. *Am J Hum Genet.* (2017) 100:216–27. doi: 10.1016/j.ajhg.2016.12.010
77. Altassan R, Radenkovic S, Edmondson AC, Barone R, Brasil S, Cechova A, et al. International consensus guidelines for phosphoglucomutase 1 deficiency (PGM1-CDG): Diagnosis, follow-up, and management. *J Inherit Metab Dis.* (2021) 44:148–63. doi: 10.1002/jimd.12286
78. Schiff M, Roda C, Monin ML, Arion A, Barth M, Bednarek N, et al. Clinical, laboratory and molecular findings and long-term follow-up data in 96 French patients with PMM2-CDG (phosphomannomutase 2-congenital disorder of glycosylation) and review of the literature. *J Med Genet.* (2017) 54:843–51. doi: 10.1136/jmedgenet-2017-104903
79. Al-Maawali AA, Miller E, Schulze A, Yoon G, Blaser SI. Subcutaneous fat pads on body MRI-an early sign of congenital disorder of glycosylation PMM2-CDG (CDG1a). *Pediatr Radiol.* (2014) 44:222–25. doi: 10.1007/s00247-013-2782-2
80. Cabezas OR, Flanagan SE, Stanescu H, García-Martínez E, Caswell R, Lango-Allen H, et al. Polycystic Kidney Disease with Hyperinsulinemic Hypoglycemia Caused by a Promoter Mutation in Phosphomannomutase 2. *J Am Soc Nephrol.* (2017) 28:2529–39. doi: 10.1681/ASN.2016121312
81. Diaz J, Kane TD, Leon E. Evidence of GMPPA founder mutation in indigenous Guatemalan population associated with alacrima, achalasia, and mental retardation syndrome. *Am J Med Genet A.* (2020) 182:425–30. doi: 10.1002/ajmg.a.61476
82. Sturla L, Fruscione F, Noda K, Miyoshi E, Taniguchi N, Contini P, et al. Core fucosylation of N-linked glycans in leukocyte adhesion deficiency/congenital disorder of glycosylation IIc fibroblasts. *Glycobiology.* (2005) 15:924–34. doi: 10.1093/glycob/cwi081
83. Etzioni A, Sturla L, Antonellis A, Green ED, Gershoni-Baruch R, Berninsone PM, et al. Leukocyte adhesion deficiency (LAD) type II/carbohydrate deficient glycoprotein (CDG) IIc founder effect and genotype/phenotype correlation. *Am J Med Genet.* (2002) 110:131–5. doi: 10.1002/ajmg.10423
84. Jaeken J, van Eijk HG, van der Heul L, Corbeel L, Eeckels R, Eggermont E. Sialic acid-deficient serum and cerebrospinal fluid transferrin in a newly recognized genetic syndrome. *Clin Chim Acta.* (1984) 144:245–47. doi: 10.1016/0009-8981(84)90059-7
85. Lefeber DJ, Morava E, Jaeken J. How to find and diagnose a CDG due to defective N-glycosylation. *J Inherit Metab Dis.* (2011) 34:849–52. doi: 10.1007/s10545-011-9370-0
86. Helander A, Eriksson G, Stibler H, Jeppsson JO. Interference of transferrin isoform types with carbohydrate-deficient transferrin quantification in the identification of alcohol abuse. *Clin Chem.* (2001) 47:1225–33. doi: 10.1093/clinchem/47.7.1225
87. Carchon HA, Chevigné R, Falmagne JB, Jaeken J. Diagnosis of congenital disorders of glycosylation by capillary zone electrophoresis of serum transferrin. *Clin Chem.* (2004) 50:101–11. doi: 10.1373/clinchem.2003.021568
88. Quintana E, Navarro-Sastre A, Hernández-Pérez JM, García-Villoria J, Montero R, Artuch R, et al. Screening for congenital disorders of glycosylation (CDG): transferrin HPLC versus isoelectric focusing (IEF). *Clin Biochem.* (2009) 42:408–15. doi: 10.1016/j.clinbiochem.2008.12.013
89. Babovic-Vuksanovic D, O'Brien JF. Laboratory diagnosis of congenital disorders of glycosylation type I by analysis of transferrin glycoforms. *Mol Diagn Ther.* (2007) 11:303–11. doi: 10.1007/BF03256251
90. Casetta B, Malvagia S, Funghini S, Martinelli D, Dionisi-Vici C, Barone R, et al. A new strategy implementing mass spectrometry in the diagnosis of congenital disorders of N-glycosylation (CDG). *Clin Chem Lab Med.* (2020) 59:165–71. doi: 10.1515/cclm-2020-0650

91. Messina A, Palmigiano A, Esposito F, Fiumara A, Bordugo A, Barone R, et al. For high throughput and isomeric N-glycan separation and characterization in Congenital Disorders Glycosylation and human diseases. *Glycoconj J.* (2021) 38:201–11. doi: 10.1007/s10719-020-09947-7
92. Abu Bakar N, Lefeber DJ, van Scherpenzeel M. Clinical glycomics for the diagnosis of congenital disorders of glycosylation. *J Inherit Metab Dis.* (2018) 41:499–513. doi: 10.1007/s10545-018-0144-9
93. Hipgrave Ederveen AL, de Haan N, Baerenfaenger M, Lefeber DJ, Wuhrer M. Dissecting total plasma and protein-specific glycosylation profiles in congenital disorders of glycosylation. *Int J Mol Sci.* (2020) 21:7635. doi: 10.3390/ijms21207635
94. Van Scherpenzeel M, Willems E, Lefeber DJ. Clinical diagnostics and therapy monitoring in the congenital disorders of glycosylation. *Glycoconj J.* (2016) 33:345–58. doi: 10.1007/s10719-015-9639-x
95. Bogdańska A, Kozłowski D, Pajdowska M, Lipiński P, Tylki-Szymańska A. Transferrin isoform analysis from dried blood spots and serum samples by gel isoelectric focusing for screening congenital disorders of glycosylation. *Acta Biochim Pol.* (2021) 68:139–42. doi: 10.18388/abp.2020_5576
96. Wolking AB, Park JH, Grüneberg M, Reunert J, Fingerhut R, Fobker M, et al. Transferrin glycosylation analysis from dried blood spot cards and capillary blood samples. *J Chromatogr B Analyt Technol Biomed Life Sci.* (2019) 1106–7:64–70. doi: 10.1016/j.jchromb.2019.01.004
97. Bogdańska A, Lipiński P, Szymańska-Rozek P, Jankowska I, Socha P, Tylki-Szymańska A. Pediatric liver disease patients and secondary glycosylation abnormalities. *Front Pediatr.* (2021) 8:613224. doi: 10.3389/fped.2020.613224
98. Jansen JC, van Hoek B, Metselaar HJ, van den Berg AP, Zijlstra F, Huijben K, et al. Screening for abnormal glycosylation in a cohort of adult liver disease patients. *J Inherit Metab Dis.* (2020) 43:1310–20. doi: 10.1002/jimd.12273
99. Lipiński P, Bogdańska A, Tylki-Szymańska A. Congenital disorders of glycosylation: Prevalence, incidence and mutational spectrum in the Polish population. *Mol Genet Metab Rep.* (2021) 27:100726. doi: 10.1016/j.ymgmr.2021.100726
100. Wopereis S, Morava E, Grunewald S, Adamowicz M, Huijben KM, Lefeber DJ, et al. Patients with unsolved congenital disorders of glycosylation type II can be subdivided in six distinct biochemical groups. *Glycobiology.* (2005) 15:1312–19. doi: 10.1093/glycob/cwj017
101. Brasil S, Pascoal C, Francisco R. Marques-da-Silva D, Andreotti G, Videira PA, et al. CDG therapies: from bench to bedside. *Int J Mol Sci.* (2018) 19:1304. doi: 10.3390/ijms19051304
102. Verheijen J, Tahata S, Kozicz T, Witters P, Morava E. Therapeutic approaches in Congenital Disorders of Glycosylation (CDG) involving N-linked glycosylation: an update. *Genet Med.* (2020) 22:268–79. doi: 10.1038/s41436-019-0647-2
103. Witters P, Cassiman D, Morava E. Nutritional therapies in congenital disorders of glycosylation (CDG). *Nutrients.* (2017) 9:E1222. doi: 10.3390/nu9111222
104. Gámez A, Serrano M, Gallego D, Vilas A, Pérez B. New and potential strategies for the treatment of PMM2-CDG. *Biochim Biophys Acta Gen Subj.* (2020) 1864:129686. doi: 10.1016/j.bbagen.2020.129686
105. Martínez-Monseny AF, Bolasell M, Callejón-Póo L, Cuadras D, Freniche V, Itzep DC, et al. AZATAX: Acetazolamide safety and efficacy in cerebellar syndrome in PMM2 congenital disorder of glycosylation (PMM2-CDG). *Ann Neurol.* (2019) 85:740–51. doi: 10.1002/ana.25457
106. Taday R, Grüneberg M, DuChesne I, Reunert J, Marquardt T. Dietary mannose supplementation in phosphomannomutase 2 deficiency (PMM2-CDG). *Orphanet J Rare Dis.* (2020) 15:258. doi: 10.1186/s13023-020-01528-z
107. Harms HK, Zimmer KP, Kurnik K, Bertele-Harms RM, Weidinger S, Reiter K. Oral mannose therapy persistently corrects the severe clinical symptoms and biochemical abnormalities of phosphomannose isomerase deficiency. *Acta Paediatr*. (2002) 91:1065–72. doi: 10.1111/j.1651-2227.2002.tb00101.x
108. Girard M, Douillard C, Debray D, Lacaille F, Schiff M, Vuillaumier-Barrot S, et al. Long term outcome of MPI-CDG patients on D-mannose therapy. *J Inherit Metab Dis.* (2020) 43:1360–69. doi: 10.1002/jimd.12289
109. Čechová A, Altassan R, Borgel D, Bruneel A, Correia J, Girard M, et al. Consensus guideline for the diagnosis and management of mannose phosphate isomerase-congenital disorder of glycosylation. *J Inherit Metab Dis*. (2020) 43:671–93. doi: 10.1002/jimd.12241
110. Mention K, Lacaille F, Valayannopoulos V, Romano S, Kuster A, Cretz M, et al. Development of liver disease despite mannose treatment in two patients with CDG-Ib. *Mol Genet Metab.* (2008) 93:40–3. doi: 10.1016/j.ymgme.2007.08.126
111. Jansen JC, Cirak S, van Scherpenzeel M, Timal S, Reunert J, Rust S, et al. CCDC115 deficiency causes a disorder of golgi homeostasis with abnormal protein glycosylation. *Am J Hum Genet.* (2016) 98:310–21. doi: 10.1016/j.ajhg.2015.12.010
112. Morelle W, Potelle S, Witters P, Wong S, Climer L, Lupashin V, et al. galactose supplementation in patients with TMEM165-CDG rescues the glycosylation defects. *J Clin Endocrinol Metab.* (2017) 102:1375–86. doi: 10.1210/jc.2016-3443
113. Dörre K, Olczak M, Wada Y, Sosicka P, Grüneberg M, Reunert J, et al. A new case of UDP-galactose transporter deficiency (SLC35A2-CDG): molecular basis, clinical phenotype, and therapeutic approach. *J Inherit Metab Dis*. (2015) 38:931–40. doi: 10.1007/s10545-015-9828-6
114. Ng BG, Buckingham KJ, Raymond K, Kircher M, Turner EH, He M, et al. Mosaicism of the UDP-galactose transporter SLC35A2 causes a congenital disorder of glycosylation. *Am J Hum Genet.* (2013) 92:632–6. doi: 10.1016/j.ajhg.2013.03.012
115. Hidalgo A, Ma S, Peired AJ, Weiss LA, Cunningham-Rundles C, Frenette PS. Insights into leukocyte adhesion deficiency type 2 from a novel mutation in the GDP-fucose transporter gene. *Blood*. (2003) 101:1705–12. doi: 10.1182/blood-2002-09-2840
116. Lühn K, Wild MK, Eckhardt M, Gerardy-Schahn R, Vestweber D. The gene defective in leukocyte adhesion deficiency II encodes a putative GDP-fucose transporter. *Nat Genet.* (2001) 28:69–72. doi: 10.1038/ng0501-69
117. Helmus Y, Denecke J, Yakubenia S, Robinson P, Lühn K, Watson DL, et al. Leukocyte adhesion deficiency II patients with a dual defect of the GDP-fucose transporter. *Blood.* (2006) 107:3959–66. doi: 10.1182/blood-2005-08-3334
118. Koch J, Mayr JA, Alhaddad B, Rauscher C, Bierau J, Kovacs-Nagy R, et al. mutations and uridine-responsive epileptic encephalopathy. *Brain*. (2017) 140:279–86. doi: 10.1093/brain/aww300

Conflict of Interest: The authors declare that the research was conducted in the absence of any commercial or financial relationships that could be construed as a potential conflict of interest.

Publisher's Note: All claims expressed in this article are solely those of the authors and do not necessarily represent those of their affiliated organizations, or those of the publisher, the editors and the reviewers. Any product that may be evaluated in this article, or claim that may be made by its manufacturer, is not guaranteed or endorsed by the publisher.

frontiers in Genetics

ORIGINAL RESEARCH
published: 09 September 2021
doi: 10.3389/fgene.2021.744884

ALG1-CDG Caused by Non-functional Alternative Splicing Involving a Novel Pathogenic Complex Allele

*Carlos Alberto González-Domínguez[1,2], Moisés O. Fiesco-Roa[3,4], Samuel Gómez-Carmona[5], Anke Paula Ingrid Kleinert-Altamirano[5,7], Miao He[6], Earnest James Paul Daniel[6], Kimiyo M. Raymond[8], Melania Abreu-González[9], Sandra Manrique-Hernández[1,2], Ana González-Jaimes[1], Roberta Salinas-Marín[1], Carolina Molina-Garay[10], Karol Carrillo-Sánchez[10], Luis Leonardo Flores-Lagunes[10], Marco Jiménez-Olivares[10], Anallely Muñoz-Rivas[10], Mario E. Cruz-Muñoz[11], Matilde Ruíz-García[12], Hudson H. Freeze[13], Héctor M. Mora-Montes[14], Carmen Alaez-Verson[10] and Iván Martínez-Duncker[1,15]**

[1] Laboratorio de Glicobiología Humana y Diagnóstico Molecular, Centro de Investigación en Dinámica Celular, Instituto de Investigación en Ciencias Básicas y Aplicadas, Universidad Autónoma del Estado de Morelos, Cuernavaca, Mexico, [2] Instituto de Biotecnología, Universidad Nacional Autónoma de México, Cuernavaca, Mexico, [3] Programa de Maestría y Doctorado en Ciencias Médicas, Universidad Nacional Autónoma de México (UNAM), Ciudad Universitaria, Mexico City, Mexico, [4] Laboratorio de Citogenética, Instituto Nacional de Pediatría, Mexico City, Mexico, [5] Centro de Rehabilitación e Inclusión Infantil Teletón, Tuxtla Gutiérrez, Mexico, [6] Palmieri Metabolic Disease Laboratory, Children's Hospital of Philadelphia, Philadelphia, PA, United States, [7] Hospital Regional de Alta Especialidad Ciudad Salud, Tapachula, Mexico, [8] Department of Laboratory Medicine and Pathology, Laboratory Genetics and Genomics, Mayo Clinic, Rochester, MN, United States, [9] Genos Médica, Mexico City, Mexico, [10] Laboratorio de Diagnóstico Genómico, Instituto Nacional de Medicina Genómica, Secretaría de Salud, Mexico City, Mexico, [11] Laboratorio de Inmunología Molecular, Facultad de Medicina, Universidad Autónoma del Estado de Morelos, Cuernavaca, Mexico, [12] Departamento de Neurología, Instituto Nacional de Pediatría, Mexico City, Mexico, [13] Human Genetics Program, Sanford Burnham Prebys Medical Discovery Institute, La Jolla, CA, United States, [14] Departamento de Biología, División de Ciencias Naturales y Exactas, Universidad de Guanajuato, Guanajuato, Mexico, [15] Sociedad Latinoamericana de Glicobiología A.C, Cuernavaca, Mexico

This study reports on a Mexican mestizo patient with a multi-systemic syndrome including neurological involvement and a type I serum transferrin profile. Clinical exome sequencing revealed complex alleles in *ALG1,* the encoding gene for the chitobiosyldiphosphodolichol beta-mannosyltransferase that participates in the formation of the dolichol-pyrophosphate-GlcNAc2Man5, a lipid-linked glycan intermediate during *N*-glycan synthesis. The identified complex alleles were NM_019109.5(ALG1): c.[208 + 16_208 + 19dup; 208 + 25G > T] and NM_019109.5(ALG1): c.[208 + 16_208 + 19dup; 1312C > T]. Although both alleles carried the benign variant c.208 + 16_208 + 19dup, one allele carried a known *ALG1* pathogenic variant (c.1312C > T), while the other carried a new uncharacterized variant (c.208 + 25G > T) causing non-functional alternative splicing that, in conjunction with the benign variant, defines the pathogenic protein effect (p.N70S_S71ins9). The presence in the patient's serum of the pathognomonic N-linked mannose-deprived tetrasaccharide marker for ALG1-CDG (Neu5Acα2,6Galβ1,4-GlcNAcβ1,4GlcNAc) further supported this diagnosis. This is the first report of an ALG1-CDG patient from Latin America.

Keywords: CDG, splicing, metabolic, glycosylation, ALG1, mutation, tetrasaccharide

OPEN ACCESS

Edited by:
Karolina Stepien,
Salford Royal NHS Foundation Trust,
United Kingdom

Reviewed by:
Domenico Garozzo,
Italian National Research Council, Italy
Patryk Lipiński,
Children's Memorial Health Institute (IPCZD), Poland

****Correspondence:***
Iván Martínez-Duncker
duncker@uaem.mx

Specialty section:
This article was submitted to Genetics of Common and Rare Diseases, a section of the journal Frontiers in Genetics

Received: *21 July 2021*
Accepted: *05 August 2021*
Published: *09 September 2021*

Citation:
González-Domínguez CA, Fiesco-Roa MO, Gómez-Carmona S, Kleinert-Altamirano API, He M, Daniel EJP, Raymond KM, Abreu-González M, Manrique-Hernández S, González-Jaimes A, Salinas-Marín R, Molina-Garay C, Carrillo-Sánchez K, Flores-Lagunes LL, Jiménez-Olivares M, Muñoz-Rivas A, Cruz-Muñoz ME, Ruíz-García M, Freeze HH, Mora-Montes HM, Alaez-Verson C and Martínez-Duncker I (2021) ALG1-CDG Caused by Non-functional Alternative Splicing Involving a Novel Pathogenic Complex Allele. Front. Genet. 12:744884. doi: 10.3389/fgene.2021.744884

INTRODUCTION

Approximately 140 inborn errors of metabolism have been classified as congenital disorders of glycosylation (CDG), a rapidly expanding group of diseases caused by defects in the synthesis and attachment of glycans to glycoproteins and glycolipids (Ondruskova et al., 2021). ALG1-CDG is a subtype with severe multiorgan involvement (OMIM 608540) caused by pathogenic variants in *ALG1*. This gene encodes for a transmembrane chitobiosyldiphosphodolichol beta-mannosyltransferase that participates in the first steps of N-glycan biosynthesis that occur in the cytosolic side of the endoplasmic reticulum involving dolichol-pyrophosphate-GlcNAc2Man5 synthesis, an intermediate of the lipid-linked precursor oligosaccharide that is subsequently transferred to nascent glycoproteins for protein N-glycosylation. ALG1 extends GlcNAc2-PP-dolichol by adding the first mannose in ß1,4-linkage using GDP-mannose as a substrate donor to generate Man1GlcNAc2-PP-dolichol (Couto et al., 1984). ALG1 is part of a multi-mannosyltransferase complex that includes ALG1, ALG2, and ALG11 involved in a five-reaction process (Gao et al., 2004; O'Reilly et al., 2006; Aebi, 2013).

In contrast to PMM2-CDG, the most prevalent CDG affecting N-glycosylation with >1,000 patients reported worldwide, <80 cases of ALG1-CDG have been reported in the literature since 2004, none from Latin America (Grubenmann et al., 2004; Kranz et al., 2004; Schwarz et al., 2004; Dupré et al., 2010; Morava et al., 2012; Rohlfing et al., 2014; Barba et al., 2016; Harshman et al., 2016; Ng et al., 2016; Marques-da-Silva et al., 2017; Pérez-Cerdá et al., 2017; Medrano et al., 2019; Lei et al., 2020; Bogdańska et al., 2021; Quelhas et al., 2021). According to the Human Gene Mutation Database (HGMD), 50 disease-causing mutations have been reported in *ALG1*, including 41 missense/non sense, 6 splicing mutations, 1 small insertion, 1 small indel, and 1 gross deletion (as of July 2021).

Here, we describe a Mexican mestizo patient with ALG1-CDG who is a compound heterozygous of two pathogenic variants. One of these variants (NM_019109.5(ALG1):c.208 + 25G > T), previously uncharacterized, in combination with a known *cis* benign variant NM_019109.4(ALG1): c.208 + 16_208 + 19dup, causes, a new intronic donor splice site resulting in partial intron 1 retention (+27 bp), producing an aminoacid substitution and insertion (p.N70S_S71ins9).

PATIENT REPORT

The patient was a 15-year-old male of Mexican ancestry with intellectual disability, seizures, hypotonic quadriplegia, and disproportionated microcephaly (height in normal centile). He was born in Tabasco State (in the southern part of Mexico). No consanguinity or endogamy was reported. The patient's parents and an older sister were healthy, but he had another sister who died at 15 years old with similar manifestations. The mother reported a history of a first-trimester spontaneous abortion. There was no other relevant family history (**Figure 1**). The patient was the product of a naturally conceived 38-week singleton pregnancy to a 33-year-old mother and 37-year-old father, uneventful pregnancy with two normal prenatal ultrasounds. Delivery was via emergency cesarean section for prolonged rupture of membranes. At birth weight the patient was 3,100 g [46th centile; −0.1 standard deviation scores (SDS)] and length was 50 cm (50th centile; 0.5 SDS); additional birth parameters and APGAR score were unknown. He did not require respiratory support or supplementary interventions. He left the hospital 2 days after delivery. He was hospitalized for 30 days at 9 months of age due to seizures. During this hospitalization he was first noted to have some developmental delay; the mother reported the loss of some abilities after the onset of seizures.

He was first seen by a geneticist at 5 years old; however, no diagnosis was integrated. He was re-evaluated by geneticists at 10.8 years old. The anthropometric features were 32.3 kg of weight (24th centile; −0.71 SDS), 151 cm of height (85th centile; + 1.05 SDS), and 49.2 cm of head circumference (< 3rd centile; −3.01 SDS) (HP:0000252); the head circumference measurement at 4 years old was 46.3 cm (< 3rd centile; −2.72 SDS), no previous head circumference evaluation was available. After a physical examination, the following findings were found: Short forehead (HP:0000350), eyebrow slightly sparse (HP:0000535), slightly prominent nasal bridge (HP:0000426), prominent cheeks (HP:0000293), wide mouth (HP:0000154), and widely spaced and misplaced teeth (HP:0000687 and HP:0006316, respectively). He had premature gray hair (HP:0002216) and one café-au-lait spot (HP:0000957) on his left forearm. The neurological evaluation found profound intellectual disability (HP:0002187), stereotypical and self-injurious behaviors (HP:0000733 and HP:0100716, respectively), sialorrhea (HP:0002307), central hypotonia (HP:0011398), hypotonic quadriplegia (HP:0002273), and generalized hyperreflexia (HP:0007034); no major motor milestones (gross motor function classification system level IV), and only guttural sounds [speech delay (alalia)] (HP:0001344). No other physical abnormality was detected.

During genetics follow-up, several investigations were performed. Metabolic screening for inborn errors of metabolism (including ammonia, lactate, plasma amino acids, and urine organic acids) was normal. Blood counts, INR, and prothrombin time were normal. No other laboratory tests were performed. An EEG performed at 10 years old showed diffuse slowing (HP:0010845), slow spike-and-wave activity (HP:0010850), and frontal intermittent rhythmic delta activity (FIRDA). The visual and brainstem-auditory evoked potentials revealed bilateral integrity of visual and auditory pathways, respectively. MRI was abnormal (**Figure 2**), showing generalized and asymmetric cortical-subcortical frontotemporal atrophy (HP:0006892) predominantly on the left, hypoplasia of the frontal lobes (HP:0007333), enlarged Sylvian cistern (HP:0100952), frontotemporal cortical dysplasia [pachygyria (HP:0001302) and polymicrogyria (HP:0002126)], asymmetric temporo-occipital ventriculomegaly (HP:0006956) predominantly on the left, hypoplastic *corpus callosum* (HP:0002079), and enlargement of *cisterna magna* (HP:0002280) without cerebellar atrophy. For the phenotype description, the Human Phenotype Ontology was used (Köhler et al., 2021).

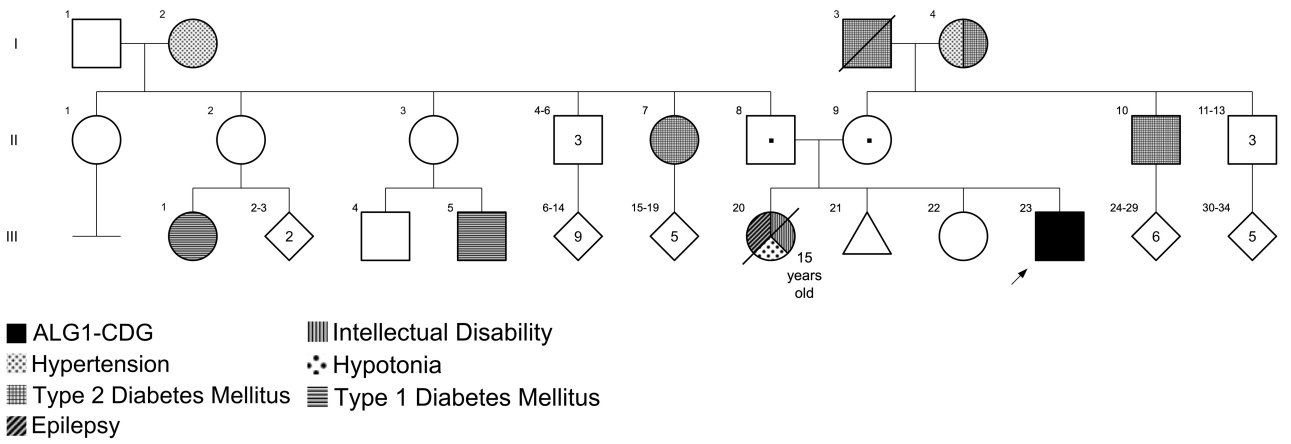

FIGURE 1 | Pedigree of the family with ALG1-CDG. Individual III:23 is the patient reported in this work with ALG1-CDG. Individual III:20 had an intellectual disability, epilepsy, and hypotonia; however, genotyping was not possible because she died at 15 years old.

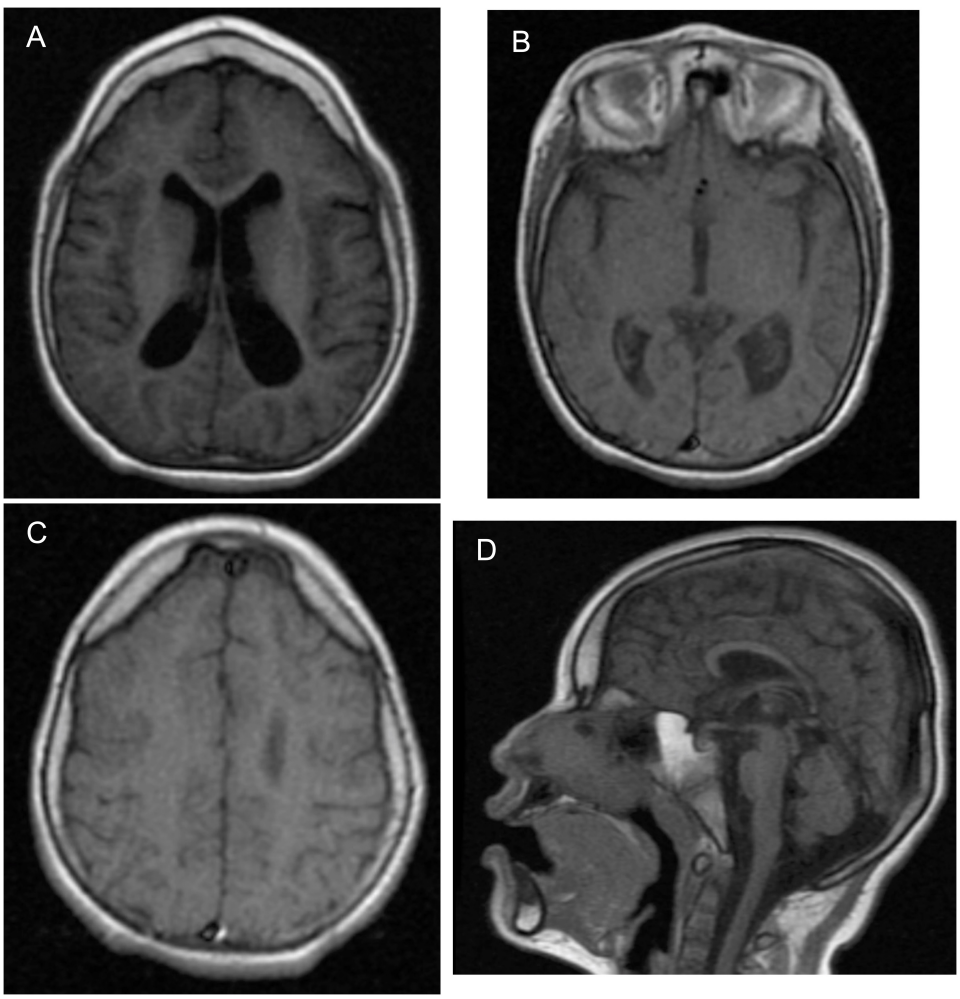

FIGURE 2 | Abnormal brain MRI of the patient at 5 years old. **(A)** Cortical–subcortical frontotemporal atrophy, hypoplasia of the frontal lobes, and ventriculomegaly predominantly on the left on axial on axial T1-weighted FLAIR MR image. **(B)** Enlarged Sylvian cistern and ventriculomegaly predominantly on the left on axial T1-weighted MR image. **(C)** Frontotemporal cortical dysplasia pachygyria and polymicrogyria on axial T1-weighted MR image. **(D)** Hypoplastic *corpus callosum* and enlargement of *cisterna magna* without cerebellar atrophy on sagittal T1-weighted MR image.

RESULTS

Based on the clinical phenotype, electrospray ionization mass spectrometry (ESI-MS) analysis of serum transferrin (Tf) was performed and a type I profile was established (mono-oligo/di-oligo = 0.90) (**Figure 3A**). To determine the genetic basis of the disease, a skin biopsy was performed to obtain a fibroblast culture. The genomic DNA (gDNA) obtained from the patient's fibroblasts was sent to clinical exome sequencing (CES), and three *ALG1* variants were found in the form of two complex alleles: one complex allele composed by a benign variant NM_019109.4(ALG1): c.208 + 16_208 + 19dup in *cis* with the known pathogenic variant NM_019109.5(ALG1):c.1312C > T (p.R438W) defined as NM_019109.5(ALG1): c.[208 + 16_208 + 19dup; 1312C > T] and a second complex allele composed by the same benign variant NM_019109.4(ALG1): c.208 + 16_208 + 19dup in *cis* with a previously not described variant c.208 + 25G > T that we termed NM_019109.5(ALG1): c.[208 + 16_208 + 19dup; 208 + 25G > T].

Sequencing of the parents' gDNA showed that the c.[208 + 16_208 + 19dup; 1312C > T] complex allele was inherited from the mother and the c.[208 + 16_208 + 19dup; 208 + 25G > T] from the father (**Figure 3B**). The Sanger sequencing of the mother's *ALG1* shows an overlap that is the result of heterozygosity for the benign c.208 + 16_208 + 19dup variant, in contrast to the father that is homozygote.

A consideration in the case of the complex allele c.[208 + 16_208 + 19dup; 208 + 25G > T] is that the c.208 + 25G > T is located + 29 bp from the donor splicing site in exon 1 due to a four base duplication (TCTG) caused by the benign variant c.208 + 16_208 + 19dup (chr16:5122072); ClinVar Variation ID 95935, dbSNP:rs35400794 (**Figure 4C**).

The c.208 + 25G > T variant was considered potentially pathogenic because it could induce a new donor splice site (GG to GT) and cause non-functional alternative splicing. Using the Human Splicing Finder prediction (HSFPro, Genomnis), it was found that this change significantly alters splicing with the following values [WT-Mut%variation] [HSF Donor site (matrix GT) 61.35 > 88.49 (44.24%) and MaxEnt Donor site 1.01 > −8.65 (756.44%)].

To further investigate the presence of alternative splicing, the patient's complementary DNA (cDNA) was synthesized and *ALG1* was polymerase chain reaction (PCR) amplified. The *ALG1* has 13 exons and codes for a 464 aminoacid protein. Amplification of *ALG1* with primers ALG1s and ALG1as encompasses the coding sequence plus short stretches from the 5′- and 3′-UTR for a predicted amplicon of 1517 bp. PCR product analysis in an agarose gel showed a slightly thicker amplicon in the patient compared to the healthy control (**Figure 3C**). Because this suggested potential splicing isoforms in the patient, subcloning and screening were performed. Three types of isoforms were identified: one with the c.1312C > T variant and constitutive splicing (c.1312C > T; p.R438W) or with the same variant (shifted to position 1201) and exon 10 skipping c.[del_962-1072;1201C > T] translated as p.[K322_G358del; R401W] and a third isoform without the c.1312C > T variant, but that presented partial intron 1 retention (+ 27 bp) without causing a frameshift and that theoretically results when translated in substitution of N70S and insertion of nine aminoacids EWPRVCLGD (p.N70S_S71ins9) (**Figures 4A–C**).

To further biochemically confirm the ALG1-CDG diagnosis, previous works have shown that ALG1-CDG patients accumulate a novel N-linked mannose-deprived tetrasaccharide considered as a pathognomonic marker for ALG1-CDG (Neu5Acα2,6Galβ1,4-GlcNAcβ1,4GlcNAc) on serum glycoproteins (Bengtson et al., 2016; Ng et al., 2016; Zhang et al., 2016; Chen et al., 2019). Total serum N-gycans were analyzed by electrospray ionization–quadrupole time-of-flight mass spectrometry (ESI-QTOF) to detect the presence of the mannose-deprived N-tetrasaccharide, finding it significantly elevated at 0.23% of total glycan (normal 0–0.03); Gal1GlcNAc2 was also increased at 0.12% (normal 0) (**Figure 5**).

DISCUSSION

This report presents a patient with a severe clinical multisystemic phenotype with neurological involvement and an ESI-MS Tf with a type I profile consistent with CDG. CES revealed two complex alleles: The NM_019109.5(ALG1): c.[208 + 16_208 + 19dup; 1312C > T], inherited from the mother, and the NM_019109.5(ALG1): c.[208 + 16_208 + 19dup; 208 + 25G > T] inherited from the father. We considered that the latter could cause non-functional alternative splicing as predicted by HSFPro (Genomnis). PCR-based analysis of the patient's *ALG1* amplicon further supported this hypothesis (**Figure 3C**).

To determine the effects of the complex alleles, the patient's *ALG1* PCR amplicon was subcloned and screened, identifying three types of isoforms (**Figure 4A**), two derived from the c.[208 + 16_208 + 19dup; 1312C > T] complex allele and the third isoform with partial intron 1 retention (+ 27 bp) that did not present the c.1312C > T variant and that we conclude is derived from the c.[208 + 16_208 + 19dup; 208 + 25G > T] complex allele.

Regarding the isoforms derived from the c.[208 + 16_208 + 19dup; 1312C > T] complex allele, inherited by the mother, one presented constitutive splicing (p.R438W) and another an unexpected alternative splicing (exon 10 skipping) that translates into a 427 aa protein lacking 37 aminoacids p.[K322_G358del;R401W]. Because no variants were found in intron/exon junctions of exon 10, we consider that the c.1312C > T variant located in exon 13 could be responsible for altering distant splicing events, although further analysis is required to make a definitive conclusion. The c.1312C > T pathogenic variant included in this complex allele has been reported in six patients as compound heterozygotes with the following pathogenic variants, c.866A > G, c.450C > A, c.1145T > C, and c.1236A > G, and has been demonstrated to have reduced function (Dupré et al., 2010; Rohlfing et al., 2014; Ng et al., 2016; Zhang et al., 2016). No deleterious effects due to the benign intronic variant were observed.

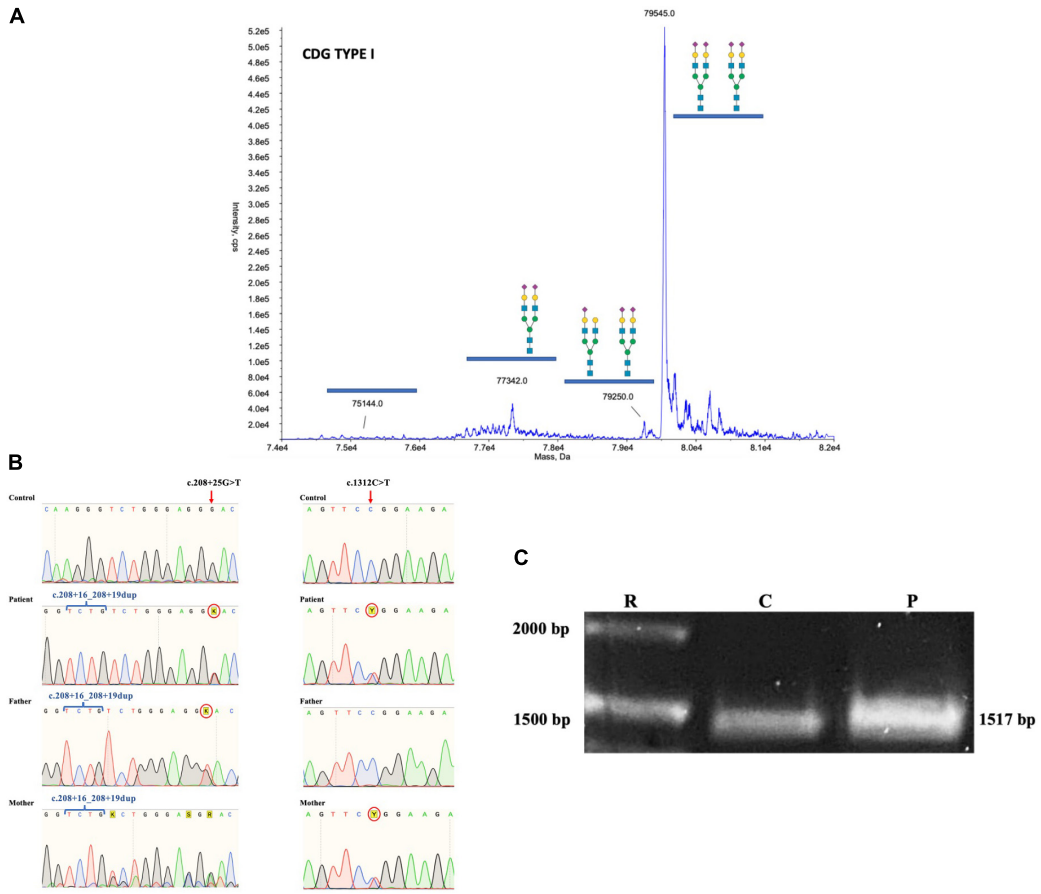

FIGURE 3 | (A) ESI-MS analysis of serum Tf isoforms. Profile of the patient showing an increase of mono-oligo Tf, peaks are annotated with the glycosylation moiety structure with the following meaning: blue box = N-acetylglucosamine; green circle = mannose; yellow circle = galactose; purple diamond = N-acetylneuraminic acid (sialic acid). **(B)** Chromatograms of gDNA sequencing from healthy control, mother, father, and patient showing the inheritance of the *ALG1* c.208 + 16_208 + 19dup, the c.208 + 25G > T, and the c.1312C > T variants. **(C)** PCR of the coding sequence of *ALG1* showing the expected wt 1517 bp size in healthy control and the patient's amplicon showing a slightly thicker band.

For the third isoform without the c.1312C > T variant and with partial intron 1 retention (+ 27 bp) we conclude that it results from the paternally inherited complex allele c.[208 + 16_208 + 19dup; 208 + 25G > T] where the c.208 + 25G > T variant induces a new donor splice site that causes partial intron 1 retention (+ 27 bp). The partial intron 1 retention does not cause a frameshift but results in aminoacid substitution (N70S) and insertion of nine aminoacids (EWPRVCLGD) (p.N70S_S71ins9) (**Figure 4C**). It is important to note that the duplication of the TCTG bases occurring at the c.208 + 16_208 + 19dup variant (chr16:5122072) shifts the position c.208 + 25G > T to + 29 bp from the donor splicing site in exon 1 which determines the length of intron retention and preservation of the ORF (**Figure 4C**). We consider that the resulting p.N70S_S71ins9 has a reduced function based on the different physicochemical properties at position 70 [acidic (N) to hydroxylic (S)] as well as the insertion of nine aminoacids, including a P residue. Also, a previously reported p.S71F variant has been shown to have reduced function (Ng et al., 2016).

The presence of the ALG1-CDG pathognomonic N-linked mannose-deprived tetrasaccharide detected by ESI-QTOF when analyzing serum total N-glycans further supports the conclusion that the resulting protein variant p.N70S_S71ins9 does not have a normal function as it is not able to compensate for the decreased function of the p.R438W pathogenic variant. The fact that the N-tetrasaccharide was not detected by ESI-MS of serum Tf (**Figure 3A**) could be explained by differential sensitivity related to types of equipment and techniques, as well as a possible increased sensitivity to detect the N-tetrasaccharide when analyzing total N-glycans versus Tf glycans alone.

It is noteworthy that the c.208 + 16_208 + 19dup variant is considered a benign variant but that the additional presence of the c.208 + 25G > T variant results in a pathogenic complex allele c.[208 + 16_208 + 19dup; 208 + 25G > T]. According to gnomAD database (Lek et al., 2016) the variant c.208 + 16_208 + 19dup is very frequent in all ethnic groups (gnomAD ExomesVersion: 2.1.1 global frequency f = 0.558), as of July 2021. Concerning the c.208 + 25G > T variant, it is absent from the genomes and exomes in the genomAD

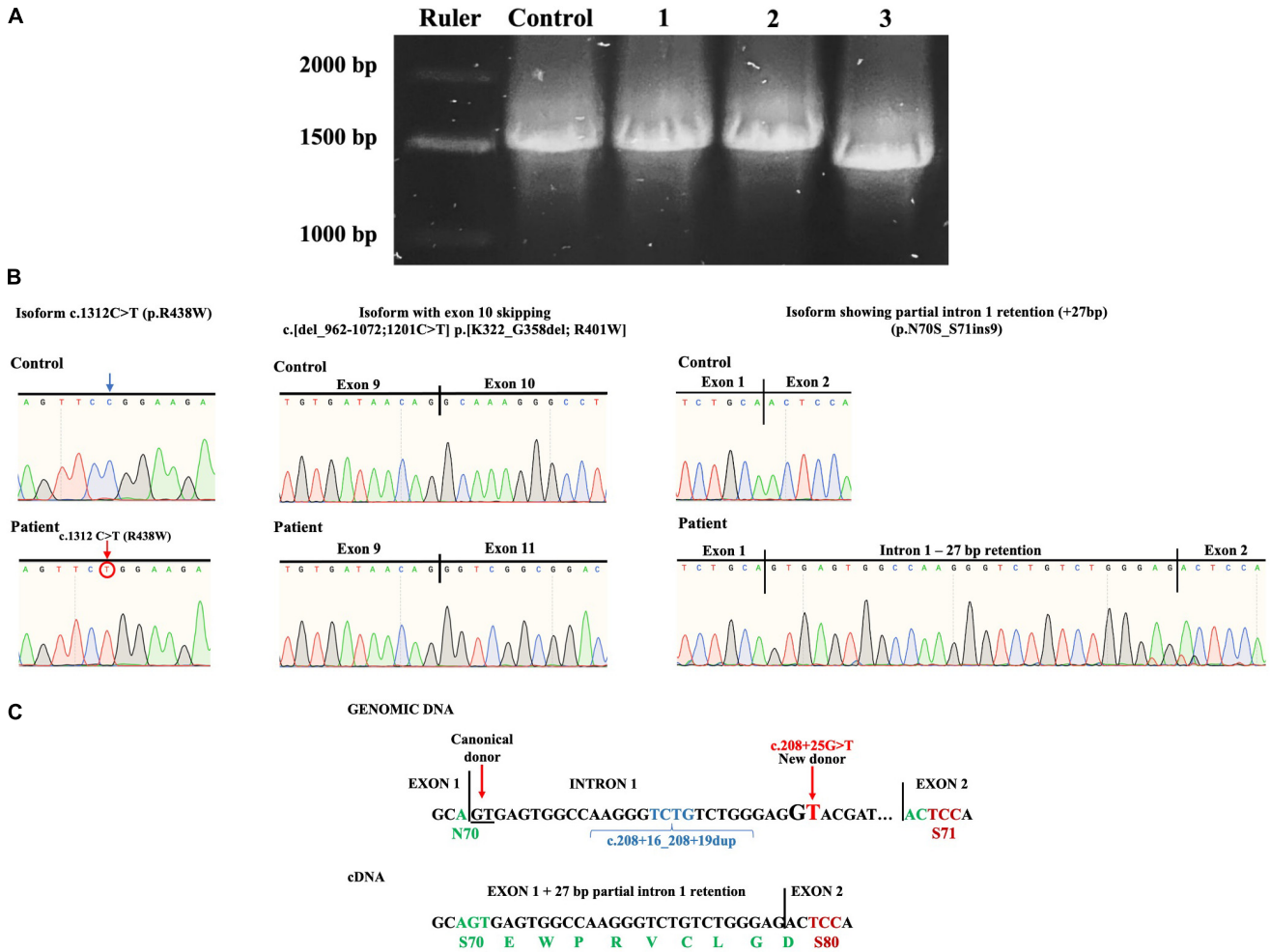

FIGURE 4 | (A) Isoforms found after PCR subcloning of the patient's *ALG1* amplicon. R, ruler; C, healthy wt control; 1, a constitutively spliced isoform bearing the c.1312C > T (p.R438W) variant; 2, an alternatively spliced isoform with partial intron 1 retention (+27bp); 3, an alternatively spliced isoform bearing the c.1312C > T variant with exon 10 skipping c.[del_962-1072;1201C > T] p.[K322_G358del; R401W]. **(B)** Sanger sequencing chromatograms of patient's isoforms showing the c.1312C > T (p.R438W) variant; exon 10 skipping c.[del_962-1072;1201C > T] p.[K322_G358del; R401W] and partial intron 1 retention (+ 27 bp) (p.N70S_S71ins9). **(C)** Splicing mechanism that induces the + 27 bp partial intron 1 retention caused by the complex allele c.[208 + 16_208 + 19dup; 208 + 25G > T]. The new donor splicing site (GG to GT) causes partial intron 1 retention (+ 27 bp) that when translated would result in aminoacid substitution N70S and insertion of nine aminoacids.

database (as of July 2021). Interestingly, in the absence of the c208 + 16_208 + 19dup, the c.208 + 25G > T variant would cause a frameshift and a premature stop codon in exon 2 which would also be pathogenic and probably more severe.

Given these results, ALG1-CDG diagnosis was clinically, biochemically, and genetically established. In most disease-related genes, variants affecting splicing are not fully characterized because variant screening is restricted to gDNA. In our experience involving ATP6V0A2-CDG and more recently PMM2-CDG, amplification of cDNA transcripts is an invaluable tool to demonstrate non-functional alternative splicing, identifying the consequence on the protein and establishing the pathogenicity mechanism (Bahena-Bahena et al., 2014; González-Domínguez et al., 2020, 2021). Of the six reported disease-causing mutations in HGMD that potentially affect splicing of *ALG1*, only one has been experimentally confirmed (**Table 1**). The c.208 + 25G > T reported in this work would be the second variant confirmed to cause alternative non-functional splicing.

This case also highlights the importance of increasing awareness and availability of technological platforms for biochemical and genetic diagnosis of rare diseases. This patient and his family had to wait 15 years to obtain a diagnosis, with a sibling who died at the same age without diagnosis. This time to diagnosis is not adequate for ALG1 patients that have an estimated premature death rate of 44% of which 65% occur at < 12 months of age (Ng et al., 2016). This is a lengthy diagnostic odyssey that is unfortunately too frequent in Latin American and most underdeveloped countries that in the era of exome sequencing can no longer be acceptable.

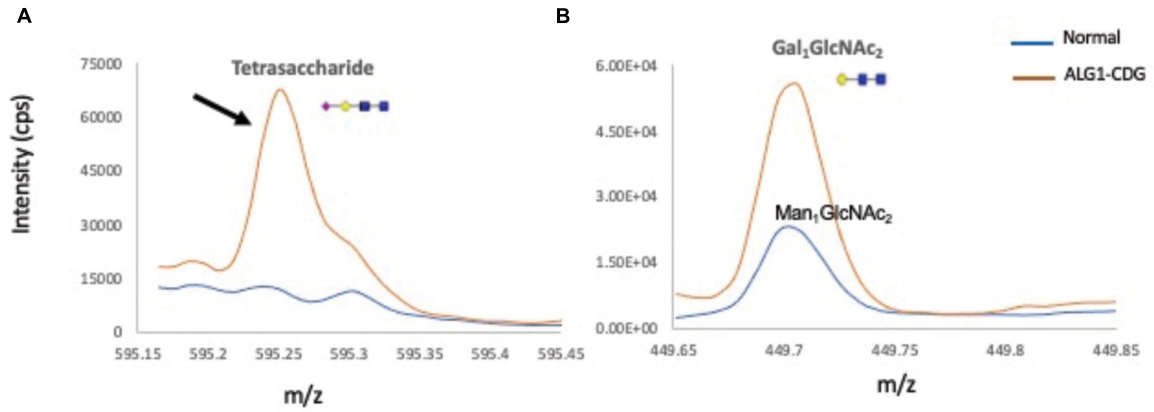

FIGURE 5 | Total ion chromatograms of N-tetrasaccharide (NeuAc1Gal1GlcNAc2) and Gal1 or Man1GlcNAc2 in serum N-glycan profiles from a normal control and the ALG1-CDG patient. Overlay of total ion chromatograms of N-linked mannose deprived tetrasaccharide **(A)**, Man1/Gal1GlcNAc2 **(B)** of a normal control plasma (in blue), and ALG1-CDG (red). Gal1GlcNAc2 is absent in total plasma proteins from normal controls, which instead have traces of Man1GlcNAc2 present. Markedly increased tetrasaccharide was detected in the ALG1-CDG patient as shown with a black arrow.

TABLE 1 | Variants of *ALG1* affecting splicing classified as disease-causing mutations in the Human Gene Mutation Database (HGMD) and the novel variant reported in this work.

Variants	Splicing site affected	Data confirming splicing	References
c.208 + 25G > T	Donor intron 1	Partial intron 1 retention	This work
c.209-1G > C	Acceptor intron 1	No	Ng et al., 2016
c.961 + 1G > C	Donor intron 9	No	Ng et al., 2016
c.1187 + 1G > A	Donor intron 11	No	Jones et al., 2013; Ng et al., 2016
c.1187 + 3A > G	Donor intron 11	Intron 11 retention	Ng et al., 2016; Bowling et al., 2017
c.1188-2A > G	Acceptor intron 11	No	Ng et al., 2016
c.1188T > A (p.Cys396Ter)	Acceptor intron 11	No	Dupré et al., 2010

It is necessary that academic and family organizations around the world pressure for a shift in global health public policy to guarantee that all patients affected by rare diseases have access to an interdisciplinary approach as well as free exome sequencing (Manickam et al., 2021).

CONCLUSION

The complex allele c.[208 + 16_208 + 19dup; 208 + 25G > T] (p.N70S_S71ins9) is pathogenic by causing non-functional alternative splicing of ALG1. Variants should be studied concerning their potential disruption of splicing, particularly if they affect canonical splicing sites. Increased awareness of rare diseases, including CDGs as well as the availability of technological platforms for genetic diagnosis, must be an international standard in public health policy.

MATERIALS AND METHODS

Informed Consent

Informed consent was obtained from both parents to perform a skin biopsy, fibroblast cultures, and all required research to obtain a molecular diagnosis and to publish other data on the patient and parents. All procedures followed were in accordance with national and institutional ethical standards on human experimentation and with the Helsinki Declaration of 1975 and revised in 2000.

Electrospray Ionization Mass Spectrometry (ESI-MS) Analysis of Serum Transferrin (Tf)

On-column immunoaffinity ESI-MS analysis of serum Tf isoforms was performed using an API-5000 triple quadrupole mass spectrometer (Applied Biosystems/MDS Sciex, Foster City, CA, United States).

Analysis of N-Linked Mannose Deprived-Tetrasaccharide

The patient's serum total N-glycans were analyzed by ESI-QTOF to detect the (Neu5Acα2,6Galβ1,4-GlcNAcβ1,4GlcNAc) N-tetrasaccharide as previously described (Chen et al., 2019).

Cell Culture

From the patient's skin biopsy, a primary culture of fibroblasts was obtained in AmnioMAX^{TM} C-100 Basal Medium (Gibco® by Life Technologies^{TM}; Life Technologies, Rockville, MD, United States) supplemented with 15% AmnioMAX^{TM} C-100 Supplement (Gibco® by Life Technologies^{TM}) and 1% penicillin/streptomycin

antibiotic (Gibco® by Life Technologies™). Fibroblast cultures were maintained at 37°C in a humidified atmosphere containing 5% CO_2. Fibroblasts were further processed to obtain genetic material.

Clinical Exome Sequencing (CES)

The gDNA was extracted from fibroblasts using Maxwell® 16 Blood DNA Purification Kit (Promega, Madison, WI, United States). The purity and concentration of the DNA samples were measured using NanoDrop 1000 spectrophotometer (Thermo Fisher Scientific, Waltham, MA, United States) and Qubit fluorometer (Thermo Fisher Scientific). Library preparation was performed using the reagents provided in the Clinical Exome sequencing panel kit, version 2 (Sophia Genetics SA, Saint Sulpice, Switzerland), according to the manufacturer's protocol. Sequencing was performed on NextSeq Instrument (Illumina, San Diego, CA, United States). Sequencing data analysis and variant annotation were performed with the Sophia DDM® software version 5.9.1.1 (Sophia Genetics SA). A bioinformatic filter was constructed, including all the genes previously reported to be related to CDG.

Predictions of the Pathogenicity of the Variants

The HSFpro software (Genomnis; Desmet et al., 2009) was used to predict the effect of variants on splicing. All predictions were made with the DYSF transcript ENST00000268261.

Polymerase Chain Reaction (PCR) and Sanger Sequencing

Total mRNA from the patient's fibroblasts was obtained using TRIzol reagent (Life Technologies) and cDNA was synthesized using M-MLV Reverse Transcriptase (Life Technologies). The cDNA-based PCR product corresponding to the coding sequence of *ALG1* was obtained using forward primer ALG1s 5′-TGACTGCTGCGGGCCAG-3′ and reverse primer ALG1as 5′-CACTGGGAGGTGCTGCTCG-3′. In the case of the patient, the amplicon was isolated in low melting point agarose gel, purified, subcloned, and screened for alternative splicing.

The inheritance of variants was determined by analyzing the patient's and parents' gDNA using primer ALG1s and reverse primer ALG1gas 5′-CTAAAGGAGCACTTCCGCC-3′ for the c.208 + 25G > T pathogenic variant and forward primer ALG1-E13s 5′-CAGGCAATGAGGTAAGCTCTG-3′ and reverse primer ALG1-E13as 5′-CAATTCTTTTACCAGGCAGTACC-3′ for the c.1312C > T pathogenic variant. Sequencing was performed by an ABI Prism 3130xl autoanalyzer (Applied Biosystems, Foster City, CA, United States), and results were visualized using SnapGene Viewer 2.2.2 (GSL Biotech LLC, Chicago, IL, United States).

DATA AVAILABILITY STATEMENT

The novel pathogenic variant observed in this study has been deposited in the ClinVar database with the accession SCV001761655.

ETHICS STATEMENT

The studies involving human participants were reviewed and approved by the Ethics Committee of the Sociedad Latinoamericana de Glicobiología. Written informed consent to participate in this study was provided by the participants' parents.

AUTHOR CONTRIBUTIONS

IM-D and CG-D conceived and designed the study. CG-D, MF-R, SG-C, AK-A, MH, ED, KR, MA-G, SM-H, AG-J, RS-M, CM-G, KC-S, LF-L, MJ-O, AM-R, MC-M, MR-G, HH-F, and CA-V contributed to data acquisition and analysis. IM-D, CG-D, CA-V, HH-F, and HM-M contributed to curation and interpretation of data. HM-M and IM-D: provided supervision. IM-D wrote the original draft. CG-D, MF-R, SG-C, A-KA, MH, ED, KR, M-AG, SM-H, AG-J, RS-M, CM-G, KC-S, LF-L, MJ-O, AM-R, MC-M, MR-G, HM-M, HH-F, CA-V, and IM-D revised, edited, and approved the final version of the manuscript.

FUNDING

IM-D and CG-D were supported by grants 293399 Red Temática Glicociencia en Salud – CONACyT and the Sociedad Latinoamericana de Glicobiología, A.C. CG-D is recipient of a scholarship 957250 from CONACYT. HH-F was supported by The Rocket Fund and National Institutes of Health Grant R01DK99551.

ACKNOWLEDGMENTS

We thank Felipe Olvera Rodríguez and Maricela Olvera Rodríguez for aiding in the production of rabbit anti-transferrin serum for IEF.

REFERENCES

Aebi, M. (2013). N-linked protein glycosylation in the ER. *Biochim. Biophys. Acta Mol. Cell Res.* 1833, 2430–2437. doi: 10.1016/j.bbamcr.2013.04.001

Bahena-Bahena, D., López-Valdez, J., Raymond, K., Salinas-Marín, R., Ortega-García, A., Ng, B. G., et al. (2014). ATP6V0A2 mutations present in two Mexican Mestizo children with an autosomal recessive cutis laxa syndrome type IIA. *Mol. Genet. Metab. Rep.* 1, 203–212.

Barba, C., Darra, F., Cusmai, R., Procopio, E., Dionisi Vici, C., Keldermans, L., et al. (2016). Congenital disorders of glycosylation presenting as epileptic encephalopathy with migrating partial seizures in infancy. *Dev. Med. Child Neurol.* 58, 1085–1091. doi: 10.1111/dmcn.13141

Bengtson, P., Ng, B. G., Jaeken, J., Matthijs, G., Freeze, H. H., and Eklund, E. A. (2016).). Serum transferrin carrying the xeno-tetrasaccharide NeuAc-Gal-GlcNAc2 is a biomarker of ALG1-CDG. *J. Inherit. Metab. Dis.* 39, 107–114. doi: 10.1007/s10545-015-9884-y

Bogdańska, A., Lipiński, P., Szymańska-Rożek, P., Jezela-Stanek, A., Rokicki, D., Socha, P., et al. (2021). Clinical, biochemical and molecular phenotype of congenital disorders of glycosylation: long-term follow-up. *Orphanet J. Rare Dis.* 16:17. doi: 10.1186/s13023-020-01657-5

Bowling, K. M., Thompson, M. L., Amaral, M. D., Finnila, C. R., Hiatt, S. M., Engel, K. L., et al. (2017). Genomic diagnosis for children with intellectual disability and/or developmental delay. *Genome Med.* 9:43. doi: 10.1186/s13073-017-0433-1

Chen, J., Li, X., Edmondson, A., Meyers, G. D., Izumi, K., Ackermann, A. M., et al. (2019). Increased clinical sensitivity and specificity of plasma protein N-glycan profiling for diagnosing congenital disorders of glycosylation by use of flow injection-electrospray ionization-quadrupole time-of-flight mass spectrometry. *Clin. Chem.* 65, 653–663. doi: 10.1373/CLINCHEM.2018.296780

Couto, J. R., Huffaker, T. C., and Robbins, P. W. (1984). Cloning and expression in *Escherichia coli* of a yeast mannosyltransferase from the asparagine-linked glycosylation pathway. *J. Biol. Chem.* 259, 378–382. doi: 10.1016/s0021-9258(17)43670-2

Desmet, F. O., Hamroun, D., Lalande, M., Collod-Bëroud, G., Claustres, M., and Béroud, C. (2009). Human Splicing Finder: an online bioinformatics tool to predict splicing signals. *Nucleic Acids Res.* 37:e67. doi: 10.1093/nar/gkp215

Dupré, T., Vuillaumier-Barrot, S., Chantret, I., Yayé, H. S., Le Bizec, C., Afenjar, A., et al. (2010). Guanosine diphosphate-mannose: GlcNAc2-PP-dolichol mannosyltransferase deficiency (congenital disorders of glycosylation type Ik): five new patients and seven novel mutations. *J. Med. Genet.* 47, 729–735. doi: 10.1136/jmg.2009.072504

Gao, X. D., Nishikawa, A., and Dean, N. (2004). Physical interactions between the Alg1, Alg2, and Alg11 mannosyltransferases of the endoplasmic reticulum. *Glycobiology* 14, 559–570. doi: 10.1093/glycob/cwh072

González-Domínguez, C. A., Raya-Trigueros, A., Manrique-Hernández, S., González Jaimes, A., Salinas-Marín, R., Molina-Garay, C., et al. (2020). Identification through exome sequencing of the first PMM2-CDG individual of Mexican mestizo origin. *Mol. Genet. Metab. Rep.* 25:100637. doi: 10.1016/j.ymgmr.2020.100637

González-Domínguez, C. A., Villarroel, C. E., Rodríguez-Morales, M., Manrique-Hernández, S., González-Jaimes, A., and Olvera-Rodriguez, F. (2021). Non-functional alternative splicing caused by a Latino pathogenic variant in a case of PMM2-CDG. *Mol. Genet. Metab. Rep.* 28:100781. doi: 10.1016/j.ymgmr.2021.100781

Grubenmann, C. E., Frank, C. G., Hülsmeier, A. J., Schollen, E., Matthijs, G., Mayatepek, E., et al. (2004).). Deficiency of the first mannosylation step in the N-glycosylation pathway causes congenital disorder of glycosylation type Ik. *Hum. Mol. Genet.* 13, 535–542. doi: 10.1093/hmg/ddh050

Harshman, L. A., Ng, B. G., Freeze, H. H., Trapane, P., Dolezal, A., Brophy, P. D., et al. (2016). Congenital nephrotic syndrome in an infant with ALG1-congenital disorder of glycosylation. *Pediatr. Int.* 58, 785–788. doi: 10.1111/ped.12988

Jones, M. A., Rhodenizer, D., da Silva, C., Huff, I. J., Keong, L., Bean, L. J. H., et al. (2013). Molecular diagnostic testing for congenital disorders of glycosylation (CDG): detection rate for single gene testing and next generation sequencing panel testing. *Mole. Genet. Metabol.* 110, 78–85. https://doi.org/10.1016/j.ymgme.2013.05.012

Köhler, S., Gargano, M., Matentzoglu, N., Carmody, L. C., Lewis-Smith, D., Vasilevsky, N. A., et al. (2021). The human phenotype ontology in 2021. *Nucleic Acids Res.* 49, D1207–D1217. doi: 10.1093/nar/gkaa1043

Kranz, C., Denecke, J., Lehle, L., Sohlbach, K., Jeske, S., Meinhardt, F., et al. (2004). Congenital Disorder of Glycosylation Type Ik (CDG-Ik): a Defect of Mannosyltransferase I. *Am. J. Hum Genet.* 74, 545–551. doi: 10.1086/382493

Lei, Y. L., Zhen, L., Xu, L. L., Yang, Y. D., and Li, D. Z. (2020). Foetal phenotype of ALG1-CDG caused by paternal uniparental disomy 16. *J. Obstet. Gynaecol.* 41, 828–830. doi: 10.1080/01443615.2020.1786031

Lek, M., Karczewski, K. J., Minikel, E. V., Samocha, K. E., Banks, E., Fennell, T., et al. (2016). Analysis of protein-coding genetic variation in 60,706 humans. *Nature* 536, 285–291. doi: 10.1038/nature19057

Manickam, K., Mcclain, M. R., Demmer, L. A., Biswas, S., Kearney, H. M., Malinowski, J., et al. (2021). Exome and genome sequencing for pediatric patients with congenital anomalies or intellectual disability: an evidence-based clinical guideline of the American College of Medical Genetics and Genomics (ACMG). *Genet. Med.* [Epub Online ahead of print]. doi: 10.1038/s41436-021-01242-6

Marques-da-Silva, D., dos Reis Ferreira, V., Monticelli, M., Janeiro, P., Videira, P. A., Witters, P., et al. (2017). Liver involvement in congenital disorders of glycosylation (CDG). A systematic review of the literature. *J. Inherit. Metab. Dis.* 40, 195–207. doi: 10.1007/s10545-016-0012-4

Medrano, C., Vega, A., Navarrete, R., Ecay, M. J., Calvo, R., Pascual, S. I., et al. (2019). Clinical and molecular diagnosis of non-phosphomannomutase 2 N-linked congenital disorders of glycosylation in Spain. *Clin. Genet.* 95, 615–626. doi: 10.1111/cge.13508

Morava, E., Vodopiutz, J., Lefeber, D. J., Janecke, A. R., Schmidt, W. M., Lechner, S., et al. (2012). Defining the phenotype in congenital disorder of glycosylation due to ALG1 mutations. *Pediatrics* 130, e1034–e1039. doi: 10.1542/peds.2011-2711

Ng, B. G., Shiryaev, S. A., Rymen, D., Eklund, E. A., Raymond, K., Kircher, M., et al. (2016). ALG1-CDG: clinical and Molecular Characterization of 39 Unreported Patients. *Hum. Mutat.* 37, 653–660. doi: 10.1002/humu.22983

Ondruskova, N., Cechova, A., Hansikova, H., Honzik, T., and Jaeken, J. (2021). Congenital disorders of glycosylation: still "hot" in 2020. *Biochim. Biophys. Acta Gen. Subj.* 1865:129751. doi: 10.1016/j.bbagen.2020.129751

O'Reilly, M. K., Zhang, G., and Imperiali, B. (2006). In vitro evidence for the dual function of Alg2 and Alg11: essential mannosyltransferases in N-linked glycoprotein biosynthesis. *Biochemistry* 45, 9593–9603. doi: 10.1021/bi060878o

Pérez-Cerdá, C., Girós, M. L., Serrano, M., Ecay, M. J., Gort, L., Pérez Dueñas, B., et al. (2017). A Population-Based Study on Congenital Disorders of Protein N- and Combined with O-Glycosylation Experience in Clinical and Genetic Diagnosis. *J. Pediatr.* 183, 170–177.e1. doi: 10.1016/j.jpeds.2016.12.060

Quelhas, D., Martins, E., Azevedo, L., Bandeira, A., Diogo, L., Garcia, P., et al. (2021). Congenital Disorders of Glycosylation in Portugal—Two Decades of Experience. *J. Pediatr.* 231, 148–156. doi: 10.1016/j.jpeds.2020.12.026

Rohlfing, A. K., Rust, S., Reunert, J., Tirre, M., du Chesne, I., Wemhoff, S., et al. (2014). ALG1-CDG: a new case with early fatal outcome. *Gene* 534, 345–351. doi: 10.1016/j.gene.2013.10.013

Schwarz, M., Thiel, C., Lübbehusen, J., Dorland, B., de Koning, T., von Figura, K., et al. (2004). Deficiency of GDP-Man:GlcNAc2-PP-Dolichol Mannosyltransferase Causes Congenital Disorder of Glycosylation Type Ik. *Am. J. Hum. Genet.* 74, 472–481. doi: 10.1086/382492

Zhang, W., James, P. M., Ng, B. G., Li, X., Xia, B., Rong, J., et al. (2016). A novel N-tetrasaccharide in patients with congenital disorders of glycosylation, including asparagine-linked glycosylation protein 1, phosphomannomutase 2, and mannose phosphate isomerase deficiencies. *Clin. Chem.* 62, 208–217. doi: 10.1373/clinchem.2015.243279

Conflict of Interest: The authors declare that the research was conducted in the absence of any commercial or financial relationships that could be construed as a potential conflict of interest.

Publisher's Note: All claims expressed in this article are solely those of the authors and do not necessarily represent those of their affiliated organizations, or those of the publisher, the editors and the reviewers. Any product that may be evaluated in this article, or claim that may be made by its manufacturer, is not guaranteed or endorsed by the publisher.

frontiers in Genetics

REVIEW
published: 10 September 2021
doi: 10.3389/fgene.2021.735348

Treatment Options in Congenital Disorders of Glycosylation

*Julien H. Park and Thorsten Marquardt**

Department of General Pediatrics, Metabolic Diseases, University Children's Hospital Münster, Münster, Germany

Despite advances in the identification and diagnosis of congenital disorders of glycosylation (CDG), treatment options remain limited and are often constrained to symptomatic management of disease manifestations. However, recent years have seen significant advances in treatment and novel therapies aimed both at the causative defect and secondary disease manifestations have been transferred from bench to bedside. In this review, we aim to give a detailed overview of the available therapies and rising concepts to treat these ultra-rare diseases.

Keywords: glycosylation, congenital disorder of glycosylation, treatment, drug repurposing, chaperone, substrate supplementation, cofactor

OPEN ACCESS

Edited by:
Karolina Stepien,
Salford Royal NHS Foundation Trust,
United Kingdom

Reviewed by:
Gerard Berry,
Division of Genetics and Genomics,
Boston Children's Hospital,
United States
Arnaud Bruneel,
Assistance Publique–Hôpitaux de Paris, France
Francois Foulquier,
UMR 8576 Unité de Glycobiologie Structurale et Fonctionnelle (UGSF), France

***Correspondence:**
Thorsten Marquardt
marquat@uni-muenster.de

Specialty section:
This article was submitted to Genetics of Common and Rare Diseases, a section of the journal Frontiers in Genetics

Received: *02 July 2021*
Accepted: *23 August 2021*
Published: *10 September 2021*

Citation:
Park JH and Marquardt T (2021) Treatment Options in Congenital Disorders of Glycosylation. Front. Genet. 12:735348. doi: 10.3389/fgene.2021.735348

INTRODUCTION

Congenital disorders of glycosylation are a group of inborn errors of metabolism affecting the synthesis, processing, and addition of carbohydrate entities to macromolecules, resulting in an extremely varied group of phenotypes affecting multiple organ systems. Initially termed "carbohydrate-deficient glycoprotein syndrome," disorders of protein *N*-glycosylation were the first to be characterized (Jaeken et al., 1984). Currently, four subgroups of glycosylation disorders are recognized: (A) disorders of *N*-linked glycosylation, (B) disorders of *O*-linked glycosylation, (C) combined *N*- and *O*-linked/multiple disorders of glycosylation, and (D) lipid and glycosylphosphatidylinositol (GPI) anchor biosynthesis defects. Disorders of *N*-glycosylation are subdivided into CDG type I affecting glycan synthesis and type II affecting glycan processing (Marquardt and Denecke, 2003). In the analysis of serum transferrin, the screening method of choice for disorders of *N*-glycosylation, these subtypes are readily distinguished (**Figure 1**): in type I CDG, di- and asialo-transferrin are elevated, while type II CDG is characterized by more or less inconstantly elevated tri-, di-, mono- and asialo-transferrin (Jaeken and Matthijs, 2001).

The analysis of transferrin glycosylation by isoelectric focusing (IEF), while still being considered the gold-standard, has been replaced by high-performance liquid chromatography (HPLC)- and capillary electrophoresis (CE)-based methods mainly due to the advantages of offering a quantitative assessment of glyco-isoforms and faster turn-around times (Lefeber et al., 2011). More detailed studies of serum transferrin glycosylation can be performed using electrospray ionization quadrupole time-of-flight (ESI QTOF) mass spectrometry of immunopurified serum transferrin (Chen et al., 2019; Wada, 2020). In recent years, mass-spectrometry based analyses of the *N*-glycome, i.e., the entirety of plasma glycan structures, have been shown to detect more subtle glycosylation abnormalities and are being discussed as a first-in-line tool for diagnosing CDG (Wada, 2006; Guillard et al., 2011).

While a plethora of new subtypes has been discovered over the course of the following years and continue to be (Ondruskova et al., 2021), treatment options remained limited to a few subtypes and showed varying success. Recently, the screening of large compound libraries and innovative

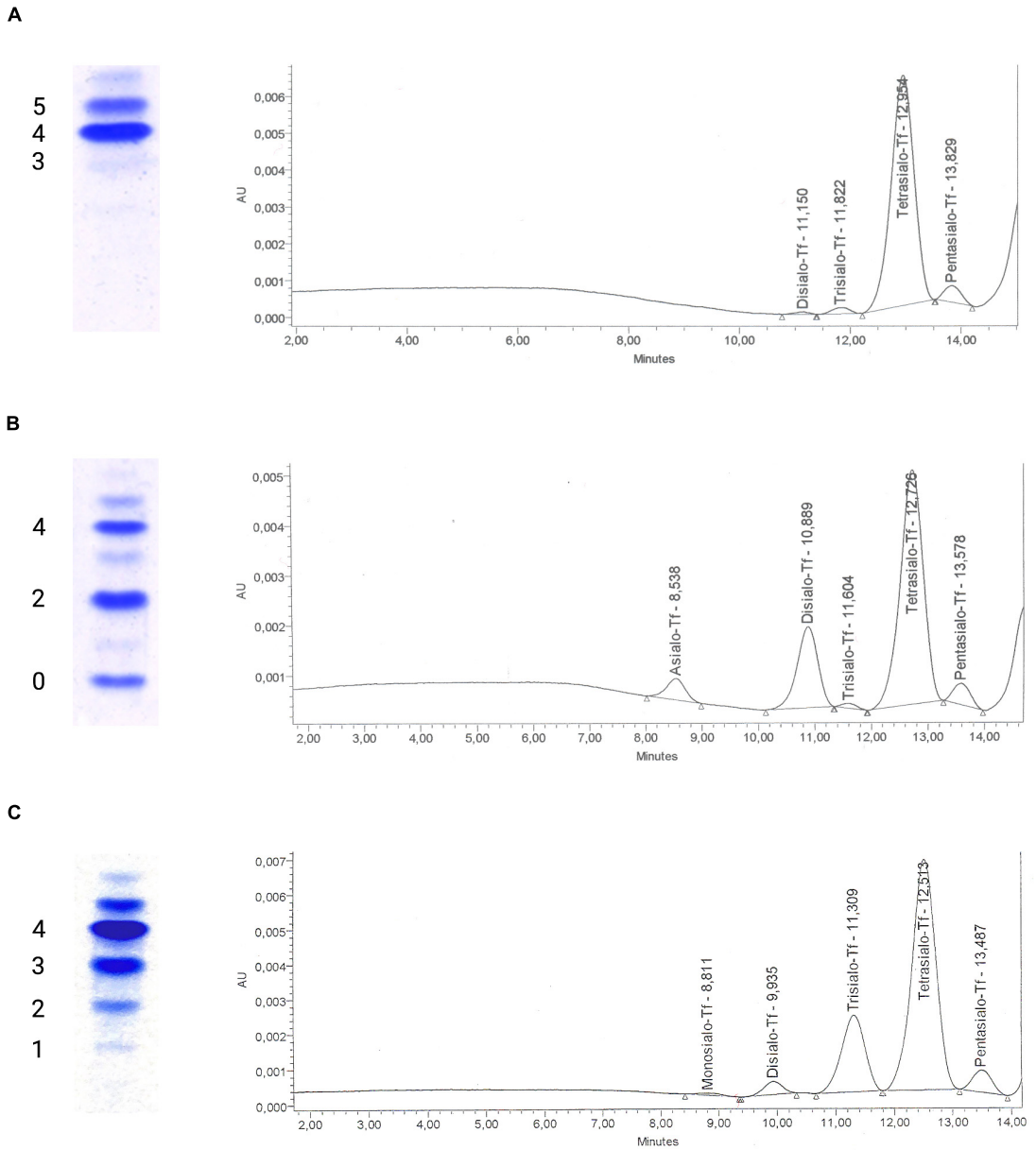

FIGURE 1 | Glycosylation analysis of serum transferrin using isoelectric focusing and high-performance liquid chromatography. Isoelectric focusing (IEF) of serum transferrin has traditionally been used to diagnose congenital disorders of *N*-glycosylation. The test separates transferrin isoforms according to their negative charge that is dependent on the amount of sialic acid residues on glycan chains, with each sialic acid residue corresponding to a negative charge. Currently, alternative methods such as high-performance liquid chromatography (HPLC) are being favored for their ease of use and ability to generate quantitative results for transferrin isoforms. **(A)** A normal glycosylation profile in IEF of serum transferrin with tetrasialo-transferrin (4-) representing the major fraction of transferrin isoforms. To the right, the corresponding HPLC curve can be seen, giving the area % for the varying transferrin subtypes (pentasialo-transferrin 4.97%, tetrasialo-transferrin 92.44%, trisialo-transferrin 1.94%, and disialo-transferrin 0.65%). **(B)** Impaired transferrin glycosylation seen in a PMM2-CDG patient, with decreased tetrasialo-transferrin and increased di-(2-) and monosialo-(1-)transferrin proportions (type I CDG pattern). HPLC identified pentasialo-transferrin (4.62%), tetrasialo-transferrin (68.02%), trisialo-transferrin (0.89%), disialo-transferrin (21.36%), and asialo-transferrin (5.1%). **(C)** In a COG6-CDG patient, increased proportions of tri- (3-), di- (2-), and monosialo-transferrin (1-) are seen in IEF. HPLC detected pentasialo-transferrin (5.2%), tetrasialo-transferrin (69.16%), trisialo-transferrin (22.03%), disialo-transferrin (2.99%), and monosialo-transferrin (0.62%). Reference intervals for HPLC of serum transferrin at our laboratory: Pentasialo (5-) 2.6–10.2%, tetrasialo (4-) 85.7–94.0%, trisialo (3-) 1.16–6.36%, disialo (2-) 0.38–1.82%, monosialo (1-) 0%, asialo (0-) 0%.

concepts have identified novel opportunities to treat several subtypes of inborn glycosylation disorders. However, the lack of randomized controlled trials continues to hamper efforts toward a standardized treatment of CDG. In this review, we aim to give a comprehensive overview of past and present approaches to therapy of CDG, stressing rising concepts and recent advances.

Special focus is put on treatment approaches to the most common subtype, PMM2-CDG.

THERAPEUTIC CONCEPTS IN THE TREATMENT OF CDG

While the ever-growing number of CDG subtypes involves a plethora of disease mechanisms in different organ systems (Jaeken, 2011), the approaches to treating this diverse group of disorders can be summarized by three basic concepts. These have been implemented in clinical care to different degrees with some being firmly established, while others remain preclinical or on a single case basis. In addition, non-specific treatment options are available (**Table 1**).

Substrate (Precursor) Supplementation and Bypassing Strategies

With the elucidation of underlying enzymatic defects, initial attempts were made to supplement substrates of the affected enzymes with the aim to shift the reaction equilibrium toward the favored product, thus improving glycosylation. In cases where the direct substrate is either not available or nor stable, precursors of this substrate have been applied or the enzymatic defect was bypassed, utilizing alternative pathways (see section "Mannose Supplementation for MPI-CDG Bypasses the Impaired Enzyme"). In analogy to this, the transported molecule ("substrate") of transport proteins has been supplemented in CDG subtypes mediated by nucleotide sugar transporter defects (**Figure 2A**; Eisenberg, 2011). While successful in several CDG subtypes such as MPI-CDG, SLC35C1-CDG, and SLC35A2-CDG (Niehues et al., 1998; Marquardt et al., 1999; Witters et al., 2020), the therapeutic principle remains disputed in the most common subtype PMM2-CDG.

Most proposed substrate supplementation therapies have been administered orally and are therefore sometimes considered to be nutritional therapies (Verheijen et al., 2020). Attempts at parenteral, i.e., intravenous, substrate supplementation have been made (Mayatepek et al., 1997; Schroeder et al., 2010; Grünert et al., 2019) but have typically been limited to critically ill patients not tolerating oral supplementation and were either unsuccessful (i.v., mannose in PMM2-CDG) or associated with adverse effects (i.v., mannose in MPI-CDG, see section "Mannose Supplementation for MPI-CDG Bypasses the Impaired Enzyme").

Cofactor Supplementation

In several CDG subtypes, supplementation of the affected enzyme with essential cofactors has been employed as a means to improve glycosylation both *in vivo* and *in vitro* (Park et al., 2018; Houdou et al., 2019). Like substrate supplementation, the addition of cofactor(s) aims at improving protein function by optimizing reaction conditions in order to shift the reaction equilibrium toward the product (**Figure 2B**). An emerging subgroup of glycosylation disorders is caused by genetic defects affecting the uptake of cofactors with glycosylation abnormalities as a secondary, "downstream" manifestation of the disorder. In these CDG, cofactor supplementation is a promising therapeutic concept that has been established for some of these (Potelle et al., 2017; Park et al., 2018).

Pharmacological Chaperones

While frameshift and non-sense mutations frequently lead to a total loss of protein function (Gorlov et al., 2006),

TABLE 1 | Overview and categorization of treatable congenital disorders of glycosylation.

Therapeutic principle	Therapeutic compound	CDG subtype	Phenotype summary
Substrate supplementation	Mannose	MPI-CDG	Liver fibrosis Protein losing enteropathy Coagulopathy Failure to thrive
	Galactose	SLC35A2-CDG	Neurodevelopmental delay Seizures Brain malformations Dysmorphic features Skeletal abnormalities
		PGM1-CDG	Myopathy Cardiomyopathy Hepatopathy Hypoglycemia Dysmorphic features Endocrinopathies
		SLC39A8-CDG*	Neurodevelopmental delay Seizures Cerebellar atrophy Cranial synostoses Visual impairment Auditory impairment Failure to thrive Leigh-like syndrome
		TMEM165-CDG*	Neurodevelopmental delay Skeletal dysplasia Hepatopathy Nephrotic syndrome Cardiac defects
	Fucose	SLC35C1-CDG	Neurodevelopmental delay Short stature Facial dysmorphism Recurring infections
		FUT8-CDG	
Cofactor supplementation	Manganese-(II)-sulfate	SLC39A8-CDG	See above
Pharmaceutical chaperones	Epalrestat	PMM2-CDG	See above
Non-causative and other treatments	Acetazolamide	PMM2-CDG	See above
	Sodium butyrate	PIGM-CDG	Seizures Thrombotic events Muscular hypotonia Macrocephaly

**Galactose supplementation in these disorders targets secondary glycosylation abnormalities (see section "Galactose Supplementation Corrects Secondary Glycosylation Abnormalities in SLC39A8-CDG and TMEM165-CDG").*

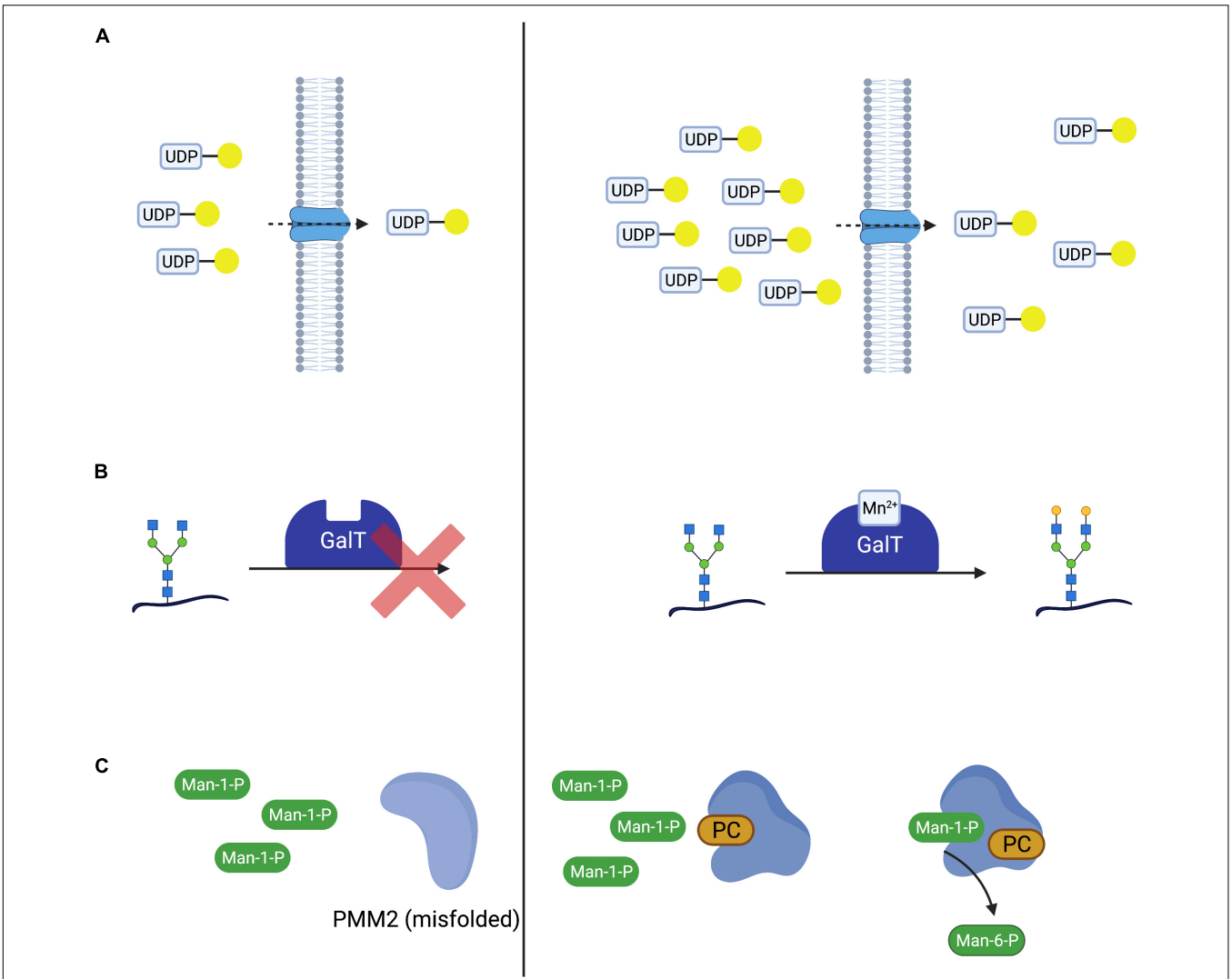

FIGURE 2 | Therapeutic concepts for congenital disorders of glycosylation. **(A)** Substrate supplementation aims at overcoming the impaired transport process or enzymatic reaction by increasing the concentration of the substrate of the respective reaction. One such treatment is galactose supplementation for SLC35A2-CDG, where oral supplementation of galactose (yellow circle) increases UDP-galactose supplies and thus transport across the defective UDP-galactose transporter SLC35A2. **(B)** In SLC39A8-CDG, defects in SLC39A8 lead to a deficiency in manganese (Mn^{2+}). Lack of this cofactor impairs the function of galactosyltransferases (GalT). Cofactor supplementation leads to an improved GalT function and thus normalized glycosylation. **(C)** Mutated and subsequentially misfolded enzymes are either degraded or impaired in function. Specific mutations in *PMM2* result in misfolded phosphomannomutase 2 **(A)**. Pharmacological chaperones (in this case epalrestat) bind and stabilize the affected enzyme, leading to increased enzyme activity and thus improved glycosylation **(B)**.

missense mutations can result in impaired protein folding (Yuste-Checa et al., 2015) and thus reduced enzyme activity. Pharmacological chaperones are small molecules capable of binding to the altered structure of mutated proteins and facilitating correct folding and thus increasing enzyme activity (**Figure 2C**). This principle has been explored in lysosomal storage disease and there are currently approved medications for Fabry disease (Fan et al., 1999; Germain et al., 2016) and Niemann-Pick C disease (Pipalia et al., 2019, 2021; Shioi et al., 2020), while such treatments for others are under investigation (Tropak et al., 2004; Parenti et al., 2014; Han et al., 2020). The advent of *in silico* screening of large compound libraries has greatly facilitated the identification of novel candidate compounds and is actively being explored in CDG (Yuste-Checa et al., 2016).

Non-causative and Other Treatments

Besides treatments aiming at correcting or improving the function of the affected protein and thus leading to normalized glycosylation, other treatments aim to correct symptoms or secondary manifestations of the disease. In the interest of brevity, only those treatments specific to symptoms of CDG are mentioned in this review.

Furthermore, the treatment of glycosylphosphatidylinositol (GPI) deficiency caused by promoter mutations in *PIGM* relies on enhanced histone acetylation, a

concept not used in any other known CDG therapy (Almeida et al., 2007).

ESTABLISHED THERAPIES FOR CONGENITAL DISORDERS OF GLYCOSYLATION

Substrate (Precursor) Supplementation and Bypassing Strategies

Mannose Supplementation for MPI-CDG Bypasses the Impaired Enzyme

Defects in mannose-6-phosphate isomerase (PMI, EC 5.3.1.8) cause MPI-CDG (**Figure 3A**), a disorder characterized by severe protein-losing enteropathy (Jaeken et al., 1998; Niehues et al., 1998), liver disease (de Koning et al., 1999), and coagulopathy resulting in recurrent thrombosis (Girard et al., 2020). In addition, hyperinsulinism occurs frequently (de Lonlay et al., 1999). Unlike in other CDG, no neurological phenotype can be observed and patients show no intellectual disabilities (de Lonlay and Seta, 2009).

Due to the loss of PMI function, the conversion of fructose-6-phosphate into mannose-6-phosphate is not possible, necessitating the direct phosphorylation of mannose by hexokinase (Niehues et al., 1998). Since the mammalian mannose transporter was found to operate at submaximal efficiency under physiological mannose concentrations (Etchison and Freeze, 1997; Panneerselvam et al., 1997) and oral incorporation of mannose was shown to raise blood levels (Alton et al., 1997), oral mannose supplementation was introduced and showed both clinical and biochemical improvement in a follow-up period of 11 months (Niehues et al., 1998; **Figure 3B**). Additional studies showed similar results (Mayatepek and Kohlmüller, 1998; de Lonlay et al., 1999; Westphal et al., 2000; Hendriksz et al., 2001; Harms et al., 2002) with improvement of intestinal and hematological symptoms, while the response of liver disease to mannose therapy might be limited (de Lonlay and Seta, 2009). Interestingly, hepatic fibrosis may be present at birth, hinting at a ante-natal onset of liver disease that might not be amenable to postnatal mannose treatment (Girard et al., 2020).

Although these results were convincing with regards to efficacy, the observed toxicity of mannose in several *Apidae* dubbed "honeybee syndrome" (Sols et al., 1960) raised concerns regarding the safety of this intervention. Mannose toxicity in these insects was found to be caused by intrinsic MPI deficiency (Sols et al., 1960) and subsequent accumulation of mannose-6-phosphate in conjunction with intracellular ATP depletion (de la Fuente et al., 1986).

In the context of mannose therapy for MPI-CDG, oral substitution is usually well tolerated but intravenous administration of mannose in a patient was associated with central nervous and hepatic dysfunction that was reversible upon increased intravenous glucose substitution (Schroeder et al., 2010). This was attributed to intracellular ATP depletion in addition to inhibited glycolysis by mannose-6-phosphate, similar to findings from animal model (DeRossi et al., 2006).

These findings culminated in the recent proposition of international consensus guidelines recommending the oral administration of mannose at a concentration of 150–170 mg/kg bodyweight four to five times per day (Čechová et al., 2020), a treatment that has been approved in both the European Union (EU) and the United States (Brasil et al., 2018). Blood mannose levels can serve to monitor treatment for dose optimization with measurements before administration and after 1 h, aiming to achieve levels of >20 and >100 μmol/L, respectively (Čechová et al., 2020). Despite the high efficacy of treatment regarding intestinal and hematological symptoms, the requirement to ingest large amounts of mannose and associated adverse effects such as diarrhea may lead to poor compliance (Girard et al., 2020). Future improvements in formulation might improve therapy adherence.

In addition to mannose, heparin has shown positive effects on protein losing enteropathy associated with MPI-CDG in a single case (Liem et al., 2008).

Galactose Supplementation Improves Defective UDP-Galactose Transport in SLC35A2-CDG

Mutations in *SLC35A2* affecting the function of the Golgi-localized UDP-galactose transporter (**Figure 2A**) are inherited in an X-linked recessive manner although most occur *de novo*, resulting in a type II CDG (Kodera et al., 2013; Ng et al., 2013). In some cases, glycan analysis indicates no abnormal glycosylation of serum transferrin (Ng et al., 2019). The phenotype is characterized by seizures often manifesting as severe infantile spasms with hypsarrhythmia, failure to thrive, dysmorphic features, and brain malformations.

Glycan analysis indicates a loss of both galactose and sialic acid structures and *in vitro* studies have shown reduced uptake and subsequently a severely reduced Golgi-localized UDP-galactose following the expression of *SLC35A2* mutations (Ng et al., 2013). On the background of these findings, oral galactose supplementation at doses of up to 1.5 g/kg bodyweight/day or higher was proposed as a potential treatment and correlated with normalized transferrin glycosylation as well as clinical improvement (Dörre et al., 2015). However, improvement of transferrin glycosylation was also observed in untreated individuals (Ng et al., 2019). On the background of the absence of dysglycosylation in a group of affected individuals, improved glycosylation can – in our view – be seen as an unreliable correlate for treatment efficacy at best. A recently published study underscored positive effects on clinical presentation, namely seizure control, as well as biochemical abnormalities, further strengthening the case for galactose supplementation as a treatment for SLC35A2-CDG (Witters et al., 2020).

Rewiring Glucose Metabolism and Glycosylation – Galactose Supplementation in PGM1-CDG

Before their identification as a cause of a glycosylation disorder in 2014 (Tegtmeyer et al., 2014), biallelic mutations in *PGM1* were identified as a cause of glycogen storage disease (GSD) type XIV (Stojkovic et al., 2009). In the index patient, rhabdomyolysis and muscle weakness along muscular glycogen accumulation were noted while PGM1 activity was severely reduced, leading to

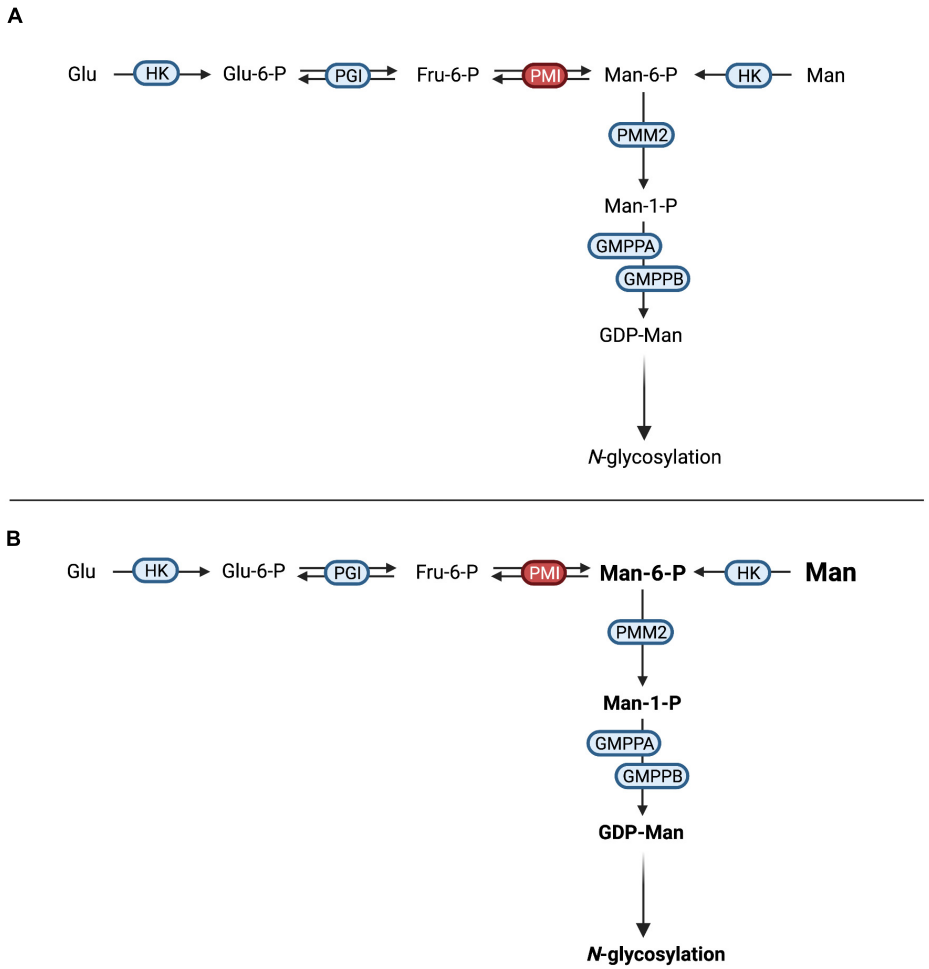

FIGURE 3 | Mannose therapy in MPI-CDG. **(A)** Mutations in *MPI* lead to an impaired function of phosphomannose isomerase (PMI), thus hindering the interconversion of fructose-6-phosphate (Fru-6-P) to mannose-6-phosphate (Man-6-P). **(B)** The oral supplementation of mannose increases the available Man-6-P following conversion of mannose (Man) by hexokinase (HK). After conversion of Man-6-P to mannose-1-phosphate (Man-1-P) by phosphomannomutase 2 (PMM2), conversion into guanosine diphosphate-mannose (GDP-Man). This can be used in *N*-glycosylation.

decreased interconversion of glucose-1-phosphate and glucose-6-phosphate.

Subsequently, a large cohort of 19 patients with biallelic *PGM1* mutations leading to abnormal glycosylation with a mixed type I and II like dysglycosylation pattern of serum transferrin was identified (Tegtmeyer et al., 2014). Additional phenotypical features included hypoglycemia, hepatopathy (transaminase elevation, abnormal coagulation parameters), growth retardation, and dilated cardiomyopathy. Endocrine abnormalities in the form of hypogonadotropic hypogonadism were present, while a bifid uvula was described as an easily recognizable clinical sign. Initially, it was believed that neurological impairment was uncommon and secondary to hypoglycemia. However, recent studies have proposed a neurological phenotype unrelated to blood sugar abnormalities (Radenkovic et al., 2018). Due to the finding of markedly decreased UDP-galactose content in patient-derived skin fibroblasts, galactose was added to the cell culture media and resulted in improved glycosylation of ICAM-1 while no effect on glycogen content was observed. This intervention does not provide the direct substrate of PGM1 but bypasses the enzymatic defect (**Figures 4A,B**), resulting in improved glycosylation (**Figure 4C**).

The subsequent galactose supplementation in a sub-cohort of six individuals of 1 g/kg bodyweight/day led to improved glycosylation as assessed by serum transferrin and total serum *N*-glycome studies. Clinically, no further episodes of rhabdomyolysis were observed and hypogonadotropic hypogonadism resolved with patients developing signs of puberty (Tegtmeyer et al., 2014).

A prospective trial in eight patients confirmed the positive effect observed previously (Wong et al., 2017). In the study, D-galactose was administered orally at incremental doses of 0.5, 1.0, and 1.5 g/kg/day for 6 weeks, respectively (total study period 18 weeks). One individual continued to receive a lesser dose of 1.0 g/kg/day for a year after the trial.

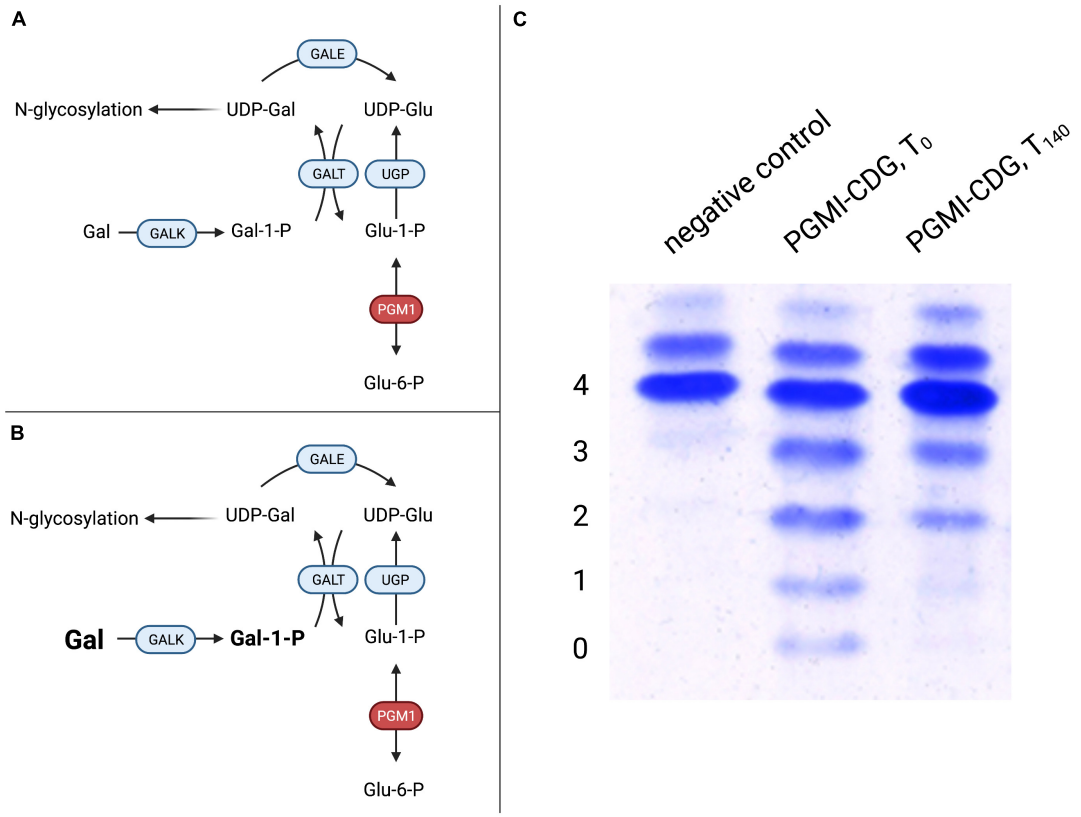

FIGURE 4 | Galactose therapy in PGM1-CDG. **(A)** A defect in PGM1 hinders conversion of glucose-1-phosphate (Glu-1-P) to glucose-6-phosphate (Glu-6-P), thus impairing hepatic glucose release. Similarly, the reverse reaction in which Glu-6-P is converted to Glu-1-P, which can serve as a substrate for UDP-glucose production by UDP-glucose pyrophosphorylase (UGP) for glycogen synthesis or glycosylation, is impaired. **(B)** Supplemented galactose is transformed to UDP-galactose (UDP-Gal) by galactose-1-phosphate uridyltransferase (GALT). UDP-Gal can serve both in glycosylation and as a substrate for UDP-galactose epimerase (GALE), supplying UDP-Gal for glycogen metabolism. **(C)** Transferrin IEF profiles during galactose substitution over 140 days in PGM1-CDG. Compared to controls, PGM1-CDG shows a characteristic, "ladder-like" pattern in IEF (PGM1-CDG, T_0). Following 20 weeks of galactose substitution at a dose of 1 g/kg bodyweight/day, significant improvement with reduced abnormal transferrin isoforms was observed (PGM1-CDG, T_{140}) (4 – tetrasialo-transferrin, 3 – trisialo-transferrin, 2 – disialo-transferrin, 1 – monosialo-transferrin, 0 – asialo-transferrin).

The absence of serious adverse events and generally good tolerance of increasing amounts of galactose indicated the general safety of the therapy. As in the previous study, transferrin glycosylation improved in all except one participant, and no further episodes of rhabdomyolysis were reported despite no clear effect on previously elevated creatine kinase levels. Endocrine abnormalities improved in all patients. In addition, liver function improved drastically, with ALT normalizing in a subset of patients and AST decreasing. Likewise, coagulation parameters improved or normalized. In a separate trial with eleven individuals, early therapy was found to be preferrable to delayed treatment, which was seen to argue for inclusion into screening programs (Conte et al., 2020). This is especially relevant since a modified Beutler test was shown to detect PGM1-CDG from dried blood spots (Tegtmeyer et al., 2014). A glycoprofiling study was able to identify specific glycomarkers, allowing early diagnosis as well as therapy monitoring using mass spectrometry-based methods (Abu Bakar et al., 2018).

The effect of galactose supplementation on cardiomyopathy has not been evaluated formally so far. In a singular case that presented with restrictive rather than dilated cardiomyopathy, galactose supplementation did not improve echocardiography and ECG results, while liver function and glycosylation improved (Donoghue et al., 2021). Similarly, there are reports of incomplete normalization of transferrin glycosylation at standard doses of galactose, possibly indicating that supplementation at higher doses as done, e.g., in SLC39A8-CDG might be needed in certain cases (Nolting et al., 2017).

Galactose Supplementation Corrects Secondary Glycosylation Abnormalities in SLC39A8-CDG and TMEM165-CDG

Both SLC39A8-CDG and TMEM165-CDG are caused by disturbed manganese metabolism and might thus be considered secondary glycosylation disorders in which the deficiency of glycosyltransferases is caused by the lack of a cofactor (see section "Manganese-Sulfate Is a Causative Treatment for SLC39A8-CDG" and "A Potential Role for Manganese in the Treatment of TMEM165-CDG," **Figure 2B**). Mass spectrometry analysis of glycan structures has identified hypogalactosylation, i.e., the lack

of galactose residues when compared to normal glycan structures, in both subtypes (Foulquier et al., 2012; Park et al., 2015).

Oral supplementation of galactose has therefore been attempted in order to improve dysglycosylation. In SLC39A8-CDG, a dose of up to 3.75 g/kg bodyweight per day (either given continuously via an enteral feeding pump or divided in five equal doses) led to near complete normalization transferrin glycosylation, while interruption of treatment resulted in an increase of abnormally glycosylated transferrin isoforms (Park et al., 2015). The relatively high doses used here were well tolerated, hinting at the possibility of higher doses in other CDG subtypes (see section "Galactose Supplementation Improves Defective UDP-Galactose Transport in SLC35A2-CDG" and "Rewiring Glucose Metabolism and Glycosylation – Galactose Supplementation in PGM1-CDG"). In addition to galactose, uridine was supplemented (150 mg/kg bodyweight/d) with the aim to increase UDP-galactose supplies. The trial design did not allow for a distinction between the possible separate effects of galactose and uridine. Similar results were seen in an independent study (Riley et al., 2017). In both cases, improvement was observed within approximately 2 weeks, indicating that transferrin synthesis might be the limiting factor (Park et al., 2015).

Similarly, galactose supplementation was studied in TMEM165-CDG. After encouraging results on both a HEK293 model with a knockout of *TMEM165* and patient-derived skin fibroblasts in which galactose corrected hypogalactosylation (Morelle et al., 2017), oral supplementation of 1 g galactose/kg/d was administered to two individuals with TMEM165-CDG. *N*-glycosylation improved and biochemical abnormalities were partly corrected, with higher doses of up to 1.5 g/kg/d having no additional beneficial effect.

L-Fucose Supplementation Increases Impaired GDP-Fucose Transport in SLC35C1-CDG

Leukocyte adhesion deficiency type II (LADII) is caused by impaired glycoconjugate fucosylation due to impaired function of SLC35C1, the GDP-fucose transporter, and is therefore named SLC35C1-CDG under the current nomenclature of glycosylation disorders. Even before the identification of the underlying genetic defect (Lübke et al., 2001; Lühn et al., 2001), reduced fucose uptake and correction by increased fucose supplementation both *in vitro* (Lübke et al., 1999; Marquardt et al., 1999) and *in vivo* (Marquardt et al., 1999; Wild et al., 2002) was demonstrated.

The phenotype is marked by severely delayed psychomotor development in conjunction with short stature, dysmorphic features, and recurrent, potentially life-threatening infections (Etzioni et al., 1992). Extreme neutrophilia (up to 20 times of normal values) due to impaired rolling is caused by the absence of sialyl-Lewis^x (sLe^x, CD15) selectin ligand carrying fucose (Etzioni et al., 1992). Similarly, patients have a Bombay blood group (hh) as defined by lacking expression of the H antigen with an alpha(1,2)linked fucose-galactose disaccharide (Wolach et al., 2019). In a subset of patients, the immunological phenotype appears to be rather mild and these individuals are frequently diagnosed with short stature and intellectual disability (Dauber et al., 2014; Knapp et al., 2020).

Oral L-fucose supplementation has been administered five times per day in escalating doses of up to 492 mg/kg bodyweight/dose and was shown to correct core fucosylation of serum proteins, followed by a reduction of peripheral neutrophil counts (Marquardt et al., 1999). During therapy, improvement of psychomotor development as assessed by the Griffiths Test (Griffiths, 1984) was observed, although no standardized trials regarding psychomotor development during fucose therapy of SLC35C1-CDG have been conducted. The involvement of blood group antigens in the phenotype necessitates careful observation during therapy: In theory, synthesis of the H-antigen might occur during fucose supplementation, causing autoimmune side effects in case anti-H-antigen antibodies are present or would be raised. However, no H-antigen expression has been observed in the original trial (Marquardt et al., 1999) or has occurred to our knowledge.

L-Fucose Supplementation Leads to Clinical Improvement and Protein-Specific Enhancement of Glycosylation in FUT8-CDG

Mutations in *FUT8* encoding the α-1,6-fucosyltransferase (EC 2.4.1.68) are associated with a severe glycosylation disorder that is characterized by a loss of core fucosylation upon glycan analysis in patient sera as well as patient-derived cells (Ng et al., 2018). All patients exhibit failure to thrive, severe developmental delay, muscular hypotonia, feeding abnormalities, with respiratory abnormalities being a distinctive feature of the disorder (Ng et al., 2020). Seizures are also frequently seen, although absence of this disease manifestation has been observed (Park et al., 2020b).

The addition of L-fucose to cell culture media of patient-derived skin fibroblasts did not improve either overall glycosylation or core fucosylation in a specific variant leading to a loss of exon 9 of the protein (Ng et al., 2018). In contrast, oral L-fucose supplementation in dizygotic twins that was escalated from 100 to 825 mg/kg/d showed a protein specific effect with increased core fucosylation of both serum transferrin and IgG in addition to an increase of a fucosylated disialo-biantennary glycan. At the same time, several truncated, non-fucosylated glycan entities (agalactosylated glycan Hex3HexNAc4, asialo glycan Hex5HexNAc4, and mono-galactosylated, Neu5Ac1Hex4HexNAc4) decreased to normal levels (Park et al., 2020b). No adverse effects were noted during follow-up and the patients could be weaned from non-invasive ventilation and showed general clinical improvement.

Sialic Acid Supplementation Is Associated With Improved Psychomotor Development in NANS-CDG

First described in 2016, NANS-CDG is caused mutations in the eponymous gene, leading to impaired function of *N*-acetyl-*D*-neuraminic acid synthase (van Karnebeek et al., 2016). Phenotypically, the disorder is characterized by global developmental delay, muscular hypotonia, short stature, and facial dysmorphisms. In a zebrafish model, sialic acid was able to partially rescue the phenotype (van Karnebeek et al., 2016). Early results indicate improved psychomotor development in NANS-CDG patients following sialic acid supplementation (den Hollander et al., 2021), with additional research still ongoing.

Impaired Nucleotide Sugar Synthesis in CAD-CDG Is Rescued by Uridine Supplementation

Mutations in *CAD* lead to a deficiency in cytoplasmic carbamoyl-phosphate synthetase 2, subsequently impairing *de novo* pyrimidine synthesis. Loss of the protein results in a reduction of nucleotide sugars, i.e., precursors of glycosylation, and reduced flux of aspartate into DNA and RNA (Ng et al., 2015). Of note, despite reduced nucleotide sugars, no abnormal glycosylation was found in fibroblasts or serum of the index patient. This was confirmed in an additional cohort of two patients (Koch et al., 2017), making the classification of CAD deficiency as a glycosylation disorder debatable. Clinically, affected individuals show global developmental delay, epileptic encephalopathy and a hematologic phenotype consisting of anemia and anisopoikilocytosis (Ng et al., 2015; Koch et al., 2017). After rescue of biochemical abnormalities *in vitro* by uridine supplementation (Ng et al., 2015), a therapeutic trial was initiated resulting in cessation of seizures as well as normalization of biochemical abnormalities (Koch et al., 2017).

Mannose Supplementation in PMM2-CDG?

PMM2-CDG was the first glycosylation disorder and was characterized in the 1980s by the Belgian Pediatrician Jaak Jaeken (Jaeken et al., 1984). Caused by a defect in the enzyme phosphomannomutase 2 (EC: 5.4.2.8), this disturbance of mannose metabolism is an archetypical glycosylation disorder and remains the most common one, with approximately 1,000 cases diagnosed to date (Witters et al., 2018).

Early on, mannose supplementation was considered as a possible therapy. However, the location of the enzyme defect within the glycosylation pathway renders a beneficial effect of exogenous mannose unlikely (**Figure 5**; Ichikawa et al., 2014). Surprisingly, treatment with mannose led to a normalization of glycosylation in patient-derived skin fibroblasts (Panneerselvam and Freeze, 1996; Rush et al., 2000). Similarly, mannose administration to pregnant mice mitigated embryonic lethality in a hypomorphic PMM2 mouse model (Schneider et al., 2011).

Early trials involving both intravenous (Mayatepek et al., 1997) and oral (Kjaergaard et al., 1998) mannose administration did not show any signs of improvement. These findings were supported by later, unrelated reports (Mayatepek and Kohlmüller, 1998; Grünert et al., 2019). In a recent retrospective analysis of longer mannose supplementation over several years, our group detected biochemical improvement as defined by improved transferrin glycosylation following treatment >1 year (Taday et al., 2020; **Figure 5B**). Although spontaneous improvement of serum transferrin glycosylation is frequently seen in PMM2-CDG (Schiff et al., 2017; Witters et al., 2018), the response regardless of age at onset of therapy and the deterioration following discontinuation of treatment argue against purely spontaneous normalization (Taday et al., 2020). Due to the retrospective nature of the study, no formal evaluation of clinical improvement was performed. However, a subset of responders showed improved nerve conduction velocities in addition to restoration of deep tendon reflexes (Taday et al., 2020). Therefore, further studies – ideally in the form of randomized-controlled trials – are needed to assess the effect of oral mannose supplementation on PMM2-CDG.

Cofactor Supplementation

Manganese-Sulfate Is a Causative Treatment for SLC39A8-CDG

In contrast to other glycosylation disorders, SLC39A8-CDG is caused by mutations in the gene encoding the eponymous divalent cation channel, that acts as the principal cellular manganese uptake transporter (He et al., 2006; Nebert and Liu, 2019). Due to the reliance of several glycosyltransferases on Mn^{2+} as a cofactor (Breton et al., 2006), mutations in *SLC39A8* resulting in intracellular manganese depletion cause secondary glycosylation defects corresponding to a type II CDG pattern of transferrin dysglycosylation. Manganese is severely reduced or absent both in blood and urine (Boycott et al., 2015; Park et al., 2015; Riley et al., 2017).

Clinically, SLC39A8-CDG is characterized by psychomotor retardation, short stature, severe seizures, cerebellar atrophy, cranial synostoses, as well as visual and auditory impairment (Boycott et al., 2015; Park et al., 2015). In addition, Leigh-like mitochondrial disease, possibly due to impaired function of manganese-dependent SOD2, has been reported (Riley et al., 2017). Indeed, additional manganese dependent enzymes might in theory be affected by manganese depletion.

While initial attempts using galactose supplementation aimed at correcting the observed hypogalactosylation and resulted in improved transferrin glycosylation (Park et al., 2015), manganese supplementation was hypothesized to be a causative treatment not only targeting impaired glycosyltransferases but also other manganese dependent enzymes like SOD2 (Flynn and Melov, 2013) and xanthine oxidase (Schroeder et al., 1966). In a trial with two individuals, oral supplementation of 15–20 mg manganese-II-sulfate ($MnSO_4.H_2O$)/kg bodyweight was able to correct transferrin glycosylation to normal levels and led to considerable clinical improvement by near normalization of EEG patterns and cessation of seizures (Park et al., 2018). However, due to the broad spectrum of clinical presentations, the doses needed for correction cannot be expected to be uniform in all patients.

Given the potential toxicity of manganese, showcased by cases of a Parkinsonian phenotype dubbed "manganism" observed in battery or steel factory workers as well as other occupational or environmental exposition (Harischandra et al., 2019; Evans and Masullo, 2020), caution is warranted in treating SLC39A8-CDG. Although no reports of adverse effects of manganese substitution exist, careful monitoring of blood manganese levels and repeated MRI studies to assess possible manganese deposits in the brain (Lucchini et al., 2000; Crossgrove and Zheng, 2004) seems prudent.

Another hindrance is the imperfect assessment of treatment efficacy. While blood manganese levels and transferrin glycosylation normalize quickly under adequate substitution (Park et al., 2018), recent research by our group has identified subtle glycosylation abnormalities in SLC39A8-CDG that are not detected by conventional methods (Park et al., 2020a). *N*-glycome profiling using matrix-assisted laser desorption

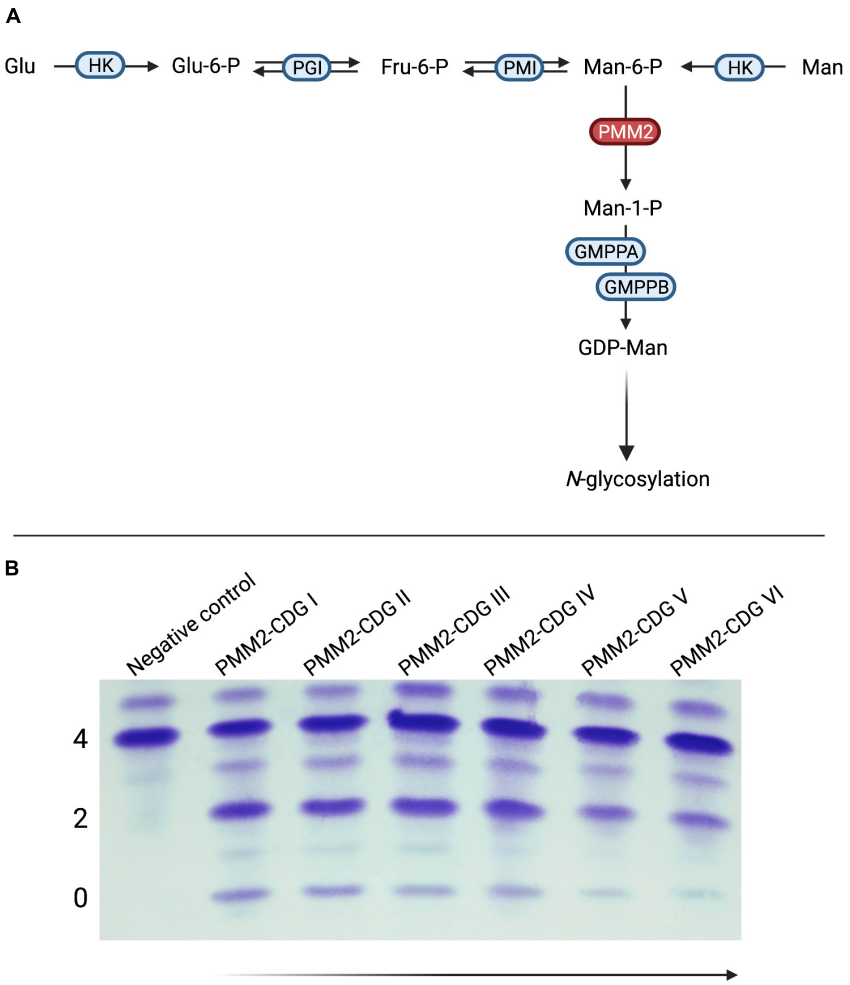

FIGURE 5 | Mannose supplementation in PMM2-CDG. **(A)** In PMM2-CDG, the conversion of mannose-6-phosphate (Man-6-P) to mannose-1-phosphate (Man-1-P) by phosphomannomutase 2 (PMM2) is impaired due to mutations in *PMM2*. **(B)** Findings for mannose supplementation in PMM2-CDG have been inconsistent. In a subgroup of patients, significant improvement of serum transferrin glycosylation can be achieved with oral supplementation of mannose. Of note, these changes occur after several months or even years and have been shown to be reversible if mannose substitution is discontinued. PMM2-CDG I and II – Pretherapeutic samples from the same patient; PMM2-CDG III–VI – Samples after 1, 2, 3, and 4 years of mannose substitution at a dose of 1 g/kg bodyweight/day (HK, hexokinase; Glu-6-P, glucose-6-phosphate; PGI, glucose-6-phosphate isomerase; Fru-6-P, fructose-6-phosphate; PMI, phosphomannose isomerase; GMPPA, Mannose-1-phosphate guanyltransferase alpha; GMPPB, Mannose-1-phosphate guanyltransferase beta).

ionization time of flight (MALDI-TOF) mass spectrometry might be more suitable to monitor the effects of manganese sulfate substitution (Park et al., 2020a).

A Potential Role for Manganese in the Treatment of TMEM165-CDG

As in SLC39A8-CDG, glycosylation defects in TMEM165-CDG are characterized by hypogalactosylation in addition to hyposialylation (Foulquier et al., 2012). Recent studies have identified abnormal manganese metabolism (Potelle et al., 2016, 2017) and provide *in vitro* evidence that manganese can correct glycosylation abnormalities in TMEM165-CDG. To date, no *in vivo* studies have been performed to assess manganese supplementation as a therapy for TMEM165-CDG.

Chaperones

While having been explored for some time, pharmacological chaperones did not reach clinical application or *in vivo* trials in CDG until recently. However, previous research indicated that glucose-1,6-bisphosphate is a natural ligand of PMM2 and increases its catalytic activity (Monticelli et al., 2019). Following screening studies on large compound libraries (Yuste-Checa et al., 2016), the aldolase inhibitor epalrestat was identified as a potent activator of several variant PMM2 proteins (Iyer et al., 2019). The effect on mutant PMM2 proteins carrying the frequent variants p.R141H/p.F182S, p.R141H/p.E139K, and p.R141H/p.N216I was assessed using a novel *Caenorhabditis elegans* model and patient-derived fibroblasts. An increase in PMM2 activity of up to 3.15-fold of baseline was observed (Iyer et al., 2019).

Due to the compounds approval as a drug for diabetic neuropathy in Japan, clinical application in CDG would represent a repurposing approach with the potential to shorted time to clinical application [for an excellent review on drug repurposing see Pushpakom et al. (2019)]. Currently, a $n = 1$ exploratory study is being conducted in the United States, with results expected to be reported shortly (A Phase I study of Epalrestat Therapy in a Single Patient with Phosphomannomutase Deficiency (PMM2-CDG), 2021). Another patient was started in Germany even earlier and is still under investigation.

Non-causative and Other Treatments

General Aspects and Clinical Recommendations for the Treatment of CDG

General recommendations for the symptomatic treatment of CDG have mainly been based on clinical experience or single case studies rather than controlled trials. A detailed summary on current specific recommendations for PMM2-CDG, MPI-CDG, and PGM1-CDG can be found in published consensus guidelines (Altassan et al., 2019, 2021; Čechová et al., 2020). However, on the background of lacking guidelines for most subtypes, general recommendations that apply to all known CDG subtypes can facilitate management of such patients.

In general, fever exerts a detrimental effect on glycosylation and has been shown to reduce the residual activity of glycosylation related enzymes further (Kjaergaard et al., 1999; Andreotti et al., 2015; Görlacher et al., 2020). Indeed, glycosylation abnormalities are sometimes only detected during or shortly after episodes of fever (Reunert et al., 2019). Therefore, aggressive management of fever with antipyretics is recommended in order to preserve glycosylation capacities. Likewise, infections should be treated liberally.

Coagulation abnormalities both in the form of thrombotic events and impaired hemostasis are frequently seen in CDG. The underlying abnormalities are complex and in many cases, a somewhat fragile equilibrium seems to exist (Stibler et al., 1996). While thrombosis can be treated with low molecular weight heparin and also rivaroxaban (Lefrère et al., 2018; Altassan et al., 2019), impaired hemostasis and bleeding diathesis should be treated using fresh-frozen plasma rather than single factor substitution in order to avoid unwanted effects (Brucker et al., 2020).

Treating Ataxia and Stroke-Like Episodes in PMM2-CDG – Acetazolamide to the Rescue

Among the multitude of symptoms found in PMM2-CDG, ataxia accounts for a considerable burden of disease. The radiographic correlate is pronounced cerebellar ataxia, oftentimes diagnosed in other subtypes as well (Barone et al., 2014). Another complication of PMM2-CDG are so called stroke-like episodes (SLE) in which hemiparesis in the absence of any ischemic or hemorrhagic intracranial lesions is observed. There is data suggesting that SLE have an epileptic origin and they frequently improve following the administration of anticonvulsive medication (Dinopoulos et al., 2007). Recent research has identified gain-of-function effects of the $Ca_V2.1$ voltage-gated calcium channel that are mediated by hypoglycosylation of both subunits α_{1A} and α_{2A} as a potential pathomechanism in SLE (Izquierdo-Serra et al., 2018).

Interestingly, dysfunction of $Ca_V2.1$ caused by mutations in *CACNA1A* has been identified in Familial hemiplegic migraine 1 (FHM1; Ophoff et al., 1996), where altered channel kinetics were identified as a pathomechanism (Kraus et al., 1998, 2000). Other diseases associated with *CACNA1A* mutations are Spinocerebellar Ataxia type 6 (SCA6; Zhuchenko et al., 1997) and Developmental and Epileptic Encephalopathy 42 (Epi4K Consortium, 2016), which all show phenotypic similarities to the symptoms observed in PMM2-CDG.

The carbonic anhydrase inhibitor acetazolamide was shown to reduce cerebellar symptoms in SCA6 (Yabe et al., 2001) and FHM1 (Athwal and Lennox, 1996). It is believed that acetazolamide reduces overactivity, i.e., a gain of function, by altering the intracellular pH (Bain et al., 1992), making it a potential treatment for cerebellar symptoms in PMM2-CDG. The landmark randomized AZATAX trial showed substantial improvement of ataxia as assessed by International Cooperative Ataxia Rating Scale (ICARS) scores and general clinical improvement, while being generally well tolerated (Martínez-Monseny et al., 2019). Due to the limited observation period, no formal assessment of the effect on SLE frequency or severity could be made, although one patient who was frequently experiencing SLE did not do so during treatment.

Histone Deacetylase Inhibition Is a Targeted Therapy for PIGM-CDG

Inherited glucosylphosphatidylinositol (GPI) deficiency or PIGM-CDG is caused by a mutation in the core promoter of *PIGM*, severely impairing the binding site of the transcription factor Sp1 and resulting in hindered transcription (Almeida et al., 2006). In affected individuals, thrombotic events, seizures, and global hypotonia are present. Prompted by the lack of histone acetylation at the *PIGM* promoter, *in vitro* studies of the effect of the histone deacetylase inhibitor sodium butyrate indicated normalized Histone 4 acetylation and increased transcriptional activity as well as restored surface expression of GPI (Almeida et al., 2007). In a single patient trial of sodium butyrate at a dose of 20 mg/kg bodyweight three times a day, *PIGM* transcription and GPI expression increased *in vivo* as well, which was accompanied by dramatic clinical improvement with absence of seizures, returning of walking abilities and restored self-feeding (Almeida et al., 2007). Higher doses of 30 mg/kg three times a day were tolerated as well. Another study in three individuals carrying the same mutation found modest clinical improvement while not demonstrating increased GPI expression. However, these results were reported to have been hampered by incomplete compliance (Pode-Shakked et al., 2019).

Transplantation of Organs and Cells

As outlined above, mannose supplementation is not successful in preventing hepatic fibrosis in MPI-CDG. This has been reported to necessitate liver transplantation in female patient (Janssen et al., 2014). The patient showed profound clinical improvement in addition to normalization of biochemical parameters. Similarly, liver transplantation in CCDC115-CDG

led to improvement in a patient although several individuals had died previously following repeated transplantations and associated complications (Jansen et al., 2016). While attempted in COG6-CDG (Rymen et al., 2015), no definite judgment on the efficacy in this subtype can be made since the patient died due to transplant associated complications.

Heart transplantation was attempted in DOLK-CDG in several cases (Kapusta et al., 2013; Klcovansky et al., 2016), showing favorable outcomes.

Due to the predominantly immunocompromised phenotype in PGM3-CDG, hematopoietic stem cell transplantation from bone marrow and cord blood was performed in two individuals, leading to correction of neutro- and lymphopenia (Stray-Pedersen et al., 2014).

Emerging Concepts

Given the successful application of antisense and gene therapy approaches in disorders such as spinal muscular atrophy and *RPE65*-mediated inherited retinal dystrophy (Finkel et al., 2017; Mendell et al., 2017; Russell et al., 2017; Day et al., 2021), similar approaches in CDG are being actively explored. However, none of the currently studied therapies has advanced to clinical or human *in vivo* application (Vega et al., 2009; Tal-Goldberg et al., 2014; Haenseler et al., 2018).

CONCLUSION

Congenital disorders of glycosylation represent an ever-growing, complex family of disorders with a severe presentation in virtually all organ systems. Although treatment options for most subtypes are still lacking, recent years have seen substantial advances in the treatment of these ultra-rare diseases. Due to the rising numbers in patients, controlled trials now seem possible and have even been attempted, thus finally producing a robust scientific basis for clinical application. Further, collaborative efforts are needed to assure optimal treatment for patients with CDG.

AUTHOR CONTRIBUTIONS

JP and TM drafted, revised, and approved the final version of the article. Both authors contributed to the article and approved the submitted version.

FUNDING

We acknowledge an unconditional grant by Nutricia Metabolics.

ACKNOWLEDGMENTS

The authors would like to acknowledge the patients affected by CDG as well as their families, who have been the driving force of the authors' research and clinical work. Marianne Grüneberg's support and expert technical assistance in glycosylation analysis studies is gratefully acknowledged. All figures were created with BioRender.com.

REFERENCES

A Phase I study of Epalrestat Therapy in a Single Patient with Phosphomannomutase Deficiency (PMM2-CDG) (2021). Available online at: https://www.mayo.edu/research/clinical-trials/cls-20491217 (accessed May 26, 2021).

Abu Bakar, N., Voermans, N. C., Marquardt, T., Thiel, C., Janssen, M. C. H., Hansikova, H., et al. (2018). Intact transferrin and total plasma glycoprofiling for diagnosis and therapy monitoring in phosphoglucomutase-I deficiency. *Transl. Res.* 199, 62–76.

Almeida, A. M., Murakami, Y., Baker, A., Maeda, Y., Roberts, I. A. G., Kinoshita, T., et al. (2007). Targeted therapy for inherited GPI deficiency. *N. Engl. J. Med.* 356, 1641–1647. doi: 10.1056/nejmoa063369

Almeida, A. M., Murakami, Y., Layton, D. M., Hillmen, P., Sellick, G. S., Maeda, Y., et al. (2006). Hypomorphic promoter mutation in PIGM causes inherited glycosylphosphatidylinositol deficiency. *Nat. Med.* 12, 846–851. doi: 10.1038/nm1410

Altassan, R., Péanne, R., Jaeken, J., Barone, R., Bidet, M., Borgel, D., et al. (2019). International clinical guidelines for the management of phosphomannomutase 2-congenital disorders of glycosylation: diagnosis, treatment and follow up. *J. Inherit. Metab. Dis.* 42, 5–28.

Altassan, R., Radenkovic, S., Edmondson, A. C., Barone, R., Brasil, S., Cechova, A., et al. (2021). International consensus guidelines for phosphoglucomutase 1 deficiency (PGM1-CDG): Diagnosis, follow-up, and management. *J. Inherit. Metab. Dis.* 44, 148–163. doi: 10.1002/jimd.12286

Alton, G., Kjaergaard, S., Etchison, J. R., Skovby, F., and Freeze, H. H. (1997). Oral ingestion of mannose elevates blood mannose levels: a first step toward a potential therapy for carbohydrate-deficient glycoprotein syndrome type I. *Biochem. Mol. Med.* 60, 127–133. doi: 10.1006/bmme.1997.2574

Andreotti, G., Monti, M. C., Citro, V., and Cubellis, M. V. (2015). Heterodimerization of two pathological mutants enhances the activity of human phosphomannomutase2. *PLoS One* 10:e0139882. doi: 10.1371/journal.pone.0139882

Athwal, B. S., and Lennox, G. G. (1996). Acetazolamide responsiveness in familial hemiplegic migraine. *Ann. Neurol.* 40, 820–821. doi: 10.1002/ana.410400526

Bain, P. G., O'Brien, M. D., Keevil, S. F., and Porter, D. A. (1992). Familial periodic cerebellar ataxia: a problem of cerebellar intracellular pH homeostasis. *Ann. Neurol.* 31, 147–154. doi: 10.1002/ana.410310205

Barone, R., Fiumara, A., and Jaeken, J. (2014). Congenital disorders of glycosylation with emphasis on cerebellar involvement. *Semin. Neurol.* 34, 357–366. doi: 10.1055/s-0034-1387197

Boycott, K. M., Beaulieu, C. L., Kernohan, K. D., Gebril, O. H., Mhanni, A., Chudley, A. E., et al. (2015). Autosomal-Recessive intellectual disability with cerebellar atrophy syndrome caused by mutation of the manganese and zinc transporter gene SLC39A8. *Am. J. Hum. Genet.* 97, 886–893. doi: 10.1016/j.ajhg.2015.11.002

Brasil, S., Pascoal, C., Francisco, R., Marques-da-Silva, D., Andreotti, G., Videira, P. A., et al. (2018). CDG Therapies: from bench to bedside. *Int. J. Mol. Sci* 19:1304. doi: 10.3390/ijms19051304

Breton, C., Snajdrová, L., Jeanneau, C., Koca, J., and Imberty, A. (2006). Structures and mechanisms of glycosyltransferases. *Glycobiology* 16, 29R–37R.

Brucker, W. J., Croteau, S. E., Prensner, J. R., Cullion, K., Heeney, M. M., Lo, J., et al. (2020). An emerging role for endothelial barrier support therapy for congenital disorders of glycosylation. *J. Inherit. Metab. Dis.* 43, 880–890. doi: 10.1002/jimd.12225

Čechová, A., Altassan, R., Borgel, D., Bruneel, A., Correia, J., Girard, M., et al. (2020). Consensus guideline for the diagnosis and management of mannose phosphate isomerase-congenital disorder of glycosylation. *J. Inherit. Metab. Dis.* 43, 671–693. doi: 10.1002/jimd.12241

Chen, J., Li, X., Edmondson, A., Meyers, G. D., Izumi, K., Ackermann, A. M., et al. (2019). Increased clinical sensitivity and specificity of plasma protein n-glycan profiling for diagnosing congenital disorders of glycosylation by use of flow injection-electrospray ionization-quadrupole time-of-flight mass spectrometry. *Clin. Chem.* 65, 653–663. doi: 10.1373/clinchem.2018.296780

Conte, F., Morava, E., Bakar, N. A., Wortmann, S. B., Poerink, A. J., Grunewald, S., et al. (2020). Phosphoglucomutase-1 deficiency: early presentation, metabolic management and detection in neonatal blood spots. *Mol. Genet. Metab.* 131, 135–146. doi: 10.1016/j.ymgme.2020.08.003

Crossgrove, J., and Zheng, W. (2004). Manganese toxicity upon overexposure. *NMR Biomed.* 17, 544–553. doi: 10.1002/nbm.931

Dauber, A., Ercan, A., Lee, J., James, P., Jacobs, P. P., Ashline, D. J., et al. (2014). Congenital disorder of fucosylation type 2c (LADII) presenting with short stature and developmental delay with minimal adhesion defect. *Hum. Mol. Genet.* 23, 2880–2887. doi: 10.1093/hmg/ddu001

Day, J. W., Finkel, R. S., Chiriboga, C. A., Connolly, A. M., Crawford, T. O., Darras, B. T., et al. (2021). Onasemnogene abeparvovec gene therapy for symptomatic infantile-onset spinal muscular atrophy in patients with two copies of SMN2 (STR1VE): an open-label, single-arm, multicentre, phase 3 trial. *Lancet Neurol.* 20, 284–293. doi: 10.1016/s1474-4422(21)00001-6

de Koning, T. J., Dorland, L., and van Berge Henegouwen, G. P. (1999). Phosphomannose isomerase deficiency as a cause of congenital hepatic fibrosis and protein-losing enteropathy. *J. Hepatol.* 31, 557–560. doi: 10.1016/s0168-8278(99)80052-x

de la Fuente, M., Peñas, P. F., and Sols, A. (1986). Mechanism of mannose toxicity. *Biochem. Biophys. Res. Commun* 140, 51–55. doi: 10.1016/0006-291x(86)91056-9

de Lonlay, P., and Seta, N. (2009). The clinical spectrum of phosphomannose isomerase deficiency, with an evaluation of mannose treatment for CDG-Ib. *Biochim. Biophys. Acta* 1792, 841–843. doi: 10.1016/j.bbadis.2008.11.012

de Lonlay, P., Cuer, M., Vuillaumier-Barrot, S., Beaune, G., Castelnau, P., Kretz, M., et al. (1999). Hyperinsulinemic hypoglycemia as a presenting sign in phosphomannose isomerase deficiency: a new manifestation of carbohydrate-deficient glycoprotein syndrome treatable with mannose. *J. Pediatr.* 135, 379–383. doi: 10.1016/s0022-3476(99)70139-3

den Hollander, B., Rasing, A., Post, M. A., Klein, W. M., Oud, M. M., Brands, M. M., et al. (2021). NANS-CDG: delineation of the genetic, biochemical, and clinical spectrum. *Front. Neurol.* 12:668640. doi: 10.3389/fneur.2021.668640

DeRossi, C., Bode, L., Eklund, E. A., Zhang, F., Davis, J. A., Westphal, V., et al. (2006). Ablation of mouse phosphomannose isomerase (Mpi) causes mannose 6-phosphate accumulation, toxicity, and embryonic lethality. *J. Biol. Chem.* 281, 5916–5927. doi: 10.1074/jbc.m511982200

Dinopoulos, A., Mohamed, I., Jones, B., Rao, S., Franz, D., and deGrauw, T. (2007). Radiologic and neurophysiologic aspects of stroke-like episodes in children with congenital disorder of glycosylation Type Ia. *Pediatrics* 119, e768–e772.

Donoghue, S. E., White, S. M., Tan, T. Y., Kowalski, R., Morava, E., and Yaplito-Lee, J. (2021). Galactose treatment of a PGM1 patient presenting with restrictive cardiomyopathy. *JIMD Rep.* 57, 29–37. doi: 10.1002/jmd2.12177

Dörre, K., Olczak, M., Wada, Y., Sosicka, P., Grüneberg, M., Reunert, J., et al. (2015). A new case of UDP-galactose transporter deficiency (SLC35A2-CDG): molecular basis, clinical phenotype, and therapeutic approach. *J. Inherit. Metab. Dis.* 38, 931–940. doi: 10.1007/s10545-015-9828-6

Eisenberg, B. (2011). Channels as enzymes: oxymoron and tautology. *arXiv* Available online at: https://www.semanticscholar.org/paper/a084e51e96c5d55d7b1120c90a538fa19df4b474 (accessed July 29, 2021),

Epi4K Consortium (2016). De novo mutations in SLC1A2 and CACNA1A are important causes of epileptic encephalopathies. *Am. J. Hum. Genet* 99, 287–298.

Etchison, J. R., and Freeze, H. H. (1997). Enzymatic assay of D-mannose in serum. *Clin. Chem.* 43, 533–538. doi: 10.1093/clinchem/43.3.533

Etzioni, A., Frydman, M., Pollack, S., Avidor, I., Phillips, M. L., Paulson, J. C., et al. (1992). Recurrent severe infections caused by a novel leukocyte adhesion deficiency. *N. Engl. J. Med.* 327, 1789–1792. doi: 10.1056/nejm199212173272505

Evans, G. R., and Masullo, L. N. (2020). Manganese Toxicity. Treasure Island, FL: StatPearls Publishing. doi: 10.1056/nejm199212173272505

Fan, J. Q., Ishii, S., Asano, N., and Suzuki, Y. (1999). Accelerated transport and maturation of lysosomal alpha-galactosidase a in fabry lymphoblasts by an enzyme inhibitor. *Nat. Med.* 5, 112–115. doi: 10.1038/4801

Finkel, R. S., Mercuri, E., Darras, B. T., Connolly, A. M., Kuntz, N. L., Kirschner, J., et al. (2017). Nusinersen versus sham control in infantile-onset spinal muscular atrophy. *N. Engl. J. Med.* 377, 1723–1732. doi: 10.1056/nejmoa1702752

Flynn, J. M., and Melov, S. (2013). SOD2 in mitochondrial dysfunction and neurodegeneration. *Free Radic. Biol. Med.* 62, 4–12. doi: 10.1016/j.freeradbiomed.2013.05.027

Foulquier, F., Amyere, M., Jaeken, J., Zeevaert, R., Schollen, E., Race, V., et al. (2012). TMEM165 deficiency causes a congenital disorder of glycosylation. *Am. J. Hum. Genet.* 91, 15–26. doi: 10.1016/j.ajhg.2012.05.002

Germain, D. P., Hughes, D. A., Nicholls, K., Bichet, D. G., Giugliani, R., Wilcox, W. R., et al. (2016). Treatment of fabry's disease with the pharmacologic chaperone migalastat. *N. Engl. J. Med.* 375, 545–555.

Girard, M., Douillard, C., Debray, D., Lacaille, F., Schiff, M., Vuillaumier-Barrot, S., et al. (2020). Long term outcome of MPI-CDG patients on D-mannose therapy. *J. Inherit. Metab. Dis.* 43, 1360–1369. doi: 10.1002/jimd.12289

Görlacher, M., Panagiotou, E., Himmelreich, N., Hüllen, A., Beedgen, L., Dimitrov, B., et al. (2020). Fatal outcome after heart surgery in PMM2-CDG due to a rare homozygous gene variant with double effects. *Mol. Genet. Metab. Rep.* 25:100673. doi: 10.1016/j.ymgmr.2020.100673

Gorlov, I. P., Kimmel, M., and Amos, C. I. (2006). Strength of the purifying selection against different categories of the point mutations in the coding regions of the human genome. *Hum. Mol. Genet.* 15, 1143–1150. doi: 10.1093/hmg/ddl029

Griffiths, R. (1984). *The Abilities Of Young Children: A Comprehensive System Of Mental Measurement For The First Eight Years Of Life. Association for Research in Infant and Child Development*. Oxford: The Test Agency Ltd.

Grünert, S. C., Marquardt, T., Lausch, E., Fuchs, H., Thiel, C., Sutter, M., et al. (2019). Unsuccessful intravenous D-mannose treatment in PMM2-CDG. *Orphanet J. Rare Dis.* 14:231.

Guillard, M., Morava, E., van Delft, F. L., Hague, R., Korner, C., Adamowicz, M., et al. (2011). Plasma N-glycan profiling by mass spectrometry for congenital disorders of glycosylation type II. *Clin. Chem.* 57, 593–602. doi: 10.1373/clinchem.2010.153635

Haenseler, W., Kuzmenko, E., Smalls-Mantey, A., Browne, C., Seger, R., James, W. S., et al. (2018). Lentiviral gene therapy vector with UCOE stably restores function in iPSC-derived neutrophils of a CDG patient. *Matters* 2018. doi: 10.19185/matters.201805000005

Han, T.-U., Sam, R., and Sidransky, E. (2020). Small molecule chaperones for the treatment of gaucher disease and GBA1-associated Parkinson Disease. *Front. Cell Dev. Biol.* 8:271. doi: 10.3389/fcell.2020.00271

Harischandra, D. S., Ghaisas, S., Zenitsky, G., Jin, H., Kanthasamy, A., Anantharam, V., et al. (2019). Manganese-Induced neurotoxicity: new insights into the triad of protein misfolding. Mitochondrial impairment, and neuroinflammation. *Front. Neurosci.* 13:654. doi: 10.3389/fnins.2019.00654

Harms, H. K., Zimmer, K. P., Kurnik, K., Bertele-Harms, R. M., Weidinger, S., and Reiter, K. (2002). Oral mannose therapy persistently corrects the severe clinical symptoms and biochemical abnormalities of phosphomannose isomerase deficiency. *Acta Paediatr.* 91, 1065–1072. doi: 10.1111/j.1651-2227.2002.tb00101.x

He, L., Girijashanker, K., Dalton, T. P., Reed, J., Li, H., Soleimani, M., et al. (2006). ZIP8, member of the solute-carrier-39 (SLC39) metal-transporter family: characterization of transporter properties. *Mol. Pharmacol.* 70, 171–180. doi: 10.1124/mol.106.024521

Hendriksz, C. J., McClean, P., Henderson, M. J., Keir, D. G., Worthington, V. C., Imtiaz, F., et al. (2001). Successful treatment of carbohydrate deficient glycoprotein syndrome type 1b with oral mannose. *Arch. Dis. Child.* 85, 339–340. doi: 10.1136/adc.85.4.339

Houdou, M., Lebredonchel, E., Garat, A., Duvet, S., Legrand, D., Decool, V., et al. (2019). Involvement of thapsigargin- and cyclopiazonic acid-sensitive pumps in the rescue of TMEM165-associated glycosylation defects by Mn2. *FASEB J.* 33, 2669–2679. doi: 10.1096/fj.201800387r

Ichikawa, M., Scott, D. A., Losfeld, M. E., and Freeze, H. H. (2014). The metabolic origins of mannose in glycoproteins. *J. Biol. Chem.* 289, 6751–6761. doi: 10.1074/jbc.m113.544064

Iyer, S., Sam, F. S., DiPrimio, N., Preston, G., Verheijen, J., Murthy, K., et al. (2019). Repurposing the aldose reductase inhibitor and diabetic neuropathy drug epalrestat for the congenital disorder of glycosylation PMM2-CDG. *Dis. Model. Mech* 12:dmm040584. doi: 10.1242/dmm.040584

Izquierdo-Serra, M., Martínez-Monseny, A. F., López, L., Carrillo-García, J., Edo, A., Ortigoza-Escobar, J. D., et al. (2018). Stroke-Like episodes and cerebellar syndrome in phosphomannomutase deficiency (PMM2-CDG): evidence for hypoglycosylation-driven channelopathy. *Int. J. Mol. Sci* 19:619. doi: 10.3390/ijms19020619

Jaeken, J. (2011). Congenital disorders of glycosylation (CDG): it's (nearly) all in it! *J. Inherit. Metab. Dis.* 34, 853–858. doi: 10.1007/s10545-011-9299-3

Jaeken, J., and Matthijs, G. (2001). Congenital disorders of glycosylation. *Annu. Rev. Genomics Hum. Genet.* 2, 129–151.

Jaeken, J., Matthijs, G., Saudubray, J. M., Dionisi-Vici, C., Bertini, E., de Lonlay, P., et al. (1998). Phosphomannose isomerase deficiency: a carbohydrate-deficient glycoprotein syndrome with hepatic-intestinal presentation. *Am. J. Hum. Genet.* 62, 1535–1539. doi: 10.1086/301873

Jaeken, J., van Eijk, H. G., van der Heul, C., Corbeel, L., Eeckels, R., and Eggermont, E. (1984). Sialic acid-deficient serum and cerebrospinal fluid transferrin in a newly recognized genetic syndrome. *Clin. Chim. Acta* 144, 245–247. doi: 10.1016/0009-8981(84)90059-7

Jansen, J. C., Cirak, S., van Scherpenzeel, M., Timal, S., Reunert, J., Rust, S., et al. (2016). CCDC115 deficiency causes a disorder of golgi homeostasis with abnormal protein glycosylation. *Am. J. Hum. Genet.* 98, 310–321. doi: 10.1016/j.ajhg.2015.12.010

Janssen, M. C. H., de Kleine, R. H., van den Berg, A. P., Heijdra, Y., van Scherpenzeel, M., Lefeber, D. J., et al. (2014). Successful liver transplantation and long-term follow-up in a patient with MPI-CDG. *Pediatrics* 134, e279–e283.

Kapusta, L., Zucker, N., Frenckel, G., Medalion, B., Ben Gal, T., Birk, E., et al. (2013). From discrete dilated cardiomyopathy to successful cardiac transplantation in congenital disorders of glycosylation due to dolichol kinase deficiency (DK1-CDG). *Heart Fail. Rev.* 18, 187–196. doi: 10.1007/s10741-012-9302-6

Kjaergaard, S., Kristiansson, B., Stibler, H., Freeze, H. H., Schwartz, M., Martinsson, T., et al. (1998). Failure of short-term mannose therapy of patients with carbohydrate-deficient glycoprotein syndrome type 1A. *Acta Paediatr.* 87, 884–888. doi: 10.1111/j.1651-2227.1998.tb01556.x

Kjaergaard, S., Skovby, F., and Schwartz, M. (1999). Carbohydrate-deficient glycoprotein syndrome type 1A: expression and characterisation of wild type and mutant PMM2 in E. coli. *Eur. J. Hum. Genet.* 7, 884–888. doi: 10.1038/sj.ejhg.5200398

Klcovansky, J., Mørkrid, L., and Möller, T. (2016). Heart transplantation in a child with congenital disorder of glycosylation. *J. Heart Lung Transplant.* 35, 1048–1049. doi: 10.1016/j.healun.2016.05.007

Knapp, K. M., Luu, R., Baerenfaenger, M., Zijlstra, F., Wessels, H. J. C. T., Jenkins, D., et al. (2020). Biallelic variants in SLC35C1 as a cause of isolated short stature with intellectual disability. *J. Hum. Genet.* 65, 743–750. doi: 10.1038/s10038-020-0764-4

Koch, J., Mayr, J. A., Alhaddad, B., Rauscher, C., Bierau, J., Kovacs-Nagy, R., et al. (2017). CAD mutations and uridine-responsive epileptic encephalopathy. *Brain* 140, 279–286.

Kodera, H., Nakamura, K., Osaka, H., Maegaki, Y., Haginoya, K., Mizumoto, S., et al. (2013). De novo mutations in SLC35A2 encoding a UDP-galactose transporter cause early-onset epileptic encephalopathy. *Hum. Mutat.* 34, 1708–1714. doi: 10.1002/humu.22446

Kraus, R. L., Sinnegger, M. J., Glossmann, H., Hering, S., and Striessnig, J. (1998). Familial hemiplegic migraine mutations change alpha1A Ca2+ channel kinetics. *J. Biol. Chem.* 273, 5586–5590. doi: 10.1074/jbc.273.10.5586

Kraus, R. L., Sinnegger, M. J., Koschak, A., Glossmann, H., Stenirri, S., Carrera, P., et al. (2000). Three new familial hemiplegic migraine mutants affect P/Q-type Ca(2+) channel kinetics. *J. Biol. Chem.* 275, 9239–9243. doi: 10.1074/jbc.275.13.9239

Lefeber, D. J., Morava, E., and Jaeken, J. (2011). How to find and diagnose a CDG due to defective N-glycosylation. *J. Inherit. Metab. Dis.* 34, 849–852. doi: 10.1007/s10545-011-9370-0

Lefrère, B., Stepanian, A., Itzhar-Baïkian, N., Charles, P., Hadj-Ali, A., Joly, B., et al. (2018). Deep venous thrombosis treated by rivaroxaban in a young patient with type Ia carbohydrate-deficient glycoprotein (CDG) syndrome. *Ann. Biol. Clin.* 76, 217–223. doi: 10.1684/abc.2018.1324

Liem, Y. S., Bode, L., Freeze, H. H., Leebeek, F. W., Zandbergen, A. A., and Paul Wilson, J. (2008). Using heparin therapy to reverse protein-losing enteropathy in a patient with CDG-Ib. *Nat. Clin. Pract. Gastroenterol. Hepatol.* 5, 220–224. doi: 10.1038/ncpgasthep1061

Lübke, T., Marquardt, T., Etzioni, A., Hartmann, E., von Figura, K., and Körner, C. (2001). Complementation cloning identifies CDG-IIc, a new type of congenital disorders of glycosylation, as a GDP-fucose transporter deficiency. *Nat. Genet.* 28, 73–76. doi: 10.1038/ng0501-73

Lübke, T., von Figura, K., Körner, C., and Marquardt, T. (1999). A new type of carbohydrate-deficient glycoprotein syndrome due to a decreased import of GDP-fucose into the Golgi. *J. Biol. Chem.* 274, 25986–25989. doi: 10.1074/jbc.274.37.25986

Lucchini, R., Albini, E., Placidi, D., Gasparotti, R., Pigozzi, M. G., Montani, G., et al. (2000). Brain magnetic resonance imaging and manganese exposure. *Neurotoxicology* 21, 769–775.

Lühn, K., Wild, M. K., Eckhardt, M., Gerardy-Schahn, R., and Vestweber, D. (2001). The gene defective in leukocyte adhesion deficiency II encodes a putative GDP-fucose transporter. *Nat. Genet.* 28, 69–72. doi: 10.1038/ng0501-69

Marquardt, T., and Denecke, J. (2003). Congenital disorders of glycosylation: review of their molecular bases, clinical presentations and specific therapies. *Eur. J. Pediatr.* 162, 359–379. doi: 10.1007/s00431-002-1136-0

Marquardt, T., Lühn, K., Srikrishna, G., Freeze, H. H., Harms, E., and Vestweber, D. (1999). Correction of leukocyte adhesion deficiency type II with oral fucose. *Blood* 94, 3976–3985. doi: 10.1182/blood.v94.12.3976.424k06_3976_3985

Martínez-Monseny, A. F., Bolasell, M., Callejón-Póo, L., Cuadras, D., Freniche, V., Itzep, D. C., et al. (2019). AZATAX: Acetazolamide safety and efficacy in cerebellar syndrome in PMM2 congenital disorder of glycosylation (PMM2-CDG). *Ann. Neurol.* 85, 740–751. doi: 10.1002/ana.25457

Mayatepek, E., and Kohlmüller, D. (1998). Mannose supplementation in carbohydrate-deficient glycoprotein syndrome type I and phosphomannomutase deficiency. *Eur. J. Pediatr.* 157, 605–606. doi: 10.1007/s004310050889

Mayatepek, E., Schröder, M., Kohlmüller, D., Bieger, W. P., and Nützenadel, W. (1997). Continuous mannose infusion in carbohydrate-deficient glycoprotein syndrome type I. *Acta Paediatr.* 86, 1138–1140. doi: 10.1111/j.1651-2227.1997.tb14825.x

Mendell, J. R., Al-Zaidy, S., Shell, R., Arnold, W. D., Rodino-Klapac, L. R., Prior, T. W., et al. (2017). Single-Dose gene-replacement therapy for spinal muscular atrophy. *N. Engl. J. Med.* 377, 1713–1722.

Monticelli, M., Liguori, L., Allocca, M., Andreotti, G., and Cubellis, M. V. (2019). β-Glucose-1,6-bisphosphate stabilizes pathological phophomannomutase2 mutants in vitro and represents a lead compound to develop pharmacological chaperones for the most common disorder of glycosylation, PMM2-CDG. *Int. J. Mol. Sci* 20:4164. doi: 10.3390/ijms20174164

Morelle, W., Potelle, S., Witters, P., Wong, S., Climer, L., Lupashin, V., et al. (2017). Galactose supplementation in patients with TMEM165-CDG rescues the glycosylation defects. *J. Clin. Endocrinol. Metab.* 102, 1375–1386. doi: 10.1210/jc.2016-3443

Nebert, D. W., and Liu, Z. (2019). SLC39A8 gene encoding a metal ion transporter: discovery and bench to bedside. *Hum. Genomics* 13:51.

Ng, B. G., Buckingham, K. J., Raymond, K., Kircher, M., Turner, E. H., He, M., et al. (2013). Mosaicism of the UDP-galactose transporter SLC35A2 causes a congenital disorder of glycosylation. *Am. J. Hum. Genet.* 92, 632–636. doi: 10.1016/j.ajhg.2013.03.012

Ng, B. G., Dastsooz, H., Silawi, M., Habibzadeh, P., Jahan, S. B., Fard, M. A. F., et al. (2020). Expanding the molecular and clinical phenotypes of FUT8-CDG. *J. Inherit. Metab. Dis.* 43, 871–879.

Ng, B. G., Sosicka, P., Agadi, S., Almannai, M., Bacino, C. A., Barone, R., et al. (2019). SLC35A2-CDG: Functional characterization, expanded molecular, clinical, and biochemical phenotypes of 30 unreported Individuals. *Hum. Mutat.* 40, 908–925.

Ng, B. G., Wolfe, L. A., Ichikawa, M., Markello, T., He, M., Tifft, C. J., et al. (2015). Biallelic mutations in CAD, impair de novo pyrimidine biosynthesis

and decrease glycosylation precursors. *Hum. Mol. Genet.* 24, 3050–3057. doi: 10.1093/hmg/ddv057

Ng, B. G., Xu, G., Chandy, N., Steyermark, J., Shinde, D. N., Radtke, K., et al. (2018). Biallelic mutations in FUT8 cause a congenital disorder of glycosylation with defective fucosylation. *Am. J. Hum. Genet.* 102, 188–195. doi: 10.1016/j.ajhg.2017.12.009

Niehues, R., Hasilik, M., Alton, G., Korner, C., Schiebe-Sukumar, M., Koch, H. G., et al. (1998). Carbohydrate-deficient glycoprotein syndrome type Ib. Phosphomannose isomerase deficiency and mannose therapy. *J. Clin. Invest.* 101, 1414–1420. doi: 10.1172/jci2350

Nolting, K., Park, J. H., Tegtmeyer, L. C., Zuhlsdorf, A., Gruneberg, M., Rust, S., et al. (2017). Limitations of galactose therapy in phosphoglucomutase 1 deficiency. *Mol Genet Metab Rep* 13, 33–40. doi: 10.1016/j.ymgmr.2017.07.010

Ondruskova, N., Cechova, A., Hansikova, H., Honzik, T., and Jaeken, J. (2021). Congenital disorders of glycosylation: still 'hot' in 2020. *Biochim. Biophys. Acta Gen. Subj.* 1865:129751. doi: 10.1016/j.bbagen.2020.129751

Ophoff, R. A., Terwindt, G. M., Vergouwe, M. N., van Eijk, R., Oefner, P. J., Hoffman, S. M., et al. (1996). Familial hemiplegic migraine and episodic ataxia type-2 are caused by mutations in the Ca2+ channel gene CACNL1A4. *Cell* 87, 543–552. doi: 10.1016/s0092-8674(00)81373-2

Panneerselvam, K., and Freeze, H. H. (1996). Mannose corrects altered N-glycosylation in carbohydrate-deficient glycoprotein syndrome fibroblasts. *J. Clin. Invest.* 97, 1478–1487. doi: 10.1172/jci118570

Panneerselvam, K., Etchison, J. R., Skovby, F., and Freeze, H. H. (1997). Abnormal metabolism of mannose in families with carbohydrate-deficient glycoprotein syndrome type 1. *Biochem. Mol. Med.* 61, 161–167. doi: 10.1006/bmme.1997.2599

Parenti, G., Fecarotta, S., la Marca, G., Rossi, B., Ascione, S., Donati, M. A., et al. (2014). A chaperone enhances blood α-glucosidase activity in Pompe disease patients treated with enzyme replacement therapy. *Mol. Ther.* 22, 2004–2012. doi: 10.1038/mt.2014.138

Park, J. H., Hogrebe, M., Fobker, M., Brackmann, R., Fiedler, B., Reunert, J., et al. (2018). SLC39A8 deficiency: biochemical correction and major clinical improvement by manganese therapy. *Genet. Med.* 20, 259–268. doi: 10.1038/gim.2017.106

Park, J. H., Hogrebe, M., Gruneberg, M., DuChesne, I., von der Heiden, A. L., Reunert, J., et al. (2015). SLC39A8 deficiency: a disorder of manganese transport and glycosylation. *Am. J. Hum. Genet.* 97, 894–903. doi: 10.1016/j.ajhg.2015.11.003

Park, J. H., Mealer, R. G., Elias, A. F., Hoffmann, S., Grüneberg, M., Biskup, S., et al. (2020a). N-glycome analysis detects dysglycosylation missed by conventional methods in SLC39A8 deficiency. *J. Inherit. Metab. Dis.* 43, 1370–1381. doi: 10.1002/jimd.12306

Park, J. H., Reunert, J., He, M., Mealer, R. G., Noel, M., Wada, Y., et al. (2020b). L-Fucose treatment of FUT8-CDG. *Mol. Genet. Metab. Rep.* 25:100680. doi: 10.1016/j.ymgmr.2020.100680

Pipalia, N. H., Saad, S. Z., Subramanian, K., Cross, A., al-Motawa, A., Garg, K., et al. (2021). HSP90 inhibitors reduce cholesterol storage in Niemann-Pick type C1 mutant fibroblasts. *bioRxiv* [Preprint] doi: 10.1101/2021.04.22.440982 2021.04.22.440982.,

Pipalia, N. H., Subramanian, K., Cross, A., Garg, K., Al-Motawa, A., and Maxfield, F. R. (2019). Targeting molecular chaperone HSP90 to treat Niemann-pick type C1 disease. *FASEB J.* 33:490.11. doi: 10.1096/fasebj.2019.33.1_supplement.490.11

Pode-Shakked, B., Heimer, G., Vilboux, T., Marek-Yagel, D., Ben-Zeev, B., Davids, M., et al. (2019). Cerebral and portal vein thrombosis, macrocephaly and atypical absence seizures in Glycosylphosphatidyl inositol deficiency due to a PIGM promoter mutation. *Mol. Genet. Metab.* 128, 151–161. doi: 10.1016/j.ymgme.2019.08.003

Potelle, S., Dulary, E., Climer, L., Duvet, S., Morelle, W., Vicogne, D., et al. (2017). Manganese-induced turnover of TMEM165. *Biochem. J.* 474, 1481–1493. doi: 10.1042/bcj20160910

Potelle, S., Morelle, W., Dulary, E., Duvet, S., Vicogne, D., Spriet, C., et al. (2016). Glycosylation abnormalities in Gdt1p/TMEM165 deficient cells result from a defect in Golgi manganese homeostasis. *Hum. Mol. Genet.* 25, 1489–1500. doi: 10.1093/hmg/ddw026

Pushpakom, S., Iorio, F., Eyers, P. A., Escott, K. J., Hopper, S., Wells, A., et al. (2019). Drug repurposing: progress, challenges and recommendations. *Nat. Rev. Drug Discov.* 18, 41–58. doi: 10.1038/nrd.2018.168

Radenkovic, S., Witters, P., and Morava, E. (2018). Central nervous involvement is common in PGM1-CDG. *Mol. Genet. Metab.* 125, 200–204. doi: 10.1016/j.ymgme.2018.08.008

Reunert, J., Rust, S., Grüneberg, M., Seelhöfer, A., Kurz, D., Ocker, V., et al. (2019). Transient N-glycosylation abnormalities likely due to a de novo loss-of-function mutation in the delta subunit of coat protein I. *Am. J. Med. Genet. A* 179, 1371–1375.

Riley, L. G., Cowley, M. J., Gayevskiy, V., Roscioli, T., Thorburn, D. R., Prelog, K., et al. (2017). A SLC39A8 variant causes manganese deficiency, and glycosylation and mitochondrial disorders. *J. Inherit. Metab. Dis.* 40, 261–269. doi: 10.1007/s10545-016-0010-6

Rush, J. S., Panneerselvam, K., Waechter, C. J., and Freeze, H. H. (2000). Mannose supplementation corrects GDP-mannose deficiency in cultured fibroblasts from some patients with Congenital Disorders of Glycosylation (CDG). *Glycobiology* 10, 829–835. doi: 10.1093/glycob/10.8.829

Russell, S., Bennett, J., Wellman, J. A., Chung, D. C., Yu, Z.-F., Tillman, A., et al. (2017). Efficacy and safety of voretigene neparvovec (AAV2-hRPE65v2) in patients with RPE65-mediated inherited retinal dystrophy: a randomised, controlled, open-label, phase 3 trial. *Lancet* 390, 849–860. doi: 10.1016/s0140-6736(17)31868-8

Rymen, D., Winter, J., Van Hasselt, P. M., Jaeken, J., Kasapkara, C., Gokçay, G., et al. (2015). Key features and clinical variability of COG6-CDG. *Mol. Genet. Metab.* 116, 163–170. doi: 10.1016/j.ymgme.2015.07.003

Schiff, M., Roda, C., Monin, M.-L., Arion, A., Barth, M., Bednarek, N., et al. (2017). Clinical, laboratory and molecular findings and long-term follow-up data in 96 French patients with PMM2-CDG (phosphomannomutase 2-congenital disorder of glycosylation) and review of the literature. *J. Med. Genet.* 54:843. doi: 10.1136/jmedgenet-2017-104903

Schneider, A., Thiel, C., Rindermann, J., DeRossi, C., Popovici, D., Hoffmann, G. F., et al. (2011). Successful prenatal mannose treatment for congenital disorder of glycosylation-Ia in mice. *Nat. Med.* 18, 71–73. doi: 10.1038/nm.2548

Schroeder, A. S., Kappler, M., Bonfert, M., Borggraefe, I., Schoen, C., and Reiter, K. (2010). Seizures and stupor during intravenous mannose therapy in a patient with CDG syndrome type 1b (MPI-CDG). *J. Inherit. Metab. Dis.* 33(Suppl. 3), S497–S502.

Schroeder, H. A., Balassa, J. J., and Tipton, I. H. (1966). Essential trace metals in man: manganese. A study in homeostasis. *J. Chronic Dis.* 19, 545–571. doi: 10.1016/0021-9681(66)90094-4

Shioi, R., Karaki, F., Yoshioka, H., Noguchi-Yachide, T., Ishikawa, M., Dodo, K., et al. (2020). Image-based screen capturing misfolding status of Niemann-Pick type C1 identifies potential candidates for chaperone drugs. *PLoS One* 15:e0243746. doi: 10.1371/journal.pone.0243746

Sols, A., Cadenas, E., and Alvarado, F. (1960). Enzymatic basis of mannose toxicity in honey bees. *Science* 131, 297–298.

Stibler, H., Holzbach, U., Tengborn, L., and Kristiansson, B. (1996). Complex functional and structural coagulation abnormalities in the carbohydrate-deficient glycoprotein syndrome type I. *Blood Coagul. Fibrinolysis* 7, 118–126. doi: 10.1097/00001721-199603000-00003

Stojkovic, T., Vissing, J., Petit, F., Piraud, M., Orngreen, M. C., Andersen, G., et al. (2009). Muscle glycogenosis due to phosphoglucomutase 1 deficiency. *N. Engl. J. Med.* 361, 425–427. doi: 10.1056/nejmc0901158

Stray-Pedersen, A., Backe, P. H., Sorte, H. S., Morkrid, L., Chokshi, N. Y., Erichsen, H. C., et al. (2014). PGM3 mutations cause a congenital disorder of glycosylation with severe immunodeficiency and skeletal dysplasia. *Am. J. Hum. Genet.* 95, 96–107.

Taday, R., Grüneberg, M., DuChesne, I., Reunert, J., and Marquardt, T. (2020). Dietary mannose supplementation in phosphomannomutase 2 deficiency (PMM2-CDG). *Orphanet J. Rare Dis.* 15:258.

Tal-Goldberg, T., Lorain, S., and Mitrani-Rosenbaum, S. (2014). Correction of the Middle Eastern M712T mutation causing GNE myopathy by trans-splicing. *Neuromolecular Med.* 16, 322–331. doi: 10.1007/s12017-013-8278-2

Tegtmeyer, L. C., Rust, S., van Scherpenzeel, M., Ng, B. G., Losfeld, M. E., Timal, S., et al. (2014). Multiple phenotypes in phosphoglucomutase 1 deficiency. *N. Engl. J. Med.* 370, 533–542.

Tropak, M. B., Reid, S. P., Guiral, M., Withers, S. G., and Mahuran, D. (2004). Pharmacological enhancement of beta-hexosaminidase activity in fibroblasts from adult Tay-Sachs and Sandhoff Patients. *J. Biol. Chem.* 279, 13478–13487. doi: 10.1074/jbc.m308523200

van Karnebeek, C. D. M., Bonafé, L., Wen, X.-Y., Tarailo-Graovac, M., Balzano, S., Royer-Bertrand, B., et al. (2016). NANS-mediated synthesis of sialic acid is required for brain and skeletal development. *Nat. Genet.* 48, 777–784.

Vega, A. I., Pérez-Cerdá, C., Desviat, L. R., Matthijs, G., Ugarte, M., and Pérez, B. (2009). Functional analysis of three splicing mutations identified in the PMM2 gene: toward a new therapy for congenital disorder of glycosylation type Ia. *Hum. Mutat.* 30, 795–803.

Verheijen, J., Tahata, S., Kozicz, T., Witters, P., and Morava, E. (2020). Therapeutic approaches in Congenital Disorders of Glycosylation (CDG) involving N-linked glycosylation: an update. *Genet. Med.* 22, 268–279. doi: 10.1038/s41436-019-0647-2

Wada, Y. (2006). Mass spectrometry for congenital disorders of glycosylation. CDG. *J. Chromatogr. B Analyt. Technol. Biomed. Life Sci.* 838, 3–8. doi: 10.1016/j.jchromb.2006.02.028

Wada, Y. (2020). Matrix-assisted laser desorption/ionization mass spectrometry to detect diagnostic glycopeptide markers of congenital disorders of glycosylation. *Mass Spectrom.* 9:A0084.

Westphal, V., Kjaergaard, S., Davis, J. A., Peterson, S. M., Skovby, F., and Freeze, H. H. (2000). Genetic and metabolic analysis of the first adult with congenital disorder of glycosylation type Ib: long-term outcome and effects of mannose supplementation. *Mol. Genet. Metab.* 73, 77–85. doi: 10.1006/mgme.2001.3161

Wild, M. K., Lühn, K., Marquardt, T., and Vestweber, D. (2002). Leukocyte adhesion deficiency II: therapy and genetic defect. *Cells Tissues Organs* 172, 161–173. doi: 10.1159/000066968

Witters, P., Honzik, T., Bauchart, E., Altassan, R., Pascreau, T., Bruneel, A., et al. (2018). Long-term follow-up in PMM2-CDG: are we ready to start treatment trials? *Genet. Med.* 21, 1181–1188. doi: 10.1038/s41436-018-0301-4

Witters, P., Tahata, S., Barone, R., Ounap, K., Salvarinova, R., Grønborg, S., et al. (2020). Clinical and biochemical improvement with galactose supplementation in SLC35A2-CDG. *Genet. Med.* 22, 1102–1107. doi: 110.1038/s41436-020-0767-8

Wolach, B., Gavrieli, R., Wolach, O., Stauber, T., Abuzaitoun, O., Kuperman, A., et al. (2019). Leucocyte adhesion deficiency-A multicentre national experience. *Eur. J. Clin. Invest.* 49:e13047. doi: 10.1111/eci.13047

Wong, S. Y.-W., Gadomski, T., van Scherpenzeel, M., Honzik, T., Hansikova, H., Holmefjord, K. S. B., et al. (2017). Oral D-galactose supplementation in PGM1-CDG. *Genet. Med.* 19, 1226–1235. doi: 10.1038/gim.2017.41

Yabe, I., Sasaki, H., Yamashita, I., Takei, A., and Tashiro, K. (2001). Clinical trial of acetazolamide in SCA6, with assessment using the ataxia rating scale and body stabilometry. *Acta Neurol. Scand.* 104, 44–47. doi: 10.1034/j.1600-0404.2001.00299.x

Yuste-Checa, P., Brasil, S., Gamez, A., Underhaug, J., Desviat, L. R., Ugarte, M., et al. (2016). Pharmacological chaperoning: a potential treatment for PMM2-CDG. *Hum. Mutat.* 38, 160–168. doi: 10.1002/humu.23138

Yuste-Checa, P., Gámez, A., Brasil, S., Desviat, L. R., Ugarte, M., Pérez-Cerdá, C., et al. (2015). The effects of PMM2-CDG-causing mutations on the folding, activity, and stability of the PMM2 protein. *Hum. Mutat.* 36, 851–860. doi: 10.1002/humu.22817

Zhuchenko, O., Bailey, J., Bonnen, P., Ashizawa, T., Stockton, D. W., Amos, C., et al. (1997). Autosomal dominant cerebellar ataxia (SCA6) associated with small polyglutamine expansions in the alpha 1A-voltage-dependent calcium channel. *Nat. Genet.* 15, 62–69. doi: 10.1038/ng0197-62

Conflict of Interest: The authors declare that the research was conducted in the absence of any commercial or financial relationships that could be construed as a potential conflict of interest.

Publisher's Note: All claims expressed in this article are solely those of the authors and do not necessarily represent those of their affiliated organizations, or those of the publisher, the editors and the reviewers. Any product that may be evaluated in this article, or claim that may be made by its manufacturer, is not guaranteed or endorsed by the publisher.

frontiers in Genetics

ORIGINAL RESEARCH
published: 17 September 2021
doi: 10.3389/fgene.2021.733048

Development and Initial Characterization of Cellular Models for COG Complex-Related CDG-II Diseases

*Farhana Taher Sumya, Irina D. Pokrovskaya and Vladimir Lupashin **

Department of Physiology and Cell Biology, University of Arkansas for Medical Sciences, Little Rock, AR, United States

Conserved Oligomeric Golgi (COG) is an octameric protein complex that orchestrates intra-Golgi trafficking of glycosylation enzymes. Over a hundred individuals with 31 different COG mutations have been identified until now. The cellular phenotypes and clinical presentations of COG-CDGs are heterogeneous, and patients primarily represent neurological, skeletal, and hepatic abnormalities. The establishment of a cellular COG disease model will benefit the molecular study of the disease, explaining the detailed sequence of the interplay between the COG complex and the trafficking machinery. Moreover, patient fibroblasts are not a good representative of all the organ systems and cell types that are affected by COG mutations. We developed and characterized cellular models for human COG4 mutations, specifically in RPE1 and HEK293T cell lines. Using a combination of CRISPR/Cas9 and lentiviral transduction technologies, both myc-tagged wild-type and mutant (G516R and R729W) COG4 proteins were expressed under the endogenous COG4 promoter. Constructed isogenic cell lines were comprehensively characterized using biochemical, microscopy (superresolution and electron), and proteomics approaches. The analysis revealed similar stability and localization of COG complex subunits, wild-type cell growth, and normal Golgi morphology in all three cell lines. Importantly, COG4-G516R cells demonstrated increased HPA-647 binding to the plasma membrane glycoconjugates, while COG4-R729W cells revealed high GNL-647 binding, indicating specific defects in O- and N-glycosylation. Both mutant cell lines express an elevated level of heparin sulfate proteoglycans. Moreover, a quantitative mass-spectrometry analysis of proteins secreted by COG-deficient cell lines revealed abnormal secretion of SIL1 and ERGIC-53 proteins by COG4-G516R cells. Interestingly, the clinical phenotype of patients with congenital mutations in the SIL1 gene (Marinesco-Sjogren syndrome) overlaps with the phenotype of COG4-G516R patients (Saul-Wilson syndrome). Our work is the first compressive study involving the creation of different COG mutations in different cell lines other than the patient's fibroblast. It may help to address the underlying cause of the phenotypic defects leading to the discovery of a proper treatment guideline for COG-CDGs.

Keywords: COG complex, congenital disorder of glycosylation, Golgi apparatus, CRISPR, vesicle tethering, glycan processing, glycosylation, mass-spectrometry

OPEN ACCESS

Edited by:
Anna Tylki-Szymańska, Children's Memorial Health Institute (IPCZD), Poland

Reviewed by:
Yao Zhang, Peking University First Hospital, China
María Eugenia De La Morena-Barrio, University of Murcia, Spain

***Correspondence:**
Vladimir Lupashin
vvlupashin@uams.edu

Specialty section:
This article was submitted to Genetics of Common and Rare Diseases, a section of the journal Frontiers in Genetics

Received: *29 June 2021*
Accepted: *06 September 2021*
Published: *17 September 2021*

Citation:
Sumya FT, Pokrovskaya ID and Lupashin V (2021) Development and Initial Characterization of Cellular Models for COG Complex-Related CDG-II Diseases. Front. Genet. 12:733048. doi: 10.3389/fgene.2021.733048

INTRODUCTION

Golgi apparatus (GA) is the central organelle within the secretory pathway composed of flattened membranes organized in a cis medial-trans fashion (Huang and Wang, 2017; Makhoul et al., 2019). Cargo proteins and lipids go to the GA where they continue to undergo post-translational modification such as glycosylation. Thereafter, the cargo is sorted and trafficked to specialized compartments within the cell or is secreted. Golgi enzymes and cargo receptors constantly recycle within the Golgi (Derby and Gleeson, 2007; Bailey Blackburn et al., 2016). Multisubunit tethering complexes (MTCs) are the key components of the intracellular trafficking machinery that tether cargo containing transport vesicles and bring them close to their target membrane. They orchestrate trafficking events by setting up multiple interactions between their individual subunits with other components of the trafficking machinery namely SNAREs, SNARE-interacting proteins, Rabs, coiled-coil tethers, and vesicular coats (Ungar et al., 2006; Bröcker et al., 2010; Bailey Blackburn et al., 2016; D'Souza et al., 2020). The Conserved Oligomeric Golgi (COG) complex is a prominent MTC that mediates intra-Golgi retrograde trafficking by interacting with several cellular constituents of the vesicle docking/fusion machinery through specific interaction sites on its subunits (Bonifacino and Glick, 2004; Laufman et al., 2013; Willett et al., 2013c; D'Souza et al., 2020). Mutations in COG subunits result in a class of human diseases known as congenital disorders of glycosylation (CDG) type II (Ungar et al., 2006; D'Souza et al., 2020). COG-CDGs are defined as multi-systemic disorders with several distinguishable symptoms, including global developmental defects, dysmorphic features, microcephaly, and failure to thrive. These disorders are often accompanied by liver and neurological impairment (Foulquier, 2009; D'Souza et al., 2020; Ondruskova et al., 2021). Nowadays, one of the major issues related to CDGs is that many cases are either underdiagnosed or misdiagnosed.

Until now, over a hundred individuals with 31 different mutations in seven different COG subunits have been identified, presenting heterogeneous clinical features and cellular phenotypes. COG mutations cause a wide range of cellular defects that directly and indirectly impact glycosylation and other trafficking processes (Climer et al., 2018; D'Souza et al., 2020). Different types of mutations in each subunit of COG have been reported, which have been studied only in patients' fibroblasts (Ferreira et al., 2018). Fibroblasts obtained from different patients could be very different in their genetic background and not a perfect representative of organ systems and cell types that are affected by COG mutations (D'Souza et al., 2020). To that end, a cellular COG disease model will benefit the molecular study of the disease, explaining the detailed sequence of the interplay between the COG complex and the trafficking machinery.

At first, we decided to develop a COG4-CDG disease model to facilitate an effective diagnosis and treatment. Two patients have been described with COG4-CDGIIj presenting clinical features such as developmental delay, hypotonia, failure to thrive, seizures, coagulopathy, liver cirrhosis, and recurrent infections. The second patient of this CDGII carried a C > T point mutation at position 2,185 in the COG4 gene resulting in R729W change (Reynders et al., 2009). Recently, a rare skeletal dysplasia has been discovered caused by a specific heterozygous COG4 substitution (p.G516R) named Saul-Wilson syndrome (SWS) (Ferreira et al., 2018; Zafra et al., 2021). Interestingly, symptoms exhibited by SWS patients are markedly different compared to COG4-CDGIIj individuals. The comparative study of two different types of COG4 mutation can potentially lead to a comprehensive understanding of the clinical phenotypes and the development of a working treatment protocol design. To create a cell-based model, we have chosen HEK293T (Stepanenko and Dmitrenko, 2015) and RPE1 as most of the COG-CDG patients exhibit neurological phenotypes as well as ocular defects (Climer et al., 2015, 2018; Blackburn et al., 2018). Moreover, these cells are non-cancerous in origin, obtain superior characteristics for microscopy imaging, and are easy to transfect as well as to study the genomic and functional properties.

In this study, we developed a cell-based COG4-CDGII disease model in RPE1 and HEK293T cell lines. Two different COG4 mutations have been introduced to benefit the molecular analysis of the disease, followed by the characterization of the developed isogenic cell lines for parameters essential for post-translational modification and regulatory secretion of the protein. We have applied biochemical, superresolution and electron microscopy, and proteomic approaches to accomplish the objectives of this study.

MATERIALS AND METHODS

Cell Culture

hTERT RPE1 (Retinal Pigment Epithelial) and HEK293T cells (a human cell line obtained from embryonic kidney but exhibiting properties of immature neurons) purchased from ATCC were cultured in Dulbecco's Modified Eagle's Medium (DMEM) containing Nutrient mixture F-12 (Corning 10–092-CV) supplemented with 10% Fetal Bovine Serum (Atlas Biologicals, CF-0500-A). Cells were incubated in a 37°C incubator with 5% CO_2 and 90% humidity.

Creation of RPE1 COG4 Knockout Cell Line

RPE1-Cas9 stable cells (Khakurel et al., 2021) were transfected by the mixture of TransEDIT-dual plasmids (Transomic) with the following target sequences.

hCOG4 TransEDIT-dual 1 (TEDH-1017241-pCL/P-dua/-SFFV-ZsGreen).

grna-a: ACTTTCTCCAACTCGACGGCAACAAGGCTA

grna-b: CTGTCAGGGAGCGAATGAGCTCAGCGGAGA

hCOG4 transEDIT-dual 2 (TEDH-1017242-pCL/P-dua/-SFFV-ZsGreen)

grna-a: CATATAAGCCAATTAGCTCCTGCATGGTAC

grna-b: CCAAGATGTCATCAGCTCTCTGAATGGCCT

Neon electroporation (Thermo Fisher) was used for transfecting cells according to the manufacturer's protocol. 48 h after transfection, cells were collected by trypsinization,

spun down at 600xg for 5 min, and resuspended in cell-sorting medium (PBS, 25 mM HEPES pH7.0, 2% FBS (heat-inactivated) 1 mM EDTA). Cell sorting was based on ZsGreen fluorescence; cells were sorted into a 96-well plate containing culture medium using a BD FACS Aria IIIu cell sorter. After sorting, colonies were expanded, and COG4KO phenotypes were confirmed by (Western Blot) WB analysis and (Immunofluorescence microscopy) IF for the absence of the COG4 protein.

Introduction of Point Mutations (G516R and R729W) in COG4 cDNA and Construction of Plasmids

COG4-2xGFP in pEntra1A, was created by PCR of hCOG4-siRES-2xGFP-FRB (Willett et al., 2013b) and (BamHI/XhoI) subcloning into pEntra1A no ccDB (Campeau et al., 2009) (Addgene #17398) vector. COG4-G516R point mutation of C to G nucleotide (resulting in amino acid change G to R) was generated using Site-Directed Mutagenesis Kit (Agilent Technologies #200523) with primers 5'-CCAGGACATCCA GCGCCGGGTGACAAGTGCCG-3' and 5' CGGCACTTG TCACCCGGCGCTGGATGTCCTGG -3'. COG4-R729W point mutation of C to T nucleotide (resulting in amino acid R to W) was generated with primers 5'-CGAGACAAGTTTGCCTGG CTCTCCCAGATG-3' and 5'- CATCTGGGAGAGCCAGGC AAACTTGTCTCG -3'.

To confirm the COG4-G516R and R729W mutation, DNA sequencing has been done by UAMS DNA Sequencing Core using the following primers:

Primer 1: 5'- CTGGGCCCCAAATAATG -3'
Primer 2: 5'- TGTCCAGCAAAGTTCGTCAG -3'
Primer 3: 5'- TTCTGTTTGAAGGGATTGCC -3'
Primer 4: 5'- GACACCTATGAGAAGGGCCA -3'
Primer 5: 5'- ACGGAGCTCAACAGCACAG -3'
Primer 6: 5'- GGATAGACTTCCGCAGTGAA -3'

COG4-WT-3myc in pEntra1A, was created by EcoRI/XbaI subcloning of pSH-hCOG4-3myc (Whyte and Munro, 2001; Kudlyk et al., 2013) fragment into COG4-2xGFP in pEntra1A.

COG4-G516R-3myc in pEntra1A was created by BglII/Kpn1 subcloning of COG4-G516R-2xGFP in pEntra1A into COG4-WT-3myc in pEntra1A. COG4-R729W-3myc in pEntra1A was created by introducing the mutation (described above) in COG4-WT-3myc in pEntra1A.

To generate pLenti COG4 promoter Neo DEST construct, a chromosomal DNA fragment encoding the COG4 promoter region was amplified from human genomic DNA by PCR using the following forward and reverse primers:

Forward: 5'-GCTTATCGATTTCCCCCACGTCTGTTTA CCA-3'Reverse: 5'- GAATTCTAGACTTGGTCCCCATTC GGCACTT -3'

Then, the amplified fragment was cloned into pLenti CMV Neo DEST (705-1) (Campeau et al., 2009) (Addgene 17292) or pLenti CMV Hygro (w117-1) (Addgene 17454), using XbaII and ClaI as restriction sites.

Plasmids were isolated from bacterial cells using the QIAprep Spin Miniprep Kit (Qiagen).

Generation of Lentiviral Particles and Stable Cell Lines

At first, COG4-WT-3myc, COG4-G516R-3myc, COG4-R729W-3myc, COG4-WT-2xGFP, COG4-G516R-2xGFP in pEntra1A were recombined into pLenti COG4 promoter destination vectors using Gateway LR Clonase II Enzyme Mix (Thermo Fisher) according to the manufacturer's instructions. HEK293FT cells were used for the generation of lentiviral particles. Three lentiviral packaging plasmids pMD2.G [a gift from Didier Trono (Addgene plasmid # 12259; http://n2t.net/addgene:12259; RRID: Addgene_12259)], pRSV-Rev, and pMDLg/pRRE (Dull et al., 1998), plus plasmid pLenti COG4 promoter DEST expressing different COG variants were used in equal amount. Then transfected HEK293FT cells were placed in serum-reduced Opti-MEM with 25 μM Chloroquine and GlutaMAX. The next day, the medium was changed to Opti-MEM supplemented with GlutaMAX. At 72 h after transfection, the medium was collected, and cell debris was removed by centrifugation at 600×g for 10 min. The supernatant was passed through 0.45 μM polyethersulfone (PES) membrane filter and the lentiviral medium was stored at 4°C overnight.

90% confluent RPE1 and HEK293T COG4KO cells growing in 6 well dishes were transduced with Lentiviral medium (200 μl per well). At 48 h after transduction of RPE1 COG4KO cells, the lentiviral medium was removed, and the cell growth media containing 600 μg/ml G418 was added for 48 h. The mixed rescued cells were expanded in media containing 200 μg/ml G418 and then cryopreserved in a freezing medium (90% FBS with 10% DMSO). In the rescued HEK293T cell line, the selection was made using 200 μg/ml Hygromycin for 48 h. The cells were expanded in media containing 50 μg/ml Hygromycin and then cryopreserved in a freezing medium (90% FBS with 10% DMSO).

Secretion Assay

Cells were grown in 15-cm dishes to 90–100% confluency, rinsed 3 times with PBS, and placed in 20 ml serum-free, chemically defined medium (BioWhittaker Pro293a-CDM, Lonza) with GlutaMAX (Gibco). After 2 h, media was replaced with fresh serum-free media. 48 h later, the conditioned media was collected and clarified by 5 min centrifugation at 3,000xg to remove detached cells. The supernatant was collected and concentrated using a 10k concentrator (Amicon® Ultra 10k, Millipore); the final concentration was 45× that of cell lysates. From these concentrated protein secretome samples (4 independent repeats for each analysis), the half amount was used for quantitative TMT mass spectrometry analysis, and the half amount was used for WB analysis.

Preparation of Cell Lysates and Western Blot Analysis

To prepare the cell lysates, cells grown on tissue culture dishes were washed three times with PBS and lysed in hot 2% SDS. Samples were mixed with 6xSDS sample buffer containing β-mercaptoethanol and heated for 10 min at 70°C.

To prepare the protein secretome sample for WB analysis, 2× SDS sample buffer was added to the concentrated sample and heated at 95°C for 10 min 10–20 μg of protein was loaded into Bio-Rad (4–15%) or Genescript (8–16%) gradient gel. Proteins were transferred onto nitrocellulose membrane using the Thermo Scientific Pierce G2 Fast Blotter. Membranes were washed in PBS, blocked in Odyssey blocking buffer (LI-COR) for 20 min, and incubated with primary antibodies for 1 h at room temperature or overnight at 4°C. Membranes were washed with PBS and incubated with secondary fluorescently-tagged antibodies diluted in Odyssey blocking buffer for 1 h. Blots were then washed with PBS and imaged using the Odyssey Imaging System. Images were processed using the LI-COR Image Studio software.

Lectin Blotting

To perform blots with fluorescent lectins, 20 μg of cell lysates or secretome samples were loaded onto Bio-Rad (4–15%) gradient gels, and proteins were transferred to nitrocellulose membrane using the Thermo Scientific Pierce G2 Fast Blotter. The membranes were blocked with Odyssey blocking buffer (LI-COR) for 20 min. Helix Pomatia Agglutinin (HPA)-Alexa 647 (Thermo Fisher) or Galanthus Nivalis Lectin (GNL) conjugated to Alexa 647 were diluted 1 : 1,000 in Odyssey blocking buffer from their stock concentration of 1 μg/μl and 5 μg/μl, respectively. Membranes were incubated with diluted HPA-Alexa 647 or GNL-Alexa 647 for 90 min and imaged using the Odyssey Imaging System.

Heparin Sulfate Proteoglycans Analysis

The cells grown on 6-well tissue culture dishes to 100% confluency were detached with 10 mM EDTA. After that cell was centrifuged at 500xg for 5 min and washed with PBS twice. Each sample was treated with 200mU of Heparinase III in 100 μl of reaction buffer (100 mM NaCl, 20 mM Tris-HCL, and 1.5 mM $CaCl_2$) for 1 hour at 37°C. Proteins from treated and untreated samples were solubilized in SDS sample buffer, resolved on 8–15% SDS-PAGE and immunoblotted with 3G10 monoclonal antibodies (AMSBio).

Superresolution AiryScan Fluorescent Microscopy

Immunofluorescence microscopy was done using the previous protocol (Willett R. A. et al., 2013) with some additional modifications. Briefly, cells grown on 12-mm round coverslips to 80–90% confluency were fixed with paraformaldehyde (PFA, freshly made from 16% stock solution) diluted in phosphate-buffered saline (PBS) for 15 min at room temperature. For the lectin staining, 1% PFA was used for fixation, followed by incubations with 50 mM ammonium chloride for 5 min and two incubations in the blocking buffer (0.1% BSA in PBS). After that, cells were incubated with HPA-647 or GNL-647 diluted in blocking buffer for 30 min. For the antibody staining cells were fixed with 4% PFA, treated with 50 mM ammonium chloride (5 min), and permeabilized with 0.1% Triton X-100 (1 min) followed by two incubations with the blocking buffer. After 45 min incubation with primary antibodies diluted in the antibody buffer (1% cold fish gelatin, 0.1% saponin in PBS), cells were washed three times in PBS and incubated with fluorescently conjugated secondary antibodies diluted in antibody buffer for 30 min. Cells were washed four times with PBS, then coverslips were dipped in PBS and water 10 times each and mounted on glass microscope slides using Prolong® Gold antifade reagent (Life Technologies). Cells were imaged with a 63× oil 1.4 numerical aperture (NA) objective of an LSM880 Zeiss Laser inverted microscope with Airyscan using ZEN software.

Flow Cytometry

Cells grown to 80–100% confluency in a 6-well dish were detached using 10 mM EDTA and transferred into an Eppendorf tube. Cells were sedimented at 500xg for 3 min, washed with PBS twice, resuspended, and incubated for 30 min in ice-cold 0.1% BSA containing the lectin of choice (GNL-647, HPA-647) at a 1 : 500 dilution. Then ice-cold 0.1% BSA (plus DAPI for viability gaiting) was added and samples were analyzed using the NxT Attune flow cytometer. Cells were gated for live cells (DAPI excluding cells), singlets for correct cell size vs complexity. Analysis was done using FlowJo software.

Mass Spectrometry (MS)

TMT mass spec analysis was performed at the UAMS IDeA National Resource for Quantitative Proteomics core. Proteins were reduced, alkylated, and purified by chloroform/methanol extraction prior to digestion with sequencing grade modified porcine trypsin (Promega). Tryptic peptides were labeled using tandem mass tag isobaric labeling reagents (Thermo) following the manufacturer's instructions and combined into three 11-plex sample groups with a common reference sample. The labeled peptide multiplexes were separated into 46 fractions on a 100 × 1.0 mm Acquity BEH C18 column (Waters) using an Ultimate 3000 UHPLC system (Thermo) with a 50 min gradient from 98 : 2 to 60 : 40 buffer A : B ratio under basic pH conditions, and then consolidated into 18 super-fractions. Each super-fraction was then further separated by reverse-phase XSelect CSH C18 2.5 um resin (Waters) on an in-line 150 × 0.075 mm column using an UltiMate 3,000 RSLCnano system (Thermo). Peptides were eluted using a 60 min gradient from 98 : 2 to 60:40 buffer A : B ratio. Eluted peptides were ionized by electrospray (2.2 kV) followed by mass spectrometric analysis on an Orbitrap Eclipse Tribrid mass spectrometer (Thermo) using multi-notch MS3 parameters with real-time search enabled. MS data were acquired using the FTMS analyzer in top-speed profile mode at a resolution of 120,000 over a range of 375–1,500 m/z. Following CID activation with a normalized collision energy of 35.0, MS/MS data were acquired using the ion trap analyzer in centroid mode and normal mass range. Using synchronous precursor selection, up to 10 MS/MS precursors were selected for HCD activation with a normalized collision energy of 65.0, followed by the acquisition of MS3 reporter ion data using the FTMS analyzer in profile mode at a resolution of 50,000 over a range of 100–500 m/z.

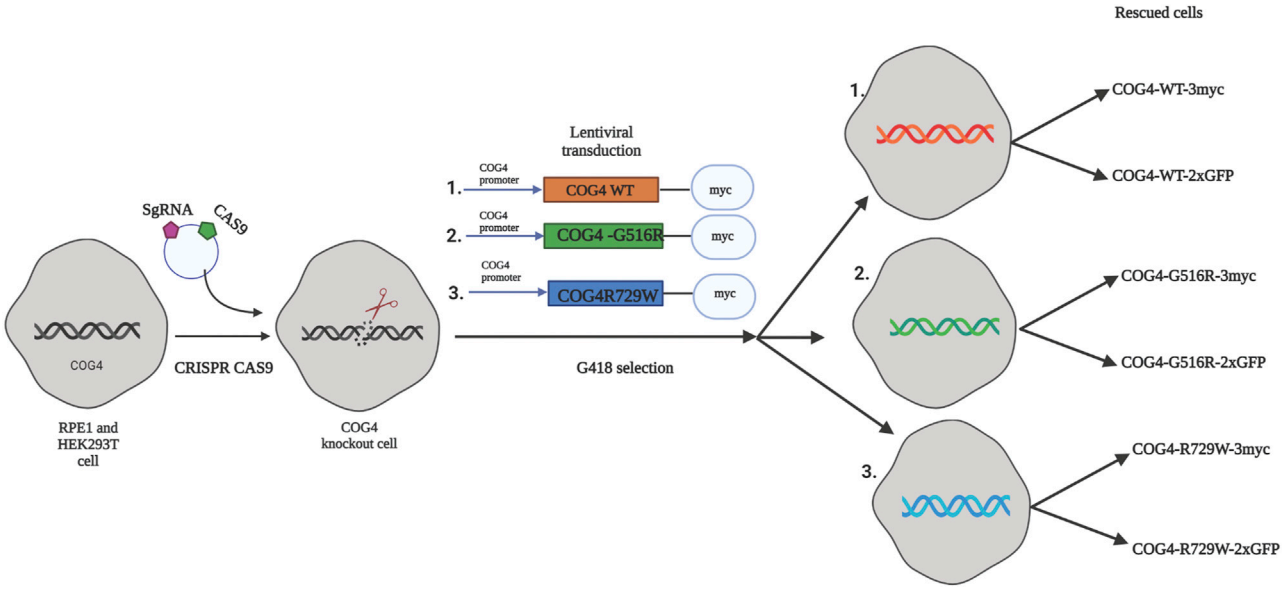

FIGURE 1 | The strategy for the creation of cellular COG-CDG models. A conceptual design of the COG4-SWS and COG4-CDGIIj cellular models. In the first step CRISPR/Cas9 protocol was used to make RPE1 and HEK293T COG4 KO cells lines. On the second step, lentiviral transduction and G418 selection was utilized to create populations of isogenic cells expressing GFP or 3myc-tagged COG4 variants under endogenous COG4 promoter.

Buffer A = 0.1% formic acid, 0.5% acetonitrile Buffer B = 0.1% formic acid, 99.9% acetonitrile. Both buffers adjusted to pH 10 with ammonium hydroxide for offline separation.

Data Analysis (MS)

Protein TMT MS3 reporter ion intensity values are assessed for quality using our in-house ProteiNorm app, a user-friendly tool for a systematic evaluation of normalization methods, imputation of missing values, and comparisons of different differential abundance methods (Graw et al., 2021). Popular normalization methods are evaluated, including log2 normalization (Log2), median normalization (Median), mean normalization (Mean), variance stabilizing normalization (VSN) (Huber et al., 2003), quantile normalization (Quantile) (Bolstad et al., 2010), cyclic loess normalization (Cyclic Loess) (Ritchie et al., 2015), global robust linear regression normalization (RLR) (Chawade et al., 2014), and global intensity normalization (Global Intensity) (Chawade et al., 2014). The individual performance of each method can be evaluated by comparing the following metrices: total intensity, Pooled intragroup Coefficient of Variation (PCV), Pooled intragroup Median Absolute Deviation (PMAD), Pooled intragroup Estimate of Variance (PEV), intragroup correlation, sample correlation heatmap (Pearson), and log2-ratio distributions. The normalized data was used to perform statistical analysis using Linear Models for Microarray Data (limma) with empirical Bayes (eBayes) smoothing to the standard errors (Ritchie et al., 2015). We performed limma differential abundance analysis using a paired sample design to evaluate differences between injured and naïve samples. Proteins with an FDR adjusted p-value <0.05 and a fold change >2 are considered significant. Significant proteins were utilized to identify important protein networks and pathways using the Ensemble of Gene Set Enrichment Analyses (EGSEA) Bioconductor package and Qiagen's Ingenuity Pathway Analysis (Alhamdoosh et al., 2017).

Transmission Electron Microscopy

Samples were treated according to Valdivia's lab protocol (Cocchiaro et al., 2008) with some modifications (Pokrovskaya et al., 2012). In short, cells were fixed for 20 min on ice with 2.5% glutaraldehyde and 0.05% malachite green (EMS) in 0.1 M sodium cacodylate buffer, pH 6.8. Samples were post-fixed for 30 min at room temperature with 0.5% osmium tetroxide and 0.8% potassium ferricyanide in 0.1 M sodium cacodylate, for 20 min on ice in 1% tannic acid, and for 1 h in 1% uranyl acetate at room temperature. Specimens were dehydrated with a graded ethanol series and embedded in Araldite 502/Embed 812 resins (EMS). Ultrathin sections were imaged at 80 kV on FEI Technai G2 TF20 transmission electron microscope. Digital images were acquired with FEI Eagle 4kX USB Digital Camera.

Antibodies

Primary and secondary antibodies used for WB or IF were commercially purchased. The list of antibodies and their dilutions are described in **Supplementary Table S2**.

Statistical Analysis

All the WB images are representative of 3 repeats and those were quantified by densitometry using the LI-COR Image Studio software. Error bars for all graphs represent standard deviation. Statistical analysis was done using one-way ANOVA using GraphPad Prism software.

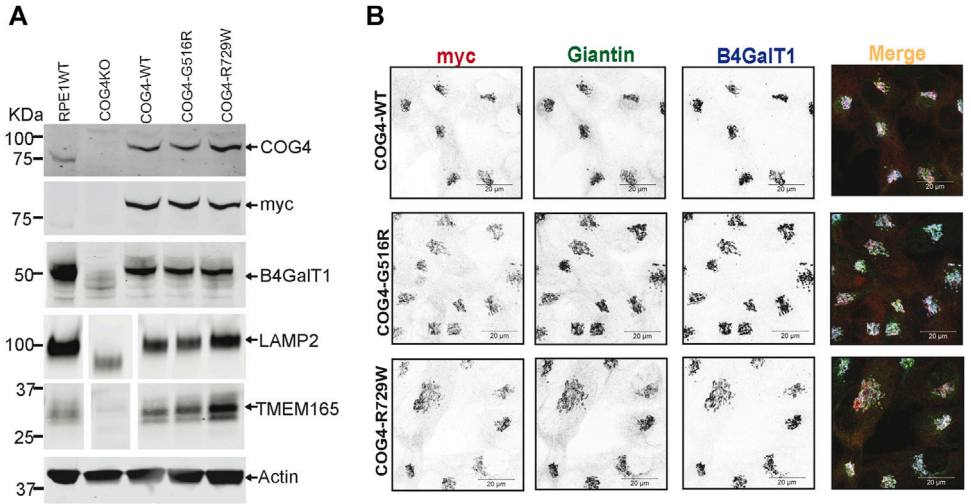

FIGURE 2 | Expression of G516R and R729W mutant proteins rescues major cellular phenotypes associated with COG4 deficiency. **(A)** WB to detect COG4, myc, B4GalT1, Lamp2, Tmem165, and actin in total cellular lysates prepared from RPE1 wild type, COG4 KO, rescued COG4-WT-3myc, COG4-G516-3myc, and COG4-R729W-3myc cells. Actin has been used as a loading control. **(B)** Airyscan superresolution IF analysis of RPE1 cells stained for myc (red), Giantin (green), B4GalT1 (blue). The red, green and infrared (blue) channels are presented in inverted black and white mode, whereas the merged view is shown in RGB mode. Scale bars, 20 μm.

RESULTS

Expression of COG4-G516R and COG4-R729W Mutant Proteins Rescued the Major COG Knockout Phenotypes

As a general strategy for the creation of mutant cell lines for functional and proteomics studies, we first knocked out the endogenous COG4 by CRISPR/Cas9 protocol in both HEK293T (Blackburn and Lupashin, 2016) and RPE1 cells and then re-introduced tagged wild-type or mutant variants of COG4 expressed under the control of the endogenous COG4 promoter (**Figure 1**). As a result, we developed a set of rescued RPE1 and HEK293T cell lines expressing COG4 (WT/G516R/R729W)-2xGFP and COG4 (WT/G516R/R729W)-3myc. Preliminary data obtained with GFP-tagged COG4 indicated that all three variants were expressed to near endogenous levels, Golgi localized, and able to rescue many COG4 KO trafficking and glycosylation defects with the exception of Cathepsin D sorting and TMEM165 stability (data not shown). We concluded that the addition of the bulky 2xGFP tag is partially compromising COG4 function and therefore focused our investigation on the COG4 constructs tagged with 3myc.

To characterize the rescued cell lines, wild-type and mutant cells have been analyzed using the biochemical and IF approaches (**Figures 2A,B**, **Supplementary Figure S1A,B**). WB analysis of the total protein revealed that the COG4 expression levels are similar in all three rescued RPE1, HEK293T cell lines and very close to the expression level of the endogenous COG4 in RPE1 and HEK293T cells, respectively, indicating that our strategy indeed resulted in the near-endogenous level of COG4-3myc expression (**Figure 2A**, **Supplementary Figure S1A**). Analysis of the myc signal confirmed a similar level of expression of all three COG4 variants, indicating that neither G516R nor R729R mutations affect the stability of COG4 protein. This result contrasts with the data previously published for COG4-G516R mutant fibroblasts (Ferreira et al., 2018). Superresolution microscopy has demonstrated that the myc tagged COG4 is Golgi localized in all rescued cell lines as myc signal colocalized with Giantin (cis-Golgi protein) and B4GalT1(trans-Golgi enzyme) (**Figure 2B**). Similarly, myc tagged COG4 is Golgi localized in all rescued HEK293T cell lines as myc signal is colocalized with GM130 (**Supplementary Figure S1B**). All analyzed cells demonstrated a similar COG4-3myc staining pattern, indicating that the rescued cell population is uniform and that cellular localization of COG4 mutants is indistinguishable from the localization of wild-type protein. Previously, we have reported that the Golgi enzyme stability and glycosylation of Lamp2 (Lysosomal membrane protein) and TMEM165 (a Golgi transmembrane glycoprotein) are altered in COG knockout cells. Western blot analysis of COG4 depleted HEK293T (Bailey Blackburn et al., 2016) and RPE1 cells show an increase in the electrophoretic mobility of Lamp2 and TMEM165 and depletion of B4GalT1enzyme (**Figure 2A**, **Supplementary Figure S1A**). Expression of wild-type and mutant COG4 rescued stability and glycosylation of all three tested proteins (**Figure 2A**, **Supplementary Figure S1A**). IF analysis of the mutant cell line also revealed no depletion or mislocalization of B4GalT1 or COG-sensitive protein Giantin (**Figure 2B**), indicating that both wild-type and a mutant version of COG4 can rescue major biochemical phenotypes associated with COG4 depletion.

Golgi Morphology Is Not Altered in Cells Expressing COG4 G516R and R729W Mutant Proteins

Previous studies suggested that COG4 mutations affect the overall structure of the Golgi apparatus. Golgi morphology was

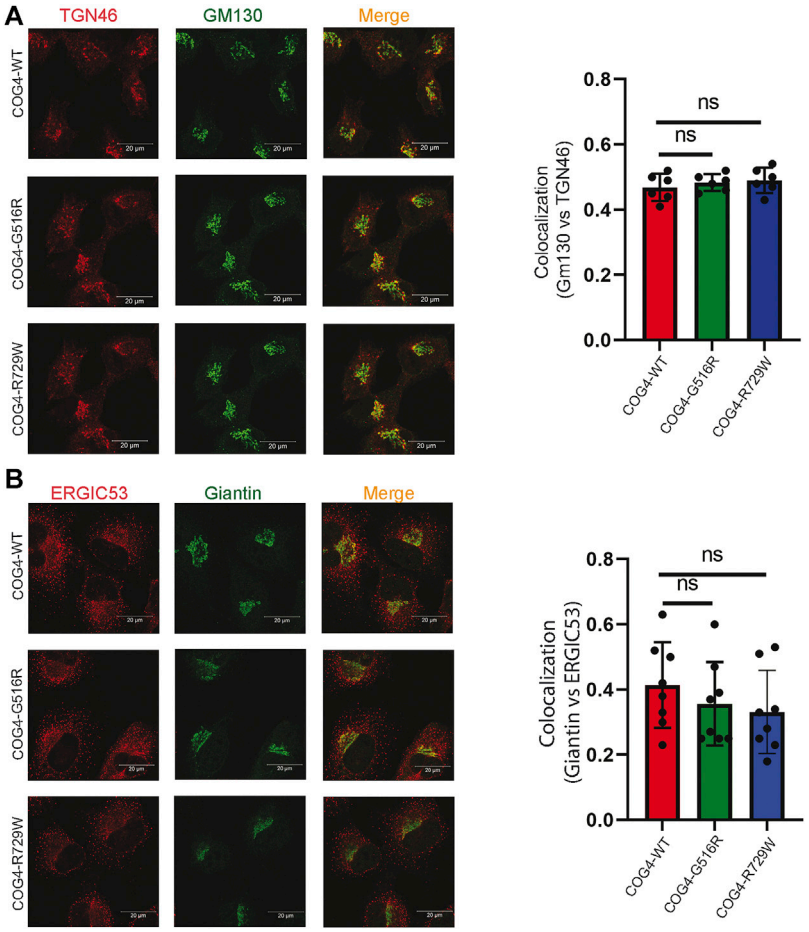

FIGURE 3 | Expression of COG4 mutants does not alter Golgi morphology. (A) Airyscan superresolution IF analysis of RPE1 COG4 wild type, G516R and R729W rescued cells stained for **(A)** GM130 (green) and TGN46 (red) and **(B)** GM130 (green) and ERGIC53 (red). Scale bars, 20 μm. Colocalization of TGN46 vs GM130 and ERGIC53 vs GM130 has been performed using Pearson's correlation coefficient (Right panel for both **(A)** and **(B)**, n = 20. Statistical significance was calculated by GraphPad Prism 8 using one-way ANOVA. $p > 0.05$, non-significant (ns). Error bar represents mean ± SD.

significantly altered in the COG4-G516R patient's fibroblast, which was determined by colocalization of GM130 and TGN46 (suggesting the collapse of the *cis*- and trans-Golgi stacks) (Ferreira et al., 2018). Moreover, undulated, fragmented, and disrupted Golgi has been observed in the COG4-R729W mutant patient's fibroblast (Reynders et al., 2009). Guided by the findings from these studies, we characterized the RPE1 COG4 mutated cell line for Golgi morphology. We applied the superresolution IF approach to check the colocalization of GM130 (peripheral membrane protein of cis-Golgi) and TGN46 (a membrane protein localized in trans-Golgi network) in the rescued mutant cell lines (both COG4-G516R and COG4-R729W). The result revealed no significant difference in relative colocalization of cis and trans-Golgi markers in comparison with the cells rescued with wild-type COG4-3myc (**Figure 3A**), indicating no collapse of *cis*- and trans-Golgi in mutant cell lines. In addition, colocalization analysis of ERGIC53 (membrane protein of the endoplasmic reticulum-Golgi intermediate compartment) and Giantin (medial-Golgi protein) revealed no significant alteration in colocalization of those markers in both mutated cell lines compared to wild type (**Figure 3B**). IF analysis of HEK293T cell lines confirms that Golgi morphology was undisturbed in cells expressing COG4 point mutants (**Supplementary Figure S2A,B**); moreover, EELS, the hallmark of COG deficiency in HEK293T cells (D'Souza et al., 2019) was not accumulated in cells expressing either G516R or R729W COG4 mutants (data not shown).

Since the resolution of the Airyscan microscopy (160 nm in x-y dimension) may not be sufficient to detect specific changes in Golgi morphology, we have employed TEM (Transmission Electron Microscopy) to analyze Golgi structure in cells bearing COG4 mutant proteins. The analysis revealed the Golgi stacks morphology and integrity were normal in all analyzed cell lines (**Figure 4**). These results suggest that altered Golgi morphology observed in patient's fibroblasts may not be directly linked to point mutations in COG4.

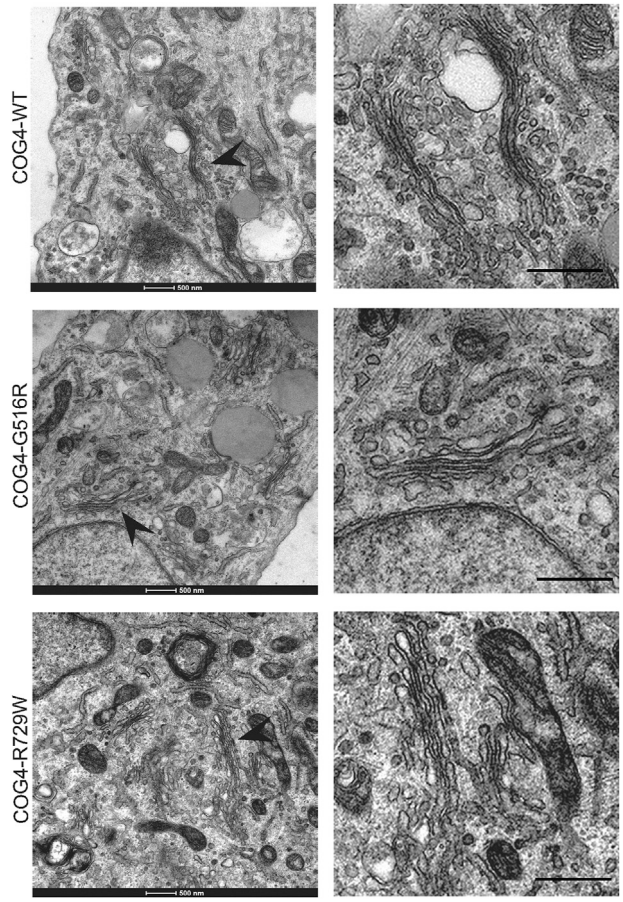

FIGURE 4 | Golgi ultrastructure is not perturbed in cells expressing COG4 mutants. Transmission Electron Microscopy has been performed to see the detailed ultrastructure of rescued RPE1 COG4-WT-3myc, COG4-G516R-3myc, and COG4-R729W-3myc cell lines. Black arrowhead indicates the Golgi. On the right side, the zoom view of the Golgi region is shown. The scale bar is 500 nm.

COG4 Mutations do Not Affect the Localization of V-SNARE GS15

GS15/Bet1L is a known COG-sensitive Golgi SNARE protein (Oka et al., 2004; Laufman et al., 2013; Blackburn et al., 2019). In the COG7-deficient patient's fibroblast, the Golgi staining for GS15 protein was substantially reduced and more dispersed as compared to control fibroblasts (Steet and Kornfeld, 2006). We were interested to see if the COG4 mutations are affecting the GS15 localization or not. IF analysis has been performed by staining the rescued COG4 (G516R and R729W) mutant and COG4WT cell lines with GM130 and GS15. The superresolution confocal microscopy revealed no significant colocalization difference of GM130 and GS15 in both mutants in comparison to wild type. In addition, the intensity of the GS15 signal was not altered in the mutant (**Figures 5A,B**). This result indicates the investigated COG4 mutations do not significantly affect GS15 localization or stability.

COG4-G516R and COG4-R729W Mutations Cause O-Glycosylation and N-Glycosylation Defects, Respectively

After finding that both G516R and R729W COG4 mutant proteins are capable of performing the major COG4 functions, we asked the question – what is altered in cells expressing COG4 point mutants? Previous studies reported that COG complex subunit knockdowns (KD) cause altered binding of several lectins due to impaired glycosylation of plasma membrane glycoconjugates (Shestakova et al., 2007; Richardson et al., 2009; Pokrovskaya et al., 2011; Climer et al., 2018). *Galanthus nivalus* lectin GNL binds to terminal α1-3 linked mannose residues exposed on immature N-glycosylated plasma membrane glycoproteins in all tested COG KD and KO cells (Pokrovskaya et al., 2011; Bailey Blackburn et al., 2016). Also, another lectin HPA (*Helix Pomatia* Agglutinin), binds to terminal N-acetylgalactosaminyl residues in immature O-glycosylated glycoproteins (Brooks, 2000). We have utilized GNL, and HPA conjugated with Alexa-647 (GNL-647 and HPA-647) to check the 'N' and 'O'-glycosylation fidelity in COG4-G516R and COG4-R729W cell lines in IF, WB, and flow cytometry approaches (**Figure 6**). IF experiment revealed that binding of HPA was significantly increased to the plasma membrane of cells expressing COG4-G516R (**Figures 6A,B**, **Supplementary Figure S3A**). The flow cytometry also confirmed that HPA-647 binding increased in cells expressing mutant COG4 (**Figure 6C**). In contrast, binding of GNL to plasma membrane of non-permeabilized cells was increased in both mutant cell lines, but most significantly in cells expressing COG4-R729W (**Figures 6A,B**, **Supplementary Figure S3B**). This lectin data is in good agreement with previously published results obtained with fibroblasts isolated from COG4-CDG (CDG-IIj) (Reynders et al., 2009) and COG4-SWS (Ferreira et al., 2018) patients. In addition, WB lectin analysis of secreted glycoproteins also revealed that HPA-647 and GNL-647 binding were significantly increased in G516R and R729W mutants correspondingly (**Figures 6D,E**).

The combined result indicates a notable O-glycosylation defect in cells expressing COG4-G516R and N-glycosylation defect in cells expressing COG4-R729W mutants.

Increased Accumulation of Core Proteins of HSPGs (Heparin Sulfate Proteoglycans) on the Cell Surface of COG4 Mutants

Proteoglycans are major components of the extracellular matrix (ECM) and comprise a large, heterogeneous group, including heparin sulfate proteoglycans (HSPGs) and chondroitin sulfate proteoglycans (CSPGs) (Xia et al., 2021). Accumulation of glypicans on the cell surface of COG4-SWS derived patient's fibroblast, and COG4-G516R zebrafish mutant has been reported previously (Ferreira et al., 2018; Xia et al., 2021). To examine potential change in proteoglycan accumulation in the cell surface of the RPE1 cells expressing different COG4 proteins, we used an antibody to HS-stubs (clone 3G10). These antibodies recognize the 3G10 neo-epitope

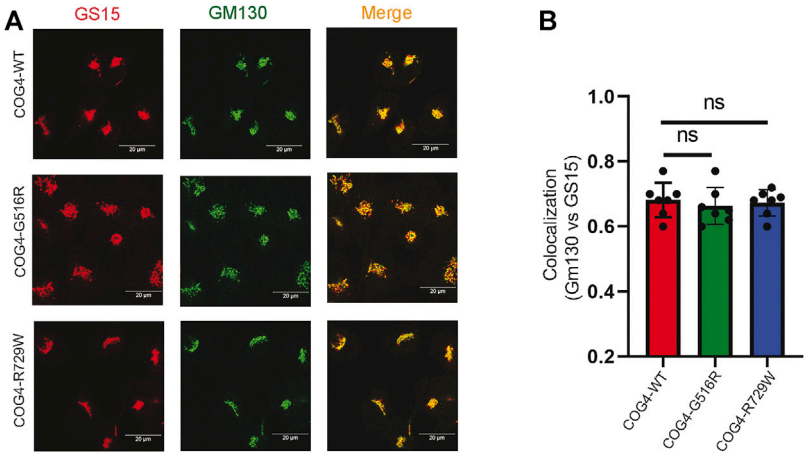

FIGURE 5 | Expression of G516R and R729W mutants do not affect the localization of v-SNARE GS15. **(A)** RPE1 rescued COG4-WT-3myc, COG4-G516R-3myc, and COG4-R729-3myc cells were stained with GM130 (green) and GS15 (red). Scale bar 20um. **(B)** Colocalization of GS15 with GM130 has been analyzed using Pearson's correlation coefficient. Quantification of colocalization in 20 cells analyzed. Statistical significance was calculated by GraphPad Prism 8 using one-way ANOVA. $p > 0.05$, nonsignificant (ns). Error bar represents mean ± SD.

(unsaturated uronic acid) exposed by digestion with heparinase III. WB revealed a significant increase in core proteins of HSPGs accumulation on the cell surface of both COG4-G516R and COG4-R729W mutant cell lines. (**Figures 7A,B**).

Abnormal Secretion of SIL1 and ERGIC53 in COG4-G516R Mutant Cell Line

COG complex is regulating intra-Golgi trafficking (Blackburn et al., 2019), and we have shown previously that COG4 depletion is significantly affecting a spectrum of secretory proteins (D'Souza et al., 2019). To test if the expression of COG4-G516R changes the spectrum of secretory proteins, we performed an unbiased analysis of the total protein secretome from RPE1 cells using a quantitative TMT mass spectrometry approach. Analysis revealed 3,404 protein signatures in both control and COG4-G516R samples. Surprisingly, more than 99% of detected proteins were released from both cell lines to the same level. Secretion of three proteins (TMCO4, S100A-1, and SERPINI1) was significantly reduced in COG4-G516R mutant, while secretion of SIL1 and LMAN1/ERGIC53 was significantly increased (**Figure 8A**). The most prominent (>10 times) increase in G516R secretome was detected for the ER luminal glycoprotein SIL1. WB analysis of the secretomes from all rescued cell lines confirmed a significant increase in the secretion of SIL1 protein by COG4-G516R and revealed that SIL1 secretion did not occur in COG4-R729W cells (**Figures 8B,C**).

DISCUSSION

We have developed a strategy for a cell-based model to compare different human mutations in the COG complex on the same genetic background. In this setup, we utilize a non-cancerous cell line in which the COG subunit is first deleted using the CRISPR/Cas9 approach and then stably restored by virus-assisted insertion of COG subunit wild-type CDG variants driven by the endogenous promoter. We have previously developed and characterized a complete set of HEK293T cells with a complete knockout of each of the COG complex subunits (Blackburn and Lupashin, 2016). To test this novel strategy, we created RPE1 and HEK293T cells expressing COG4 mutations COG4-G516R (Saul-Wilson syndrome) and COG4-R729W (COG-CDG type IIj) under the endogenous COG4 promoter. Saul-Wilson syndrome due to COG4 G516R mutation results in a rare skeletal dysplasia which is not categorized as CDG as defined in COG4 mutation R729W (Ferreira et al., 2018; D'Souza et al., 2020). It has been suggested that COG4-R729W mutation presents a partial loss of COG4 function, whereas the G516R mutation shows an abnormal gain of COG4 function (Reynders et al., 2009; Ferreira et al., 2018). Patient fibroblasts are traditionally used to reveal cellular defects associated with COG complex human mutations (Steet and Kornfeld, 2006, 7; Reynders et al., 2009; Ferreira et al., 2018). The major limitation of fibroblasts-based studies is potential heterogeneity resulting from a diverse genetic background of the patients. Another limitation is linked to the fibroblast's cell physiology which may not reveal specific defects manifested in nervous, ocular, bone, and other tissues severely affected in COG patients (D'Souza et al., 2020). The presented cellular model mostly overcomes these limitations by providing tissue-specific uniform genetic background, allowing side-by-side comparison of different COG mutations.

Comparison of COG4 G516R and R729W variants expressed in both RPE1 and HEK293T cells under COG4 promoter revealed that both mutant proteins are properly Golgi localized and expressed at the wild-type level. Moreover, we did not find any significant disruption of Golgi structure resulting from the expression of these COG mutants as

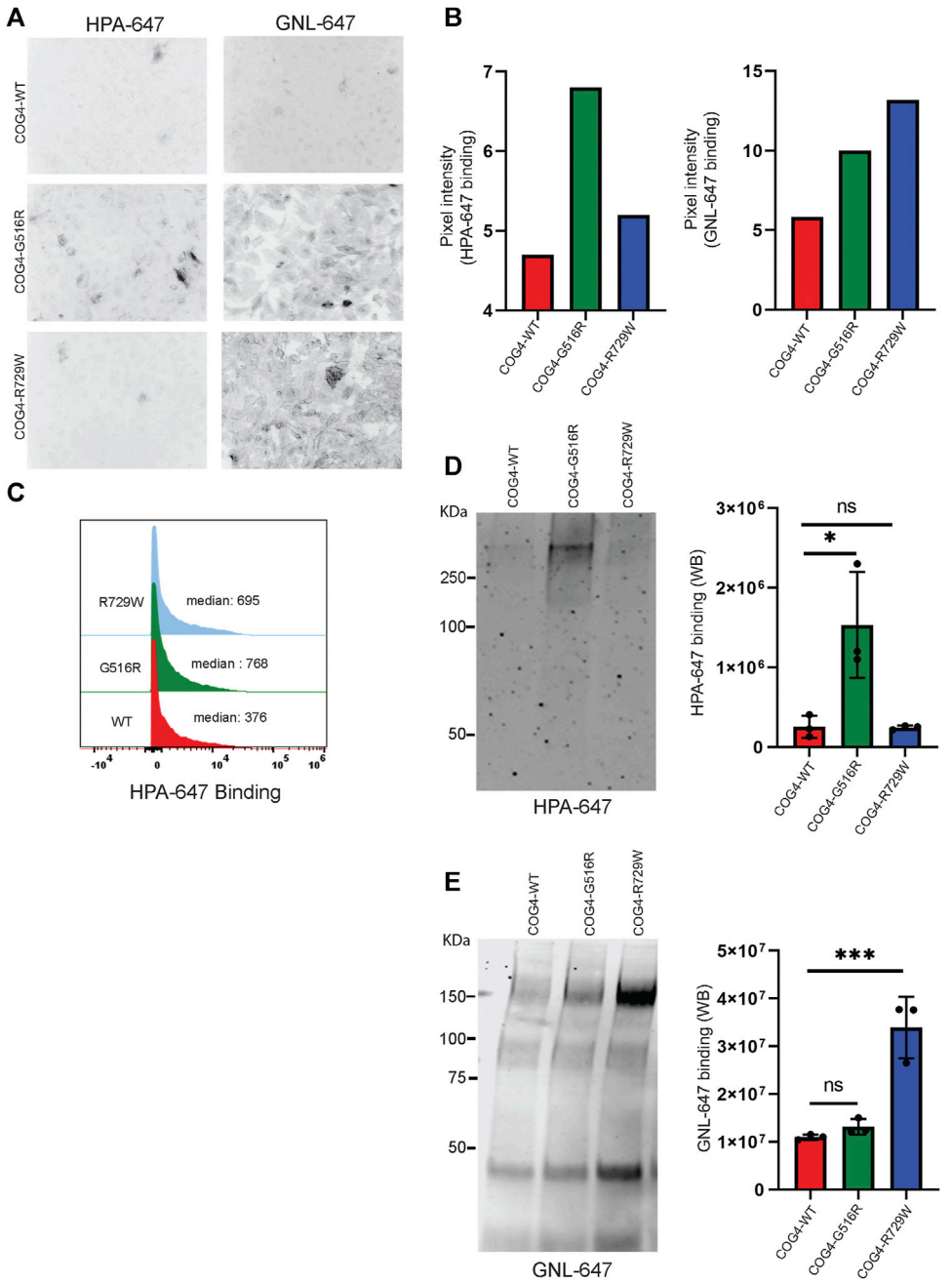

FIGURE 6 | COG4-G516R and COG4-R729W mutations are causing O-glycosylation and N-glycosylation defects, respectively**. (A)** Non-permeabilized RPE1 rescued COG4-WT-3myc, COG4-G516R-3myc, and COG4-R729W-3myc cells were stained with the fluorescently conjugated lectins HPA-647 (specific for terminal GalNAc residues) and GNL-647 (specific for terminal α-D-mannosyl residues). The images were taken by Zeiss Axiovert 200M fluorescent microscope using a ×20 objective. **(B)** The pixel intensity of the full image for each cell line has been measured using ImageJ software. The bar graph has been presented with statistical value to provide intensity difference for each lectin (HPA-647, GNL-647) binding among the rescued cell line. **(C)** Flow cytometry histogram of HPA-647 fluorescence intensity in COG4-WT-3myc (red), COG4-G516R-3myc (green), and COG4-R729W-3myc (blue) population after gating for live and single cells. **(D)** Western blot analysis of the secretion from the rescued cells has been performed by probing with the HPA-647 antibody **(left panel).** Quantification of the lectin HPA-647 binding intensity **(Right panel).** Statistical significance was calculated by GraphPad Prism 8 using One-way Anova. *$p \leq 0.05$, **$p \leq 0.01$ and non-significant (ns) $p > 0.05$. Error bar represents mean ± SD. **(E)** Western blot analysis of the secretion from the rescued cells has been performed by probing with the GNL-647 antibody **(left panel).** Quantification of the lectin GNL-647 binding intensity **(Right panel).** Statistical significance was calculated by GraphPad Prism 8 using One-way ANOVA. *$p \leq 0.05$, **$p \leq 0.01$ and non-significant (ns) $p > 0.05$. Error bar represents mean ± SD.

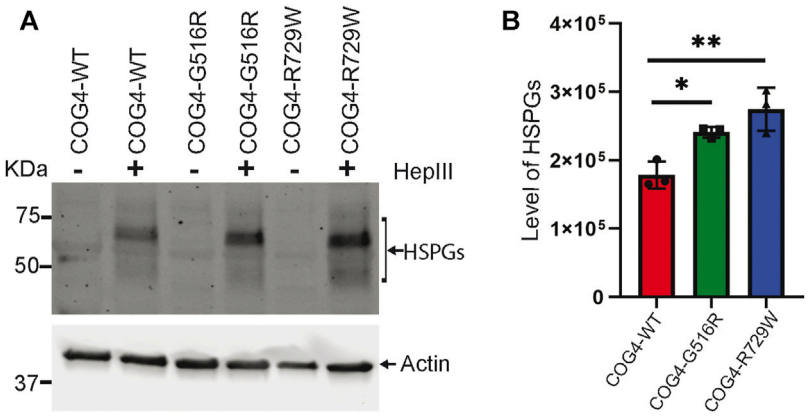

FIGURE 7 | Increased accumulation of core proteins of HSPGs (Heparin sulfate proteoglycans) on the cell surface of rescued mutant (G516R and R729W) RPE1 cell line. **(A)** RPE1 rescued COG4-WT-3myc, COG4-G516R-3myc, and COG4-R729W-3myc cells were digested by the Heparinase III enzyme. Western blot analysis with 3G10 antibody to the core proteins of proteoglycan (HSPGs). **(B)** Quantitative analysis of the core proteins of HSPGs accumulation. Statistical significance was calculated by GraphPad Prism 8 using One-way ANOVA. $^{**}p \leq 0.01$, $^{***}p \leq 0.001$. Error bar represents mean ± SD.

previously observed in some of the patients' fibroblasts (Reynders et al., 2009; Ferreira et al., 2018), indicating that both mutants enter the COG complex and capable of restoring the majority of cellular defects observed in cells completely depleted for COG4 protein. Our finding agrees with the recent study of COG4-G516R mutation in the worm model (Zafra et al., 2021), but is different from disrupted and less rigid Golgi stack found in R729W patients' fibroblasts (Reynders et al., 2009) and "collapsed" Golgi stacks observed in G516R patients' fibroblasts (Ferreira et al., 2018). Our results indicate that structural Golgi changes observed in some patients' fibroblasts are cell-type dependent and do not represent the prevailing cellular phenotype associated with G516R and R729W mutations. On the other hand, we did confirm O-glycosylated defects associated with G516R mutation and N-glycosylated defects associated with R729W mutation. The N-glycosylation defects have been reported in HeLa cells bearing R729W mutation (Richardson et al., 2009). Specific defect in N-glycosylation observed in cells bearing R729W mutation may be due to the loss of the subset of intra-Golgi recycling vesicles carrying MGAT1, medial Golgi enzyme responsible for the addition of the first GlcNAc residue in the Golgi (Kumar et al., 1990). The exact mechanism of MGAT1 recycling is still an enigma, but we have shown previously that this protein is mislocalized in cells depleted for COG4 proteins (Pokrovskaya et al., 2011). It is less clear why cells bearing G516R mutation are preferentially deficient in O-glycosylation. The HPA lectin recognizes exposed α-N-acetyl-d-galactosamine residue (Irimura et al., 1981) in immature O-glycosylated proteins. The staining for this lectin is significantly increased in cells deficient for the Golgi-to-ER recycling of polypeptide N-acetylgalactosaminyl transferases (GalNac-Ts) (Gill et al., 2010). One possibility is that the COG4 G516R mutant is defective in recognition of a subset of vesicles recycling GalNac-Ts. Depletion of COG complex subunits results in rapid accumulation of CCD (COG complex dependent) vesicles (Zolov and Lupashin, 2005; Shestakova et al., 2006); future investigation of CCD vesicle population should reveal distinct subsets regulated by different COG subunits and arrangements.

Ocular involvement has been reported in 60% of CDG with a pure O-glycosylation defect (Francisco et al., 2018). G516R mutated patients also have ocular phenotypes, which are well aligned with our findings revealing O-glycosylation defects. On the other hand, different N-glycosylation defects include phenotypes such as intellectual disability, speech disorder, and abnormal gait (Wolthuis et al., 2014), similar to our findings showing N-glycosylation defects in the R729W mutated cell line. We also confirmed the accumulation of heparin sulfate proteoglycans on the surface of cells expressing COG4-G516R mutation (Xia et al., 2021); however, our studies revealed an even greater accumulation of HSPGs in cells expressing the COG4-R729W variant. This result indicates that HSPGs accumulation alone may not be sufficient to explain the unique SWS phenotype associated with COG4 G516R mutation. Moreover, it was recently reported that HSPG modifications are severely altered in HEK293T cells depleted for six different COG complex subunits (Adusmalli et al., 2021).

Our previous work revealed an abnormal protein secretion in COG4 deficient cells (Blackburn et al., 2018). This observation prompted us to investigate the protein secretome of COG4-G516R expressing cells. Unbiased quantitative mass-spectrometry analysis revealed no difference in secretion of 99.9% of detected proteins. Importantly, two proteins, SIL1 and ERGIC53 were released from COG4-G516R cells at a much higher level as compared to wild-type cells or cells expressing COG4-R729W. SIL1/BAP is the ER-resident soluble glycoprotein that is usually not secreted from cells. Its ER localization is thought to be mediated by tetra-peptide (KELR) at the C terminus (Chung et al., 2002), but the exact mode of SIL1 intracellular retention has not been studied in detail. SIL1 functions as a nucleotide exchange factor and co-chaperone for ER lumenal chaperone HSPA5/GRP78/BIP which is

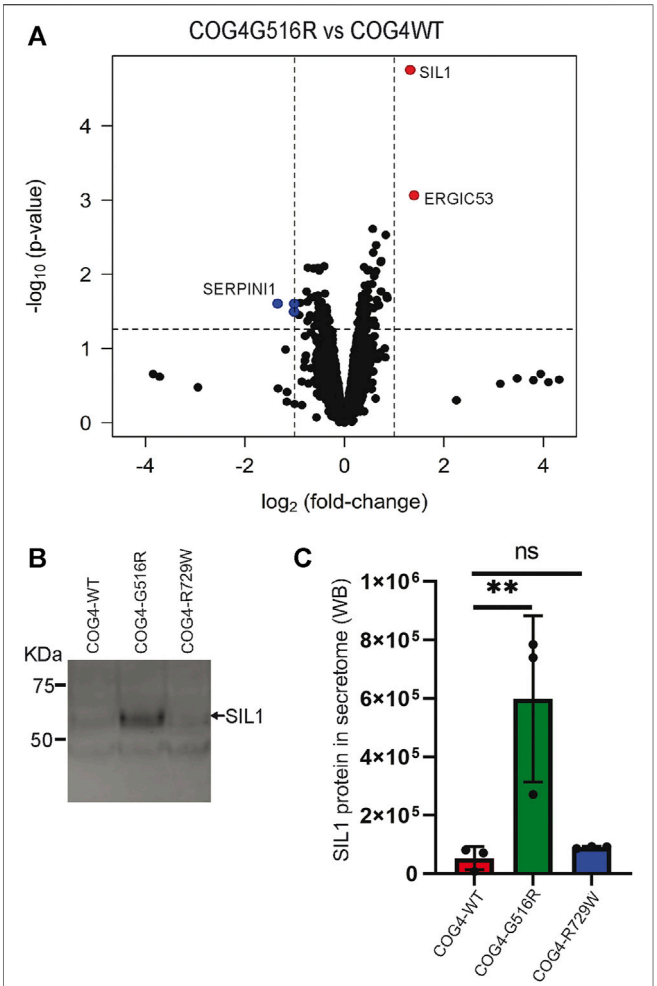

FIGURE 8 | Abnormal secretion of SIL1 and ERGIC53 from COG4-G516R mutant cell line. **(A)** Volcano plot obtained from quantitative mass spectrometry analysis of protein secretome from RPE1 rescued COG4-WT-3myc and COG4-G516R-3myc cell lines (x-axis represents the log2 of the fold change, the y-axis represents the negative decade logarithm of the significance value). Red dots and blue dots represent proteins that are significantly upregulated and downregulated **(B)** Western blot analysis of the secretome from three rescued cell lines respectively and stained with the SIL1 antibody. **(C)** Quantitative analysis of secreted SIL1 protein level. Statistical significance was calculated by GraphPad Prism 8 using One-way ANOVA. $^{**}p \leq 0.01$ and non-significant (ns) $p > 0.05$. Error bar represents mean ± SD.

required for protein translocation and folding (Ichhaporia and Hendershot, 2021). Our proteomic analysis did not detect abnormal secretion of HSPA5, or any other ER-resident proteins retained by the KDEL-based mechanism. Interestingly, SIL1 overexpression causes the disturbance of the Golgi structure (Labisch et al., 2018), indicating a potential link between SIL1 and COG trafficking machinery.

SIL1 is ubiquitously expressed in different tissues but at a different level. Though the co-chaperone mutation might affect highly secretory tissues, such as the kidney, liver, placenta, and plasma cells but SIL1 mutation significantly affect the neuronal cell, lens epithelial cell, and skeletal muscle (Krieger et al., 2013; Ichhaporia et al., 2015; Ichhaporia and Hendershot, 2021). Interestingly, the Saul-Wilson syndrome presents skeletal and ocular defects similar to SIL1 mutation (loss of function) phenotypes. Therefore, SIL1 mutation could be the major contributing factor to Saul-Wilson syndrome. ERGIC53/LMAN1 is a transmembrane glycoprotein that shuttles between ER and the Golgi apparatus and is the hallmark of the ERGIC/IC compartment (Zhang et al., 2009). It acts as a secondary quality control mechanism complementary to the ER folding machinery (Zhang et al., 2009). Importantly, ERGIC53 is a mannose-binding lectin (Baines and Zhang, 2007), and therefore ERGIC53 abnormal release from COG4-G516R cells may be connected to the elevated release of SIL1 glycoprotein.

Two commonly used non-cancerous diploid (RPE1) and triploid (HEK293T) cell lines were utilized for our initial studies. We realized that the choice of cell lines could limit our understanding of skeletal and liver defects common for COG-CDG patients. To overcome these potential limitations, similar experiments with skeletal hFOB and human iPSC cell lines were recently initiated. A more sophisticated alternative to our approach is the use of CRISPR/Cas9 gene-editing strategy to introduce known COG-CDG mutation directly into the genome (Hsu et al., 2014) of a chosen cell line. This strategy avoids potential off-target effects and may be more suitable for mutations that affect the splicing of COG subunits (Hsu et al., 2014). At the same time, the correct bi-allelic introduction of desired mutations is far more complicated as compared to the strategy presented in this work and would require single-cell cloning, introducing potential genome heterogeneity. Moreover, CRISPR editing requires homolog-driven repair (HDR). It has been reported previously that the low efficiency of HDR decreases its utility for precise gene editing, and to increase the HDR efficiency, NHEJ (non-homologous end joining) needs to be inhibited (Uddin et al., 2020).

In the future, we aim to extend this strategy to other COG mutations and expand the model system to the bone cell line hFOB as well as to stem cells. We also plan to characterize Golgi and plasma membrane glycoproteins and glycolipids using quantitative mass-spectrometry techniques. We hope that this approach will help in the identification of key problems in different COG mutants and ultimately will help in the treatment strategy for COG-CDG patients.

DATA AVAILABILITY STATEMENT

The datasets presented in this study can be found in online repositories. The names of the repository/repositories and accession number(s) can be found below: Data are available via ProteomeXchange with identifier PXD027202.

AUTHOR CONTRIBUTIONS

FS wrote the article and made substantial contributions to conception and design, acquisition of data, analysis, and interpretation of data. IP drafted the article, performed EM and other experiments and analyzed

the data. VL wrote the article made substantial contributions to conception and design.

FUNDING

This work was supported by the National Institute of Health grant R01GM083144 for VL.

ACKNOWLEDGMENTS

We are thankful to Hudson Freeze, Wei Guo, as well as others who provided reagents. We also would like to thank Zinia D'Souza for cloning the COG4 promoter, initial input, and critical reading of the manuscript. We are thankful to Amrita Khakurel for initial input and critical reading of the manuscript and Tetyana Kudlyk for excellent technical support. We would also like to thank the UAMS IDeA National Resource for Quantitative Proteomics, sequencing, flow cytometry, and microscopy core facilities for the use of their facilities and expertise.

SUPPLEMENTARY MATERIAL

The Supplementary Material for this article can be found online at: https://www.frontiersin.org/articles/10.3389/fgene.2021.733048/full#supplementary-material

REFERENCES

Adusmalli, R., Åsheim, H.-C., Lupashin, V., Blackburn, J. B., and Prydz, K. (2021). Proteoglycan Synthesis in Conserved Oligomeric Golgi Subunit Deficient HEK293T Cells Is Affected Differently, Depending on the Lacking Subunit. *Traffic Cph. Den.* doi:10.1111/tra.12804

Alhamdoosh, M., Ng, M., Wilson, N., Sheridan, J., Huynh, H., Wilson, M., et al. (2017). Combining Multiple Tools Outperforms Individual Methods in Gene Set Enrichment Analyses. *Bioinformatics* 33, 414–424. doi:10.1093/bioinformatics/btw623

Bailey Blackburn, J., Pokrovskaya, I., Fisher, P., Ungar, D., and Lupashin, V. V. (2016). COG Complex Complexities: Detailed Characterization of a Complete Set of HEK293T Cells Lacking Individual COG Subunits. *Front. Cel Dev. Biol.* 4. doi:10.3389/fcell.2016.00023

Baines, A. C., and Zhang, B. (2007). Receptor-mediated Protein Transport in the Early Secretory Pathway. *Trends Biochem. Sci.* 32, 381–388. doi:10.1016/j.tibs.2007.06.006

Blackburn, J. B., D'Souza, Z., and Lupashin, V. V. (2019). Maintaining Order: COG Complex Controls Golgi Trafficking, Processing, and Sorting. *FEBS Lett.* 593, 2466–2487. doi:10.1002/1873-3468.13570

Blackburn, J. B., Kudlyk, T., Pokrovskaya, I., and Lupashin, V. V. (2018). More Than Just Sugars: COG Complex Deficiency Causes Glycosylation-independent Cellular Defects. *Traffic Cph. Den.* 19, 463–480. doi:10.1111/tra.12564

Blackburn, J. B., and Lupashin, V. V. (2016). Creating Knockouts of Conserved Oligomeric Golgi Complex Subunits Using CRISPR-Mediated Gene Editing Paired with a Selection Strategy Based on Glycosylation Defects Associated with Impaired COG Complex Function. *Methods Mol. Biol. Clifton NJ*, 145–161. doi:10.1007/978-1-4939-6463-5_121496

Bolstad, H. M., Botelho, D. J., and Wood, M. J. (2010). Proteomic Analysis of Protein–Protein Interactions within the Cysteine Sulfinate Desulfinase Fe–S Cluster Biogenesis System. *J. Proteome Res.* 9, 5358–5369. doi:10.1021/pr1006087

Bonifacino, J. S., and Glick, B. S. (2004). The Mechanisms of Vesicle Budding and Fusion. *Cell* 116, 153–166. doi:10.1016/s0092-8674(03)01079-1

Bröcker, C., Engelbrecht-Vandré, S., and Ungermann, C. (2010). Multisubunit Tethering Complexes and Their Role in Membrane Fusion. *Curr. Biol.* 20, R943–R952. doi:10.1016/j.cub.2010.09.015

Brooks, S. A. (2000). The Involvement of Helix Pomatia Lectin (HPA) Binding N-Acetylgalactosamine Glycans in Cancer Progression. *Histol. Histopathol.* 15, 143–158. doi:10.14670/HH-15.143

Campeau, E., Ruhl, V. E., Rodier, F., Smith, C. L., Rahmberg, B. L., Fuss, J. O., et al. (2009). A Versatile Viral System for Expression and Depletion of Proteins in Mammalian Cells. *PLoS One* 4, e6529. doi:10.1371/journal.pone.0006529

Chawade, A., Alexandersson, E., and Levander, F. (2014). Normalyzer: A Tool for Rapid Evaluation of Normalization Methods for Omics Data Sets. *J. Proteome Res.* 13, 3114–3120. doi:10.1021/pr401264n

Chung, K. T., Shen, Y., and Hendershot, L. M. (2002). BAP, a Mammalian BiP-Associated Protein, Is a Nucleotide Exchange Factor that Regulates the ATPase Activity of BiP. *J. Biol. Chem.* 277, 47557–47563. doi:10.1074/jbc.M208377200

Climer, L. K., Dobretsov, M., and Lupashin, V. (2015). Defects in the COG Complex and COG-Related Trafficking Regulators Affect Neuronal Golgi Function. *Front. Neurosci.* 9, 405. doi:10.3389/fnins.2015.00405

Climer, L. K., Hendrix, R. D., and Lupashin, V. V. (2018). Conserved Oligomeric Golgi and Neuronal Vesicular Trafficking. *Handb. Exp. Pharmacol.* 245, 227–247. doi:10.1007/164_2017_65

Cocchiaro, J. L., Kumar, Y., Fischer, E. R., Hackstadt, T., and Valdivia, R. H. (2008). Cytoplasmic Lipid Droplets Are Translocated into the Lumen of the *Chlamydia trachomatis* Parasitophorous Vacuole. *Proc. Natl. Acad. Sci. U. S. A.* 105, 9379–9384. doi:10.1073/pnas.0712241105

Derby, M. C., and Gleeson, P. A. (2007). *International Review of Cytology*. Academic Press, 47–116. doi:10.1016/S0074-7696(07)61002-XNew Insights into Membrane Trafficking and Protein Sorting

D'Souza, Z., Blackburn, J. B., Kudlyk, T., Pokrovskaya, I. D., and Lupashin, V. V. (2019). Defects in COG-Mediated Golgi Trafficking Alter Endo-Lysosomal System in Human Cells. *Front. Cel Dev. Biol.* 7, 118. doi:10.3389/fcell.2019.00118

D'Souza, Z., Taher, F. S., and Lupashin, V. V. (2020). Golgi inCOGnito: From Vesicle Tethering to Human Disease. *Biochim. Biophys. Acta BBA - Gen. Subj.* 1864, 129694. doi:10.1016/j.bbagen.2020.129694

Dull, T., Zufferey, R., Kelly, M., Mandel, R. J., Nguyen, M., Trono, D., et al. (1998). A Third-Generation Lentivirus Vector with a Conditional Packaging System. *J. Virol.* 72, 8463–8471. doi:10.1128/JVI.72.11.8463-8471.1998

Ferreira, C. R., Xia, Z.-J., Clément, A., Parry, D. A., Davids, M., Taylan, F., et al. (2018). A Recurrent De Novo Heterozygous COG4 Substitution Leads to Saul-Wilson Syndrome, Disrupted Vesicular Trafficking, and Altered Proteoglycan Glycosylation. *Am. J. Hum. Genet.* 103, 553–567. doi:10.1016/j.ajhg.2018.09.003

Foulquier, F. (2009). COG Defects, Birth and Rise!. *Biochim. Biophys. Acta BBA - Mol. Basis Dis.* 1792, 896–902. doi:10.1016/j.bbadis.2008.10.020

Francisco, R., Pascoal, C., Marques-da-Silva, D., Morava, E., Gole, G. A., Coman, D., et al. (2018). Keeping an Eye on Congenital Disorders of O-Glycosylation: a Systematic Literature Review. *J. Inherit. Metab. Dis.*. doi:10.1007/s10545-017-0119-2

Gill, D. J., Chia, J., Senewiratne, J., and Bard, F. (2010). Regulation of O-Glycosylation through Golgi-To-ER Relocation of Initiation Enzymes. *J. Cel Biol.* 189, 843–858. doi:10.1083/jcb.201003055

Graw, S., Chappell, K., Washam, L. C., Gies, A., Bird, J., Robeson, S., et al. (2021). Multi-omics Data Integration Considerations and Study Design for Biological Systems and Disease. *Mol. Omics* 17, 170–185. doi:10.1039/D0MO00041H

Hsu, P. D., Lander, E. S., and Zhang, F. (2014). Development and Applications of CRISPR-Cas9 for Genome Engineering. *Cell* 157, 1262–1278. doi:10.1016/j.cell.2014.05.010

Huang, S., and Wang, Y. (2017). Golgi Structure Formation, Function, and post-translational Modifications in Mammalian Cells. *F1000Research* 6, 2050. doi:10.12688/f1000research.11900.1

Huber, L. A., Pfaller, K., and Vietor, I. (2003). Organelle Proteomics. *Circ. Res.* 92, 962–968. doi:10.1161/01.RES.0000071748.48338.25

Ichhaporia, V. P., and Hendershot, L. M. (2021). Role of the HSP70 Co-chaperone SIL1 in Health and Disease. *Int. J. Mol. Sci.* 22, 1564. doi:10.3390/ijms22041564

Ichhaporia, V. P., Sanford, T., Howes, J., Marion, T. N., and Hendershot, L. M. (2015). Sil1, a Nucleotide Exchange Factor for BiP, Is Not Required for Antibody Assembly or Secretion. *Mol. Biol. Cel* 26, 420–429. doi:10.1091/mbc.E14-09-1392

Irimura, T., Tsuji, T., Tagami, S., Yamamoto, K., and Osawa, T. (1981). Structure of a Complex-type Sugar Chain of Human Glycophorin A. *Biochemistry* 20, 560–566. doi:10.1021/bi00506a018

Khakurel, A., Kudlyk, T., Bonifacino, J. S., and Lupashin, V. V. (2021). The Golgi-Associated Retrograde Protein (GARP) Complex Plays an Essential Role in the Maintenance of the Golgi Glycosylation Machinery. *Mol. Biol. Cell, Mbc.* E21-04–0169. doi:10.1091/mbc.E21-04-0169

Krieger, M., Roos, A., Stendel, C., Claeys, K. G., Sonmez, F. M., Baudis, M., et al. (2013). SIL1 Mutations and Clinical Spectrum in Patients with Marinesco-Sjögren Syndrome. *Brain* 136, 3634–3644. doi:10.1093/brain/awt283

Kudlyk, T., Willett, R., Pokrovskaya, I. D., and Lupashin, V. (2013). COG6 Interacts with a Subset of the Golgi SNAREs and Is Important for the Golgi Complex Integrity. *Traffic Cph. Den.* 14, 194–204. doi:10.1111/tra.12020

Kumar, R., Yang, J., Larsen, R. D., and Stanley, P. (1990). Cloning and Expression of N-Acetylglucosaminyltransferase I, the Medial Golgi Transferase that Initiates Complex N-Linked Carbohydrate Formation. *Proc. Natl. Acad. Sci. U. S. A.* 87, 9948–9952. doi:10.1073/pnas.87.24.9948

Labisch, T., Buchkremer, S., Phan, V., Kollipara, L., Gatz, C., Lentz, C., et al. (2018). Tracking Effects of SIL1 Increase: Taking a Closer Look beyond the Consequences of Elevated Expression Level. *Mol. Neurobiol.* 55, 2524–2546. doi:10.1007/s12035-017-0494-6

Laufman, O., Hong, W., and Lev, S. (2013). The COG Complex Interacts with Multiple Golgi SNAREs and Enhances Fusogenic Assembly of SNARE Complexes. *J. Cel Sci.* 126, 1506–1516. doi:10.1242/jcs.122101

Makhoul, C., Gosavi, P., and Gleeson, P. A. (2019). Golgi Dynamics: The Morphology of the Mammalian Golgi Apparatus in Health and Disease. *Front. Cel Dev. Biol.* 7. doi:10.3389/fcell.2019.00112

Oka, T., Ungar, D., Hughson, F. M., and Krieger, M. (2004). The COG and COPI Complexes Interact to Control the Abundance of GEARs, a Subset of Golgi Integral Membrane Proteins. *Mol. Biol. Cel* 15, 2423–2435. doi:10.1091/mbc.e03-09-0699

Ondruskova, N., Cechova, A., Hansikova, H., Honzik, T., and Jaeken, J. (2021). Congenital Disorders of Glycosylation: Still "hot" in 2020. *Biochim. Biophys. Acta Gen. Subj.* 1865, 129751. doi:10.1016/j.bbagen.2020.129751

Pokrovskaya, I. D., Szwedo, J. W., Goodwin, A., Lupashina, T. V., Nagarajan, U. M., and Lupashin, V. V. (2012). *Chlamydia trachomatis* Hijacks Intra-golgi COG Complex-dependent Vesicle Trafficking Pathway: COG Complex and Chlamydial Development. *Cell. Microbiol.* 14, 656–668. doi:10.1111/j.1462-5822.2012.01747.x

Pokrovskaya, I., Willett, R., Smith, R., Morelle, W., Kudlyk, T., and Lupashin, V. (2011). COG Complex Specifically Regulates the Maintenance of Golgi Glycosylation Machinery. *Glycobiology* 21, 1554–1569. doi:10.1093/glycob/cwr028

Reynders, E., Foulquier, F., Leão Teles, E., Quelhas, D., Morelle, W., Rabouille, C., et al. (2009). Golgi Function and Dysfunction in the First COG4-Deficient CDG Type II Patient. *Hum. Mol. Genet.* 18, 3244–3256. doi:10.1093/hmg/ddp262

Richardson, B. C., Smith, R. D., Ungar, D., Nakamura, A., Jeffrey, P. D., Lupashin, V. V., et al. (2009). Structural Basis for a Human Glycosylation Disorder Caused by Mutation of the COG4 Gene. *Proc. Natl. Acad. Sci.* 106, 13329–13334. doi:10.1073/pnas.0901966106

Ritchie, M. E., Phipson, B., Wu, D., Hu, Y., Law, C. W., Shi, W., et al. (2015). Limma powers Differential Expression Analyses for RNA-Sequencing and Microarray Studies. *Nucleic Acids Res.* 43, e47. doi:10.1093/nar/gkv007

Shestakova, A., Suvorova, E., Pavliv, O., Khaidakova, G., and Lupashin, V. (2007). Interaction of the Conserved Oligomeric Golgi Complex with T-SNARE Syntaxin5a/Sed5 Enhances Intra-golgi SNARE Complex Stability. *J. Cel Biol.* 179, 1179–1192. doi:10.1083/jcb.200705145

Shestakova, A., Zolov, S., and Lupashin, V. (2006). COG Complex-Mediated Recycling of Golgi Glycosyltransferases Is Essential for normal Protein Glycosylation. *Traffic Cph. Den.* 7, 191–204. doi:10.1111/j.1600-0854.2005.00376.x

Steet, R., and Kornfeld, S. (2006). COG-7-deficient Human Fibroblasts Exhibit Altered Recycling of Golgi Proteins. *Mol. Biol. Cel* 17, 2312–2321. doi:10.1091/mbc.e05-08-0822

Stepanenko, A. A., and Dmitrenko, V. V. (2015). HEK293 in Cell Biology and Cancer Research: Phenotype, Karyotype, Tumorigenicity, and Stress-Induced Genome-Phenotype Evolution. *Gene* 569, 182–190. doi:10.1016/j.gene.2015.05.065

Uddin, F., Rudin, C. M., and Sen, T. (2020). CRISPR Gene Therapy: Applications, Limitations, and Implications for the Future. *Front. Oncol.* 10, 1387. doi:10.3389/fonc.2020.01387

Ungar, D., Oka, T., Krieger, M., and Hughson, F. M. (2006). Retrograde Transport on the COG Railway. *Trends Cel Biol* 16, 113–120. doi:10.1016/j.tcb.2005.12.004

Whyte, J. R., and Munro, S. (2001). The Sec34/35 Golgi Transport Complex Is Related to the Exocyst, Defining a Family of Complexes Involved in Multiple Steps of Membrane Traffic. *Dev. Cel* 1, 527–537. doi:10.1016/s1534-5807(01)00063-6

Willett, R. A., Pokrovskaya, I. D., and Lupashin, V. V. (2013a). Fluorescent Microscopy as a Tool to Elucidate Dysfunction and Mislocalization of Golgi Glycosyltransferases in COG Complex Depleted Mammalian Cells. *Methods Mol. Biol. Clifton NJ* 1022, 61–72. doi:10.1007/978-1-62703-465-4_6

Willett, R., Kudlyk, T., Pokrovskaya, I., Schönherr, R., Ungar, D., Duden, R., et al. (2013b). COG Complexes Form Spatial Landmarks for Distinct SNARE Complexes. *Nat. Commun.* 4, 1553. doi:10.1038/ncomms2535

Willett, R., Ungar, D., and Lupashin, V. (2013c). The Golgi Puppet Master: COG Complex at center Stage of Membrane Trafficking Interactions. *Histochem. Cel Biol.* 140, 271–283. doi:10.1007/s00418-013-1117-6

Wolthuis, D. F. G. J., Janssen, M. C., Cassiman, D., Lefeber, D. J., Morava, E., and Morava-Kozicz, E. (2014). Defining the Phenotype and Diagnostic Considerations in Adults with Congenital Disorders of N-Linked Glycosylation. *Expert Rev. Mol. Diagn.* 14, 217–224. doi:10.1586/14737159.2014.890052

Xia, Z.-J., Zeng, X.-X. I., Tambe, M., Ng, B. G., Dong, P. D. S., and Freeze, H. H. (2021). A Single Heterozygous Mutation in COG4 Disrupts Zebrafish Early Development via Wnt Signaling. *bioRxiv*, 443307. doi:10.1101/2021.05.23.443307

Zafra, I., Nebenfuehr, B., and Golden, A. (2021). Saul-Wilson Syndrome Missense Allele Does Not Show Obvious Golgi Defects in a *C. elegans* Model. *Micropublication Biol.* 2021. Available at: https://www.micropublication.org/journals/biology/micropub-biology-000373/ (Accessed June 20, 2021).

Zhang, Y. C., Zhou, Y., Yang, C. Z., and Xiong, D. S. (2009). A Review of ERGIC-53: its Structure, Functions, Regulation and Relations with Diseases. *Histol. Histopathol.* 24, 1193–1204. doi:10.14670/HH-24.1193

Zolov, S. N., and Lupashin, V. V. (2005). Cog3p Depletion Blocks Vesicle-Mediated Golgi Retrograde Trafficking in HeLa Cells. *J. Cel Biol.* 168, 747–759. doi:10.1083/jcb.200412003

Conflict of Interest: The authors declare that the research was conducted in the absence of any commercial or financial relationships that could be construed as a potential conflict of interest.

Publisher's Note: All claims expressed in this article are solely those of the authors and do not necessarily represent those of their affiliated organizations, or those of the publisher, the editors and the reviewers. Any product that may be evaluated in this article, or claim that may be made by its manufacturer, is not guaranteed or endorsed by the publisher.

frontiers in Pediatrics

BRIEF RESEARCH REPORT
published: 11 October 2021
doi: 10.3389/fped.2021.717864

Stroke-Like Episodes in PMM2-CDG: When the Lack of Other Evidence Is the Only Evidence

Mercedes Serrano [1,2]*

[1] Department of Neuropediatric, Institut de Recerca Hospital Sant Joan de Déu, Barcelona, Spain, [2] U-703 Center for Biomedical Research on Rare Diseases (CIBER-ER), Hospital Sant Joan de Déu, Instituto de Salud Carlos III, Barcelona, Spain

Phosphomannomutase 2 deficiency (PMM2-CDG) is the most frequent congenital disorder of glycosylation. PMM2-CDG patients develop chronic cerebellar atrophy as a neurological hallmark. However, other acute neurological phenomena such as stroke-like episodes (SLE), epilepsy, migraine, and cerebrovascular events, may also occur, and they are frequently the cause of disability and impaired quality of life. Among these, SLE are among the most stressful situations for families and doctors, as their risk factors are not known, their underlying pathomechanisms remain undiscovered, and clinical guidelines for diagnosis, prevention, and treatment are lacking. In this paper, the recent SLE experiences of two PMM2-CDG patients are examined to provide clinical clues to help improve diagnosis through a clinical constellation of symptoms and a clinical definition, but also to support a neuroelectrical hypothesis as an underlying mechanism. An up-to-date literature review will help to identify evidence-based and non-evidence-based management recommendations. Presently neuropediatricians and neurologists are not capable of diagnosing stroke-like episodes in an unequivocal way, so there is still a need to perform invasive studies (to rule out other acute diseases) that may, in the end, prove unnecessary or even harmful. However, reaching a correct and early diagnosis would lead not only to avoidance of invasive tests but also to better recognition, management, and understanding of the disease itself. There is a great need for understanding of SLE that may ultimately be very informative for the detection of patients at risk, and the future development of preventive and management measures.

Keywords: channelopathies, congenital disorders of glycosylation, *CACNA1A*, PMM2-CDG, stroke-like, coma

OPEN ACCESS

Edited by:
Aleksandra Jezela-Stanek, National Institute of Tuberculosis and Lung Diseases, Poland

Reviewed by:
Magdalena Sandu, Spitalul Clinic de Copii Doctor Victor Gomoiu, Romania
Justyna Paprocka, Medical University of Silesia, Poland

***Correspondence:**
Mercedes Serrano
mserrano@hsjdbcn.org

Specialty section:
This article was submitted to Genetics of Common and Rare Diseases, a section of the journal Frontiers in Pediatrics

Received: *31 May 2021*
Accepted: *17 September 2021*
Published: *11 October 2021*

Citation:
Serrano M (2021) Stroke-Like Episodes in PMM2-CDG: When the Lack of Other Evidence Is the Only Evidence. Front. Pediatr. 9:717864. doi: 10.3389/fped.2021.717864

INTRODUCTION

Congenital disorders of glycosylation (CDG) are a rapidly expanding group of metabolic disorders with defects in the synthesis of glycans and their attachment to proteins and lipids. To date, over 150 CDG types have been described (1). PMM2-CDG (MIM# 212065), caused by *PMM2* mutations, is by far the most frequent congenital disorder of N-linked glycosylation, with more than 900 patients in the literature (2).

PMM2-CDG patients develop cerebellar atrophy and a chronic cerebellar syndrome (3, 4). However, other acute neurological phenomena such as stroke-like episodes (SLE), epilepsy, migraine, movement disorders, and cerebrovascular events, may also occur (5–13), and they

are frequently the cause of disability and impaired quality of life. Among these, SLEs are particularly stressful for families and doctors, as their risk factors are not known, their underlying pathomechanisms remain undiscovered, and clinical guidelines for diagnosis, prevention and treatment are lacking (5–12).

The term SLE was initially coined for MELAS syndrome to stress its non-ischemic origin (14) but it has been used for different neurological diseases associated with focal deficits that mimick, clinically but not neuroradiologically, an ischemic injury. This is the case of PMM2-CDG and some channelopathies related to *CACNA1A*, *ATP1A2*, and *SCN1A* mutations, leading to episodes called familial hemiplegic migraine (FHM). FHM is, actually, very similar clinically to SLE, as episodes are triggered by metabolic stress or cranial trauma, they present after a symptom-free period, and they progress to irritability, somnolence, focal deficits with hyperpyrexia, and, frequently epileptic seizures, eventually ending in clinical resolution after a period of time from hours to days (8, 12, 15, 16). These clinical resemblances may correspond to common biological disturbances, as was recently demonstrated through the experimental generation of impaired N-glycosylation at the $Ca_V2.1$ (encoded by *CACNA1A*); impaired N-glycosylation led to a gain-of-function on the $Ca_V2.1$ channel (8), similar to those mutations causing FHM (17, 18).

Historically, it has been hypothesized that SLE have a vascular origin, due to the frequent abnormalities in coagulation in CDG patients (13, 19). However, many clinical and neuroradiological features of SLE remain unexplained, while the vascular hypothesis and several symptoms are incongruous.

In this paper, the recent SLE experiences of two PMM2-CDG patients that were exhaustively evaluated during the episodes and who were able to communicate their symptoms are described. These experiences, together with an up-to-date literature review, will provide clinical clues to help improve diagnosis through a proposed clinical constellation of symptoms. A literature review will help to identify evidence-based management recommendations, and the vascular and neuroelectrical hypotheses will be discussed as potential underlying mechanisms in SLE.

METHOD

Two patients with confirmed PMM2-CDG and suffering SLE episodes during the previous 24 months were evaluated. The episodes of each fulfilled the following SLE definition: "Acute event consisting of sudden onset of a focal neurological deficit, irritability or decreased consciousness that may associate with seizures, headache or other transient symptoms, in the absence of another diagnosis explaining these symptoms" (8).

Personal direct interview with the patients during the episodes, serial neurological evaluations, laboratory tests, cranial magnetic resonance (MRI) images, and videoelectroencephalogram (video-EEG) were performed during the acute phase of the SLE. MRI was performed with a 1.5 or 3 T scanner (GE Healthcare, Milwaukee, WI, USA or similar). The MRI clinical protocol and sequences included anatomical T1-weighted, T2 weighted fast spin-echo Images, fast-spin echo with fluid-attenuated inversion recovery (FLAIR) coronal, and diffusion weighted images (DWI). VideoEEG recordings were made with plate electrodes fixed on the scalp via "10–20 International System", and using a digital system with monopolar and differential fittings, which also provides track visualization after recording.

Written informed consent for publication was obtained from the parents and the adult patient, and assent was obtained from the adolescent patient.

For the literature review a search in PubMed for articles on PMM2, PMM2-CDG, CDG-Ia, congenital disorders of glycosylation, and stroke-like as search terms, was performed, from January 1, 1982, and May 29, 2021, with different combinations of the terms.

CASE REPORTS

Subject 1

An 11-year-old girl affected by PMM2-CDG (P113L/P113L) was taken to the emergency department for refractory fever up to 39°C of 36 h evolution, along with vomiting and low oral intake. Blood and urine tests were uninformative and the process was cataloged as a viral infectious one causing gastroenteritis.

Eight hours later, despite ibuprofen therapy, the hyperthermia persisted, and the patient suffered a left-sided headache, somnolence, right-arm monoparesis, and particular difficulties in denomination. The patient returned to the emergency department, and, despite suspicion of an SLE, due to febrile neurological symptoms, a ruling-out protocol for treatable disorders was applied. Cranial tomography and MRI scan (**Figure 1**) were performed, showing no abnormalities on supratentorial structures and demonstrating the expected cerebellar atrophy. Coagulation tests were normal. Lumbar puncture was initially planned but 3 h later, the patient showed improvement, with a normalization of body temperature, increased right arm strength (4/5), normal alertness, and disappearance of the headache. During the next 24 h, the clinical situation oscillated, with limited periods of left-side intense headache associated with coincident worsening of right-arm monoparesis. The MRI obtained at 18 h from the first motor symptoms included T1- and T2-weighted images and FLAIR, DWI, and an arterial and venous angiographic study. There was no abnormal finding other than the cerebellar atrophy. Video-EEG was performed, showing asymmetric slow brain activity with delta waves predominantly in the left hemisphere [see **Figure 2** showing left temporal intermittent rhythmic delta waves of short duration resembling TIRDA (temporal intermittent rhythmic delta activity)] and theta rhythms predominantly in the right, as well as low voltage beta rhythms, with a diffuse distribution. No paroxysms were recorded. This episode was the first acute neurological event for this patient.

Fourteen months later, at the age of 13, she suffered a head trauma. Fifteen minutes after the head contusion she showed left arm paresis and incoherent speech followed by a progression of the paresis, reaching the left leg. She began with headache, vomiting, and increasing irritability. At the emergency room she received a total dose of 15 mg of midazolam (5 mg intramuscular,

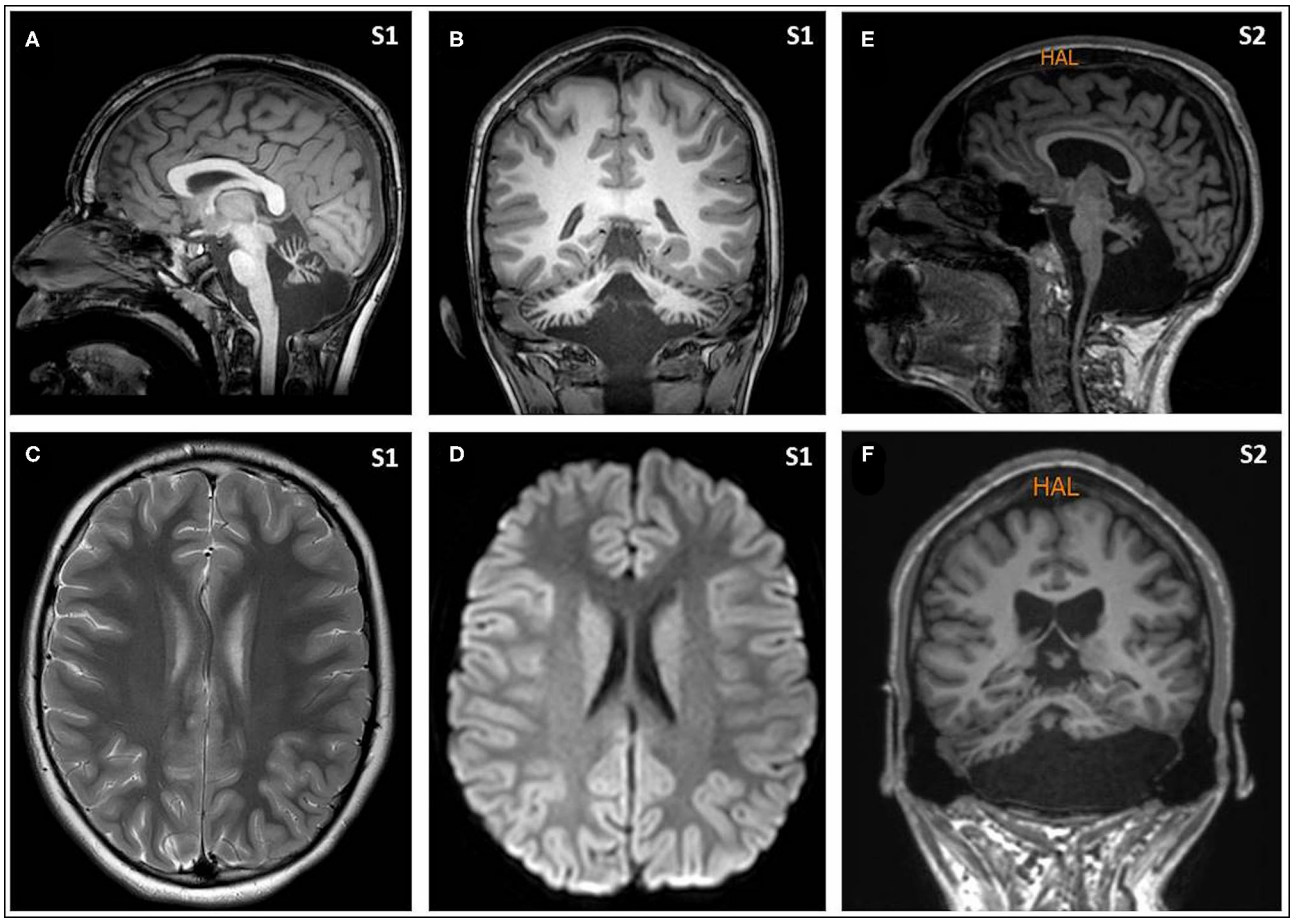

FIGURE 1 | Magnetic resonance imaging (MRI) from Subjects included T1- and T2-weighted images and FLAIR, diffusion weighted images, and an arterial and venous angiographic study, performed with a 3 T and 1.5 T scanners, respectively. There was no abnormal finding other than the cerebellar atrophy. Sagittal [**(A)** from Subject 1, and **(E)** from Subject 2] and coronal images [**(B)** from Subject 1, and **(F)** from Subject 2] show the small cerebellar vermis with enlarged interfolial spaces representing atrophy and secondary enlargement of the fourth ventricle. Axial supratentorial images **(C)**, including diffusion weighted images **(D)**, from Subject 1 show no other abnormalities.

10 mg intranasal), and a CT scan was performed, showing no supratentorial abnormalities. Six hours after the head trauma, physical exploration was normal, headache had disappeared, and the patient had coherent speech but with slowed thought and response. Eighteen hours after the beginning of SLE the patient was discharged with no abnormal findings compared to her baseline physical exploration. In recent months she has been receiving topiramate (50 mg every 12 h) to control behavioral disturbances. Topiramate was chosen to take advantage of the resemblance of its mechanism of action to that of acetazolamide (20), recently used in a clinical trial for PMM2-CDG (21).

Subject 2

A 24-year-old young man affected by PMM2-CDG (V44A/R141H) went to the emergency room with intense right-side migraine, propulsive vomiting, photophobia, and, on physical examination, a left hemiparesis. At the outset of the episode with the initiation of the right-side headache, the patient reported a fluctuation of strength on his left side; when he was recovering strength in the lower limb he noted a worsening in the upper limb. No decrease in consciousness or epileptic seizures was detected upon initial examination at the emergency room. However some hours later the patient showed confusion, irritability, and a decrease in alertness. As with Subject 1, lab tests were normal, neuroimaging showed the already known cerebellar atrophy, and video EEG showed right-hemispheric slow brain activity. The full episode lasted approximately 12 hours; the patient was given analgesics (ketorolac and metamizol) and antiemetics (metoclopramide) during the hospitalization.

From infancy the patient had presented with recurrent episodes of somnolence and irritability of several hours' duration, triggered in particular by infection and with associated hyperthermia and epileptic seizures. Antiepileptic treatment with carbamazepine was initiated at 2 years of age and continued until the age of fourteen, after which levetiracetam was prescribed and maintained until the age of eighteen, but it did not seem to prevent SLE recurrence. There was no increase in the rate of occurrence after antiepileptic drug withdrawal. On the contrary,

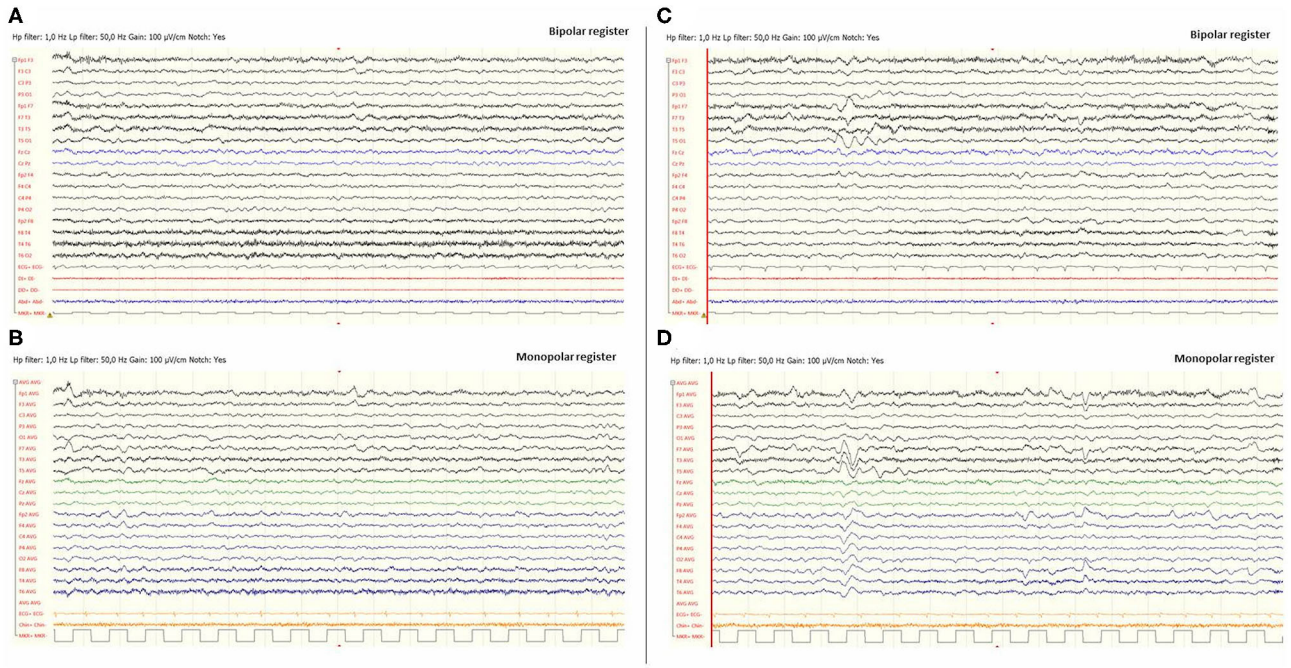

FIGURE 2 | Video-EEG performed during the first episode of Subject 1. EEG was done 12 h after the beginning of the focal deficit and once midazolam had been administered. The EEG was acquired with the eyes open and the patient being awake. EEG showed slow brain activity with subtle asymmetries, delta waves predominantly in the left hemisphere and theta rhythms predominantly in the right [left images **(A)** and **(B)**]. No paroxysms were recorded. Images **(C)** and **(D)**, on the right, include EEG register fragments that show some left temporal intermittent rhythmic delta waves of short duration resembling TIRDA (temporal intermittent rhythmic delta activity).

the family reported a subsequent increase in alertness and attention skills.

From adolescence the stroke-like episodes presented with a frequency of one to three times per year and were triggered mainly by heat and dehydration or emotional stress. They were characterized mainly by one-side intense headache with somnolence and irritability, but without epileptic seizures. The fluctuations in strength described in this last episode were previously experienced by the patient and he explained that they occurred for 2–3 h at a time. Headache similarly affected both sides during the different episodes. Motor deficits always presented opposite to the migraine location, and sometimes involved the tongue and mouth movement. The family reported affected speech and denomination when the migraine affected the left side. At the present time the patient is not receiving any pharmacological therapy but the parents limit his exposure to sun and heat and offer him frequent hydrating beverages. He has presented no additional episodes of SLE in the last 18 months.

DISCUSSION

Clinical situations described in the present report, including experiences of patients in their own voice and exhaustive clinical evaluations, allow us to probe deeper into the phenomenology of SLE, one of the most stressful acute situations for families living with PMM2-CDG.

Remarkably, although it has been reported that up to 50% of PMM2-CDG patients may suffer at least one episode (6, 7), only a few papers on SLE in CDG are indexed in PubMed and there are no cohorts of SLE in PMM2-CDG patients other than a couple of short series (8, 9). Moreover, that SLE is restricted to PMM2-CDG is uncertain, since families of other types of CDG patients share similar episodes as evidenced on social networks and meetings (data unpublished).

SLE are little-known events occurring in a very rare condition, they have been scarcely published and they are probably underdiagnosed. A limitation of the present study is the description of SLE episodes suffered by two patients. However, despite the sample size, this is the first time that a first-person description, including the patients' voice, and the interesting finding of a fluctuation and coincidence of a constellation of symptoms are reported, leading to new mechanistic hypothesis.

SLE are characterized by a confused mental state, focal deficits (mono- or hemiparesis, dysphagia, amaurosis, etc.), hyperthermia, epileptic seizures, and severe encephalopathy in some cases (5, 8–12). Full recovery is expected in most cases in the following days; however, long-term sequelae have also been reported (5, 6, 8, 9, 12).

SLE can present at any age, and seem to occur independently of the clinical global severity (8, 12). Interestingly, recurrent SLE can be the only manifestation of an otherwise asymptomatic child with PMM2-CDG, as has recently been reported (12). Preliminary studies of epidemiological, clinical, laboratory, and

neuroimaging findings revealed no differences between PMM2-CDG patients with SLE and those without, and in terms of the genotype, all the pathogenic variants were distributed among both groups (5, 8–12).

In the scientific literature, there are two main trigger factors for SLEs in PMM2-CDG: head trauma and infection (5, 8–12). The role of both conditions in triggering encephalopathic episodes is also described in other inborn errors of metabolism, as well as some channelopathies (14, 15). However the mechanism whereby the mechanical stimulus or the metabolic stress precipitates an SLE is unknown. Although head trauma is a common situation in children with ataxia and hypotonia, due to clumsiness, why only some PMM2-CDG patients develop SLE after cranial trauma is currently unknown.

Unfortunately, there is no specific constellation of clinical symptoms or biomarker that unequivocally characterizes SLE. Clinical, radiological, and electrophysiological findings [including hemispheric EEG diffuse slowing (8–10, 13)] are unspecific and routine lab studies are not informative. Frequently, families suggest the diagnosis to the emergency doctor, so that they can contact the referring doctors, who, however, cannot offer evidence-based clinical guidelines for the management of SLE. Both clinicians and families need accessible and contrasted information.

Due to the absence of positive markers supporting the diagnosis, clinicians are obliged to perform all the tests to rule out treatable disorders, such as central nervous system infections or vascular events, requiring invasive studies such as lumbar puncture and neuroimaging under sedation that may in the end prove unnecessary and sometimes dangerous for the SLE, as has been described (5). Altogether, the scarce scientific evidence and the complex differential diagnosis lead to an absence or a delay in the diagnosis, hindering our knowledge about the real incidence of SLE.

Refractory hyperpyrexia has been described as associated consistently with SLE, probably due to a central origin, as it is often not correlated with inflammatory parameters such as PCT or PCR, or increase in white blood cells (7, 8, 12), and may be refractory to common antipyretics such as ibuprofen and paracetamol (acetaminophen).

The coexistence of migraine, focal neurologic deficits, hemispheric slow EEG trace and refractory hyperpyrexia without laboratory signs of infection make up a characteristic but unspecific tetrad (5, 7–12). In this difficult clinical context, both for diagnosis, but also for the challenging task of increasing scientific knowledge, the use of an accepted clinical definition probes essential (8).

Concerning treatment, there are no evidence-based management guidelines, other than symptomatic measures like antiepileptic drugs, for which concrete publications report an improvement in both seizures and focal deficits (8, 9) similar to that experienced by Subject 1. In this respect, the phenomenology of the SLE described here in which the patients referred a fluctuant headache coincident with a worsening of the motor paresis reinforces the idea of an electric basis for the pathogenesis of SLE and supports the use of antiepileptic drugs. With PMM2-CDG, Dinopoulos' group was the first to indicate the possibility of hemiparesis caused by an active epileptic inhibitory process, supported by EEG findings in three patients during SLE and suggesting, accordingly, anticonvulsant agents for SLE management. The three patients received intravenous lorazepam (0.1–0.2 mg/kg) with an improvement in the EEG recording of one of the patients shortly after administration (9). In our experience, we have seen positive responses to midazolam, as in Subject 1. Although larger samples of patients with SLE in PMM2-CDG are needed to support an evidence-based recommendation, the use of lorazepam or midazolam seems advisable. In addition, the possibility to perform both repeated video-EEG and MRI, from the early detection or suspicion of SLE, before and after the antiepileptic drug administration and later during the SLE resolution, could detect unreported abnormalities and also shed light on the underlying pathophysiology and the best practices for therapeutic management.

As noted above, the term SLE was initially coined for MELAS syndrome (14), stressing its non-ischemic origins. In MELAS, these events are probably explained by an energy failure and the nitric oxide precursor L-arginine seems to exhibit a beneficial effect on the extension, progression, duration, and outcome of a SLE (22). But SLE has also been used for different acute neurological events clinically but not neuroradiologically mimicking an ischemic injury. The events called FHM related to *CACNA1A*, *ATP1A2*, and *SCN1A* mutations are an example of this (15, 16); clinically they are similar to SLE related to PMM2-CDG and hence, FHM should be in the complex differential diagnosis as reported recently (12). In FHM events it is known that there are underlying electric mechanisms; an inhibitory cortical transmission called "cortical spreading depression" (17). In the FHM murine model, a decreased triggering threshold for cortical spreading depression has been demonstrated (23). In FHM, hemispheric EEG abnormalities, similar to those found in PMM2-CDG SLE (8), have been reported (15, 16). Interestingly, the cortical depression mechanism is also the basis of the migraine pathogenesis (24), explaining the hemispheric electric EEG abnormalities, but also the one-sided headache.

During the acute episodes of SLE and FHM, there are clinical, electrophysiological, and neuroradiological similarities. Episodes in both conditions (i) may be triggered by head traumatisms, (ii) may present after a period free of symptoms, (iii) hyperthermia is frequent (with the absence of any sign of infection in blood or CSF), (iv) abnormal EEG findings may be present, and finally, (v) hemispheric vasogenic edema may occur (8, 15). Interestingly, chronically speaking, clinical, neuroimaging, and neurophysiological features of PMM2-CDG and *CACNA1A* related phenotypes are also similar, including, ataxia, ocular motor disturbances (particularly nystagmus and tonic upgaze deviation), and progressive cerebellar atrophy (3, 8, 25).

Finally, there are also similarities from the pharmacological point of view. Acetazolamide has been used in CACNA1A patients to prevent FHM (26), and a recently designed non-commercial clinical trial using acetazolamide in PMM2-CDG to improve cerebellar syndrome also showed improvement in a treated patient who suffered from almost weekly SLE episodes together with migraine. The patient saw a disappearance of SLE at the beginning of acetazolamide treatment, which returned when the therapy was discontinued following the protocol (21).

In the search for the biological link between PMM2-CDG and FHM, there is some evidence, using experimental generation of impaired N-glycosylation at *CACNA1A* channel and evaluating the subsequent gating abnormalities, that impaired N-glycosylation leads to a gain-of-function on CACNA1A channel, similar to mutations causing FHM (8).

For many years the most widely accepted hypothesis for the pathogenesis of SLE in PMM2-CDG was based on the high frequency of coagulation abnormalities and the very prevalent vascular events (2, 13, 19). However, no significant correlations have been found in a number of studies between the presence of abnormal coagulation and occurrence of SLE (8–12). Furthermore, the majority of patients with SLEs (i) do not show vascular occlusion on magnetic resonance angiography, (ii) have edema images that are not congruent with a cytotoxic edema, but rather a vasogenic edema, (iii) do not follow well-defined vascular territories on brain magnetic resonance images (MRI), and (iv) have lesions that do not reveal restricted diffusion in DWI (signal-intensity changes can be detected within minutes of arterial occlusion with DWI) (8–12). Moreover, the pathomechanisms suggested such as hypoperfusion or ischemia do not explain the nature and temporal course of neuronal dysfunction (8–12).

Despite this lack of evidence, anti-aggregants such as aspirin have been widely used in the attempt to prevent recurrence of SLE, without a scientifically sound basis and running the risk of iatrogenesis while also increasing the risk of developing a bleeding complication. In some patients reported, the use of anti-aggregant doses of aspirin did not prevent the recurrence of SLE (7, 12).

To further complicate matters, from the clinical point of view, the differential diagnosis between SLE, epileptic seizures, a real cerebrovascular event, and a migraine with aura (all prevalent in this group of patients) is a real challenge in PMM2-CDG patients. Moreover, there is a well-studied overlap of biological mechanisms and a known comorbidity among vascular stroke, epilepsy, and migraine (27, 28), since they may share some pathogenic mechanisms.

Head trauma triggering is common not only to channelopathies such as CACNA1A (15, 16), but also to other rare neurological conditions such as vanishing white matter disease (29), and it does not seem to be completely explained merely by a metabolically stressful situation. As occurred in the second SLE of our Subject 1, head trauma is a known trigger for SLE (5, 8, 12), but interestingly, SLE-related neurological symptoms start after a symptom-free interval ranging between one and 24 h (8). Neurons have mechanoreceptors capable of transducing mechanical forces, some of which are N-glycosylated, and abnormalities in N-glycosylation have been proven to alter their functions (30). But after the mechanical stimulus, the symptom-free period reported in these patients points toward the generation of a cascade of changes in the brain until it affects the whole neurological clinical picture, which probably involves the modification of expression of several genes. If this is the case, knowledge of this cascade will discover to us how to treat SLE and prevent progression from a mechanistic point of view.

In conclusion, there is a characteristic but unspecific tetrad of symptoms made up of migraine, focal neurologic deficits, hemispheric slow EEG trace and refractory hyperpyrexia without laboratory signs of infection. However, for clinicians there is an urgent need to positively and unequivocally detect SLE episodes in the group of patients at risk, and based not merely on the ruling out of other acute neurological processes. Invasive studies such as lumbar puncture and neuroimaging under sedation often prove unnecessary and sometimes dangerous for the SLE evolution.

At the present time there is a lack of sound scientific evidence to categorically affirm what the underlying mechanisms beneath SLE are, and therefore evidence-based recommendations for management are very limited, but there is some biological and clinical evidence supporting the use of antiepileptic drugs such as the benzodiazepines lorazepam and midazolam.

Scientific knowledge is still lacking concerning the needs of patients and their families at risk of SLE; a very prevalent and stressful clinical situation that needs to be urgently addressed by researchers.

DATA AVAILABILITY STATEMENT

The original contributions presented in the study are included in the article/supplementary material, further inquiries can be directed to the corresponding author.

ETHICS STATEMENT

The studies involving human participants were reviewed and approved by CEIC Fundació Sant Joan de Déu. Written informed consent to participate in this study was provided by the participants' legal guardian/next of kin. Written informed consent was obtained from the minor(s)' legal guardian/next of kin for the publication of any potentially identifiable images or data included in this article.

AUTHOR CONTRIBUTIONS

MS conceptualized and designed the text, drafted the initial manuscript, and reviewed and revised the manuscript.

FUNDING

PMM2-CDG research was supported by National Grants PI14/00021, PI17/00101, and PI21/00068 from the National Plan on I+D+I, cofinanced by ISCIII (Subdirección General de Evaluación y Fomento de la Investigación Sanitaria) and FEDER (Fondo Europeo de Desarrollo Regional). MS research work was supported by a grant from the Generalitat de Catalunya (PERIS SLT008/18/00194).

ACKNOWLEDGMENTS

I thank the patients and patients' families for their collaboration and consent. I want to acknowledge the help of Dr. Valera-Dávila with the EEG evaluation.

REFERENCES

1. Ng BG, Freeze HH. Perspectives on glycosylation and its congenital disorders. *Trends Genet.* (2018) 34:466–76. doi: 10.1016/j.tig.2018.03.002
2. Altassan R, Péanne R, Jaeken J, Barone R, Bidet M, Borgel D, et al. International clinical guidelines for the management of phosphomannomutase 2-congenital disorders of glycosylation: Diagnosis, treatment and follow up. *J Inherit Metab Dis.* (2019) 42:5–28. doi: 10.1002/jimd.12024
3. de Diego V, Martínez-Monseny AF, Muchart J, Cuadras D, Montero R, Artuch R, et al. Longitudinal volumetric and 2D assessment of cerebellar atrophy in a large cohort of children with phosphomannomutase deficiency (PMM2-CDG). *J Inherit Metab Dis.* (2017) 40:709–13. doi: 10.1007/s10545-017-0028-4
4. Serrano NL, De Diego V, Cuadras D, Martinez Monseny AF, Velázquez-Fragua R, López L, et al. A quantitative assessment of the evolution of cerebellar syndrome in children with phosphomannomutase deficiency (PMM2-CDG). *Orphanet J Rare Dis.* (2017) 12:155. doi: 10.1186/s13023-017-0707-0
5. Barone R, Carrozzi M, Parini R, Battini R, Martinelli D, Elia M, et al. A nationwide survey of PMM2-CDG in Italy: high frequency of a mild neurological variant associated with the L32R mutation. *J Neurol.* (2015) 262:154–64. doi: 10.1007/s00415-014-7549-7
6. Kjaergaard S, Schwartz M, Skovby F. Congenital disorder of glycosylation type Ia (CDG-Ia): phenotypic spectrum of the R141H/F119L genotype. *Arch Dis Child.* (2001) 85:236–39. doi: 10.1136/adc.85.3.236
7. Schiff M, Roda C, Monin ML, Arion A, Barth M, Bednarek N, et al. Clinical, laboratory and molecular findings and long-term follow-up data in 96 French patients with PMM2-CDG (phosphomannomutase 2-congenital disorder of glycosylation) and review of the literature. *J Med Genet.* (2017) 54:843–51. doi: 10.1136/jmedgenet-2017-104903
8. Izquierdo-Serra M, Martínez-Monseny AF, López L, Carrillo-García J, Edo A, Ortigoza-Escobar JD, et al. Stroke-like episodes and cerebellar syndrome in PMM2-CDG: evidence for hypoglycosylation-driven channelopathy. *Int J Mol Sci.* (2018) 19:619. doi: 10.3390/ijms19020619
9. Dinopoulos A, Mohamed I, Jones B, Rao S, Franz D. deGrauw T. Radiologic and neurophysiologic aspects of stroke-like episodes in children with congenital disorders of glycosylation type-1a. *Pediatrics.* (2007) 119:768–72. doi: 10.1542/peds.2006-0763
10. Ishikawa N, Tajima G, Ono H, Kobayashi M. Different neuroradiological findings during two stroke-like episodes in a patient with a congenital disorder of glycosylation type Ia. *Brain Dev.* (2009) 31:240–3. doi: 10.1016/j.braindev.2008.03.012
11. Miossec-Chauvet E, Mikaeloff Y, Heron D, Merzoug V, Cormier-Daire V, de Lonlay P, et al. Neurological presentation in pediatric patients with congenital disorders of glycosylation type Ia. *Neuropediatrics.* (2003) 34:1–6. doi: 10.1055/s-2003-38614
12. Farmania R, Jain P, Sharma S, Aneja S. Unusual presentation of PMM2-congenital disorder of glycosylation with isolated strokelike episodes in a young girl. *J Child Neurol.* (2019) 34:410–4. doi: 10.1177/0883073819833543
13. Arnoux JB, Boddaert N, Valayannopoulos V, Romano S, Bahi-Buisson N, Desguerre I, et al. Risk assessment of acute vascular events in congenital disorder of glycosylation type Ia. *Mol Genet Metab.* (2008) 93:444–9. doi: 10.1016/j.ymgme.2007.11.006
14. Sproule DM, Kaufmann P. Mitochondrial encephalopathy, lactic acidosis, and strokelike episodes: basic concepts, clinical phenotype, and therapeutic management of MELAS syndrome. *Ann N Y Acad Sci.* (2008) 1142:133–58. doi: 10.1196/annals.1444.011
15. Hart AR, Trinick R, Connolly DJ, Mordekar SR. Profound encephalopathy with complete recovery in three children with familial hemiplegic migraine. *J Paediatr Child Health.* (2009) 45:154–7. doi: 10.1111/j.1440-1754.2009.01465.x
16. Malpas TJ, Riant F, Tournier-Lasserve E, Vahedi K, Neville BG. Sporadic hemiplegic migraine and delayed cerebral oedema after minor head trauma: a novel de novo CACNA1A gene mutation. *Dev Med Child Neurol.* (2010) 52:103–4. doi: 10.1111/j.1469-8749.2009.03493.x
17. Vecchia D, Tottene A, van den Maagdenberg AM, Pietrobon D. Mechanism underlying unaltered cortical inhibitory synaptic transmission in contrast with enhanced excitatory transmission in CaV2. *1 knockin migraine mice Neurobiol Dis.* (2014) 69:225–34. doi: 10.1016/j.nbd.2014.05.035
18. Tottene A, Fellin T, Pagnutti S, Luvisetto S, Striessnig J, Fletcher C, et al. Familial hemiplegic migraine mutations increase Ca(2+) influx through single human CaV2. 1 channels and decrease maximal CaV21 current density in neurons. *Proc Natl Acad Sci U S A.* (2002) 99:13284–9. doi: 10.1073/pnas.192242399
19. Linssen M, Mohamed M, Wevers RA, Lefeber DJ, Morava E. Thrombotic complications in patients with PMM2-CDG. *Mol Genet Metab.* (2013) 109:107–11. doi: 10.1016/j.ymgme.2013.02.006
20. Supuran CT. An update on drug interaction considerations in the therapeutic use of carbonic anhydrase inhibitors. *Expert Opin Drug Metab Toxicol.* (2020) 16:297–307. doi: 10.1080/17425255.2020.1743679
21. Martínez-Monseny AF, Bolasell M, Callejón-Póo L, Cuadras D, Freniche V, Itzep DC, et al. AZATAX: Acetazolamide safety and efficacy in cerebellar syndrome in PMM2 congenital disorder of glycosylation (PMM2-CDG). *Ann Neurol.* (2019) 85:740–51. doi: 10.1002/ana.25457
22. Koga Y, Povalko N, Inoue E, Nakamura H, Ishii A, Suzuki Y, et al. Therapeutic regimen of L-arginine for MELAS: 9-year, prospective, multicenter, clinical research. *J Neurology*. (2018) 265:2861–74. doi: 10.1007/s00415-018-9057-7
23. Dehghani A, Karatas H. Mouse models of familial hemiplegic migraine for studying migraine pathophysiology. *Curr Neuropharmacol.* (2019) 17:961–73. doi: 10.2174/1570159X17666190513085013
24. Choudhuri R, Cui L, Yong C, Bowyer S, Klein RM, Welch KM, et al. Cortical spreading depression and gene regulation: relevance to migraine. *Ann Neurol.* (2002) 51:499–506. doi: 10.1002/ana.10158
25. Izquierdo-Serra M, Fernández-Fernández JM, Serrano M. Rare CACNA1A mutations leading to congenital ataxia. *Pflugers Arch.* (2020) 472:791–809. doi: 10.1007/s00424-020-02396-z
26. Pelzer N, Stam AH, Haan J, Ferrari MD, Terwindt GM. Familial and sporadic hemiplegic migraine: diagnosis and treatment. *Curr Treat Options Neurol.* (2013) 15:13–27. doi: 10.1007/s11940-012-0208-3
27. Kurth T, Chabriat H, Bousser MG. Migraine and stroke: a complex association with clinical implications. *Lancet Neurol.* (2012) 11:92–100. doi: 10.1016/S1474-4422(11)70266-6
28. Keezer MR, Bauer PR, Ferrari MD, Sander JW. The comorbid relationship between migraine and epilepsy: a systematic review and meta-analysis. *Eur J Neurol.* (2015) 22:1038–47. doi: 10.1111/ene.12612
29. van der Knaap MS, Pronk JC, Scheper GC. Vanishing white matter disease. *Lancet Neurol.* (2006) 5:413–23. doi: 10.1016/S1474-4422(06)70440-9
30. Li J, Ng CA, Cheng D, Cox CD. Modified N-Linked Glycosylation Status Predicts Trafficking Defective Piezo1 Channel Mutations. *Biophysical J.* (2021) 120:p236a−237a. doi: 10.1016/j.bpj.2020.11.1562

Conflict of Interest: The author declares that the research was conducted in the absence of any commercial or financial relationships that could be construed as a potential conflict of interest.

frontiers in Genetics

ORIGINAL RESEARCH
published: 01 December 2021
doi: 10.3389/fgene.2021.737094

SRD5A3-CDG: Emerging Phenotypic Features of an Ultrarare CDG Subtype

Nazreen Kamarus Jaman[1†], Preeya Rehsi[1†], Robert H. Henderson[2,3], Ulrike Löbel[4], Kshitij Mankad[4] and Stephanie Grunewald[1,5]*

[1]Metabolic Department, Great Ormond Street Hospital NHS Foundation Trust, London, United Kingdom, [2]Ophthalmology Department, Great Ormond Street Hospital, London, United Kingdom, [3]Ophthalmology Department, Moorfields Eye Hospital, London, United Kingdom, [4]Department of Radiology, Great Ormond Street Hospital for Children, London, United Kingdom, [5]Institute for Child Health, NIHR Biomedical Research Center (BRC), University College London, London, United Kingdom

Background: SRD5A3-CDG is a rare N-glycosylation defect caused by steroid 5 alpha reductase type 3 deficiency. Its key feature is an early severe visual impairment with variable ocular anomalies often leading to diagnosis. Additional symptoms are still poorly defined. In this case study, we discuss 11 genetically confirmed cases, and report on emerging features involving other systems in addition to the eye phenotype.

Methods: In total, 11 SRD5A3-CDG patients in five sets of sibships were included in the study. Data on 9 of 11 patients are as of yet unpublished. Patients' results on biochemical and genetic investigations and on in-depth phenotyping are presented.

Results: Key diagnostic features of SRD5A3-CDG are ophthalmological abnormalities with early-onset retinal dystrophy and optic nerve hypoplasia. SRD5A3-CDG is also characterized by variable neurological symptoms including intellectual disability, ataxia, and hypotonia. Furthermore, ichthyosiform skin lesions, joint laxity, and scoliosis have been observed in our cohort. We also report additional findings including dystonia, anxiety disorder, gastrointestinal symptoms, and MRI findings of small basal ganglia and malrotated hippocampus, whereas previous publications described dysmorphic features as a common finding in SRD5A3, which could not be confirmed in our patient cohort.

Conclusion: The detailed description of the phenotype of this large cohort of patients with SRD5A3-CDG highlights that the key clinical diagnostic features of SRD5A3-CDG are an early onset form of ophthalmological problems in patients with a multisystem disorder with variable symptoms evolving over time. This should aid earlier diagnosis and confirms the need for long-time follow-up of patients.

Keywords: SRD5A3-CDG, steroid 5 alpha reductase deficiency, emerging phenotypic features, retinal dystrophy, congenital disorder of glycosylation, CDG

OPEN ACCESS

Edited by:
Karolina Stepien, Salford Royal NHS Foundation Trust, United Kingdom

Reviewed by:
Scott Brodie, NYU Langone Health, United States
Kristin Kantautas, Ela Capital Inc., Canada

***Correspondence:**
Nazreen Kamarus Jaman
nazreen.kamarusjaman@gosh.nhs.uk

[†]*These authors share first authorship*

Specialty section:
This article was submitted to Genetics of Common and Rare Diseases, a section of the journal Frontiers in Genetics

Received: *06 July 2021*
Accepted: *25 October 2021*
Published: *01 December 2021*

Citation:
Kamarus Jaman N, Rehsi P, Henderson RH, Löbel U, Mankad K and Grunewald S (2021) SRD5A3-CDG: Emerging Phenotypic Features of an Ultrarare CDG Subtype. Front. Genet. 12:737094. doi: 10.3389/fgene.2021.737094

INTRODUCTION

Congenital disorders of glycosylation (CDG) are genetic diseases with an extremely broad spectrum of clinical presentation. They occur due to defective glycosylation of glycoproteins or glycolipids, and the genetic defects affect several glycosylation pathways (Ondruskova et al., 2021). Initial steps in the glycosylation pathways result in a stepwise build-up of monosaccharide and oligosaccharide chains. Dolichol acts as a carrier of the oligosaccharide precursor during the assembly, occuring initially at

the outside and, subsequently, at the inside of the endoplasmic reticulum (ER) membrane. Dolichol biosynthesis defects lead to a congenital disorder of glycosylation. The first step in the dolichol synthesis is dehydrodolichyl diphosphate synthase (DHDDS), which forms a complex with the nuclear undecaprenyl pyrophosphate synthase 1 (NUS), forming polyprenol pyrosphosphate from farnesyl and isoprenenyl diphosphate. Mutations in their encoding genes lead to DHDDS- and NUS1-CDG, respectively (Buczkowska et al., 2015). The polyprenol is then reduced by steroid 5 alpha reductases type 3 (SRD5A3) to dolichol. SRD5A3-CDG (previously known as CDG-Iq) (Canatgrel et al., 2010) (MIM:612379) is caused by deleterious mutations in the *SRD5A3* gene and in patients with SRD5A3-CDG, and an increase of polyprenols has been shown (Gründahl et al., 2012; Online Mendelian inherita, 2021). Dolichol is further phosphorylated by dolichol kinase (DOLK), and mutations in the *DOLK* gene cause DOLK-CDG. The phosphorylated dolichol might also act as a carrier for monosaccharides such as mannose and glucose used as donors in N-glycosylation as well as O-mannosylation, C-mannosylation, and GPI anchor synthesis.

SRD5A3-CDG is an ultrarare CDG subtype caused by autosomal recessive inheritance and has been reported so far in 38 patients. Key diagnostic features of SRD5A3-CDG are ophthalmological abnormalities such as retinitis pigmentosa/retinal dystrophy and optic nerve hypoplasia presenting at early onset. SRD5A3-CDG is also characterized by variable neurological symptoms including intellectual disability, cerebellar abnormalities, and hypotonia.

We report on the in-depth phenotyping of eleven SRD5A3-CDG patients of five sets of sibships that are followed up at our center. We compare their clinical and molecular findings to those cases reported in the literature.

MATERIALS AND METHODS

In total, 11 SRD5A3-CDG patients of five sets of sibships were included in the study. Data on 9 of 11 patients are yet unpublished. Siblings from family 5 were reported by Al-Gazali et al. (2008). Patients' results on biochemical and genetic investigations and in-depth phenotyping were collected by retrospective review of the patients' medical records and an additional questionnaire. Informed consent was taken from the legal representatives of previously unpublished cases. The clinical characteristics of these eight females and three male patients, with current ages ranging from 5 to 23 years, are summarized in **Table 1**. More detailed patient descriptions can be found in **Supplementary Information S1**.

RESULTS

Demographics

A total of 11 patients with SRD5A3-CDG are included in our cohort, with a female to male ratio of 8:3. The current ages ranged from 5 to 23 years.

Clinical Features

All 11 patients in our cohort came to the attention of clinicians due to parental concerns regarding developmental delay and visual abnormalities noted from as early as birth. Despite the early presentation of symptoms (average 3.5 months of age), the mean time to obtaining a diagnosis was 8 years (range 1–14.5 years) from symptom onset. The frequency of symptoms experienced by our cohort has been summarized in **Figure 1**, while in **Figure 2**, we illustrate the timing of onset of certain clinical features, which were identifiable from clinical documentation. The earliest clinical feature identified was nystagmus (average onset 3 months, range 0–18 months). This was followed by motor delay (average onset 15 months, range 6–30 months). Speech delay was a documented feature in nine patients with an onset of 26 months (range 12–64 months). Eye signs then progressed further to retinal dystrophy at an average onset of 32 months (range 9–84 months).

The multi-systemic, heterogeneous nature of SRD5A3-CDG is evident from the clinical features observed. Key diagnostic features are ophthalmic abnormalities experienced in all (11/11) individuals of our cohort, including nystagmus, retinal dystrophy, optic nerve hypoplasia, and colobomas. Non-specific visual symptoms such as nystagmus are present from very early onset (e.g., from birth), followed by early-onset retinal dystrophy. **Figure 3** illustrates the ophthalmological findings in two of our families.

Both siblings in family 2 were born with signs of infantile-onset retinal dystrophy: they had a pendular nystagmus, photophobia, and reduced visual behaviors. Electrodiagnostic testing was difficult and limited, secondary to their developmental delay, but revealed attenuated responses to both rod and cone stimulation with delayed 30 Hz flicker, suggesting widespread retinal dysfunction. Their central vision has remained largely stable over the years, but the presence of a hyper-autofluorescent ring and the loss of the ellipsoid layer seen on OCT, outside the perifoveal region, indicate a widespread and significant retinal dystrophy. In patient 3-1, the OCT scans show loss of the photoreceptors (ellipsoid) inside the macula that was detectable from the age of 11. She had a dystrophy identified on electrodiagnostics from the age of 3; however, similar to family 2, she had an early-onset retinal dystrophy. In summary, the data from the two families in **Figure 3** suggest a reasonably coherent phenotype: all have an early onset rod–cone dystrophy on electrodiagnostics, with a hyperfluorescent ring visible on fundus autofluorescence in their late teenage years indicating advanced retinal dystrophy. The progression of the disease, despite being onset during infancy, suggests that patients retain the capacity for moderate central vision into their 20s.

SRD5A3-CDG is also characterized by variable neurological symptoms including hypotonia (10/11), ataxia (5/11), anxiety disorder (5/11), autism (3/11), and movement disorder (dystonia in 2/11). Patient 3-2 has also developed sensorimotor neuropathy. Global developmental delay and subsequent learning disabilities are experienced by all of our patients. Cutaneous and musculoskeletal features such as ichthyosis/psoriasis (4/11, **Figure 4**), scoliosis (6/11), and joint laxity (3/11) have been observed.

TABLE 1 | Clinical characteristics of patients with SRD5A3-CDG in our cohort of 11 patients.

Phenotypic presentation of 11 patients with SRD5A3-CDG											
Patient ID/Age	1-1/20 y	1-2/14.9 y	2-1/23 y	2-2/19 y	3-1/16 y	3-2/8.5 y	4-1/15 y	4-2/12 y	4-3/5 y	5-1/20 y*	5-2/17 y*
Gender	F	F	F	F	F	M	F	F	M	F	M
Ethnicity	Pakistani	Pakistani	Indian	Indian	Kurdish	Kurdish	Pakistani	Pakistani	Pakistani	Baluchi	Baluchi
Consanguinity	+	+	+	+	+	+	+	+	+	+	+
Age at onset (months)	9 m	Birth	18 m	Birth	2 m	6 m	6 weeks	3 weeks	6 weeks	Birth	Birth
Age at diagnosis (years)	15 y	2 y	16 y	12 y	11 y	4 y	13 y	8 y	4 y	~5 y	~1 y
Genetics	*SRD5A3 c.943C > T p.(Pro315Ser)* Homozygous	*SRD5A3 c.943C > T p.(Pro315Ser)* Homozygous	*SRD5A3 c.57G > A p.(Trp19Ter)* homozygous	*SRD5A3 c.57G > A p.(Trp19Ter)* homozygous	*SRD5A3 c.57G > A p.(Trp19Ter)* homozygous	*SRD5A3 c.57G > A p.(Trp19Ter)* homozygous	*SRD5A3 c.57G > A p.(Trp19Ter)* homozygous	*SRD5A3 c.57G > A p.(Trp19Ter)* homozygous	*SRD5A3 c.57G > A p.(Trp19Ter)* homozygous	*SRD5A3 p.Gln96delinsX* homozygous deletion	*SRD5A3 p.Gln96delinsX* homozygous deletion
Dysmorphic features	No	No	No	No	No	No	No	No	No	Yes	Yes
Ophthalmic findings	RD Squint	RD	RD, Nystagmus	RD, Nystagmus	RD Nystagmus Astigmatism	RD Nystagmus Astigmatism	RD Nystagmus	RD Nystagmus	RD Nystagmus Optic nerve hypoplasia	Squint Bilateral optic nerve colobomas	Bilateral iris and chorioretinal colobomas
Neuro-development	GDD, mild LD	GDD, severe LD, ASD	GDD, LD	GDD, LD	GDD, severe LD, ASD	GDD, severe LD, ASD	GDD, moderate LD	GDD, Mild LD	GDD, severe LD	GDD, LD	GDD, LD
Hypotonia	+	+	+	+	+	+	+	–	+	+	+
Seizures	–	–	–	–	–	–	–	–	–	–	–
Dystonia	–	–	–	–	–	+	–	–	+	–	–
Behavior	–	Anxiety	–	Anxiety	Anxiety	–	Mood swings	Anxiety	–	–	–
Ataxia	–	+	+	–	+	+	+	–	–	–	–
Cutaneous	Psoriasis	Ichthyosis, collodion baby	–	Mild hyperkeratosis	–	–	Eczema	Dry skin	–	Ichthyosis Hypertrichosis	Ichthyosis Hypertrichosis
Cardiac	Palpitations	Palpitations	–	–	AR, Prolonged QT	AR	–	–	–	TGA	sASD
Gastrointestinal	IBS	IBS, cyclical vomiting	–	Unexplained weight loss	–	Constipation, dairy allergy	–	–	Poor feeding, dysphagia, Gastrostomy	–	–
Renal	–	–	–	–	–	–	–	–	–	Right duplex kidney	–
Infection	–	–	–	–	–	Recurrent URTI and LRTI, on prophylactic azithromycin	–	–	Recurrent LRTI Prophylactic azithromycin	–	–
Endocrine	Primary Ovarian Failure	–	–	–	Irregular menstruation	–	–	–	–	Small AP, SOD	Small AP
Spinal scoliosis	–	–	+	+	+	+	+	–	+	–	–
Joint laxity	–	–	–	–	+	+	–	–	+	–	–
Dental	–	–	–	Crowding, difficult hygiene	–	–	Dental extractions	–	Premature loss of milk teeth	–	–
Investigations											
Transferrin isoelectric focusing	Abnormal type 1 pattern	Abnormal type 1 pattern	nk	Nk	Normal	Abnormal type 1 pattern	Abnormal type 1 pattern	Abnormal type 1 pattern	Abnormal type 1 pattern	Abnormal type 1 pattern	Abnormal type 1 pattern
Clotting	Normal	Normal	nk	nk	Normal	Prol. APTT	nk	nk	nk	nk	nk
TFT	Normal	Normal	nk	nk	Nk	Normal	nk	nk	Normal	Norm	Normal
Testosterone	3.8 (H)	Nk	nk	nk	Nk	nk	nk	nk	nk	nk	nk
FSH/LH	4.3/15.3	3.4/15.0	nk	nk	Normal	nk	nk	nk	nk	nk	nk
GH	Nk	Normal	nk	nk	Nk	Normal	nk	nk	nk	Norm	nk
Liver test	Normal	Normal	nk	Normal	Normal	Elevated	Normal	nk	Elevated	Norm	Elevated
MRI brain	Findings suggestive of demyelination	Cavum septum pellucidum et vergae, small basal ganglia, mild cerebellar hypoplasia and dysplasia, thick corpus callosum, punctate white matter lesions	Not done	Not done	Normal apart from non-specific subcortical white matter foci in the frontal lobe	Malrotation of hippocampus, retro-cerebellar cyst, thin cervical cord, immature myelin, basal ganglia small (LN)	Not done	Not done	Small cerebral white matter volume, small cerebellum and pons, delayed myelination, small basal ganglia (LN), small optic nerves, malrotation of hippocampus	Small AP, left microphthalmia and atrophic visual pathways	Cerebellar vermis hypoplasia, b/l severe frontal microgyria, delayed myelination

(+), present; (–), not present; (*), patients lost to follow up; RD, retinal dystrophy; GDD, global developmental delay; LD, learning difficulties; ASD, Autism spectrum disorder; AR, abnormal repolarisation; TGA, transposition of the great arteries; sASD, secundum atrial septal defect IBS, irritable bowel syndrome; URTI, upper respiratory tract infection; LRTI, lower respiratory tract infection; AP, anterior pituitary; SOD, septo-optic dysplasia; APTT, activate partial thromboplastin time; TFT, thyroid function; LN, lentiform nucleus; nk, not known.

We have also seen that around half of our patients have gastrointestinal symptoms (5/11). Cardiac abnormalities have been described in 6/11 patients varying from structural abnormalities to conduction abnormalities and palpitations reported by patients. Interestingly dysmorphic features were only present in 2/11 patients. In two female patients from different families, we observed primary ovarian failure and menstruation irregularities. Pituitary abnormalities were seen in 2/11 patients. Comparing the clinical symptoms of siblings in our cohort of five families, with either two or three affected individuals, there is clear intra-familiar variability of signs and symptoms.

Genetics

All our patients were diagnosed by non-targeted whole-exome sequencing and/or *via* the 100,000 genome project, a UK government project funded by the NHS. SRD5A3-CDG is an autosomal recessive disorder, though interestingly, in our cohort, all our families have affected siblings, where four out of five sibships were duos, and one family presented with three affected children. The commonest SRD5A3-CDG mutation reported so far is *c.57G > A p.(Trp19Ter) p.W19X*, also found in seven patients in our cohort (Morava et al., 2010; Gründahl et al., 2012; Kara et al., 2014; Tuysuz et al., 2016; Taylor et al., 2017; Gupta et al., 2018). These families are of Kurdish, Indian, or Pakistani background. Family 1, also of Pakistani origin, was found to be homozygous for the *c.943C > T p.(Pro315Ser)* variant. Interestingly this mutation has not yet been reported. Family 5, of Baluchi origin, were found to carry the *p.Gln96delinsX* homozygous deletion, which resulted in a frameshift and premature termination at amino acid 96 of 318 of the SRD5A3 protein.

Laboratory

Isoelectric focusing of transferrin (IEF), the commonly used screening test for N-glycosylation disorders, was performed in nine patients and was found to be abnormal in 8. The abnormal IEF results showed a type I pattern, characterized by an increase of di- and asialotransferrin, pointing to an early assembly defect in the dolichol-linked glycosylation. Additional biochemical parameters, often found to be abnormal in CDG patients, were variably performed in at least 9/11 patients. These include thyroid function tests, liver enzymes, clotting, and sex hormones. We only observed one patient with a prolonged APTT that later normalized. Three patients had elevated liver enzymes but all patients investigated had normal thyroid function. Premature ovarian failure and irregularity of menstruation were reported for patients 1-1 and 3-1, respectively.

Neuroimaging

Neuroimaging findings were variable in our cohort with intra-familiar variability. MRI brain was performed in seven patients (four families). Detailed descriptions are found in **Table 1** with MRI brain images in **Figure 5**. Findings included cerebellar and cerebellar vermis hypoplasia, severe frontal microgyria, delayed myelination, small cerebral white matter volume loss, drooping splenium and small pons, small basal ganglia (lentiform nucleus), and mal-rotated hippocampus. The latter two features have not previously been described in association with glycosylation disorders. Other findings include evidence of demyelination in patient 1-1, who has a second diagnosis of multiple sclerosis.

DISCUSSION

SRD5A3-CDG is an ultrarare CDG diagnosis with 38 cases reported so far (Jaeken et al., 2020). The clinical spectrum of SRD5A3-CDG is still evolving, and the diagnosis of patients is often only established by untargeted extended mutational screening. Delineating these features remains a challenge due to the small number of patients and limited individual case data available.

We present here the in-depth phenotyping of another nine unpublished cases of five sets of siblings with SRD5A3-CDG from unrelated families of different ethnic backgrounds. Transferrin isoelectric focusing (IEF), as a screening test for N-glycosylation defects, will usually show a type 1 pattern in SRD5A3-CDG. However, affected patients with a normal pattern have also been reported, as seen in patient 3-1. All our patients were diagnosed by non-targeted whole-exome sequencing and/or *via* the 100,000 genome project. Interestingly, despite early symptom onset, there is an average delay of almost 8 years between the first symptom and diagnosis. There is an apparent phenotypic variability in the clinical features among patients with SRD5A3-CDG. This variability interestingly extends to affected siblings within the same families, carrying the same genetic mutation as we demonstrate in our patient cohort. As each set of siblings comes from a background of consanguineous parents, there is an increased probability of additional inherited genetic factors contributing to the patients' signs and symptoms. However, no other gene variants of particular concern were reported in our patients.

The ophthalmological findings in SRD5A3-CDG are already well delineated in the literature. Each of our patients is affected by eye changes which include nystagmus, retinal dystrophy, optic nerve hypoplasia, squint, and colobomas. In our cohort, nystagmus was the most common presenting feature early in infancy, and therefore an important though unspecific diagnostic sign. Seven of 11 patients were diagnosed with early-onset retinal dystrophy with onset as early as 9 months of age. This is comparable to a previous case series which reported early-onset (≤3 years) retinal dystrophy in SRD5A3-CDG patients carrying a common mutation (*c.57G > A p.(Trp19Ter)* homozygous) (Taylor et al., 2017). This is the same mutation carried by the seven of 11 patients in our cohort diagnosed with early-onset retinal dystrophy. Using our cohort, and those described in the literature, we can suggest that nystagmus followed by the development of early retinal dystrophy and visual impairment forms part of the natural disease history in SRD5A3-CDG patients. It has been hypothesized that hypo-glycosylation of rhodopsin expressed in rod photoreceptor cells could be responsible for the early onset changes on the retina. Rhodopsin has two N-glycosylation sides, and mutations

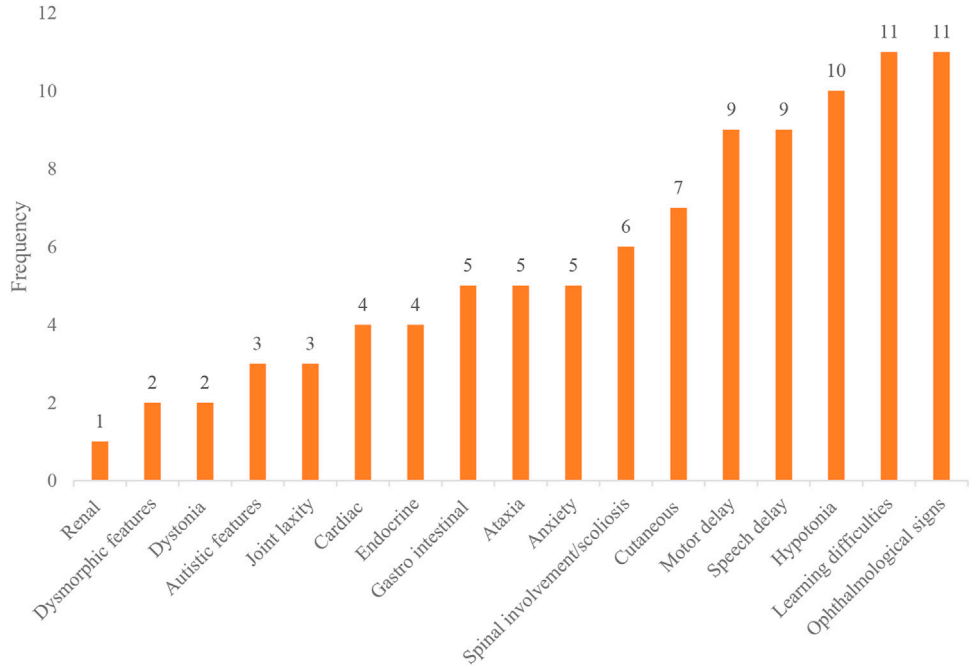

FIGURE 1 | Frequency of symptoms affecting our SRD5A3-CDG cohort. This bar chart demonstrates the number of patients affected by each clinical feature/organ involvement. Learning difficulties (11/11), ophthalmological signs (11/11), hypotonia (10/11), speech delay (9/11), motor delay (9/11), cutaneous (7/11), scoliosis (6/11), anxiety (5/11), ataxia (5/11), gastrointestinal (5/11), cardiac (4/11), endocrine (4/11), autistic features (3/11), joint laxity (3/11), dystonia (2/11), dysmorphism (2/11), and renal (1/11).

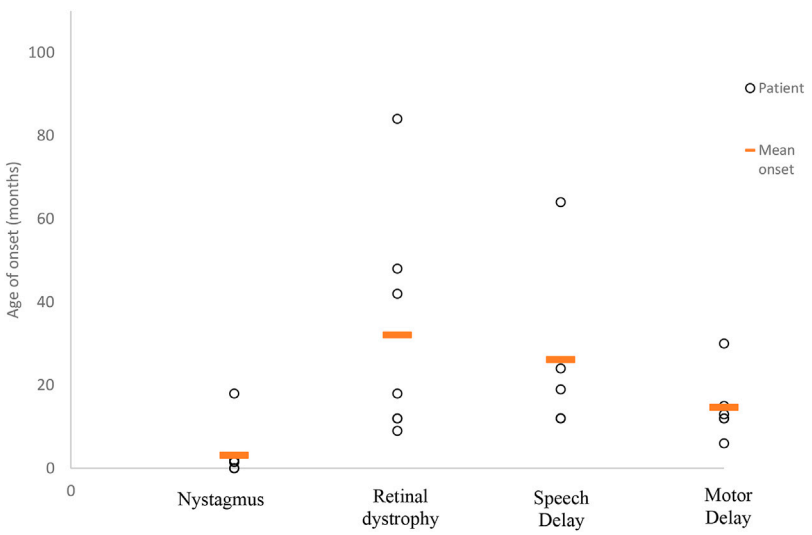

FIGURE 2 | Average age at symptom onset. This scatter graph illustrates the timing of symptom onset ascertained from patient records as documented. Timing of symptom onset was not identifiable for all clinical features. Therefore, those included are as follows (number of patients/mean age of onset in months): nystagmus (6 of 7/3 months), retinal dystrophy (7 of 9/32 months), speech delay (5 of 9/26 months), and motor delay (6 of 9/15 months).

in the *SRD5A3* gene leading to abnormal glycosylation of rhodopsin might affect its normal incorporation and function in the rod outer segment. This could then subsequently lead to defective phototransduction, loss of vision, and development of retinal dystrophy (Taylor et al., 2017). The other patients harboring different mutations also had profound retinal or structural changes of the eye. Siblings from family 1 presented with retinal dystrophy in early childhood, whereas patients in family 5 were found to have colobomas. Colobomas have been described in four

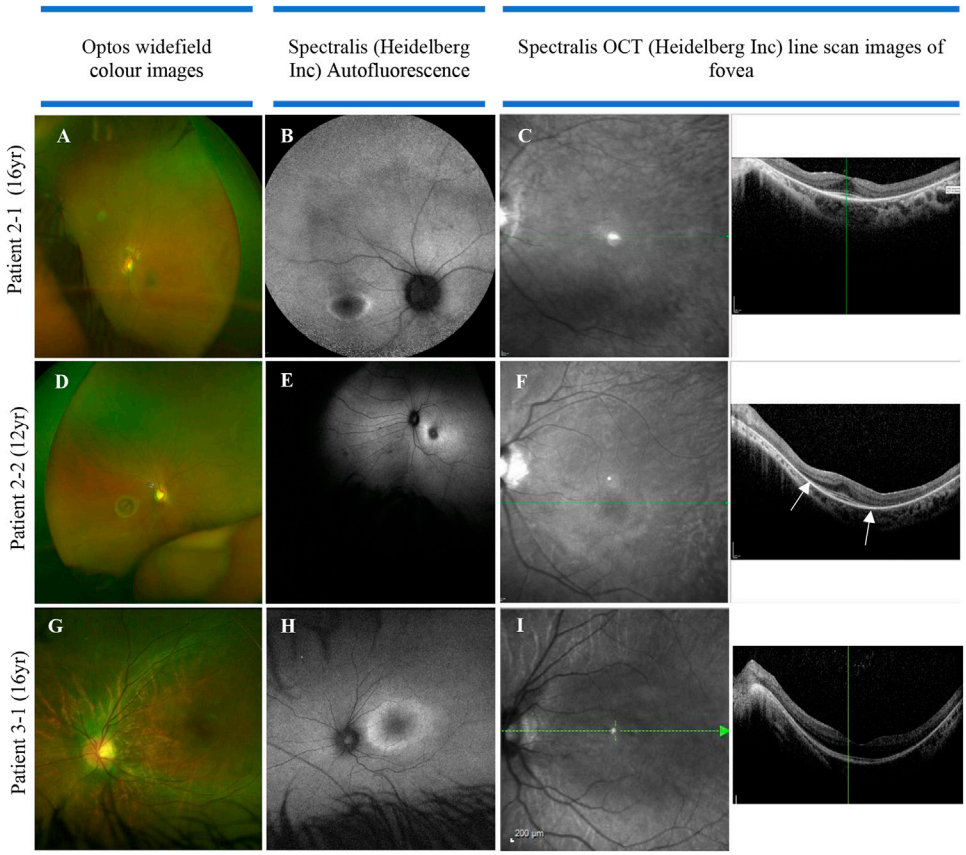

FIGURE 3 | Color fundus, autofluorescence, infrared, and OCT images in three individuals of two families with SRD5A3-CDG. **(A)** Optos image of eye with nystagmus (leading to some distortion of the image), demonstrating mild vascular attenuation, myopic oval disc morphology, and subtle macula reflex abnormalities. The peripheral retina does not reveal any pigmentary abnormalities; **(B)** delineating "watershed" zone between relatively preserved central retina, and dystrophic periphery; **(C)** loss of ellipsoid outside the perifoveal region in both eyes; **(D)** myopic discs, retinal nerve fiber layer reflexes constrained to macula, subtle vascular attenuation, and no significant retinal pigmentation migration suggestive of retinal dystrophy. **(E)** Abnormal macula with hyper-autofluorescent ring around fovea; **(F)** loss of ellipsoid—the outer retinal layers beyond the fovea (as highlighted by arrows). **(G)** Color image of left eye; **(H)** hyper-autofluorescent ring illustrating watershed area between preserved central macula function and dystrophic retinal periphery; **(I)** loss of ellipsoid layer outside the perifoveal retina.

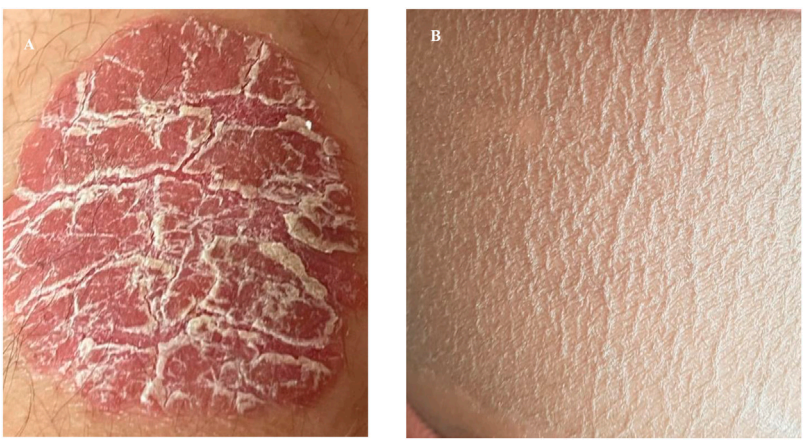

FIGURE 4 | Examples of skin changes seen in SRD5A3-CDG. **(A)** Well demarcated erythematous and scaly plaque classical of psoriasis seen in patient 1–1. **(B)** Excessively dry scaly skin representative of ichthyosis seen in patient 1–2 who was born as a collodion baby.

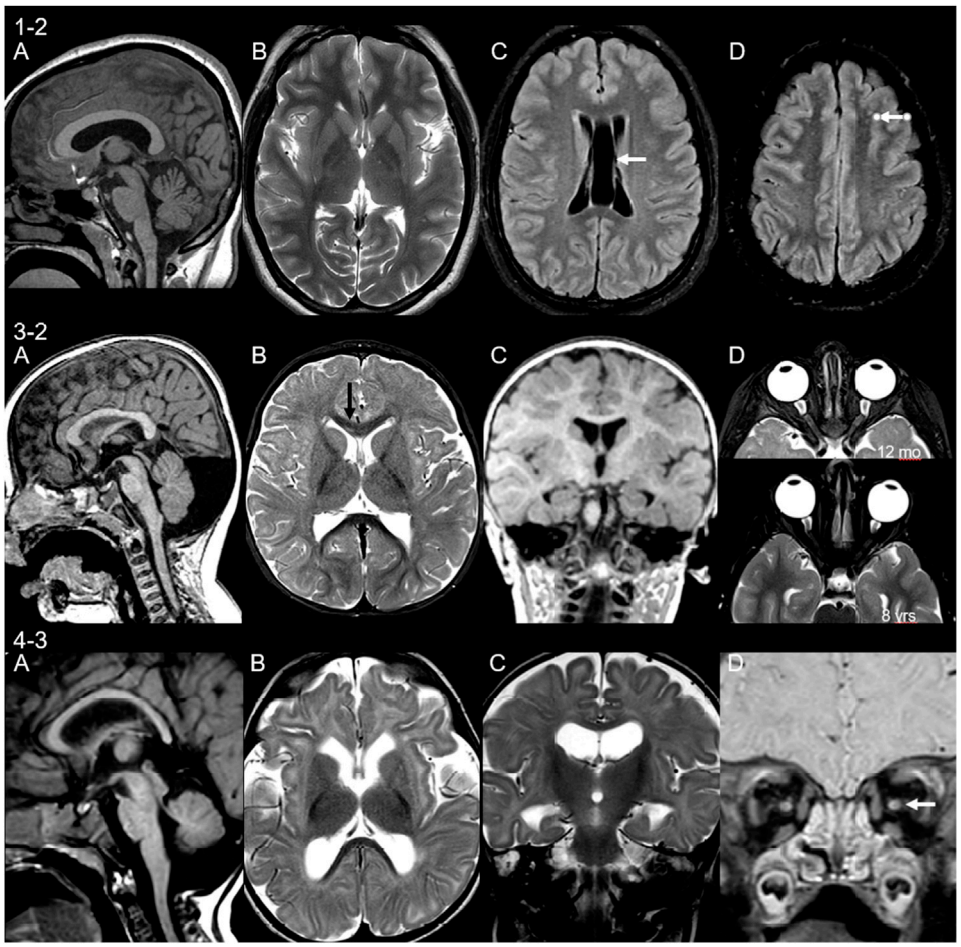

FIGURE 5 | Neuroimaging findings in three unrelated patients. **MRI of patient 1-2** at age 15 years shows **(A)** thick corpus callosum and mild cerebellar hypoplasia, **(B)** small basal ganglia, **(C)** cavum septum pellucidum et vergae (arrow), and **(D)** non-specific punctate white matter lesions on fluid-attenuated inversion recovery (FLAIR) sequences (arrow). **Patient 3-2** scanned at 12 months of age shows **(A)** retrocerebellar cyst and thin cervical cord, **(B)** signal change of the genu of corpus callosum (immature myelin, black arrow) and small lentiform nucleus, **(C)** malrotation of hippocampi, and **(D)** asymmetry of the globes, more prominent on follow-up (lower image). **Patient 4-3** at 7 months of age shows **(A)** small cerebellum and pons and drooping splenium, **(B)** microcephaly with volume loss of the white matter, delayed myelination, and volume loss of the lentiform nucleus, **(C)** malrotation of hippocampi, and **(D)** volume loss of the optic nerves.

other families each carrying different mutations in the *SRD5A3* gene (Canatgrel et al., 2010).

There is also some phenotypic overlap with other congenital disorders of glycosylation, resulting in an early disruption of the dolichol pathway: patients with *DHDDS*-CDG (MIM 613861) have been found to have isolated non-syndromic retinitis pigmentosa (Zelinger et al., 2011) or severe multisystem disease (Sabry et al., 2016). Suppression of DHDDS expression in zebrafish leads to the loss of photoreceptor's outer segments and visual function, supporting the hypothesis that insufficient DHDDS function leads to retinal degeneration (Wen et al., 2014). In two siblings diagnosed with NUS1-CDG, alongside severe neurological impairment, epilepsy, and hearing deficit, these children had visual impairment with discrete bilateral macular lesions at the age of 4 years (Park et al., 2014). The spectrum of ocular involvement from early onset highlights the role and importance of the dolichol biosynthesis pathway in the normal development of the eyes.

Global developmental delay and learning difficulties are known features of SRD5A3-CDG, with each of our patients affected to some degree. There appears to be obvious variability among affected siblings; family numbers 1 and 4 are a good example of this with individuals on the severe spectrum of learning difficulties, in comparison to their siblings who are either requiring minimal support or managed to pursue higher education. Three patients with severe learning difficulties are also affected by autism spectrum disorder, two of whom are siblings. In addition, anxiety or mood alteration appears to be a feature in females, with over 60% (5/8) of our female cohort affected. Anxiety appears to be an evolving feature and may be at least partially secondary to visual impairment, and therefore affecting those with a lesser degree of intellectual disability and higher

functionality. In contrast, anxiety may not be well recognized in those with a more severe intellectual disability and less independently functional, as all of our patients are affected by a degree of visual impairment.

Other neurological findings include hypotonia, and all except one of our cohort suffer from this to varying degrees, which is evident in their slow progression, or lack of progression of gross motor skills. It is hypothesized that mutations in the *SRD5A3* gene also disrupt O-mannosylation, which is essential for muscular tissue maintenance, which could be contributing to the muscular symptoms seen in our patient cohort (Endo, 2019). Only one patient in our cohort (4-1) has reported normal tone with normal mobility and posture despite her siblings being affected by marked hypotonia. Six of our patients with hypotonia have developed or have signs of early emerging scoliosis. The degree of scoliosis and its early onset in childhood may not be fully attributable to hypotonia, which is only mild in some of our cases. Two of our male patients described also suffer from dystonia requiring medical management. Dystonia might, therefore, be an additional neurological feature that needs to be evaluated in SRD5A3-CDG patients. Dystonia is rarely described in other CDG subtypes. Nevertheless, a single case report from Prietsch et al. (2002) describes a female patient who developed dystonic hand movements, and dystonia has been described in cases of PMM2-CDG (Prietsch et al., 2002; Mostile et al., 2019). Patient 3-2 has also developed a sensorimotor neuropathy, a feature not previously described in this ultrarare condition, and possibly also needs to be recognized as a new manifestation of this disorder.

The variable frequency and diversity of brain developmental abnormalities is a known feature in CDGs, and this is demonstrated in our cohort. Proper protein glycosylation is essential for normal brain development and function, thereby explaining the variety of features seen in CDG patients. Malformations described include cortical malformations, midline brain structure and volume anomalies, myelination disorders, and venous sinus thrombosis (Paprocka et al., 2021). Classically, type 1 CDG patients demonstrate patterns of cerebellar, pontocerebellar, and cerebellar vermis hypoplasia and atrophy. Cantagrel et al. (2010) summarized MRI findings of five families with the loss of function mutations in the *SRD5A3* gene that were found to have signs of cerebellar atrophy or vermis malformations (Canatgrel et al., 2010). This may provide an explanation for the early onset nystagmus as well as ataxia seen in SRD5A3-CDG patients; we see a high prevalence of ataxia in our cohort (5/11) with intra-familiar variability. Medina-Cano et al. (2018) observed motor coordination defects and abnormal granule cell development in a cerebellum-specific knockout mouse for *SRD5A3*. Their proteomic studies confirmed that *SRD5A3* loss affects a specific subset of glycoproteins, namely, those highly glycosylated. They observed, for example, impaired IgSF-CAM–mediated neurite growth and axon guidance in the cerebellum of their *SRD5A3* mutant mice (Medina-Cano et al., 2018). Interestingly, in addition to the central nervous system, highly glycosylated IgSF-CAM members also play critical roles in other systems such as the developing eye (Morava et al., 2009), which might explain both the cerebellar and ocular signs and symptoms in patients with SRD5A3-CDG. The finding of severe frontal microgyria in patient 5-2 is intriguing. Neuronal migration defects are common features of a subgroup of O-glycosylation defects, namely, O-mannosylation defects leading to dystroglycanopathies. As O-mannosylation might also be hampered in SRD5A3-CDG, this might contribute to the misfolding of the cortex (Schiller et al., 2020). The findings of the mal-rotated hippocampus and small brainstem are features not previously described in SRD5A3-CDG or other glycosylation defects. The cause of a mal-rotated hippocampus itself is unexplained although thought to be a result of the failure of the normal infolding process during development *in utero*. The mechanism, if this failure is unclear, could be a result of acquired or genetic factors (Fu et al., 2021). White matter abnormalities are not a typical characteristic in CDGs although they have been described in only a few patients (Paprocka et al., 2021). Similarly in our cohort, white matter volume loss was only described in a single patient.

In total, 5 of 11 patients in our cohort displayed skin changes, and among those affected, symptoms varied from generalized dryness and eczematous changes to psoriasis and ichthyosiform changes. At the severe end of the spectrum, a single patient presented at birth with ichthyosis with troublesome symptoms in infancy easing with older age (1–2). Interestingly, his sibling, affected with the same genetic mutation, has a milder cutaneous involvement with the development of psoriasis at a later age. Variable skin involvement has been previously reported, and the most common findings are those of ichthyosiform changes, hyperpigmentation, and palmoplantar keratoderma (Wheeler et al., 2016). The very first steps in the dolichol synthesis pathway share those of the sterol pathway up to the formation of farnesyl-PP. It has been suggested that the accumulation of toxic sterol precursors could contribute to the cutaneous phenotype of SRD5A3-CDG, and could also explain ichthyosis being observed in DOLK-CDG (Rymen and Jaeken, 2014).

Gastroenterological symptoms have been reported in 5/11 patients in our cohort. Siblings in family 1 have symptoms of presumed irritable bowel syndrome. The youngest sibling in family 4, with a more severe phenotype, was noted to have difficulties with feeding from 3 weeks of age, and he had episodes of recurrent vomiting and was gastrostomy fed from approximately 1 year of age. He also suffers from severe hypotonia and remains immobile. The *SRD5A3* gene is expressed in the duodenum so disruption of its function might impact gut mucosa maintenance, intestinal motility, and absorption contributing to this phenotype (Morava et al., 2010). As these symptoms are rather non-specific, gastrointestinal symptoms could be an under-reported feature.

Cardiac phenomena have been described only sporadically in cases of SRD5A3-CDG. Though in our cohort, we have 6/11 patients with cardiac involvement varying from clinical symptoms and conduction abnormalities to structural abnormalities. Siblings from family 1 are symptomatic of palpitations although cardiac investigations have been normal so far. Patient 1-2 also suffers from anxiety of which palpitations may be a manifestation. There is a history of abnormal

repolarisation in family 3, and this includes unaffected family members. Siblings in family 5 have a history of structural heart defects as described. As the *SRD5A3* gene is expressed in cardiac tissue, and although its exact role is yet to be understood, its impact on dolichol synthesis and N- and O-glycosylation within cardiac tissue could explain these emerging phenotypes (Morava et al., 2010).

Endocrine dysfunction, particularly hypergonadotropic hypogonadism in CDG disorders, has been described in the literature, and the patient's pubertal development should be monitored (Miller and Freeze, 2003). Interestingly, patient 1-1 has primary ovarian failure, and 3-1 has irregular menstrual periods, which need further investigation. Siblings in family 5 have evidence of small anterior pituitary glands with patient 5-1 suffering from a variation of septo-optic dysplasia. Growth abnormalities have not been described in our cohort.

It is questionable if the uncommonly described feature of recurrent infections is linked to the diagnosis of SRD5A3-CDG. Two of our patients from unrelated families have a history of recurrent upper and lower respiratory tract infections requiring prophylactic azithromycin. Patient 3-2 has been extensively investigated for underlying immune deficiencies, of which all results are normal. There was symptomatic improvement in patient 4-3 after gastrostomy insertion, suggesting recurrent aspiration from unsafe swallow was the likely cause for these recurrent lower respiratory tract infections.

Isoelectric focusing (IEF) of transferrin is commonly used to screen for glycosylation disorders. In our patient cohort, eight out of nine patients that had IEF showed a type I pattern, whereas in one family the older sibling had a normal result. This phenomenon has been seen in other patients with SRD5A3-CDG, so normal glycosylation screening does not rule out SRD5A3-CDG. Variable and age-dependent changes in glycosylation patterns have also been reported in other CDG subtypes (Mohamed et al., 2011).

In summary, patients with SRD5A3-CDG present with signs and symptoms of early ophthalmological abnormalities, developmental delay and intellectual disability, neurological symptoms, cutaneous changes, and spinal involvement, and fewer described cardiac and endocrine manifestations. Furthermore to the range of symptoms already prescribed, we report on emerging additional manifestations such as dystonia, anxiety disorder, and gastrointestinal symptoms. The genotypic and phenotypic spectrum of *SRD5A3*-CDG is evolving, and we also note intra-familiar variability. Genotype-phenotype analyses are hampered due to the limited number of patients being diagnosed so far. In addition, some of those diagnosed carry compound heterozygous mutations, making it even more difficult to predict an outcome. The presence of residual enzyme activity in some patients could provide an explanation for the different severity of patients' presentation, and it has also been suggested that there might be an alternative biosynthetic pathway for dolichol synthesis in patients (Canatgrel et al., 2010). Mutant mouse model studies have shown the activation of the mevalonate pathway suggesting a positive feedback mechanism to overcome the lack of dolichol synthesis in some *SRD5A3* mutants by increasing substrate production (Canatgrel et al., 2010). Overall, SRD5A3-CDG manifests on a wide range of organs, which is likely to reflect the fact that *SRD5A3* gene mutations not only affect N-glycosylation but as dolichol is also required for the synthesis of O-mannose linked glycans, C-mannosylation, and glycophospholipid anchor synthesis, and disruption in these pathways may also explain part of the phenotypic spectrums. Further studies on cell and animal models and delineation of disrupted glycosylation pathways in humans will provide better insight into the different pathology of signs and symptoms in SRD5A3-CDG patients.

CONCLUSION

The detailed description of the phenotype of this large cohort of patients with SRD5A3-CDG highlights that the key clinical diagnostic features of SRD5A3-CDG are early onset of ophthalmological problems. However, SRD5A3-CDG is a multi-systemic disorder also characterized by variable neurological symptoms including intellectual disability, hypotonia, and ataxia. In addition, we demonstrate the presence of cutaneous lesions as well as spinal, cardiac, and endocrine involvement. In our study population, new emerging clinical features include dystonia, anxiety disorder, gastrointestinal symptoms, and MRI findings of small basal ganglia and mal-rotated hippocampus. Dysmorphic features have been key to SRD5A3-CDG cases described in the literature, in contrast to our nine new patients where dysmorphic faces are not described. Furthermore, we newly observe clear intra-familiar variability in our cohort. This, alongside the evolving clinical spectrum of SRD5A3-CDG, makes it even more difficult to predict long-term prognosis, and there is a need for long-time follow-up of these patients. SRD5A3-CDG and other CDG subtypes in the early dolichol pathway should be considered as a cause of early-onset retinal dystrophy, particularly if patients present with multisystem disease. This would aid early diagnosis, inform genetic counseling, and would eventually provide patients access to emerging therapies. Disease-specific registries will help to capture the disease-specific manifestations and are particularly essential in such an ultrarare CDG subtype. Further delineation of the phenotypic spectrum should help to aid earlier diagnosis and guide clinicians to target long-term follow-up of SRD5A3-CDG patients.

DATA AVAILABILITY STATEMENT

The original contributions presented in the study are included in the article/**Supplementary Materials**; further inquiries can be directed to the corresponding authors.

AUTHOR CONTRIBUTIONS

NKJ: As a first author, participated in the design of the work, data collection, data analysis and interpretation, and drafting

the article, and has taken part in the completion of the article alongside coauthors. PR: As a first author, participated in the design of the work, data collection, data analysis and interpretation, and drafting the article, and has taken part in the completion of the article alongside coauthors. RHH: as coauthor, participated in the ophthalmology aspects of data collection, interpretation and analysis, critical review and revision. UL: as coauthor, participated in the neuro-imaging/radiology aspects of data collection, interpretation and analysis, critical review and revision. KM: as coauthor, participated in the neuro-imaging/ radiology aspects of data collection, interpretation and analysis, critical review and revision. SG: As a senior author, helped in conception, participated in the design of the work, provided guidance in data collection, data analysis and interpretation, drafting the article, critical review, revision, and submission, and taken part in the completion of the article alongside coauthors.

ACKNOWLEDGMENTS

We are particularly grateful for all families that have agreed to participate in the study, and to their clinicians and geneticists providing access to patients' clinical information.

SUPPLEMENTARY MATERIAL

The Supplementary Material for this article can be found online at: https://www.frontiersin.org/articles/10.3389/fgene.2021.737094/full#supplementary-material

REFERENCES

Al-Gazali, L., Hertecant, J., Algawi, K., El Teraifi, H., and Dattani, M. (2008). A New Autosomal Recessive Syndrome of Ocular Colobomas, Icthyosis, Brain Malformations and Endocrine Abnormalities in an Inbred Emirati Family. *Am. J. Med. Genet. Part. A.* 146A, 813–819. doi:10.1002/ajmg.a.32114

Buczkowska, A., Swiezewska, E., and Lefeber, D. J. (2015). Genetic Defects in Dolichol Metabolism. *J. Inherit. Metab. Dis.* 38 (1), 157–169. doi:10.1007/s10545-014-9760-1

Canatgrel, V., Lefeber, D. J., Ng, B. G., Guan, Z., Silhavy, J. L., Bielas, S. L., et al. (2010). SRD5A3 Is Required for Converting Polyprenol to Dolichol and Is Mutated in a Congenital Glycosylation Disorder. *Cell* 142 (2), 203–217. doi:10.1016/j.cell.2010.06.001

Endo, T. (2019). Mammalian O-Mannosyl Glycans: Biochemistry and Glycopathology. *Proc. Jpn. Acad. Ser. B, Phys. Biol. Sci.* 95 (1), 39–51. doi:10.2183/pjab.95.004

Fu, T. Y., Ho, C. R., Lin, C. H., Lu, Y. T., Lin, W. C., and Tsai, M. H. (2021). Hippocampal Malrotation: A Genetic Developmental Anomaly Related to Epilepsy? *Brain Sci.* 11 (4), 463. doi:10.3390/brainsci11040463

Gründahl, J. E. H., Guan, Z., Rust, S., Reunert, J., Müller, B., Du Chesne, I., et al. (2012). Life with Too Much Polyprenol: Polyprenol Reductase Deficiency. *Cell Mol. Genet. Metab.* 105 (4), 642–651. doi:10.1016/j.ymgme.2011.12.017

Gupta, N., Verma, G., Kabra, M., Bijarnia-Mahay, S., and Ganapathy, A. (2018). Identification of a Case of SRD5A3-Congenital Disorder of Glycosylation (CDG1Q) by Exome Sequencing. *Indian J. Med. Res.* 147, 422–426. doi:10.4103/ijmr.IJMR_820_16

Jaeken, J., Lefeber, D. J., and Matthijs, G. (2020). SRD5A3 Defective Congenital Disorder of Glycosylation: Clinical Utility Gene Card. *Eur. J. Hum. Genet.* 28 (9), 1297–1300. doi:10.1038/s41431-020-0647-3

Kara, B., Ö, Ayhan., Gökçay, G., Başboğaoğlu, N., and Tolun, A. (2014). Adult Phenotype and Further Phenotypic Variability in SRD5A3-CDG. *BMC Med. Genet.* 15, 10. doi:10.1186/1471-2350-15-10

Medina-Cano, D., Ucuncu, E., Nguyen, L. S., Nicouleau, M., Lipecka, J., Bizot, J.-C., et al. (2018). High N-Glycan Multiplicity Is Critical for Neuronal Adhesion and Sensitizes the Developing Cerebellum to N-Glycosylation Defect. *Elife* 7, e38309. doi:10.7554/eLife.38309

Miller, B. S., and Freeze, H. H. (2003). New Disorders in Carbohydrate Metabolism: Congenital Disorders of Glycosylation and Their Impact on the Endocrine System. *Rev. Endocr. Metab. Disord.* 4 (1), 103–113. doi:10.1023/a:1021883605280

Mohamed, M., Cantagrel, V., Al-Gazali, L., Wevers, R. A., Lefeber, D. J., and Morava, E. (2011). Normal Glycosylation Screening Does Not Rule Out SRD5A3-CDG. *Eur. J. Hum. Genet.* 19, 1019. doi:10.1038/ejhg.2010.260

Morava, E., Wevers, R. A., Cantagrel, V., Hoefsloot, L. H., Al-Gazali, L., Schoots, J., et al. (2010). A Novel Cerebello-Ocular Syndrome with Abnormal Glycosylation Due to Abnormalities in Dolichol Metabolism. *Brain* 133, 3210–3220. doi:10.1093/brain/awq261

Morava, E., Wosik, H. N., Sykut-Cegielska, J., Adamowics, M., Guillard, M., Wevers, R. A., et al. (2009). Ophthalmological Abnormalities in Children with Congenital Disorders of Glycosylation Type I. *Br. J. Ophthalmol.* 93, 350–354. doi:10.1136/bjo.2008.145359

Mostile, G., Barone, R., Nicoletti, A., Rizzo, R., Martinelli, D., Sturiale, L., et al. (2019). Hyperkinetic Movement Disorders in Congenital Disorders of Glycosylation. *Eur. J. Neurol.* 26 (9), 1226–1234. doi:10.1111/ene.14007

Ondruskova, N., Cechova, A., Hansikova, H., Honzik, T., and Jaeken, J. (2021). Congenital Disorders of Glycosylation: Still "hot" in 2020. *Biochim. Biophys. Acta Gen. Subj.* 1865 (1), 129751. doi:10.1016/j.bbagen.2020.129751

Online Mendelian inheritance in Man (2021). *Online Mendelian Inheritance in Man, OMIM*. Baltimore, MD: Johns Hopkins University. MIM Number: {# 612379} Marla J. F. O'Neill : 10/29/2008 , Cassandra L. Kniffin - updated : 9/9/2010.

Paprocka, J., Jezela-Stanek, A., Tylki-Szymańska, A., and Grunewald, S. (2021). Congenital Disorders of Glycosylation from a Neurological Perspective. *Brain Sci.* 11 (1), 88. doi:10.3390/brainsci11010088

Park, E. J., Grabińska, K. A., Guan, Z., Stránecký, V., Hartmannová, H., Hodaňová, K., et al. (2014). Mutation of Nogo-B Receptor, a Subunit of Cis-Prenyltransferase, Causes a Congenital Disorder of Glycosylation. *Cell Metab.* 20 (3), 448–457. doi:10.1016/j.cmet.2014.06.016

Prietsch, V., Peters, V., Hackler, R., Jakobi, R., Assmann, B., Fang, J., et al. (2002). A New Case of CDG-X with Stereotyped Dystonic Hand Movements and Optic Atrophy. *J. Inherit. Metab. Dis.* 25, 126–130. doi:10.1023/a:1015628810892

Rymen, D., and Jaeken, J. (2014). Skin Manifestations in CDG. *J. Inherit. Metab. Dis.* 37 (5), 699–708. doi:10.1007/s10545-014-9678-7

Sabry, S., Vuillaumier-Barrot, S., Mintet, E., Fasseu, M., Valayannopoulos, V., Héron, D., et al. (2016). A Case of Fatal Type I Congenital Disorders of Glycosylation (CDG I) Associated with Low Dehydrodolichol Diphosphate Synthase (DHDDS) Activity. *Orphanet J. Rare Dis.* 11 (1), 84. doi:10.1186/s13023-016-0468-1

Schiller, S., Rosewich, H., Grünewald, S., and Gärtner, J. (2020). Inborn Errors of Metabolism Leading to Neuronal Migration Defects. *J. Inherit. Metab. Dis.* 43 (1), 145–155. doi:10.1002/jimd.12194

Taylor, R. L., Gavin, A., Poulter, J. A., Khan, K. N., Morarji, J., Hull, S., et al. (2017). Association of Steroid 5α-Reductase Type 3 Congenital Disorder of Glycosylation with Early-Onset Retinal Dystrophy. *JAMA Ophthalmol.* 135 (4), 339–347. doi:10.1001/jamaophthalmol.2017.0046

Tuysuz, B., Pehlivan, D., Özkök, A., Jhangiani, S., Yalcinkaya, C., Zeybek, Ç. A., et al. (2016). Phenotypic Expansion of Congenital Disorder of Glycosylation Due to SRD5A3 Null Mutation. *JIMD Rep.* 26, 7–12. doi:10.1007/8904_2015_478

Wen, R., Dallman, J. E., Li, Y., Züchner, S. L., Vance, J. M., Peričak-Vance, M. A., et al. (2014). Knock-down DHDDS Expression Induces Photoreceptor Degeneration in Zebrafish. *Adv. Exp. Med. Biol.* 801, 543–550. doi:10.1007/978-1-4614-3209-8_69

Wheeler, P. G., Ng, B. G., Sanford, L., Sutton, V. R., Bartholomew, D. W., Pastore, M. T., et al. (2016). SRD5A3-CDG: Expanding the Phenotype of a Congenital Disorder of Glycosylation with Emphasis on Adult Onset Features. *Am. J. Med. Genet. A.* 170 (12), 3165–3171. doi:10.1002/ajmg.a.37875

Zelinger, L., Banin, E., Obolensky, A., Mizrahi-Meissonnier, L., Beryozkin, A., Bandah-Rozenfeld, D., et al. (2011). A Missense Mutation in DHDDS, Encoding Dehydrodolichyl Diphosphate Synthase, Is Associated with Autosomal-Recessive Retinitis Pigmentosa in Ashkenazi Jews. *Am. J. Hum. Genet.* 88 (2), 207–215. doi:10.1016/j.ajhg.2011.01.002

Conflict of Interest: The authors declare that the research was conducted in the absence of any commercial or financial relationships that could be construed as a potential conflict of interest.

Publisher's Note: All claims expressed in this article are solely those of the authors and do not necessarily represent those of their affiliated organizations, or those of the publisher, the editors, and the reviewers. Any product that may be evaluated in this article, or claim that may be made by its manufacturer, is not guaranteed or endorsed by the publisher.

frontiers in Genetics

ORIGINAL RESEARCH
published: 08 December 2021
doi: 10.3389/fgene.2021.719624

Fatal Neonatal DOLK-CDG as a Rare Form of Syndromic Ichthyosis

Katalin Komlosi[1], Olivier Claris[2,3†], Sophie Collardeau-Frachon[4,5†], Julia Kopp[1], Ingrid Hausser[6], Juliette Mazereeuw-Hautier[7], Nathalie Jonca[8,9], Andreas D. Zimmer[1], Damien Sanlaville[10,11] and Judith Fischer[1]*

[1]Institute of Human Genetics, Medical Center, Faculty of Medicine, University of Freiburg, Freiburg, Germany, [2]Department of Neonatology, Hospices Civils de Lyon, Hôpital Femme Mère Enfant, Bron, France, [3]Claude Bernard University, Lyon, France, [4]Hospices Civils de Lyon, Hôpital Femme Mère Enfant, Institut de Pathologie, Bron, France, [5]Faculté de médecine Lyon Est, Claude Bernard University, Lyon, France, [6]Institute of Pathology, Heidelberg University Hospital, Heidelberg, Germany, [7]Dermatology Department, Reference Center for Rare Skin Diseases, CHU Larrey, Université Paul Sabatier, Toulouse, France, [8]Infinity, CNRS, Inserm, UPS, Université Toulouse, Toulouse, France, [9]CHU Toulouse, Hôpital Purpan, Laboratoire de Biologie Cellulaire et Cytologie, Institut Fédératif de Biologie, Toulouse, France, [10]Hospices Civils de Lyon, Hôpital Femme Mère Enfant, Service de Génétique, Bron, France, [11]Institut Neuromyogène, Université de Lyon, Lyon, France

OPEN ACCESS

Edited by:
Anna Tylki-Szymańska, Children's Memorial Health Institute (IPCZD), Poland

Reviewed by:
Julien H. Park, University of Münster, Germany
Hasan Orhan Akman, Columbia University Irving Medical Center, United States
Daisy Rymen, University Hospitals Leuven, Belgium

***Correspondence:**
Katalin Komlosi
katalin.komlosi@uniklinik-freiburg.de

†These authors have contributed equally to this work

Specialty section:
This article was submitted to Genetics of Common and Rare Diseases, a section of the journal Frontiers in Genetics

Received: *02 June 2021*
Accepted: *02 November 2021*
Published: *08 December 2021*

Citation:
Komlosi K, Claris O, Collardeau-Frachon S, Kopp J, Hausser I, Mazereeuw-Hautier J, Jonca N, Zimmer AD, Sanlaville D and Fischer J (2021) Fatal Neonatal DOLK-CDG as a Rare Form of Syndromic Ichthyosis. Front. Genet. 12:719624. doi: 10.3389/fgene.2021.719624

Neonatal collodion baby or ichthyosis can pose a diagnostic challenge, and in many cases, only additional organ involvement or the course of the disease will help differentiate between non-syndromic and syndromic forms. Skin abnormalities are described in about 20% of the congenital disorders of glycosylation (CDG). Among those, some rare CDG forms constitute a special group among the syndromic ichthyoses and can initially misdirect the diagnosis towards non-syndromic genodermatosis. DOLK-CDG is such a rare subtype, resulting from a defect in dolichol kinase, in which the congenital skin phenotype (often ichthyosis) is later associated with variable extracutaneous features such as dilatative cardiomyopathy, epilepsy, microcephaly, visual impairment, and hypoglycemia and may lead to a fatal course. We report two neonatal cases of lethal ichthyosis from the same family, with distal digital constrictions and a progressive course leading to multi-organ failure and death. Postmortem trio whole-exome sequencing revealed the compound heterozygous variants NM_014908.3: c.1342G>A, p.(Gly448Arg) and NM_014908.3: c.1558A>G, p.(Thr520Ala) in the *DOLK* gene in the first affected child, which were confirmed in the affected sibling. Reduced staining with anti-α-Dystroglycan antibody was observed in frozen heart tissue of the second child as an expression of reduced O-mannosylation due to the dolichol kinase deficiency. In addition to the detailed dermatopathological changes, both cases presented hepatic and extrahepatic hemosiderosis on histological examination. Our patients represent an early and fatal form of DOLK-CDG with a striking presentation at birth resembling severe collodion baby. Both cases emphasize the phenotypic variability of glycosylation disorders and the importance to broaden the differential diagnosis of ichthyosis and to actively search for organ involvement in neonates with ichthyosis.

Keywords: DOLK, congenital disorders of glycosylation, whole exome sequencing, Mendelian disorders of cornification, syndromic ichthyosis

INTRODUCTION

Pediatric disorders leading to perinatal death still present a challenge for genetic counseling when rapid whole exome/whole genome sequencing (WES/WGS) in the neonatal setting is not available. Affected children often die before a genetic diagnosis can be established and phenotypic descriptions are often insufficient. Complete and rigorous autopsy with multiple tissue sampling of affected fetuses or children is of great importance for detecting all anomalies that can indicate a potential diagnosis, and providing frozen tissue for genetic and functional analysis. A definitive diagnosis always requires a multidisciplinary approach including clinical data, autopsy findings, and genetic results, especially for correct interpretation of the pathogenicity of the identified DNA variants. A confirmed genetic defect is the requirement for targeted carrier testing in parents and prenatal or preimplantation genetic diagnosis in further pregnancies.

Inherited ichthyoses are classified as Mendelian disorders of cornification (MEDOC), which are further defined on the basis of clinical and genetic features and can be divided into non-syndromic and syndromic forms. To date, mutations in more than 50 genes are known to result in various types of ichthyoses (Fischer and Bourrat, 2020). The syndromic ichthyoses are generally very rare and are classified based on the mode of inheritance, and can be further subdivided according to the predominant symptoms (Oji et al., 2010; Fischer and Bourrat, 2020).

Rare forms of congenital disorders of glycosylation (CDG) are among the inborn errors of metabolism presenting at birth with ichthyosis. CDG are due to deficient glycosylation of proteins and lipids and are characterized by multi-organ symptoms with a wide range of clinical severity, from mild symptoms to severe multisystem dysfunction, and even a fatal course (Francisco et al., 2019). The spectrum of clinical manifestations comprises psychomotor delay and intellectual disability, muscle hypotonia, seizures, endocrine and coagulation abnormalities, ophthalmologic anomalies, failure to thrive, and variable dysmorphic features. Skin abnormalities are described in only about 20% of the different CDG forms (Rymen et al., 2012; Haijes et al., 2020; Komlosi et al., 2020). Generally, the skin manifestations represent only a single feature within a much broader phenotype and include orange peel skin, ichthyosis, increased skin laxity, hypo/hyperpigmentation, tumoral calcinosis, aplasia cutis congenita, hypohidrosis, hyperthermia, lipodystrophy, and psoriasis (Rymen et al., 2012; Kouwenberg et al., 2014; Alsubhi et al., 2017; Van Damme et al., 2017; Haijes et al., 2020; Komlosi et al., 2020). CDG linked to ichthyosis or ichthyosiform dry skin with variable neurologic and multi-organ involvement are due to deficiencies within the dolichol (DOLK-, SRD5A3-CDG) and the GPI (glycosylphosphatidylinositol) anchor biosynthesis pathway (PIGL-CDG, MPDU1-CDG) (Schenk et al., 2001; Kranz et al., 2007; Kahrizi et al., 2011; Lefeber et al., 2011; Kapusta et al., 2013; Jaeken et al., 2014; Rymen and Jaeken, 2014; Rush et al., 2017; Thiel et al., 2018; Hall et al., 2020; Ng et al., 2021). Recently, mild manifestations were also observed in a patient with COG5-CDG (Rymen et al., 2012). We recently described a family with two affected children with COG6-CDG in whom very dry, tight, and rigid skin with hyperkeratosis and scaling was the prominent skin feature at birth (Komlosi et al., 2020).

Construction of the complex N-linked glycan chains on proteins starts with production of the lipid carrier dolichyl phosphate, which serves to anchor the nascent oligosaccharide to the endoplasmic reticulum. It is known that dolichol and dolichyl phosphate metabolites are expressed ubiquitously in humans and are localized to the endoplasmic reticulum but also present in other organelles such as the Golgi apparatus, mitochondria, and lysosomes. In addition to their critical role in glycan synthesis, dolichols have a number of other proposed functions including modulating physiochemical properties of lipid bilayers and shielding of cellular lipids from oxidative damage (Cantagrel et al., 2010; Buczkowska et al., 2015). Dolichol kinase deficiency (DOLK-CDG, OMIM #610768) is an autosomal recessive disorder that results from deficiency of the enzyme responsible for the terminal step in the synthesis of dolichol phosphate. The range of symptoms and age at presentation are highly variable in the patients described so far (Kranz et al., 2007; Lefeber et al., 2011; Kapusta et al., 2013; Rush et al., 2017; Hall et al., 2020). The phenotypic spectrum encompasses three major forms with (1) neurological abnormalities with hypotonia, microcephaly, seizures, and visual impairment with or without ichthyosis; (2) isolated cardiomyopathy; and (3) multiorgan involvement, which can also include ichthyosis (Kranz et al., 2007; Lefeber et al., 2011; Helander et al., 2013; Kapusta et al., 2013; Lieu et al., 2013; Rush et al., 2017; Hall et al., 2020; Paprocka et al., 2021). A few cases with biallelic pathogenic variants in *DOLK* (OMIM *610746) with severe multi-organ involvement encompassing profound muscular hypotonia, ichthyosiform skin, nystagmus, epilepsy, and pulmonary infections leading to death within the first months of life have also been described (Kranz et al., 2007; Lefeber et al., 2011; Lieu et al., 2013; Rush et al., 2017; Hall et al., 2020).

We present two children of a non-consanguineous French couple with compound heterozygous variants in the *DOLK* gene presenting with severe ichthyosis, distal digital constrictions, cardiomegaly, thrombocytopenia, diffuse coagulation defect, and progressive multi-organ failure, which resulted in death in the neonatal period. They represent two additional cases of the early and fatal form of DOLK-CDG with a striking presentation at birth resembling autosomal recessive congenital ichthyosis with progressive multi-organ failure.

MATERIALS AND METHODS

Clinical Report

Patient 1

The study was conducted according to the guidelines of the Declaration of Helsinki, and approved by the Ethics Committee of the University of Freiburg (ethical code number: 436/17). The parents of the patients gave written informed consent to the publication of the clinical information and the pictures.

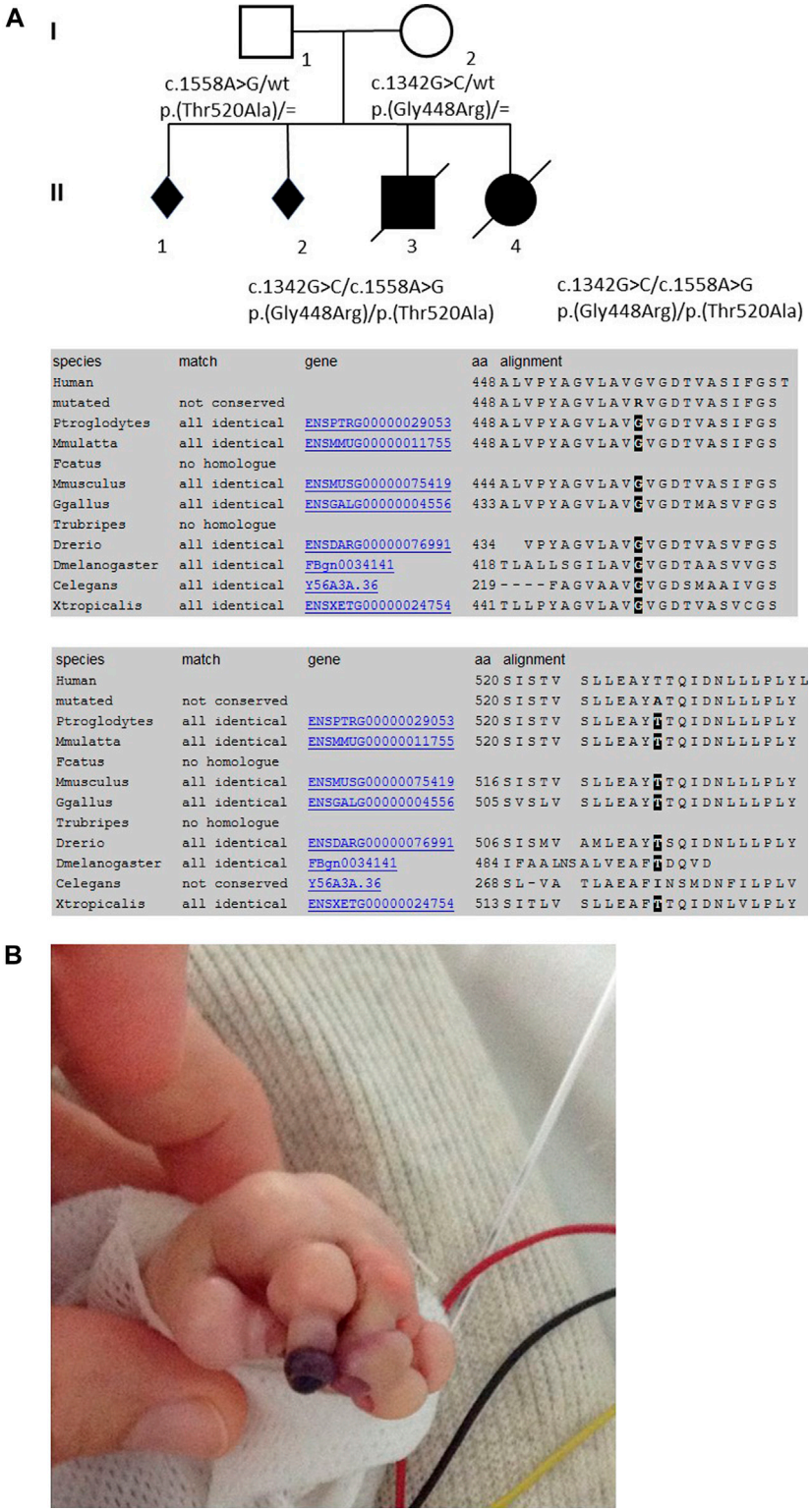

species	match	gene	aa	alignment
Human			448	ALVPYAGVLAVGVGDTVASIFGST
mutated	not conserved		448	ALVPYAGVLAVRVGDTVASIFGS
Ptroglodytes	all identical	ENSPTRG00000029053	448	ALVPYAGVLAVGVGDTVASIFGS
Mmulatta	all identical	ENSMMUG00000011755	448	ALVPYAGVLAVGVGDTVASIFGS
Fcatus	no homologue			
Mmusculus	all identical	ENSMUSG00000075419	444	ALVPYAGVLAVGVGDTVASIFGS
Ggallus	all identical	ENSGALG00000004556	433	ALVPYAGVLAVGVGDTMASVFGS
Trubripes	no homologue			
Drerio	all identical	ENSDARG00000076991	434	VPYAGVLAVGVGDTVASVFGS
Dmelanogaster	all identical	FBgn0034141	418	TLALLSGILAVGVGDTAASVVGS
Celegans	all identical	Y56A3A.36	219	----FAGVAAVGVGDSMAAIVGS
Xtropicalis	all identical	ENSXETG00000024754	441	TLLPYAGVLAVGVGDTVASVCGS

species	match	gene	aa	alignment
Human			520	SISTV SLLEAYTTQIDNLLLPLYL
mutated	not conserved		520	SISTV SLLEAYATQIDNLLLPLY
Ptroglodytes	all identical	ENSPTRG00000029053	520	SISTV SLLEAYTTQIDNLLLPLY
Mmulatta	all identical	ENSMMUG00000011755	520	SISTV SLLEAYTTQIDNLLLPLY
Fcatus	no homologue			
Mmusculus	all identical	ENSMUSG00000075419	516	SISTV SLLEAYTTQIDNLLLPLY
Ggallus	all identical	ENSGALG00000004556	505	SVSLV SLLEAYTTQIDNLLLPLY
Trubripes	no homologue			
Drerio	all identical	ENSDARG00000076991	506	SISMV AMLEAYTSQIDNLLLPLY
Dmelanogaster	all identical	FBgn0034141	484	IFAALNSALVEAFTDQVD
Celegans	not conserved	Y56A3A.36	268	SL-VA TLAEAFINSMDNFILPLV
Xtropicalis	all identical	ENSXETG00000024754	513	SITLV SLLEAFTTQIDNLVLPLY

FIGURE 1 | Pedigree of the family, conservation of the AAs among the diverse species (from MutationTaster, www.mutationtaster.org), and skin manifestations of the first child in the neonatal period.

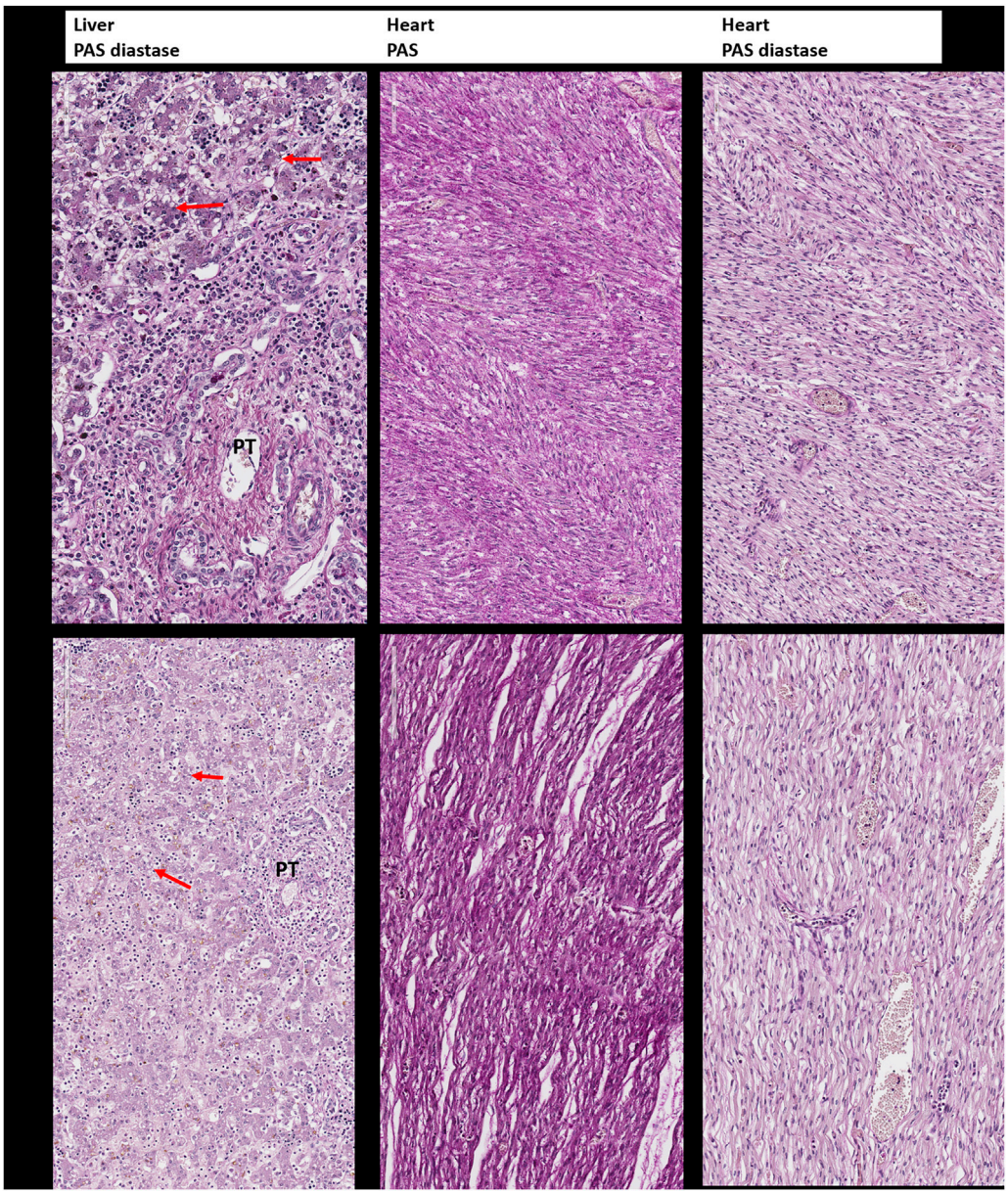

FIGURE 2 | Periodic Acid–Schiff (PAS) and Periodic Acid–Schiff–diastase (PAS-D, PAS diastase) staining for the detection of glycogen. Upper panel: Liver and heart tissue of the first child: no evidence of glycogen storage and diffuse small vacuoles of steatosis in the hepatocytes (arrow). PT: portal tract. Lower panel: Liver and heart tissue of the second child with the same findings as in the brother.

Patient 1 was male and the first child of healthy French European parents (**Figure 1A**). The mother was a 30-year-old with a history of two spontaneous abortions. Pregnancy was complicated by oligohydramnios and intrauterine growth retardation. Prenatal ultrasound examinations did not show any malformation and the couple did not wish further prenatal genetic diagnosis. Pregnancy was marked by rupture of the amniotic membrane at 31 + 2 weeks of gestation and administration of antenatal corticosteroids. The infant was born prematurely at 35 + 1 weeks of gestation by vaginal delivery with a birth weight of 1,840 g (3rd percentile), length of 42.5 cm (3rd percentile), and occipitofrontal circumference (OFC) of 31.2 cm (10th percentile). Apgar scores were 10/10/10/10 at 1, 3, 5, and 10 min, respectively. Physical examination showed a congenital anomaly of all four extremities resembling amniotic bands with extremity edema and tendinous retractions at the level of the joints (**Figure 1B**), underdeveloped thenar, rigid fingers, signs of oligohydramnios with low-set ears, hypertelorism, broad forehead and flat nose, a narrow chest, and arthrogryposis (**Supplementary Figure S1A**). The most prominent feature was the very dry, nonelastic, and hard skin. Chest x-ray showed a narrow thorax and lung hypoplasia as a

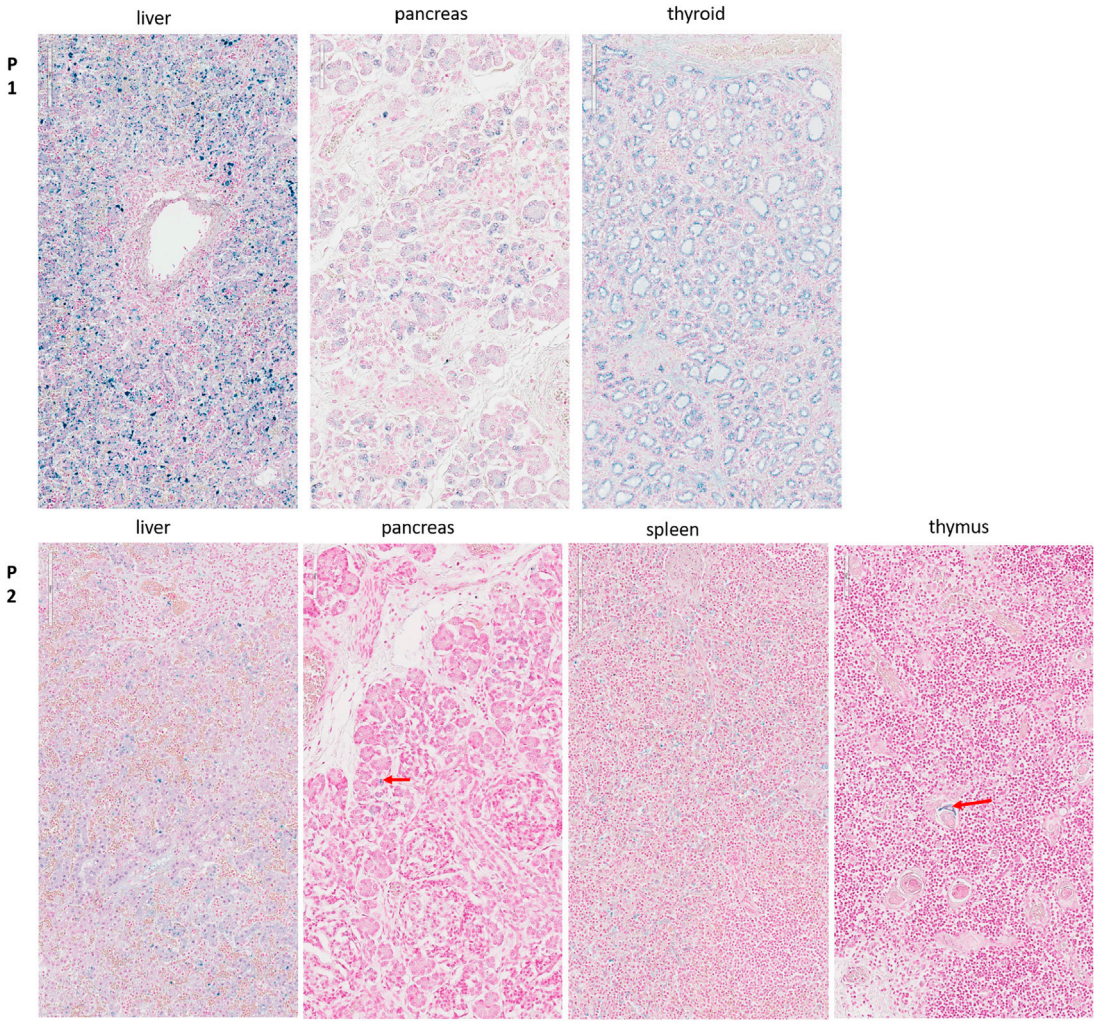

FIGURE 3 | Perls staining for the detection of hemosiderosis. Upper panel (P1): Diffuse hemosiderosis in liver parenchyma, thyroid follicles, and pancreatic acini of the first child. Lower panel (P2): Liver: relatively diffuse hemosiderosis in liver parenchyma, less intense than in her brother; Pancreas: focal hemosiderosis in a few acini (arrow); Spleen: diffuse hemosiderosis in macrophages; Thymus: focal hemosiderosis in a few Hassal corpuscles (arrow).

consequence of the oligohydramnios and cardiomegaly with right deviation of the heart. There was no sign of hepatosplenomegaly on physical examination, with no abdominal ultrasound performed. After an initial stable cardiac and respiratory state, the neonate developed progressive respiratory failure at 12 h of age and was transferred to a level III Neonatal Intensive Care Unit. He was difficult to ventilate adequately, and developed pneumomediastinum and pneumothorax requiring exsufflation. He was subsequently switched from conventional ventilation to high-frequency oscillatory ventilation. Sequential echocardiographs were performed showing severe persistent pulmonary hypertension, a large right-to-left shunting patent ductus arteriosus, and a mild but significant left ventricle hypokinesia with mild mitral and aortic insufficiency. Despite administration of dobutamine and norepinephrine, hypotension persisted and the child developed multi-organ failure after 48 h, with anuria, severe metabolic acidosis (pH 6.97), elevated lactate (15 mmol/L), thrombocytopenia (64 G/L), elevated transaminases, necrosis of the digits (**Figure 1B**), and a progressive respiratory failure. He died on postnatal day 3. The immediate cause of death was hemodynamic instability, ventricular fibrillation, and severe metabolic acidosis.

Patient 2

Patient 2 was female, born to the same parents 20 months after patient 1 (**Figure 1A**). The pregnancy was complicated by prenatal ultrasound findings of hyperechogenic intestines in gestational week 23. Conventional karyotyping and array CGH analysis from amniotic fluid was normal; *CFTR* screening revealed a heterozygous paternal mutation. After premature rupture of the amniotic membrane and chorioamnionitis, the infant was born prematurely at 32 + 4 weeks of gestation by vaginal delivery with a birth weight of 1,800 g (25th–50th percentile), a length of 44.5 cm (50th–75th percentile), and

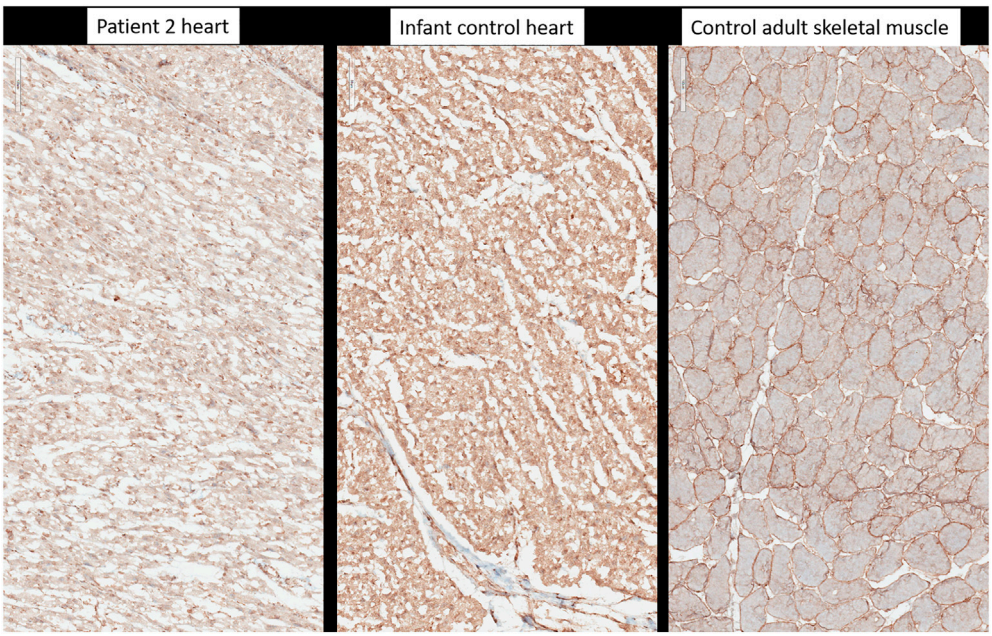

FIGURE 4 | Immunohistochemistry with anti-alpha-dystroglycan (clone VIA4-1, Sigma-Aldrich-Merck, Germany). Heart tissue of patient 2, heart tissue of a healthy age-matched control, control from adult skeletal muscle.

OFC of 29 cm (25th percentile). Apgar scores were 9/8/8/10 at 1, 3, 5, and 10 min, respectively. Physical exam showed collodion membrane with tight and hard skin with fissures, no ectropion or eclabion, and edema of the extremities (**Supplementary Figures S1A,B**). The fingers and toes were fixed in rigid volar/plantar flexion (**Supplementary Figure S1B**) and there was a blackish appearance of some fingers, raising the possibility of necrosis. Relieving incisions of the fingers (fingers II to V of both hands) were performed on day 4. There was no evidence of respiratory distress syndrome and the child was maintained on nasal CPAP (continuous positive airway pressure) until she developed apneic episodes and intubation was indicated. Although initially stable hemodynamically, on postnatal day 5, she developed several bradycardic episodes. There was no sign of hepatosplenomegaly and abdominal ultrasound was normal. Laboratory investigations revealed a diffuse coagulation defect (thrombocyte count: 201 G/L; total coagulation activity: 5.29xT, normal range: 0.8–1.2; Fibrinogen 1.8 g/L; Factor II: 9%, Factor V: 7%, Factor VII: 8%, Factor X: 16%) and plasma transfusion was administered. Ophthalmological examination showed extensive retinal hemorrhage of the right eye. On postnatal day 7, following episodes of crying and recurrent vomiting, the child developed a sudden cardiopulmonary arrest leading to death.

Molecular Genetic Analyses

Since there was no confirmed genetic diagnosis during the neonatal period in either of the siblings, postmortem genetic analyses were performed. With the clinical suspicion of congenital syndromic ichthyosis, a multi-gene panel was initially performed from DNA extracted from a postmortem liver sample of the second child of the family. Mutation analysis of 66 genes associated with non-syndromic and syndromic ichthyosis (in-house designed HaloPlex Custom Kit, Agilent Technologies, Inc. Santa Clara, CA, United States) detected no pathogenic alterations.

For further analysis, trio whole-exome sequencing of the first child and the parents was performed using DNA extracted from a postmortem thymus sample and from peripheral blood of the healthy parents. Target enrichment of all coding genomic regions (exome) was performed with a Twist Human Core Exome Kit (Twist Bioscience) and sequencing was run on an Illumina platform (NextSeq500 System, San Diego, United States) with 150-bp paired-end reads. Candidate causative variants were validated by Sanger sequencing.

Histopathological Analyses

Histopathological examination of the skin (H&E staining) was performed from the abdominal wall along the incision that was performed for internal examination in the first child (**Figure 5A**) and from the right inner thigh and the scalp of the second affected child (**Figures 5B,C**).

To assess glycogen storage in the liver and heart tissue of the first and second child, Periodic Acid–Schiff (PAS) and Periodic Acid–Schiff–diastase (PAS diastase) stainings were performed on FFPE tissues. For the detection of hemosiderosis, Perls staining was performed on FFPE of liver, spleen, pancreas, renal, thyroid, and thymus samples.

O-mannosylation was assessed by immunohistochemistry on frozen heart tissue sample of the second child with anti-α-Dystroglycan antibody (clone VIA4-1, Sigma-Aldrich Merck, Germany) directed against the O-mannosyl glycans of alpha-dystroglycan. As a control, a normal heart tissue sample from a

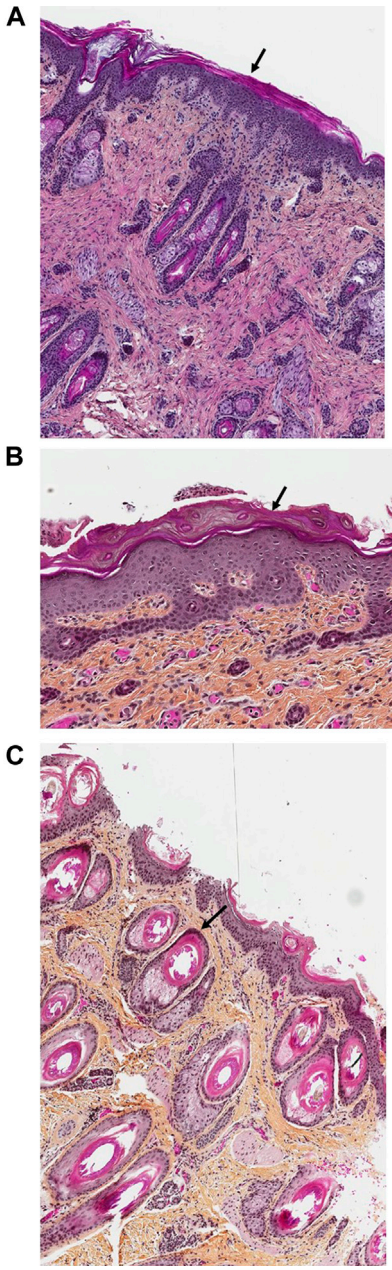

FIGURE 5 | (A–C). Skin histology of Patients 1 and 2. In the histopathological examination of the skin (H&E staining) from the abdominal wall along the incision that was performed for internal examination in the first child (**Figure 5A**, magnification ×40) and from the right inner thigh of the second affected child (**Figure 5B**, magnification ×100), the epidermis exhibited global compact orthohyperkeratosis with moderate to severe hyperplasia of the stratum corneum (arrows). The granular layer encompassed one cellular layer; there was acanthosis and no epidermal or sub-epidermal detachment (no bullae) and no inflammatory infiltrate with leucocytes or erythrocyte. Pronounced follicular plugging with onion scale-like keratin deposits were seen in the hair follicle orifices from the second child (**Figure 5C**, magnification ×100, arrow).

healthy proband of the same age was used. To determine whether the antibody worked, a tissue sample from adult skeletal muscle was used.

RESULTS

Molecular Genetic Results

Trio whole-exome sequencing revealed the compound heterozygous variants NM_014908.3:c.1342G>C, p.(Gly448Arg) and NM_014908.3:c.1558A>G, p.(Thr520Ala) in the *DOLK* gene in the affected first child. Sanger sequencing confirmed both variants in the DNA of the second child (**Figure 1A**). The variant NM_014908.3:c.1342G > C, p. (Gly448Arg), which is maternally derived, has not been described in the literature so far, nor is it listed in clinical databases (ClinVar or HGMD® Professional 2020.3). In the population database gnomAD (the Genome Aggregation Database v2.1.1; http://gnomad.broadinstitute.org/), it is listed in heterozygous state in one individual (heterozygous carriers 1/251,402, allele frequency 0.0004%). Several *in silico* algorithms predict a deleterious effect of the variant and even an effect on splicing is predicted. Residue 448 is highly conserved among eukaryotes (**Figure 1A**). According to the ACMG guidelines (Richards et al., 2015) this variant was classified as likely pathogenic (class 4). The second variant NM_014908.3:c.1558A > G, p. (Thr520Ala), which is paternally derived, was already described (Retterer et al., 2016; Rush et al., 2017 and HGMD CM1618868) as pathogenic and results in a non-conservative amino acid substitution of a polar, hydrophilic threonine with a nonpolar, hydrophobic alanine residue. The Threonine-520 residue contributes to a highly conserved cytoplasmic domain (Rush et al., 2017, **Figure 1A**). Data from gnomAD suggest that this variant is rare, with an allele frequency of 0.004% (heterozygous carriers 9/251,490).

No further causative or possibly causative variants were identified in the trio analysis that would explain the striking phenotype in the siblings. Biallelic pathogenic variants in the *DOLK* gene are known to be responsible for DOLK-CDG (OMIM #610768).

Results of the Macroscopic and Histopathological Analyses

In addition to the clinical anomalies previously described in Patient 1 (dry skin, pterygium, arthrogryposis of joints of all limbs, IUGR, cardiomegaly, and pulmonary hypoplasia, **Supplementary Figure S1A**), autopsy revealed a hypotrophic liver with diffuse steatosis (**Figure 2**, arrow) and hemosiderosis (**Figure 3**). There was no evidence of glycogen storage on PAS diastase staining in the liver (**Figure 2**). The heart weight was increased (18 g, normal value for age = 9.6 ± 2.4 g) without malformation, but ventricle wall measurement did not reveal hypertrophy and no steatosis or glycogen storage was seen on microscopic examination (**Figure 2**). Extrahepatic epithelial hemosiderosis was observed on Perls stainings in pancreatic acini and thyroid follicles (**Figure 3**, lower panel).

On postmortem examination of the second child, there was no IUGR, but pterygium and arthrogryposis of all limbs and joints, as well as skin anomalies described at birth (**Supplementary Figures S1B,C**). In addition, autopsy highlighted cardiomegaly: the heart weighed 24 g (normal = 12.6 ± 2.9 g) with mildly increased right ventricular thickness (5 mm, normal = 3.2 ±

TABLE 1 | Clinical and laboratory comparison of eight DOLK-CDG cases with fatal neonatal or early infantile course.

	Patient 1	Patient 2	Rush et al., 2017 Patient 1	Rush et al., 2017 Patient 2	Hall et al., 2020, P1	Hall et al., 2020, P2	Hall et al., 2020, P3	Hall et al., 2020, P4
Gender	M	F	F	F	M	M	M	F
Age at presentation	Prenatal	Prenatal	At birth	Prenatal	Prenatal/at birth			
Age at death	2 days	7 days	8 days	2 months	9.5 h	24 h	26 h	6 days
Consanguinity	No	No	No	No	No			
DOLK variants	c.1342G > C, *p*. (Gly448Arg)/c.1558A > G, *p*. (Thr520Ala)	c.1342G > C, *p*. (Gly448Arg)/c.1558A > G, *p*. (Thr520Ala)	c.951C > A, *p*. (Tyr327*)/c.1558A > G, *p*. (Thr520Ala)	c.951C > A, *p*. (Tyr327*)/c.1558A > G, *p*. (Thr520Ala)	c.1262T > C, *p*. (Leu421Pro)/c1373G > T, *p*. (Gly458Val)			
Pregnancy history of the mother	Two spontaneous abortions	Two spontaneous abortions	Four spontaneous abortions	Four spontaneous abortions	Two early spontaneous abortions			
Pregnancy complications	Oligohydramnios and intrauterine growth retardation	Hyperechogenic intestines	Polyhydramnios	Polyhydramnios and apparent camptodactyly	Polyhydramnios, maternal hypoglycemia (2/4), reduced fetal activity (4/4)			
Gestational weeks at birth	35 + 1	32 + 4	32 + 3	33 + 1	39	40	38	36
Birth measurements Weight Length OFC	1,840 g (3rd *p*) 42.5 cm (3rd *p*) 31.2 cm (10th *p*)	1,800 g (25th–50th *p*) 44.5 cm (50th-75th *p*) 29 cm (25th *p*)	2,060 g (50th *p*) 48 cm (>97th *p*) NR	NR	2,580 g (3rd *p*) 45 cm (<3rd *p*) 33 cm (10th *p*)	2,720 g (5th *p*)	2,320 g (3rd *p*) 47 cm (10th *p*) 31 cm (3rd *p*)	2,381 g (25th *p*) 48 cm (50th *p*) 32 cm (25th *p*)
Facial dysmorphism	Low-set ears, large earlobe, hypertelorism, broad forehead, and flat nose	No, especially no ectropion or eclabion	Taut, shiny skin over the face, slightly downward slanting palpebral fissures	NR	Skin creases on forehead	NR	Relatively normal face	Normal face with forehead creases
Skin (macroscopic)	Collodion membrane with very dry, nonelastic skin	Collodion membrane with tight skin with fissures	Collodion membrane with taut, shiny skin over the entire body	Collodion membrane with taut, shiny skin	Generalized hyperkeratosis, thick skin, linear skin creases	NR	NR	Very thick and cracked soles
Skin histology	Diffuse global hyperkeratosis, compact orthokeratosis, hyperplasia of the stratum corneum, thin granular layer	Diffuse global hyperkeratosis, hyperplasia of the stratum corneum, dilated follicular ostiums, and pronounced follicular plugging	NR	Compact hyperkeratosis with focal parakeratosis, a normal granular layer, minimal dermal inflammation EM: lipid droplets in the stratum corneum	NR	NR	Hyperkeratosis of the skin	NR
Growth retardation	Yes	No	No	NR	3/4 yes			
Microcephaly	No	No	NR	NR	No			
Brain anomalies	NR	Periventricular hemorrhage	No	NR, autopsy declined	NR			

(Continued on following page)

TABLE 1 | (*Continued*) Clinical and laboratory comparison of eight DOLK-CDG cases with fatal neonatal or early infantile course.

	Patient 1	**Patient 2**	**Rush et al., 2017 Patient 1**	**Rush et al., 2017 Patient 2**	**Hall et al., 2020, P1**	**Hall et al., 2020, P2**	**Hall et al., 2020, P3**	**Hall et al., 2020, P4**
Cardiac pathology	Cardiomegaly	Cardiomegaly	Right ventricular hypertrophy, biventricular dilation, moderate-severe atrial dilation	Dilatative cardiomyopathy, first-degree heart block	Heart block, cardiomegaly			
Pulmonary manifestations	Pulmonary hypoplasia with focal alveolar bleeding	Thrombosis of the pulmonary arteries with calcification of the vascular walls	Lung development in the late canalicular or early saccular phase, delayed for age	NR	NR			
Gastrointestinal tract manifestations	Hypotrophic liver and steatosis hepatis	Episodic vomiting, hypotrophic liver, and steatosis hepatis	Hepatosplenomegaly with fibrosis, elevated transaminases	Elevated transaminases	NR	Hepatosplenomegaly	Hepatosplenomegaly	Splenomegaly
Digital and joint anomalies	Congenital anomaly of all four extremities resembling amniotic bands with extremity edema and tendinous retractions at the level of the joints, rigid fingers	Edema of the extremities, fingers, and toes fixed in rigid volar/plantar flexion, necrosis of the fingers	Necrosis of the distal phalanges of the hands and feet, sparing the thumbs and halluces fingers and toes fixed in rigid volar/plantar flexion	Milder digital constrictions, less severe digital amputation	Joint flexion, 10-digit circumferential skin constrictions with hypoplastic, absent, and/or clubbed nails	Additionally right knee contracture	Mild contractures of the large joints	Soft tissue lesion protruding from the dorsal surface of the distal phalanx of the second digit of the right hand
Hematologic abnormalities	Coagulation defect, bleeding, and necrosis	Diffuse coagulation defect	NR	Anemia thrombocytopenia	Anemia thrombocytopenia	NR	NR	Thrombocytopenia
Metabolic abnormalities	Severe metabolic acidosis, lactacidemia	Severe metabolic acidosis, lactacidemia	Hypothyroidism	Hypothyroidism	Hypoglycemia hypokalemia	NR	Hyperbilirubinemia	Hypoglycemia

1 mm) without microscopic anomalies. No glycogen storage was seen on PAS and PAS diastase stainings (**Figure 2**). Immunohistochemistry with α-Dystroglycan antibody on frozen heart tissue showed a reduced expression compared to an age-matched control (**Figure 4**).

Liver weight in the second child was normal but diffuse steatosis (**Figure 2**) and hemosiderosis, less intense than in the brother, were present (**Figure 3**). Extrahepatic hemosiderosis was also seen on Perls staining in macrophages of spleen (diffuse hemosiderosis), while there was focal hemosiderosis in the thymus, in a few Hassal corpuscles (arrow), and in the pancreatic acini (**Figure 3**).

On histopathological examination of the skin from the abdominal wall (**Figure 5A**) of Patient 1, the epidermis exhibited global compact orthohyperkeratosis with moderate to severe hyperplasia of the stratum corneum (**Figure 5A**, arrow). The granular layer encompassed one cellular layer, and there was acanthosis and no epidermal or sub-epidermal detachment (no bullae) and no inflammatory infiltrate with leucocytes or erythrocyte (no signs of erythroderma). Histopathology from the right inner thigh of the second child was similar to those of her brother (**Figure 5B**); from the scalp, it showed pronounced follicular plugging with onion scale-like keratin deposits in hair follicle orifices (**Figure 5C**, arrow).

DISCUSSION

Here, we present two new cases of a lethal neonatal phenotype of DOLK-CDG whose severe ichthyosis at birth initially misdirected diagnostic efforts towards an autosomal recessive congenital ichthyosis. However, the combination of severe skin phenotype, distal digital constrictions, cardiomegaly, thrombocytopenia, coagulation defect, and multi-organ failure led to reconsideration and suspicion of an inborn error of metabolism. If CDG is suspected or considered early in the differential diagnosis of severely ill neonates, transferrin isoelectric focusing can be performed to screen for N-linked glycosylation defects as a rapid biochemical first-tier investigation. Due to the rapid fatal course in both of our patients, unfortunately, no isoelectric focusing of serum transferrin was performed. However, we attempted to show the effects of the compound heterozygous mutations of the dolichol kinase gene on reduced O-mannosylation in the second child. Dolichol-phosphate is converted to dolichol-phosphate-mannose, the monosaccharide donor for N-glycosylation inside the ER lumen and for O-mannosylation of alpha-dystroglycan. Immunohistochemistry with anti-α-Dystroglycan antibody directed against the O-mannosyl glycans of α-Dystroglycan on frozen heart tissue sample of the second child showed a reduced expression as an evidence of deficient protein mannosylation.

Dolichol kinase deficiency (DK) can present with a wide range and severity of symptoms (Kranz et al., 2007; Lefeber et al., 2011; Lieu et al., 2013; Rush et al., 2017; Hall et al., 2020). It can often be fatal, particularly when manifesting with cardiomyopathy. At the most severe end of the spectrum, two independent families with two and four affected children each, presenting with a lethal neonatal course including severe ichthyosis, digit skin constriction rings, dilated cardiomyopathy/cardiomegaly, hepatosplenomegaly, thrombocytopenia, hypoglycemia, and hypothyroidism, have been reported (Rush et al., 2017; Hall et al., 2020). Review of those most severely affected cases shows symptoms partly overlapping with those of our patients (**Table 1**). Besides presenting with striking congenital ichthyosis, both of our patients had a narrow chest and evidence of pulmonary hypoplasia on autopsy. In both children, evidence of hepatic and extrahepatic (spleen, thymus, thyroid, and pancreas) hemosiderosis was seen, which has only been described in a few cases of CDG so far (Agarwal et al., 2007; Léticée et al., 2010) and can lead to hematological, endocrinological, and immunological abnormalities. Endocrinopathy has already been described in other DOLK-CDG cases. Both of our patients had cardiomegaly; however, due to the rapid fatal course, they did not yet manifest signs of a dilatative cardiomyopathy. Deficient O-mannosylation of α-Dystroglycan in the heart tissue also points to a functional defect of the heart muscle in our second patient. Since altered glycosylation of certain coagulation factors can alter their plasma levels and thus influence the coagulation profile (Hansson and Stenflo, 2005), diffuse coagulopathies are often observed in CDG. The first child of the family showed necrosis of the digits already on the second day of his life probably due to thrombosis possibly caused by deficient glycosylation of clotting factors, e.g., Protein C and Protein S. The second child showed a severe diffuse coagulation defect with strongly decreased coagulation factor activities as an expression of a glycosylation defect and consequent intraretinal hemorrhage and required plasma transfusion.

It is interesting to note that the mothers in all three families reported with severe neonatal DOLK-CDG children had previous early miscarriages (Rush et al., 2017; Hall et al., 2020 and our family). In our family, no additional genetic cause was detected in the trio-exom sequencing, raising the possibility of a contribution of the *DOLK* mutation. Other prenatal manifestations in the fatal neonatal cases were IUGR (2/8), oligohydramnios (2/8), polyhydramnios (5/8), hyperechogenic intestines (in our case), and unexplained hypoglycemia of the mother during the pregnancy (2/8) (Rush et al., 2017; Hall et al., 2020 and **Table 1**).

Skin abnormalities have been described in about 20% of the different CDG forms (Rymen et al., 2012; Haijes et al., 2020; Komlosi et al., 2020). Recently, some rare forms have also been classified among the syndromic ichthyosis due to their characteristic skin manifestations (Fischer and Bourrat, 2020). Both siblings described here showed a striking congenital ichthyosis as previously described in this disease by Rush et al. (2017) and mentioned by Kranz et al. (2007) while in the four siblings with fatal neonatal DOLK-CDG recently described by Hall et al. (2020), less severe ichthyosis was seen. The pathomechanisms for the skin involvement in dolichol kinase deficiency are still not fully understood and there is only one previous report describing the detailed dermatopathological changes in this disease (Rush et al., 2017) while Hall et al. shows only the hyperkeratosis in one of the four siblings (Hall et al., 2020). Most theories explaining skin involvement are based on the assumption of the instability of key glycoproteins in skin. Since dolichol biosynthesis follows

the sterol pathway up to the formation of farnesyl-PP, it has also been proposed that accumulation of toxic sterol precursors could contribute to the phenotype in patients with SRD5A3- and DOLK-CDG (Gründahl et al., 2012; Rymen and Jaeken, 2014). Since the diagnosis of a CDG disorder was established in our cases on postmortem samples, 3 years after the death of the second child in the family, no fresh tissue sample was available to assess the accumulation of a possible toxic metabolite precursor. Glycogen storage was not observed in the liver and heart tissue of both children on microscopic examination. One missense mutation found in our patients [*DOLK* NM_014908.3:c.1558A>G, p.(Thr520Ala)] was also found in a patient published by Rush et al. (2017), and the reported dermatopathological changes in this patient concurred with ours as well. Histopathology in our cases was typical for ichthyosis with global compact orthohyperkeratosis, thin granular layer, and follicular plugging (**Figures 5A–C**). Unfortunately, no skin specimen was available anymore for further ultrastructural analysis in our case. In the previous report by Denecke and Kranz (2009), electron microscopy of a skin biopsy sample revealed hyperkeratosis (Kranz et al., 2007), while Rush et al. showed evidence of abnormal lipid droplet accumulation in the stratum corneum and keratinocytes (Rush et al., 2017). With increasing awareness for rare metabolic disorders including CDG and with the expanding possibilities of rapid genetic diagnoses even in the neonatal setting, it will be very important to further elucidate the pathomechanism of skin and organ involvement in future confirmed DOLK-CDG cases.

CONCLUSION

Our two cases presenting a detailed histopathology besides the clinical data expand the prenatal and postnatal phenotype of DOLK-CDG. They illustrate the broad differential diagnosis of neonatal syndromic ichthyosis and emphasize the importance to actively search for organ involvement in neonates with ichthyosis and to consider the congenital disorders of glycosylation among the possible diagnoses. Congenital ichthyosis with cardiac involvement and distal digital constrictions in combination with multi-organ failure and coagulation defects should prompt strong consideration of DOLK-CDG. In case of suspicion, a rapid first-tier screening using transferrin isoelectric focusing can be performed, followed by genetic analyses. Trio exome sequencing in children with severe disease course and early perinatal death can be valuable in informing the reproductive options of the affected families and allowing them access to prenatal and preimplantation genetic diagnosis.

DATA AVAILABILITY STATEMENT

The original contributions presented in the study are included in the article/**Supplementary Material**. Further inquiries can be directed to the corresponding author.

ETHICS STATEMENT

The studies involving human participants were reviewed and approved by Ethics Committee of the University of Freiburg (ethical code number: 436/17). Written informed consent to participate in this study was provided by the participants' legal guardian/next of kin. Written informed consent was obtained from the minor(s)' legal guardian/next of kin for the publication of any potentially identifiable images or data included in this article.

AUTHOR CONTRIBUTIONS

JF conceived the manuscript. OC performed the clinical diagnosis and treatment of the neonate, and OC, JM-H, and NJ initiated the genetic diagnostics and DS carried out the genetic counseling and further genetic diagnostics of the proband and their parents; SC-F carried out the macroscopic and microscopic pathological examinations; JK and JF carried out the molecular analyses and reviewed the molecular genetic results; AZ performed the bioinformatic analyses; KK and JF planned the manuscript; KK, JF, and IH interpreted the results and researched the literature; KK and JF prepared the manuscript. OC, SC-F, DS, IH, JK, AZ, and JF edited and reviewed the manuscript; JF contributed substantially to the conception, design, and critical revision of the work for important intellectual content. KK drafted the paper and coordinated writing of the manuscript. All authors discussed, read, and approved the manuscript. All authors approve the version to be published and agree to be accountable for all aspects of the work in ensuring that questions related to the accuracy or integrity of any part of the work are appropriately investigated and resolved.

FUNDING

This work was partially supported by the German Research Foundation, Grant/Award Number: FI1767/3-1. The authors confirm independence from the sponsors; the content of the article has not been influenced by the sponsors in any way.

ACKNOWLEDGMENTS

We wish to thank the family for their consent to the publication. We also thank the team of the molecular genetic laboratory of the Institute of Human Genetics Freiburg, Germany, and the team of Institute of Pathology of the Hôpital Femme Mère Enfant, Hospices Civils de Lyon, France for technical assistance in the analyses.

SUPPLEMENTARY MATERIAL

The Supplementary Material for this article can be found online at: https://www.frontiersin.org/articles/10.3389/fgene.2021.719624/full#supplementary-material

REFERENCES

Agarwal, B., Ahmed, A., Rushing, E. J., Bloom, M., Kadom, N., Vezina, G., et al. (2007). Congenital Disorder of Glycosylation-X: Clinicopathologic Study of an Autopsy Case with Distinct Neuropathologic Features. *Hum. Pathol.* 38, 1714–1719. doi:10.1016/j.humpath.2007.05.028

Alsubhi, S., Alhashem, A., Faqeih, E., Alfadhel, M., Alfaifi, A., Altuwaijri, W., et al. (2017). Congenital Disorders of Glycosylation: The Saudi Experience. *Am. J. Med. Genet.* 173, 2614–2621. doi:10.1002/ajmg.a.38358

Buczkowska, A., Swiezewska, E., and Lefeber, D. J. (2015). Genetic Defects in Dolichol Metabolism. *J. Inherit. Metab. Dis.* 38, 157–169. doi:10.1007/s10545-014-9760-1

Cantagrel, V., Lefeber, D. J., Ng, B. G., Guan, Z., Silhavy, J. L., Bielas, S. L., et al. (2010). SRD5A3 Is Required for Converting Polyprenol to Dolichol and Is Mutated in a Congenital Glycosylation Disorder. *Cell* 142, 203–217. doi:10.1016/j.cell.2010.06.001

Denecke, J., and Kranz, C. (2009). Hypoglycosylation Due to Dolichol Metabolism Defects. *Biochim. Biophys. Acta (Bba) - Mol. Basis Dis.* 1792, 888–895. doi:10.1016/j.bbadis.2009.01.013

Fischer, J., and Bourrat, E. (2020). Genetics of Inherited Ichthyoses and Related Diseases. *Acta Derm. Venereol.* 100, adv00096. doi:10.2340/00015555-3432

Francisco, R., Marques-da-Silva, D., Brasil, S., Pascoal, C., Dos Reis Ferreira, V., Morava, E., et al. (2019). The challenge of CDG Diagnosis. *Mol. Genet. Metab.* 126, 1–5. doi:10.1016/j.ymgme.2018.11.003

Gründahl, J. E. H., Guan, Z., Rust, S., Reunert, J., Müller, B., Du Chesne, I., et al. (2012). Life with Too Much Polyprenol: Polyprenol Reductase Deficiency. *Mol. Genet. Metab.* 105, 642–651. doi:10.1016/j.ymgme.2011.12.017

Haijes, H. A., Jaeken, J., and Hasselt, P. M. (2020). Hypothesis: Determining Phenotypic Specificity Facilitates Understanding of Pathophysiology in Rare Genetic Disorders. *Jrnl Inher Metab. Disea* 43, 701–711. doi:10.1002/jimd.12201

Hall, B. D., Stevenson, R. E., and Jones, J. R. (2020). Fatal Hyperkeratosis Syndrome in Four Siblings Due to Dolichol Kinase Deficiency. *Am. J. Med. Genet.* 182, 1421–1425. doi:10.1002/ajmg.a.61574

Hansson, K., and Stenflo, J. (2005). Post-translational Modifications in Proteins Involved in Blood Coagulation. *J. Thromb. Haemost.* 3, 2633–2648. doi:10.1111/j.1538-7836.2005.01478.x

Helander, A., Stödberg, T., Jaeken, J., Matthijs, G., Eriksson, M., and Eggertsen, G. (2013). Dolichol Kinase Deficiency (DOLK-CDG) with a Purely Neurological Presentation Caused by a Novel Mutation. *Mol. Genet. Metab.* 110, 342–344. doi:10.1016/j.ymgme.2013.07.002

Jaeken, J., Rymen, D., and Matthijs, G. (2014). Congenital Disorders of Glycosylation: Other Causes of Ichthyosis. *Eur. J. Hum. Genet.* 22, 444. doi:10.1038/ejhg.2013.168

Kahrizi, K., Hu, C. H., Garshasbi, M., Abedini, S. S. S., Ghadami, S., Kariminejad, R., et al. (2011). Next Generation Sequencing in a Family with Autosomal Recessive Kahrizi Syndrome (OMIM 612713) Reveals a Homozygous Frameshift Mutation in SRD5A3. *Eur. J. Hum. Genet.* 19, 115–117. doi:10.1038/ejhg.2010.132

Kapusta, L., Zucker, N., Frenckel, G., Medalion, B., Gal, T. B., Birk, E., et al. (2013). From Discrete Dilated Cardiomyopathy to Successful Cardiac Transplantation in Congenital Disorders of Glycosylation Due to Dolichol Kinase Deficiency (DK1-CDG). *Heart Fail. Rev.* 18, 187–196. doi:10.1007/s10741-012-9302-6

Komlosi, K., Gläser, S., Kopp, J., Hotz, A., Alter, S., Zimmer, A. D., et al. (2020). Neonatal Presentation of COG6-CDG with Prominent Skin Phenotype. *JIMD Rep.* 55, 51–58. doi:10.1002/jmd2.12154

Kouwenberg, D., Gardeitchik, T., Mohamed, M., Lefeber, D. J., and Morava, E. (2014). Wrinkled Skin and Fat Pads in Patients with ALG8-CDG: Revisiting Skin Manifestations in Congenital Disorders of Glycosylation. *Pediatr. Dermatol.* 31, e1–e5. doi:10.1111/pde.12233

Kranz, C., Jungeblut, C., Denecke, J., Erlekotte, A., Sohlbach, C., Debus, V., et al. (2007). A Defect in Dolichol Phosphate Biosynthesis Causes a New Inherited Disorder with Death in Early Infancy. *Am. J. Hum. Genet.* 80, 433–440. doi:10.1086/512130

Lefeber, D. J., de Brouwer, A. P. M., Morava, E., Riemersma, M., Schuurs-Hoeijmakers, J. H. M., Absmanner, B., et al. (2011). Autosomal Recessive Dilated Cardiomyopathy Due to DOLK Mutations Results from Abnormal Dystroglycan O-Mannosylation. *Plos Genet.* 7, e1002427. doi:10.1371/journal.pgen.1002427

Léticée, N., Bessières-Grattagliano, B., Dupré, T., Vuillaumier-Barrot, S., de Lonlay, P., Razavi, F., et al. (2010). Should PMM2-Deficiency (CDG Ia) Be Searched in Every Case of Unexplained Hydrops Fetalis? *Mol. Genet. Metab.* 101, 253–257. doi:10.1016/j.ymgme.2010.06.009

Lieu, M. T., Ng, B. G., Rush, J. S., Wood, T., Basehore, M. J., Hegde, M., et al. (2013). Severe, Fatal Multisystem Manifestations in a Patient with Dolichol Kinase-Congenital Disorder of Glycosylation. *Mol. Genet. Metab.* 110, 484–489. doi:10.1016/j.ymgme.2013.09.016

Ng, B. G., Hackmann, K., Jones, M. A., Eroshkin, A. M., He, P., Wiliams, R., et al. (2021). Mutations in the Glycosylphosphatidylinositol Gene PIGL Cause CHIME Syndrome. *Am. J. Hum. Genet.* 90, 685–688. doi:10.1016/j.ajhg.2012.02.010

Oji, V., Tadini, G., Akiyama, M., Blanchet Bardon, C., Bodemer, C., Bourrat, E., et al. (2010). Revised Nomenclature and Classification of Inherited Ichthyoses: Results of the First Ichthyosis Consensus Conference in Sorèze 2009. *J. Am. Acad. Dermatol.* 63, 607–641. doi:10.1016/j.jaad.2009.11.020

Paprocka, J., Jezela-Stanek, A., Tylki-Szymańska, A., and Grunewald, S. (2021). Congenital Disorders of Glycosylation from a Neurological Perspective. *Brain Sci.* 11, 88. doi:10.3390/brainsci11010088

Retterer, K., Juusola, J., Cho, M. T., Vitazka, P., Millan, F., Gibellini, F., et al. (2016). Clinical Application of Whole-Exome Sequencing across Clinical Indications. *Genet. Med.* 18, 696–704. doi:10.1038/gim.2015.148

Richards, S., Aziz, N., Aziz, N., Bale, S., Bick, D., Das, S., et al. (2015). Standards and Guidelines for the Interpretation of Sequence Variants: a Joint Consensus Recommendation of the American College of Medical Genetics and Genomics and the Association for Molecular Pathology. *Genet. Med.* 17, 405–423. doi:10.1038/gim.2015.30

Rush, E. T., Baker, C. V., and Rizzo, W. B. (2017). Dolichol Kinase Deficiency (DOLK-CDG): Two New Cases and Expansion of Phenotype. *Am. J. Med. Genet.* 173, 2428–2434. doi:10.1002/ajmg.a.38287

Rymen, D., and Jaeken, J. (2014). Skin Manifestations in CDG. *J. Inherit. Metab. Dis.* 37, 699–708. doi:10.1007/s10545-014-9678-7

Rymen, D., Keldermans, L., Race, V., Régal, L., Deconinck, N., Dionisi-Vici, C., et al. (2012). COG5-CDG: Expanding the Clinical Spectrum. *Orphanet. J. Rare. Dis.* 7, 94. doi:10.1186/1750-1172-7-94

Schenk, B., Imbach, T., Frank, C. G., Grubenmann, C. E., Raymond, G. V., Hurvitz, H., et al. (2001). MPDU1 Mutations Underlie a Novel Human Congenital Disorder of Glycosylation, Designated Type if. *J. Clin. Invest.* 108, 1687–1695. doi:10.1172/jci200113419

Thiel, C., Wortmann, S., Riedhammer, K., Alhaddad, B., Mayatepek, E., Prokisch, H., et al. (2018). Severe Ichthyosis in MPDU1-CDG. *J. Inherit. Metab. Dis.* 41, 1293–1294. doi:10.1007/s10545-018-0189-9

Van Damme, T., Gardeitchik, T., Mohamed, M., Guerrero-Castillo, S., Freisinger, P., Guillemyn, B., et al. (2017). Mutations in ATP6V1E1 or ATP6V1A Cause Autosomal-Recessive Cutis Laxa. *Am. J. Hum. Genet.* 100, 216–227. doi:10.1016/j.ajhg.2016.12.010

Conflict of Interest: The authors declare that the research was conducted in the absence of any commercial or financial relationships that could be construed as a potential conflict of interest.

Advantages of publishing in Frontiers

OPEN ACCESS
Articles are free to read for greatest visibility and readership

FAST PUBLICATION
Around 90 days from submission to decision

HIGH QUALITY PEER-REVIEW
Rigorous, collaborative, and constructive peer-review

TRANSPARENT PEER-REVIEW
Editors and reviewers acknowledged by name on published articles

Frontiers
Avenue du Tribunal-Fédéral 34
1005 Lausanne | Switzerland

Visit us: www.frontiersin.org
Contact us: frontiersin.org/about/contact

REPRODUCIBILITY OF RESEARCH
Support open data and methods to enhance research reproducibility

DIGITAL PUBLISHING
Articles designed for optimal readership across devices

FOLLOW US
@frontiersin

IMPACT METRICS
Advanced article metrics track visibility across digital media

EXTENSIVE PROMOTION
Marketing and promotion of impactful research

LOOP RESEARCH NETWORK
Our network increases your article's readership